

Advances in Science, Technology & Innovation
IEREK Interdisciplinary Series for Sustainable Development



Helder I. Chaminé
José Augusto Fernandes *Editors*

Advances in Geoengineering, Geotechnologies, and Geoenvironment for Earth Systems and Sustainable Georesources Management

Proceedings of the 1st Conference on Georesources,
Geomaterials, Geotechnologies and Geoenvironment
(4GEO), Porto, 2019

Advances in Science, Technology & Innovation

IEREK Interdisciplinary Series for Sustainable Development

Editorial Board

Anna Laura Pisello, Department of Engineering, University of Perugia, Italy

Dean Hawkes, University of Cambridge, Cambridge, UK

Hocine Bougdah, University for the Creative Arts, Farnham, UK

Federica Rosso, Sapienza University of Rome, Rome, Italy

Hassan Abdalla, University of East London, London, UK

Sofia-Natalia Boemi, Aristotle University of Thessaloniki, Greece

Nabil Mohareb, Faculty of Architecture—Design and Built Environment,
Beirut Arab University, Beirut, Lebanon

Saleh Mesbah Elkaffas, Arab Academy for Science, Technology and Maritime Transport,
Cairo, Egypt

Emmanuel Bozonnet, University of La Rochelle, La Rochelle, France

Gloria Pignatta, University of Perugia, Italy

Yasser Mahgoub, Qatar University, Qatar

Luciano De Bonis, University of Molise, Italy

Stella Kostopoulou, Regional and Tourism Development, University of Thessaloniki,
Thessaloniki, Greece

Biswajeet Pradhan, Faculty of Engineering and IT, University of Technology Sydney,
Sydney, Australia

Md. Abdul Mannan, Universiti Malaysia Sarawak, Malaysia

Chaham Alalouch, Sultan Qaboos University, Muscat, Oman

Iman O. Gawad, Helwan University, Egypt

Anand Nayyar , Graduate School, Duy Tan University, Da Nang, Vietnam

Series Editor

Mourad Amer, International Experts for Research Enrichment and Knowledge Exchange
(IEREK), Cairo, Egypt

Advances in Science, Technology & Innovation (ASTI) is a series of peer-reviewed books based on important emerging research that redefines the current disciplinary boundaries in science, technology and innovation (STI) in order to develop integrated concepts for sustainable development. It not only discusses the progress made towards securing more resources, allocating smarter solutions, and rebalancing the relationship between nature and people, but also provides in-depth insights from comprehensive research that addresses the **17 sustainable development goals (SDGs)** as set out by the UN for 2030.

The series draws on the best research papers from various IEREK and other international conferences to promote the creation and development of viable solutions for a **sustainable future and a positive societal** transformation with the help of integrated and innovative science-based approaches. Including interdisciplinary contributions, it presents innovative approaches and highlights how they can best support both economic and sustainable development, through better use of data, more effective institutions, and global, local and individual action, for the welfare of all societies.

The series particularly features conceptual and empirical contributions from various interrelated fields of science, technology and innovation, with an emphasis on digital transformation, that focus on providing practical solutions to **ensure food, water and energy security to achieve the SDGs**. It also presents new case studies offering concrete examples of how to resolve sustainable urbanization and environmental issues in different regions of the world.

The series is intended for professionals in research and teaching, consultancies and industry, and government and international organizations. Published in collaboration with IEREK, the Springer ASTI series will acquaint readers with essential new studies in STI for sustainable development.


ASTI series has now been accepted for Scopus (September 2020). All content published in this series will start appearing on the Scopus site in early 2021.

Helder I. Chaminé • José Augusto Fernandes
Editors

Advances in Geoengineering, Geotechnologies, and Geoenvironment for Earth Systems and Sustainable Georesources Management

Proceedings of the 1st Conference
on Georesources, Geomaterials,
Geotechnologies and Geoenvironment
(4GEO), Porto, 2019

Editors

Helder I. Chaminé 
Department of Geotechnical Engineering
and LABCARGA—Laboratory of Cartography
and Applied Geology
School of Engineering—ISEP
Polytechnic of Porto
Porto, Portugal

José Augusto Fernandes
Department of Geotechnical Engineering
and LGMC—Laboratory of Geotechnics
and Construction Materials
School of Engineering—ISEP
Polytechnic of Porto
Porto, Portugal

ISSN 2522-8714 ISSN 2522-8722 (electronic)
Advances in Science, Technology & Innovation
IEREK Interdisciplinary Series for Sustainable Development
ISBN 978-3-031-25985-2 ISBN 978-3-031-25986-9 (eBook)
<https://doi.org/10.1007/978-3-031-25986-9>

© The Editor(s) (if applicable) and The Author(s), under exclusive license to Springer Nature
Switzerland AG 2023

This work is subject to copyright. All rights are solely and exclusively licensed by the Publisher, whether the whole or part of the material is concerned, specifically the rights of translation, reprinting, reuse of illustrations, recitation, broadcasting, reproduction on microfilms or in any other physical way, and transmission or information storage and retrieval, electronic adaptation, computer software, or by similar or dissimilar methodology now known or hereafter developed.

The use of general descriptive names, registered names, trademarks, service marks, etc. in this publication does not imply, even in the absence of a specific statement, that such names are exempt from the relevant protective laws and regulations and therefore free for general use.

The publisher, the authors, and the editors are safe to assume that the advice and information in this book are believed to be true and accurate at the date of publication. Neither the publisher nor the authors or the editors give a warranty, expressed or implied, with respect to the material contained herein or for any errors or omissions that may have been made. The publisher remains neutral with regard to jurisdictional claims in published maps and institutional affiliations.

Disclaimer: Despite the independent peer-review process, the authors of individual chapters are solely responsible for ideas, views, data, figures, maps, and geographical boundaries presented in the respective chapters of this book, and these have not been endorsed, in any form, by the publisher, the guest editors, and the author of Foreword, or other Chapters.

This Springer imprint is published by the registered company Springer Nature Switzerland AG
The registered company address is: Gewerbestrasse 11, 6330 Cham, Switzerland

Committees

Scientific Committee

Chairs

Helder I. Chaminé, ISEP, Portugal
José Augusto Fernandes, ISEP, Portugal

Board

Acacia Naves, UC, Spain
Agostinho Mendonça, Soares da Costa & DEG|ISEP, Portugal
Alberto Gomes, FLUP, Portugal
Alcides J.S.C. Pereira, FCTUC, Portugal
Alexandre Pinto, IST|UL, Jetsj & SPG, Portugal
Amélia Dionísio, IST|UL, Portugal
Ana Cláudia Teodoro, FCUP, Portugal
Ana Cristina Meira, DM|ISEP, Portugal
Ana Malheiro, LREC, Azores, Portugal
Ana Maria Castañón, ULE, Spain
Ana Pires, LSA|ISEP-INESC TEC, Portugal
André Dias, LSA|ISEP-INESC TEC, Portugal
Anna Ostręga, AGH, Poland
António Gomes Correia, UM, Portugal
António Guerner Dias, FCUP, Portugal
António José Roque, LNEC, Portugal
António Mouraz Miranda, IST|UL, Portugal
António Pinho, UÉ, Portugal
António Rodrigues Vieira, Mota-Engil Africa, Mozambique
António Vega y de La Fuente, DEG|ISEP, Portugal
Ary Pinto de Jesus, FCUP, Portugal
Atiye Tugrul, IU, Turkey
Augusto Pérez-Alberti, USC, Spain
Barbara Tora, AGH, Poland
Cândido Freitas, DEC|ISEP, Portugal
Carlos Baião, TPF, Portugal
Carlos Costa, EGIAMB, Portugal
Carlos Dinis da Gama, IST|UL, Portugal
Carlos Leal Gomes, UM, Portugal
Celeste Jorge, LNEC, Portugal
Cino Viggiani, UG, France

Cristina Delerue-Matos, DEQ|ISEP, Portugal
Cristina Rodrigues, UFP, Portugal & UAN, Angola
Eda Freitas de Quadros, BGTech, Brazil
Eduardo Ferreira da Silva, UA, Portugal
Eduardo Fortunato, LNEC, FEUP & SPG, Portugal
Elisabete Costa, DEG|ISEP, Portugal
Felipe Macías, AMBIO SOL & USC, Spain
Fernando Marques, FCUL, Portugal
Fernando Pedro Figueiredo, FCTUC, Portugal
Fernando Rocha, UA, Portugal
Francisco Javier Elorza, UPM, Spain
Frederic L. Pellet, INSA|UL, France
Giorgio Lollino, IRPI|CNR, Italy
Gustavo Paneiro, IST|UL, Portugal
Isabel Duarte, UÉ, Portugal
Isabel Fernandes, FCUL & SPG, Portugal
Isik Yilmaz, CU, Turkey
Joana Ribeiro, FCTUC, Portugal
João Coroado, IPT, Portugal
João Paulo Meixedo, DEG|ISEP, Portugal
João Santos Baptista, FEUP, Portugal
Jorge Carvalho, FEUP, Portugal
Jorge Luis Loredo, UO, Spain
Jorge Relvas, FCUL, Portugal
José António Simões Cortez, FEUP, Portugal
José Filinto Trigo, DEC|ISEP, Portugal
José Lopes Velho, UA, Portugal
José Manuel Marques, IST|UL, Portugal
José Martins Carvalho, DEG|ISEP, Portugal
José Neves, IST|UL & SPG, Portugal
José Soeiro Carvalho, FEUP, Portugal
José Teixeira, FLUP, Portugal
Kaan Erarslan, KDU, Turkey
Kerim Aydiner, KTU, Turkey
Krzysztof Broda, AGH, Poland
Leandro R. Alejandro, UVg, Spain
Lídia Catarino, FCTUC, Portugal
Luís Ferreira Gomes, UBI, Portugal
Luis González de Vallejo, UCM, Spain
Luís Lopes, UÉ, Portugal
Luís Ribeiro e Sousa, FEUP, Portugal
Manuel Abrunhosa, IAH|GP, Portugal
Manuel Francisco Costa Pereira, IST|UL, Portugal
Manuel G. Romana, UPM, Spain
Manuel João Lemos de Sousa, UFP, Portugal
Manuela Carvalho, DEG|ISEP, Portugal
Manuela Simões, UNL, Portugal
Maria de Lurdes Dinis, FEUP, Portugal
Maria Eugénia Lopes, DEG|ISEP, Portugal
Maria João Fernandes, LAQV, GRAQ|ISEP, Portugal
Maria José Afonso, DEG|ISEP, Portugal
Mário Quinta-Ferreira, FCTUC, Portugal
Mercedes Fuertes-Fuente, UO, Spain

Nick Barton, NB|HSRE, Norway
Norberto Jorge-Bejerman, ASAGAI, Argentina
Nuno Pimentel, FCUL, Portugal
Orquídia Neves, IST|UL, Portugal
Paulo Sá Caetano, UNL, Portugal
Pedro Santarém Andrade, FCTUC, Portugal
Rafael Fernández-Rubio, UPM, Spain
Raúl Pistone, COBA & CPT|SPG, Portugal
Ricardo Oliveira, UNL & COBA, Portugal
Richard Přikryl, CUP, Czech Republic
Romeu Vieira, FMG, Portugal
Rosário Carvalho, FCUL, Portugal
Rui Baptista, GALP & FCUL, Portugal
Sílvia Costa Spínola, DEG|ISEP, Portugal
Telma Barroso, GEO, Portugal
Tiago Miranda, UM, Portugal

Organizing Committee

General Chair

José Augusto Fernandes, ISEP & OET, Portugal

Advisor Board

António Sequeira Correia, OET, Portugal
Mário Gil Abrunhosa, OET, Portugal
António Fernandes, OET, Portugal
António Rodrigues Vieira, OET & Mota-Engil, Portugal

Local Organizing Committee

Sílvia Costa Spínola, DEG|ISEP, Portugal
Maria Eugénia Lopes, DEG|ISEP, Portugal
Maria João Fernandes, LAQV-GRAQ|ISEP, Portugal
Isilda Costa, LGMC|ISEP, Portugal
Helen Meerkhan, LABCARGA|ISEP & GeoBioTec|UA, Portugal

Foreword

This volume integrates an impressive set of contributions from authors showing an ever-increasing awareness of the importance of interrelated fields: geomaterials, georesources, geotechnologies and geoenvironment. All these disciplines have an essential role in solving major problems for the industrial world, minimising the resulting adverse effects, keeping economic stability and contributing to society's health and welfare. Indeed, the book encompasses studies associated with geosciences, georesources, engineering geology, geotechnical engineering, rock engineering and the environment, which are paramount for solving engineering and societal problems. Thus, the book includes topical research related to (i) functional geomaterials and applications in geotechnics, georesources and environment; (ii) emerging technologies in engineering geosciences and learned lessons by large engineering works and geohazards; (iii) geoenvironment issues and climate change, including groundwater engineering and geothermic applications.

The volume materialises crucial developing research topics that reshape the recent disciplinary frontiers in science, engineering, and innovation to improve combined concepts for sustainability and earth systems resilience. Moreover, the book's scope provides an in-depth understanding of comprehensive research that focuses on some of the key "Sustainable Development Goals" (SDGs) and interrelated targets established by the UN for 2030. That promotes the following SDGs: "SDG 7: Affordable and Clean Energy", "SDG 9: Industry, Innovation and Infrastructure", "SDG 11: Sustainable Cities and Communities", "SDG 12: Responsible Consumption and Production" and "SDG 13: Climate Action". Thus, the book underlines the improvement of workable results for a sustainable outlook and an enlightened societal change with the practical support of combined applied geosciences, geotechnics and georesources. In addition, it comprises interdisciplinary contributions that highlight the best support for socioeconomic, eco-responsibility, and sustainable progress for the well-being of communities.

This book, entitled "Advances in Geoengineering, Geotechnologies, and Geoenvironment for Earth Systems and Sustainable Georesources Management", mainly results from selected peer-review contributions presented at the "1st Conference on Georesources, Geomaterials, Geotechnologies and Geoenvironment" (4GEO), Porto, on 7–8 November 2019 and the pre-conference meeting "The Sustainability of the Environmental Compartments: Soil, Water, and Air" co-organised by APEMETA–LNEC–ISEP. These remarkable conference papers represent the value of applied geosciences, geoengineering, geomaterials and geoenvironment in sustainability and earth systems management. In summary, this volume is informative and updates the explanation of the current advances in the above-interrelated disciplines and will overwhelmingly aid the researchers, practitioners and students. Furthermore, it is an impressive contribution to lessening the gap between academia, research and industry. That helpful

approach in the search to understand and contribute to solving environmental issues and balanced resilient engineering designing solutions with environment.

Lastly, it is fair to recognise the author's valuable contributions included in this volume, as well as the scientific committee and guest editors' efforts to ensure the volume quality. This book will be an excellent asset for the Springer publisher included in the series of Advances in Science, Technology & Innovation (ASTI), an IEREK Interdisciplinary Series for Sustainable Development. Furthermore, the readers will find a vivid source of practical knowledge and inspiration for future and trending research works.

Guimarães, Portugal
July 2021

António Gomes Correia
Professor and Researcher at ISISE
University of Minho
Braga, Portugal

Preface

(...) many geological 'products' seem so simple that it is, for both the general public and decision makers, often difficult to understand how complex the activities are that are needed for making these apparently very simple raw materials available. A good example is aggregate, probably the simplest geological product. The understanding of aggregate characteristics requires a profound knowledge of the rock properties and of the variation of these properties.

—(van Loon 2002)

Rocks and soils are natural material that forms the earth's crust. The fluids flow through pores and ground fissures. Thus, the natural materials are formed in a continuous geodynamic cycle through geological time. In engineering practice, geological materials—from igneous, metamorphic, sedimentary and weathered rocks, including residual soils—can be outlined into hard rocks, soft rocks and soils (e.g. De Freitas 2009; Chaminé et al. 2013). Lately, anthropic rocks have been considered a shared term for rock materials and construction materials altered or relocated by humans (Underwood 2001), which is well illustrated in urban areas continuously assembled and reassembled by the materials that shift into it from elsewhere (Edensor 2020). Human activities have induced profound and rapid changes to the earth's surface in the last centuries. Additionally, the earth's systems are dominated by climate variability and anthropic actions (e.g. Lyell 1830–1833; Marsh 1865; Stoppani 1873). This anthropic footprint shaped the so-called Anthropocene (e.g. Crutzen and Stoermer 2000; Crutzen 2002; Ehlers and Krafft 2006; Glikson and Groves 2016; Thomas et al. 2020). Since the dawn of time, the first human settlements and civilisations used natural raw materials leading to a society acting as a dynamic geomorphic agent (e.g. Marsh 1865; Sherlock 1922; Thomas 1956; Hooke 2000; Ambrose 2001). Nowadays, society demands a balanced and better response of all activities and operations related to a green footprint for responsible and sustainable resources management, i.e. the path shall be transitioning from a mining life cycle to a sustainable georesource management living cycle (e.g. Tilton 1996; Giurco and Cooper 2012; Danielsen and Kuznetsova 2016; Nurmi 2017; Gorman and Dzombak 2018; Smol et al. 2020; Mudd 2021; and references therein). Because of all that, the communication and dissemination of geosciences and engineering with the public must be clear and direct within a geoethical context (Moore 1997; Di Capua et al. 2021).

Georesources, geomaterials, geotechnologies and geoenvironment are challenging and interrelated subjects in modern society. This deserves a deeper reflection by academia, practitioners, authorities, policy-makers and the public. That is necessary for proper sustainable resource management and an engineering design with nature within a geoethical framework. That approach must combine technical-scientific integrity, eco-responsibility, sustainability, functionality and communication with society.

In a broad sense, georesources are understood as geological and energetic resources of great importance to a sustainable and developing society. Minerals, rocks, water and energy have assumed an essential role in societies' technological development. Given the increase in population and the rising needs and intensification of their use, it is crucial to ensure sustainable management and responsible solutions designed with nature, geohazards and society (McHarg 1992; González de Vallejo 2012; Chaminé et al. 2013).

Natural sand, gravel and crushed rock aggregates are essential to the societal environment and represent a large proportion of the materials used in the construction industry (Smith and Collis 2001; van Loon 2002). The earth's materials were designated by Fookes (1991) as geomaterials. Therefore, geomaterials are processed or unprocessed soils, rocks or minerals used in the construction of buildings or structures, including man-made construction materials manufactured from soils, rocks or minerals. More recently, Prikry et al. (2016) termed geomaterials as “inorganic raw materials derived from the earth's crust and used in construction after appropriate processing to make a natural and functionally varied group of mineral resources”. In addition, the geomaterials for construction shall encompass sustainability and functionality as the primary mineral raw materials exploited, processed, and used by society. Consequently, geomaterials are functional geological materials artificially processed for the generality of the activities developed by man (e.g. Fookes 1991; Smith and Collis 2001; van Loon 2002; Fernandes et al. 2016; Prikry et al. 2016). The functional geomaterials may include rock, clay, granular materials, treated soils and industrial waste.

Site appraisal for geotechnics must be shaped by understanding earth systems and ground conditions (e.g. Glossop 1968; De Freitas 2009; Griffiths 2014; Chaminé et al. 2021). Geotechnical practitioners aim to contribute to properly studying soils and rocks' ground behaviour and their applications in sustainable design with nature and the society. Geotechnologies are an essential tool for supporting the collection, mapping and geospatial analysis of data with geographical information systems, high-resolution digital imagery developed by unmanned aerial vehicles, high-precision global position systems, remote sensing, and additional techniques used in the most diverse geoenvironmental fields, including supporting the monitoring and prediction of natural hazards.

The geoenvironment is a traversal field that identifies the continuous changes resulting from the transformations of the contemporary world and finds solutions to the resulting socio-economic and environmental changes impacting health and life. Yong et al. (2015) state that “the geoenvironment is a specific compartment of the environment and concerns itself with the various elements and interactions occurring in the domain defined by a significant portion of the geosphere and portions of the atmosphere, hydrosphere, biosphere, and anthroposphere”. In addition, climate change, industrialisation and human activity are, among others, factors of pressure and alteration of the natural environment, so it is necessary to minimise impacts and emerging hazards and risks.

This book contains the selected presentations submitted at the “1st Conference on Georesources, Geomaterials, Geotechnologies and Geoenvironment” (4GEO). That conference was held in Porto, Portugal, from 7 to 8 November 2019 and held in the School of Engineering (ISEP), Polytechnic of Porto, based in Porto city, a UNESCO World Heritage Site. This event was a joint organisation by the Geotechnical and Mining Engineering Body from the Order of Technical Engineers (OET) from Portugal and the Department of Geotechnical Engineering of ISEP. In addition, it includes some geoenvironmental topical works from the pre-conference meeting “The Sustainability of the Environmental Compartments: Soil, Water, and Air”, 6 November 2019, co-organised by APEMETA—Portuguese Association of Environmental Technology Companies, LNEC (National Laboratory for Civil Engineering) and ISEP.

Various contributions to this special volume confirm the challenges of a balanced earth systems management and design with nature, geohazards and society. In this volume were considered three major sections (Fig. 1):

1. Geomaterials, Geotechnics and Georesources. The main topics were (i) functional materials and raw materials; applications and advanced laboratory geotechnical testing; site geotechnical characterisation and evaluation; (ii) mineral deposits; mineral resources availability; exploration, mining design and sustainable project.



Fig. 1 Word cloud based on keywords of the special volume on “Advances in Geoengineering, Geotechnologies, and Geoenvironment for Earth Systems and Sustainable Georesources Management” (generated using <http://www.edwordle.net>)

2. Geotechnologies, Engineering Geosciences and Geohazards. The main themes were surveying and planning management; engineering geology and rock engineering; geohazards; offshore mining; ground modelling, GIS mapping, photogrammetry and geopositioning, unmanned aerial systems and techniques.
3. Geoenvironment, Water and Climate Change. The main subjects were geoenvironment and contaminated soils; geoenvironmental technologies and applications; groundwater engineering; geothermic, water and climate change.

These challenges reinforce the need to promote geoengineering integration, including characterisation, analysis, evaluation, and modelling within a geoethical, environmental and societal framework. This volume provides new insights on geoengineering in model regions in Southern Africa, Asia, America and Europe but focuses on the Iberian Peninsula. It offers new perceptions of the interrelated fields of geotechnics, geomaterials, georesources, geotechnologies and geoenvironment. It includes critical studies illustrating earth systems’ role in fostering a sustainable environment and the most refined engineering design. Furthermore, the volume discusses the latest advances in geoengineering, georesources, functional geomaterials and geoenvironmental issues from varied environments and highlights the influence of climate variability and technologies on earth systems.

The special volume has a core of 47 conference papers mainly grounded on scientific sessions. During the sessions was performed five outstanding keynote lectures by Luis González de Vallejo (Complutense University of Madrid, Spain), Richard Příkryl (Charles University of Prague, Czech Republic), Felipe Macías (University of Santiago de Compostela, Spain), Isabel Fernandes (University of Lisbon, Portugal) and Ana Pires (ISEP–INESC TEC, Portugal). The keynote speakers gave interesting insights into the following topics: lessons learned on geological and geotechnical hazards in large engineering infrastructures, functional geomaterials as critical mineral raw materials and their service for a modern society, applications of technosols in environmental problems aiming for a better solution, the role of engineering geosciences focused on concrete studies for construction purposes, as well as the recent developments of geotechnologies in harbour, coastal and marine geotechnics and hardness rock material studies in the space environment. The volume met over 135 authors from the academy, research centres and state laboratories or industry and was assigned over 97 reviewers to revise and improve the presented works during the peer-review process.



Fig. 2 Overview during the sessions from the 1st Conference on Georesources, Geomaterials, Geotechnologies and Geoenvironment (4GEO) at ISEP, *Porto* keynote lectures, communications and a musical moment by ISEP Academic Tuna before the closing ceremony

The book interests scholars and practitioners in engineering geosciences, geotechnics, georesources, raw materials, geomaterials, geoenvironmental and water sciences. Also, students and environment-related practitioners will find the volume a valuable source for further research. Regarding the interference of society with nature, the words of Marsh (1865) are topical: “(...) to suggest the possibility and the importance of the restoration of disturbed harmonies and the material improvement of waste and exhausted regions”. Conversely, Sherlock (1922) highlights a sound principle “(...) the dictum that we cannot be said to know anything until we have measured it, applies to geology as much as to physics, and we should aim at obtaining as near an approximation to the true figures as circumstances permit”. Or, in short, by the inspiring words of Hoek (1999) are still present: “putting numbers to geology”. The reader of this book will find the conference papers topical and quantitative, supported by this approach to understanding nature better to lead to balance, resilient and eco-responsible solutions. The book covers the scope of the “Sustainable Development Goals” (SDGs) and interconnected targets established by the UN for 2030, namely “SDG 7: Affordable and Clean Energy”, “SDG 9: Industry, Innovation and Infrastructure”, “SDG 11: Sustainable Cities and Communities”, “SDG 12: Responsible Consumption and Production” and “SDG 13: Climate Action”. The diverse topics published in this unique volume contribute to the clear shift of the environmental geotechnologies, green functional geomaterials and natural resources footprint paradigm based on the design of sustainable and resilient solutions. It demands better geosciences, geoengineering, georesources and geoenvironment in mapping, characterising, evaluating, modelling and designing solutions with nature, geohazards and society.

Porto, Portugal
July 2021

Helder I. Chaminé
José Augusto Fernandes

References

- Ambrose SH (2001) Paleolithic technology and human evolution. *Science* 291:1748–1753
- Chaminé HI, Afonso MJ, Teixeira J, Ramos L, Fonseca L, Pinheiro R, Galiza AC (2013) Using engineering geosciences mapping and GIS-based tools for georesources management: lessons learned from rock quarrying. *Eur Geol J* 36:27–33
- Chaminé HI, Afonso MJ, Trigo JF, Freitas L, Ramos L, Carvalho JM (2021) Site appraisal in fractured rock media: coupling engineering geological mapping and geotechnical modelling. *Eur Geol J* 51:31–38
- Crutzen PJ, Stoermer EF (2000) The ‘Anthropocene’. *IGBP Newsletter* 41:17–18
- Crutzen, PJ (2002) Geology of mankind. *Nature* 415:23
- Danielsen SW, Kuznetsova E (2016) Resource management and a best available concept for aggregate sustainability. In: Pírkryl R, Török Á, Theodoridou M, Gomez-Heras M, Miskovsky K (eds) *Sustainable Use of Traditional Geomaterials in Construction Practice*. Geological Society, London, Special Publications 416:59–70
- De Freitas MH (2009) Geology: its principles, practice and potential for geotechnics. *Quart J Eng Geol Hydrogeol* 42:397–441
- Di Capua G, Bobrowsky PT, Kieffer SW, Palinkas C. (2021) Introduction: geoethics goes beyond the geoscience profession In: Di Capua G, Bobrowsky PT, Kieffer SW, Palinkas C. (eds.), *Geoethics: Status and Future Perspectives* Geological Society, London, Special Publications, 508:1–11
- Edensor T (2020) *Stone: stories of urban materiality*. Palgrave Macmillan, Springer Nature, Singapore
- Ehlers E, Krafft T (eds.) (2006) *Earth system science in the Anthropocene: emerging issues and problems*. Springer, Berlin
- Fernandes I, Ribeiro MA, Broekmans MATM, Sims I (eds) (2016) *Petrographic atlas: characterisation of aggregates regarding potential reactivity to alkalis*. Springer, Dordrecht
- Fookes PG (1991) Geomaterials. *Quart J Eng Geol Hydrogeol* 24:3–15
- Giurco D, Cooper C (2012) Mining and sustainability: asking the right questions. *Min Eng* 29:3–12
- Glikson AY, Groves C (2016) *Climate, fire and human evolution: the deep time dimensions of the Anthropocene*. Springer, Cham
- Glossop R (1968) The rise of geotechnology and its influence on engineering practice. *Géotechnique* 18:105–150

- González de Vallejo LI (2012) Design with geohazards: an integrated approach from engineering geological methods. *Soils Rocks, Int J Geotech Geoenviron Eng* 35(1):1–28
- Gorman MR, Dzombak DA (2018) A review of sustainable mining and resource management: transitioning from the life cycle of the mine to the life cycle of the mineral. *Resour Conserv Recyc* 137:281–291
- Griffiths JS (2014) Feet on the ground: engineering geology past, present and future. *Quart J Eng Geol Hydrogeol* 47(2):116–143
- Hoek E (1999) Putting numbers to geology: an engineer's viewpoint. *Quart J Eng Geol* 32(1):1–19
- Hooke RL (2000) On the history of humans as geomorphic agents. *Geol* 28:843–846
- Lyell C (1830–1833) *Principles of geology*. 3 Vols., J. Murray, London
- Marsh GP (1865) *Man and nature: or physical geography as modified by human action*. Scribner, New York
- McHarg IL (1992) *Design with nature*. 25th anniversary edition, Wiley series in sustainable design. Wiley, New York
- Moore EM (1997) Geology and culture: a call for action. *GSA Today* 7:7–11
- Mudd GM (2021) Sustainable/responsible mining and ethical issues related to the Sustainable Development Goals (SDGs). In: Di Capua G, Bobrowsky PT, Kieffer SW, Palinkas C (eds.), *Geoethics: Status and Future Perspectives* Geological Society, London, Special Publications, 508:187–199
- Nurmi PA (2017) Green mining: a holistic concept for sustainable and acceptable mineral production. *Ann Geophys* 60:1–7
- Přikryl R, Török Á, Theodoridou M, Gomez-Heras M, Miskovsky K (2016) Geomaterials in construction and their sustainability: understanding their role in modern society. Geological Society, London, Special Publications 416(1):1–22
- Sherlock RL (1922) *Man as a geological agent: an account of his action on inanimate nature*. H. F. & G. Witherby, London
- Smith MR, Collis L (eds) (2001) *Aggregates: sand, gravel and crushed rock aggregates for construction purposes*. 3rd ed., Engineering Geology Special Publications, Vol. 17. The Geological Society of London, London
- Smol M, Marcinek P, Duda J, Szoldrowska D (2020) Importance of sustainable mineral resource management in implementing the circular economy (CE) model and the European green deal strategy. *Resour* 9(5):55
- Stoppani A (1873) *Corso di geologia*. Vol. 2, G. Bernardoni & G. Brigola, Milan
- Thomas JA, Williams M, Zalasiewicz J (2020) *The Anthropocene: a multidisciplinary approach*. Polity, Cambridge
- Thomas WL (ed) (1956) *Man's role in changing the face of the earth*. The University of Chicago Press, Chicago, USA
- Tilton JE (1996) Exhaustible resources and sustainable development. *Resour Polic* 22(1–2): 91–97
- Underwood J (2001) Anthropogenic rocks as a fourth basic class. *Environ Eng Geosci* 7(1):104–110
- van Loon A (2002) The complexity of simple geology. *Earth-Sci Rev* 59(1–4):287–295
- Yong RN, Mulligan CN, Fukue M (2015) *Sustainable practices in geoenvironmental engineering*. 2nd ed., CRC Press, Taylor & Francis Group, Boca Raton

Acknowledgements

We thank the authors, keynote speakers and presenters of the 4GEO Conference for producing high-quality contributions. In addition, we thank the scientific committee for their outstanding hard work in enhancing the quality of the chapters. The book benefitted enormously from their critical suggestions and corrections. The authors and reviewers demonstrate remarkable resilience during these strange and challenging times because of the COVID-19 pandemic.

Our thanks are due to the OET (A. Sequeira Correia, M. G. Abrunhosa, A. Fernandes, A. R. Vieira), APEMETA (C. Jorge, C. Costa, C. Iglézias, R. Veríssimo) and ISEP (M. J. Viamonte, A. Vega y de la Fuente) to fully support the 4GEO Conference and APEMETA pre-Conference Meeting. Also, thanks are extended to the colleagues of the local organizing committee, particularly Maria João Fernandes and Sílvia Spínola, for their continuous support. Thanks to colleague Augusto Pérez-Alberti (USC, Spain) for gently sharing the remarkable image on the book's front cover with the young researcher Alejandro Gómez-Pazo working on the Galician rocky coast. The front cover symbolises these resilient times because of the global pandemic.

Special thanks to António Gomes Correia, Emeritus Professor of the University of Minho, for the insightful foreword. The guest editors are also grateful for the assistance of the publishing staff of IEREK, Springer Nature and the Springer production team.

Contents

Geomaterials, Geotechnics, and Georesources	
The Contribution of Engineering Geosciences to the Durability of Concrete Structures	3
Isabel Fernandes, Mário Quinta-Ferreira, and Helder I. Chaminé	
Comparative Analysis of Clinker Manufactured in Two Cement Plants in Spain: Use of Alternative Fuels	7
A. M. Castañón, V. Contreras, and A. Guerrero	
Sludges from the Ornamental Rock Primary Cut: Mortar Incorporation Study	15
João Dixo, Sílvia Spínola, and Adriano Teixeira	
Soil Stabilisation Using Third Generation Polymers	21
Ana Vieira, Telma Barroso, and José Augusto Fernandes	
Applying Soil Thermal Regime to Improve Storage Conditions of Temperature-Sensitive Materials in Camping Tents	31
Jorge Espinha Marques, Carlos Pacheco, Hernâni Gonçalves, Catarina Mansilha, Armindo Melo, and Isabel Ferreira	
Impact of the New European Standardisation on Soil Laboratory Routines and Test Results: The Case of Grain Size Distribution Analysis	37
Camila Afonso, Eduardo Neves, Adriano Teixeira, and Manuela M. Carvalho	
Soil Particle Density Determination According to EN ISO 17892-3: 2015: Some Difficulties in Laboratory Practices	43
Camila Afonso, Eduardo Neves, Adriano Teixeira, and Manuela M. Carvalho	
Physical and Chemical Characterisation of Fillers for the Manufacture of Bituminous Mixtures	49
Bruno Santos, Adriano Teixeira, and José Augusto Fernandes	
Case Study of an Inert Steel Aggregate in Road Construction: Characterization and Monitoring of the Structural Behaviour	57
Eduardo Fortunato, António José Roque, and António Gomes Correia	
Review on Laboratory Testing for Hydraulically Bound Mixtures Used in Road Applications	63
José Neves	
Absolute Permeability of Codaçal Porous Limestone Under Different Pressure and Temperature Conditions	69
Gustavo Paneiro and Alirza Orujov	

Geotechnical Properties of the Miocene Rocks of Central Algarve (Portugal)	75
Fernando Marques	
Rock Quarries in Critical Situation in Portugal: An Overview	81
Mário Quinta-Ferreira, Isabel Fernandes, and Helder I. Chaminé	
Methodological Approach of Georesources Sustainability for Northern Portuguese Industrial Rocks	85
Paulo Pita and José Augusto Fernandes	
Marble and Limestone Dimension Stone By-Products	91
Ruben Martins, Luís Lopes, and Tiago Alves	
Petrographic and Geochemical Characterisation of Organic Matter of Precambrian Black Shales from Ossa-Morena Zone, South of Portugal	97
Vanessa Laranjeira, Joana Ribeiro, Noel Moreira, Pedro Nogueira, João Graciano Mendonça Filho, and Deolinda Flores	
Components of Lithium Depletion from Starting Spodumene—Petalite Assemblages in <i>Subsolidus</i> Evolution of Portuguese Pegmatites	103
Carlos Leal Gomes and Pedro Amorim	
Nodular Sulphides in Cerdeirinha Stratiform Metasomatic Deposit—LA-ICP-MS Composition of Typomorphic Minerals	107
Ana Sofia Souto, Carlos Leal Gomes, Wolfgang Bach, and Patrick Monien	
Calc-silicate Gemstones from the Meluco Region, Cabo Delgado, Mozambique	111
Carlos Leal Gomes	
Conceptual Genetic Model for the Primary Occurrence of Garnet and Corundum Gemstones in the Miteda Region, Cabo Delgado Province, Mozambique	117
Carlos Leal Gomes	
Geotechnologies, Engineering Geosciences, and Geohazards	
Polish Experience in Offshore Mining: The New Concept of Transport Deep-Sea Concretions and Processing	125
Krzysztof Broda, Wiktor Filipek, and Barbara Tora	
Recovery of Non-ferrous Metals from Oceanic Nodules by Pyro and Hydrometallurgical Methods	131
Stanisław Pietrzyk, Andrzej Piotrowicz, and Barbara Tora	
Slope Inclinometers: Qualitative Evaluation of Probe Inclinometer Data—An Update	137
Luís Coimbra, Francisco Salgado, and João Paulo Meixedo	
Application of Photogrammetry for Geotechnical and Structural Characterization of Carbonated Rock Mass	141
João Duarte, Nuno Coelho, Fernando Figueiredo, and Pedro Andrade	
GeoTec: A System for 3D Reconstruction in Underground Environment (Aveleiras Mine, Monastery of Tibães, NW Portugal)	147
Ana Pires, André Dias, Paulo Rodrigues, Pedro Silva, Tiago Santos, Alexandre Oliveira, António Ferreira, José Almeida, Alfredo Martins, Helder I. Chaminé, and Eduardo Silva	

Rock Surveys for Geological and Geotechnical Assessment in a Basic Rock Quarry (SW Dili, East Timor)	155
Roberto R. Varela, Luís Ramos, José Augusto Fernandes, and Helder I. Chaminé	
Cut Slope Stabilization Proposals at A03 Karimbala Road, Liquiça Municipality, Timor-Leste	161
Oktoviano V. Tilman de Jesus and Mário Quinta-Ferreira	
Rock Slope Instability Risk Assessment in Open-Pit Quarries: A Comprehensive Approach	167
João Brissos, Leonor Mata, João Cruz, João Saúde, Paulo Sá Caetano, Carlos Costa, and Daniel Vendas	
Geological and Geotechnical Hazards in Large Infrastructures in Spain: Lessons Learned from Pajares Railway Tunnels and Castor Underground Gas Storage Project	173
L. I. González de Vallejo	
Multiscale and Modelling Hydraulic Properties of Rock Mass Foundations: Decision Tools for Design and Construction	179
Vasco Gavinhos, Jorge Carvalho, João Paulo Meixedo, and Helder I. Chaminé	
RMR₁₄ Versus RMR₈₉: A Methodological Approach for Rock Mass Excavations (N Portugal)	187
Suse Mateus, Maria José Afonso, Isabel Fernandes, and Helder I. Chaminé	
Drilling Parameters in the Evaluation of Rock Mass Quality	193
Marcelo Pereira, Isabel Fernandes, Rui Moura, and Nadir Plasencia	
Methodologies for the Geological–Geotechnical Characterisation of Weathering Profiles of Granite: A Case Study	197
Rita Lamas, Isabel Fernandes, Jorge Espinha Marques, and António Viana da Fonseca	
Characterisation of Coastal Granitic Sector Using Geomorphological and Hardness Measurements (Galicia, NW Iberian Peninsula)	203
Alejandro Gómez-Pazo and Augusto Pérez-Alberti	
Hardness Tester for Analog Planetary Rocks: A Preliminary Assessment in Microgravity Flight	209
Ana Pires, Catarina Costa, Rui Moura, Aaron H. Persad, Jason Reimuller, Derek Gowanlock, Shahrukh Alavi, Heather Wright Beatty, José Almeida, Fernando Almeida, Eduardo Silva, Augusto Pérez-Alberti, and Helder I. Chaminé	
Geoenvironment, Water, and Climate Change	
Environmental and Productive Applications of Tailor-Made Technosols: Biosphere Learnings	219
Felipe Macías García, Isabel Macías García, and Felipe Macías Vázquez	
The Multi-incremental Sampling Methodology in the Study of Potential Contaminated Sites	227
Celeste Jorge	
Contaminated Soil Management in Urban Earthworks in Portugal: Solutions for Treatment and Valorisation of Hazardous and Non-hazardous Wastes	231
Carlos Costa and Daniel Vendas	

Decommissioning of Potentially Polluting Activities in São Paulo: A Petrol Station Case Study	237
Erika von Zuben and Carlos Costa	
Tailings Dams: The Environmental Risks and Failures Management	243
Maria de Lurdes Dinis and António Fiúza	
Geochemical Background in Heavy Metals on Basaltic Soils from the Lisbon Volcanic Complex	247
Andrei Spiridon, Paulo Sá Caetano, Graça Brito, André Sanches, and Ricardo Manuel	
Bioaugmentation and Biostimulation for Remediation of BTEX—Polluted Soils: Study Case	253
Manuela M. Carvalho, Maria Cristina Vila, Teresa Oliva-Teles, Cristina Delerue-Matos, and António Fiúza	
Microplastic-Like Debris and Biomarkers in the Fish <i>Pseudochondrostoma duriense</i>: Preliminary Findings	259
M. A. Martins, L. R. Vieira, L. G. A. Barboza, J. Costa, C. Antunes, and L. Guilhermino	
Impact of Agriculture and Livestock on Quality of the Tagus Alluvial Groundwater Body: Evolution of Nitrate Concentration	263
Joel Zeferino, Maria do Rosário Carvalho, Ana Rita Lopes, Rosário de Jesus, José Martins Carvalho, and Helder I. Chaminé	
Use of Drill Cuttings for Hydrogeological Water Well Logging Reconstruction: A Practical Approach	269
José Teixeira, José Martins Carvalho, and Helder I. Chaminé	
A Case Study on the Use of Ground Source Heat Pumps (GSHP) in Heating and Climatization of the Military Academy—Amadora Quartering (Portugal) ...	275
Diogo Gonçalves, Rui Costa Neto, José Manuel Marques, Paula Figueiredo, Paula Carreira, and Maria Orquídia Neves	
The Hydromineral and Geothermal Field of Chaves (NE Portugal): A Prospective Approach Updated	281
José Martins Carvalho and Helder I. Chaminé	

About the Editors



Helder I. Chaminé is a skilled Geologist and Professor of engineering geosciences at the School of Engineering (ISEP) of the Polytechnic of Porto, with over 33 years of experience in multidisciplinary geosciences research, consultancy and practice. He studied geological engineering and geology (B.Sc., 1990) at the Universities of Aveiro and Porto (Portugal), respectively. He received his Ph.D. in geology (structural geology and regional mapping) at the University of Porto in 2000 and spent his postdoctoral research in applied geosciences at the University of Aveiro (2001–2003). In 2011, he received his Habilitation (D.Sc.) in geosciences (structural geology and rock mechanics) from the University of Aveiro. Before joining the academy, he worked for over a decade on international projects for mining, geotechnics, groundwater industry and/or academia related to geodynamics and regional geology, hard-rock hydrogeology and water resources, engineering geosciences and applied geomorphology, rock engineering and georesources. His research interests span fundamental to applied fields: GIS mapping techniques for applied geology, structural geology and regional geology, engineering geosciences and rock engineering, slope geotechnics, mining geology and hydrogeomechanics, hard-rock hydrogeology, urban groundwater and hydromineral resources. He is interested in mining geoheritage, the history of cartography, military geosciences and higher-education dissemination, skills, and core values. Presently, he is Head of the Laboratory of Cartography and Applied Geology (LABCARGA|ISEP), Senior Researcher at Centre GeoBioTec|U.Aveiro and Centre IDL|U.Lisbon, as well as belongs to the executive board of the M.Sc.+B.Sc. Geotechnical and Geoenvironmental Engineering Programmes (OE+EUR-ACE Label) and the Department of Geotechnical Engineering (ISEP). He belongs to SPG's board of the Technical Commission of Environmental Geotechnics. He was a Board Member of APGeom—Portuguese Association of Geomorphologists (2009–2013), SPG—Portuguese Geotechnical Society (2016–2020), APG—Portuguese Association of Geologists (2020–April 2021), and AIH-GP—Portuguese Chapter of the International Association of Hydrogeologists (2019–2023). He was a consultant and or responsible for over 75 projects of applied geology, hydrogeomechanics, slope geotechnics, mining geology, exploration hydrogeology, hard-rock hydrogeology, water resources, urban groundwater and applied mapping

(Mozambique, Portugal and Spain). He has co-authored over 220 publications in indexed journal articles, conference proceedings/full papers, chapters, technical and professional papers. He co-edited over 16 special volumes and is presently involved in editing themed issues for some international journals (e.g. Environmental Earth Sciences, Springer Nature Applied Sciences, Discover Water, Arabian Journal of Geosciences and Water). He has a broad activity as a referee for several international journals in applied mapping, geosciences, geotechnics and rock engineering, hydrogeology, water resources and geohazards. He served as Invited Expert Evaluator of the Bologna Geoscience Programme for DGES (Portugal) and Scientific Projects Evaluation for NCST, 2017–2019 (Kazakhstan), and NRF|RISA, 2019 (South Africa), as well as Coordinator of “Geology on Summer|Ciência Viva” Programme at ISEP (2005–2019) for geoscience dissemination. He has also been active in teaching and supervising many Ph.D., M.Sc., and undergraduate students. He has been on the editorial board, among others, of the Springer Nature Applied Sciences, Arabian Journal of Geosciences, Geotechnical Research, Geosciences, Mediterranean Geoscience Reviews, Hydrogeology Journal, Euro-Mediterranean Journal for Environmental Integration, Discover Water, Revista Geotecnia and Geología Aplicada a la Ingeniería y al Ambiente. He integrates as Moderator or Session Chair in several conferences, workshops and meetings. He was the Scientific Chair of the 1st International Conference on Georesources, Geomaterials, Geotechnologies and Geoenvironment, 4GEO (Porto, Portugal, 7–8 November 2019). Currently, he is on the organizing and scientific committees of the 4th International Workshop on Natural Hazards—NATHAZ’25 (Azores, May 2025), focused on geotechnical hazards and risks.



José Augusto Fernandes is a skilled Geotechnical Engineer and Professor of georesources at the School of Engineering (ISEP) of the Polytechnic of Porto, with over 36 years’ experience in interdisciplinary geotechnics, soil mechanics, mining and georesources consultancy, practice, and research. He holds a PhD in Geosciences (Georesources speciality), an M.Sc. in Industrial Minerals and Rocks from the University of Aveiro, and a degree in Geotechnical Engineering from the School of Engineering (ISEP), Polytechnic of Porto. Currently is a Coordinator Professor in the Department of Geotechnical Engineering at ISEP, where he teaches, among other subjects, georesources, soil mechanics, geomaterials, and nuclear energy raw materials and production plants design. Presently, he is Head of the Department of Geotechnical Engineering and Director of the Laboratory of Geotechnics and Construction Materials (LGMC|ISEP). He was the Director of the BSc Geotechnical and Geoenvironmental Engineering programme (OE+EURACE label). He regularly integrates several doctoral and master’s thesis juries and was the supervisor of 2 PhD and over 50 MSc dissertations. Researcher member at the Centre GeoBioTec (3G Group—Georesources, Geotechnics and

Geomaterials), University of Aveiro. He was the Principal Investigator of the R&D projects (IPP, 2007): P1—Study of shape variation of the aggregates produced in fragmentation equipment considering different particle sizes and power adjustments (CSS), and P2—Evaluation of thermal behaviour of natural stones. He also participates, as a researcher, in the R&D project “Optical systems monitorisation in the shape of particles with irregular extended size distribution”. He has experience in geotechnical engineering and mining industrial projects, geotechnics (in-situ site investigations, soil mechanics and foundations), georesources, geomathematics and resources modelling and exploitation, and mining (open pit and underground) and ore processing and geomaterials. During his professional activity, held in private companies based in Portugal, the positions of (i) General Manager at Tracomine Ltd.; (ii) Technical Consultant at Unimil Minerais Ltd. and Unizel Minerais Ltd.; (iii) Technical Director at Euroquartzo-Portugal Ltd., a subsidiary of French Multinational Group DAM (Denain Anzin Minéraux); (iv) Production Manager in ECC Portugal—Minerais Industriais Inc., a subsidiary of Multinational Group ECC (English China Clay); (v) Production Engineer in Anglo-Portuguesa de Caulinos de Viana, Ltd.; (vi) Chief Mine Engineer in Empresa Nacional de Urânio (ENU), Urgeiriça and (vii) Internship Engineer in Sociedade Mineira de França, Monteseinho Mine, Bragança. Member of SPG (Portuguese Geotechnical Society), AP3E (Portuguese Association of Engineering Studies and Explosives), AIESMIN (Asociación Iberoamericana de Enseñanza Superior de la Minería), member and president of Portuguese geotechnical and mining engineering body of OET (Order of Technical Engineers). Currently, he is the chairman of the Portugal Mineral Resources Cluster. Author and co-author of several publications in conference proceedings and articles in national and international journals. He was an invited speaker and moderator for some conferences, workshops and seminars. He was the General Chair of the 1st International Conference on Georesources, Geomaterials, Geotechnologies and Geoenvironment, 4GEO (Porto, Portugal, 7–8 November 2019).

Geomaterials, Geotechnics, and Georesources



The Contribution of Engineering Geosciences to the Durability of Concrete Structures

Isabel Fernandes, Mário Quinta-Ferreira, and Helder I. Chaminé

Abstract

Although concrete has been considered for decades as a long-lasting building material, deterioration processes were recognised in many structures worldwide since early in the twenty century. The causes of deterioration can be the chemical, mechanical or biological origin and usually result in cracking, misalignments of structural elements, steel corrosion, discolouration and exudations contributing to the shortening of the lifetime of large critical structures such as dams, bridges and buildings. In some cases, it is difficult or even impossible to identify the leading cause of degradation. In diagnosing the causes of deterioration, which involves different scales and phases, petrographic methods play a relevant role. Concrete petrography applies the techniques traditionally used in the study of rocks to identify the concrete components (aggregates and cement type) and detect the manifestations of deterioration. It also allows the characterisation of the products formed in consequence of internal chemical reactions, therefore contributing to the diagnosis of the mechanism involved. Different petrographic techniques can concur to the diagnosis of the deterioration of concrete. A revision is made of these methods and their applicability to identifying internal chemical reactions in concrete.

Keywords

Petrographic methods • Aggregates • Concrete • Alkali-silica reactions • Sulphides

1 Introduction

Concrete is composed of aggregate particles, binder (cement), water and additives. The main volume of concrete is composed of aggregate particles with adequate physical and chemical characteristics. Concrete structures can deteriorate due to several different mechanisms. The deterioration is usually due to cycles of freeze/thaw, carbonation, chloride penetration, sulphate and sulphide attack, and Alkali–Aggregate Reaction (AAR). Attack mechanisms can work synergistically, and, very often, it is difficult to conclude which is the main cause of deterioration, jeopardising the definition of the rehabilitation strategies.

The geologist is responsible for selecting aggregates, both from quarries or from natural deposits, defining the available volume and studying the chemical and mineralogical composition as well as the texture and fabric. The mineral composition is of utmost importance as aggregates mainly contain components that cause deleterious internal reactions. The most common type of AAR occurs when reactive forms of silica are present in the aggregate called alkali-silica reaction (ASR). Alkali-silica reaction is a deleterious internal chemical reaction involving silica contained in the aggregates and ions OH^- , Na^+ and K^+ from the interstitial fluids in the concrete, and it can occur just a few years after construction (2–5 years) or take some decades to develop (10–20 years). It results in the formation of an expansive hygroscopic product called alkali-silica gel. The reaction's effects can be observed in hand specimens and at the structure scale (Godart et al. 2014), with map cracking as the most common feature. At the microscope scale, cracks form in the aggregate particles' interior and extend to the cement

I. Fernandes (✉)

Department of Geology, IDL—Instituto Dom Luiz,
University of Lisbon, Lisbon, Portugal
e-mail: mifernandes@ciencias.ulisboa.pt

M. Quinta-Ferreira

Department of Earth Sciences, CGeo—Geosciences Center,
University of Coimbra, Coimbra, Portugal

H. I. Chaminé

Laboratory of Cartography and Applied Geology,
Department of Geotechnical Engineering, School of Engineering
(ISEP), Polytechnic of Porto, Porto, Portugal

Centre GeoBioTec|UA, Aveiro, Portugal

© The Author(s), under exclusive license to Springer Nature Switzerland AG 2023

H. I. Chaminé and J. A. Fernandes (eds.), *Advances in Geoengineering, Geotechnologies, and Geoenvironment for Earth Systems and Sustainable Georesources Management*, Advances in Science, Technology & Innovation, https://doi.org/10.1007/978-3-031-25986-9_1

paste. Also, a matter of concern regarding the concrete deterioration in the presence of sulphides in the aggregate particles can originate damage due to the formation of expansive minerals: ettringite, thaumasite and gypsum. Pyrrhotite was found to originate expansion in concrete foundations in Canada and the USA (e.g. Rodrigues et al. 2016), involving a considerable amount of money in rehabilitation. The diagnosis of internal chemical reactions involves the petrographic study of thin polished sections of concrete samples obtained from the structures by drill coring. This analysis identifies the aggregate involved in the reaction and the characterisation of the alkali-silica products formed inside the cracks and filling the voids.

The present study aims to explain the work carried out by petrographers to identify potentially reactive aggregates (Fernandes et al. 2016) and concrete petrography (Poole and Sims 2016) concerning the main objectives that can be achieved under the different scales of observation.

2 Materials and Methods

2.1 Aggregates

The characterisation of aggregates for concrete is a process that involves visual methods (petrography) and several physical laboratory tests. Based on the petrographic characterisation, the visual methods are the first to be carried out regarding preventing AAR and sulphide oxidation. The study can be based on hand-picking of particles to identify the type of rock; analysis of thin sections under polarised light microscope eventually with automated point counting to quantify deleterious minerals. The analysis, both from natural deposits and quarries, requires representative samples to be sent to the laboratory.

2.2 Concrete

The diagnosis of deterioration of concrete demands that core drilling of the damaged structures is performed after macroscopic visual inspection of the structure. In the laboratory, the petrographer registers the existence of cracks, voids, “sweat spots”, the presence of materials filling the cracks and voids, disintegrated or de-bonded aggregate particles and, eventually, exudations. The cores are then cut lengthwise for the preparation of specimen for the petrographic methods. Damage Rating Index (DRI) is determined using stereomicroscope on cores cut half-wise. The polished surface of the

concrete is divided into a grid of 10×10 mm (Sanchez et al. 2016), and the number of damage features is registered in each square area, and its frequency is multiplied by a weighting factor. The final DRI value is normalised to 100 cm^2 , allowing the comparison between different samples.

The petrographic analysis is performed using a polarised light microscope under plane polarising (PPL) and cross polarising (XPL) light. To highlight the cracks and voids and to obtain the water/cement ratio, a yellow fluorescence dye is added to the resin. The thin sections are observed using ultra-violet light (UV). To characterise the products of the reaction (alkali-silica gel, ettringite, thaumasite, gypsum), either broken pieces of concrete, sputtered with Au-Pd, or thin polished sections, without cover glass and sputtered with carbon, can be used for observation under a scanning electron microscope with chemical analysis by energy-dispersive X-ray spectroscopy (SEM/EDS) and Electron Probe Micro-Analyzer (EPMA). Recently, synchrotron radiation micro-computed tomography (SR Micro CT) has been used for quantitative details on the 3D-morphology of the reaction products (Dähn et al. 2016). Also, Raman microscopy constitutes a promising technique in cementing and identifying the AAR products (Leemann 2017). Table 1 presents a summary of the use of the different petrographic methods used to study damaged concrete.

3 Results and Discussion

3.1 Aggregates

On a commercial basis, grains from polymictic deposits, such as alluvial materials, are hand split. However, for fine-grained lithologies and deposits used for the first time, thin sections are prepared, and point counting is performed to quantify the deleterious minerals present in the batch, such as polymorphs silica and minerals that contain alkalis. However, the classification as innocuous or potentially reactive to alkalis is not always easy. Deformation of minerals can show different stages, as described in Ramos et al. (2016), concluding that the quartz crystals with intense undulatory extinction and deformation bands present more favourable conditions to ASR occurrence. The identification of silica polymorphs may need complementary methods such as X-ray, Electron Probe Micro-Analysis (EPMA), SEM/EDS with element maps and bulk chemical analysis to quantify the content of free silica. These complementary methods are, however, rarely used on a commercial basis.

Table 1 Petrographic methods and their objectives in the diagnosis of concrete deterioration

		DRI	Polarising microscope	SEM/EDS	Synchrotron	Raman
Cracks	In aggregates	X	X	X	X	
	In cement paste	X	X	X	X	
De-bonding		X	X	X	X	
Alkali-silica gel	In cracks	X	X	X	X	Structure
	In voids	X	X	X	X	
Ettringite/thaumasite		X	X	X	X	Structure

Sulphides are unstable under oxidising conditions, leading to expansive secondary minerals such as oxide/hydroxide/oxyhydroxide, iron sulphate and gypsum. The identification of pyrite and/or pyrrhotite may require that EPMA obtains analysis. The subject is covered, for example, in EN 12,620, defining a maximum content of SO_3 and S for aggregates to prevent the reaction with sulphides.

3.2 Concrete

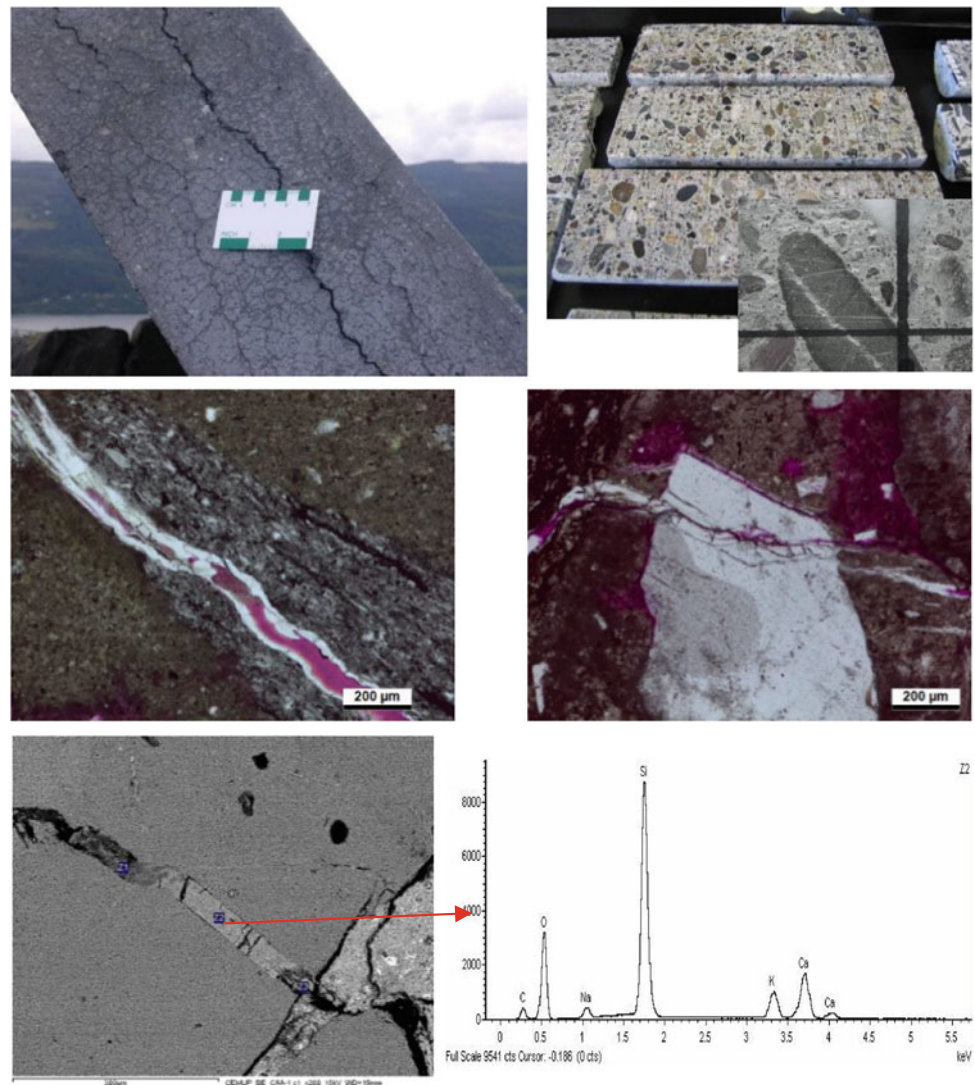
The diagnosis of deterioration of concrete implies that different scales are used, as summarised in Fig. 1. The structures' visual analysis allows identifying cracks, deformation, discolouration, misalignments, exudations and pop-outs. Deterioration leads to the loss of concrete's mechanical characteristics, therefore reducing the project service life of the structures. The visual features observed at the structure scale are usually also visible in the concrete cores. As already referred, this analysis is performed under a stereomicroscope to quantify the features that indicate deterioration, mainly related to an internal chemical reaction, which gives the DRI result. Under an optical microscope, besides the identification of the aggregates involved in the reactions in hardened concrete and the characterisation of reaction products, concrete petrography can provide further information, namely the w/c ratio and the type of cement used (ordinary Portland cement, filler, fly ash, blast furnace slag, silica fume, metakaolinite, etc.). The products of deterioration are usually detected and identified at this scale, mainly for commercial purposes. However, research goes deeper

into the analysis to understand the reaction mechanism and evaluate the future development of the structures' internal reactions. The stress that the reaction products can apply to concrete is still a matter of investigation. In this concern, the heterogeneous distribution of the structures' reactions is a drawback of accepting the petrographic method. According to this, Alkali-silica gel (ASR products) can be amorphous or crystalline, depending on its location along the cracks, and is mainly composed of Si with variable content of Ca, K and Na, the results obtained under SEM/EDS and EPMA. Raman microscopy and synchrotron radiation micro-computed tomography have been applied in the characterisation of the reaction products (Leemann 2017), and researchers concluded that these are powerful tools to investigate the structure of reaction products and explain their behaviour.

4 Concluding Remarks

The present work aims at summarising the petrographic methods that can be used in the study of concrete and its components. These methods are essential in two stages: selecting aggregates to prevent deleterious internal reactions; during the service life of the structures for the diagnosis of the cause of damage. Besides optical microscopy, SEM/EDS and EPMA, Raman spectroscopy and synchrotron seem to be quite valuable in explaining the mechanisms involved in the deterioration. Work is needed to use technologies that can be applied commercially with reasonable costs for the construction industry.

Fig. 1 Different scales of observation of concrete to determine the cause of deterioration: example of a structure in Norway; the lengthwise halves of the concrete cores (diameter of the cores = 100 mm), with 100 mm² grid to obtain DRI; photomicrographs obtained under the optical microscope showing cracks and gel in aggregate particles; image obtained by SEM with an EDS spectrum of gel



Acknowledgements The author would like to acknowledge the financial support of FCT through project UIDB/50019/2020—IDL. The SEM/EDS results were obtained in the equipment available at CEMUP, which were financed by REEQ/1062/CTM/2005 and REDE/1512/RME/2005 of FCT. MQF was funded by CGeo|UC (FCT-UIDB/00073/2020). HIC was supported partially by LABCARGA|ISEP re-equipment program (IPP-ISEP|PAD'2007/08) and Centre GeoBio-Tec|UA (FCT-UID/GEO/04035/2020).

References

- Dähn R, Arakcheeva A, Schaub Ph, Pattison P, Chapuis G, Grolimund D, Wieland E, Leemann A (2016) Application of micro X-ray diffraction to investigate the reaction products formed by the alkali-silica reaction in concrete structures. *Cem Concr Res* 79:49–56. <https://doi.org/10.1016/j.cemconres.2015.07.012>
- Fernandes I, Ribeiro MA, Broekmans MATM, Sims I (2016) *Petrographic atlas: characterisation of aggregates regarding potential reactivity to alkalis*. Springer, Dordrecht
- Godart B, Rooij M, Wood, JGM (eds) (2014) *RILEM AAR-6.1 Guide to diagnosis and appraisal of AAR damage to concrete structures, Part 1: diagnosis*. Springer, Dordrecht
- Leemann A (2017) Raman microscopy of alkali-silica reaction (ASR) products formed in concrete. *Cem Concr Res* 102:41–47
- Poole AB, Sims I (2016) *Concrete petrography, a handbook of investigative techniques*, 2nd edn. CRC Press, London
- Ramos V, Fernandes I, Noronha F, Santos Silva A, Soares D, Leal S, Fournier B (2016) Assessment of the potential reactivity of granitic rocks: petrography and expansion tests. *Cem Concr Res* 86:63–77
- Rodrigues A, Duchesne J, Fournier B, Durand B, Shehata MH, Rivard P (2016) Evaluation protocol for concrete aggregates containing iron sulfide minerals. *ACI Mat J* 113(3):349–359
- Sanchez L, Fournier B, Jolin M, Bedoya M, Bastien J, Duchesne J (2016) Use of damage rating index to quantify alkali-silica reaction damage in concrete: fine versus coarse aggregate. *ACI Mat J* 113(4):395–407



Comparative Analysis of Clinker Manufactured in Two Cement Plants in Spain: Use of Alternative Fuels

A. M. Castañón, V. Contreras, and A. Guerrero

Abstract

The construction industry is based on the use of cement as the main axis of its activity. The manufacture of cement constitutes a process with significant emissions of harmful substances to the environment, derived from its high energy consumption. Large amounts of raw materials are used, especially minerals from the upper part of the Earth's crust, known as geomaterials. In this study, the quality results of four clinker from two Spanish factories are compared. Different techniques have been used to understand their characteristics better and, thus, determine the correlation between the sintering temperature, alternative fuels, and the quality of the clinker. Using alternative fuels from different sources is presented as a solution to obtain more eco-efficient cement clinker without losing any of their properties for their use in the construction sector.

Keywords

Geomaterials • Clinker • Cement • Alternative fuels • Eco-efficient

1 Introduction

The construction industry has been one of the most influential in the economy throughout the twentieth and twenty-first centuries. The productive activity of the construction sector is currently undergoing a paradigm shift.

A. M. Castañón (✉) · V. Contreras
Department of Mining, Topography and Structures, University of León (ESTIM), León, Spain
e-mail: amcasg@unileon.es

A. Guerrero
Construction Eco-Efficient Materials, Eduardo Torroja Institute for Construction Sciences, IETcc-CSIC, Madrid, Spain

The idea of a circular economy rather than a linear one is a critical challenge to be accomplished by 2030. Development, both in advanced economies and emerging ones, implies substantial growth in this sector, which must be unfailingly sustainable, efficient, and compliant with the Sustainable Development Goals (SDGs), amongst other aspects, protecting the planet. This model entails an overhaul of the sector through innovation and industrialisation in its constructive processes via new technological breakthroughs and more efficient materials. The quintessential material most widely used in the construction sector is cement. Cement is a geomaterial comprised of, mainly, silicon oxide (SiO₂), calcium oxide (CaO), iron (III) oxide (Fe₂O₃) and aluminium oxide (Al₂O₃). The manufacture of cement grows exponentially and uses materials drawn from the Earth's crust. This production runs alongside a sizeable amount of greenhouse gas (GHG) emissions which must be minimised (Přikryl et al. 2016; Přikryl 2017). In line with the SDGs and international agreements for the conservation of the planet, it is necessary to study strategies that reduce the adverse effects this sector causes on the environment and society (Castañón et al. 2012; Mokhtar et al. 2020). In this sense, the cement industry has placed sustainability as the main axis of its activity, making important changes in its production process that have reduced GHG emissions to the environment and maximised the energy efficiency of its plants (Guerrero et al. 2008). In order to advance in the search for efficient solutions to ensure that the construction sector is sustainable and applying the concepts of circular economy, work is being done on the incorporation of waste as a substitute for raw materials or fuels (e.g. Hashem et al. 2019, El-Salamony et al. 2020, Daya et al. 2021). This work presents the effect that alternative fuels from different sources and other improvements made in cement plants can have on the manufacture of cement clinker. The clinker manufactured in two cement factories is studied, using different techniques to analyse and compare the quality results with the alternative fuels and the sintering temperature of the furnace.

2 Materials and Methods

2.1 Materials

Four clinkers (C-1, C-2, C-3 and C-4) have been chosen from two factories located in the North of Spain to undertake this study. For the manufacture of clinker, alternative fuel sources of different origins have been used: used tyres, used vehicles, plastics, animal meal and textiles waste, Table 1.

2.2 Experimental Methods

Therefore, to carry out quality testing on the clinker and assess the effect of alternative fuels on clinkers' properties, diverse technical instruments have been used. The chemical composition of the four clinkers was determined by X-Ray Fluorescence Spectrometry (XRF). A boron glass bead was prepared with each sample of ash powder. That was done by melting in an induction microwave oven, mixing the Merck Spectromelt A12 flux and the sample in proportions of approximately 20:1. The chemical analyses of the beads were performed in a vacuum atmosphere, using a PANalytical Axios wavelength dispersive X-ray fluorescence (WDXRF) sequential spectrometer equipped with an Rh tube and three detectors (gaseous flow, scintillation and Xe sealing). Well-characterised international rock and mineral standards were used to prepare the calibration line. Further, each sample's loss-on-ignition (LOI) was calculated after subjecting an aliquot part of each sample to 1050 °C for one hour in a muffle furnace. X-Ray Diffraction (XRD) has been performed using a Diffractometer manufactured by Panalytical, CUBIX PRO AMT-ME/A model without monochromator and Cu radiation support provided by Analytical software.

Morphological and compositional analyses were performed using a JEOL 6100LV scanning electron microscope (SEM) equipped with energy-dispersive X-ray spectroscopy (EDX).

3 Results

The use of alternative fuels together with other improvements made in cement plants, such as burners with lower NOx emissions, could have or lead to substantial shifts in the kiln's parameters, such as the sintering temperature, entry of NOx and the temperature of secondary air into the cooling chamber. These parameters significantly influence the clinker's quality markers, such as C₃S and CaO free (Castañón 2011).

All the data that appear in this work are experimental data that have been obtained from the factories studied.

The average results of the feeding at the entrance to the furnace of the clinker are observed in Table 2.

The rest of the flour components are loss to fire, and a small part of minority elements, in both factories.

3.1 Chemical and Mineralogical Composition

Table 3 shows the chemical composition of the principal oxides present in the four clinkers (C-1, C-2, C-3 and C-4) obtained by XRF. These data correspond to mean results from all of the samples under study to appraise the effect of alternative fuel sources of diverse origin. All the data are real and have been obtained from the analysis of the cement company. Once the chemical composition of the oxides was known, in order to perform and oversee suitably the chemical control of the dosage of the raw materials and admixtures, the cement modules are calculated using the: lime saturation factor (LSF), silica ratio (SR) and alumina ratio (AR). These modules are (Taylor 1997):

$$\text{LSF} = \text{Lime Saturation Factor} = \text{CaO}/(2.8\text{SiO}_2 + 1.2\text{Al}_2\text{O}_3 + 0.65\text{Fe}_2\text{O}_3).$$

$$\text{SR} = \text{Silica Ratio} = \text{SiO}_2/(\text{Al}_2\text{O}_3 + \text{Fe}_2\text{O}_3).$$

$$\text{AR} = \text{Alumina Ratio} = (\text{Al}_2\text{O}_3)/(\text{Fe}_2\text{O}_3).$$

Table 1 Percentage replacement of fossil fuels by alternative fuel sources

Precalciner-combustion chamber			
	<i>Clinker 1–2</i>	<i>Clinker 3</i>	<i>Clinker 4</i>
Petcoke (%)	<28	100	55
Alternative fuels ⁽¹⁾ (%)	>72	0	45*
Main burner (%)			
	<i>Clinker 1–2</i>	<i>Clinker 3–4</i>	
Petcoke (%)	>80	<60	
Alternative fuels ⁽²⁾ (%)	<20	>40*	

⁽¹⁾Combustion Chamber: Clinker 1 and 2: used tyres, used vehicles and SRF. Clinker 4: used tyres and plastic. ⁽²⁾Main Burner: Clinker 1 and 2: textiles waste. Clinkers 3 and 4 are animal food and plastics

Table 2 Average feed to the oven

Components	Clinker 1–2 (%)	SD (%)	Clinker 3–4 (%)	SD (%)
CaO	41.79	0.09	43.64	0.28
SiO ₂	13.05	0.25	13.99	0.19
Al ₂ O ₃	3.58	0.06	3.19	0.14
Fe ₂ O ₃	2.20	0.22	2.18	0.16
MgO	0.93	0.01	0.91	0.09
Na ₂ O	0.32	0.02	0.14	0.03
K ₂ O	0.67	0.01	0.5	0.03
SO ₃	0.75	0.03	1.07	0.11

Table 3 Chemical Composition (%)

	SiO ₂	Al ₂ O ₃	Fe ₂ O ₃	CaO	MgO	SO ₃	Na ₂ O	K ₂ O	LSF	SR	AR	Free CaO
C-1	20.5	5.3	4.1	63.4	1.4	1.5	1.0	0.5	95.52	2.18	1.30	1.24
C-2	21.0	5.2	3.4	64.1	1.5	1.5	0.9	0.4	95.56	2.45	1.54	0.51
C-3	21.4	4.61	3.5	65.7	1.4	2.3	0.22	0.67	97.20	2.64	1.32	1.10
C-4	21.6	4.05	3.7	66.4	1.2	1.9	0.23	0.63	98.00	2.78	1.08	1.48

The LSF is related to the clinker reactivity. The optimum values for a clinker are in the region of 92.98. The value of the SR module is linked to the number of calcium silicates in the clinker. The standard values range between 2 and 3. The AR module determines the relationship between the clinker's aluminate and ferritic phases; its standard values oscillate between 1 and 4.

Concerning high-temperature reactions in the clinkerization kiln, the presence of these oxides is the determining factor for the quality of the raw meal obtained. CaO free is another essential parameter in the production process of Portland clinker. The ideal amount is for its percentage to be close to 0.8%–1.5%. However, this would mean that the temperature of the clinkerization process had been overly high, along with its time in the kiln. Under these conditions, energy consumption would be very high. The clinker's mineralogical composition is comprised chiefly of four phases: Tricalcium silicate (3CaO·SiO₂) or alite (C₃S), bicalcium silicate (3CaO·SiO₂) or belite (C₂S), tricalcium aluminate (3CaO·Al₂O₃) or (C₃A) and tetracalcium aluminoferrite (4CaO·Al₂O₃·Fe₂O₃) or (C₄AF).

The chemical composition of standard Portland clinker is 67% CaO, 22% SiO₂, 5% Al₂O₃, 3% Fe₂O₃ and 3% formed by other components (Castañón 2011). Our study's four clinkers assessed have their main oxides: SiO₂ with values of 20.5–21.6%, Al₂O₃: 3.4–5.3%, Fe₂O₃: 3.4–4.1% and CaO: 63.4–66.5%. These oxides allow us to know the reactivity, aptitude to the firing of crudes elements and, therefore, a clinker's quality through the cement modules named and described in Sect. 2.2: LSF, SR and AR. In our study, all the clinkers display an average LSF value of 96.57. Concerning the value of the SR module, these clinkers show an average

value of 2.5. The AR module in our study has value of 1.31. Upon viewing the average values, it can be ascertained that the four clinker falls within limits established through regulations in force. About the CaO-free content, its value is found to be within the range of 0.51–1.48%, whereby its average is 1.08%.

The determination of the mineralogical composition can be calculated through Bogue equations or using the refinement of X-ray diffraction, opting for the Rietveld method for this. By Rietveld analysis, it is difficult to obtain significant CaO results when the average values in the weight are very low. As has been stated in other works (Castañón 2011; Castañón et al. 2012), in which it has been proven that it is possible to perform a quantitative analysis of the clinker phases using X-ray diffraction in a laboratory setting and the Rietveld method offering acceptable levels of accuracy and exactitude.

In Table 4, the mineralogical composition of the four clinkers calculated following the Rietveld method is listed. More than 1,000 diffractograms have been analysed.

The two most significant parameters that appraise a clinker's quality are C₃S and CaO-free content. In our study, the four clinkers examined displayed optimum values concerning C₃S and CaO to be considered quality clinker appropriate to be used in the construction sector.

3.2 Effect on NO_x Emissions and Sintering Temperature

In some experimental studies carried out by this research group, a decrease in NO_x at the furnace outlet has been

Table 4 Quantification results using Rietveld on the clinker (%)

Sample	C ₃ S	C ₂ S	C ₃ A	C ₄ AF	CaO free	MgO	C ₃ S/C ₂ S
Clinker 1	77.22	7.33	3.16	11.90	1.10	0.00	10.53
Clinker 2	80.20	4.99	3.31	11.47	0.69	0.00	16.07
Clinker 3	59.20	23.50	1.80	9.80	1.10	0.20	2.52
Clinker 4	63.20	20.50	1.70	9.20	1.50	0.00	3.08

Table 5 C₃S values, free CaO and Sintering Temperature of the clinker studied

	Sintering temperature (°C)	C ₃ S (%)	CaO free (%)
Clinker 1	1160	77.22	1.1
Clinker 2	1240	80.2	0.69
Clinker 3	1000	59.2	1.1
Clinker 4	1000	63.2	1.5

verified using alternative fuels (NFUs) compared to fossil fuels. In the case of clinker 1–3, a reduction of NO_x levels (measured under normal conditions) of 531 mg/Nm³, 700 mg/Nm³ and 420 mg/Nm³ is achieved, respectively. For clinker 4, reductions of 373 mg/Nm³ are obtained. Below, the changes in the chemical and mineralogical composition of the clinker under study are displayed.

The sintering temperature values for clinker 1 and clinker 2 are 1160 °C (SD = 62.8 °C) and 1240 °C (SD = 49.2 °C), respectively. For clinker 3 and clinker 4, the mean value of the annual sintering temperature is 1000 °C with a standard deviation of 148.2 °C.

Table 5 shows the sintering temperature and the Alite and CaO-free quality parameters (Table 4) for the four clinkers.

3.3 Scanning Electron Microscopy

The clinker morphology was determined by SEM. Upon comparison of the four samples, it can be seen how the general appearance of the clinker's microstructure (Fig. 1) features more impurities than clinker without the use of alternative fuel sources (Castañón 2011; Castañón et al. 2012).

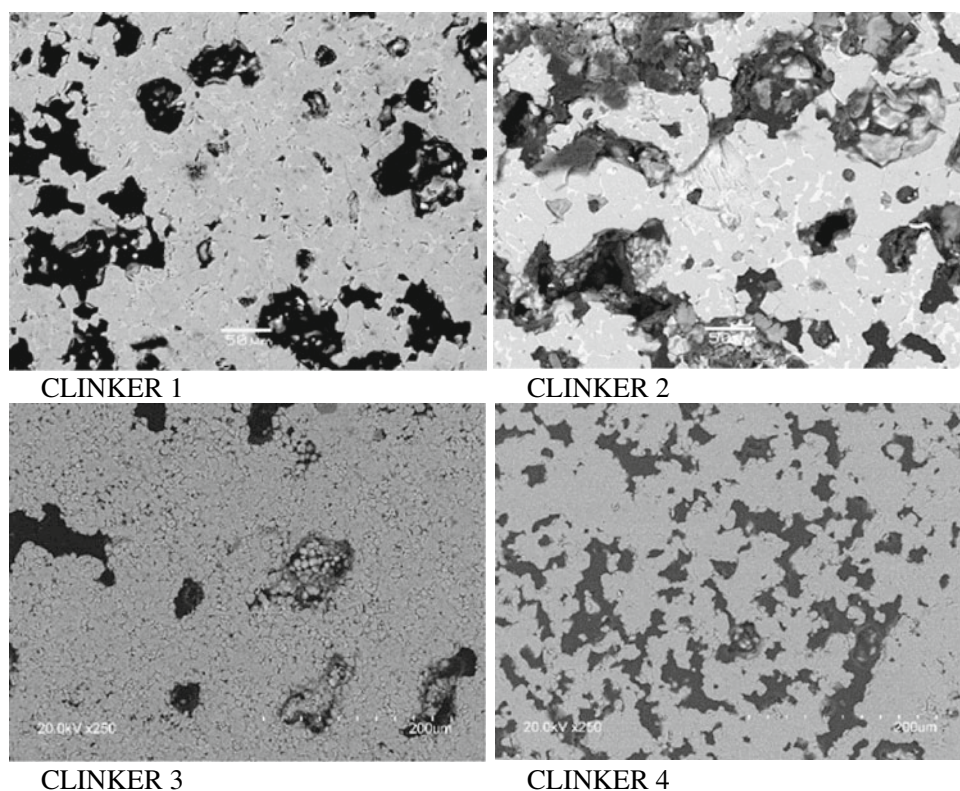
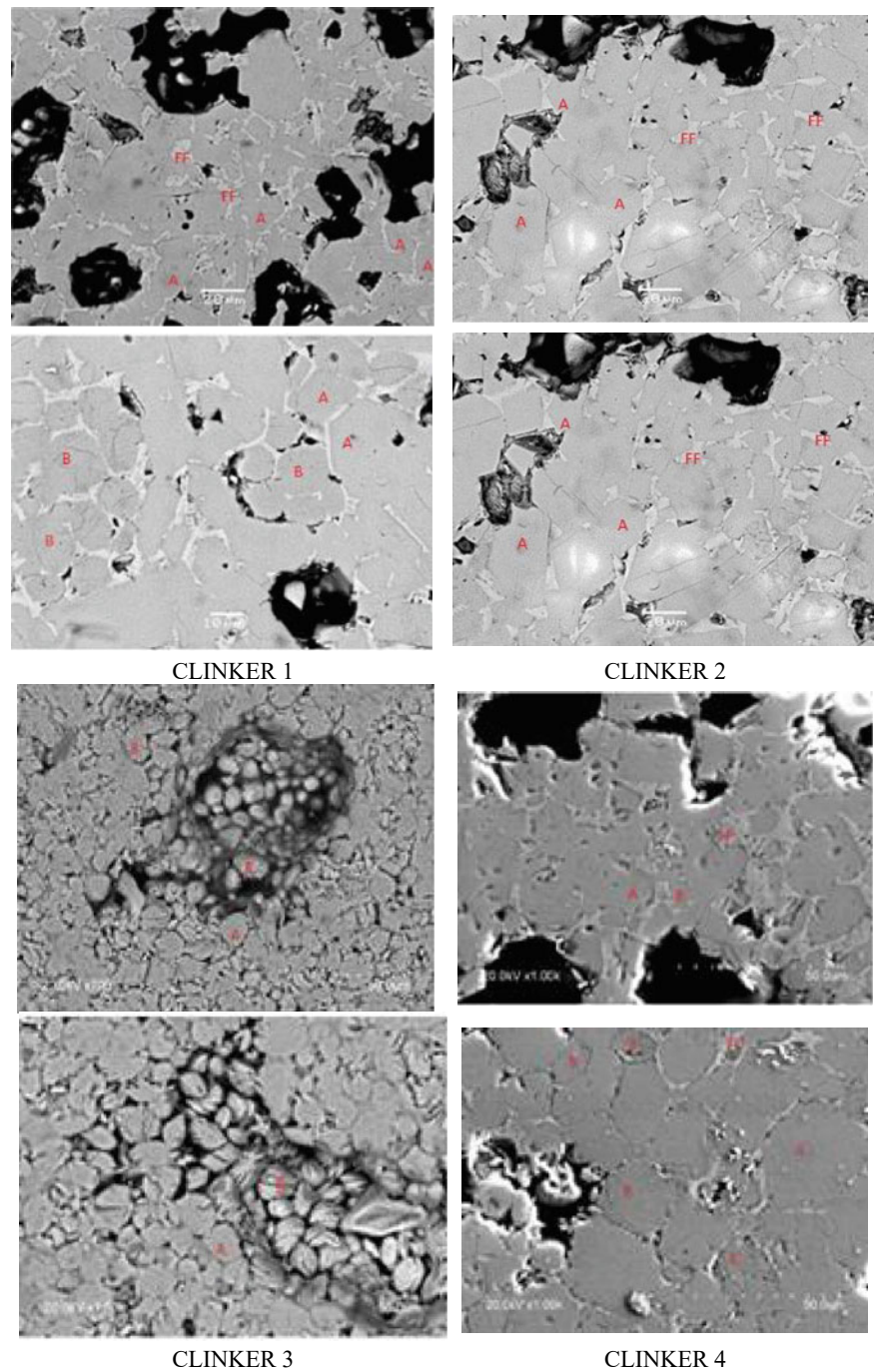
Fig. 1 The general appearance of the clinker samples

Fig. 2 The general appearance of the clinker: Clinker 1, Clinker 2, Clinker 3 and Clinker 4



Concerning the effect produced by the alternative fuels in the different clinker's phases: C_3S (Alite) (denoted by A in the micrographs), C_4AF (denoted by FF in the micrographs) and C_2S (Belite) (denoted by B in the micrographs), in Fig. 2, it is showing a series of comparative micrographs showing the four clinkers used. In the case of clinkers 1 and 2, the major phase is the C_3S (Alite) (A) which appears as highly defined angular crystals with rectangular and hexagonal sections that co-exist during the ferritic phase C_4AF (FF).

The C_2S (Belite) phase, found to a lesser degree, appears localised in highly specified areas of the microstructure.

In the case of clinkers 3 and 4, a different and uneven microstructure is visible, featuring a reduced definition of the C_3S (A), C_2S (B) and C_4AF (FF) phases. The C_3S (A) crystals display rounded edges, thus losing their angular appearance. Two types of C_2S (B) crystals can be identified, some more dendritic and others with a more laminate structure in the clinker.

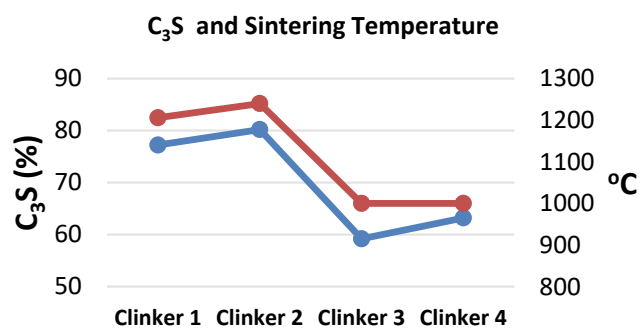


Fig. 3 Representation of the Alite of the four samples, compared to the Sintering Temperature

4 Discussion

From statistical studies carried out with more than 3000 data from Clinker (Castañón (2011)), it has been shown that the main parameter of the production process that influences the quality parameters of Alite and free lime is the sintering temperature of the furnace. The relationship between the sintering temperature of the furnace and the Alite phase can be verified in Fig. 3. The Clinker with the highest temperature corresponds to the highest value of the Alite quality parameter.

The composition of the flour of the clinker, as can be seen in Table 2, is very similar in the four samples. Therefore, this parameter in these samples is not decisive for their result, as it is similar in the four cases.

This study's findings show that using alternative fuels of diverse origin in the manufacture of cement clinker based on geomaterials such as SiO_2 , Al_2O_3 , Fe_2O_3 , and CaO is an efficient solution to achieve sustainability in the construction sector. Incorporating plastics alongside tyres in the clinkerization kilns contributes to reducing the percentage of NO_x in the kiln entrance, reaching values of 373 mg/Nm^3 . This reduction does not negatively affect the clinker's quality. The C_3S content is greater than 60% in clinkers 1, 2 and 4. In clinker 3, cement is produced with greater content in the C_2S phase, which fosters the formulation of belite cement. This type of cement has differentiated properties to standard Portland, required for certain applications due to enhanced durability compared to sulphate ions, dam constructions, and radioactive waste storage with medium and low radioactivity (Guerrero et al. 2008). The high C_2S content is relevant as it provides long-term resistance (>180 days) to cement.

5 Concluding Remarks

The main remarks carried out with this study are

1. The use of tyres and plastics as alternative fuel sources reduces traditional fossil fuels and reduces the NO_x percentage in the kiln to a value of 373 mg/Nm^3 . All of the previous leads to a positive on the manufacture of cement.
2. The variation of sintering temperature and alternative fuels in the manufacturing process plays a role in the mineralogical structure of the clinker's major phases, C_3S , C_2S and C_4AF , C-1 and C-2 ver-sus C-3 and C-4.
3. The quality parameters that have been considered for appraising the clinker's quality were the content in C_3S (Alite) and CaO free (free lime). A direct correlation is observed between the sintering temperature of the furnace and the Alite. These quality parameters are markedly influenced by the percentage of NO_x in the kiln. Reducing the NO_x content at the kiln entrance could cause an increase in the amount of free lime and a drop in the C_3S content, but always maintaining the established quality values.
4. The decrease noted in C_3S (Alite) and CaO -free content in the clinker has no negative bearing on its quality. In the four cases is above the standard content.
5. The use of tyres and plastics as alternative fuel sources allows us to obtain more eco-efficient cement clinkers with enhanced properties in durability, notably for dam construction.

Acknowledgements The authors would like to thank the two factories for supplying the clinker. Special thanks also to the Central Analysis Service, IETcc, and the Microscopy Service of the University of León for the technical support.

References

- Castañón A (2011) Optimización del proceso de producción de clinker: aplicación a la factoría de Tudela Veguín. Universidad de León, León, Spain (PhD Thesis)
- Castañón A, García S, Guerrero A, Gómez F (2012) A research of the mineralogy phases of clinker in a Spanish cement using the method of Rietveld. *Dyna* 79(173):41–47
- Daya DR, Sit SP, Layzell DB (2021) Alternative fuels co-fired with natural gas in the pre-calciner of a cement plant: energy and material flows. *Fuel* 295:120544

- El-Salamony A-HR, Mahmoud HM, Shehata N (2020) Enhancing the efficiency of a cement plant kiln using modified alternative fuel. *Environ Nanotech Monit Manage* 14:100310
- Guerrero A, Goñi S, Lorenzo MP (2008) Long term durability at 40 °C of eco-efficient belite cement-mortar exposed to sulfate attack. *Adv Cem Res* 20(4):139–144
- Hashem FS, Razeq TA, Mashout HA (2019) Rubber and plastic wastes as alternative refused fuel in cement industry. *Constr Build Mater* 21:275–282
- Mokhtar A, Nasooti M (2020) A decision support tool for cement industry to select energy efficiency measures. *Energy Strat Rev* 28:100458
- Přikryl R (2017) Constructional geomaterials: versatile earth resources in the service of humankind—introduction to the thematic set of papers on challenges to supply and quality of geomaterials used in construction. *Bull Eng Geol Environ* 76:1–9
- Přikryl R, Török A, Gomez-Heras M, Miskovsky K, Theodoridou M (eds) (2016) Sustainable use of traditional geomaterials in construction practice, vol 416. Geological Society, London, pp 1–22
- Taylor HFW (1997) *Cement chemistry*. Thomas Telford Services Ltd, London



Sludges from the Ornamental Rock Primary Cut: Mortar Incorporation Study

João Dixo, Sílvia Spínola, and Adriano Teixeira

Abstract

One of mankind's main challenges is to study the benefits of the mining, extractive and manufacturing industries and the environmental impacts caused by their activity. The natural stones sector generates high amounts of sludge. This work aims to complement existing research to find sustainable solutions for this problem. For that purpose, a physical and chemical characterisation was made of four sludges from a Portuguese industry, generated in the sawing and primary cut of natural stones, known as LCA, LARM, FPPEM and FPMP. The tests included grading analysis by sieving and sedimentation (X-ray attenuation method), determining density, the quality of fine particles (methylene blue test), and finally, quantitative chemical measurements by X-ray fluorescence. After that, the sludges were incorporated in mortars, replacing part of the cement (20% and 40%) in those mortars' manufacture. To investigate this possibility, tests of resistance to compression and bending were carried out on the mortars at different ages. Based on the results, the objective of characterising the sludges was fulfilled, and it was concluded that it would be possible to incorporate them in mortars.

Keywords

Sludge • Primary cut • Natural stone • Characterisation • Utilisation

J. Dixo · S. Spínola (✉)

Laboratory of Geotechnics and Construction Materials (LGMC),
School of Engineering (ISEP), Polytechnic of Porto, Porto,
Portugal
e-mail: scs@isep.ipp.pt

A. Teixeira

CICOPN—Centro de Formação Profissional da Indústria da
Construção Civil e Obras Públicas do Norte, Maia, Portugal

Department of Geotechnical Engineering, School of Engineering
(ISEP), Polytechnic of Porto, Porto, Portugal

1 Introduction

The transformation of ornamental stones produces a high amount of sludge and waste due to multiple processes, such as sewing, cutting, and polishing the rocks. The sludge is then treated in a batching sludge tank, where the solid particles are removed by sedimentation by using flocculants. The water resulting thereof is reused in the manufacturing process, and the sludge is sent to a filter-press, where it is dehydrated, and its volume is reduced, after which it is sent to a landfill.

One of the main challenges of the natural stone processing industry is to reconcile the benefits with the environmental impacts caused by its activities, namely the production of a high volume of sludge and waste, which constitutes an environmental issue. Aiming to complement previous studies, four distinct samples of sludge were collected from an industrial facility. They were submitted to laboratory characterisation in terms of their physical and chemical properties, thus concluding the possibility of their use as a by-product (Dixo 2018). Next, a study was carried out to evaluate the possibility of incorporating the sludge in mortars' production as a replacement for cement, in two distinct percentages: 20% and 40%. This aim was carried out in other studies such as Moura et al. (2002, 2006), Cruz et al. (2003) and Tenório et al. (2005).

2 Materials and Methods

The four sludges under consideration were collected at an industrial facility in the Centre of Portugal. Two of those samples were obtained next to the sawing equipment (primary cut), and they result from the cut of Cinza Antas granite (LCA) and Amarelo Rio Mel granite (LARM). The other two samples come from material resulting from the filter-presses: one from the multi-blade machines, which saws different types of granites (FPPEM), and the other from

Fig. 1 Sampling locations of the studied sludges



waste from the primary cut of different types of marbles and limestones (FPMC) (Fig. 1).

After sampling, the material was weighed, disaggregated and separated, using test sieve no. 200 of ASTM series, to obtain two particle size fractions (>0.075 mm and <0.075 mm), which were then oven-dried (100 ± 5 °C). The percentage of particles above 0.075 mm corresponds to the following values: 90% (LCA), 91% (LARM), 92% (FPFM) and 92% (FPMC). This particle-size distribution was kept in the methodologies for sludge characterisation and use. Tests were performed for particle size distribution by sieving (LNEC E239 1970) and quantitative chemical analysis by X-ray fluorescence spectrometry (portable equipment), according to LGMC's procedure for the fraction below 0.075 mm. The fraction was submitted to particle size analysis tests by sedimentation (method of X-ray attenuation—sedigraph), tests for determination of density (LNEC E64 1979) and methylene blue tests (EN 933-9:2009+A1: 2013), for determination of the fine quality, according to the current standards. That procedure was performed in the Laboratory of Geotechnics and Construction Materials (LGMC) of ISEP.

Following this characterisation, a study was performed at CICCOPN (Centro de Formação Profissional da Indústria da Construção Civil e Obras Públicas do Norte) for the incorporation of the sludge in mortars. A standard mortar was prepared as a reference without the incorporation of sludge. For each of the sludges under consideration (LCA, LARM, FPFM and FPMC), two mortars were prepared, with the same amount of water and sand, but with part of the cement (20% and 40%) being replaced by the incorporation of the sludge. The water/cement (a/c) ratio was 0.50. After

moulding the test specimens, they were placed in a humidity chamber for 24 h, at a controlled temperature of $20.0 (\pm 1.0)$ °C, with relative humidity not below 90%. Then they were demoulded, weighed and immersed in a tank filled with water at a temperature of $20.0 (\pm 1.0)$ °C, where they stayed until the testing. In total, 9 mortars and 27 test specimens were prepared. For the characterisation of the mortars in the hardened state, to evaluate the influence of each type of sludge according to their properties, the specimens were tested to bending and compression, according to standard EN 196-1: 2016 after 7, 28 and 56 days. For all test specimens, the water absorption was also determined.

3 Results and Discussion

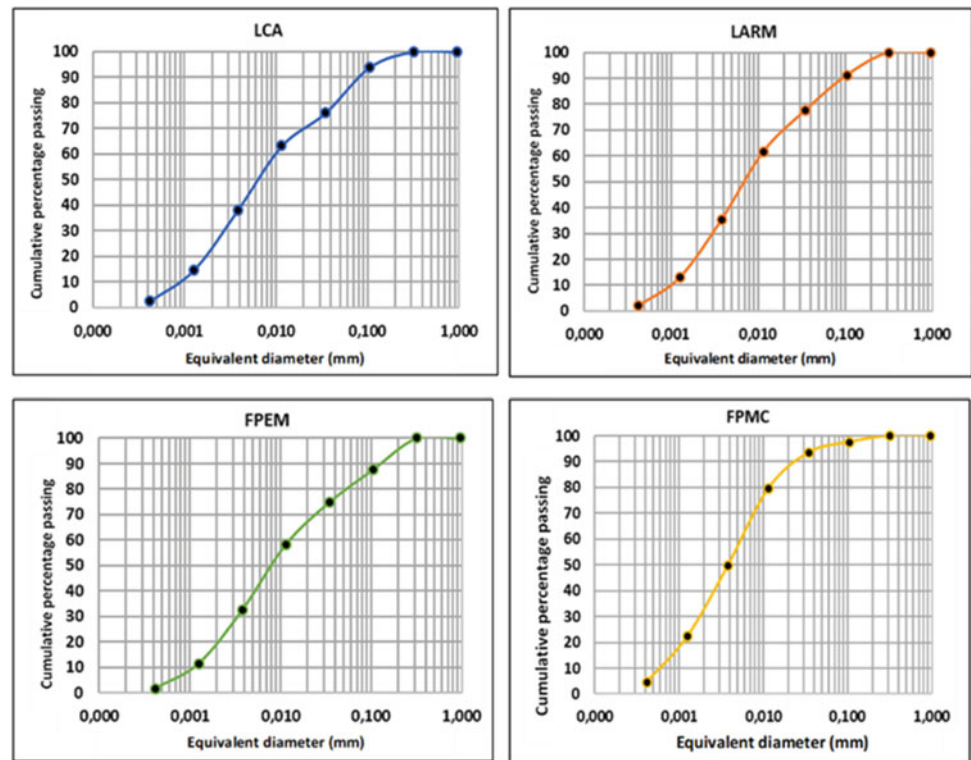
3.1 FRX Chemical Analysis

The FRX chemical analysis (portable equipment) allowed us to determine that the sludge is composed of silica (SiO_2) and alumina (Al_2O_3), besides iron (Fe_2O_3) and calcium (CaO), and that it also contains other chemical elements in smaller quantities, such as MgO , K_2O , MnO and TiO_2 .

3.2 Particle Size Distribution by Sedimentation (<0.075 mm)

The results obtained from the particle size distribution tests showed that the sludge respects the particle size distribution specification in terms of materials for industrial purposes,

Fig. 2 Particle size distribution charts



which, generally speaking, is below 1 mm; also, since their dimension is mostly below 0.063 mm (LCA = 85%; LARM = 85%; FPEM = 80%; FPMC = 90%), they may be classified as filler as well. The (D_{50}) was similar for all four samples (Fig. 2).

3.3 Density and Fines Quality (Methylene Blue)

For the density, values between 2.64 g/cm^3 and 2.78 g/cm^3 were obtained, which are below the density of cement ($>3.05 \text{ g/cm}^3$) and above that of sand (2.51 g/cm^3). As for the methylene blue values, all samples had 1.7 g/kg , which points out that they are not very active and belong to the “MBF10” category, according to standard EN 13,043:2002/AC: 2004 (Figs. 3 and 4).

3.4 Mechanical Resistance to Bending and Compression

Table 1 shows the results obtained for the mechanical resistance to bending and compression:

The results obtained show that all mortars with the incorporation of sludge have a lower resistance to bending when compared to the standard mortar. In contrast, the

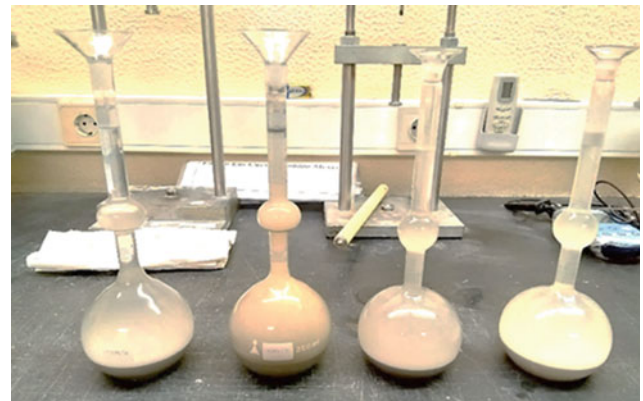


Fig. 3 Pycnometers used in density tests

incorporation of 20% is the one with the highest resistance to both bending and compression, regardless of the sludge sample and age.

Also, in terms of the mechanical resistance to compression, it is possible to conclude that all mortars have a lower resistance to compression when compared to the standard mortar, regardless of age. However, when comparing the two percentages of incorporation, 20% is the one with the highest resistance to compression, regardless of the sludge sample and the age at which the test was performed.

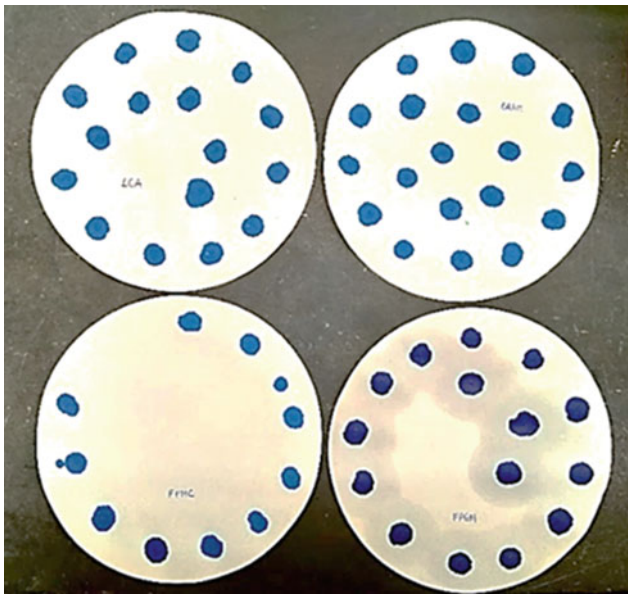


Fig. 4 Paper filters: methylene blue tests

3.5 Water Absorption

Figure 5 shows the values of water absorption obtained for the several mortars in this study. The results show that they have lower water absorption when compared to the standard mortar. The incorporation of 40% is the one with the lowest value of water absorption, which may be explained by the higher quantity of sludge incorporated, accounting for a decrease in the permeability.

4 Concluding Remarks

This study allowed the sludge’s characterisation resulting from the primary cut of ornamental rocks. It pointed out that they may be incorporated in mortars since they have particle size characteristics similar to those of a filler. They have low iron (Fe_2O_3) content. Compared to the standard mortar, all mortars showed a lower mechanical resistance, both to bending and to compression, regardless of the sample age.

Table 1 Values of the mechanical resistance to bending and compression (MPa)

Mortar	Incorporation (%)	Resistance to bending			Resistance to compression		
		7 days	28 days	56 days	7 days	28 days	56 days
Standard	0	7.73	7.03	8.95	45.47	53.19	59.80
LCA	20	7.26	7.33	6.26	39.60	45.06	46.96
LARM	20	6.16	6.98	6.33	37.86	44.77	45.69
FPEM	20	6.68	6.61	7.50	36.88	44.39	45.82
FPMC	20	7.52	6.96	7.45	41.61	46.90	48.64
LCA	40	5.09	5.46	6.16	26.95	31.29	30.96
LARM	40	5.06	5.23	4.99	27.55	30.17	32.10
FPEM	40	5.20	5.60	5.60	25.23	29.95	28.58
FPMC	40	5.72	6.35	6.75	27.10	33.02	34.30

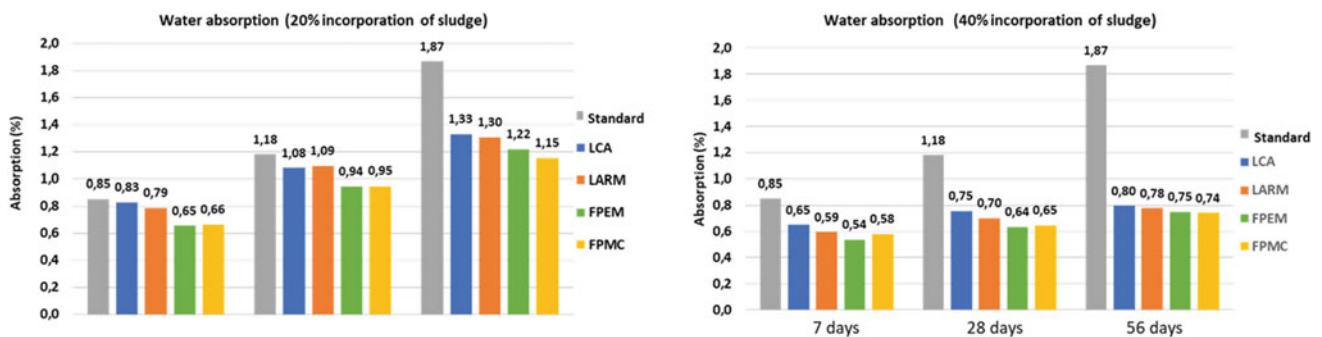


Fig. 5 Water absorption of the mortars for 20% and 40% incorporation of sludge

The mortars with 20% incorporation were the ones that presented the highest values of the resistances studied when compared to the mortars with 40% of incorporation. The resistance to compression of the standard mortar (52.5 MPa) was not reached in any of the samples at any age. The sample with the best behaviour is FPMC, which comes from the filter-press receiving the waste from the sludge of the primary cut of marbles and limestones. That is possibly due to the similarity to cement characteristics, above all, in its chemical composition.

The tests show that it is possible to obtain better results with lower values of sludge incorporation, bringing this closer to what has been shown in other studies referenced above, which mention lower incorporations of about 5 to 15%. It is also recommended that more tests be performed at later ages, at least until six months, to understand better how the mechanical characteristics and permeability evolve with time.

References

- Cruz DFM, Lameiras RM, Barboza ASR, Lima LA (2003) Estudo das propriedades mecânicas de argamassas produzidas utilizando-se resíduo do corte de mármore e granito. In: VI Seminário Desenvolvimento Sustentável e a Reciclagem na Construção Civil Proceedings, p 14. São Paulo, Brasil
- Dixo J (2018) Caracterização e aproveitamento das lamas geradas no corte primário de rocha ornamental. Instituto Superior de Engenharia do Porto, Porto (MSc Dissertation)
- EN 13043:2002/AC (2004) Aggregates for bituminous mixtures and surface treatments for roads, airfields, and other trafficked areas
- EN 196-1 (2016) Methods of testing cement—Part 1: Determination of strength
- EN 933-9:2009+A1 (2013) Tests for geometrical properties of aggregates—Part 9: Assessment of fines—Methylene blue test
- LNEC E 239 (1970) Solos. Análise Granulométrica por peneiração Húmida, Lisboa
- LNEC E 64 (1979) Cimentos. Determinação da Massa Volúmica, Lisboa
- Moura W, Gonçalves JP, Leite RS (2002) Utilização do resíduo de corte de mármore e granito em argamassas de revestimento e confeção de lajetas para piso. In: Sítienbus, Feira De Santana, Brasil 26:49–61
- Moura W, Lima MBL, Calmon JL, Moratti M, Souza FLS (2006) Utilização de resíduo de serragem de rochas ornamentais (RSRO) como substituição parcial do cimento na produção de blocos pré-moldados de argamassa. Proceedings Encontro Nacional De Tecnologia Do Ambiente Construído, Porto Alegre, Brasil 11:4217–4226
- Tenório JLL, Lameiras RM, Lima LA (2005) Desempenho de argamassas produzidas com resíduos do beneficiamento de chapas de granito (RBCG). In: Proceedings VI Seminário Brasileiro de Tecnologia das argamassas e I International Symposium on Mortars Technology, Florianópolis, Brasil, pp 34–44



Soil Stabilisation Using Third Generation Polymers

Ana Vieira, Telma Barroso, and José Augusto Fernandes

Abstract

Currently, the demand for ground engineering techniques that do not interfere negatively with the environment is a priority. The stabilisation of soils is no exception. This work reflects the study of third generation polymers to stabilise wall holes, a backup application to bentonite that does not cause any environmental disturbance in the region. Since the stabilisation of soils is influenced by many factors, the present work refers to the realisation of various laboratory tests to characterise five different soils (A to E) to assess the behaviour of the polymer in different scenarios (blends soil/polymer). Laboratory tests were carried out for soil characterisation. Based on the study carried out, it was possible to conclude that the polymer used in this work could ensure stabilisation in sandy soils. However, the existence of fines in its composition interferes with its effectiveness. The silty and the polymer clay soils improve the ability of sedimentation, as well as the limits of consistency, though, can connect these soil particles neither bring better stabilisation. It was also possible to verify that the application of only 0.5 g of polymer in 1 L of water brings significant benefits for both sedimentation and the equivalent of sand. For this reason, other blend ratios were tested, trying to use a lower concentration of polymer in order to optimise the cost-benefit of the entire process.

A. Vieira · J. A. Fernandes (✉)
Laboratory of Geotechnical and Construction Materials (LGMC),
School of Engineering (ISEP), Polytechnic of Porto, Porto,
Portugal
e-mail: jap@isep.ipp.pt

T. Barroso
GEO—Ground Engineering Operations, Seixal, Portugal

J. A. Fernandes
Department of Geotechnical Engineering, School of Engineering
(ISEP), Polytechnic of Porto, Porto, Portugal
GeoBioTec|UA, Aveiro, Portugal

Keywords

Soil stabilisation • Polymer • Soil mechanics • Ground

1 Introduction

The progress of technology has led to the evolution of construction and engineering works, making them increasingly demanding. However, the soil can be a major obstacle in carrying out the work, and it is increasingly common to apply soil stabilisation techniques to improve soil characteristics. Soil stabilisation consists of applying methods that aim to change the intrinsic characteristics of the soil and thus improve its behaviour (Mendonça 2016). To change soil properties, mechanical, physical or chemical means can be chosen, which, according to Medina and Motta (2005), have as main objectives: to increase soil resistance, to increase or decrease soil permeability, according to the purpose of the work, and reduce the compressibility of the soil.

Due to the diversity of methods, there are several solutions for the same type of soil, and one of the biggest challenges in soil stabilisation is to select, depending on the objectives, which technique will present the best results. Thus, Table 1 presents some of the techniques applicable to each case. However, it is essential to note that the technique addressed in this work relies on the addition of polymers, a chemical stabilisation technique in a strand of stabilisation fluid for carrying out excavation and drilling.

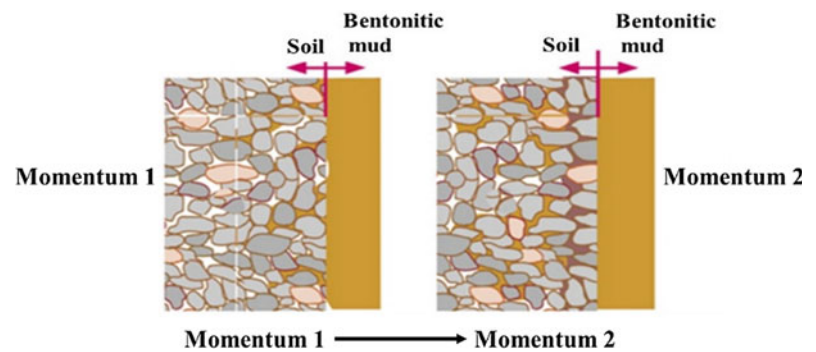
This work had as its main objective the study of the behaviour of a polymeric product, the PolyMud, which corresponds to the base component of a 3rd generation when added to different types of soils.

In the context of site construction, namely in the stabilisation of soils in the scope of piles and moulded wall preparation, as a stabilising fluid to enable the excavation of

Table 1 Soil stabilisation techniques (adapted from Coelho 1996, Soliz 2007, Cruz and Jalali 2010, Matos Fernandes 2012, Welling 2012, Mendonça 2016, SPFE 2021)

General methods	Specific methods	
Mechanics	Compaction Compaction with explosives Dynamic compaction Vibro-compaction Preload Overload Drains Dynamic consolidation	
Physics	Electro-osmosis Heating Freezing Vacuum method Soil mixing Jet grouting	
Chemicals	Chemical treatments	With cement With bitumen With lime With salt (sodium or calcium chloride) With synthetic or natural polymers
	Injections	

Fig. 1 Formation of an impermeable film with the use of bentonite (adapted from Pinto 2008)



the soil, the fluid guarantees the stabilisation of the soil excavation walls. Thus, both bentonite and the use of polymers have the same objectives: through hydrostatic pressure, prevent the passage of water into the excavation, and sustain the stresses exerted by the land adjacent to the excavation (Barbosa 2006; Pinto 2008) (Fig. 1).

Polymeric fluids have the same function as bentonite but behave differently. Once applied, the polymeric sludge penetrates the excavation walls and creates connections with the soil particles due to a difference in electrical charge, creating a membrane film (Trindade 2010) (Fig. 2). To ensure the presence of the membrane throughout the excavation area, it is necessary to ensure that the water pressure in the soil is never higher than the pressure exerted by the polymeric mud. Otherwise, water will seep into the excavation, breaking the formed membrane, altering the excavation stability and contributing to the rupture (Pinto 2008).

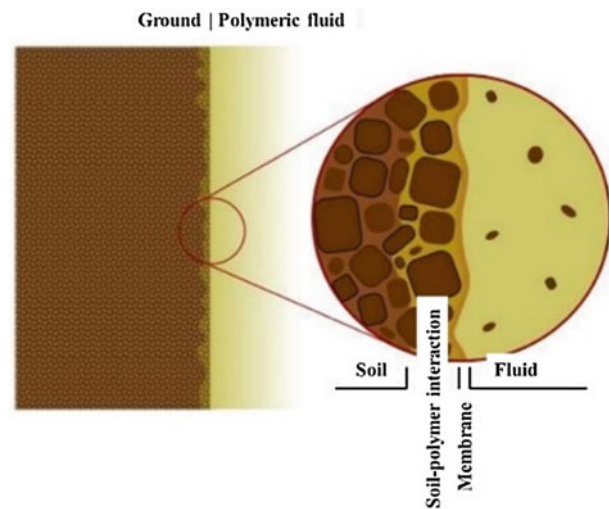


Fig. 2 Soil-polymer interaction (adapted from Trindade 2010)

2 Materials and Methods

The soil samples used in this work were prepared according to the standard (LNEC 1967a) and have the designations A, B, C, D and E. The tests carried out on the samples of the studied soils, considered as the most relevant in the interaction of the soil with the polymer, were the following: particle size distribution by wet sieving, Atterberg limits, sedimentation, water content and specific weight, sand equivalent, methylene blue, shear resistance, electrical conductivity, quantitative chemical analysis by X-ray fluorescence spectrometry (portable equipment), pH and Brookfield viscosity.

The characteristics of the soils under study are presented in Table 2. The company GEO (Ground Engineering Operations, Seixal, Portugal) uses a concentration of 0.1% of polymer on-site. This concentration will be abbreviated throughout the work as 1/1, 1 g of polymer applied in 1 L of water. However, in this study, concentrations of 0.05% and 0.15% were also used to verify the polymer concentration's implication in soil characteristics (in the different soil parameters to be studied). These concentrations will be abbreviated throughout the paper as 0.5/1 and 1.5/1.

Regarding the soils studied in this work, soil A was the only one characterised as clay, while the remaining soils correspond to sands. However, they are all quite different in their composition, with soil D being the one with the most significant amount of fines within the sands. The objective was to verify how the polymer performs in terms of stabilisation for different scenarios: the improvement in soil behaviour with sands, silts and clays.

3 Results and Discussion

3.1 Soil Distribution Size and Classification

The soil distribution size (LNEC E-196: 1970) is shown in Fig. 3, and soil classifications, uniformity and curvature coefficients in Table 2. According to the uniformity coefficient, soil B corresponds to a well-graded soil, with the remaining values for the other soils being low, which is an indicator of poorly graded soils.

The studied scenarios were sands, silts and clays. So the soils B, C and E will contribute to sands since soil B

comprises coarse to medium sand and C of medium to fine sand, while E presents a considerable percentage of pebbles (29%). Soil D corresponds to silt; however, it still presents 45% sand, but 37% of that sand is fine. Finally, although corresponding to clayey sand, soil A was the only one that presents clay, but in small quantities (ASTM 2016).

3.2 Soil Particle Sedimentation

The soil particle sedimentation test (LNEC E-196: 1966) was conducted without and with the application of polymer. Figure 4 presents the corrected densimeter values according to the time in which they were obtained. As shown in Fig. 4, some tests do not present the values for all recording moments because the solution tested was not in the densimeter reading grid. It was not possible to obtain any value for soil A and soils B+1.5P, C+1P and C+1.5P with a reduced number of data. It was verified that faster sedimentation for all the soils with the proportion of 0.5/1 and slower when the quantity 1.5/1 was used. The proportion 1/1 presented a sedimentation velocity between the two ratios already mentioned. For soil A without polymer was not possible to obtain results.

3.3 Consistency Limits of Soils Without Polymer and with Different Polymer Incorporations

Regarding the consistency limits of soils (NP-143:1969), the LL (liquidity limit) shows that the greater the amount of polymer applied, the greater the value obtained, i.e., the sample needed more water to reach its liquidity limit (Table 3). However, the LP (plasticity limits) should follow the same logic of thought, which does not occur, apparently resulting from the change in viscosity of the medium.

3.4 Water Content and Specific Weight

Table 4 represents the water content (NP-84: 1965a) of soils and the specific weight (NP-83: 1965b) obtained for each specimen without applying the polymer. Again, soil A stands out for its water content, much higher than the other soils. It is also possible to verify that the specimen with the

Table 2 Soil classifications, uniformity and curvature coefficients

Classification	Soil A	Soil B	Soil C	Soil D	Soil E
ASTM	SC clayey sand	SM silty sand	SM silty sand	ML sandy silt	SM silty sand with gravel
C_U^*	–	75.0	7.3	6.3	–
C_C^{**}	–	10.1	3.0	1.4	–

* C_U —uniformity coefficient, ** C_C —curvature coefficient

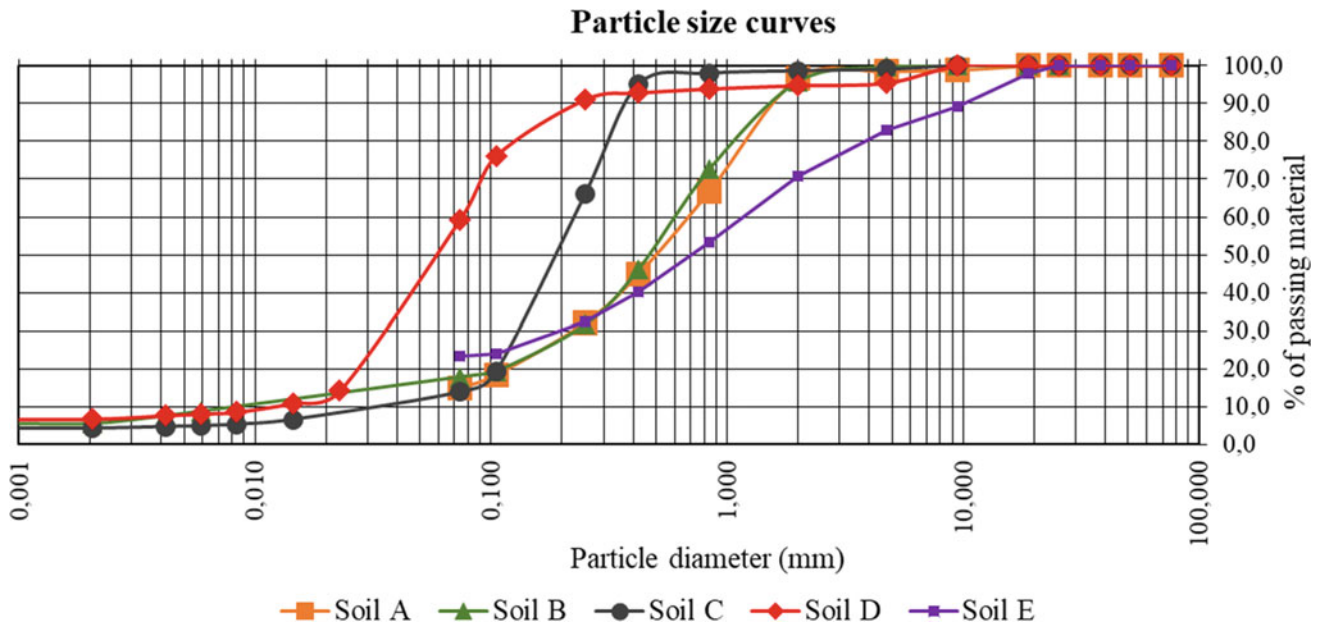


Fig. 3 Soil distribution size curves

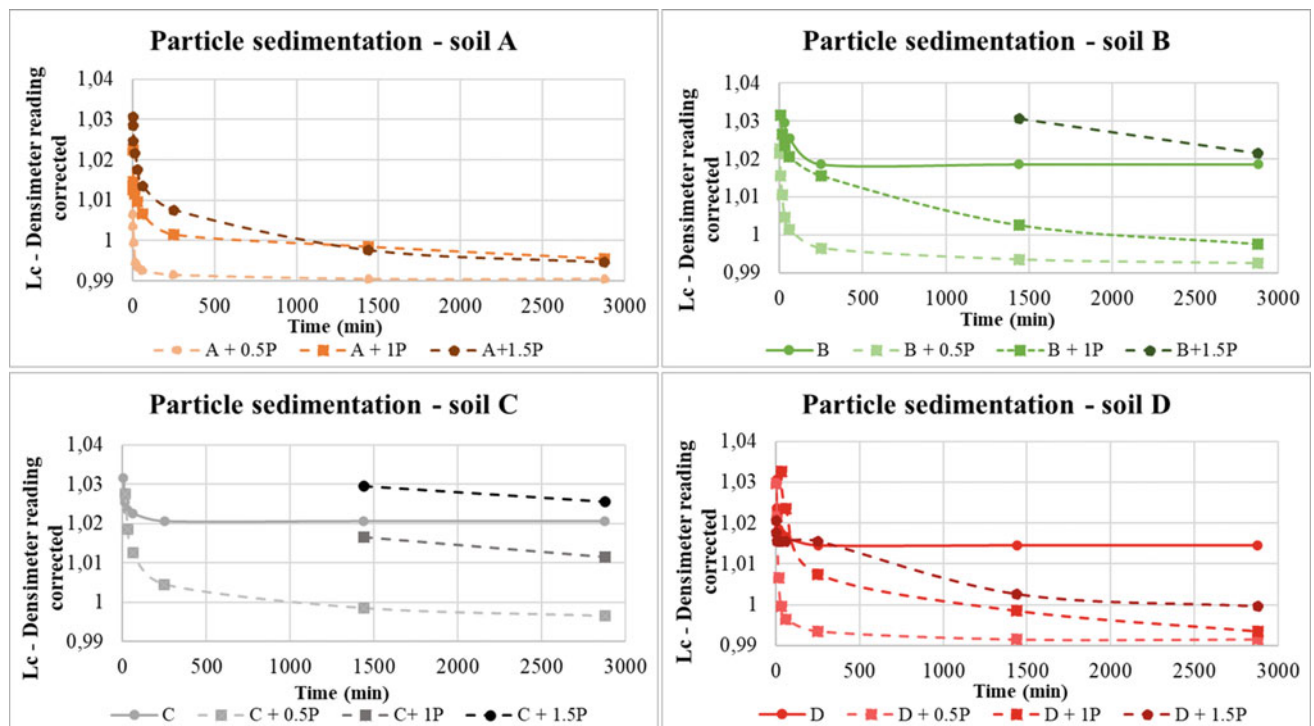


Fig. 4 Particle sedimentation of soils without and with polymer addition

Table 3 Liquidity limit, plasticity limits and index plasticity without polymer and with different polymer incorporations

Soil	Soil limits	Soil without polymer	Soil with polymer		
			0.5P/1	1P/1	1.5P/1
A	LL* (%)	49.6	56.9	63.5	71.1
	LP** (%)	25.8	32.4	29.9	36.5
	IP***	23.8	24.7	33.6	34.6

*LL—liquidity limit, **LP—plasticity limit, ***IP—plasticity index

Table 4 Water content and specific weight

Soil	A	B	C	D	E
Water content (%)	4.1	0.3	0.1	0.4	0.3
Specific weight (g/cm ³)	2.1	2.0	2.3	2.1	2.1

Table 5 Values of sand equivalent obtained in each soil

	Sand equivalent (%)				
	Soil A	Soil B	Soil C	Soil D	Soil E
Soil	19.8	44.5	61.4	4.4	–
Soil +polymer 0.5/1	51.9	50.0	92.2	71.6	–
Soil +polymer 1/1	42.1	94.7	78.3	52.6	–
Soil +polymer 1.5/1	5.3	72.0	2.5	3.6	–

highest specific weight corresponds to C and, on the other hand, the one with the lowest mass is B.

3.5 Sand Equivalent

Table 5 shows the sand equivalent (LNEC E-199:1967a) values obtained for each soil, considering the quantities of polymer used. Figure 5 represents graphically the values presented in Table 5.

The approximate value of polymer to obtain the highest percentage of sand equivalent is 0.7 for soil A, 1.0 for soil B, 0.6 for soil c and 0.7 for soil D.

From Fig. 5 and Table 5, it was possible to verify a non-linear increase in the percentage of sand equivalent, the most significant being that of soil D, which after polymer addition increases by 67.3%; it is sand equivalent. Soil D was considered as clay material, and after is designated as sandy material. It is possible to ascertain from Fig. 5 that there is a polynomial trend in the values obtained, except for soil B. Using the obtained polynomial trends, it was possible to analyse which polymer value should be used to achieve the highest percentage of sand equivalent. For soils A and D, a concentration of soils 0.7/1 was selected. For soils B and

C, the concentration of 1/1 and 0.6/1 were chosen, respectively. Considering these values of sand equivalent (Table 5), an average was performed to obtain the polymer mass that would best adapt to the different soils studied. The obtained value was 0.75 g of polymer for 1 L of water. The polymer can increase the sedimentation velocity of the particles, which leads to an increase in the values of the sand equivalent test, as it is possible to verify it in the data analysed.

This property is dependent on the type of soil and the concentration of polymer used. A medium with a high polymer concentration does not benefit all soils with fines since it gives rise to an obstructed sedimentation, i.e., the medium in which they are found has a high viscosity that hinders their sedimentation. However, in soils mostly sandy, like soil B, sedimentation is possible even in media with higher viscosity. Thus, by analysing the values, it is possible to see that, concerning this attribute, a concentration of 1.5/1 is not feasible because the fines will remain in suspension in the polymeric slurry, which will interfere with the execution of the works on-site. The characteristics that influence the yield of the polymeric sludge are density, sand content, pH and viscosity. Regarding sand equivalent, it was found that the polymer can increase sedimentation and, consequently,

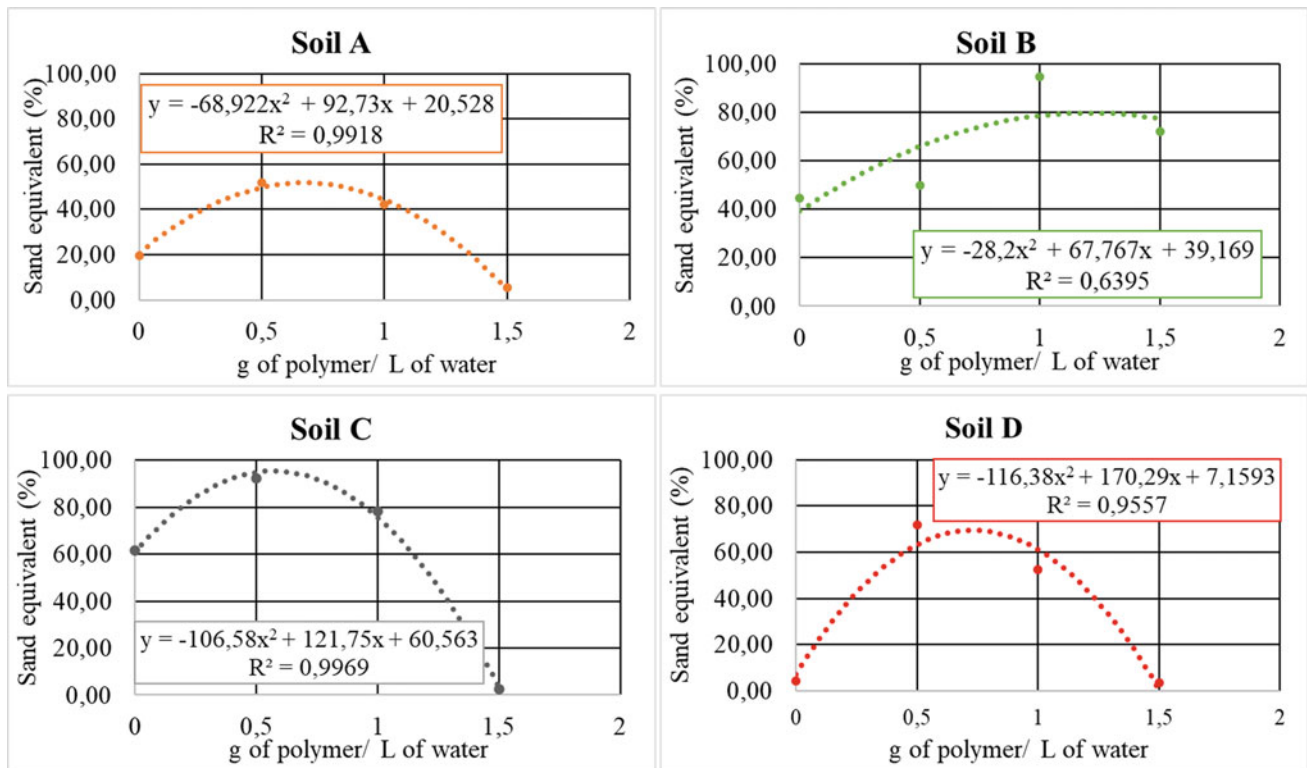


Fig. 5 The sand equivalent of soils for different blends of polymer

the sand equivalent. As such, the ideal proportion of polymer, considering only this property, would be 0.75/1.

3.6 Shear Strength

To carry out the shear strength test, it was necessary to consider the value of the vertical tension to be applied to the soil samples, and the use of polymer as a technique for supporting the walls in site operations does not generally exceed 50 m. Therefore, it was decided to apply a vertical force of 100, 200 and 400 kPa, for Specimen 1 (P1), Specimen 2 (P2) and Specimen 3 (P3), respectively. Thus, the different stresses were applied to the same material, without and with polymer, to verify whether the polymer will influence the shear strength, as well as the friction and cohesion angle of each material. The results are presented in Table 6. However, this test was carried out only by applying

the 1/1 polymer proportion. So, it will only be possible to verify if there is an improvement after the polymer application, and it will not be possible to compare which proportion is the best to benefit this property.

Since the test samples are stirred, the respective cohesion values are considered to be null. Unlike soil A, soil B proves that the polymer behaves better when it comes to shear stress, i.e., a more significant shear stress is required for the same displacement for sands with a lower amount of fines, as is the case of soil B which has 18%. On the other hand, soil C showed an increase in shear strength after polymer application. This fact is justified by the increase in cohesion, clearly proving the purpose of the polymer regarding stabilisation, i.e., interconnecting the particles, which leads to an increase in the cohesion of the soil under study.

Soil D shows no significant changes with the application of the polymer. The cohesion is null for both the soil with polymer and the soil without polymer. However, there is an

Table 6 Resistance parameters obtained from the shear stress test

	Soil A	Soil A+polymer	Soil B	Soil B+polymer	Soil C	Soil C+polymer	Soil D	Soil D+polymer	Soil E	Soil E+polymer
Friction angle (°)	32.0	28.2	33.0	40.0	35.7	6.7	37.0	43.3	38.8	46.3
Cohesion (kPa)	0.0	0.0	0.0	24.8	0.0	292.2	0.0	0.0	0.0	28.8

Table 7 Electrical conductivity of soil and blends of soil with polymer

Soil	Electrical conductivity ($\mu\text{S}/\text{cm}$)			
	Soil without polymer	Soil with polymer		
		0.5/1	1/1	1.5/1
A	98.5	177.2	250.0	259.0
B	19.2	77.2	186.3	216.0
C	81.4	176.2	270.0	336.0
D	140.0	179.0	259.0	287.0
E	154.4	215.0	294.0	335.0

increase in the friction angle, which indicates a positive influence on the polymer. Soil E presents an angle of friction of 39° , which agrees with the data obtained in the granulometric analysis. The resistance values obtained for soil E indicate that the polymer could interconnect the respective soil particles, but not as effectively as in soil C since there was no significant increase in cohesion.

3.7 Electrical Conductivity

Table 7 shows the values of electrical conductivity obtained for each soil (DSNR 2013) without and with polymer application. It can be seen that the values of electrical conductivity increase according to the amount of polymer applied, i.e., the higher concentration of polymer gives greater electrical conductivity.

Electrical conductivity is related to the tendency of ions to associate with soil particles. This particularity may explain why soil E shows better results in the direct shear test than soil B. Both soils are sands, but soil E has an electrical conductivity eight times higher than soil B (i.e., more ionic interconnections in soil E), which facilitates the interconnection of the polymer with the soil. Thus, although soil E has a minor percentage of fines (without clay) than soil B, its electrical conductivity value is substantially higher, contributing to soil stability. From this test, it was possible to prove that the electrical conductivity of soil can compromise the efficiency of chemical stabilisation.

Table 8 pH of soils and blends of soils with polymer

Soil	pH			
	Soil without polymer	Soil with polymer		
		0.5/1	1/1	1.5/1
A	7.9	7.7	7.9	7.9
B	7.0	7.3	7.4	7.2
C	9.7	8.7	9.0	9.1
D	9.1	8.7	8.9	8.9
E	9.3	8.7	8.9	8.7

3.8 Chemical Analysis

The chemical composition (oxides) of the soils before and after the polymer addition were analysed. The main found oxides were, in both cases, CaO, FeO, Fe₂O₃, K₂O and TiO₂. The results showed that the chemical composition (oxides) of the soils tested before and after the application of the polymer did not show any changes.

3.9 pH

This topic aims to verify the changes in the pH of the leachate after the addition of the different proportions of polymer. To this end, Table 8 represents the pH values (LNEC E-203:1967b) obtained for the different soils, and different amounts of polymer applied.

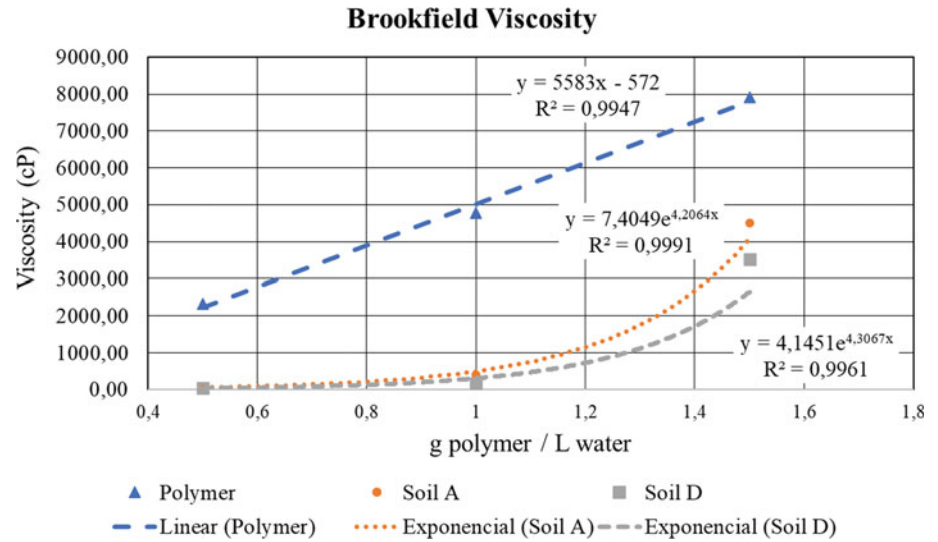
From the values in Table 8, it can be seen that, regardless of the amount of polymer used, the soil-polymer solution presents the pH of the soil. Therefore, on-site, to know if the pH after applying the polymeric slurry in the borehole will present the advisable range of values, i.e., ranging 9–12, it is sufficient to check the pH of the soil in which the polymer will act.

3.9.1 Brookfield Viscosity

In Table 9, it is possible to check the viscosity of the polymer and the polymer employed in the soil. Figure 6 graphically represents the obtained values. Firstly, it is

Table 9 Brookfield viscosity values obtained

Polymer +water	Polymer solution			Soil+0.5/1 polymer		Soil+1/1 polymer		Soil+1.5/1 polymer	
	1/0.5	1/1	1/1.5	Soil A	Soil D	Soil A	Soil D	Soil A	Soil D
Viscosity (cP)	2337	4776	7920	67	48	407	173	4500	3528

Fig. 6 Brookfield viscosity of polymer and soils A and D

possible to see that the joining of the soil with the polymer leads to a reduction of the polymer viscosity, and the greater the amount of polymer applied to the soil, the greater the viscosity of the mixture.

Additionally, it can be observed that, under normal site conditions and for the same amount of polymer applied, soil A presents a higher viscosity than soil D, i.e., with a polymer ratio of 1/1, the viscosity of soil A is twice that of soil D. However, it should be noted that, when applying a polymer ratio of 1/1.5, soil A compared to the ratio 1/1 increases its viscosity by 10 times, while soil D increases it by approximately 20 times.

4 Concluding Remarks

This work allowed verifying that the application of the polymer PolyMud, as a chemical treatment for soil stabilisation, presents benefits in sands, namely the increase of the sedimentation speed, when the proportion 0.5/1 is used, for any of the tested sands and the increase of soil cohesion associated with the bonding of the particles. It also improves the sand equivalent but with better results for a 0.75/1 ratio and guarantees the stability of the excavation walls. However, more than 15% of fines (<0.074 mm) is not advisable in the constitution of the sand since they occupy the empty spaces that the polymer needs to guarantee the

interconnection of the particles. It was also found that the sedimentation velocity decreases when the proportion of 1/1 is applied in fine sands and that soil with low electrical conductivity can interfere with the effectiveness of the polymer.

In silts and clays, the application of the polymer enables the sedimentation of the particles and improves the Atterberg limits. In other words, a more significant amount of water is needed for the soil to reach the plasticity and liquidity index and, as the sedimentation process is accelerated, the application of the polymer improves the sand equivalent of clayey and silty soils. It is important to note that properties such as sedimentation and sand equivalent showed significant results for the 0.5/1 ratio, so it would be essential to check if this concentration guarantees the stabilisation of the soil, as this factor could make the application of polymer even more profitable.

Silts and clays revealed similar behaviours, not showing changes in strength after the application of polymer. Though the sedimentation speed of the particles increased, the water content necessary to reach the plasticity limit and liquidity were higher. On the other hand, it does not cause changes in the cohesion value. It cannot occupy the empty spaces between the clay particles and create a connection between them; it decreases the viscosity of the soil-polymer solution, does not change the values of the shear resistance of soil and does not bring stability benefits.

Acknowledgements The authors acknowledge GEO—Ground Engineering Operations and LGMC|ISEP to support and use the facilities.

References

- ASTM (2016) Designation: D2166/D2166M-16—Standard test method for unconfined compressive strength of cohesive soil. American Society for Testing and Materials, USA
- Barbosa MIR (2006) Bentonitas aditivadas com polímeros para aplicação em fluidos de perfuração. Universidade Federal de Campina Grande, Brasil, URL: <http://dspace.sti.ufcg.edu.br:8080/jspui/handle/riufcg/10745> (MSc Dissertation)
- Coelho S (1996) Tecnologia de fundações. Edições E. P. Gustave Eiffel, Amadora
- Cruz ML, Jalali S (2010) Melhoramento do desempenho de misturas de solo-cimento com recurso a activadores de baixo custo. Geotecnia, Revista SPG, ABMS & SEMSIG 120:49–64
- DSNR (2013) Soil survey standard test method: electrical conductivity (C1A/3). Department of Sustainable Natural Resources, Australia
- LNEC (1966) Especificação E 196-1966, Solos - Análise granulométrica. Laboratório Nacional de Engenharia Civil, Lisboa
- LNEC (1967a) Especificação E 199-1967, Solos—Ensaio de equivalente de areia. Laboratório Nacional de Engenharia Civil, Lisboa
- LNEC (1967b) Especificação E 203-1967, Solos—Determinação do pH. Laboratório Nacional de Engenharia Civil, Lisboa
- LNEC (1970) Especificação E 239-1970, Análise granulométrica por peneiração húmida. Laboratório Nacional de Engenharia Civil, Lisboa
- Matos Fernandes M (2012) Mecânica dos solos: conceitos e princípios fundamentais. 3ª Ed., Vol. 1, Edições U.Porto, Porto
- Medina J, Motta LMG (2005) Mecânica dos pavimentos. 3ª Edição. COPPE, pp 48–53
- Mendonça A (2016) Reforço e contenção de terrenos. Instituto Superior de Engenharia do Porto, Porto
- NP (1965a) Norma portuguesa NP—83, Solos - Determinação do peso específico das partículas sólidas. Lisboa
- NP (1965b) Norma portuguesa NP—84, Solos - Determinação do teor em água. Lisboa
- NP (1969) Norma portuguesa NP—143, Solos—Determinação dos limites de consistência. Lisboa
- Pinto RNMG (2008) Sistemas construtivos de estruturas de contenção multi-apoiadas em edifícios. Faculdade de Engenharia da Universidade do Porto, Porto. <http://hdl.handle.net/10216/57929> (MSc Dissertation)
- Soliz VVP (2007) Estudo de três solos estabilizados com emulsão asfáltica. Universidade Federal do Rio de Janeiro, Brasil. <http://dspace.sti.ufcg.edu.br:8080/jspui/handle/riufcg/1879> (MSc Dissertation)
- SPFE – Sociedade Portuguesa de Fundações Especiais (2021) Estacas escavadas sem uso de lama bentonítica ou polímero. Sociedade Portuguesa de Fundações Especiais <http://www.spfe.com.pt/semlama.html>. Accessed Jan 2021
- Trindade EMA (2010) Uso de polímero como substituto da bentonite na estabilização de escavações em solos. Universidade de Évora, Évora. <http://hdl.handle.net/10174/21033> (MSc Dissertation)
- Welling EG (2012) Engineering performance of polymer amended soils. Faculty of California Polytechnic State University, USA. <https://digitalcommons.calpoly.edu/theses/856/> (MSc Thesis)



Applying Soil Thermal Regime to Improve Storage Conditions of Temperature-Sensitive Materials in Camping Tents

Jorge Espinha Marques, Carlos Pacheco, Hernâni Gonçalves, Catarina Mansilha, Armindo Melo, and Isabel Ferreira

Abstract

Every year, camping tents are used as shelters for several hundreds of millions of overnight stays. The indoor air temperature in camping tents may be above 50 °C, which is inadequate for storing temperature-sensitive materials. The research objective was to develop and assess a method to create a safe storage zone in camping tents exposed to direct solar radiation. An experimental camping site was set up with three trekking dome tents: in tent A (conventional fabric), the stored items were totally exposed to the incoming solar radiation and the indoor air, whereas in tents B (conventional fabric) and C (reflective fabric) the stored items were insulated using ordinary camping materials. A set of temperature sensors was installed, and readings were recorded every minute for six days. The thermal conditions in tent A were inadequate for storage since the stored items' temperature reached values above 40 °C during the warmest part of the day. In contrast, in tents B and C, the stored items' temperature was kept below 25 °C throughout the day due to the influence of the insulation cover combined with soil

temperature. Also, the measured effect of the reflective fabric on the temperature of the stored item was negligible.

Keywords

Soil temperature • Air temperature • Thermal insulation • Food products • Medical products

1 Introduction

Several recreational outdoor activities (e.g., Cordell 2012), namely trekking, mountain bicycling, hunting, scouting, mountaineering and camping, require the use of camping tents for the shelter of people as well as for gear storing, which usually includes temperature-sensitive items such as food products, medical products and gas cartridges. The precise number of outdoor outings which take place every year is difficult to determine. However, several organisms' statistics allow us to estimate the worldwide occurrence of several hundreds of millions of overnight stays in camping tents per year (e.g., TOF 2018). Camping tents are also used in other types of recreational and non-recreational activities, such as educational camps, religious pilgrimages and music festivals, and as temporary shelters in refugee camps, military camps and emergency camps. For example, the Scout Movement, the world's largest educational youth organization, has around 54 million members (WOSM 2020), most of who attend, every year, several camping activities of regional, national or international scope, especially during spring and summer.

Despite their wide use, camping tents have poor thermal performance, with indoor air temperature reaching values above 50 °C, usually much higher than outdoor air temperature (Zhang et al. 2017), affecting the occupants' health as the stored items. Since in campsites the use of refrigeration is usually not available, temperature-sensitive items may

J. Espinha Marques (✉)

Earth Sciences Institute (ICT), Department of Geosciences, Environment and Land Planning, Faculty of Sciences, University of Porto, Porto, Portugal
e-mail: jespinha@fc.up.pt

C. Pacheco

INESC TEC—Institute for Systems and Computer Engineering, Technology and Science, Porto, Portugal

H. Gonçalves

Department of Community Medicine, Information and Health Decision Sciences/CINTESIS, Faculty of Medicine, University of Porto, Porto, Portugal

C. Mansilha · A. Melo

LAQV|REQUIMTE, Department of Environmental Health, National Institute of Health Dr. Ricardo Jorge, Porto, Portugal

I. Ferreira

LAQV|REQUIMTE, Faculty of Pharmacy, University of Porto, Porto, Portugal

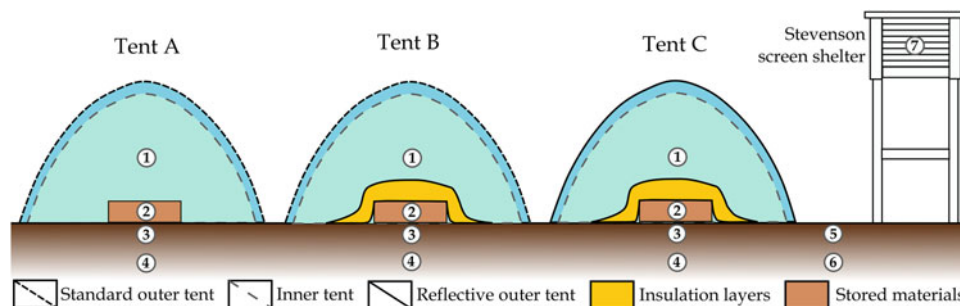


Fig. 1 Schematic representation of the experimental campsite. Temperature sensors: indoor air (1), stored materials (2), indoor soil at 2 cm depth (3), indoor soil at 10 cm depth (4), outdoor soil at 2 cm depth (5),

outdoor soil at 10 cm depth (6) and outdoor air (7). Note: no vertical or horizontal scale

deteriorate and seriously harm human health, for instance, by poisoning resulting from the ingestion of food or medicinal products. Also, these conditions are not recommended for the safe storage of gas cartridges. Previous studies on the thermal behaviour of several types of tents have highlighted the effect of intense solar radiation on the indoor thermal environment (e.g., Obyn et al. 2015; Zhang et al. 2017). Some of these studies have assessed possible solutions to mitigate the problem by applying shading materials or reflective layers outside the tents and improving tent design.

Soil temperature has been used for centuries to support food storage in underground cellars. It is still applied as an alternative to modern refrigeration systems or where these systems are not available (e.g., Brubaker et al. 2009; Mazarrón et al. 2012). Soil thermal regime encompasses daily and annual fluctuations controlled by a complex system of internal and external factors. Soil temperature fluctuations decrease with depth, and daily temperature fluctuations are hardly measurable below 50 cm from the surface. In contrast, at 10 m of depth, the ground temperature is nearly constant throughout the year (Hillel 2004; SSDS 2017).

The research objective was to develop and assess a simple, yet efficient method to create a safe storage zone for temperature-sensitive materials in camping tents exposed to direct solar radiation. For that purpose, an experimental campsite consisting of three tents under different indoor temperature settings was set up for one week in July 2018, in the village of Junça, Central Portugal. During the experiment, the temperature was continuously recorded at selected points of the campsite in order to assess the method implemented for insulating temperature-sensitive materials from high indoor air temperatures in camping tents.

2 Materials and Methods

The study was carried out at the village of Junça (Almeida municipality, Central Portugal), during summer, from 21 to 26 July 2018. The experimental campsite was located on a

plateau at 755 m a.s.l., with coarse-grained granite bedrock and Regosol soil type with Ap-C-R profile. The study site's Köppen-Geiger climate classification is Csb, which corresponds to a Mediterranean temperate climate with dry and temperate summer. The mean annual air temperature is 12.4 °C, the coldest month is January (4.7 °C) and the warmest month is July (21.5 °C). The mean annual precipitation is 499 mm, the wettest month is March (65 mm) and the driest month is July (6 mm).

The campsite consisted of three trekking dome tents (tents A, B and C) with identical dimensions (base: 190 cm × 200 cm; height: 130 cm) and double skin structure, including a waterproof outer tent and an inner tent for sleeping and storage purposes (Fig. 1). Tents A and B are made of standard materials with a low ability to block solar radiation. In tent C, the outer tent is made of reflective fabric with a high ability to block solar radiation. A similar set of water bottles and fruit juice packages was placed at the central part of the tent's floor in all tents.

In tent A, the stored items were totally exposed to the incoming solar radiation and the air inside the tent. In tents B and C, the stored items were covered with the following thermal insulation layers: at the bottom, a self-inflating sleeping mattress with an R-value of 2.3 (with an outer fabric composed of thermoplastic polyurethane and polyester and an internal polyurethane foam), the intermediate layer consisted of a polyester sleeping bag (with comfort and limit temperatures of 10 °C and 5 °C, respectively) and the top layer comprised a survival blanket (composition: 4% of resin, 92% of polyethylene terephthalate and 4% of aluminium). These thermal insulation materials were selected among the items usually carried by trekkers in order to avoid extra weight and volume in their rucksacks. The insulating layer function blocks out sunlight and insulates the temperature-sensitive items from the tent's hot air. This way, the temperature of the stored items is closer to the temperature of the underlying soil.

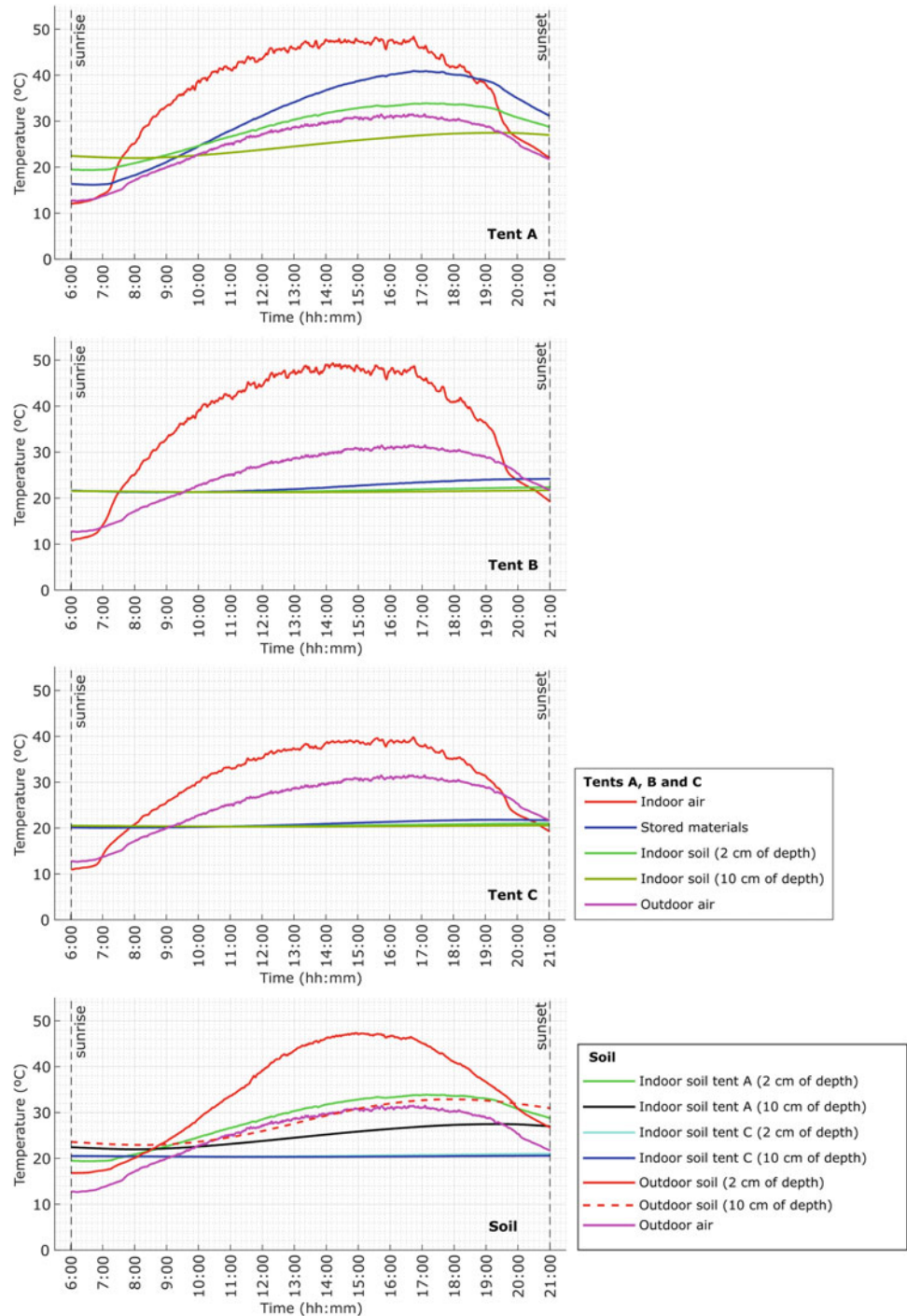
A set of semiconductor temperature sensors (from Maxim Integrated, model DS18B20+PAR) was installed in the

experimental campsite's selected points (Fig. 1), and readings were recorded every minute using data loggers. Inside the tents, a sensor was placed at 60 cm of height and another at the stored items. Soil temperature sensors were placed at 2 cm and 10 cm depth under each tent and in an outdoor spot. The outdoor air temperature was measured at 1.5 m above the ground, using a sensor placed in a Stevenson screen shelter.

3 Results and Discussion

Temperature measurements on tents A, B and C and all soil and outdoor measurements are presented in Fig. 2 for the average day of the period of the experiment. These temperatures are similar to those verified within each day. The vertical dashed lines indicate the limits of the time selected for comparison purposes, between 6:00 (sunrise) and 21:00 (sunset)

Fig. 2 Temperature variation for the average day between 6:00 (sunrise) and 21:00 (sunset)



(sunset). Data are presented as minimum, maximum, median, first (Q1) and third (Q3) quartiles.

The temperature of the stored materials in tent A monotonically increased from 8:00 until around 19:00, ranging from 16.2 °C to 40.9 °C. Afterwards, it was approximately 7 °C higher than the indoor air until sunrise of the next day. The median temperature was 33.6 °C, and Q1 and Q3 were respectively 23.7 °C and 39.0 °C. On the other hand, the temperature of the stored materials in tent B was consistently much smaller than the indoor air, ranging from 21.2 °C to 24.2 °C, with a median temperature of 22.1 °C and (Q1, Q3) of (21.4 °C, 23.5 °C). Additionally, this range of values was near those of the soil measured at 2 cm depth. Although tent C provides conditions for a lower indoor air temperature (Fig. 2), the temperature of the stored materials was similar to that of tent B, with values ranging from 20.1 °C to 21.8 °C, a median of 20.8 °C and the (Q1, Q3) of (20.2 °C, 21.6 °C). Concerning the soil temperature on tents A and C and its comparison with the outdoor air and soil temperatures, the outdoor soil at 2 cm depth presented the highest values, followed by the indoor soil at 2 cm depth on tent A, outdoor air, outdoor soil at 10 cm depth and indoor soil at 10 cm depth on tent A.

On the other hand, much lower temperatures were observed on tent C's indoor soil at both 2 cm and 10 cm depth (Fig. 2). An illustrative example is provided by the temperatures measured at 16:02 on July 25. At this hour, the indoor air temperature was 50.2 °C in tent A, 51.5 °C in tent B and 41.3 °C in tent C, even though the outdoor air temperature was 31.9 °C. Simultaneously, the temperature of the stored items was 41.1 °C in tent A, 23.9 °C in tent B and 21.6 °C in tent C, while the soil temperature at 2 cm depth was 33.3 °C in tent A, 22.3 °C in tent B and 20.8 °C in tent C.

These results demonstrate that the thermal conditions in tent A were inadequate for storage since the temperature of the stored items reached values above 40 °C during the warmest part of the day. In contrast, the indoor air temperature reached values above 45 °C (Fig. 2). On the other hand, the thermal conditions in tents B and C were much more suitable for storage since the stored items' temperatures were kept, even during the warmest part of the day, below 25 °C. As a result of the reflective outer tent, the indoor air temperature in tent C during the warmest period of the day is around 10 °C lower than in tents A and B (Fig. 2). However, the temperature of the stored items in tents B and C is very similar and, at the same time, close to soil

temperature, highlighting the major effect of the overlying insulating layers and the minor effect of the reflective outer tent.

4 Concluding Remarks

Camping tents are used in a wide range of activities. However, the thermal performance of camping tents, especially when exposed to direct sunlight, is often inappropriate for storing temperature-sensitive materials. This study intended to develop and assess a simple method for creating a safe storage zone in camping tents using the combined effect of an insulating layer and soil thermal regime. The results demonstrated this method's efficiency since the insulated items were kept under 25 °C, close to soil temperature, even when the indoor air temperature reached values above 50 °C. By contrast, the non-insulated items consistently reached temperature values above 40 °C during the warmest part of the day. Therefore, this method can significantly improve the storage conditions of sensitive-temperature materials in camping tents, which may be of great interest in situations where refrigeration is not an option.

Future research on this subject may focus on the influence of a wider set of factors on camping tents' storage conditions, like air humidity, wind speed, soil moisture, tent ventilation and different insulation materials. A comparative study encompassing the tent storage method and an alternative storage method for camping sites, consisting of a shallow hole dug in the topsoil (around 20–30 cm depth), covered with an insulating layer, could also be performed.

Acknowledgements This work was developed under the ICT (project UIDB/04683/2020) with the reference POCI-01-0145-FEDER-007690. The authors thank the anonymous reviewers, whose comments and suggestions helped improve the manuscript.

References

- Brubaker M, Bell J, Rolin A (2009) Climate change effects on traditional Inupiat food cellars. *Cent Clim Healt Bull* 1:1–6
- Cordell HK (2012) Outdoor recreation trends and futures. General Technical Report SRS-150. US Department of Agriculture Forest Service, Southern Research Station, Asheville
- Hillel D (2004) Introduction to environmental soil physics. Academic Press, Amsterdam
- Mazarrón FR, Cid-Falceto J, Cañas I (2012) An assessment of using ground thermal inertia as passive thermal technique in the wine industry around the world. *Appl Therm Eng* 33–34:54–61

- Obyn S, van Moeseke G, Virgo V (2015) Thermal performance of shelter modelling: Improvement of temporary structures. *Energy Build* 89:170–182
- SSDS—Soil Science Division Staff (2017) Soil survey manual. USDA Handbook 18. Government Printing Office, Washington, DC
- TOF—The Outdoor Foundation, (2018) Outdoor participation report 2018. The Outdoor Foundation, Washington, DC
- WOSM—World Organization of the Scout Movement. <https://www.scout.org/worldwide>. Accessed 06 May 2020
- Zhang L, Meng X, Liu F, Xu L, Long E (2017) Effect of retro-reflective materials on temperature environment in tents. *Cas Stud Therm Eng* 9:122–127



Impact of the New European Standardisation on Soil Laboratory Routines and Test Results: The Case of Grain Size Distribution Analysis

Camila Afonso, Eduardo Neves, Adriano Teixeira, and Manuela M. Carvalho

Abstract

Soil is widely used for supporting foundations and as an excavation or construction material, making the study of its properties and performance essential. Soil characterisation is performed using geotechnical evaluation techniques and, depending on the intended purpose of the soil use, in situ and/or laboratory tests. These activities should be performed following technical standards that define the methodology to be applied in each of these procedures. Recently, new European soil characterisation standards are being implemented to develop comparable methodologies in the different countries of the European Union. This work presents a study of the main changes in the new standardisation to determine particle size distribution. In this study, to evaluate the impact of the new standard methodologies on the routine of the laboratories and the results obtained, about 30 laboratory tests were carried out, and two soil types were used: granitic residual soil and kaolinitic clay soil. From these tests, it was possible to verify that some modifications introduced by the new standardisation do not guarantee uniformity of testing practices or fundamental accuracy in this type of determination.

Keywords

Soils • Standardisation • Laboratory testing • Particle size distribution

1 Introduction

New standards are being implemented to unify the different methodologies of lab characterisation of soils used in the European Union countries. To determine particle size distribution, the standard to be implemented is EN ISO 17892-4: 2016, with the general title: “Geotechnical investigation and testing—Laboratory testing of soils—Part 4: Determination of particle size distribution”. This standard describes sieving methods, sedimentation methods and a combination of both. In Portugal, the determination of particle size distribution has been executed for some decades according to the standards LNEC E 239: 1970 and E 196: 1966, preceded by the application of E 195: 1966.

When comparing the new standardisation to be implemented with the one currently used in Portugal, it was found that (i) in the sieve method, there are differences in the aperture sizes of the sieves, in the specimen preparation and the test performance; (ii) in the sedimentation method, the differences are related to the characteristics of the dispersing agent used in the specimen preparation, to the hydrometer specified for the test execution, in the fact that the new standard does not specify the time and intensity for stirring the suspension in the dispersing agent and also in the change in reading times during the sedimentation process (Santos 2019). Therefore, it is important to verify how these changes influence the precision and repeatability of the test method and the results.

2 Methods

The procedures adopted are those described in EN ISO 17892-4: 2016. Tests were carried out on two different soils: Soil A—granitic residual soil and Soil B—kaolinitic clay soil. Both soils have more than 10% of particles smaller than 0.063 mm and more than 10% of particles larger than 0.063 mm, so, according to the standard, they were tested by

C. Afonso · A. Teixeira · M. M. Carvalho (✉)
Department of Geotechnical Engineering, School of Engineering (ISEP), Polytechnic of Porto, Porto, Portugal
e-mail: mmc@isep.ipp.pt

E. Neves · A. Teixeira
Centro de Formação Profissional da Indústria da Construção Civil e Obras Públicas do Norte (CICCOPN), Maia, Portugal

Table 1 Designation of the particle size distribution tests

Designation	Test
PSv_2_A	Determination of particle size distribution by the combination of sieving and sedimentation with vigorous mixing (18,000 rpm for 10 min) using two different specimens—Soil A
PSv_2_B	Determination of particle size distribution by the combination of sieving and sedimentation with vigorous mixing (18,000 rpm for 10 min) using two different specimens—Soil B
PSs_2_A	Determination of particle size distribution by the combination of sieving and sedimentation with gentle mixing (300 rpm for 4 h) using two different specimens—Soil A
PSs_2_B	Determination of particle size distribution by the combination of sieving and sedimentation with gentle mixing (300 rpm for 4 h) using two different specimens—Soil B
PSv_1_A	Determination of particle size distribution by the combination of sieving and sedimentation with vigorous mixing (18,000 rpm for 10 min) using the same specimen—Soil A
PSv_1_B	Determination of particle size distribution by the combination of sieving and sedimentation with vigorous mixing (18,000 rpm for 10 min) using the same specimen—Soil B
PSs_1_A	Determination of particle size distribution by the combination of sieving and sedimentation with gentle mixing (300 rpm for 4 h) using the same specimen—Soil A
PSs_1_B	Determination of particle size distribution by the combination of sieving and sedimentation with gentle mixing (300 rpm for 4 h) using the same specimen—Soil B
E196:1966	Determination of particle size distribution by the combination of sieving and sedimentation using the specification LNEC E196: 1966—Soil B

combining both methods, sieving and sedimentation on separate specimens from the same sample. Sequential sieving and sedimentation tests were also carried out on a single specimen from each sample.

The sieving tests were carried out using wet preparation, in triplicate, for each soil. In the Soil A specimen preparation for the sieving test, no dispersing agent was used since it is a granular soil, and the particles disperse easily. For Soil B, a hexasodium hexametaphosphate solution with a concentration of 2 g/l was used. During sieving, the material was passed through a batch of test sieves according to ISO 3310-1 and ISO 3310-2, with the following aperture sizes: 63.0 mm, 37.5 mm, 20.0 mm, 10.0 mm, 6.3 mm, 2.0 mm, 0.60 mm, 0.20 mm and 0.063 mm.

The sedimentation tests by the hydrometer method were performed for each specimen in the fraction passing 0.063 mm, in a temperature-controlled room equipped with a calibrated temperature measuring device for recording maximum and minimum temperatures. For each of the tested variations, at least three repetitions were performed. The specimens were deflocculated with a hexasodium hexametaphosphate solution with a concentration of 40 g/l. As the standard does not specify the agitation conditions to be applied to achieve full soil particle dispersion, two types of agitation were tested to understand whether, or not, the agitation influences the results obtained: (i) vigorous mixing in a short time—mechanical stirrer at 18,000 rpm for 10 min and (ii) gentle and prolonged mixing—magnetic stirrer at 300 rpm for 4 h. After that mixing, as specified, the soil suspensions were placed in sedimentation cylinders, and

hydrometer readings were taken at 0.5 min, 1 min, 2 min, 4 min, 8 min, 30 min, 1 h, 2 h, 6 h and 24 h.

Table 1 presents a summary of the various tests carried out and their designations.

3 Results

Figures 1 and 2 shows the granulometric curve obtained by combining the sieving and sedimentation methods. The results obtained in the tests with two specimens from the same sample, one for sieving and the other for sedimentation as specified in the standard EN ISO 17892-4: 2016, are presented, as well as the results obtained in tests with a single specimen for sieving and sedimentation. Corrected graphs are also presented in both cases, removing the first sedimentation point since these presented values are higher than the ones found with the last sieve.

Figure 1 shows the granulometric curves obtained for the three repetitions in the tests performed with different specimens for sieving and sedimentation on both soil types (A and B), with vigorous mixing and gentle mixing. The corrected graphs are shown on the right side, adjusting the transition zone between sieving and sedimentation.

Figure 2 shows the granulometric curves obtained for the three repetitions in the tests performed with the same specimen for sieving and sedimentation on both soil types (A and B), with vigorous mixing and gentle mixing. The corrected graphs are shown on the right side, adjusting the transition zone between sieving and sedimentation.

Fig. 1 Granulometric curves obtained by sieving and sedimentation, with vigorous and gentle mixing, for the tests using two different specimens for Soil A (PSv_2_A and PSs_2_A) and for Soil B (PSv_2_B and PSs_2_B)

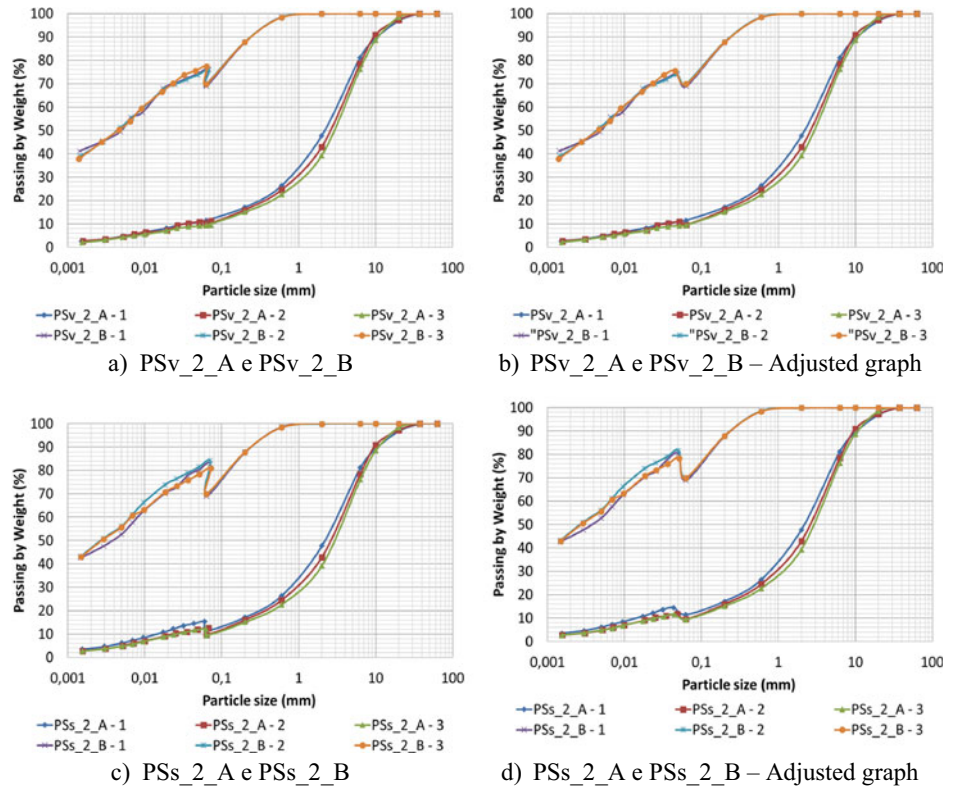
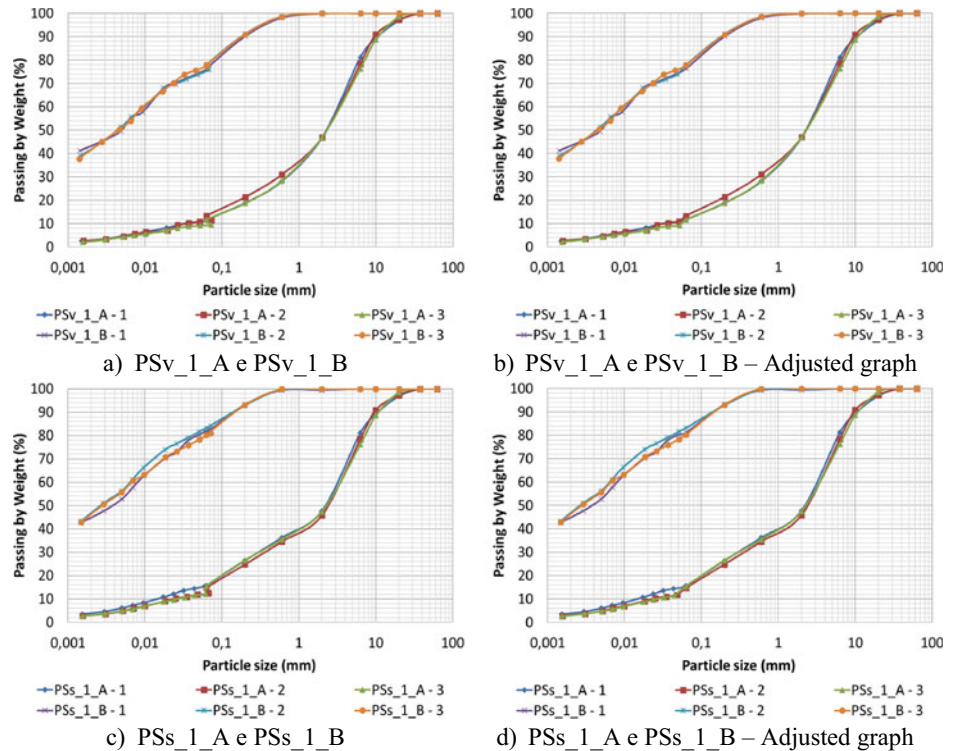


Fig. 2 Granulometric curves obtained by sieving and sedimentation, with vigorous and gentle mixing, for the tests using the same specimen for Soil A (PSv_1_A and PSs_1_A) and for Soil B (PSv_1_B e PSs_1_B)



4 Discussion

The results obtained for both soils were analysed for the influence of the two different agitation types applied in the sample preparation on the sedimentation method and the influence of using a single specimen or two different specimens, one for sieving and the other for sedimentation.

In Fig. 3, it is possible to observe the average curves obtained in the sedimentation test with vigorous (Sv_A and Sv_B) and gentle (Ss_A and Ss_B) mixing. Comparing the values obtained for the two soils, it is possible to observe that (i) the results differ depending on the method chosen for the dispersion of the particles; (ii) the percentage of particles smaller than the equivalent diameter assumes slightly higher values for the gentle mixing. This behaviour can be related to the suspension's reaction time with the dispersing agent, 4 h in gentle mixing and 10 min in vigorous mixing; the longer contact with the dispersing agent can cause a greater dispersion of the particles. This difference is more pronounced for Soil B.

The standard European states that the tests must be carried out separately with different specimens taken from the same sample regarding the combination of sieving and sedimentation. As is possible to observe (Fig. 1), the results obtained do not constitute smooth continuous curves in the transition zone. For both agitation methods, the point determined by the first reading of the hydrometer, at 30 s, presents values of diameter very close to or larger than the aperture size of the last sieve used in the sieving test (0.063 mm). This may be related to the shape of soil particles: if there are particles with a lamellar shape, one of the dimensions is larger than the others, the particles can pass through the sieve but have one side with a dimension larger than 0.063 mm; however, this dimension can be detected through the hydrometer readings. On the other hand, this discontinuity may also be related to inaccuracies in the

calculation methodology since the particle diameter is determined by Stokes' Law which relates the fall velocity of the particles to their equivalent diameter.

In all cases where two specimens are used, even after removing the first point obtained by sedimentation (adjusted curves), the granulometric curves remain with a slight discontinuity in the transition between sieving and sedimentation, which may be related to the different particle dispersing methodologies applied to the specimens. When comparing the percentage of material that passes through the 0.063 mm sieve, in tests where a single specimen is used, this value is higher than that obtained in tests with two different specimens, as shown in Fig. 4. It is also possible to observe that these percentages were higher when gentle mixing was used, in which the soil remains in contact with the dispersing agent longer. Combining the curves obtained by sieving and sedimentation, it is observed that in tests using a single specimen with the same preparation, the curve is smoother and more continuous than when different specimens are used.

Finally, to compare the values obtained using the European standardisation with those obtained using the Portuguese specification (E196:1966), the determination of particle size distribution of soil B was performed according to E196:1966. This standard recommends using the same specimen for sedimentation and sieving. All material goes through the same preparation process, with the same concentration of dispersant agent. When comparing the result obtained by applying both standards (E196:1966 and EN ISO 17892-4:2016), it is noted that the granulometric curve obtained by E196:1966 has a different behaviour from that obtained by EN ISO 17892-4:2016, for both gentle and vigorous mixing, as shown in Fig. 5a). Comparing the curve defined by E196:1966 with the results obtained in the tests PSv_1_B and PSs_1_B, where only one specimen was used too, it appears that the curves present a similar behaviour as shown in Fig. 5b).

Fig. 3 Comparison between the average curves obtained in the sedimentation tests with vigorous mixing and with gentle mixing

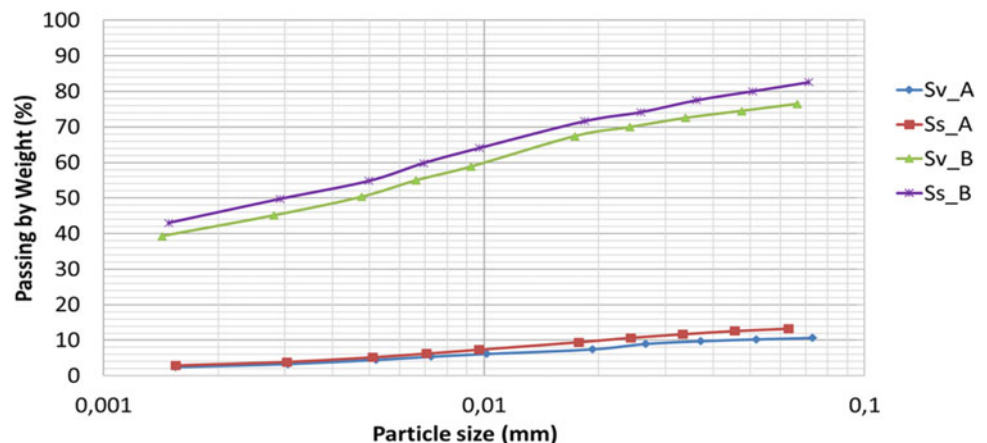


Fig. 4 Comparison between the average granulometric curves, obtained with **a** vigorous mixing and **b** gentle mixing, using a single specimen per soil and using two specimens

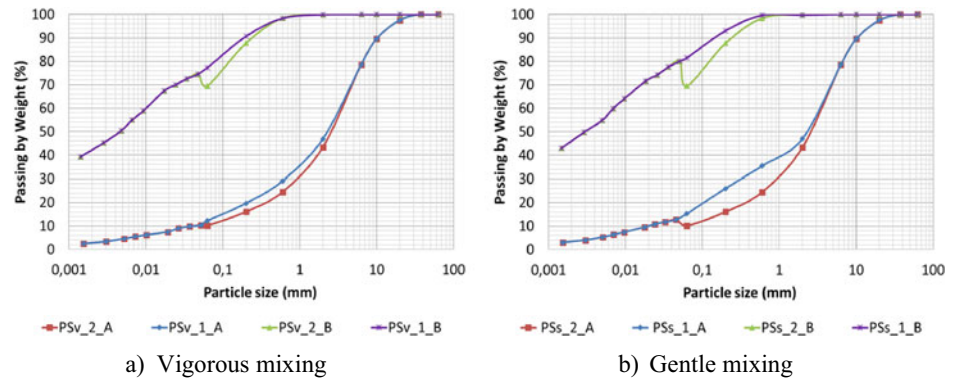
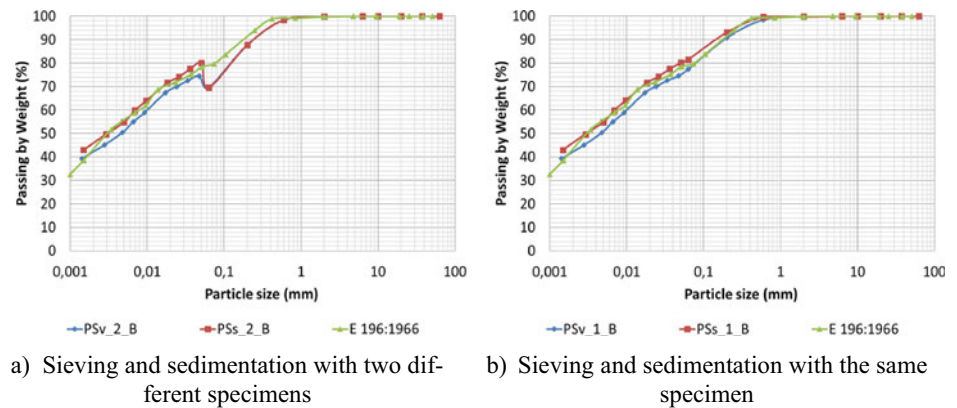


Fig. 5 Comparison between the granulometric curves obtained by E196:1966 and EN ISO 17892-4:2016—Soil B



5 Concluding Remarks

Regarding the sedimentation test using the hydrometer method, for the two types of soils studied, it is possible to conclude that in the first reading, at 30 s, the equivalent diameter obtained is very close to or larger than the aperture of the last sieve used in the sieve test (0.063 mm). This can be related to the particle shape or the calculation methodology. Combining the results obtained by sedimentation and sieving made it necessary to exclude this reading to reduce the irregular transition. According to E196:1966, currently used in Portugal, the first sedimentation reading is at 1 min, and this anomalous situation does not occur.

For both soil types, the gentle and prolonged mixing resulted in better dispersion of the particles than the vigorous and short mixing. In these cases, the fraction of particles smaller than the equivalent diameter was slightly higher when compared to more vigorous mixing. These results allow us to conclude that, without precisely defining the method to be applied for the dispersion of particles, standard EN ISO 17892-4:2016 allows the results obtained to be influenced by the knowledge and experience of the laboratory operator, which may lead to obtaining very different results.

When it is necessary to combine the sieve test with the sedimentation test, the European standard establishes the use of different specimens from the same sample, which are prepared with different concentrations of dispersant agent and the combination of the results in a single smooth and continuous curve. In the present work, in both studied soils, this was not possible when different specimens were used and prepared with different concentrations of dispersant agent—the combination of results did not result in a single smooth, and continuous curve since the percentage of material smaller than 0.063 mm is higher in the sedimentation method than in the sieve method. However, it was possible when a single specimen with the same preparation procedure was used (contrary to what is specified by the standard); in this case, the curve obtained was smooth and continuous in the transition between the methods.

Finally, it is possible to recommend revising the methodology described in EN ISO 17892-4:2016, both in terms of the combination of tests by sieving and sedimentation and the procedure for carrying out the sedimentation test using the densimeter, particularly in terms of the number of specimens to be used per sample, the methodology to be applied in the preparation of the samples, the definition of the most appropriate method for the dispersion of the particles and also regarding the relevance of the first reading in the sedimentation, at 30 s of testing.

References

- E 195:1966 Solos—Preparação por via seca de amostras para ensaios de identificação. Laboratório Nacional de Engenharia Civil, LNEC, Lisboa, Portugal
- E 196:1966 Solos—Análise granulométrica. Laboratório Nacional de Engenharia Civil, LNEC, Lisboa, Portugal
- EN ISO 17892-4:2016 Geotechnical investigation and testing – Laboratory testing of soils—Part 4: Determination of particle size distribution. European Committee for Standardization, Brussels
- Santos C (2019) Análise comparativa de diferentes métodos laboratoriais na caracterização física de solos utilizados em obras de engenharia civil. Instituto Superior de Engenharia do Porto, Porto. (Master's dissertation)



Soil Particle Density Determination According to EN ISO 17892-3: 2015: Some Difficulties in Laboratory Practices

Camila Afonso, Eduardo Neves, Adriano Teixeira, and Manuela M. Carvalho

Abstract

Soils are used as raw material and to provide support in various human activities. In the scope of civil and geotechnical engineering, their characterization is indispensable for a significant number of design and construction situations, such as foundations, earthworks and excavations. Soil characterization is performed in the field and laboratory using tests that must be standardized to ensure adequate technical standards and repeatability procedures. To develop comparable methodologies in European countries, the European Union has been defining test standards for laboratory soil characterization. This work presents the main changes resulting from applying this new standardization to the soil particle density determination. To evaluate the impact of the new standard methodologies on the laboratories' routine and the results obtained, about 230 laboratory tests were carried out, and two types of soil were used: a granitic residual soil and a kaolinitic clay soil. From these tests, it was possible to notice that some new standardization changes do not guarantee uniformity in the testing practices or determination precision.

Keywords

Soils • Standardizations • Laboratory testing • Particle size distribution

1 Introduction

In Portugal, the determination of soil particle density has been carried out for decades following standard NP-83:1965. In order to unify the test methodologies used in different countries of the European Union (EU), a new standardization is being implemented to determine the soil particle density, the EN ISO 17892-3:2015, with the proposed general title: “Geotechnical investigation and testing—Laboratory testing of soils—Part 3: Determination of the particle density”.

When comparing this new standardization with the one used for decades in Portugal, some changes were observed in the testing methodology (Santos 2019). The current standard (NP-83:1965) determines that the specimen shall have at least 25 g of dry mass and shall rest in the pycnometer covered with distilled water to about three-quarters of the capacity, at least for 12 h, before extracting the air in the vacuum pump, with the values of vacuum pressures, application time and boiling time defined; the need of a water bath in any stage is not mentioned. The new standard (EN ISO 17892-3:2015) determines the use of a test specimen with at least 10 g of dry mass. It defines that the pycnometer must be kept in the water bath for at least 1 h to control the pycnometer calibration temperature and test execution. However, it does not mention the procedure to be adopted for the 12 h rest phase, nor does it specify how to remove the air. Martins (2018) concluded that the particle density values obtained by the new standardization are slightly lower than those obtained by the current standard, and the difference in results may be related to the fact that the new standard does not specify how to remove the air trapped in the specimen. Therefore, several tests were carried out to analyze the influence of different methodologies for removing the trapped air. The correct perception of the factors that influence the soil particle density's laboratory determination is essential to guarantee the results' reliability.

C. Afonso · A. Teixeira · M. M. Carvalho (✉)
Department of Geotechnical Engineering, School of Engineering (ISEP), Polytechnic of Porto, Porto, Portugal
e-mail: mmc@isep.ipp.pt

E. Neves · A. Teixeira
Centro de Formação Profissional da Indústria da Construção Civil e Obras Públicas do Norte (CICCOPN), Maia, Portugal

2 Methods

Two soil types were tested, a granitic residual soil (Soil A) and a kaolinitic clay soil (Soil B), and about 230 determinations were made. The procedures adopted for carrying out the tests are those described in EN ISO 17892-3:2015. The soils were tested by the fluid pycnometer method. The particle density determination is done based on the soil particles' dry mass and the difference in the volume of liquid required to fill the pycnometer with and without the sample present. The tests were performed using oven-dried specimens (method A) and moist (method B).

The new standard does not define how the trapped air must be removed from the specimen; it only recommends agitation, slight heating, boiling or vacuum application. Therefore, the primary variable in the tests performed was removing the trapped air; thus, it will be possible to observe its influence on the results obtained. In the present work, for both soils, five methods were tested to remove the air trapped in the specimens: (i) vacuum at 40 hPa, for 10 min; (ii) vacuum at 133 hPa, for 10 min; (iii) slight heating (below 50 °C), for 10 min; (iv) boiling for 10 min and (v) manual agitation for 1 min.

The standard requires at least two determinations in each test and, if the values do not agree within 0.03 Mg/m³, the test shall be repeated. In the present work, to validate the results obtained for each soil, at least five repetitions were performed for each method of removing the trapped air, both for the oven-dried specimen and the moist one.

3 Results

As previously described, the determination of density was performed for Soil A and Soil B in oven-dried and moist specimens. Five different methods were tested to remove the air trapped in the specimen. The results obtained are presented below, with the following graphs (Figs. 1, 2, 3 and 4) showing the results obtained in the tests carried out on both soils. The values obtained on each repetition, the mean value and the standard deviation for each test series are presented.

4 Discussion

The results obtained for both soils can be analyzed from three different perspectives: (i) repeatability of the tests for each studied case; (ii) comparison between the values obtained for method A (oven-dried specimens) and method B (moist specimens) and (iii) comparison between the different methods to remove the air trapped in the specimens.

For soil A, it is possible to observe that, except for the removal of air by light heating in method B, there was a divergence of 0.05 Mg/m³. The values obtained in the repetitions do not differ from 0.03 Mg/m³. For soil B, it was found that the repetitions diverge more than 0.03 Mg/m³ in the tests in which the air was removed by vacuum at 133 hPa and by manual agitation, both in method A and method B. In these cases, the standard determines that the values can be ignored for calculation purposes. However, for

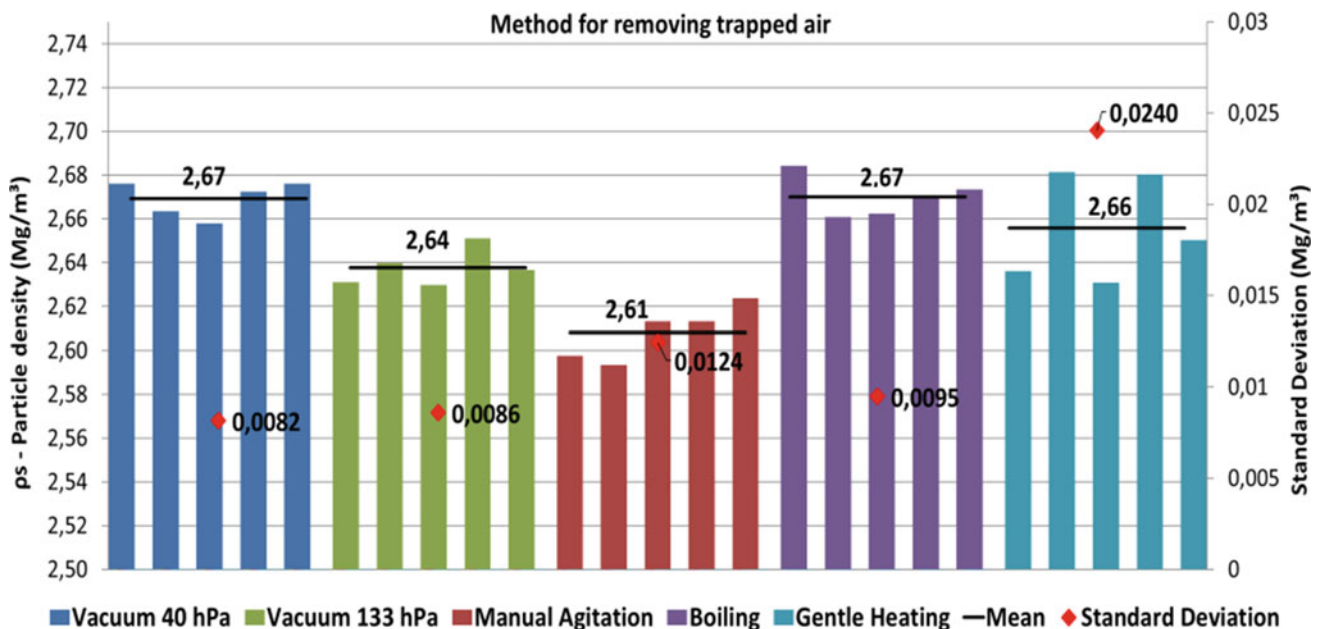


Fig. 1 Particle density—Soil A—Method A (oven-dried specimens): five different methodologies for removing the air trapped in the specimens

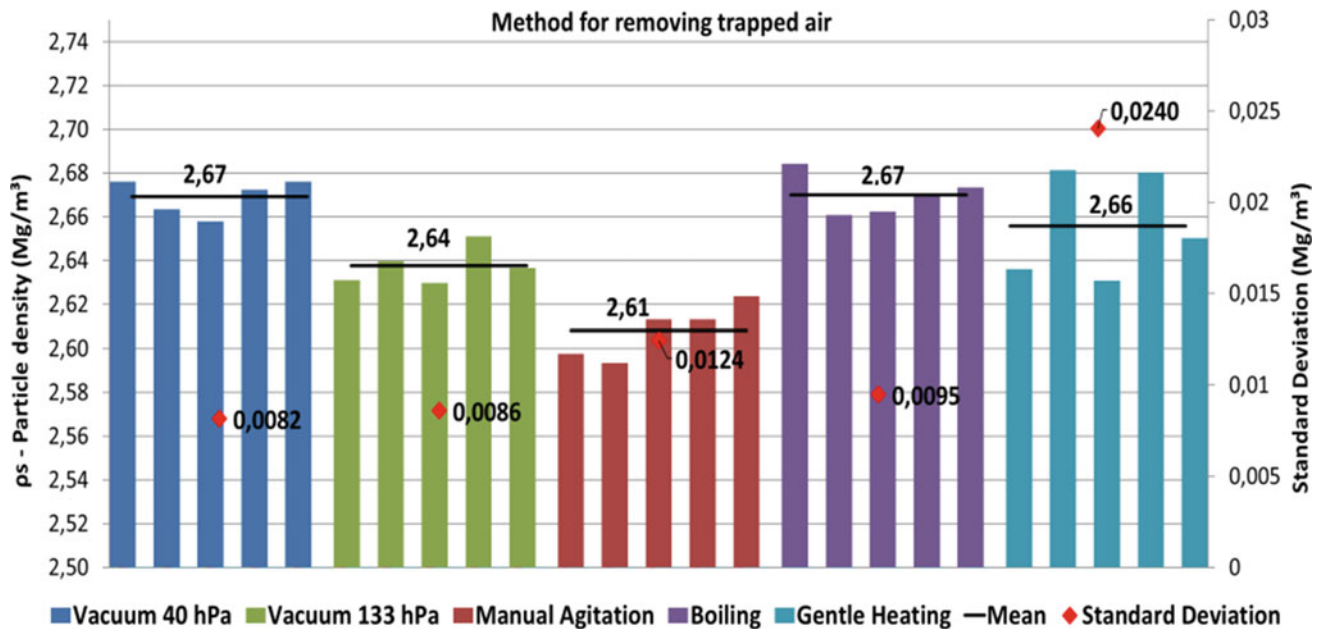


Fig. 2 Particle density—Soil A—Method B (moist specimens): five different methodologies for removing the air trapped in the specimens

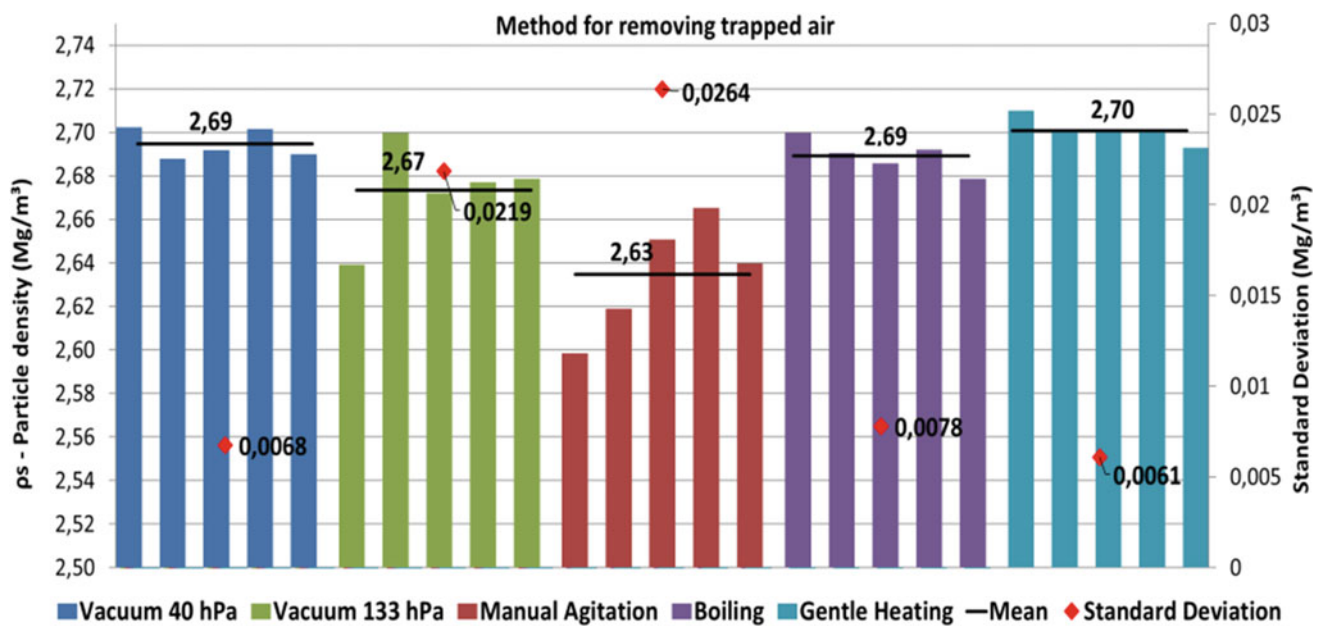


Fig. 3 Particle density—Soil B—Method A (oven-dried specimens): five different methodologies for removing the air trapped in the specimens

this work, all the determined values were considered to compare better the influence of the different methodologies applied since the divergence can be related not only to the test steps but also to the efficiency of the method for removing the air.

Regarding the soil water content, comparing the results obtained for method A and method B, very similar values were obtained for the two soils. Thus, the chosen method

(oven-dried specimens or moist specimens) did not influence the results obtained.

When comparing the results obtained with the different air removal methods, it is possible to see a significant difference between the values. Table 1 shows the different forms of air removal, both for method A and method B, the minimum and the maximum values obtained for particle density, the mean, the variance and the standard deviation.

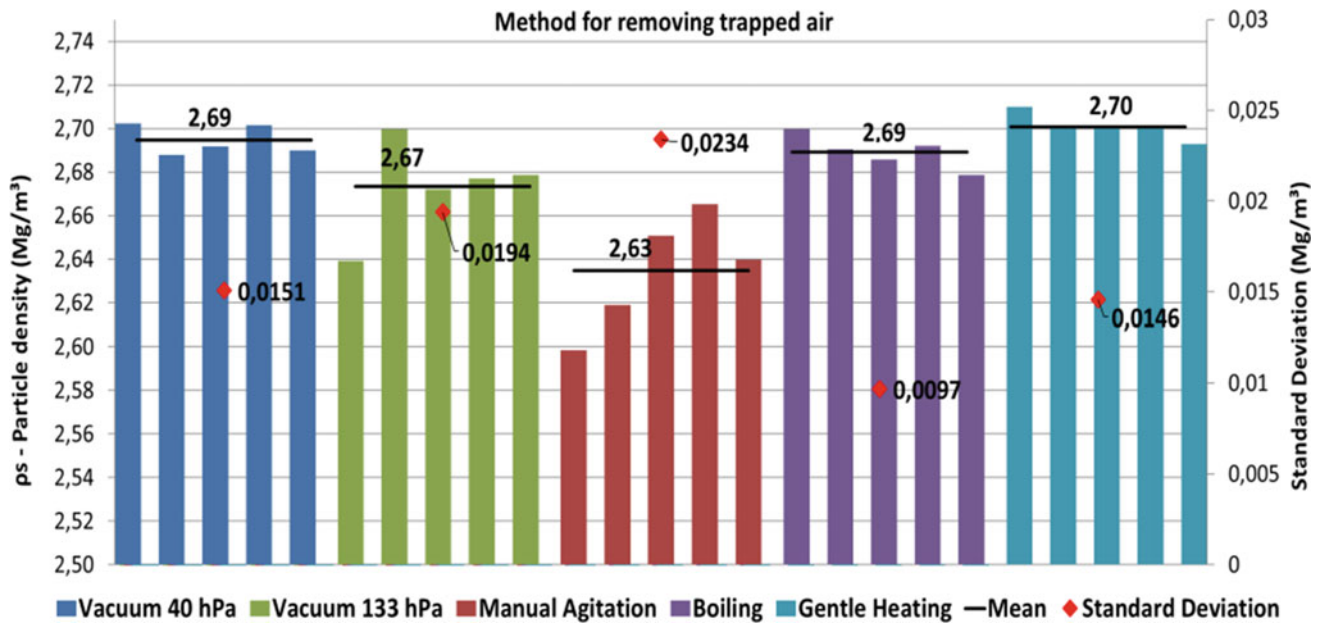


Fig. 4 Particle density—Soil B—Method B (moist specimens): five different methodologies for removing the air trapped in the specimens

Table 1 Comparison of the different methods for removing air

Method for removing trapped air	Soil A		Soil B	
	Method A	Method B	Method A	Method B
Vacuum—40 hPa (10 min)	2.66	2.67	2.69	2.68
Vacuum—133 hPa (10 min)	2.66	2.64	2.67	2.69
Manual agitation (1 min)	2.61	2.61	2.63	2.63
Boiling (10 min)	2.66	2.67	2.69	2.69
Gentle heating (10 min)	2.67	2.66	2.70	2.68
<i>Minimum</i>	2.61	2.61	2.63	2.63
<i>Maximum</i>	2.67	2.67	2.70	2.69
<i>Mean</i>	2.65	2.65	2.68	2.67
<i>Variance</i>	0.0006	0.0007	0.0007	0.0006
<i>Standard deviation</i>	0.0239	0.0259	0.0265	0.0245

In Soil A, for both methods, the different specimens' mean values varied between 2.61 Mg/m³ and 2.67 Mg/m³. For Soil B, in method A, the different specimens' mean values were between 2.63 Mg/m³ and 2.70 Mg/m³, while in method B, the different specimens' mean values of the particle density varied between 2.63 Mg/m³ and 2.69 Mg/m³.

In both soils and methods, the lowest value obtained occurred in the specimens with trapped air removed by manual agitation. The manual agitation was not sufficient for

the total removal of the air trapped in the specimen. Consequently, the value of the particle density is lower. It was possible to notice this effect during the tests since when the pycnometer was moving, air particles emerged from the specimen. The emergence of air particles from the specimen also occurred when the vacuum at 133 hPa and slight heating was applied. For the tests in which the air was removed by vacuum at 40 hPa or by boiling, it was found that the values obtained were more similar and consistent, showing that the removal of air was more efficient in these cases.

5 Concluding Remarks

The European standard, EN ISO 17892-3:2015, does not define the procedure for removing the air trapped in the specimen, leaving the operator with the method's choice to be applied. In this way, the results obtained vary according to the chosen technique and its application time.

In this study, for both soils (granitic residual soil and kaolinitic clay soil), the removal of air by vacuum at 133 hPa for 10 min, by slight heating for 10 min or by manual agitation for 1 min, was not efficient. When the trapped air was removed by vacuum at 40 hPa for 10 min or by boiling for 10 min, the results were more consistent, and air removal was more efficient.

The new standard allows different technical procedures for removing air trapped in the specimen because they are not entirely specified, thus allowing the results to depend on the operator's knowledge and experience. This situation can lead to significant differences; the necessary standardization

and reliability for this type of test are not guaranteed. The new standard must be revised before its global implementation to ensure the methodology's uniformity and the results obtained in the different labs and countries where it will be adopted.

References

- EN ISO 17892-3:2015 Geotechnical investigation and testing—Laboratory testing of soil—Part 3: determination of particle density. European Committee for Standardization, Brussels
- Martins C (2018) Caracterização laboratorial de solos: nova normalização. Instituto Superior de Engenharia do Porto, Master's dissertation, Porto
- NP 83:1965 Solos—Determinação da densidade das partículas. IPQ—Instituto Português da Qualidade, Caparica
- Santos C (2019) Análise comparativa de diferentes métodos laboratoriais na caracterização física de solos utilizados em obras de engenharia civil. Instituto Superior de Engenharia do Porto, Master's dissertation, Porto



Physical and Chemical Characterisation of Fillers for the Manufacture of Bituminous Mixtures

Bruno Santos, Adriano Teixeira, and José Augusto Fernandes

Abstract

This work aims to contribute to a better understanding of the influence of the physical and chemical properties of the filler used in the composition of bituminous mixtures, thus ensuring that their behaviour is the most appropriate. The filler plays a relevant role in the behaviour of mixtures, contributing to the filling of voids between the coarse aggregates and changing the properties of binders. As a basis for the study, and following the standard NP EN 13043:2004, several tests were performed, which allowed characterising of the geometric, physical and chemical requirements, and the regularity of filler production, in the following types of filler: (A) Filler RC 480, (B) Filler RC 590, (C) Filler recovered limestone powder, (D) Filler recovered granite powder, (E) Filler limestone C100, (F) Filler recovered, (G) Hydrated lime and (H) Hydraulic lime. Finally, the results obtained in the characterisation tests of the fillers are presented and discussed, concluding the relative merits of each of the samples analysed. A methodology of analysis is also proposed. For the studied fillers, the determination of the void content of the dry compacted filler revealed to be the test that best characterises them, also showing strong correlation with the number of bitumens and variation of the ring and ball softening temperature, allowing to characterise the filler regarding its stiffening power.

B. Santos · J. A. Fernandes (✉)
Laboratory of Geotechnical and Construction Materials, School of Engineering (ISEP), Polytechnic of Porto, Porto, Portugal
e-mail: jap@isep.ipp.pt

A. Teixeira
CICCO PN—Centro de Formação Profissional da Indústria da Construção Civil e Obras Públicas do Norte, Maia, Portugal

A. Teixeira · J. A. Fernandes
Department of Geotechnical Engineering, School of Engineering (ISEP), Polytechnic of Porto, Porto, Portugal

GeoBioTec|UA, Aveiro, Portugal

Keywords

Filler · Bituminous mixtures · Physical–chemical characterisation · Road pavements

1 Introduction

As a consequence of economic and social development, mobility needs to evolve and grow exponentially in recent years. Even their patterns have undergone significant changes in the last decades, with greater relevance to the particular case of urban areas. The result of an increase in the residential urban exodus and the decentralisation of some business activities and services provided, mobility appears to be a primordial requirement in what is called quality of life.

Metropolitan regions today are a very diversified and complex reality, marked essentially by the massive use of individual transport, resulting from the inefficiency of the public transport network, which may have adverse effects on future generations in terms of noise exposure, as well as the deterioration of energy sustainability and atmospheric pollution conditions. Furthermore, transport represents a sector that presents the emissions of pollutant gases such as carbon dioxide and the consumption of fossil fuels, which in turn contributes to global warming (DGT 2015).

The replacement of fossil fuels with alternative energy sources will offer a safer, reliable and affordable alternative to our energy needs. It could even provide everything that fossil fuel currently offers, but without pollution. Several Portuguese cities are already pioneering projects, including ecological buses powered by hydrogen and electric energy (Ponce de Leão et al. 2020).

The national road network comprises main routes, complementary routes, national and regional roads and motorways, with the pavement as its most relevant infrastructure, subject to the most severe actions, particularly from traffic and climate. For this reason, much of the investment made in

construction is directed towards this component of the road network, conservation and rehabilitation, as well as in fundamental and applied research to reduce these investments and optimise the design (IF 2021).

In Portugal, in the last two decades, there was a high investment in the extension of the national road network, which has been stagnating as a result of the current financial crisis that the country is undergoing, causing a sharp decrease in construction and a consequent increase in maintenance and rehabilitation works (Pereira et al. 2007).

Road pavements are designed to respond to the demands of traffic and weather for a given period (20–40 years) from a perspective of technical–economic–environmental sustainability and defined certain quality standards, structural and functional. Their conservation aims at promoting an improvement of their characteristics (essentially structural), faced with new demands for a new period of life, namely with higher traffic than that considered for the previous period. As a result, there is often a need for interventions, not foreseen, before the end of the life period for which they were designed and built, with high costs for both the respective road administration and, particularly for users, or even the environment (Morais 2001).

In this context, the road should be an infrastructure that allows safe circulation, comfort and the reduction of environmental impacts, contributing directly to the increase in quality of life.

2 Materials and Methods

2.1 Physical and Chemical Characterisation of Fillers

Road pavements are subject to different actions, which may lead to various types of degradation. The solution to these problems is to increase the knowledge of the effects of fillers, with the development of better criteria for the conception of mixtures and the control of the main factors during the execution of the pavements.

Bituminous mixtures applied in road pavements are composed of a mineral fraction formed by particles of variable sizes, between 5 and 30 mm. According to the specifications of EP (2014), the term filler is given to any aggregate whose majority passes the 0.063 mm sieve, and that can be added to construction materials to give them specific properties. The use of fillers in bituminous mixtures requires the fulfilment of several requirements in order to comply with the general requirements of standard NP EN 13043:2004 and the EP (2014) specifications. The filler is used as a material to fill the voids between coarse and fine aggregates, contributing to the completion of the mixture, modifying characteristics such as workability, resistance to

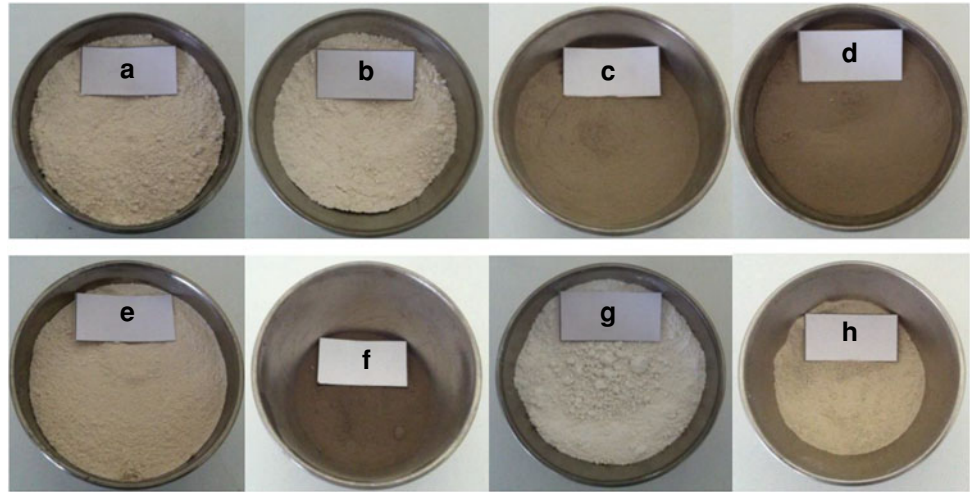
water and resistance to deterioration due to the reduced size of its particles and its surface characteristics. The process of manufacturing filler may result from the recovery of fines using suitable filter systems (dust extractors and recovered filler) in bituminous mix plants, or it can be produced separately in a crushing plant with a controlled production process (commercial fillers). The nature of commercial fillers should be calcareous, Portland cement, hydraulic lime or fly ash and the recovered filler may have any petrographic origin, as it will depend on the nature of the aggregate used to manufacture the bituminous mix.

According to Hesp et al. (2001), different types of fillers in apparently equal bituminous mixtures often lead to very different behaviour of these bituminous mixtures in the pavement. That is because each filler's physical and chemical properties directly affect the mechanical properties of the mixture. The change that each filler causes occurs through variations in the chemical and physical properties of the binder, which depends on the following factors: type of filler (size, grain shape, etc.), nature of the filler (a physical and chemical activity that affects the affinity with bitumen) and concentration of the filler in the mixture. Due to the importance of the properties above in the different types of fillers to be used in bituminous mixtures, Craus et al. (1978) studied the physico-chemical characteristics of different types of fillers and evaluated their influence on the behaviour of the bituminous mixtures, and concluded that the geometric irregularity of the filler (shape and surface texture) plays a relevant role in the bituminous mixtures, affecting the optimum bitumen percentage (average of the sum of the percentages of bitumen corresponding to the maximum breaking force, the maximum specific weight and the average porosity), the filler-bitumen bonds and the rheological behaviour of bituminous mastics.

Craus et al. (1978) consider that, among the various physico-chemical aspects of the asphalt-filler-binder interaction, the essential factor in characterising the filler is the adsorption intensity (adhesion of molecules of a fluid to a solid surface). Increased adsorption leads to the greater irregularity of the filler, forcing an increase in the percentage of bitumen in the bituminous mix without any benefit in terms of mechanical behaviour. Therefore, when there is a significant increase in bitumen, this type of filler become economically unviable and should not be used.

The study aimed to test a wide variety of fillers with different petrographic characteristics and manufacturing processes to achieve a broader range of analyses. The samples tested are granite (Samples: D and F) and limestone (Samples: A, B, C and E). Apart from the materials from crushing and recovery in the bituminous plants, hydrated lime (Sample: G) and hydraulic lime (Sample: H) were also tested (Fig. 1).

Thus, the tests performed that led to the study of physical, chemical and geometric characteristics of each of the fillers

Fig. 1 Filler samples

were (1) grain size of the filler (air-jet sieving—Retsch AS 200 jet) (EN 933-10:2009), (2) fines quality—Methylene Blue—NP EN 933-9:2011 (Annex A), (3) volume weight of filler (NP EN 1097-7:2012), (4) voids index of dry compacted filler (NP EN 1097-4:2012, NP EN 1097-7:2012), (5) specific weight of filler in paraffin (NP EN 1097-3:2002), (6) softening range ring and ball (NP EN 13179-1:2010), (7) apparent viscosity (Bitumen Number—NP EN 13179-2:2010), (8) chemical analysis by X-ray fluorescence spectrometry (Niton XL3t), 9) water solubility (EN 1744-1:2009) and (10) water susceptibility (EN 1744-4:2005).

3 Results and Discussion

From the analysis of the results obtained, it was possible to realise the most significant characteristics and possible correlations between them.

3.1 Filler Size Distribution (Sieving by Air-Jet)

The experimental determination of the particle size composition of the different fillers was carried out through the air-jet sieving method, and the results are presented in Table 1, in which the percentages of passes through sieves of 2 mm, 0.125 mm and 0.063 mm are indicated.

On the influence of particle size, of the eight analysed fillers, hydrated lime (Sample G) followed by granite powder recovered filler (Sample F) and lime filler RC 590 (Sample B) were those that showed the highest percentage (greater than or equal to 90%) of particles smaller than 0.063 mm, being these the particles that contribute to obtaining the particle size requirements of bituminous mixtures in their finest zone and that contribute to the stiffening

Table 1 Results of the grain size analysis

Sample	% Passed 2 mm	% Passed 0.125 mm	% Passed 0.063 mm
A	100	97	78
B	100	100	90
C	100	86	67
D	100	83	69
E	100	98	79
F	100	98	93
G	100	100	99
H	100	95	80

of bitumen in this type of mixtures. On the other hand, the one that showed the highest percentage of particles larger than 0.063 mm was the limestone powder recovered filler (Sample C) and the granite powder recovered filler (Sample D). Thus, although there is no uniformity of the values of material that passed through the 0.063 mm sieve among the studied samples, the existing difference is not significant (standard deviation of 11%).

According to the particle size requirements for commercial fillers (Samples A, B, E, G and H) and according to standard NP EN 13043:2004, the values obtained are within limits imposed and within the values specified in the product datasheets.

3.2 Fines Quality (Methylene Blue Test)

The methylene blue adsorption test is an efficient, simple, fast and economical alternative to evaluate the cleanliness of an aggregate, allowing to estimate the amount and type of clays present in its fine fraction. The results can be seen in Table 2.

Table 2 Methylene blue content

Sample	MBF (ml/g)	Sample	MBF (ml/g)
A	1.67	E	1.67
B	1.67	F	7.33
C	1.67	G	3.27
D	3.33	H	1.66

Table 3 Summary of the categories and conformity of requirements for the values obtained

Sample	A	B	C	D	E	F	G	H
MBF	1.7	1.7	1.7	3.3	1.7	7.3	3.3	1.7
MBF category (NP EN 13043:2004)	MBF10	MBF10	MBF10	MBF10	MBF10	MBF10	MBF10	MBF10
Requirements Standards*	✓	✓	✓	✓	✓	✓	✓	✓

*According to EP (2014)—Table 14.03.0-3b

After the test, it was possible to verify that the test presents reduced sensitivity when applied to materials with low clay content in fillers. Profiling is not very relevant because the levels obtained are always very low.

Table 3 shows the categories (standard NP EN 13043:2004) corresponding to the values of the methylene blue test for each sample of filler and presents the requirements defined in the specifications of EP (2014) for fillers to be included in bituminous mixtures.

3.3 Filler Density

The determination of the density of the fillers was done through the pycnometer method. It was found that the density values of limestone-based fillers, RC 480 limestone filler (Sample A), RC 590 limestone filler (Sample B), recovered limestone dust filler (Sample C), C100 limestone filler (Sample E), hydraulic lime (Sample H), varied between 2.70 Mg/m^3 and 2.74 Mg/m^3 , as well as granite-based fillers, granite powder recovered filler (Sample D) and granite powder recovered filler (Sample F), vary between 2.62 Mg/m^3 and 2.64 Mg/m^3 , which does not present a highlighted difference in both cases. The same does not happen for hydrated lime (sample G), which has a density

value (2.24 Mg/m^3) significantly lower; this fact can be explained by the high porosity of the particles, a consequence of a high percentage of voids of this material, as will be seen in the next Sect. 3.4.

3.4 Voids Index of the Dry Compacted Filler

The percentage of filler voids obtained is shown in Table 4. The difference between hydrated lime and the other fillers may be related to its structural configuration of hydrated lime, high porosity and lower density, originating a smaller particle arrangement during compaction and consequent increase in volume. The voids in dry compacted fillers are classified according to the Portuguese standard NP EN 13043:2004, which establishes categories to a table of void ranges. However, the product standard is not prepared to classify fillers with high percentages of voids in volume, as in hydrated lime (Sample G).

Table 5 presents the categories (standard NP EN 13043:2004) of corresponding values of the percentage of filler void and verification of compliance with the requirements defined in the specifications of Estradas de Portugal (2014) for fillers to be included in bituminous mixtures.

Table 4 Percentage of filler voids

Sample	Filler voids (%)	Sample	Filler voids (%)
A	29.40	E	28.07
B	31.19	F	46.73
C	35.45	G	59.12
D	31.94	H	45.68

Table 5 Summary of the categories and conformity of requirements for the values obtained

Sample	A	B	C	D	E	F	G	H
Filler voids (%)	29.40	31.19	35.45	31.94	28.07	46.73	59.12	45.68
Category v (NP EN 13043:2014)	v28/38	v28/38	v28/38	v28/38	v28/38	v44/55	v44/55	v44/55
Requirement standards*	✓	✓	✓	✓	✓	✓	✓	✓

*According to EP (2014)—Table 14.03.0-3b

3.5 Specific Weight of Filler in Paraffin

The paraffin-specific weight was performed on all the filler samples. The results obtained show that the recovered limestone powder (Sample C—0.77 Mg/m³), granite powder (Sample D—0.67 Mg/m³) and granite powder (Sample F—0.67 Mg/m³) had the highest values, followed by commercial fillers, as limestone filler C100 (Sample E—0.50 Mg/m³), hydraulic lime (Sample H—0.50 Mg/m³) and hydrated lime (Sample G—0.15 Mg/m³) with the lowest values.

3.6 Softening Temperature Point Ring and Ball

Obtained values show it is possible to notice that the stiffening effect values are similar in the samples: RC 480 lime filler (Sample A—11.40 °C), RC 590 lime filler (Sample B—12.40 °C), limestone filler C100 (Sample E—12.80 °C), limestone powder recovered filler (Sample C—14.80 °C), increasing slightly in the recovered granitic dust filler (Sample D—21.20 °C), hydraulic lime (Sample H—21.90 °C) and the filler recovered from granitic powder (Sample F— ≥ 33.00 °C).

3.7 Apparent Viscosity

The results obtained for the apparent viscosity of a bituminous mixture (Bitumen Number—% by mass), for the different fillers, made it possible to realise that the results with the lowest values are related to commercial lime fillers: RC 480 limestone filler (Sample A—26), C100 limestone filler (Sample E—26) and RC 590 limestone filler (Sample B—28), followed by recovered limestone dust filler (Sample C—36), recovered granite dust filler (Sample D—40), hydraulic lime (Sample H—46), granite powder recovered filler (Sample F—52), ending with hydrated lime (Sample G—108), as the highest values with some disparity from the others.

3.8 Chemical Analysis by X-ray Fluorescence Spectrometry

From the observation of the results obtained and of the elements with more significant representation, it was

possible to verify that the samples of RC 480 limestone filler (Sample A), RC 590 limestone (Sample B), recovered limestone powder (Sample C), limestone filler C 100 (Sample E), hydrated lime (Sample G), and hydraulic lime (Sample H) have CaO (calcium oxide) values that vary between 52% and 73%, while the fillers recovered from granite dust (Sample D and F) register a lower variation, between 1% and 2%.

In hydrated lime, which consists mainly of calcium oxides and hydroxides (CaO and Ca(OH)₂), the value obtained seems lower than expected. In the other element of greater relevance, the silica dioxide (SiO₂) presented higher registers, between 56 and 57% in the fillers recovered from granitic dust (Sample D and F), and lower between 0.3% and 8% in RC 480 limestone filler (Sample A), RC 590 limestone filler (Sample B), recovered limestone dust filler (Sample C), C100 limestone filler (Sample E), hydrated lime (Sample G) and hydraulic lime (Sample H).

3.9 Water Solubility

Table 6 shows the categories (standard NP EN 13043:2004) corresponding to the values obtained for bitumen number and the verification of the requirements defined in the specifications of Estradas de Portugal (2014) for fillers to be included in bituminous mixtures. The value observed in filler G's case may be because this filler contains particles of a smaller diameter than the pore diameter of the filter used in the filtration.

3.10 Water Susceptibility

When determining the water susceptibility of the fillers, that is, evaluating the higher or lower resistance to separation of filler from bitumen in the presence of water, it was possible to confirm that all the samples submitted to testing demonstrated non-susceptibility to water, with no need for the execution of any calculation or advance for obtaining values according to the standard.

Finally, and based on the characterisation results of the fillers obtained, the possible existence of a correlation between the values of the various tests was evaluated, and

Table 6 Summary of the categories corresponding to the test values obtained

Sample	A	B	C	D	E	F	G	H
Solubility in water (% by mass)	2.1	2.7	0.1	1.2	1.2	1.5	5.1	2.5
Category WS (NP EN 13043:2004)	WS10	WS10	WS10	WS10	WS10	WS10	WS10	WS10

the variations of the three characteristics that presented the best correlation are shown in Fig. 2. Thus, it seems possible to determine only one characteristic to approximate the other two without performing the tests. Obviously, for a more definitive conclusion on this matter, it would be necessary to carry out a more comprehensive campaign of tests for other samples of fillers.

4 Concluding Remarks

This study performed the physical–chemical characterisation of several fillers commonly used in the manufacture of bituminous mixtures. In the experimental work, several tests were performed, according to standard NP EN 13043:2004

(Aggregates for Bituminous Mixtures), on fillers with different characteristics (commercial limestone filler, recovered granite filler, recovered limestone filler, hydrated lime and hydraulic lime), using the fraction passed through the 0.125 mm sieve.

From the results achieved in this study, starting with the grain size distribution of one of the most appropriate properties of its characterisation, it was found that the commercial one was within limits imposed by the standard and according to the specifications indicated in the technical sheets of the different products.

In the evaluation of the fillers' performance regarding the fines quality, through the methylene blue test, it was verified that all fillers complied with the requirements of the *Estradas de Portugal* (EP) and that the highest values were related

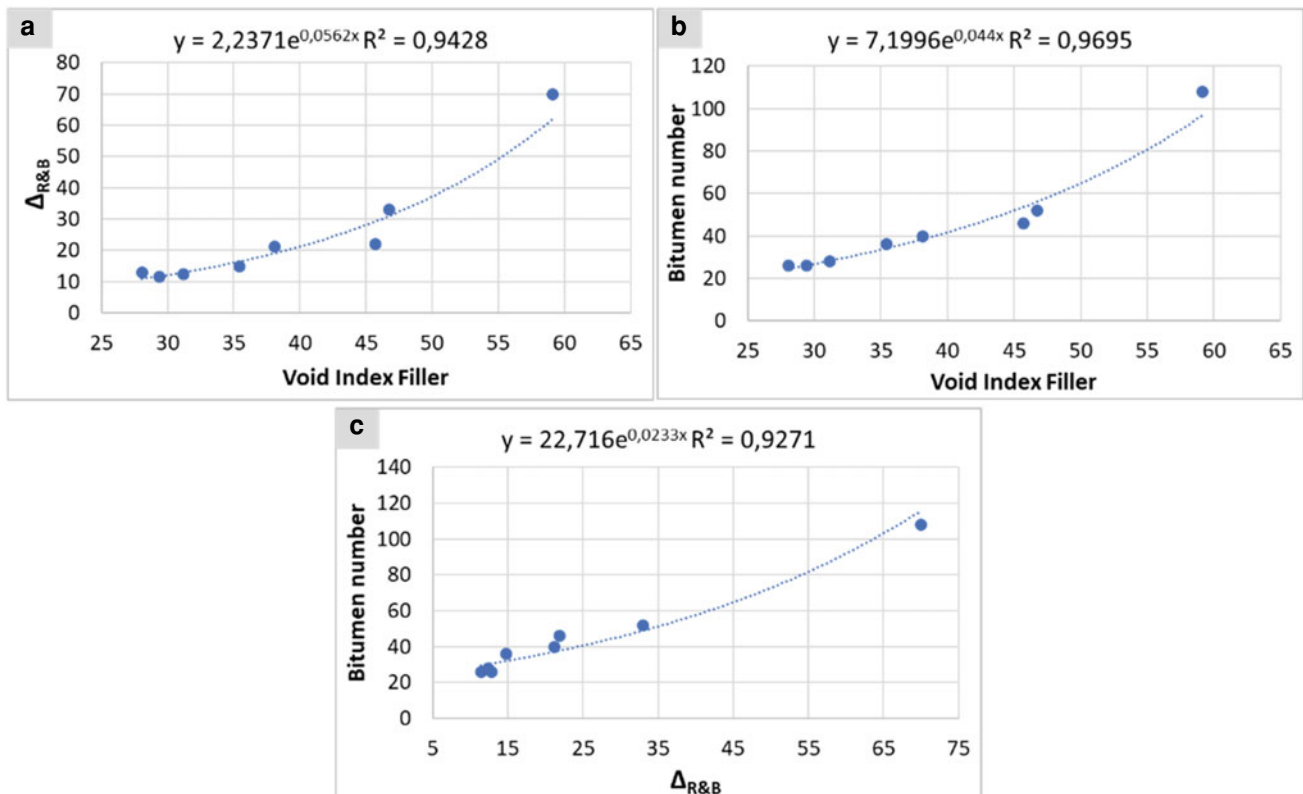


Fig. 2 Correlations between **a** filler void ratio/ring and ball temperature variation ($\Delta_{R\&B}$), **b** filler void ratio/bitumen number and **C** bitumen number/ring and ball temperature variation

to fillers recovered from granitic materials, which may indicate that the values may be associated with the geological characteristics, namely the presence of micas.

Determining the void content of dry compacted fillers proved to be one of the tests that best characterises the fillers, associating the best quality materials, commercial fillers, to lower values of the void content. An excellent correlation between the bitumen number and the softening temperature ring and ball variation was found. There is a strong correlation between the results of the Rigden voids test, the softening temperature variation of the ring and ball and the viscosity of the filler (bitumen number). It would be necessary to perform more tests with fillers with other values, but everything indicates that it is possible to find correlation laws between the three parameters, characterising the filler as stiffening power only with the behaviour before a test. In this case, it seems the Rigden test is the most advisable because it presents better repeatability and reproducibility, it is not necessary to work with bitumen, and therefore, there are no safety problems, and the equipment required is low.

It was found that the fillers present very different behaviours so their performance in the different bituminous mixtures must be studied appropriately so that each one of them can be used judiciously, depending on the purpose in view and not forgetting that these materials are used in bituminous mixtures for the following purposes: (i) to contribute with their granulometry and to the granulometry of the aggregate mixture; (ii) to form with bitumen a mastic that is stiffer than bitumen, a mastic that will bind the aggregates.

However, given the characteristics of each of these materials, they can be used to achieve other goals, such as increasing the stiffness of bituminous mixtures, especially at high temperatures, increasing the adhesion of the binder to the aggregate and allowing an increase in the bitumen dosage, improving the fatigue behaviour of the bituminous mixture and increasing its durability without compromising the behaviour of permanent deformation.

According to the specifications of EP (2014), all fillers meet the requirements of grain size and methylene blue. However, some of the fillers cannot be used in bituminous mixtures: recovered granite powder filler (Sample F), hydrated lime (Sample G) and hydraulic lime (Sample H), because they do not meet the requirement concerning the voids of the compacted dry filler. The impossibility of performing the temperature variation of the ring and ball test of hydrated lime (Sample G) was a consequence of the high

porosity of the particles and the high volume of voids between the particles.

Acknowledgements The authors gratefully acknowledge the support provided by the technical teams of the following laboratories: CIC-COPN, Laboratory of Geotechnics and Construction Materials (LGMC) of the Geotechnical Engineering Department (ISEP) and Laboratory of the Chemical Engineering Department (ISEP) and of the companies Amândio Carvalho, MonteAdriano, Lusical and Secil for providing filler samples; without their cooperation it would not have been possible to carry out this study.

References

- Craus J, Ishai I, Sides A (1978) Some physico-chemical aspects of the effect and the role of the filler type and properties. *J Assoc Asph Pav Technol* 47:558–588
- DGT (2015) *Cidades sustentáveis 2020*. Ministério do Ambiente, Ordenamento do Território e Energia, Direção-Geral do Território, Lisboa
- EN 1744-1:2009+A1:2012 (Ed. 1) Tests for chemical properties of aggregates. Part 1: Chemical analysis, European Standard—English Version
- EN 1744-4:2005 Tests for chemical properties of aggregates. Determination of water susceptibility of fillers for bituminous mixtures, European Standard—English Version
- EN 933-10:2009 (Ed. 2) Tests for geometrical properties of aggregates. Part 10: Assessment of fines—Grading of filler aggregates (air-jet sieving), European Standard—English Version
- EP (2014) *Caderno de encargos tipo obra 14.03 - Pavimentação - Características dos materiais*. Estradas de Portugal S.A. Lisboa 3: 1–125
- Hesp S, Smith B, Hoare T (2001) Effect of the filler particle size on the low. *J Assoc Asph Pav Technol* 70:492–508
- IF (2021) *Plano rodoviário nacional*. Infraestruturas de Portugal, SA. <https://www.infraestruturasdeportugal.pt/pt-pt/rede/rodoviaria/prn>. Accessed June 2021
- Morais H (2001) *Estudo da fundação dum pavimento rodoviário flexível*. Instituto Politécnico de Bragança, MSc Dissertation, Bragança. <http://hdl.handle.net/10198/6827>
- NP EN 1097-3:2002 Ensaio das propriedades mecânicas e físicas dos agregados. Parte 3: Determinação da Baridade e do Volume de vazios, European Standard—Portuguese Version
- NP EN 1097-4:2012 (Ed. 2) Ensaio das propriedades mecânicas e físicas dos agregados. Parte 4: Determinação dos vazios do filler seco compactado, European Standard—Portuguese Version
- NP EN 1097-7:2012 (Ed. 2) Ensaio das propriedades mecânicas e físicas dos agregados. Parte 7: Determinação da massa volúmica do filler. Método do picnómetro, European Standard—Portuguese Version
- NP EN 13043:2004 Aggregates for bituminous mixtures and surface treatments for roads, airfields and other trafficked areas, European Standard—Portuguese Version

- NP EN 13179-1:2010 (Ed. 1) Ensaios de fileres utilizados em misturas betuminosas. Parte 1: Variação da temperatura de amolecimento de anel e bola, European Standard—Portuguese Version
- NP EN 13179-2:2010 (Ed. 1) Ensaios de fileres utilizados em misturas betuminosas. Parte 2: Viscosidade aparente (Número de betume), European Standard—Portuguese Version
- NP EN 933-9:2011 (Ed. 3) Ensaios das propriedades geométricas dos agregados. Parte 9: Avaliação dos finos. Ensaio do azul de metileno, European Standard—Portuguese Version
- Pereira P, Pais JC, Freitas EF, Silva HMD, Oliveira JRM (2007) A reabilitação da rede rodoviária no século XXI. Engenharia Civil, Revista da Universidade do Minho 28:19–36
- Ponce de Leão T, Gonçalves H, Catarino J, Picado A (2020) Fórum energias renováveis em Portugal 2020. LNEG, Lisbon



Case Study of an Inert Steel Aggregate in Road Construction: Characterization and Monitoring of the Structural Behaviour

Eduardo Fortunato, António José Roque, and António Gomes Correia

Abstract

The use of alternative materials, in particular industrial by-products and waste materials, in the construction of transport infrastructures and geotechnical works, has been promoted across the world. Nonetheless, considering that, in most situations, the application of some of these materials is fairly recent, little information is available on the long-term performance of the infrastructures in which they were used. This work mentions some characteristics of the Inert Steel Aggregate for Construction (ISAC). It presents some results related to the evolution in the surface characteristics and the structural behaviour of a field trial built on a road section in Portugal. ISAC was used in the embankments and pavement layers. The visual inspection, the results of the mechanical tests performed, and the values of the settlements measured on the surface markings about ten years after the section is open to traffic led to conclude that the pavement in the zone where ISAC was used as a construction material is, in general, in a better condition and presents better structural performance than the adjacent areas built with natural materials. The embankment's maximum settlements in the areas with ISAC were similar to the ones observed in the adjacent areas.

Keywords

Inert Steel Aggregate for Construction (ISAC) • Mechanical properties • Structural behaviour • Long-term performance

1 Introduction

Steel slag, a by-product resulting from steel manufacturing, has been the object of studies developed worldwide aiming to promote its use, particularly as artificial aggregate, in geotechnical works and transport infrastructures. It has been demonstrated that, after due treatment (Roque et al. 2007), this by-product may be an excellent alternative to natural aggregates as construction material (Sofilić et al. 2012). Apart from its adequate technical performance and from its use being associated with some economic advantages for the projects in which it is employed, its application in this type of work, in particular when significant volumes are used, may offer an advantage in sustainability terms because this will represent an opportunity to reuse the 400 million tons of slag produced every year across the world (Worldsteel 2016).

In Portugal, two steel plants are equipped with electric arc furnaces, one in Maia and another in Seixal, which generate steel slag, among other by-products. Within the framework of a research project developed between 2005 and 2009, the material obtained from the processing of such slag—Inert Steel Aggregate for Construction (ISAC)—was studied to assess the feasibility of application to the construction of road infrastructures, namely embankment layers, capping layers, as well as base and sub-base layers.

An overall analysis of results from the laboratory tests performed within such a project's framework made it possible to conclude that, compared to natural materials, which are typically used in embankment layers, capping layers, and base and sub-base layers, ISAC demonstrated to have better mechanical properties. As referred to the chemical

E. Fortunato (✉)
Transportation Department, Laboratório Nacional de Engenharia Civil (LNEC), Lisboa, Portugal
e-mail: efortunato@lneec.pt

A. J. Roque
Geotechnical Department, Laboratório Nacional de Engenharia Civil (LNEC), Lisboa, Portugal

A. G. Correia
Escola de Engenharia, ISISE, Universidade do Minho, Guimarães, Portugal

characterization of the eluate analysis (after leachate of 20 slag samples), for several parameters considered as relevant for evaluating the environmental impacts of slags (if placed in landfills), it was concluded that all results demonstrated the inert character of the material, in light of the legislation in force. Apart from the extensive laboratory characterization, a full-scale field trial was also designed, built, instrumented, and monitored (Gomes Correia et al. 2012).

This work refers, in general terms, to the characteristics of the studied material and presents some results related to the structural behaviour exhibited by the field trial ten years after being open to traffic.

2 Characteristics of the Full-Scale Field Trial Under Analysis

Between October and November 2007, an embankment full-scale field trial was constructed in Portugal, with a 60 m length and a maximum height of 3.5 m. The purposes were to validate the properties of the materials studied in the laboratory and assess their performance in the base layer, capping layer, and embankment layer. The field trial was constructed at km 13 + 600 of the route linking Fafe to Cabeceiras de Basto (EN 311). This route has two lanes (a platform with 11.5 m width, comprising a 7.0 m carriageway and two shoulders) and an Annual Average Daily Traffic (AADT) of heavy vehicles in the range from 300 to 500 (Gomes Correia et al. 2012).

The field trial included three separate sections, as shown in Fig. 1: (i) a section corresponding to the traditional road construction materials, consisting of residual granite soil (GRS), in the body of the embankment and capping layer and crushed granite aggregate (GA) in the base layer; (ii) a section with residual granite soil in the embankment body and capping layer and ISAC in the base layer; and (iii) the last section with embankment, granular capping layer, and base layer built with ISAC. The particle size distribution of the materials is presented in Fig. 2. The construction of residual granite soil, ISAC, and crushed granite aggregate

layers led to compaction values higher than 95% of the modified Proctor test's reference value.

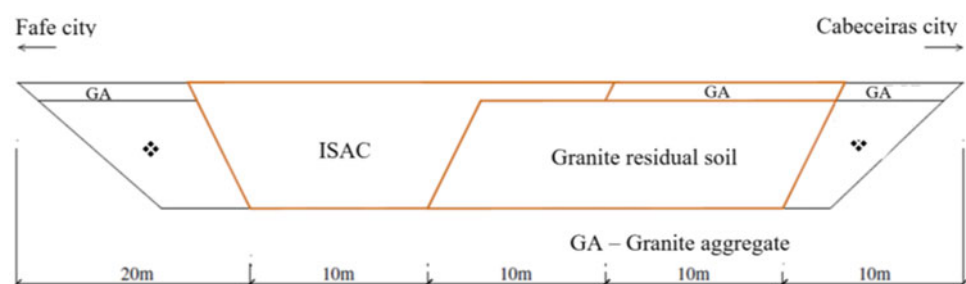
The results obtained during the quality control of the construction and for approximately two and a half years after completion of the field trial, in particular, as referred to the mechanical behaviour of the pavement layers and foundation, have demonstrated that the layers with ISAC material had a better performance than the layers with natural materials (soil and crushed granite aggregate). Such behaviour was particularly evident when the pavement was tested with the Falling Weight Deflectometer (FWD). Indeed, the deflections recorded at the surface of the area built on the ISAC were about five times less than the ones recorded on the areas built on natural materials.

The results of the environmental monitoring regarding the chemical composition of leachate samples collected from the two lysimeters installed on the field (one in the section built with ISAC and the other in the section built with the traditional material—granite residual soil) have shown that ISAC, from a leachate viewpoint, can be considered as an inert material. That means that the construction of transport infrastructures with ISAC is neither expected to contribute to the degradation of the environmental quality, namely of soils and surface and ground waters, nor expected to pose a risk to public health (Gomes Correia et al. 2012).

3 Evaluation of the Long-Term Behaviour of the Field Trial

About ten years after the construction of the field trial, a visual inspection and a testing campaign were carried out on the pavement to analyse its mechanical performance, particularly the deflections observed on the pavement surface as a result of imposed loads. In this case, bearing tests with FWD were performed on various pavement areas on both lanes (Fig. 3). In each test, three load levels were successively employed (30 kN and 47 kN) on a 0.45 m diameter plate. Figure 4 presents the maximum deflections measured under the load plate for the two loads.

Fig. 1 Longitudinal profile of the full-scale field trial (Gomes Correia et al. 2012)



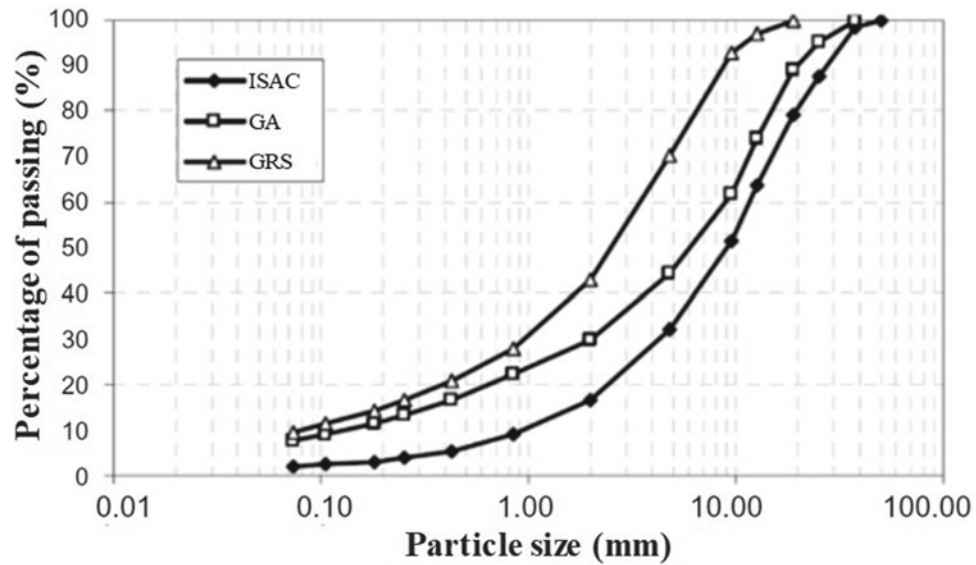


Fig. 2 Particle size distribution of the materials used in the full-scale field trial (Gomes Correia et al. 2012)



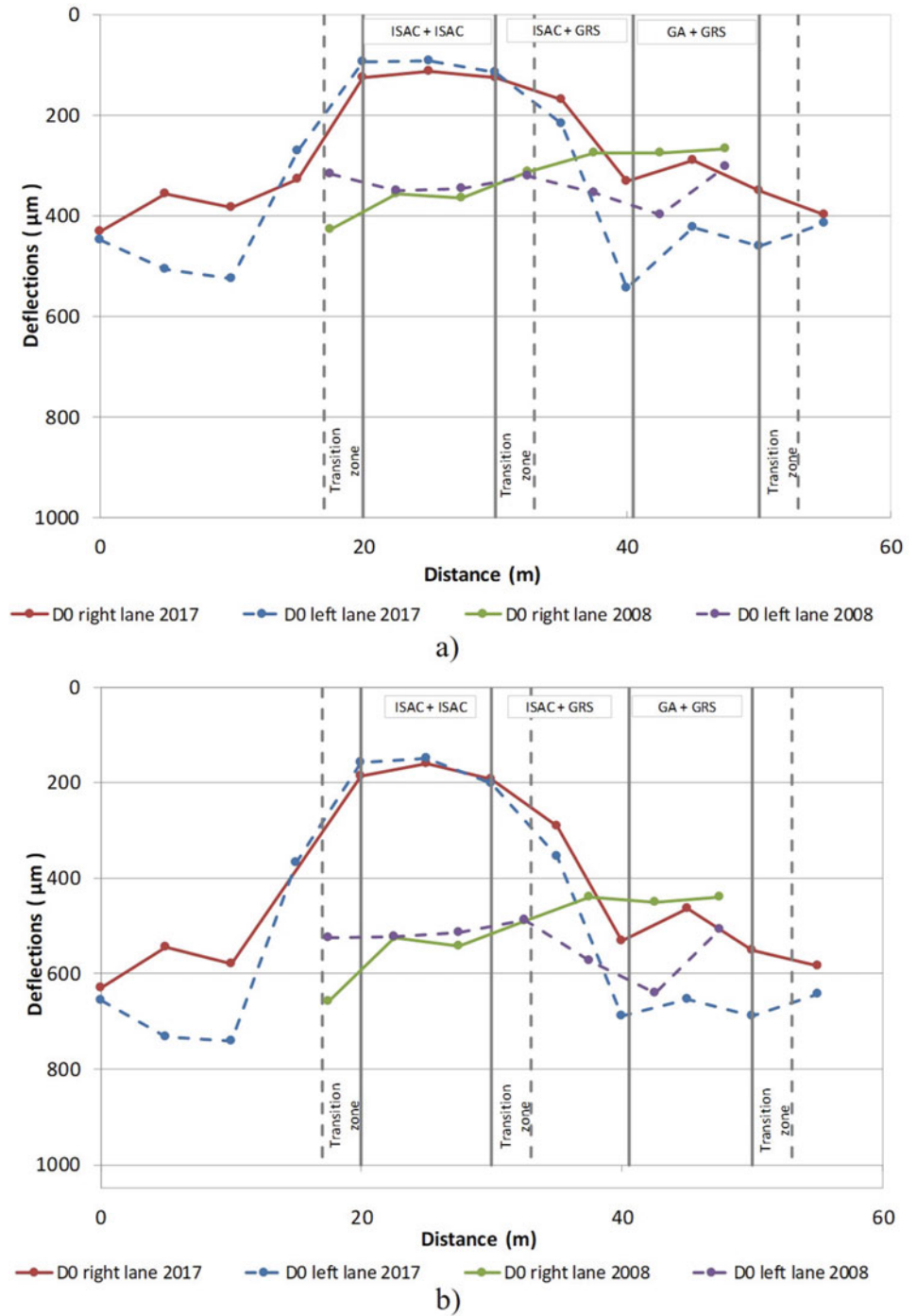
Fig. 3 Aspects of the field trial and FWD testing

Also, a precision geodetic levelling campaign was carried out on the levelling line installed during the embankment construction to determine the permanent vertical displacements that occurred. Considering a campaign performed in October 2007, maximum vertical displacements of approximately 8.2 mm were measured in 2017 on the surface markings installed on the embankment, both in the section with ISAC and in the section with residual granite soil.

4 Discussion

From the analysis of the results, it can be concluded that in the field trial zones with ISAC, the deflections were lower, indicating a better performance of the pavement in those zones. That was more significant for higher values of the applied load, emphasizing the low deformability of ISAC

Fig. 4 Maximum deflections (D0) measured with the FWD in the direction Fafe-Cabeceiras de Basto in 2008 and in 2017, on both lanes: **a** applied load of 30 kN; **b** applied load of 47 kN



since, for higher load values, the deepest pavement layers are also involved (base and capping layers). When comparing the maximum deflections (D_0) measured in this campaign, for applied load values of 30 and 47 kN, with those measured in 2008, it can be concluded that in the zone where ISAC was used, the deflections are now significantly less than the ones measured in 2008. In contrast, in the other zones, the present deflections are higher than those measured in 2008. The results seem to indicate that, over time, the pavement structure became more rigid in the zones where ISAC was employed and more flexible in the other zones.

In general, the pavement cracks, particularly longitudinal cracks and alligator cracking, were less severe and less frequent in the zones where ISAC was used.

The maximum permanent vertical displacements of the embankment (8.2 mm), measured on surface markings, corresponded to maximum deformations of approximately 0.25%, ten years after. That indicates a good performance of the structure compared with one of the other road embankments (Fortunato and Veiga Pinto 1998).

Hence, from the analysis of data, it can be concluded that the pavement of the field trial during 10 years in service, in the zone where ISAC was employed as construction material, was generally in better condition (as referred to the existence of cracks) and exhibited better structural performance than the adjacent zones constructed with natural materials.

5 Concluding Remarks

The visual inspection and the results of the mechanical tests performed about ten years after a field trial built with Inert Steel Aggregate for Construction (ISAC) started operating made it possible to conclude that the pavement in the zone with ISAC was in better condition and exhibited better structural performance than the one in the adjacent zones

constructed with natural materials. In terms of the embankment's maximum settlements, no significant differences were observed when comparing the zones with ISAC with the other zones.

Hence, the studies reported in this work, which were conducted to assess the ISAC characteristics, and the performance of layers constructed with it, made it possible to conclude that this material has similar or even better characteristics than the natural materials, when considering the requirements imposed for the construction of embankment layers, and capping and base layers of pavements.

The environmental monitoring results have demonstrated that ISAC can be considered an inert by-product. It neither contributes to the degradation of the environmental quality, namely of soils and surface and ground waters, nor poses relevant risk to public health.

Acknowledgements Thanks are due to the company Megasa for their permission to publish the results.

References

- Fortunato E, Veiga Pinto A (1998) Structural behaviour of soil-rockfill mixtures embankments. In: 2nd international symposium on the geotechnics of hard soils—Soft rocks, Naples, vol 2, pp 1101–1107
- Gomes Correia A, Roque AJ, Reis Ferreira SM, Fortunato E (2012) Case study to promote the use of industrial by-products: the relevance of performance tests. *J ASTM Int* 9(2):1–18
- Roque AJ, Fortunato E, Gomes Correia A, Ferreira SM, Pardo de Santayana F, Castro F, Trigo L (2007) The geotechnical reuse of Portuguese inert siderurgical aggregate. In: XIII Panamerican conference on soils mechanics and geotechnical engineering, Margarita Island, Venezuela, pp 429–434
- Sofilić T, Sofilić U, Brnardić I (2012) The significance of iron and steel slag as by-product for utilization in road construction. In: 12th international foundrymen conference. sustainable development in foundry materials and technologies, Opatija, Croatia, pp 419–436
- Worldsteel (2016) Steel industry co-products. <https://www.worldsteel.org>. Last Accessed 02 Oct 2020



Review on Laboratory Testing for Hydraulically Bound Mixtures Used in Road Applications

José Neves

Abstract

Hydraulically bound mixtures are mixtures containing a hydraulic binder responsible for the fast setting and hardening properties of the material. These mixtures are designed to attain structural integrity in the base, sub-base, and subgrade of road pavements. The main objective of this work is to present a general overview of the existing European framework on laboratory test methods related to the performance of the hydraulically bound mixtures regarding road applications. The main test methods for mechanical and durability properties are described, including the preparation of test specimens.

Keywords

Durability • Hydraulically bound mixtures • Pavement • Road

1 Introduction

Hydraulically Bound Mixtures (HBM) are mixtures where the binder is responsible for the fast setting and hardening characteristics of the material (EN 14227–1:2013). Despite being a traditional technology that has been applied for a long time, HBM continues to be currently promoted as base, sub-base, and subgrade materials of road and airfield pavements and for other trafficked areas (e.g., parking areas) (Walters and Edwards 2009, Majarrez 2013, Liu et al. 2020). The most current HBM applied in road pavements are Cement-Bound Granular Mixtures (CBGM) and soil treated by cement (SC). The construction of pavements

using HBM can be an economical and environmentally advantageous technique where sufficient natural geomaterials are unavailable or unsupportable transportation costs. In general, shallow stabilisation improves the local materials' properties and enhances the pavement performance through an increase in bearing capacity, stability, and durability over the road infrastructure's life cycle (Antunes et al. 2016). This pavement technology results in the conservation and/or enhancement of local and natural resources, thus contributing to more sustainable construction practices and promoting the circular economy (Gomes-Correia et al. 2016; Plati 2019). Furthermore, this technology has also been used successfully in natural materials and waste materials (Xuan et al. 2010; Pérez et al. 2013; Stehlik et al. 2015; Pasetto and Baldo 2016).

HBM is designed to attain structural integrity in the pavement, measured by strength and elastic modulus tests. In Europe, the EN 14227 standard series includes the specifications on the mechanical performance of HBM for roads and other transportation infrastructures: CBGM is specified in Part 1 (EN 14227–1:2013) and SC is specified in Part 15 (EN 14227–15:2015). EN 14227 also covers bound granular mixtures of slag (Part 2), fly ash (Part 3), and hydraulic road binder (Part 5). Hydraulic-stabilised soils, covered by EN 14227–15, include soils not only treated by cement but also treated by lime, slag, fly ash, and hydraulic road binder. These specifications are supported by test methods covered by the EN 13286 standard series. This standardisation framework has been developed by the Working Group WG 4—Hydraulic bound and unbound mixtures (including by-products and waste materials)—of the TC 227—Road materials—of the European Committee for Standardisation (CEN@ 2020).

EN 14227–1 considers five types of CBGM based on geometrical and mechanical requirements of the mixture: grading, compacity, and immediate bearing index. CBGM are designated according to their type and the main laboratory characteristics: particle size (d/D), grading category (G),

J. Neves (✉)

CERIS, Department of Civil Engineering, Architecture, and Georesources, Instituto Superior Técnico, Universidade de Lisboa, Lisboa, Portugal
e-mail: jose.manuel.neves@tecnico.ulisboa.pt

and mechanical performance classification (T). EN 14227–1 presents an example: CBGM 2 0/20 – G2 – T3.

The main objective of this work is to present a review of the most commonly used framework for the laboratory test methods on the mechanical performance and durability of CBGM and SC. The study also describes the preparation and characterisation of the fresh mixture and the manufacturing methods of the test specimens. The work is based on the global review and analysis of the different parts of EN 14227 and EN 13286, most closely related to the characteristics mentioned above.

2 Test Specimens

HBM mostly consists of aggregates and binders mixed with water and secondary constituents, which are added to improve certain properties of the mixture (e.g., stability, impermeability, and hardening). The aggregates used in HBM could be natural, artificial, recycled, or a combination of these. The aggregates must be in conformity with EN 13242:2002 + A1:2007, which covers requirements in terms of geometrical, physical, chemical, and durability properties. These requirements are related to the coarse and fine aggregates. Sampling and sample reduction of aggregates for HBM are described in EN 932–1 (1996), EN 932–2 (1999), and EN 13286–1 (2021, 2003) (Annex A). The properties of the cement used as a binder must be in conformity with EN 197–1 (2011).

Prior to test specimen manufacturing, laboratory dry density, and water content must be determined. Indeed, the dry density depends on the effective compaction energy applied and the amount of water in the mixture. Proctor compaction (EN 13286–2:2010/AC:2012) and vibrating hammer compaction (EN 13286–4:2021, 2003) are the most current methods for the laboratory determination of the relationship between the dry density and the water content. Other possible methods are vibrocompression (EN 13286–3:2003) and vibrating table compaction (EN 13286–5:2003). These methods will estimate HBM density and water content for test specimen manufacturing and quality control during road construction.

The tests for HBM strength and modulus of elasticity determinations are carried out in cubic or cylindrical specimens manufactured according to the following test methods: Proctor equipment or vibrating table compaction (EN 13286–50:2004); vibrating hammer compaction (EN 13286–51:2004); vibrocompression (EN 13286–52:2004); and axial compression (EN 13286–53:2004). The first step in the manufacturing of test specimens is preparing the aggregates and cement portions (EN 932–2:1999), followed by the mixture and the addition of the required

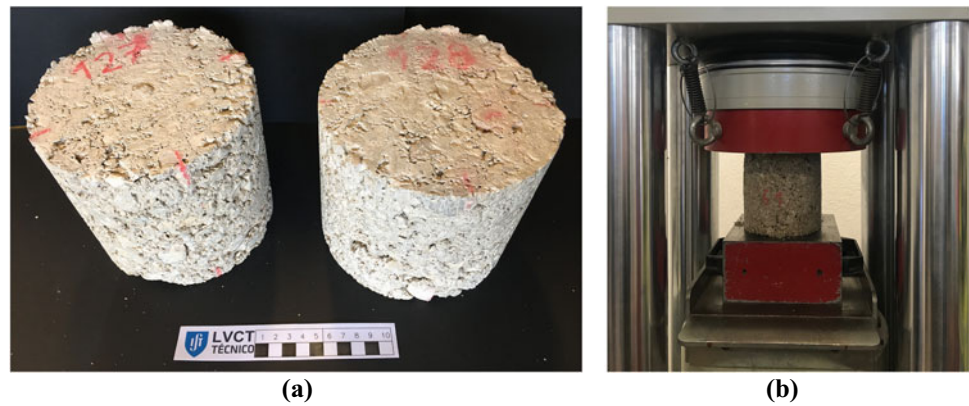
amount of water to attain the final moisture level of the specimen. Prior to this procedure, the determination of the water content of the aggregates by drying them in a ventilated oven may be necessary (EN 1097–5:2008).

Besides the proportion of the constituents, grading, water content, dry density, and compaction, other properties related to the fresh mixture that should be attained by the mixture design developed in the laboratory may be important. Depending on the material and the application, these may include the workability period (EN 13286–45:2003), moisture condition value (EN 13286–46:2003), immediate bearing index (EN 13286–47:2012), and degree of pulverisation (EN 13286–48:2005). The workability period is the duration of time since the end of the mixing process up until the moment that the binder setting is practically null. The moisture condition value is relative to the compaction of HBM. The immediate bearing index is the immediate California Bearing Ratio (CBR) determined without surcharge. The CBR is a well-known and empirical parameter used to characterise the bearing capacity of a mixture, normally after a period of four days of immersion in water curing. The degree of pulverisation has to do with the effectiveness of the mixing, in particular the possibility of the cohesive material being mixed efficiently with the binder. The moisture condition value and the degree of pulverisation are most common in the case of hydraulically stabilised soils.

The cylindrical and cubical moulds used to manufacture HBM test specimens must conform to EN 13286–2/AC (2012) and EN 12390–1 (2021), respectively. Metal or plastic moulds can be used. The moulds can also be integer or split. However, they must be rigid enough during compaction to rule out deformations. Normally the specimens are compacted in layers. The surface of each layer should be scarified before the compaction of the next layer to promote good adherence and the final rigidity of the test specimen. The final top face of the specimen must be regular, eventually involving removing excess mixture and filling in depressions with a fine mixture. The top and bottom faces must also be parallel, and a process to cap the specimen can be adopted if necessary (e.g., a thin layer of plaster). Figure 1a shows cylindrical specimens of CBGM compacted using a vibrating hammer (diameter: 150 mm; height: 150 mm).

After compaction and before demoulding, specimens are maintained at a temperature of 20 °C for hardening for at least 20 h, in the proper conditions for preserving moisture and temperature. After that time, the specimens are extracted from moulds through a process ensuring the structural integrity and stored for the duration of the curing time, which is typically, 7, 14, and 28 days. Temperatures during curing are typically 20 or 40 °C. The specimens are conditioned vertically and protected against moisture loss. After

Fig. 1 Cylindrical test specimens (a) and unconfined compressive strength test (b)



the curing time and the evaluation of dimensions and mass, test specimens can be submitted to the mechanical tests. In the case of durability tests, other curing conditions can be specified before testing.

3 Mechanical Performance

Resistance is the most important parameter to be considered when evaluating the mechanical performance of HBM (PCA 1992). Indeed, the presence of the binder has a significant strengthening effect on the hydraulic mixture. The resistance is generally evaluated through compressive and tensile strengths. The most popular and easy parameter is the unconfined compressive strength (UCS), which is commonly a key design parameter for cement-stabilised layers of road pavements (EN 13286-41:2021, 2003) (Fig. 1b). However, tensile strength is also an especially important resistance factor for pavement bound layers due to traffic loading. The test methods for tensile strength determination are direct tensile strength (EN 13286-40:2003) and indirect tensile strength (EN 13286-42:2003). The laboratory mechanical performance can be divided into two classification systems according to EN 14227-1 (2013) and EN 14227-15 (2015): (1) compressive strength; and (2) combination of the strength and the modulus of elasticity. In the case of the compressive strength (R_c) classification, the class of resistance (C) is obtained in combination with the specimen geometry: cylindrical specimens with a height to diameter ratio (H/D) of 2; and cubes or cylindrical specimens with H/D = 1. The class is related to the minimum compressive strength (in MPa) and ranges from $C_{0.4/0.5}$ to $C_{36/38}$ for CBGM (EN 14227-1:2013). The first and second numbers in the notation are the minimum resistance for both types of specimens, respectively.

In fact, a better approach to mechanical performance would be possible if the methodology were based simultaneously on strength and deformability and not only exclusively based on material resistance. Figure 2a presents the

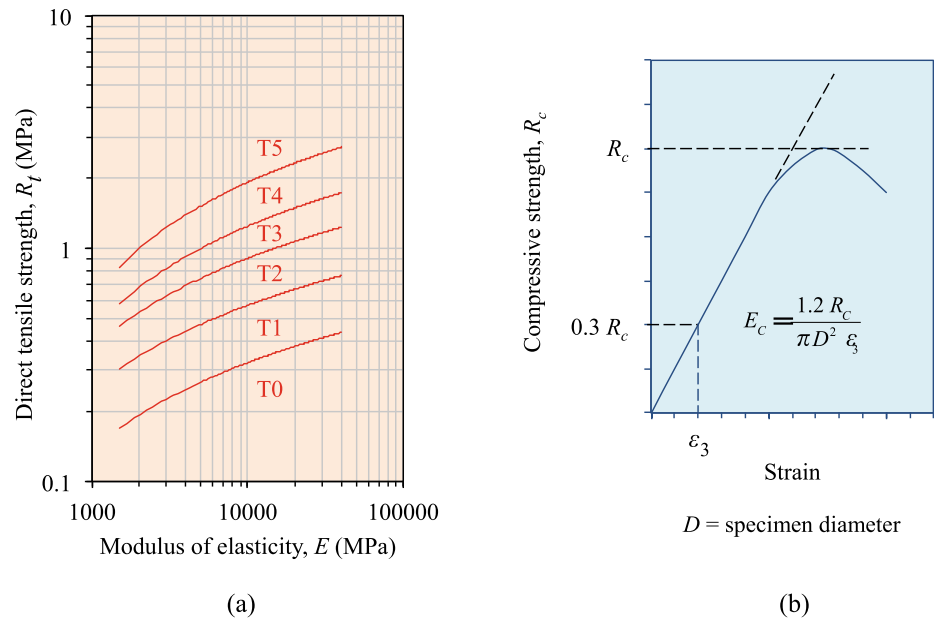
classification of CBGM and SC based on the direct tensile strength (R_t) and the modulus of elasticity (E): categories T5, T4, T3, T2, and T1. The modulus of elasticity is determined following the procedure in EN 13286-43 (2003), which should also apply to the tensile testing method used for the mechanical performance classification. Figure 2b illustrates the procedure to determine the modulus of elasticity (E_c), measured in compressive strength (R_c). When using the indirect tensile strength, the values are estimated by the relationships: $R_t = 0.8 R_{it}$ and $E = E_{it}$ (R_{it} and E_{it} are measured in indirect tension).

The strength and the modulus of elasticity should be the average result of a minimum of three specimens. If any test result exceeds more than 20% of the mean value, it should be discarded (EN 14227-1:2013). HBM resistance depends on the specimen geometry and density. So, it is extremely important that the resistance should always be associated with the test specimens' manufacturing method. All compaction methods are suitable for evaluating the strength and the modulus of elasticity. However, vibrocompression compaction is recommended if direct tensile testing is adopted.

4 Durability

The durability of HBM has a considerable influence on the performance of semi-rigid pavements. The durability assessment must be related to the aggregate and the mixture performance itself. The most important factors impacting the durability of HBM are the volumetric changes (thermal expansion) and the sensitivity to water (frost heave). Other factors may also be important, such as the drying shrinkage and the presence of organic material. Assessment of the durability of HBM is a complex matter. Generally speaking, the latest current laboratory methods are mainly based on wet-dry and freeze-thaw cycling tests (Biswal et al. 2018). These tests could be a primary indicator of the long-term performance of SC. In general, the specimens are submitted

Fig. 2 Classification of the mechanical performance (a) (adapted from EN 14227-1 and EN 14227-15) and determination of the modulus of elasticity (b) (adapted from EN 13286-43)



to several cycles of conditioning under a standard protocol. In the wet-dry test, one cycle comprises the immersion in water, followed by the drying in a ventilated oven. After each cycle, the specimens are brushed, and the mass loss is assessed.

In accordance with EN 14227-1 and EN 14227-15, the durability of HBM is judged using the resistance to water tests: strength after immersion in water, linear swelling after soaking in water (EN 13286-47:2012) or volumetric swelling after water immersion (EN 13286-49:2004). The strength after immersion in water test is applied to both CBGM and SC. This test assesses the decrease in resistance after the conditioning of the specimens in sealed curing followed by full immersion curing in water. Annex A of EN 14227-15 presents examples of the age of classification and curing regimes of treated soils (duration and temperature of sealed and immersion in water curing). The linear swelling after soaking in water is the classic expansion obtained in the CBR test. The volumetric swelling after water immersion is the expansion measured at the end of a set period of accelerated curing (a maximum of 14 days) using special storage of the specimens. Both tests are suitable for SC durability evaluation.

CEN/TS 13286-54 (2014) is dedicated to assessing HBM frost susceptibility by determining the resistance to the cyclic action of freezing and thawing. The test determines the retained strength ratio, in compression or tensile test, between conditioned and unconditioned specimens. The conditioning consists of 10 freeze-thaw cycles (1 day each) at a specified temperature in the first stage. After these

cycles, the specimens are unwrapped and returned to a second stage curing regime for 1 day at 20 °C to complete thawing.

5 Concluding Remarks

This study has reviewed the laboratory test methods for hydraulically bound mixtures (HBM) used in road applications. The main focus of the work was the cement bound granular mixtures, following EN 14227-1, and the soils treated by cement, for which the specifications are defined in EN 14227-15.

Procedures for specimens manufacturing were presented concerning all the test methods for mechanical performance covered by the EN 13286 standards series: Proctor, vibrating hammer, vibrocompression, and vibrating table.

In general, unconfined compressive strength is most commonly used for the characterisation of HBM. In addition to this, the work has also outlined the direct and indirect tensile strength tests. The mechanical performance classification based simultaneously on strength and deformability (modulus of elasticity) was presented. Durability tests were also included, considering the importance of durability for the global performance of HBM. The work was based on the European standardisation framework. Other countries have equivalent test methods for laboratory-manufactured cement materials, such as the USA (ASTM and AASHTO) and Australia (Austroads).

Acknowledgements The author is grateful for the support of the Foundation for Science and Technology (FCT) through funding FCT-IDB/04625/2020 from the research unit CERIS (Center of Civil Engineering Research and Innovation for Sustainability).

References

- Antunes ML, Marecos V, Neves J, Morgado J (2016) Decision to pavement solutions in road infrastructures based on life-cycle assessment. *Baltic J Road Brid Eng* 11(1):43–52
- Biswal DR, Sahoo UC, Dash SR (2018) Durability and shrinkage studies of cement stabilised granular lateritic soils. *Int J Pav Eng* 20(12):1451–1462
- CEN Homepage, European Committee for Standardization. <https://standards.cen.eu>. Accessed 18 Nov 2020
- CEN/TS 13286-54:2014 – Unbound and hydraulically bound mixtures. Test method for the determination of frost susceptibility. Resistance to freezing and thawing of hydraulically bound mixtures. CEN, Brussels
- EN 197-1:2011 – Cement. Composition, specifications and conformity criteria for common cements. CEN, Brussels
- EN 932-1:1996 – Tests for general properties of aggregates. Methods for sampling. CEN, Brussels
- EN 932-2:1999 – Tests for general properties of aggregates. Methods for reducing laboratory samples. CEN, Brussels
- EN 1097-5:2008 – Tests for mechanical and physical properties of aggregates. Determination of the water content by drying in a ventilated oven. CEN, Brussels
- EN 12390-1:2021 – Testing hardened concrete. Shape, dimensions and other requirements for specimens and moulds. CEN, Brussels
- EN 13242:2002+A1:2007 – Aggregates for unbound and hydraulically bound materials for use in civil engineering work and road construction. CEN, Brussels
- EN 13286-1:2021 – Unbound and hydraulically bound mixtures. Test methods for laboratory reference density and water content. Introduction, general requirements and sampling. CEN, Brussels
- EN 13286-2:2010/AC:2012 – Unbound and hydraulically bound mixtures. Test methods for laboratory reference density and water content. Proctor compaction. CEN, Brussels
- EN 13286-3:2003 – Unbound and hydraulically bound mixtures. Test methods for laboratory reference density and water content. Introduction, general requirements and sampling. CEN, Brussels
- EN 13286-4:2021 – Unbound and hydraulically bound mixtures. Test methods for laboratory reference density and water content. Vibrating hammer. CEN, Brussels
- EN 13286-5:2003 – Unbound and hydraulically bound mixtures. Test methods for laboratory reference density and water content. Vibrating table. CEN, Brussels
- EN 13286-40:2003 – Unbound and hydraulically bound mixtures. Test method for the determination of the direct tensile strength of hydraulically bound mixtures. CEN, Brussels
- EN 13286-41:2021 – Unbound and hydraulically bound mixtures. Test method for the determination of the compressive strength of hydraulically bound mixtures. CEN, Brussels
- EN 13286-42:2003 – Unbound and hydraulically bound mixtures. Test method for the determination of the indirect tensile strength of hydraulically bound mixtures. CEN, Brussels
- EN 13286-43:2003 – Unbound and hydraulically bound mixtures. Test method for the determination of the modulus of elasticity of hydraulically bound mixtures. CEN, Brussels
- EN 13286-45:2003 – Unbound and hydraulically bound mixtures. Test method for the determination of the workability period of hydraulically bound mixtures. CEN, Brussels
- EN 13286-46:2003 – Unbound and hydraulically bound mixtures. Test method for the determination of the moisture condition value. CEN, Brussels
- EN 13286-47:2012 – Unbound and hydraulically bound mixtures. Test method for the determination of California bearing ratio, immediate bearing index and linear swelling. CEN, Brussels
- EN 13286-48:2005 – Unbound and hydraulically bound mixtures. Test method for the determination of degree of pulverisation. CEN, Brussels
- EN 13286-49:2004 – Unbound and hydraulically bound mixtures. Accelerated swelling test for soil treated by lime and/or hydraulic binder. CEN, Brussels
- EN 13286-50:2004 – Unbound and hydraulically bound mixtures. Method for the manufacture of test specimens of hydraulically bound mixtures using Proctor equipment or vibrating table compaction. CEN, Brussels
- EN 13286-51:2004 – Unbound and hydraulically bound mixtures. Method for the manufacture of test specimens of hydraulically bound mixtures using vibrating hammer compaction. CEN, Brussels
- EN 13286-52:2004 – Unbound and hydraulically bound mixtures. Method for the manufacture of test specimens of hydraulically bound mixtures using vibrocompression. CEN, Brussels
- EN 13286-53:2004 – Unbound and hydraulically bound mixtures. Methods for the manufacture of test specimens of hydraulically bound mixtures using axial compression. CEN, Brussels
- EN 14227-1:2013 – Hydraulically bound mixtures. Specifications. Cement bound granular mixtures. CEN, Brussels
- EN 14227-15:2015 – Hydraulically bound mixtures. Specifications. Hydraulically stabilised soils. CEN, Brussels
- Gomes-Correia A, Winter MG, Puppala AJ (2016) A review of sustainable approaches in transport infrastructure geotechnics. *Transport Geotech* 7:21–128
- Liu Y, Su P, Li M, You Z, Zhao M (2020) Review on evolution and evaluation of asphalt pavement structures and materials. *J Traf Transport Eng* 7(5):573–599
- Majarrez FP (2013) Semi-rigid pavement performance and construction techniques for semiarid areas. *Road Mat Pav Desig* 14(3):615–637
- PCA (1992) Soil-cement laboratory handbook. Portland Cement Association, USA
- Pasetto M, Baldo N (2016) Recycling of waste aggregate in cement bound mixtures for road pavement bases and sub-bases. *Constr Build Mat* 108:112–118
- Pérez P, Agrela F, Herrador R, Ordoñez J (2013) Application of cement-treated recycled materials in the construction of a section of road in Malaga, Spain. *Constr Build Mat* 44:593–599
- Plati C (2019) Sustainability factors in pavement materials, design, and preservation strategies: a literature review. *Constr Build Mat* 211:539–555
- Stehlik D, Dasek O, Hyzl P, Coufalik P, Krcmova I, Varaus M (2015) Pavement construction using road waste building material: from a model to reality. *Road Mat Pav Desig* 16:314–329
- Walters CE, Edwards J (2009) Increasing the use of hydraulically bound mixtures in construction. Final report, WRAP, Banbury
- Xuan D, Houben LJM, Molenaar AAA, Shui Z (2010) Cement treated recycled demolition waste as a road base material. *J Wuhan Univ Techn-Mat Sci Ed* 25(4):696–699



Absolute Permeability of Codaçal Porous Limestone Under Different Pressure and Temperature Conditions

Gustavo Paneiro and Alirza Orujov

Abstract

Thermal-enhanced oil recovery is becoming a widely applied practice on increasing oil productivity. Applied temperature and depletion of pressure with production might affect the source rock's petrophysical characteristics, especially around the wellbore. This work presents an experimental study of core flooding tests over Codaçal limestones core samples from the Lusitanian Basin as reservoir rock analogues. The samples were subjected to a set of tests where the first step is porosity determination. Afterwards, brine flooding was performed in brine-saturated limestone core samples, considering different temperature and pressure conditions. The results show the influence of temperature and confinement pressure on the tested cores' absolute permeability, having a more considerable influence on permeability reduction.

Keywords

Core flooding • Carbonates • Portuguese limestone • Permeability • Temperature • Pressure

1 Introduction

Thermal-enhanced oil recovery becoming a widely applied practice on increasing oil productivity. Although the method has a long-known history, its application was not considered economically feasible since the availability of vast oil reserves and other economic reasons (Thomas 2007). However, increasing demand for hydrocarbons leads to

maximising reservoir productivity in all possible ways, including thermal enhancement that shows inevitable adversities to overcome.

The effects of temperature and pressure depletion with production might affect the reservoir rock's petrophysical characteristics, especially around the wellbore and fluid flow. The most prominent flow parameter is absolute permeability which is directly in charge of fluid flow through pores. The temperature on petrophysical parameters was already investigated for different types of rocks, including carbonates.

Sanyal et al. (1974) showed that increasing temperature significantly affects pore volume compressibility, permeability, electrical resistivity, and capillary pressure behaviour of reservoir rocks. Also, Zekri and Chaalal (2001), based on experimental work, observed a permeability reduction of 50% due to increasing temperature at 150°C for non-fractured cores. The temperature effect leads to the thermal expansion of solid grains and skeleton and, consequently, to various fluid mass content at drained conditions (Palciauskas and Domenico 1982; Guéguen and Boutéca 2004). Similarly, Benzagouta and Amro (2009) developed an experimental study under carbonate rock samples that shows a substantial effect of pressure and temperature on permeability. Song et al. (2018) and Aadland et al. (2019) drew out the same conclusions.

The Lusitanian Basin (LB) in coastal west-central Portugal has been studied as an analogue for the less well-known Peniche Basin in the deep offshore (Pimentel and Pena dos Reis 2016), with several petroleum systems and potential hydrocarbon reservoirs (Fainstein and Duarte 2018). Given this, the present study investigates the effect of temperature and pressure in the context of a specific Middle Jurassic carbonate rock (Codaçal limestone). According to Azerêdo et al. (2020), the Middle Jurassic successions of the LB offer a wide range of outcrop analogues, including the Codaçal limestone from the Santo António-Candeeiros formation.

The present work presents the results obtained in core flooding experimental over three core samples of Codaçal

G. Paneiro (✉)
DER—Departamento de Engenharia de Recursos Minerais e Energéticos e CERENA, Técnico Lisboa, Universidade de Lisboa, Lisboa, Portugal
e-mail: gustavo.paneiro@tecnico.ulisboa.pt

A. Orujov
DIATI, Politécnico Di Torino, Torino, Italy

limestone. Each of the samples was subjected to four different temperatures and three confinement pressure conditions during the flooding, resulting in 12 flooding tests for each sample. The influence of temperature and confinement pressure conditions are analysed and quantified.

2 Materials and Methods

For this work, temperature and pressure effects on the samples were investigated in absolute permeability changes. Since absolute permeability represents the essential flowing parameter of the fluids inside the rock, it is significant to be examined (Benzagouta and Amro 2009; Amro and Benzagouta 2009).

Limestone samples were collected in a quarry outcrop that belongs to the Pé da Pedreira formation. That corresponds to a thin layer that is a part of the Santo António--Candeiros formation, a large geomorphological unit deposited in the LB (Fig. 1).

Core samples are specifically extracted and handled from the field to GeoLab of CERENA, Técnico ULisboa, Portugal. Then they were sampled according to International Society for Rock Mechanics (ISRM) recommendations (Franklin 1977) by a rotary core drill with a 38 mm diameter and 100 mm length. The cuttings were performed parallel to the stratification. Then the specimens were labelled and ready for routine core analyses.

The experimental work's first and foremost step starts with measuring the weights and geometrical parameters (length and diameter) of each sample according to ISRM

(Franklin 1977). Each measurement should be repeated at least 5 times, and an average value should be obtained to minimising the errors. After the measurements, all samples are put in the oven at a constant temperature of 105 °C for at least 24 h to dry all the moisture. A dry mass was obtained before saturating them with 35 g/L saline water (brine). The sample is weighted again on a highly sensitive electronic scale, and a fully saturated weight is obtained after sample saturation. These are the key parameters to determine the effective porosity of the samples according to EN (1936:2001) and using the following relation:

$$\varnothing = \frac{\text{Saturated Weight} - \text{Dry weight}}{\text{Brine density} * \text{specimen volume}} * 100\% \quad (1)$$

After porosity calculations, the samples are carefully placed inside a Hassler core holder, and temperature is applied using an electric mantle, which covers the core holder. A simplified scheme of the entire flooding process is described in Fig. 1.

Before starting flooding, temperature conduction time was considered. Inlet pressure and flow rate measurements have been taken with a 10-min frequency. 35 g/l concentration of brine was used for injection with a 5 ml/h injection rate applied. 12 total tests were performed for each sample under three different confinement pressures (P_c) and four different temperatures. Darcy's law was applied for absolute permeability calculation for each flooding test.

Permeability reduction factor (PRF) was also calculated concerning initial permeability at 20 °C and 100 bar confinement pressure. Therefore, all the PRF (%) values are determined by the following equation for all different runs.

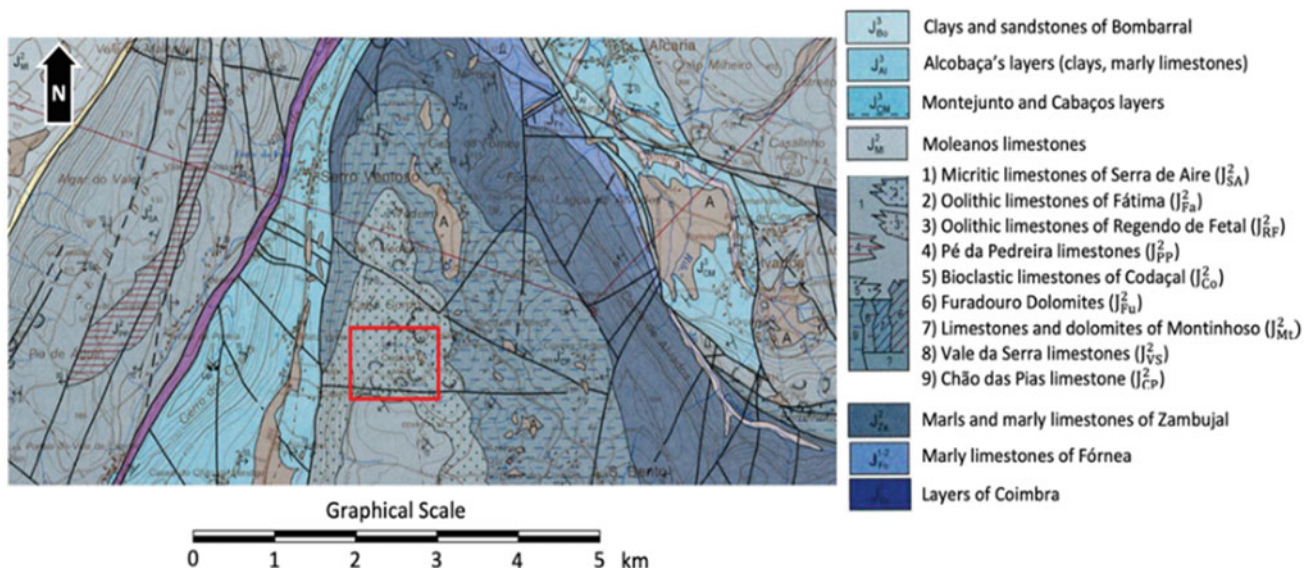


Fig. 1 Geological map of the studied area (adapted from Manuppella et al. 2000)

$$PRF = 1 - \left(\frac{K_n}{K_i}\right) \quad (2)$$

where K_i is initial permeability at 20 °C temperature and 100 bar confinement pressure (P_c) and K_n the permeability at any considered temperature and pressure step.

3 Results and Discussion

Table 1 resumes the dry and saturated weights, lengths, and effective porosity values for the three tested samples following the described methodology.

Table 1 indicated that the open porosities are similar, with a maximum value of 12.60% for AL1 and a minimum of 11.65% for AL6.

From the flooding tests performed on each of the considered samples, absolute permeabilities, and permeability reduction factors were calculated according to Eq. 2. It is worth mentioning that the considered flow rate is 5 ml/h. L and A are the sample geometrical parameters, the inlet pressure was periodically recorded by a pressure gauge at the

inlet (until it is stabilised), the outlet pressure is the constant atmospheric pressure, and the dynamic viscosity, which is the function of brine salinity and temperature, was calculated based on empirical values that can be found in El-Dessouky and Ettouney (2002). The obtained results for each sample, AL4, AL5, and AL, are summarised in Tables 2, 3, and 4, respectively.

The tables show that absolute permeability generally decreases with increasing temperature, and there is a minor effect of pressure on permeability reduction, particularly for sample AL6.

Figure 3 shows the overall absolute permeability variation for increasing confinement pressures and the different temperatures, considering the obtained results.

Figure 2 shows that the absolute permeability variation tends to be higher for lower temperatures. This variation tends to vanish for higher temperatures, indicating that the effect of thermal expansion on the reduction of porosity probably reaches a stable value, and its impacts on absolute permeability became less significant. The same results were obtained by Benzagouta and Amro (2009). The results could be the same if considering PRF, as shown in Fig. 4a.

Table 1 Dry and brine-saturated weight and open porosity values were obtained for the tested samples

Sample	Dry weight (g)	Saturated weight (g)	Effective porosity (%)
AL4	258.28	272.80	12.60
AL5	262.47	275.99	11.67
AL6	261.47	274.90	11.65

Table 2 Absolute permeabilities and PRF values were obtained for sample AL4

P_c (bar)	Temperature (°C)							
	20		40		60		80	
	K (mD)	PRF (%)	K (mD)	PRF (%)	K (mD)	PRF (%)	K (mD)	PRF (%)
100	0.2245	–	0.2222	1.01	0.1820	18.95	0.1621	27.77
150	0.1924	14.31	0.1777	20.86	0.1591	29.11	0.1569	30.11
200	0.1924	14.31	0.1777	20.86	0.1591	29.11	0.1569	30.11

Table 3 Absolute permeabilities and PRF values were obtained for sample AL5

P_c (bar)	Temperature (°C)							
	20		40		60		80	
	K (mD)	PRF (%)	K (mD)	PRF (%)	K (mD)	PRF (%)	K (mD)	PRF (%)
100	0.1345	–	0.1109	17.57	0.1059	21.25	0.0970	27.84
150	0.1222	9.10	0.1109	17.57	0.1059	21.25	0.0970	27.84
200	0.1120	16.69	0.1109	17.57	0.1059	21.25	0.0970	27.84

Table 4 Absolute permeabilities and PRF values were obtained for sample AL6

P _c (bar)	Temperature (°C)							
	20		40		60		80	
	K (mD)	PRF (%)	K (mD)	PRF (%)	K (mD)	PRF (%)	K (mD)	PRF (%)
100	0.1347	0	0.1110	17.57	0.1107	17.82	0.1080	19.80
150	0.1347	0	0.1110	17.57	0.1107	17.82	0.1080	19.80
200	0.1224	9.10	0.1110	17.57	0.1061	21.25	0.1023	24.03

Fig. 2 Simplified scheme of the core flooding apparatus

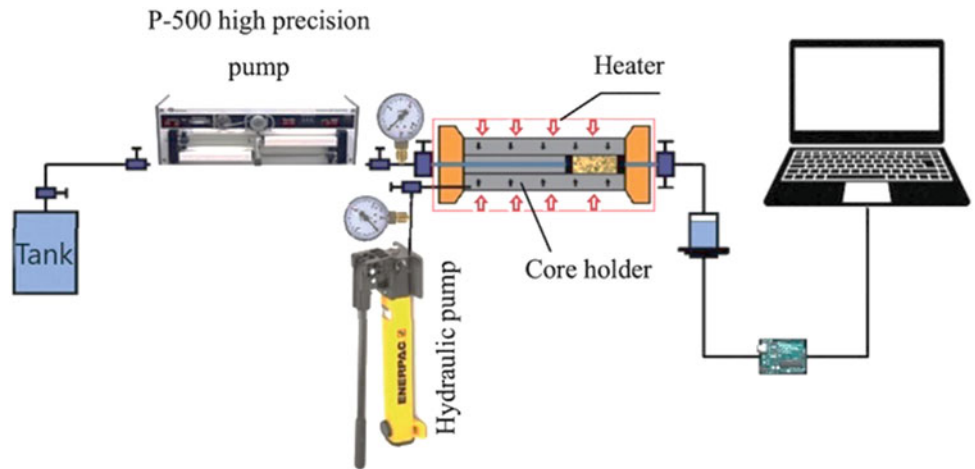
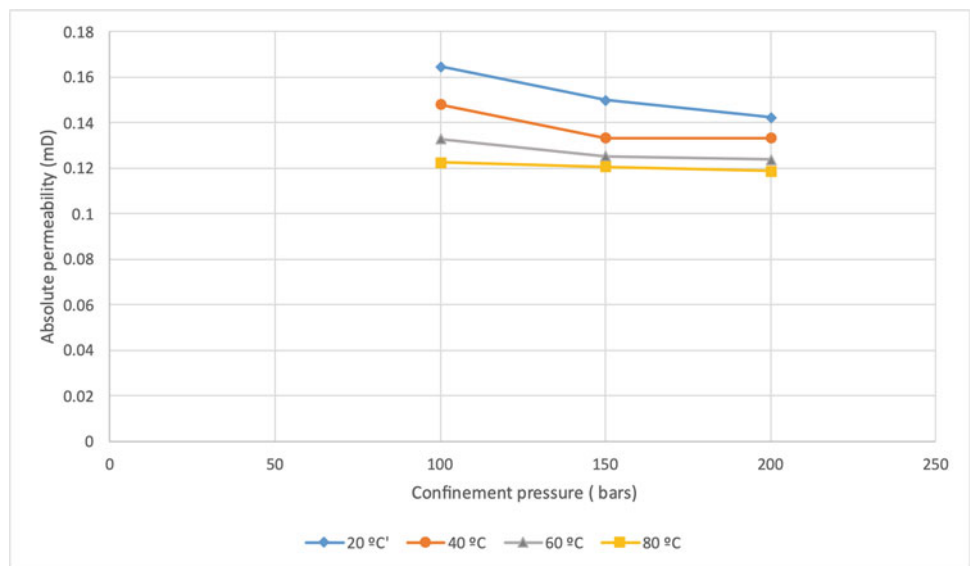


Fig. 3 Variation of the brine absolute permeability at increasing confinement pressure, considering the different temperatures



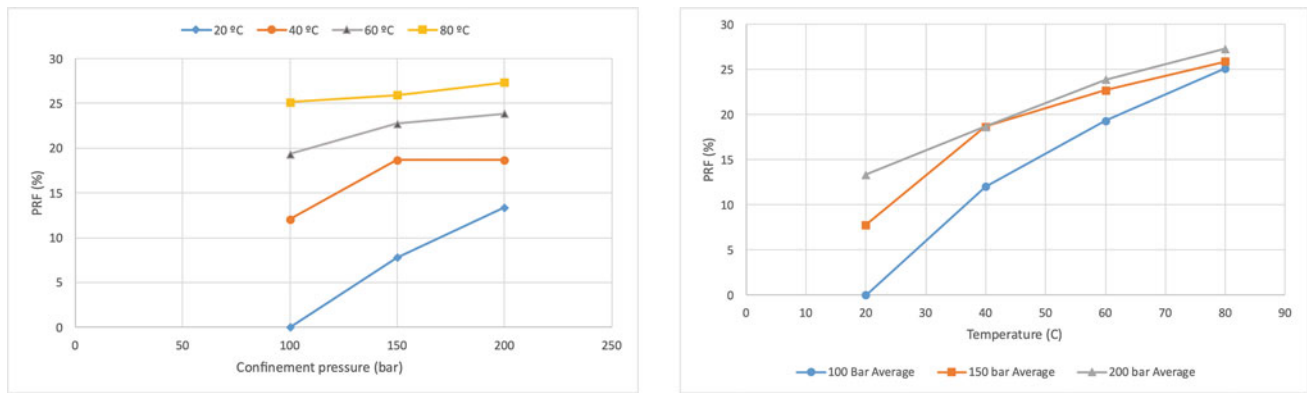


Fig. 4 Variation of PRF at **a** increasing confinement pressure, considering the different temperatures; **b** increasing temperature, considering the different confinement pressures

However, considering Fig. 4b, it becomes clear that permeability has a significant variation with temperature for the studied confinement pressures.

4 Concluding Remarks

The effects of the temperature and confinement pressures on the absolute permeability of Codaçal limestones are investigated through experimental work.

During the experiment, a reduction of permeabilities was observed with increasing temperature steps on each constant confinement pressure. This reduction rate is more significant from 20 to 40 °C and 40 to 60 °C rather than 60 to 80 °C. That can be explained by the nonlinear viscosity reduction of brine with increasing temperature, but, considering the referred literature, for higher temperatures, the reduction of porosity in a confinement state probably reaches a stable value, and its consequent impacts on absolute permeability tend to vanish.

At constant temperature, permeability reduction rates are higher in between 100 bars—150 bars range than 150 bars—200 bars, meaning a reduction of permeability is related to more significant porosity reductions in the first stage of compression. The original cause of it can be due to compaction and primary pore collapse. These rates are also higher at lower temperatures due to decreasing in brine viscosity with increasing temperature.

Acknowledgements The authors gratefully acknowledge the support of CERENA—Center for Natural Resources and Environment (strategic project FCT-UIDB/04028/2020) and Politecnico di Torino. The authors would like to acknowledge the comments presented by the reviewers.

References

- Aadland, RC, Jakobsen TD, Heggset EB, Long-Sanouiller H, Simon S, Paso KG, Syverud K, Torsaeter O (2019) High-temperature core flood investigation of nanocellulose as a green additive for enhanced oil recovery. *Nanomat* 9(5):665
- Amro MM, Benzagouta MS (2009) Effect of pressure and temperature on petrophysical characteristics in the case of carbonate reservoirs. *Oil Gas Eur Mag* 35(29):74–78
- Azerêdo AC, Inês N, Bizarro P (2020) Carbonate reservoir outcrop analogues with a glance at pore-scale (middle Jurassic, Lusitanian Basin, Portugal). *Marit Petrol Geol* 111:815–851
- Benzagouta MS, Amro MM (2009) Pressure and temperature effect on petrophysical characteristics: carbonate reservoir case. In: SPE Saudi Arabia Section Technical Symposium, Al-Khobar, Saudi Arabia
- El-Dessouky HT, Ettouney HM (2002) *Fundamentals of salt water desalination*. Elsevier Science, Amsterdam
- European Committee for Standardization (2001) EN 1936:2001 Natural stone test methods. Determination of real density and apparent density, and total and open porosity. <https://www.cen.eu/>
- Fainstein R, Duarte B (2018) Geophysics definition of Peniche Basin, un-explored Atlantic Margin edge offshore Portugal. In: AAPG Europe regional conference, global analogues of the Atlantic Margin, Lisbon
- Franklin JA (1977) Suggested methods for determining water content, porosity, density, absorption and related properties and swelling and slake-durability index properties. In: Ulusay R, Hudson JA (eds) *The complete ISRM suggested methods for rock characterization, testing*

- and monitoring:1974–2006. International society for rock mechanics, commission on testing methods, Ankara, Turkey
- Guéguen Y, Boutéca M (2004) *Mechanics of fluid saturated rocks*. Elsevier Academic Press, Amsterdam
- Manuppella G, Antunes A, Almeida CAC, Azerêdo AC, Barbosa B, Cardoso JL, Crispim JA, Duarte LV, Henriques MH, Martins LT, Ramalho MM, Santos V, Terrinha P (2000) *Notícia Explicativa da Carta Geológica de Portugal, escala 1:50000, Folha 27-A – Vila Nova de Ourém, 2ª edição*, Instituto Geológico Mineiro, Lisboa
- Palciauskas V, Domenico PA (1982) Characterisation of drained and undrained response of thermally loaded repository rocks. *Water Resour Res* 18(2):281–290
- Pimentel N, Pena dos Reis R (2016) Petroleum systems of the west Iberian margin: a review of the Lusitanian Basin and the deep offshore Peniche Basin. *J Petrol Geol* 39(3):305–326
- Sanyal SK, Marsden Jr. SS, Ramey Jr JR (1974) Effect of temperature in petrophysical properties of reservoir rocks. In: SPE California regional meeting, San Francisco, California
- Song, Y, Kuang, Y, Fan, Z, Zhao, Y, Zhao, J (2018) Influence of core scale permeability on gas production from methane hydrate by thermal stimulation. *Int J Heat Mass Transf* 121:207–214. <https://doi.org/10.1016/j.ijheatmasstransfer.2017.12.157>
- Thomas S (2007) Enhanced oil recovery: an overview. *Oil Gas Sci Technol* 63(1):9–19
- Zekri AY, Chaalal O (2001) Thermal stress of carbonate rocks: an experimental approach. In: SPE western regional meeting, bakersfield, California



Geotechnical Properties of the Miocene Rocks of Central Algarve (Portugal)

Fernando Marques

Abstract

The calcarenite rocks of the Miocene age form the bedrock of the southern part of the central Algarve. These are generally soft to very soft rocks, heavily affected by karst features, with these aspects being a considerable constraint for engineering projects. This work presents laboratory test results to assess unit weight, calcium carbonate content, water content, ultrasonic velocity, uniaxial compressive strength, and indirect tensile strength (Brazilian test). The strength test results indicate that there is a significant strength decay between dry and wet conditions. The results obtained and their influence on the expected behaviour of these rocks are discussed.

Keywords

Soft rock • Calcarenite • Miocene • Uniaxial compression • Indirect tensile strength • Ultrasonic velocity

1 Introduction

The Miocene rocks form the rocky substrate of much of the coast of the central Algarve and are the main lithological support of the coastal cliffs (Fig. 1). They comprise layers of fine calcarenites alternating with fossiliferous calcarenites, locally lumachelic, which generally correspond to rocks of low to very low resistance. Miocene rocks were affected by intense karst dissolution. The karst cavities are usually filled with red Plio-Pleistocene silty sands with clay intercalations, forming a discontinuous cover of the Miocene rocky

substrate. The presence of a low strength rocky substrate, affected by abundant karst features, often hidden by a sandy cover with much lower strength than the substrate, produces relevant geotechnical conditioning for engineering projects in the region and the stability of the coastal cliffs. The intense and growing human occupation in the region, especially along the coast, gives relevance to those geotechnical conditions.

This study presents several campaigns of laboratory tests for geotechnical characterization of Miocene calcarenites, including identification and strength tests which may be a source of valuable data for future projects considering the almost inexistent record of geotechnical data published on these rocks.

2 Geological Setting

The Miocene rocks occupy a large extension of the central Algarve (Fig. 1) and correspond essentially to the Lagos-Portimão Formation (lower Miocene, Aquitanian–Burdigalian) (Rocha et al. 1981, 1983; Antunes and Pais 1993). It is mainly composed of alternating beds of fine-grained biocalcarenes and biocalcarenes with abundant remains of macrofossils. Bedding planes do not generally correspond to mechanical discontinuities but sharp transitions from layers of fine-grained calcarenites with few remains of macrofossils to layers with debris and moulds of macrofossils, surrounded by fine calcarenite matrix. Often, the coarsest beds correspond to lumachel. The upper part of the rock mass has suffered dissolution and precipitation of calcite, which led to the formation of calcretes, with frequently much higher strength than the underlying rocks (Marques 1994, 1997).

The unit thickness does not exceed 50 m west of Albufeira and increases southeast up to 85 m in the Balaia region. Near Vilamoura, the unit was detected under the Plio-Pleistocene cover, in a borehole, with a measured

F. Marques (✉)
Departamento de Geologia, Instituto D. Luiz (IDL), Faculdade de Ciências, Universidade de Lisboa, Lisboa, Portugal
e-mail: fsmarques@fc.ul.pt

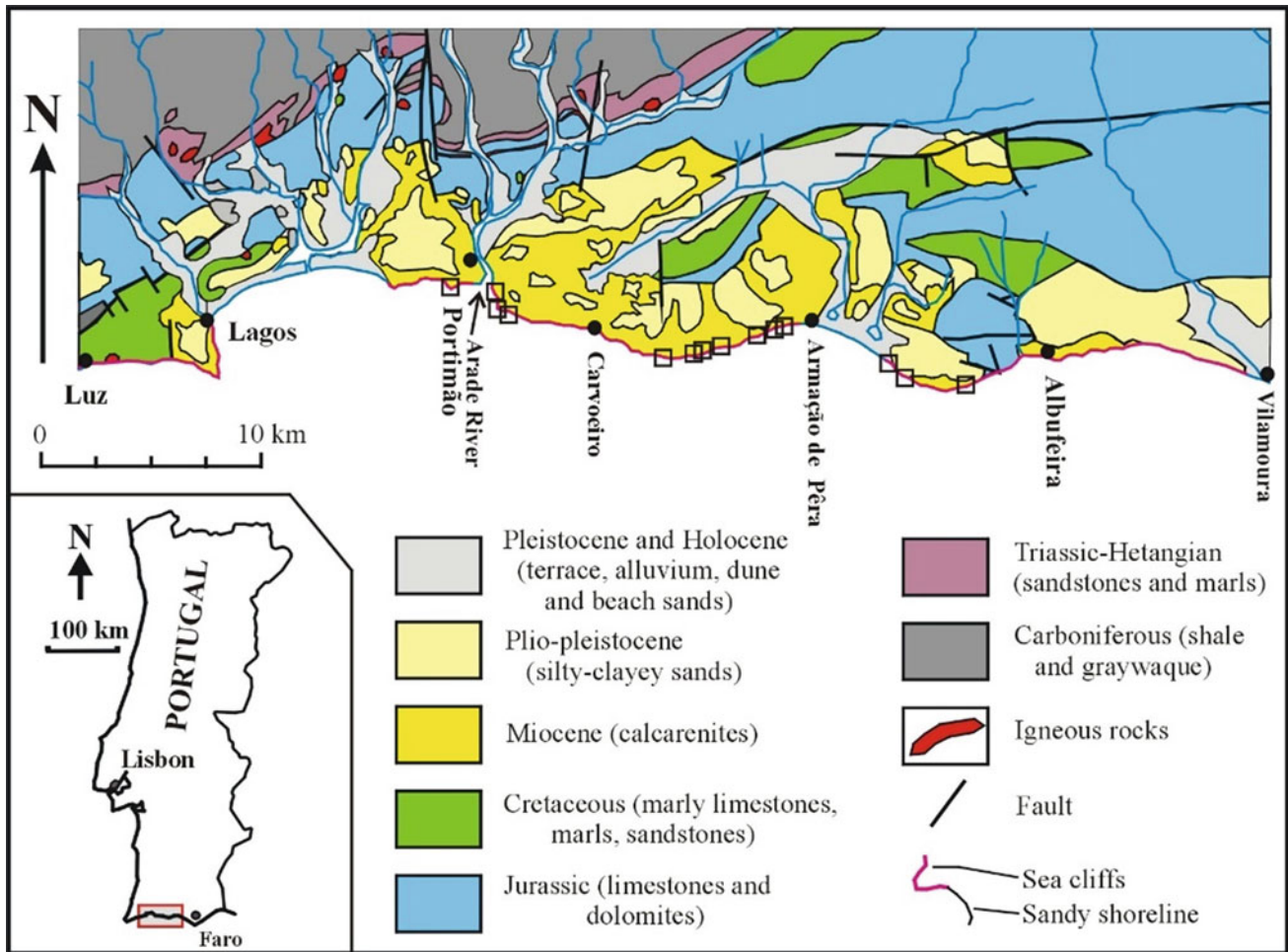


Fig. 1 Localization and geological map of the Central Algarve (details in Rocha et al. 1981, 1983). Square marks indicate locations of sample collection. From west to east: Pintadinho beach, Altar Point; Caneiros

beach; Alfanzina W; Carvalho beach; Benagil; Marinha beach; Algar Capitão-Caramujeira; Albandeira beach; Galé beach; Castelos point; S. Rafael beach

thickness exceeding 80 m (Silva 1988). The beds generally dip less than 6° to the east or south, except near Ponta dos Castelos (SW Portimão), with dip up to 15° – 20° to the west, due to a major N-S fault, and near Ponta da Atalaia (SW Albufeira) with dips also up to 18° .

The Miocene rocks were affected by intense karstification with variable morphological characteristics. Westwards of Arade River and eastwards of Armação de Pêra, the karst morphology is characterized by a high frequency of sinkholes, with diameters of a few to tens of metres their bottom located below the current mean sea level, with less frequent karst galleries. Limestone precipitations usually harden the sinkhole walls with strength much higher than the surrounding rocks. They are filled with Plio-Pleistocene reddish sandy-clay deposits, with little resistance to erosion. On the coast, the rapid erosion of the karst filling motivates its exhumation, which produces a highly irregular coastline,

with frequent sea stacks (see Marques 1997). In the sector between the mouth of Arade River and Armação de Pêra, along the coast, the karstification is dominated by galleries, sometimes with large sections (width of up to 30 m and visible heights of the order of 20 m) and the sinkholes present often correspond to the collapse of the gallery ceilings.

3 Methods, Results and Discussion

The laboratory tests were performed on block samples collected in the field in several locations (Fig. 1). The tests carried out included uniaxial compressive strength (σ_c); indirect tensile strength (Brazilian test) (σ_t); ultrasonic P wave velocity (v_{us}); water content; calcium carbonate content; dry unit weight (γ_d). The strength tests were made

considering the ISRM suggested methods (ISRM 2015) and adaptations imposed by the rocks' low strength and friable character. Also, in some of the σ_c tests, some specimens with height less than 2.5 times the diameter were used due to specimen preparation difficulties. The specimen for strength tests was drilled to provide cores with diameters of 53.5 mm and 44.5 mm. The rocks observed in several outcrops and sampled were grouped into four lithological types, which include: 1) Lumachelic calcarenite (CL); 2) Fine-grained calcarenite with macrofossils (CFM); 3) Fine-grained calcarenite (CF); 4) Calcrete (CC). The tests were made in several fields and laboratory campaigns made over the past two decades. Due to the varied availability of test equipment, it was not possible to follow the same testing protocol, i.e. using the same tests for all the rock samples collected in the field. In consequence, test results relations and comparisons are made within the ones which were made according to the same testing protocol.

The summary of test data is in Table 1. The results obtained indicate that these rocks are mainly composed of calcium carbonate, mainly composed of bioclasts weakly cemented, with a quite variable macrofossil content, and

correspond to calcarenites, despite other designations be found in the geological literature. As expected, test results show a very wide range of variations due to the large textural heterogeneity of these rocks. Dry unit weight varied widely, reflecting the variety of voids' density and volume in the matrix and the macrofossils moulds. The same happened with the ultrasonic P wave velocity, which corresponds mainly to a generally low strength rock. The σ_c values obtained for dry specimen were quite varied (Fig. 2) with more frequent results between 1 MPa and 7.5 MPa, with higher, less frequent values resulting from local stronger cementation. In contrast, the wet specimen provided much lower, more frequent values between 0.4 MPa and 4 MPa (Fig. 3).

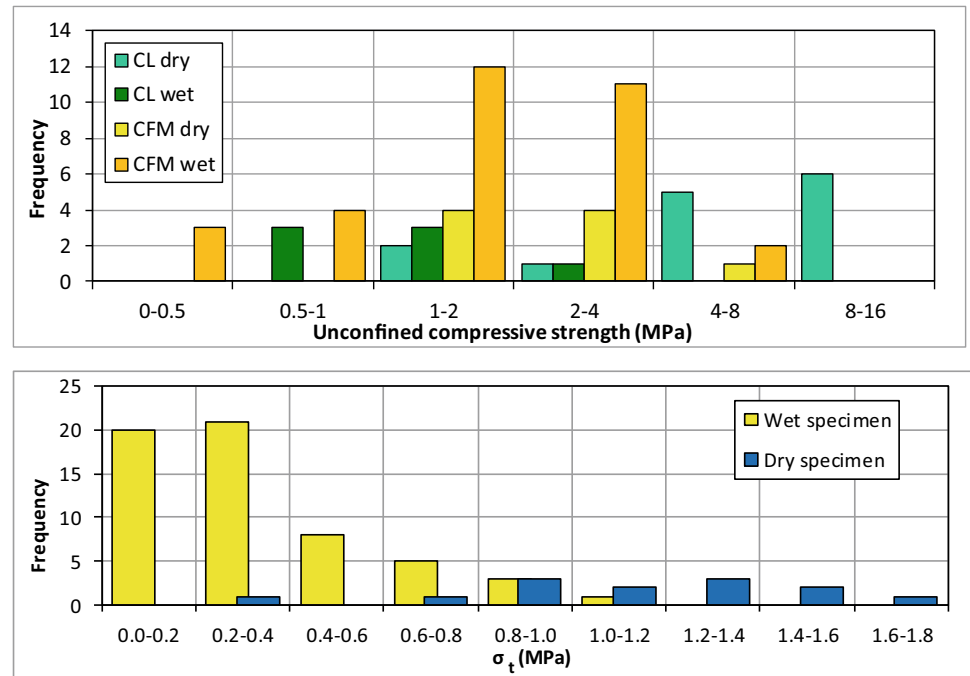
The median uniaxial compression test values indicate a strength decay of about 35% for CFM and 85% for CL. The Brazilian test results also indicate a strength reduction by wetting, with more frequent dry values between 0.8 MPa and 1.6 MPa. The corresponding wet values between 0.08 MPa and 0.8 MPa, providing a strength reduction of about 77% for CFM and 48% for CL, in opposition to the σ_c test values. The compressive to tensile strength ratio is low

Table 1 Summary of statistical data of the Miocene rocks testing

Property	Lithology	Median	Mean	Sd ¹	Min	Max	N ²
CaCO ₃ (%)	CL	89.4	86.8	9.9	64.8	98.1	52
CaCO ₃ (%)	CFM	74.9	72.9	11.0	53.1	93.7	56
CaCO ₃ (%)	CF	97.6	97.8	0.3	97.6	98.1	3
CaCO ₃ (%)	CC	93.8	92.9	2.1	90.0	95.4	6
γ_d (kN/m ³)	CL	18.4	18.8	1.9	16.2	25.1	71
γ_d (kN/m ³)	CFM	17.7	18.0	1.1	16.1	21.6	74
γ_d (kN/m ³)	CF	20.5	20.3	0.9	18.4	21.5	10
γ_d (kN/m ³)	CC	17.0	17.5	2.2	15.3	21.9	13
v_{us} (m/s)	CL	2742	2806	991	1510	5503	21
v_{us} (m/s)	CFM	1852	1946	391	1565	3070	18
σ_c dry (Mpa)	CL	8.40	11.62	13.05	1.26	54.64	14
σ_c dry (Mpa)	CFM	2.44	2.75	1.63	1.04	6.76	10
σ_c wet (Mpa)	CL	1.25	1.50	1.20	0.52	3.98	7
σ_c wet (Mpa)	CFM	1.56	1.89	1.22	0.34	5.79	32
σ_t dry (MPa)	CL	1.46	1.33	0.34	0.70	1.71	7
σ_t dry (MPa)	CFM	1.15	1.11	0.36	0.32	1.60	13
σ_t wet (MPa)	CL	0.76	0.97	0.83	0.09	4.55	93
σ_t wet (MPa)	CFM	0.26	0.32	0.22	0.07	1.09	86
σ_t wet (MPa)	CF	2.52	2.76	1.18	1.16	5.29	10
σ_t wet (MPa)	CC	0.85	1.11	0.89	0.30	3.47	13

¹—Standard deviation; ²—Number of tests

Fig. 2 Unconfined compressive (top) and indirect tensile (bottom) plot for dry and wet specimen



for the context of rocks, with a general value of about 6 for CFM and less than 2 in CL. These values and relations with the opposite character for the same lithology are quite puzzling, requiring further analysis and may reflect significant variations in the strength parameters mainly due to variations in cement content and fissures size and density in the same lithology. However, a not neglectable number of tests provided σ_c values lower than 1 MPa, suggesting that particular care must be taken when analysing field conditions for specific projects. This aspect is relevant mainly because, in the more current engineering projects, strength data tends to be only derived from SPT, which tend to provide N values above 60 blows, which does not provide a reliable picture of its strength.

In many cases, the SPT tests are made with the rock dry or near dry due to the local climatic conditions and rock mass saturation in rainy periods implies a considerable rock strength reduction. Were found some relations between wet specimen uniaxial compressive strength and CaCO_3 content and ultrasonic velocity (Fig. 3), with other relations, namely with dry unit weight, providing poor correlations, which are also due to the very heterogeneous character of these rocks.

4 Concluding Remarks

The Miocene calcarenites of the central Algarve are mainly soft to very soft rocks, which suffer a considerable strength reduction with wetting. The unconfined strength reduction depends on the rocks' fossil content, from circa 35% for CFM to 85% for CL, while in the indirect tensile tests, the rocks exhibited an opposite behaviour (less 77% for CFM and 48% for CL). Compressive to tensile strength ratios are lower than common values for most rock types, varying between 6 for CFM and less than 2 in CL. The results of the tests presented in this study may be a helpful reference and guidance for site investigation projects in the region. However, it is felt that further studies are required to get a more comprehensive knowledge of the geotechnical behaviour of the rock masses composed by these rocks. The low strength of the Miocene rocks coupled with the very frequent and extensive karst features indicate that the use of geophysical methods such as Ground Penetrating Radar (GPR) is highly recommendable, especially bearing in mind the low strength of these rocks, which may not be able to withstand heavy construction loads located near or over open karst voids.

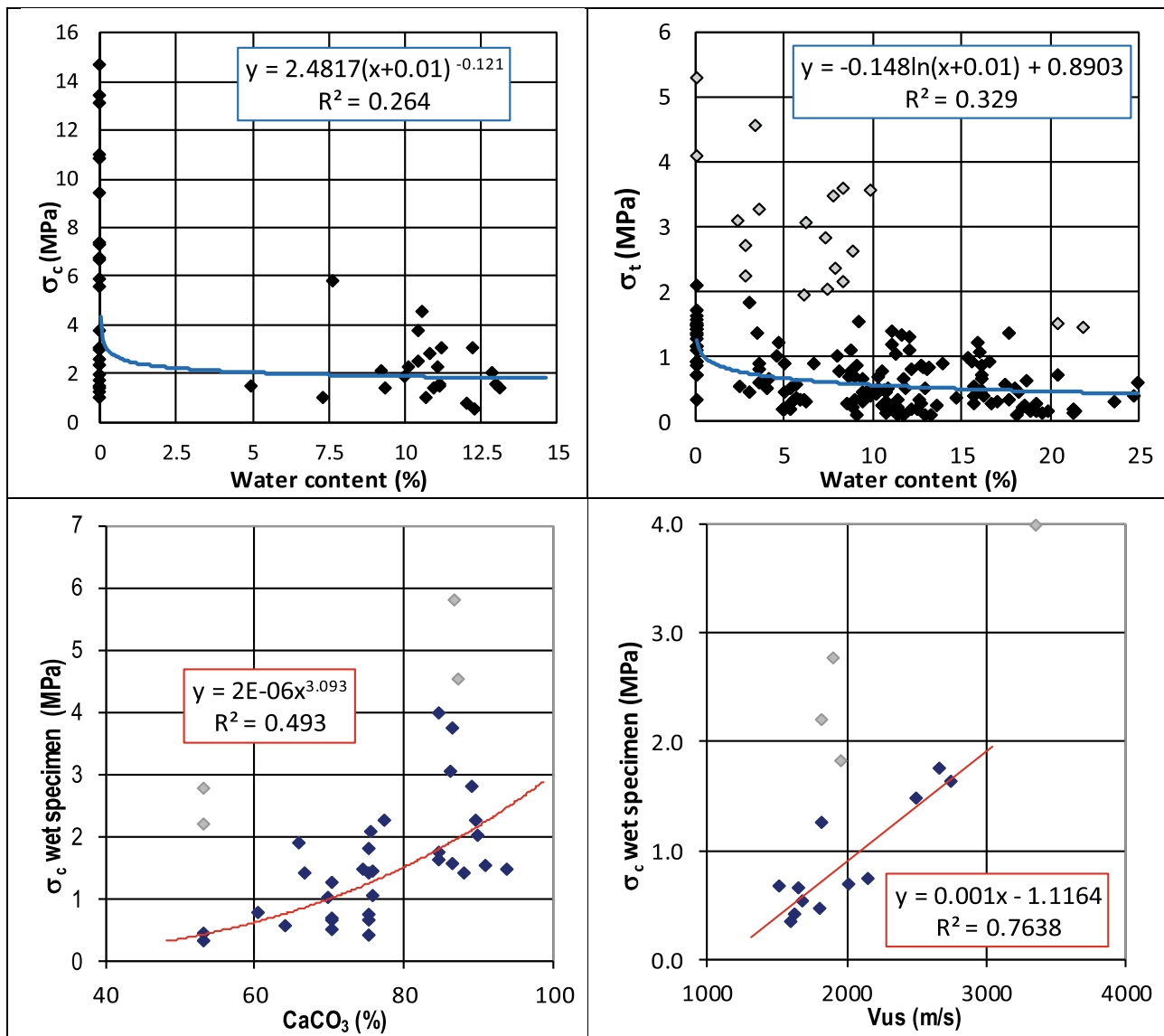


Fig. 3 σ_c (top left) and σ_t (top right) variation with water content. CaCO_3 (bottom left) and v_{us} (bottom right) variations with σ_c of the wet specimen. Grey marks indicate data points not used for correlations

Acknowledgements Acknowledgements are due to two anonymous reviewers, which helped to improve the manuscript. This work was funded by the Portuguese Fundação para a Ciência e a Tecnologia (FCT) I.P./MCTES through national funds (PIDDAC)–UIDB/50019/2020.

References

- Antunes MT, Pais J (1993) The Neogene of Portugal. *Ciências Da Terra*, UNL 12:7–22
- ISRM – International Society for Rock Mechanics (2015) The ISRM suggested methods for rock characterisation, testing and monitoring: 2007–2014. In: Ulusay R (ed.), Suggested methods prepared by the commission on testing methods, ISRM. Springer, Cham
- Marques FMSF (1994) Sea cliff evolution and related hazards in Miocene terranes of Algarve (Portugal). In: Oliveira R, Rodrigues LF, Coelho AG, Cunha AP (eds.), Proceedings of the 7th International Congress of the IAEG, Lisbon, A.A. Balkema 4:3109–3118
- Marques FMSF (1997) As arribas do litoral do Algarve: dinâmica, processos e mecanismos. University of Lisbon, Lisbon (PhD thesis)
- Rocha RB, Manuppella G, Marques B (1981) Geological map of Portugal in 1:50,000 scale, sheet 52-B, Albufeira. Serviços Geológicos de Portugal, Lisbon
- Rocha RB, Ramalho MM, Antunes MT, Coelho AVP (1983) Geological map of Portugal in 1:50,000 scale, sheet 52-A, Portimão. Serviços Geológicos de Portugal, Lisbon
- Silva ML (1988) Hidrogeologia do Miocénico do Algarve. University of Lisbon, Lisbon (PhD thesis)



Rock Quarries in Critical Situation in Portugal: An Overview

Mário Quinta-Ferreira, Isabel Fernandes, and Helder I. Chaminé

Abstract

Following a serious accident killing five people, resulting from a steep quarry slope failure in November 2018, the Portuguese authorities required that 191 “critical quarries” implement urgent procedures to achieve safe operating conditions. Frequent problems encountered in “critical quarries” are the lack of compliance with protection distances, the absence of fences, the existence of quite high rock slopes, insufficient stabilization procedures, unstable excavation slopes, poor drainage, and unsatisfactory planning. The characteristics of the ground, the permeability, discontinuity network or low strength seams must be studied, and preventive measures must be taken in time, avoiding accidents. As quarrying tends to create slopes, which, when not properly designed, can lead to unstable conditions, it is required that “critical quarries” must adopt urgent transition procedures to improve safety along with the exploitation process, assuring their economic viability. Quarrying must be carried out with the utmost respect for safety and the environment. The recovered areas can be an essential asset for urban occupation, waste deposition in landfills, recycling, or recreational areas.

Keywords

Quarry • Safety • Rehabilitation • Mineral mass • Portugal

1 Introduction

Quarries are fundamental to societies’ development and well-being as they provide irreplaceable raw materials for numerous economic activities, such as construction, ceramic, and chemical industries. In addition, quarry operations allow the extraction of a large variety of mineral materials, namely aggregates, ornamental stones, rock blocks, sands, clays, and plaster (e.g., Smith and Collis 2001; Bell 2004; Allington and Jarvis 2014). As defined by the Portuguese legislation (Decreto-Lei n.º 340/2007), a quarry is a set formed by any mineral mass subject to licensing, facilities, and associated areas.

Most of the Earth population lives in cities, requiring the availability of huge amounts of quarry products like aggregates, rock, and sand for the construction and maintenance of buildings and engineering infrastructures (e.g., Quinta-Ferreira and Trindade 1998; Smith and Collis 2001; Langer et al. 2004). For example, for the city of Istanbul in Turkey, 90 million tonnes/year of aggregates are produced (Tuğrul and Yilmaz 2018), which is almost three times the total aggregate produced in one year in Portugal (UEPG 2019).

Therefore, the consumption of processed mineral materials, of which aggregates are a good indicator, tends to accompany the economic progress and is dependent on economic and investment cycles (Quinta-Ferreira and Trindade 1998; Langer et al. 2004). The European Union (EU) has a low average aggregate consumption, around 4 tonnes per capita, with a downward trend (Langer et al. 2004). China’s strong economic growth has led to a large increase in aggregate production, reaching close to 17 tonnes

M. Quinta-Ferreira (✉)

Department of Earth Sciences, Faculty of Sciences and Technology, University of Coimbra, Coimbra, Portugal
e-mail: MarioQuinta-Ferreira@dct.uc.pt

I. Fernandes

Department of Geology, IDL - Instituto Dom Luiz, University of Lisbon, Lisbon, Portugal

H. I. Chaminé

Laboratory of Cartography and Applied Geology, Department of Geotechnical Engineering, School of Engineering (ISEP), Polytechnic of Porto, Porto, Portugal

Centre GeoBioTec|UA, Aveiro, Portugal

© The Author(s), under exclusive license to Springer Nature Switzerland AG 2023

H. I. Chaminé and J. A. Fernandes (eds.), *Advances in Geoenvironment, Geotechnologies, and Geoenvironment for Earth Systems and Sustainable Georesources Management*, Advances in Science, Technology & Innovation, https://doi.org/10.1007/978-3-031-25986-9_13

per capita, around four times the average EU production. The production of aggregates tends to be higher in higher-income countries.

2 Critical Quarries

On November 19, 2018, an accident killing two workers and three people travelling on a public road adjacent to a deep quarry in Portugal provoked an energetic reaction from state authorities, requiring that 191 quarries fully comply with the quarry law ensuring safe operating conditions. The so-called “critical quarries” were considered to contain one or more critical factors for people, assets, and the environment, resulting from their activity and their impact on the environment, regardless of the current state of licencing or activity (DGEG 2019).

Currently, there are approximately 2500 quarries in Portugal, of which 1074 (43%) correspond to quarries of class 3 and 4, which means that they are under the responsibility of the local administration, while the remaining 1426 quarries (57%) are from class 1 and 2 and are under the responsibility of the central administration (DGEG 2019). The 191 “critical quarries” correspond to 13% of the quarries of classes 1 and 2.

Of the 1426 quarries under central administration supervision, 51% have a complete licencing process, while 28% have to license but do not comply with the current administrative obligations of licencing, and 21% are in the licencing process. About 67% of the quarries are in

exploitation or recovery concerning their activity situation, 19% with the activity suspended, without authorization or abandoned. In comparison, 8% of the quarries are suspended with authorization, and only 6% are in the closing stage.

Considering the distribution by the “critical quarries” administrative licencing status, they are distributed by three main equal categories, with 32% each, namely licenced quarries, in-licencing process, and licenced but do not meet current administrative licencing obligations. There is still 4% of quarries where it was not possible to obtain information (DGEG 2019). Considering the distribution by activity situation of the “critical quarries”, it was concluded that 71% (136) are in exploration or recovery, that 15% of the quarries have suspended activities without authorization, that 4% (8) are closed, and that another 4% do not have conclusive information (DGEG 2019).

3 Critical Factors

Considering the Critical Factors for the 191 quarries (DGEG 2019), in 30% of the cases, the critical factor is the non-compliance with the minimum safety distance (see Fig. 1), while 70% result from other non-compliance technical requirements related to the quarry activity and other external occurrences. For 93% of the quarries (178), it is necessary to develop studies or projects to improve their safety. In comparison, 87% (166) need to improve signalling, and 74% (141) need to raise fences according to the

Fig. 1 Example from an insufficient safety distance of a high vertical quarry slope to a public road (photo: MQF)



stipulated law. Concerning the priority level for implementing the procedures, 34 quarries have a high level, a moderate level is for 76 quarries, and a reduced level applies to 81 quarries.

4 Plan for Intervention in Quarries in Critical Situation

Administrative procedures for notifying explorers and landowners were launched through DGEG (Directorate-General for Energy and Geology), so they assume their responsibilities and obligations without prejudice to the Portuguese inspection authorities' intervention and law enforcement authorities infringements are attributed to quarry operators. The Portuguese Mining Development Company (EDM, S.A.) ensures the acquisition and placement of signs in quarries in a critical situation representing a cost of 150,000 €. This action will be developed in articulation with the competent City Councils and other entities. At the expense of the explorers and landowners, the estimate for the interventions is 14.2 M€, considering 10.5 M€ for fences, and 3.7 M€ for preliminary studies and/or design. In addition, the Portuguese Environmental Fund will provide about 2 M€/year for EDM, S.A., to intervene in non-compliance by the owners, triggering a legal process to recover the funds used (DGEG 2019).

Implementing the stabilization procedures was not estimated because it requires a detailed design adjusted to the exploitation plan, under the responsibility of the quarry technical manager. Indeed, this is the largest amount of all the expenses involved in improving safety for the critical quarries and will be done at the expense of the quarry owners.

5 Most Frequent Problems

Among the most common problems encountered in "critical quarries" are the reduced protection distances (Fig. 1), which is considered the most critical issue, and unstable excavation slopes or relatively high rock slopes, making it challenging to implement stabilization procedures. Deficient drainage and insufficient planning of extractive activities are also very frequent.

Quarrying processes tend to create slopes mainly by excavation and fill, which can present unstable conditions when not properly designed or constructed. In quarry operation, it is also necessary to consider the characteristics of the rock mass, as discontinuities or low strength seams or layers must be fully studied. When necessary, preventive procedures can be taken in due time, avoiding accidents.

The lack of distance to protect objects and structures surrounding a quarry is a serious problem. In addition, the reduced space of high slopes frequently prevents or makes it difficult to achieve adequate stabilization, increasing costs. These situations usually require the construction of fill slopes to meet the law requirements, increasing the quarry's protection distance.

It is advisable that the quarries urgently adopt transition procedures to improve safety and the exploration process, assuring the quarries' economic viability. If producers cannot implement the stabilization procedures, the quarrying licence would be cancelled, creating a serious risk to unfinish the required works due to a lack of financial capacity. Many quarry owners find themselves with insufficient financial stability because of past conditions and procedures and the previous construction crisis. Suppose the interventions necessary to promote adequate safety will be forced to a large extent and in a short period. In that case, they will seriously compromise the economic viability of most quarries. Therefore, it is strongly recommended that all the works necessary to implement the required legal framework should be integrated into future extraction procedures during a reasonable span of time to allow the quarries companies to adjust to the legal requirements without a financial rupture. To achieve this goal, the role and guidance of the quarry's technical directors are crucial.

Looking to the past, in order to prepare for the future, it is clear that the work methodology of a large number of quarries must be improved in order to be prepared for a more demanding legal framework regarding safety, environment protection, and improvement of the quality of the quarry products. These challenges require better quarry management and a more efficient technical approach to maintain the quarry companies' long-term economic stability.

The fundamental role of the extractive industry in the progress and the lifestyle of societies must be discussed. Most citizens are not aware of the provenance and importance of commodities essential to their day-by-day comfort. However, they are sensitive to the environmental impacts, creating a basic antipathy to the extractive industry. This unsuitable framework must also be improved, leading to sharing responsibilities between producers, consumers, and legislators. The technical and legal frameworks will continue to be more and more demanding. However, we would like to address whether we are adequately preparing our higher education students for this difficult reality shortly.

The new quarry legislation that has already undergone public discussion and will be in force soon presents more demanding requirements for licencing and operation, including the protection distances that increase 50% to 100%, like for "rustic, urban or mixed neighbouring buildings, walled or not" passing from the present 10 m to 20 m (RP 2019).

Numerous other questions are still without an answer. However, the problems for quarries of classes 3 and 4 could be worst, as the local enforcing authorities tend to be more permissive, or even absent, on the surveillance processes.

6 Recommendations and Concluding Remarks

Quarrying must be carried out with the utmost respect for the environment, and it must be noted that impressive thought by Langer et al. (2004): “the disturbed terrain to build a community or a highway is about 100 times larger than the disturbed terrain to provide aggregate for these purposes”. Besides, the construction of infrastructure or community is permanent. Simultaneously, the exploitation of a quarry is transitory, allowing the recovery of the disturbed area, which can even be an asset for urban occupation by creating platforms for easier use and construction, as found in almost any city in the world. As a relevant example, in the city of Braga, in NW Portugal, we have a worldwide known football stadium that was built on a quarry site, that provided a suitable flat area for the field and slopes for benches for the spectators, significantly reducing the rock excavations and the earth moving operations. Furthermore, quarry sites can also be used for other essential uses for societies, like processing and depositing recycled materials and wastes, and new uses like recreational areas.

Knowing the critical situation in which many quarries owners find themselves because of past exploration conditions, incorrect procedures, and the economic crisis, the required interventions in the “critical quarries” will promote safety and a significant economic effort. It is possible that, if forced to a large extent and in a short period, it will seriously compromise the economic viability of most companies, now already very fragile. If producers cannot implement the stabilization procedures, the quarrying licence would be cancelled, creating a severe risk of incomplete the required rehabilitation due to lack of financial capacity. Therefore, the quarries should adopt urgent transition procedures to

improve safety and a more efficient exploitation process, assuring their economic viability and future activity.

Acknowledgements This work was supported by FCT—Fundação para a Ciência e a Tecnologia, through Portuguese funds, in the research project UIDB/00073/2020 of the Geosciences Centre of the University of Coimbra, UID/GEO/50019/2020—Instituto Dom Luiz and UID/GEO/04035/2020—Centre GeoBioTEC|UA.

References

- Allington R, Jarvis D (2014) A quarry design handbook. David Jarvis Associates, GWP Consultants, London
- Bell FG (2004) Engineering geology and construction. Taylor & Francis, Abingdon, UK
- Decreto-Lei n.º 340/2007 (2007) Revelação e aproveitamento de massas minerais. Ministério da Economia e da Inovação. Diário da República, 1.ª série — N.º 197 — 12 de Outubro de 2007, pp 7337–7374
- DGEG (2019) Plano de intervenção nas pedreiras em situação crítica. Direção Geral de Energia e Geologia, DGEG, Ministério do Ambiente e da Transição Energética, Lisboa. https://www.ccdra.gov.pt/docs/ccdra/gestao/Plano%20de%20Intervencao_nas%20pedreiras_em_situacao_critica.pdf. 11 March 2019
- Langer WH, Drew LJ, Sachs JS (2004) Aggregate and the environment: production, construction, and reclamation. In: American geological institute, environmental awareness series, vol 8. Alexandria, VA
- Quinta-Ferreira M, Trindade MF (1998) Alguns dados sobre a produção de geomateriais granulares. Comunicações dos Serviços Geológicos de Portugal 84(2): F66–F69. ISSN 0873-948X
- RP – República Portuguesa (2019) Consulta pública relativa ao projeto de Decreto-Lei que procede à regulamentação da Lei n.º 54/2015, de 22 de junho, no que respeita às massas minerais. https://www.consultalex.gov.pt/ConsultaPublica_Detail.aspx?Consulta_Id=157. Accessed 25 Feb 2021
- Smith MR, Collis L (eds) (2001) Aggregates: sand, gravel and crushed rock aggregates for construction purposes, vol 17, 3rd edn. Engineering Geology Special Publications, Geological Society, London
- Tuğrul A, Yılmaz M (2018) Aggregate mining in megacities and existing problems: an example from İstanbul, Turkey. In: Shakoor A, Cato K (eds) IAEG/AEG annual meeting proceedings, San Francisco, California, Springer Nature, Cham, vol 3, pp 85–89
- UEPG – Union Européenne des Producteurs de Granulats / European Aggregates Association (2019) Current trends for the European aggregates sector. [<https://uepg.eu/pages/trends>] (last accessed 2019/11/03)



Methodological Approach of Georesources Sustainability for Northern Portuguese Industrial Rocks

Paulo Pita and José Augusto Fernandes

Abstract

The sustainable development of mineral resources is currently one of the most significant challenges facing the global world, as it contributes significantly to the world economy and the preservation of raw materials. In order to add value to companies and promote the sustainable development of the extractive sector, several international initiatives have been trying to establish Sustainability Indexes for mining activity. Furthermore, current industrial policies seek economic goals with social and environmental rights by implementing sustainable development policies. The coordinated management of these three concerns is intended to contribute to the well-being and progressive improvement of citizens' quality of life. The implementation of an evaluation system for quarries that produce crushed stone, based on the integrated analysis of sectoral indicators in the economic, social, and environmental areas was the main objective of this work, which resulted from the development of an evaluation method that allows a qualitative and quantitative analysis of the performance of quarries from the point of view of their sustainability, in order to help improve the economic, environmental, and social performance of the country. The creation and adoption of economic, social, and environmental indicators adapted to Portuguese aggregate-producing quarries were developed. After analysing the referred sectorial indicators, a calculation method for creating a Sustainability Index was proposed, which was applied to 50 aggregate production quarries in northern Portugal.

Keywords

Sustainability • Indicators • Evaluation • Quarrying industry

1 Introduction

Sustainability is a subject that should be addressed in an interdisciplinary way. Sustainably inhabiting the world is a current obligation (Soares 2011). The concept of sustainable development may be considered generically a pattern of economic development in which the use of resources aims to meet human needs, preserving the environment so that these needs may be met not only in the present but also for future generations. The term “sustainable development” was used by the UN-WCED (1987), creating what has become the most quoted definition of sustainable development, namely: “Sustainable development is that which satisfies present needs without compromising the ability of future generations to satisfy their needs” (UN-WCED 1987).

Sustainable development no longer incorporates ecological and social problems but adopts multiple models with parallel economic viability and ecological viability. The concept of development thus became much more comprehensive, developing in parallel the redefinition of relations between human society and nature and, as such, a substantial change in the civilisational process itself (Jackson and Anderson 2009; Jackson 2013).

The concept of sustainability was created to imply a necessary interrelationship between social justice, quality of life, environmental balance, and the need for development with a carrying capacity that allows the viability of development processes. Furthermore, understanding environmental problems from a perspective more focused on natural sciences to a more comprehensive perspective, including in parallel the social issues, expanded the issues to a socio-environmental dimension, not ignoring the cultural

P. Pita
DGEG—Direção Geral de Energia e Geologia, Ministério do Ambiente e da Transição Energética, Porto, Portugal

J. A. Fernandes (✉)
Department of Geotechnical Engineering, School of Engineering (ISEP), Polytechnic of Porto, Porto, Portugal
e-mail: jap@isep.ipp.pt

GeoBioTec|UA, Aveiro, Portugal

issues and consequent adoption of more comprehensive public policies.

The challenge currently facing contemporary society is, on the one hand, to create jobs with sustainable environmental practices and, on the other hand, to raise the level of environmental awareness, enabling populations to participate more intensely and effectively in decision-making processes as a means of strengthening their co-responsibility in the supervision and control of the agents responsible for socio-environmental degradation. No less critical will be the need to ensure that an agenda for environmental sustainability does not ignore access to information by the communities, not ignoring that this is often difficult to understand and very dispersed. The communities' ease of access to information in implementing sustainable development concepts should be part of a policy to strengthen the various actors involved (Soares 2011). On the other hand, the sustainable development process is also described as economic development and poverty reduction while preserving the environment. By ensuring the preservation of the environment, we will be guaranteeing the longevity and long-term viability of ecosystems. At the same time, we will ensure social development and thus human potential.

To meet the objectives of sustainable development, the whole decision-making process must be equitable between the parties involved, transparent, and participated in by all the actors who are directly or indirectly called upon to take part in the decision-making processes, namely the populations as the main stakeholders in the actions to be developed. Thus, the planning and decision-making processes should ideally be supported on systematised analyses of structural and legal factors. Furthermore, within the structural factors, the analysis of technical/operational, economic, and management issues will be of primary importance to ensure the competitiveness and sustainability of the industrial activity.

Relating the issue of creating new sustainable development indicators with the particular activity of the quarrying industry for aggregate production, as it is known, this is an industry that exploits mineral masses and, given the exhaustible nature of these geological resources, it is necessary to create indicators that specifically allow the economic, social, and environmental performance of these industries to be evaluated. Nevertheless, on the other hand, this type of industry, given its intrinsic nature, requires that its analysis consider the stages of exploitation of natural resources and the stages related to the closure and post-closure operations of the exploited areas (Pita et al. 2009).

Concerning the quarrying industry in particular, within the scope of application of sustainable development policies, it is essential that for current generations, as well as for future generations, quarrying activity minimises environmental impacts through the adoption of corrective and mitigation measures, while at the same time contributing to the

promotion of the socio-economic well-being of the communities, directly and indirectly, involved, leading to the creation of wealth and jobs.

Thus, companies linked to this industrial activity are subjected not only to compliance with legal norms that regulate the access and exercise of this economic activity but, desirably, in addition to the compliance mentioned above with the various legal regulations, demonstrate that they have a sustainable industrial policy in the economic, social, and environmental performance (Viana 2012).

The objective of this work will be the presentation of a proposal for the adoption of a series of indicators that allow for an individual assessment, in an integrated way, of the economic, environmental, and social performance of each project (granite quarries), subsequently allowing, after the treatment of the information resulting from the analysis of the adopted indicators, the creation of a Sustainability Index. Thus, in a simple, practical, clear, and direct way, companies can assess their performance from the sustainability of their economic activity. Furthermore, this procedure will also allow companies to make an internal evaluation of the effectiveness of the adopted measures and, at the same time, allow third parties to have an objective, transparent, and impartial evaluation of the analysed projects (details in Pita 2014).

2 Indicators for the Evaluation of Quarry Producers of Aggregates

The work carried out was supported by the survey and analysis of data relating to 50 aggregate production quarries located in the North region of Portugal, in the Districts of Viana do Castelo-Vc, Braga-Bg, Vila Real-Vr, Bragança-Bgç, Porto-Prt, Aveiro-Av, Viseu-Vis and Guarda-G (Fig. 1).

The indicators adopted allowed selection parameters to assess compliance with the company's improvement goals within a certain period. In view of the foregoing, and for the indicators to be comparable, the results of the data analysis related to the enterprises reality must be tangible, observable, and quantitatively and qualitatively assessed, having the main following characteristics (Villas Bôas 2006; Pita 2014): (1) be easily measurable, accurately and precisely, being its selection indicator of better or worse performance of the actions that are intended to evaluate; (2) be easily observable; (3) be sensitive and reflect changes that occur during the over time; (4) be a guaranteed source of a quality of the data obtained for its determination; (5) be intelligible, in order to be easily perceptible in their construction and understanding by the analyst; (6) be easy to assign in order to determine who is responsible for their performance; (7) be selective and should be assisted with the analysis services or



Fig. 1 Location of the quarries studied in northern Portugal

processes, focusing on the relevant points and measuring their capacity and the characteristics of their use; (8) be comprehensive and must be compatible with what is expected of the company; (9) be easily comparable through the existence of reliable standards, and (10) be constant, allowing periodic performance evaluations of the companies over time, facilitating historical comparisons.

The indicators used to determine the Sustainability Index of aggregate production processes are related to three areas: economic, social, and environmental. Thirty indicators were adopted (10 economic indicators, 10 environmental indicators, and 10 social indicators) that allowed the evaluation of the individual performance of each quarry in an integrated way, scaling them according to their performance in each of the three areas indicated. Each indicator had a range of quantitative benchmarks whose minimum value is zero, and the maximum value is 1. In addition, strictly equal weight was adopted for each of the three areas evaluated, using 10 indicators from each area, all with the same individual weight. In this way, reading the indicators was made more accessible and intuitive (Fig. 2).

The economic indicators adopted for creating a Sustainability Index are intended to relate the economic performance of the quarries studied, with the creation of financial and patrimonial reserves that allow facing the environmental issues originated by the work of this type of industry. At the same time, these indicators allowed to relate economic and environmental issues to social issues directly and indirectly related to the activity of these industrial units (Fig. 3).

From the analysis of the 10 economic indicators used, 6 indicators, according to the scales used, had an Insufficient evaluation, and 1 indicator had a Very Insufficient evaluation. That is, 7 indicators had a negative evaluation (70%). On the other hand, only 3 indicators had a positive evaluation, one with Very Good performance, one Good, and another with Sufficient performance (30%). Finally, for the final calculation of each quarry's Sustainability Index, the sum of the averages of all the analysed economic indicators reached the total value of 4.72, which, according to the qualitative evaluation used, indicates a value of the overall performance of economic indicators Insufficient. It is recalled that the result of the 10 indicators should have a value between 0 and 10 (0 to 1 for each indicator individually).

Social indicators are quantities. Usually, statistics are used to translate social concepts quantitatively, sometimes conceptual, to produce information about the social reality analysed for research purposes, or in the present study, to monitor and evaluate the quarries' performance (Fig. 4).

From the analysis of the 10 economic indicators used, 3 indicators, according to the scales used, had a Very Insufficient evaluation, and 4 indicators had an Insufficient evaluation. That is, 7 indicators had a negative evaluation (70%). On the other hand, only 3 indicators had a positive evaluation with Very Good performance (30%). Finally, for the final calculation of each quarry's Sustainability Index, the sum of the average of each social indicator analysed reached a total value of 5.39, which, according to the qualitative evaluation used, indicates a value of the overall performance of social indicators Sufficient. It is recalled that the result of the 10 indicators should have a value between 0 and 10 (0 to 1 for each indicator individually).

Environmental indicators are quantified, easily understood information used in decision-making processes at all levels of society. They present characteristics of tools to evaluate certain phenomena, presenting their trends and



Fig. 2 Qualitative evaluation of indicators

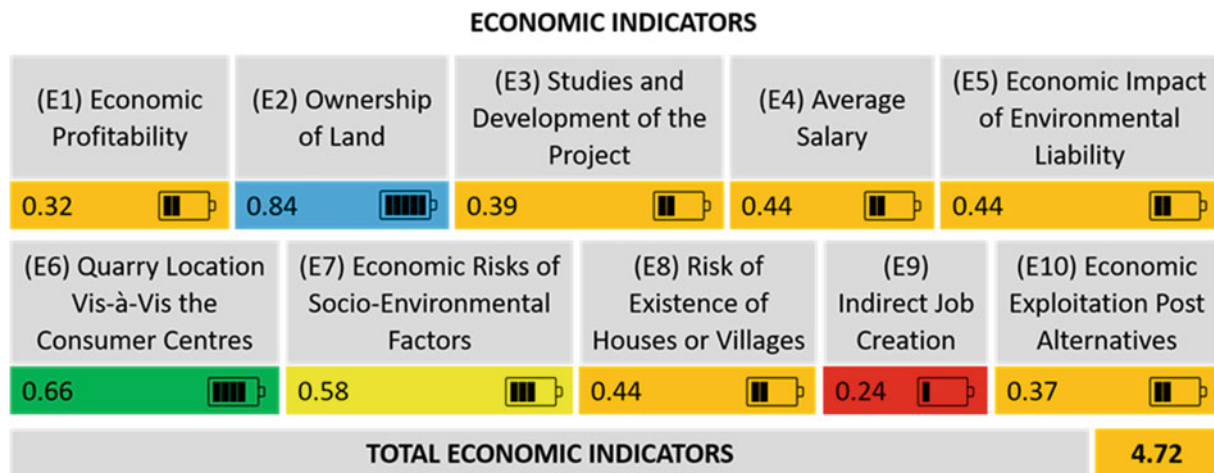


Fig. 3 Quantitative and qualitative performance of the economic indicators analysed

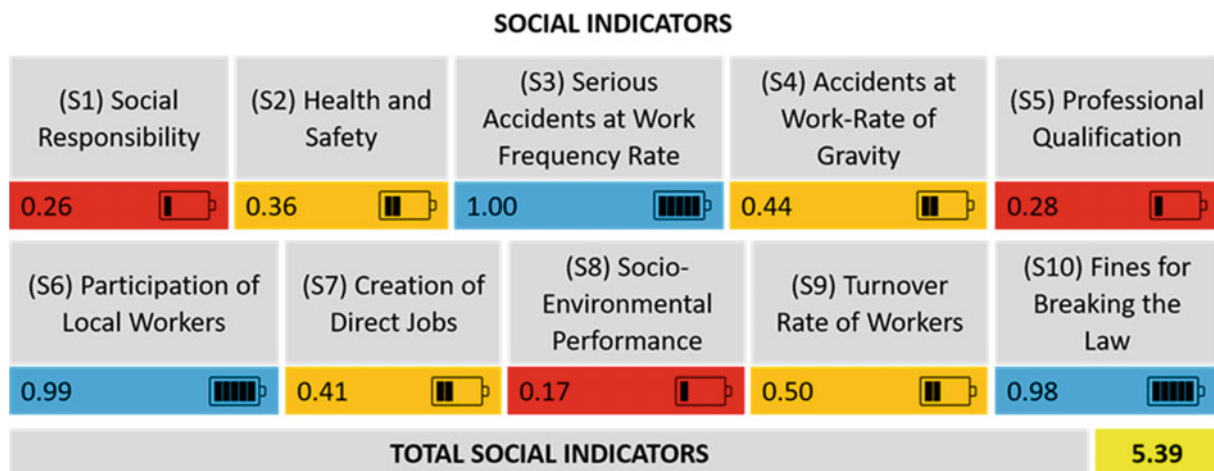


Fig. 4 Quantitative and qualitative performance of the social indicators analysed

progress that may change over time. They should simplify the level of information contained to illustrate a given reality simply and clearly. Environmental indicators are selected statistical quantities representing or summarising some aspects of the environment, natural resources, and human activity that interact with them (Fig. 5).

From the analysis of the 10 environmental indicators used, 5 indicators, according to the scales used, had a Sufficient evaluation, and 2 indicators had a Very Good evaluation, that is, 5 indicators had a positive evaluation (50%). On the other hand, only 5 indicators had a negative evaluation, 2 with Very Insufficient performance and 3 with Insufficient performance (50%).

Finally, for the final calculation of each quarry's Sustainability Index, the sum of the averages of each environmental indicator analysed reached a total value of 5.34, which, according to the qualitative evaluation used, indicates a value of the overall performance of environmental

indicators Sufficient. It is recalled that the result of the 10 indicators should have a value between 0 and 10 (0 to 1 for each indicator individually).

3 Sustainability Index: Analysis of the Results

An integrated analysis of these three sectorial assessments was also made to obtain a Sustainability Index for each analysed project. The creation of this Index intends to allow for integrated analysis of the industry's performance to respond to the new evaluation needs arising from applying the principles underlying the concept of Sustainable Development.

After calculating the economic, social, and environmental indices for each of the 50 quarries analysed, a global analysis of the results obtained for each studied area and a proposal for calculating the Sustainability Index is presented. From

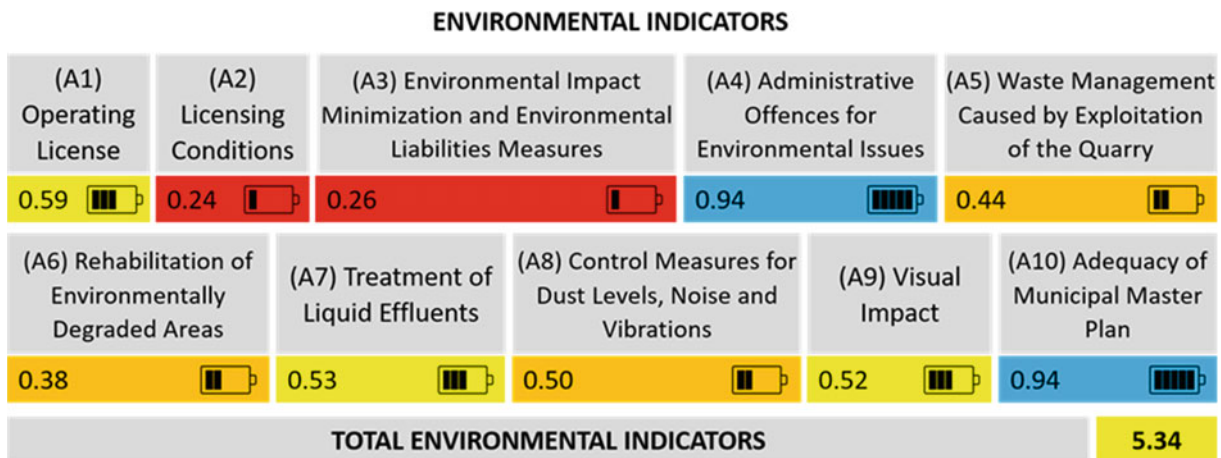


Fig. 5 Quantitative and qualitative performance environmental indicators of the indicators analysed

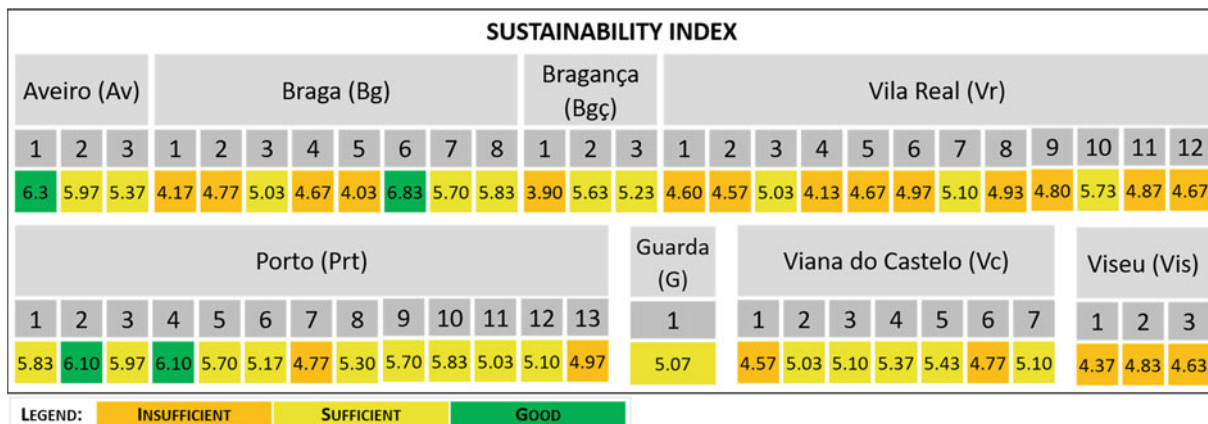


Fig. 6 Calculation of sustainability indices for the quarries analysed

the analysis of Fig. 6, which summarises the values of Sustainability Indexes calculated for each of the 50 quarries evaluated, it can be concluded that 29 achieved a positive assessment, which is 58%. Of these, 25 have obtained a

Sufficient rating and 4 a classification of Good. None of the quarries got a Very Good rating. The remaining 21 quarries obtained negative notes, having all obtained Insufficient classification. No quarry was rated Very Insufficient (Fig. 7).

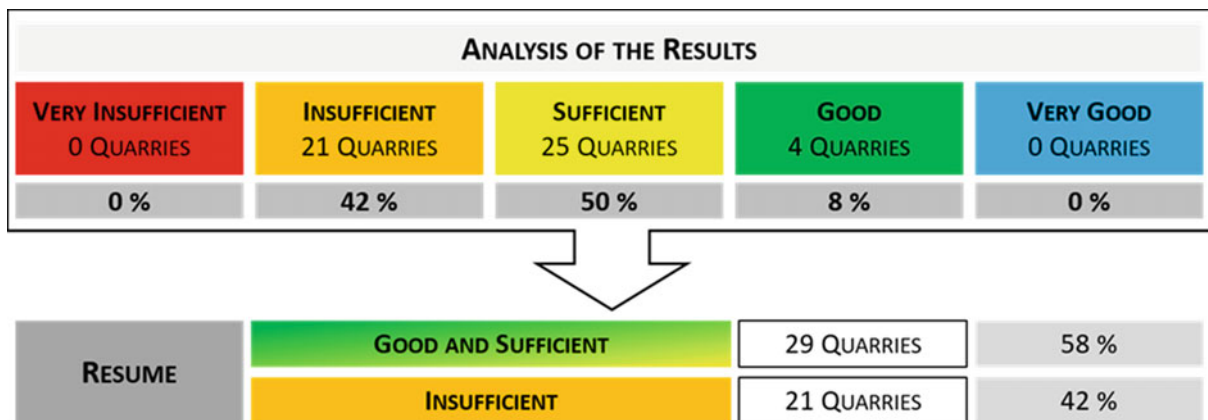


Fig. 7 Analysis of global results

4 Concluding Remarks

The calculated Sustainability Index allowed the integration and linkage of several sectoral indexes to be undertaken and quantitative and qualitative analyses of the 50 quarries' performance. In this way, it was possible to verify that the districts of Aveiro and Porto are above the global average of 5.15, registering a positive deviation and the remaining districts were below the referred global average, registering negative deviations. From these, the districts that have more positive results (Aveiro and Porto) are situated in the coastal zone that is more developed than the interior districts of the country. In this point, the geographic situation of the companies that have the most significant dimension in the coastal region, compared to the companies in the northern part of Portugal, is decisive.

From the analysis of the final results, it can be seen that most of the studied companies persist in not taking advantage of the gains that a good environmental performance can induce in the economic performance of the studied industrial units through improvements in the efficiency of the work methods optimised by the realisation of alternative projects that could generate economic gains in the companies that exploit the quarries. It should also be remembered that quarries with a better environmental performance at implementing integrated environmental management systems are generally more economically competitive from being better prepared to compete in a competitive market.

It should be noted that a good environmental performance will certainly allow better and easier integration of the quarry companies in the community where they are located, and they should invest more in the dissemination of their economic, social, and environmental activities internally and externally. It is also worth highlighting that in the 10

environmental indicators adopted. There is an imbalance between the results obtained for each indicator, leading to companies' worse economic and social performance. Therefore, the improvement of the environmental performance of the companies, if the actions for their realisation are carried out in a balanced and interconnected way, will allow an improvement in the overall performance of the companies.

References

- Jackson T (2013) Prosperidade sem crescimento. In: *Economia para um Planeta Finito*. Edições Tinta da China, Lda., Lisboa
- Jackson T, Anderson V (2009) Redefining prosperity. *Essays in Pursuit of a Sustainable Economy*, London
- Pita P (2014) Sustentabilidade dos georrecursos: proposta de definição de índice de sustentabilidade para pedreiras produtoras de agregados. Instituto Superior de Engenharia do Porto, Porto. <http://hdl.handle.net/10400.22/6254> (MSc Dissertation)
- Pita P, Farinha Ramos JM, Pereira AP, Teixeira Torgal MC, Lourenço GT (2009) PROT-n: plano regional do ordenamento do território. Recursos Geológicos e Hidrogeológicos da Região Norte, CCRN – Comissão de Coordenação da Região Norte, Porto
- Soares C (2011) Desenvolvimento sustentável versus vida sustentável. In: Soares C, Martins N (eds) *A sustentabilidade do Planeta. Leça da Palmeira, Letras e Coisas – Livros, Arte e Design*, Soc. Unipessoal, Lda., pp 51–71
- UN-WCED – United Nations World Commission on Environment and Development (1987) *Our common future*. Report of the world commission on environment and development (document A/42/427), Brundtland commission, vol 4. Oxford University Press, New York
- Viana MB (2012) Índice de sustentabilidade da mineração (ISM). Universidade de Brasília, Brasília, Brazil (PhD Thesis)
- Villas Bôas RC (2006) Sustainable indicators for the extraction minerals industries. CETEM – Centro de Tecnologia Mineral, Rio de Janeiro, *Série Estudos e Documentos*, 68:1–33



Marble and Limestone Dimension Stone By-Products

Ruben Martins, Luís Lopes, and Tiago Alves

Abstract

The Portuguese carbonated dimension stones industry is annually responsible for one million tonnes of by-products, whose feasibility of application in other industries is the target of this study. With extraction yields values particularly in the Alentejo marble quarries vary between 10 and 25% (very different and lower in marbles than in the limestones), 1,251,540 tonnes of marbles and limestones were quarried in 2019 by the Portuguese Directorate-General for Energy and Geology (DGE). So, there is undoubtedly an enormous potential associated with those by-products. Large-scale industrial application is strongly conditioned by the distance between the extractive and processing units and any subsidiary industries that could use them, thus contributing to the more rational use of these raw materials, it is essential, therefore, to demonstrate their experimental behaviour with the aim of captivating companies to quantify the costs inherent in their use and include them in their production processes. Some physical and chemical properties of the residual soils (“*terra rossa*”, “*red soil*”), cutting, sawdust, polishing sludge, and non-dimensional blocks, usually accumulated in heaps, were determined in order to indicate possible and/or economically viable uses for these raw materials. For example, the application tests in the ceramic industry; manufacturing tiles; in compact marbles; in the paper industry; as a sealant in municipal

solid waste landfills and traditional ceramic applications of “*terra rossa*” are presented.

Keywords

Dimension stone by-products • Estremoz marble • Portuguese limestone • Life cycle assessment

1 Introduction

Any extractive industry is characterised by its high environmental impact, the dimension stone is no exception, being responsible for producing a large amount of by-products because the extraction yields are relatively low (ASSIMAGRA 2001). Its processing also produces huge quantities of small fragments and slurries (carbonated sludges) for cutting and polishing. Extraction and processing continuously produce rock fragments, considered rejected mineral mass accumulated in “heaps” in the open sky. The slurries usually undergo sedimentation processes for water reuse. The concentrated solid charge is then also accumulated in open sky deposits. On the other hand, because of the initial exploitation phases, corresponding to uncovering the top layers of the soil, for the cavities expansions, the residual soils called “*terra rossa*” are also accumulated in heaps, usually close to cavities, without any treatment or industrial use.

2 Materials and Methods

2.1 Carbonated Sludges (Slurries)

Tests conducted with different samples of slurries collected in sawmills located in the Estremoz Anticline allowed a detailed characterisation of these by-products, which are extremely thin by granulometric standards, almost 99.80%

R. Martins · L. Lopes (✉) · T. Alves
Departamento de Geociências, Escola de Ciências e Tecnologia,
Universidade de Évora, Évora, Portugal
e-mail: lopes@uevora.pt

L. Lopes
Instituto de Ciências da Terra (ICT), Pólo de Évora, Évora,
Portugal

T. Alves
Direção Geral de Energia e Geologia, Divisão de Pedreiras do Sul,
Évora, Portugal

of its particles are less than 40 μm , thus increasing the possibility of its direct application in other industries. Furthermore, chemical analysis revealed a high degree of purity material, well-illustrated in the calcium oxide amounts ($\text{CaO} > 50\%$) and loss on ignition tests ($\text{CO}_2 > 40\%$). However, to be used as raw material, their deposits stay as “pure” as possible, without any other contamination.

2.2 Residual Soil Deposits (“*Terra Rossa*”)

“*Terra rossa*” is a residual soil resulting from carbonate rocks’ dissolution with depleting of silica and enrichment in iron oxides and hydroxides. The mineralogical, chemical and physical characteristics give this material a high plasticity index and good workability. Therefore, it can be used as a good raw material for the ceramic application, particularly in traditional pottery. The research was based on the formulation of various ceramic pastes with different percentages of “*terra rossa*” and slurries after a physical and technological characterisation of these two raw materials. The characterisation tests (granulometric analysis, Atterberg limits, expansion test, organic matter test and mineral composition) were realised at the Geosciences Department laboratories. The technological tests were carried out in CENCAL (Training Centre for Industrial Ceramics in Caldas da Rainha), including shaping, drying, baking samples, the percentage of linear retraction, and the water absorption percentage flexural strength thermal-dilatometric analysis. In the end, it was also conducted an industrial test at the Olaria XT pottery in Redondo village, which aim to evaluate the shaping and conformation of the ceramic pieces on the potter’s wheel the capabilities to dry them at room temperature, and then subsequently the baking of the pieces at temperatures of 900, 1000 and 1100 $^{\circ}\text{C}$.

2.3 Heaps of Dimension Stones Industry By-Products

Rock fragments of heterogeneous dimensions constitute the heaps’ deposits. The older ones’ cores can have smaller dimension fragments due to the lesser load capacity of the vehicles used at that time. These deposits have massive volumetric blocks, sometimes exceeding 1 m^3 , disorderly arranged in the flanks and slopes with many gradients, enhancing the sliding risk. Except for situations where the cavities are found near urban centres or already had reached the lower limit of the rock deposit, the filling process of the cavities can make the quarry unviable for the resumption of the operations so, it is strongly not recommended. However, using these stone materials in road and railway construction or other calcium carbonate consumer industries seems to be

the logical point of view, thus mitigating the environmental impacts of this kind of deposits. Furthermore, the possibilities of using abandoned quarry cavities for other purposes are numerous, transforming them into simple water reservoirs, play areas, adventure tourism, etc.

3 Results

Carbonate slurries can operate as a flux in an earthenware paste and as a degreasing product by reducing excessive plasticity induced by the clay component and a consequent contraction of the ceramic body facilitating the drying process. As stated before, it has almost entirely made up of calcium oxide. In low quantities but with significant concentrations for possible industrial applications, silica (SiO_2) and aluminium (Al_2O_3) oxides are also present. The magnesium oxide content varies with the degree of dolomitisation of the samples. By the pycnometer method, the slurries showed an average density value of 2.72, and 99.80% of the particles are less than 40 μm , therefore considered an extremely thin material.

The whiteness degree is a fundamental characteristic of the industry that uses calcium carbonate as a raw material (Delgado 1995). Therefore, the brightness (expressed by the reflectance measured in the blue filter, $\lambda = 457 \text{ nm}$), and the yellowness (expressed between the reflectance measured on the blue filter and the reflectance measured on the yellow filter $\lambda = 570 \text{ nm}$), are expeditious measurements used for its evaluation. According to the ISO standard, two pressed tablets for each sample were tested in a Zeiss Datacolor Elrepho 2000 optical tester. Average values of 82.06% brightness and 7.81% yellowing for unprocessed sludges, 81.72% brightness and 8.25% yellowing for sludges with a granulometric cut of fewer than 10 μm were obtained.

Regarding the consistency limits, the plasticity index values are very low, between 1 and 3%, giving this material a non-plastic behaviour. According to the calculation of the group index (Martins 1996), in which a nominal value of 8 was obtained, being considered as silty, non-plastic or slightly plastic materials, classifying reasonable this product for landfill foundations if it is integrated into bituminous mixtures for road construction works will have better performance (Martins 1996).

The slurries expandability characterisation test is mandatory in road and civil construction, sealing landfills in the cement industry. The test was focused on unprocessed samples and a 38 μm granulometric cut sample. It was verified that these materials have a very rapid expansion during the first minutes and then decrease until stabilising after a few hours. Values ranging from 4 to 8% of expandability were obtained with water content levels close to 24%. As a comparative term, clays have slower but longer

expandability, sometimes over 48 h, with values above 20%. However, and as an example, a silty-clay material may already have expandability values in the order of 10% (Martins 1996).

3.1 Ceramic Industry—Ceramics

The tests' result enhances the flexural strength value when baked at a temperature of 1005 °C, which was 328.2 kgf/cm². This value is even better than the value found for a default folder which is 313.1 kgf/cm². Another point to note was that the experiment has a dry retraction/baked value at 1005 °C of 0.37%, which is lower than the default folder's value (0.62%). The ceramic pieces' demoulding time took 10 min less than the time measured for the default paste, an essential parameter regarding the industrial feasibility (Martins 1996).

3.2 Ceramic Industry—Manufacturing Tile Flooring for Fast Single Firing

The micronised calcium carbonate is currently embedded in contents not exceeding 15% on clay-based binders used to manufacture ceramic coating tiles by the single-fired process. These tests were performed in SORGILA company, where a default paste "E1" was served compared to the other five ceramic pastes. In E2, E3 and E4 ceramic paste, the traditionally used calcite (13%) was entirely replaced by slurries from three marble sawmills. In E5 and E6 ceramic pastes, half of the calcite was replaced by carbonated sludge. For the temperature of 1100 °C and a cooking cycle of 65 min, E3, E4 and E5 pastes are more advantageous than the default paste E1 because the measured resistance values are about 100 kgf/cm² higher. For the other parameters, it was possible to verify that they have lower water absorption. Additionally, they contain percentage values of baked-dry shrinkage of around 1%, within the allowable limit of <2% (Ventura 2007). Of all the studied ceramic pastes, it was possible to obtain the pastes' best values where the slurries were introduced rather than the default ones.

3.3 Compact Marbles for Flooring and Coverings

Several trials were conducted at a laboratory scale in the RMC company. The calcium carbonate produced from the lime grinding was substituted by a carbonated sludge mix from marble and limestone dimension stones plants. These tests also used rock fragments, polyester resin and a colourant that confers to the matrix the desired shade. The

studies culminated in the preparation of a 70.265 m³ (3.00 × 1.25 × 0.70) m block. After drying, this block was cut into polish plates. It was found that the rock-mass connection was perfect, without revealing any ridges or grooves at the interfaces. There was a good response for the polishing, with a balanced brightness over the entire plate. The tests showed that the fabricated plates assembled the requirements to be sold (Martins 1996).

3.4 Paper Industry

Tests performed in RAIZ—Instituto de Investigação da Floresta e Papel used slurries as filler, which suffered a wet dimension cut to 38 µm and reduced to 10 µm by suspended sedimentation. Several printing and writing paper sheets of approximately 80 g/m² were manufactured, replacing the kaolin commonly used for the carbonated sludge in 0% (containing only cellulosic fiber), 10, 20 and 30%. Weight, thickness, density and index hand, ashes, optical properties, mechanical properties (burst index and tensile breaking by tearing), porosity and air permeability and smoothness tests were conducted. The results were less than expected, given some randomness. For example, the paper sheet with 20% mineral filler did not obey the general behaviour in the weight test. In the thickness test, the sample with 30% mineral filler revealed an abnormal value, having also checked disparate values in density and the hand index in papers with 20 and 30% of mineral filler. However, despite these anomalous values, it may be considered that overall, the test was positive, so it would be interesting to continue this research (Martins 1996).

3.5 Sealant in Landfills of Solid Urban Waste

This study intended to carry out the accreditation of marble slurries as a confining material for solid urban waste in substituting the usual synthetic materials and other clay materials. Nevertheless, first, it is essential to clarify that using these materials in the dumps can help contain debris, prevent it from being blown away by the wind, and minimise the washing of waste by rainwater and its infiltration.

The determination of the natural water content, the Atterberg limits, the determination of the maximum dry apparent density and the optimum water content tests were carried out on slurries samples collected in Estremoz and Vila Viçosa plants. In addition, groundwater analysis to evaluate possible contaminations were done. Cylindrical specimens with 1032 mm diameter and 117 mm height were used to determine the permeability coefficient, reconstituted in the laboratory with the compaction energy corresponding to the normal proctor test and the water contents that varied

between 14 and 19%. These test pieces were mounted in triaxial chambers, applying a 100 kPa pressure confinement, followed by the test pieces' saturation, with a constant load using a hydraulic gradient of 15. After these tests, it was possible to verify that the carbonated sludge collected has a non-plastic behaviour. Regarding permeability, the values obtained are lower than the values described in the specifications for sealing works, which is suitable for its application for covering the surfaces of the dumps (Martins 1996).

Perforated 80 cm columns were used in the “in situ” permeability test, subsequently saturated with water, to make the permeability calculation. The values were later compared with other methods already recognised, where it was found that although the slurries are not impermeable, their use can be considered in situations where the degree of confinement to be required is less than that conferred by artificial materials, such as clays, geotextiles and geosynthetic materials (Martins 1996). Therefore, the existing amount of slurries in the Estremoz Anticline, coupled with the lack of clay exploration in the district, increase the hypothesis of using these materials as sealing material, even because the application of these by-products still represents a cost almost three times lower in the construction of this type of containment solutions in dumps. This way, in addition to obtaining an environmental benefit, we also obtain a financial advantage (Martins 1996).

3.6 Residual Soil in Traditional Pottery

For this study, three samples: Biblio VV, Borba VV and Lagoa, were analysed. After industrial tests, it was concluded that the Biblio VV and Lagoa samples offered an excellent response to various requests, revealing themselves as fat clays (very plastic) and having improved workability

when compared to traditionally ceramic pastes used by the potters. Alone they can also be considered ceramic paste. However, it is advisable to mix them with more thin clays (Alves 2015). All samples had a very fine granularity, with a strong clay fraction component, which varies between 54% in the Biblio VV sample and 66% in the Lagoa sample, with a good granulometric distribution. The main difference between them is the parameter D50 of the soil, where 50% of the Biblio VV sample particles are less than 15 μm , 50% of the particles of the Borba VV sample are less than 25 μm . Finally, 50% of the particles of the Lagoa sample are less than 10 μm . In terms of plasticity, the Lagoa sample proved to be the most plastic with a plasticity index equal to 25%. On the other hand, the Borba VV sample showed the lowest plasticity value (13%). Regarding the expandability test, Biblio VV is the highest one (13%), Borba VV and Lagoa samples showed expansibilities of 4% and 8%, respectively (Alves 2015). The mineralogical semi-quantitative determination revealed a strong contribution of phyllosilicates (Biblio VV—73.75%, Borba VV—48.16%, Lagoa—54.36%). The Biblio VV sample is essentially illite, while the Borba VV and Lagoa samples have a representative percentage of illite and kaolinite. In addition, all the samples revealed quartz (Biblio VV—15.04%; Borba VV—36.10%; Lagoa—31.85%), K-Feldspar (Biblio VV—3.05%; Borba VV—11.56%; Lagoa—5.46%) and goethite (Biblio VV—8.16%; Borba VV—4.19%; Lagoa—8.32%) (Alves 2015). Technological results showed excellent workability, namely in the respective test pieces' extrusion and conformation (Table 1).

The bigger MRB (mechanical resistance to bending) values are associated with the higher clay containing raw materials. As smaller the retraction value is, the greater the absorption percentage value, which is justified by densification and closing of the ceramic piece's porosity. Also,

Table 1 “*Terra rossa*” technological test results (adapted from Alves 2015)

Cooking level (°C)	% Retraction dry/cooked	% Retraction total	MRB (kgf/cm ²)	% Absorption
900	Biblio VV—1.86 Borba VV—1.08 Lagoa—0.97	Biblio VV—7.46 Borba VV—6.24 Lagoa—7.03	Biblio VV—136.92 Borba VV—78.60 Lagoa—116.00	Biblio VV—25.1 Borba VV—20 Lagoa—22
1000	Biblio VV—8.88 Borba VV—4.54 Lagoa—6.92	Biblio VV—14.68 Borba VV—9.70 Lagoa—11.88	Biblio VV—319.58 Borba VV—161.08 Lagoa—291.93	Biblio VV—9.3 Borba VV—12.3 Lagoa—9.6
1100	Biblio VV—11.19 Borba VV—5.12 Lagoa—9.46	Biblio VV—16.31 Borba VV—10.88 Lagoa—14.17	Biblio VV—409.78 Borba VV—184.84 Lagoa—374.34	Biblio VV—4.3 Borba VV—8.5 Lagoa—4.9

Table 2 Composition of the formulated pastes (adapted from Alves 2015)

Pastes	Composition
1	50% Borba VV + 50% Biblio VV
2	80% Biblio VV + 20% of silica sand
3	65% Lagoa + 35% Borba VV
4	88% Lagoa + 12% marble “cream”
5	65% Lagoa + 23% Borba VV + 12% marble “cream”

when more significant total retraction values occur, higher values of mechanical resistance and therefore lower absorption, thus reflecting more closed structures with smaller pores as it increases the cooking temperature. Despite the low values of mechanical resistance to bending in raw, it was possible to handle the ceramic pieces without causing defects, with a substantial increase of these values with the rising cooking temperatures, up 950 °C (cooking temperature used by the potters). The study continued with the formulation of five different pastes (Table 2) and a comparison between them and the others traditionally used by potters, Interpastas (Portuguese) and Pasta Collet (Spanish).

Regarding the formulations, all the pastes showed excellent workability. The plasticity of paste 1 allows the rise of the pottery pieces in height. Paste 2 is more plastic, and therefore not advisable to use it in clay pieces with open parts, and in this case, it also requires an addition of a higher percentage of degreasing product (20%). The paste 3 proved to be similar to the potter’s traditionally used potter (Mestre Xico Tarefa) and revealed itself more refractory than the pastes mentioned before, which is crucial to sustaining the thermal shock firing process at higher temperatures. Paste 4 was considered the ceramic paste with higher plasticity and relatively low flexural strength values, although the pieces are easily manipulated during and after the drying process. Finally, paste 5 presented excellent workability, and it was less plastic than the previous ones. It was also noticed that the lower values of total retraction percentage in the dry and cooked pieces are associated with the use of the marble slurries, which acts as a degreasing agent, reducing the ceramic pastes (Alves 2015).

4 Discussion

In the particular case of carbonate dimension stone extractive industry, there is no chemical, environmental impacts. Nevertheless, substantial changes to the original topography due to quarry cavities and rock heaps cause visual impacts in the landscape. In addition, the use of abrasive material for ornamental stones polishing, giving them a final shine finish,

as well as the application of flocculating products to promote the solid load precipitation in decantation tanks, may compromise the use of carbonated sludge, particularly in more demanding industrial sectors, such as chemical and pharmaceutical industries.

Chemical analysis carried out on carbonated marble sludge mentions that metallic elements, possibly from the metal alloys of the cutting and polishing tools, are present in trace amounts, such as Cd (<5 ppm), Co (<25 ppm), Cu (19 ppm), Ni (21 ppm), Pb (21 ppm), W (8 ppm), MnO (<200 ppm), TiO₂ (<200 ppm), Fe₂O₃T (<200 ppm) (Martins 1996). However, it seems necessary to develop studies in order to ascertain the real potential of these by-products in industries that are more demanding from a compositional point of view.

Despite the technical application proof of these by-products, geographical distances between extractive production centres and possible industries that can process it make its industrial application unfeasible, mainly due to transportation costs. The potential use of “*terra rossa*” is undoubtedly for covering filled cavities regarding its environmental recovery. Also, “*terra rossa*” deposits proliferate, and many of them will never be used for the purpose mentioned above. Its use as a ceramic raw material, especially for pottery in regional pottery centres, is a well-tested possibility (Alves 2015). For this purpose, the deposits must remain uncontaminated with other materials.

Despite the mining industry’s aggressiveness, the wildlife remains in the captive zone of the Estremoz Anticline. The heaps covered with a portion of soil can have some regenerative capacity, serving as a refuge for many animal species. The study of Germano (2013) proves that inactive quarries and surroundings nature form a mosaic landscape that benefits and promotes the diversity of birds and the development of new biotopes, thus contributing to a greater variety of plant communities. According to Annexe II of the Berne Convention, fifty-three birds were recorded, most of them considered strictly protected fauna. Like the animals, the flora has a great diversity in the area, and it is possible to count about two hundred and fourteen species, where some of them are vulnerable and very scarce in Portugal (Germano 2013).

5 Concluding Remarks

Since this industrial sector is characterised by the consumption of large amounts of energy, to which is added the important environmental factor and visual impact of these deposits, many academic works and research that address this theme have been developed, in a constant search for solutions and alternatives of using these by-products. Many possible applications can pass through the gravel production

sector in road construction, ceramic industry, additives for plastic paints, agricultural uses (regularisation of the pH content), and hydric uses (regularisation of water pH). However, even if it is not yet possible to apply marble slurries in industrial quantities due to the substantial costs associated with its transport to the industrial poles, it is necessary to continue promoting its collection and proper packaging instead of spreading it in the heaps.

The difficulty of finding out clay deposits adequate both in quality and size, able to supply the traditional pottery industry, could be easily over-passed using the clay-rich “*terra rossa*” that overlies the marble deposits in the Estremoz Anticlinal, as well as other clay-rich residual soils, as pottery raw materials. Regarding the slurries, it was technically possible to prove that using these raw materials is feasible in many different applications. The values obtained are promising, some of them even capable of competing with the results corresponding to the commercial products typically used.

References

- Alves T (2015) Formulação de pasta cerâmica a partir de matérias-primas: argilas dos municípios de Vila Viçosa e Redondo para a produção de cerâmica tradicional. MSc dissertation, Universidade de Évora, Évora
- ASSIMAGRA (2001) Guia de gestão ambiental do sector das pedras naturais. Resíduos, vol 3. Direcção-Geral de Energia e Geologia, DGEG, Lisboa
- Delgado H (1995) Potencialidades dos carbonatos de cálcio portugueses para aplicação como carga no papel. PhD thesis, Universidade de Aveiro, Aveiro
- Germano DLC (2013) Análise da evolução da recuperação ecológica de pedreiras de mármore inactivas no anticlinal de Estremoz: avifauna, flora e vegetação. MSc dissertation, Universidade de Évora, Évora
- Martins R (1996) Aplicações industriais de natas resultantes da indústria de fabricação de rochas ornamentais carbonatadas. MSc dissertation, Universidade de Aveiro, Aveiro
- Ventura A (2007) Pastas cerâmicas: ladrilhos utilizados na fabricação de revestimentos, para monocozedura rápida. Final BSc report, Universidade de Évora, Évora



Petrographic and Geochemical Characterisation of Organic Matter of Precambrian Black Shales from Ossa-Morena Zone, South of Portugal

Vanessa Laranjeira, Joana Ribeiro, Noel Moreira, Pedro Nogueira, João Graciano Mendonça Filho, and Deolinda Flores

Abstract

Black shale (BS) lithologies are represented in Precambrian (Ediacaran) of Ossa-Morena Zone, SW of Iberian Massif, through the *Série Negra* lithological succession. The organic matter (OM) investigation in BS is relevant to understanding the mechanisms and depositional paleoenvironments related to that genesis. This study aims to characterise the OM in BS from the *Série Negra* succession through petrographic and geochemical methodologies. The petrographic study allowed the identification of organic particles with variable abundance, size and shape in all samples. The maximum reflectance indicates that the OM corresponds to anthracite to semi-graphite. OM maturation variation in the *Série Negra* succession is related to variable burial evolution and metamorphic/metasomatic processes in the Ossa-Morena Zone sectors.

Keywords

Ediacaran • Black shale • Organic matter reflectance • Carbon content

V. Laranjeira (✉) · D. Flores
Department of Geosciences, Environment and Spatial Planning,
University of Porto, Porto, Portugal
e-mail: vanessa.laranjeira@fc.up.pt

V. Laranjeira · J. Ribeiro · D. Flores
Institute of Earth Sciences—Pole of Porto, Porto, Portugal

J. Ribeiro
Department of Earth Sciences, University of Coimbra, Coimbra,
Portugal

N. Moreira · P. Nogueira
Department of Geosciences, University of Évora and Institute of
Earth Sciences—Pole of Évora, Évora, Portugal

J. G. Mendonça Filho
Laboratory of Palynofacies and Organic Facies (LAFO),
Department of Geology, Institute of Geosciences, Federal
University of Rio de Janeiro, Rio de Janeiro, Brazil

1 Introduction and Geological Framework

Black shale (BS) occurrence is frequent in the sedimentary record throughout the geological history since Archean. These shales are characterised by the presence of organic matter (OM) that had been accumulated in anoxic environmental conditions presenting total organic carbon (TOC) content above 0.5 wt. % (Huyck 1989; Trabucho-Alexandre 2014).

The Ediacaran lithostratigraphic succession of the Ossa-Morena Zone (OMZ) (Fig. 1a), usually denominated as *Série Negra* succession, is a metasedimentary dominated sequence, containing several dark lithotypes (greywackes, black shales and black cherts/lydites) (e.g., Oliveira et al. 1991; Pereira et al. 2006). Several lithostratigraphic sectors were established in the OMZ and, although, with similar lithological features, the *Série Negra* succession acquires local designations (Oliveira et al. 1991; Pereira et al. 2006): Mosteiros Fm. (Alter do Chão-Elvas Sector and Blastomylonite Belt), Mares Fm. (Estremoz Anticline) and Águas de Peixe Fm. (Montemor-Ficalho Sector).

These Ediacaran Series have distinct tectono-thermal evolution depending on their location within the OMZ, either from Cadomian or Variscan Cycles (Oliveira et al. 1991; Eguíluz et al. 2000; Pereira et al. 2006). The Cadomian thermal events are not constrained due to the superimposition of the Variscan ones. However, the Ediacaran Series is generally highly deformed compared with the Palaeozoic Series, resulting from the Cadomian Orogeny (Apalategui et al. 1990; Oliveira et al. 1991). The Variscan metamorphic conditions are well-constrained, conditioned by first-order structures of the OMZ (Moreira et al. 2014a). The Mosteiros Fm. in Blastomylonite Belt was affected by high strain sinistral shearing during Early Carboniferous times, generally imposing high-temperature metamorphism, although with significant disparate metamorphic conditions (Pereira et al. 2012a). The Variscan regional metamorphism in the Alter do Chão-Elvas sector is low-grade,

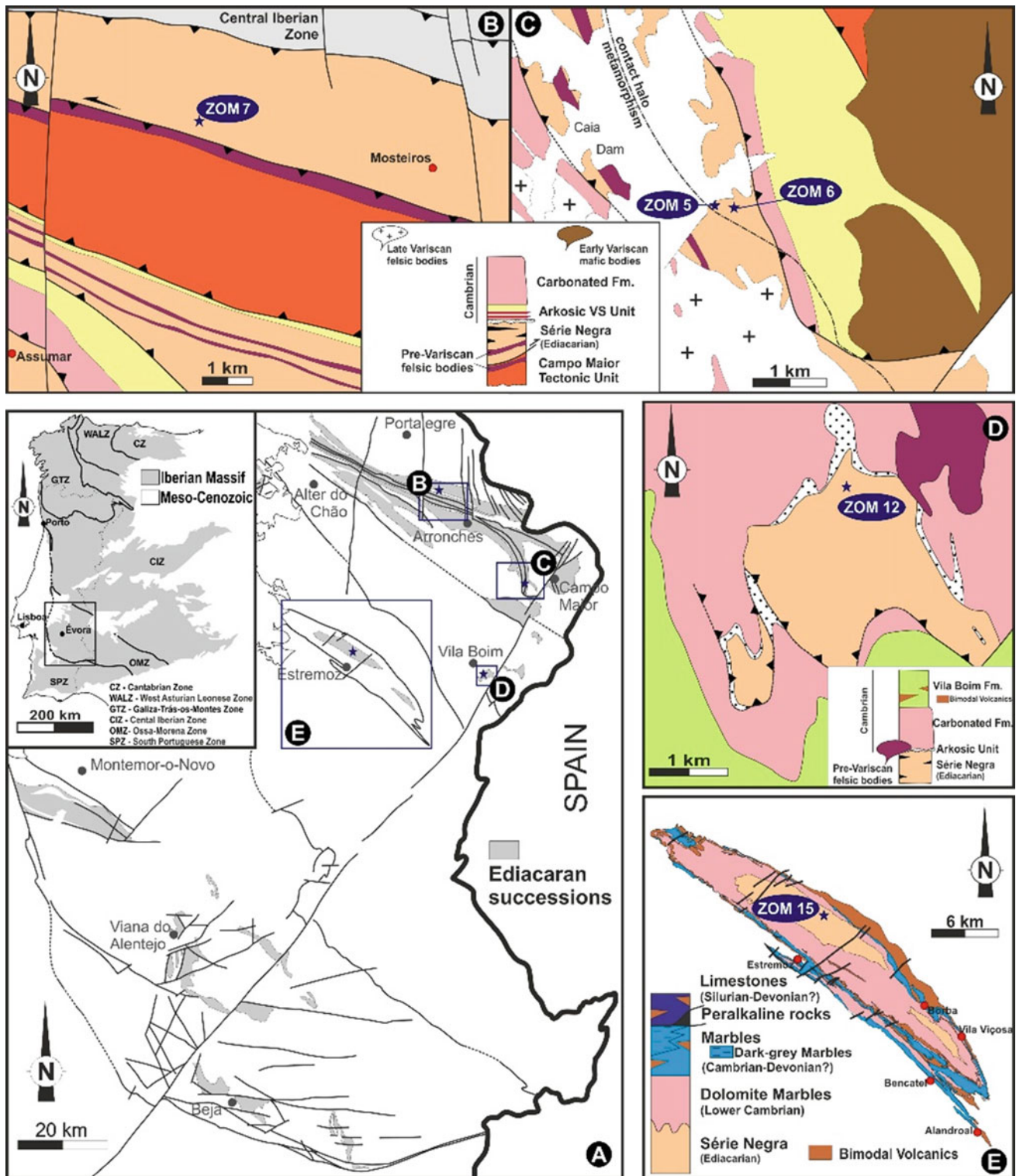


Fig. 1 Geological setting of the studied area and location of samples (geological maps adapted from: **a** LNEG 2010; **b** and **c** LNEG 2010, Pereira et al. 2010, 2012b; **d** Moreira et al. 2014b; **e** Moreira et al. 2019)

corresponding to the greenschist facies (Moreira et al. 2014b) described in the Estremoz Anticline for Mares Fm. (Pereira et al. 2012b; Moreira et al. 2019).

Previous investigations approached the petrographic and geochemical characterisation of the inorganic fraction of the *Série Negra* successions (Pereira et al. 2006; Chichorro et al.

2008), and the OM is only referred to as graphite (Pereira et al. 2006). The petrographic study, including the OM identification and characterisation and reflectance measurement, was never performed in the *Série Negra* organic-rich lithologies. Therefore, this study aims to characterise the OM in BS from the *Série Negra* succession using petrographic and geochemical methodologies. It is expected to contribute to the depositional paleoenvironmental conditions and the geodynamic evolution that conditioned the BS genesis.

2 Materials and Methodology

Five samples were collected in outcrops of Ediacaran BS from *Série Negra* succession of the OMZ (Fig. 1). The samples ZOM 5, ZOM 6, ZOM 7 (Blastomylonite belt) and ZOM 12 (Alter do Chão-Elvas Sector) belong to Mosteiros Fm. and the sample ZOM 15 to Mares Fm. (Estremoz Anticline).

The OM's petrographic characterisation was performed through optical microscopy to identify and characterise the organic and inorganic matter and measure the reflectance of the OM. The petrographic analyses were performed on whole-rock polished blocks prepared under standard procedures (ISO 7404-2 2009). The identification and characterisation of OM followed the ICCP system (Kwiecinska and Petersen 2004). The random and maximum reflectance of organic particles (R_r and R_{max}) were measured following ASTM D7708-14 (2014). The standard protocol refers that

at least 20–30 particles should be measured. However, in some of the studied samples, it was not possible to find the minimum number of organic particles to perform the analysis. The geochemical characterisation included the determination of TOC and total sulfur (S_t) using a LECO SC 144 analyser after samples acidification, following ASTM D 4239-08 (2008) and NCEA-C-1282, EMASC-001 (US–EPA 2002) standards.

3 Organic Matter Characterisation

The petrographic observations allowed the identification of organic particles in all samples. These particles are generally small, thin and elongated, occurring interbedded along with mineral matter. Figure 2 shows some petrographic features of the studied samples. In samples ZOM 5 and ZOM 6, organic particles are more abundant. In sample ZOM 5, the organic particles are larger and exhibit graphitic features (Fig. 2). Graphitic structures were also observed in samples ZOM 7 and ZOM 12. The graphitic structures in samples ZOM 5, ZOM 7 and ZOM 12 occur principally as disseminated flakes associated with iron oxides (Fig. 2). The petrographic observation of sample ZOM 6 revealed small organic particles, sometimes with rounded shapes (Fig. 2), which can be acritarch remains. In the *Série Negra*, Acritarchs near the Caia dam (where samples ZOM 5 and ZOM 6 were collected) were previously described by Gonçalves and Palácios (1984).

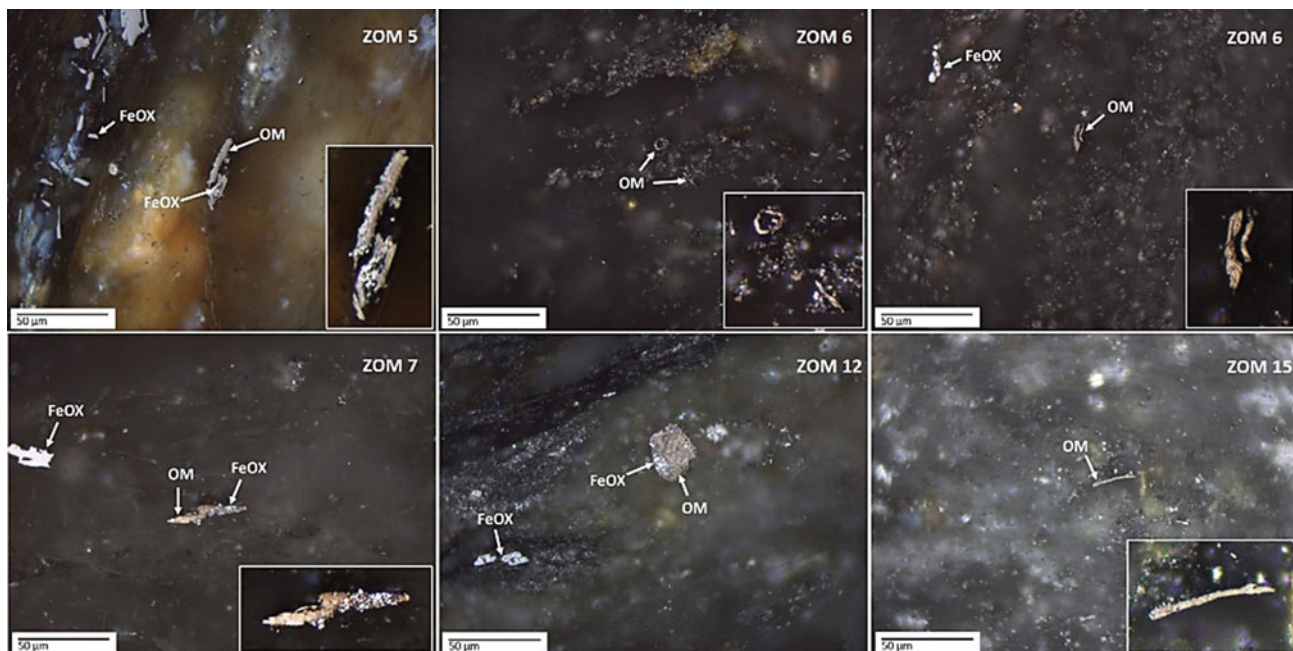


Fig. 2 Photomicrographs of the studied samples exhibiting organic particles occurring within mineral matter (OM—organic matter; FeOx—iron oxides)

Table 1 Random (R_r) and maximum reflectance (R_{max}) of organic particles, number of measured organic particles (N), the standard deviation of random reflectance (SD), TOC and S_t contents

	ZOM 5	ZOM 6	ZOM 7	ZOM 12	ZOM 15
R_r %	3.71	3.18	3.34	3.31	2.41
R_{max} %	6.60	5.17	5.19	5.37	4.13
N	21	21	7	6	4
SD	0.65	0.40	0.55	0.77	0.17
TOC %	0.20	1.53	0.29	1.08	0.76
S_t %	0.011	0.017	<0.010	<0.010	<0.010

The inorganic fraction is essentially composed of detrital derived minerals (mainly phyllosilicates and quartz), but the presence of iron oxides is common (Fig. 2). In samples ZOM 5 and ZOM 12, the presence of iron oxides is quite evident. This inorganic composition is consistent with other authors (Pereira et al. 2006; Chichorro et al. 2008).

The organic particles present R_r ranging from 2.41% to 3.71% and R_{max} varying between 4.13% and 6.60% (Table 1). Generally, samples from Mosteiros Fm. (ZOM 5, ZOM 6, ZOM 7 and ZOM 12) have higher OM reflectance ($R_r > 3\%$ and $R_{max} > 6\%$), demonstrating higher maturation than OM in a sample from Mares Fm. (ZOM 15) that has R_r and R_{max} of 2.41% and 4.13%, respectively. The R_{max} values indicate that the OM corresponds to anthracite ($R_{max} < 5\%$) in sample ZOM 15, and meta-anthracite in samples ZOM 5, ZOM 6, ZOM 7 and ZOM 12 ($5\% < R_{max} < 6.5\%$) (Kwiecinska and Petersen 2004). Graphitization begins at a temperature of at least 300 °C, within the greenschist facies chlorite zone. It is completed before the amphibolite facies at temperatures from 380 to 450 °C (Kwiecinska and Petersen 2004). Therefore, temperatures above 300 °C were expected in the studied *Série Negra* succession.

The TOC varies between 0.20% and 1.53% (Table 1). According to the classification of Huyck (1989) and Trabuco-Alexandre (2014), BS contain TOC higher than 0.5%, which is noted for samples ZOM 6, ZOM 12 and ZOM 15. Despite these TOC values, OM's petrographic observation was more evident in samples ZOM 5 and ZOM 6, as can also be inferred based on the number of measured particles (N; Table 1). The S_t values are low, close to the detection limit in all samples (Table 1).

4 Discussion and Concluding Remarks

Black shales from Ediacaran are represented in OMZ through the *Série Negra* succession. The petrographic and geochemical characterisation of the OM in BS from *Série Negra* was the aim of this study. The petrographic observations reveal the presence of organic particles of variable size and shape in all samples. The TOC content varies between 0.20% and 1.53%, and only three of the studied

samples have TOC content higher than 0.5%, thus being considered BS.

The reflectance indicates the presence of organic particles of anthracite to semi-graphite, formed during the graphitisation, at temperatures above 300 °C, accompanying the burial experienced by the sediments in the basin and metamorphic/metasomatic processes. The OM maturation in Mosteiros Fm. (ZOM 5, ZOM 6 and ZOM 7), included in the Blastomylonite belt, together with data from the bibliography, can be interpreted as related to the Early Carboniferous metamorphic event during Variscan Cycle (Pereira et al. 2012a), which according to Pereira et al. (2010), can reach temperatures higher than 500 °C in the Blastomylonite belt. The higher R_{max} in samples ZOM 5 and ZOM 12 can be associated with the proximity to plutonic bodies (Fig. 1c, d) and the metasomatic fluid percolation evidenced by the greater amounts of iron oxides, and also recognised in the *Série Negra* succession near the location of sample ZOM 5 (Cruz 2013). The maturation observed in sample ZOM 15 should represent the effect of the regional Variscan metamorphism in greenschists facies (ca. 300–400 °C; Pereira et al. 2012b; Moreira et al. 2019).

Acknowledgements This work was supported by national funds through FCT—Fundação para a Ciência e a Tecnologia, under the project UIDB/04683/2020, Institute of Earth Sciences. V. Laranjeira is also grateful to the financial support granted by FCT and the EU through national funds and European Social Fund with a PhD scholarship (SFRH/BD/137567/2018). Finally, N. Moreira and P. Nogueira acknowledge the contribution of the project ALT20-03-0145-FEDER-000028, funded by Alentejo 2020 through the FEDER/FSE/FEEI.

References

- Apalategui O, Eguiluz L, Quesada C (1990) Ossa-Morena zone: structure. In: Dallmeyer RD, Martínez-García E (eds) Pre-Mesozoic Geology of Iberia. Springer-Verlag, Berlin-Heidelberg, Germany, pp 280–292
- ASTM D 4239-08 (2008) Standard test methods for sulfur in the analysis sample of coal and coke using high-temperature tube furnace combustion methods. ASTM International
- ASTM D 7708-14 (2014) Standard test method for microscopical determination of the reflectance of vitrinite dispersed in sedimentary rocks. ASTM International

- Chichorro M, Pereira MF, Díaz-Azpiroz M, Williams IS, Fernandez C, Pin C, Silva JB (2008) Cambrian ensialic rift-related magmatism in the Ossa-Morena Zone (Évora-Aracena metamorphic belt, SW Iberian Massif): Sm-Nd isotopes and SHRIMP zircon U-Th-Pb geochronology. *Tectonophysics* 461:91–113
- Cruz C (2013) Efeitos metamórficos e fluidos do Complexo Plutónico de Santa Eulália. University of Porto, Porto (MSc Dissertation)
- Eguiluz L, Gil Ibarguchi JI, Abalos B, Apraiz A (2000) Superposed Hercynian and Cadomian orogenic cycles in the Ossa-Morena zone and related areas of the Iberian Massif. *Geol Soc Am Bull* 112:1398–1413
- Gonçalves F, Palácios T (1984) Novos elementos paleontológicos e estratigráficos sobre o Proterozóico Português da Zona de Ossa-Morena. *Mem Acad Ciênc Lisboa*, pp 226–235
- Huyck HLO (1989) When is a metalliferous black shale not a black shale? In: *Metalliferous Black Shales and Related Ore Deposits—Proceedings, United States Working Group Meeting, International Geological Correlation Program Project 254*. U. S. Geological Survey Circular 1058, pp 42–56
- ISO 7404-2 (2009) Methods for the petrographic analysis of Coals—Part 2: Methods of preparing coal samples
- Kwiecinska B, Petersen HI (2004) Graphite, semi-graphite, natural coke, and natural char classification-ICCP system. *Int J Coal Geol* 57:99–116
- LNEG (2010) Geological map of Portugal at 1:1 000 000, 3rd edn. Laboratório Nacional de Energia e Geologia, Lisbon
- Moreira N, Araújo A, Pedro JC, Dias R (2014a) Geodynamic evolution of Ossa-Morena Zone in SW Iberian context during the Variscan cycle. *Comun Geol* 101 (I):275–278
- Moreira N, Dias R, Pedro JC, Araújo A (2014b) Interference between Variscan deformation events in Torre de Cabedal structure: Alter-do-Chão – Elvas sector (Ossa-Morena Zone). *Comun Geol* 101(I):279–282
- Moreira N, Pedro J, Santos JF, Araújo A, Dias R, Ribeiro S, Romão J, Mirão J (2019) $^{87}\text{Sr}/^{86}\text{Sr}$ applied to age discrimination of the Palaeozoic carbonates of the Ossa-Morena Zone (SW Iberia Variscides). *Int J Earth Sci (Geol Rundsch)* 108(3):963–987
- Oliveira JT, Oliveira V, Piçarra JM (1991) Traços gerais da evolução tectono-estratigráfica da Zona de Ossa Morena, em Portugal. *Cuad Lab Xeol Laxe, Coruña* 16:221–250
- Pereira MF, Apraiz A, Chichorro M, Silva JB, Armstrong RA (2010) Exhumation of high-pressure rocks in northern Gondwana during the Early Carboniferous (Coimbra–Cordoba shear zone, SW Iberian Massif): tectonothermal analysis and U-Th–Pb SHRIMP in-situ zircon geochronology. *Gondw Res* 17:440–460
- Pereira MF, Chichorro M, Linnemann U, Eguiluz L, Silva JB (2006) Inherited arc signature in Ediacaran and early Cambrian basins of the Ossa-Morena Zone (Iberian Massif, Portugal): paleogeographic link with European and North African Cadomian correlatives. *Precamb Res* 144:297–315
- Pereira MF, Silva JB, Chichorro M, Ordóñez-Casado B, Lee JKW, Williams IS (2012a) Early Carboniferous wrenching, exhumation of high-grade metamorphic rocks and basin instability in SW Iberia: constraints derived from structural geology and U-Pb and ^{40}Ar - ^{39}Ar geochronology. *Tectonophysics* 558–559:28–44
- Pereira MF, Solá AR, Chichorro M, Lopes L, Gerdes A, Silva JB (2012b) North-Gondwana assembly, break up and paleogeography: U-Pb isotope evidence from detrital and igneous zircons of Ediacaran and Cambrian rocks of SW Iberia. *Gondw Res* 22(3–4):866–881
- Trabucho-Alexandre J (2014) More gaps than shale: erosion of mud and its effect on preserved geochemical and palaeobiological signals. *Geol Soc, London, Special Publication* 404(1):251
- US – EPA (2002) Methods for the determination of Total Organic Carbon (TOC) in soils and sediments. United States Environmental Protection Agency (U. S. EPA), Office of Research and Development, National Exposure Research Laboratory, Las Vegas, NV. NCEA-C-1282, EMASC-001



Components of Lithium Depletion from Starting Spodumene—Petalite Assemblages in *Subsolidus* Evolution of Portuguese Pegmatites

Carlos Leal Gomes and Pedro Amorim

Abstract

In Portugal, especially in the NW region, mineral assemblages with spodumene after petalite and petalite only are hosted in pegmatite bodies, which intrude metasedimentary to metavolcanic, Silurian, or earlier formations. Regardless of the region in which they occur, this paragenesis and the pegmatites that support them are affected by evolutionary trends of deuteritic to supergenic alteration that may lead to lithium leaching and severe depletion of early contents sequestered in starting materials. That has relevant consequences for the recovery of Li resources, not only by the generalized lowering of the Li grades of pegmatite deposits but also by the multiplication of Li-specific carrier phases, which penalizes the recovery percentages during any mineralurgy routines. Predictably, recovered grades will be significantly lower than those obtained by chemical analysis of whole rock and channel pegmatite samples.

Keywords

Petalite • Spodumene • Metasomatism • Weathering

1 Introduction

Since the early eighties of the twentieth century, the Portuguese production of ceramic raw materials introduced quartz-feldspar blends with lithium minerals, mainly lepidolite. Besides this primary Li-rich ceramic material, which came from de Viseu–Guarda–Castelo Branco region, in

C. L. Gomes (✉) · P. Amorim
School of Sciences, Department of Earth Sciences, University of Minho, Braga, Portugal
e-mail: carloslealdb@gmail.com

C. L. Gomes
Landscapes, Heritage and Territory Laboratory, University of Minho, Braga, Portugal

1984, some feldspar producers draw their attention to the considerable waste dumps, with highly comminuted tailings, that resulted from an earlier cycle of tin-tungsten mining in some of the significant pegmatite deposits. The main waste dumps considered were: Vieiros and Seixoso in the Amarante region, Rebentão, Lousadela in the Vila Nova de Paiva region and Ribeiro do Seixalvo, Moreira de Lima in the Ponte de Lima region. All the tailings underwent a beneficiation process of iron decontamination by electromagnetic extraction of iron minerals. Some minor waste dumps in the Beça mining field, in the region of Montalegre, were also studied but discarded, owing to severe dispersion of the tailings, its high degree of defilement and high distance to consumption centres for ceramic pastes (Fig. 1a).

In general, the industrial melting assays of these materials showed good characteristics as melting depressors, achieving a good to excellent whitening degree of the test specimens, which also showed good percentages of contraction compared to the assays of some low-grade feldspars. Leal Gomes (1985) called attention to the fact that this excellent behaviour could be related to the presence, in the comminuted debris, of variable amounts of Li minerals, not exclusively Li phyllosilicates, but mainly, petalite and its *subsolvus* decay products (spodumene) and *subsolvus* equilibrium products to secondary lithium assemblages. In the fuse tests carried out, it was found that regardless of the mineralogical diversity and Li contents' heterogeneity, all products with Li minerals showed better melting behaviour. Afterwards, this trend was confirmed in more detail (Dias and Leal Gomes 2005).

On the contrary, when a pegmatitic paragenesis is seen as a source of metallic lithium, the diversity and the number of mineral phases carrying Li and the levels of Li leaching that pegmatitic materials undergo is of critical importance for the deduction of eventual economic feasibility.

Thus, this study aims to clarify the diversity of daughter phases during the evolution of primary anhydrous silicates

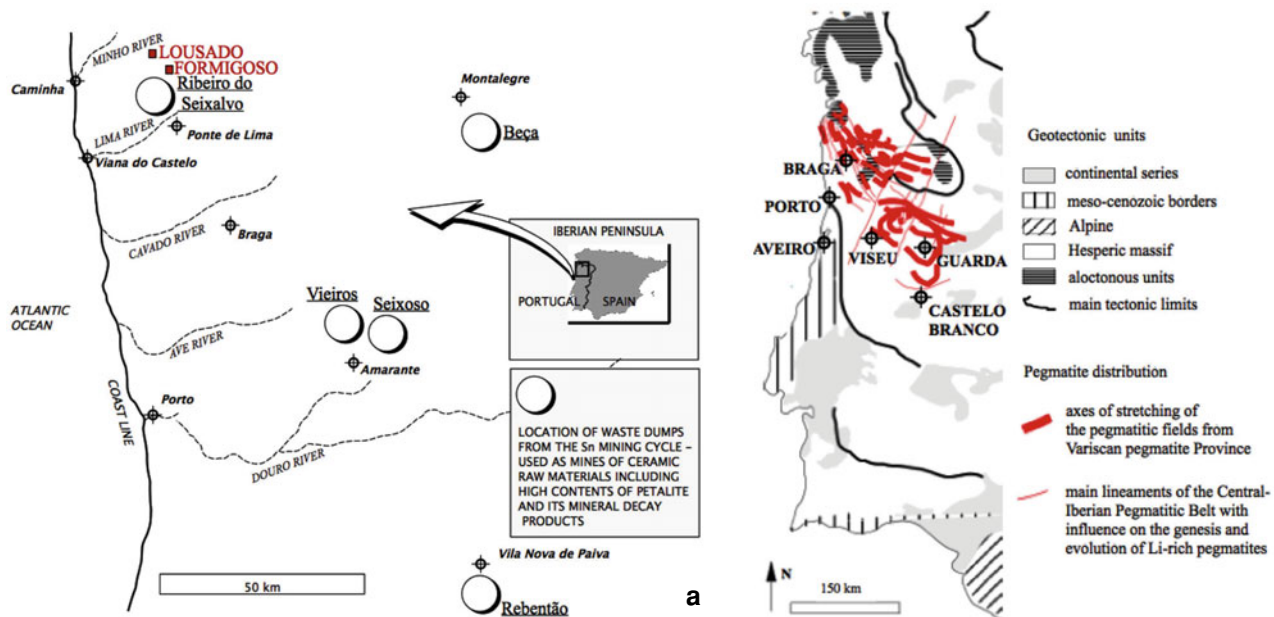


Fig. 1 Regional distribution of lithium-bearing pegmatites in North-western Portugal. **a** Location of the main Sn pegmatite tailings used as ceramic raw materials in Northern Portugal. Note: these tailings hold petalite as the prevalent Li mineral, and several Li-minerals decay products; the same locations are representative centres of

petalite-bearing pegmatites showing decay assemblages and Li-leached secondary lithotypes; red squares indicate key sites with the most complex Li-bearing paragenesis—Lousado and Formigoso; **b** Regional divisions, pegmatite swarm distribution and main lineaments of Central-Iberian Pegmatite Belt

and the corresponding depreciation of potential Li recovery from replaced-metasomatized and weathered pegmatites.

underwent chemical analysis by inductively coupled plasma mass spectrometry (ICP-MS) and atomic absorption (AAS) with special consideration of Li contents as Li_2O .

2 Materials and Methods

Li-rich minerals and mineral assemblages are envisaged as Li-rich mixed ceramic raw materials. Therefore, different hard rock pegmatites were analyzed from a mineral-chemical point of view as a tentative to establish and systematize their utility as lithium-ores. The studied pegmatites belong to the Central-Iberian Pegmatite Belt, a tectonic division of the Variscan Pegmatite Province expressed in Northwestern Portugal, as quoted in Leal Gomes (1994) (Fig. 1b).

Departing from petrography and fabric analysis, some selected assemblages—mainly from Lousado and Formigoso pegmatite groups (Fig. 1a)—were subjected to whole rock X-ray diffractometry (XRD).

According to Černý (1990) and Černý and Ercit (2005) these pegmatites, are classified as follows: Lousado—LCT family, lepidolite + tourmaline, type; Formigoso—LCT family, petalite ± spodumene type.

The main goal was to discriminate the mineralogy of lithium and the screening of lithium bearers and non-lithium phases related to petalite decay. These same assemblages

3 Results

Once established the mineralogy and paragenesis of representative and potential lithium ores, we tried to attribute a chemical—mineralogical systematic of the most persistent, metastable to stable assemblages, which are frequent at the mining fronts, considering paragenetic persistence and modal content criteria and considering its location within or at the periphery of internal pegmatitic units with prevailing primary petalite or spodumene after petalite.

Leal Gomes (2015) and Leal Gomes and Dias (2018) refer to the maximum lithium that is to be expected in these pegmatites and the trends of subsolidus evolution responsible for the decay of its content. Following these works and with the methodologies now adopted, we seek to clarify the characteristic sequestration levels of each of the materials discriminated in the studied mine fronts.

Table 1 synthesizes the conjugation of whole-rock XRD data with values obtained by chemical analysis of Li for

Table 1 Mineralogy and Li content of representative phases and mineral assemblages from different isochemical (isoc.), deuteric (deut.) to supergenic (sup.) stages of evolution—Li contents are average values for combined Lousado and Formigoso case studies (ICP-MS and AAS)

Stage	Start assemblages or minerals (XRD)	Li content (weight % Li ₂ O)	End products (XRD)—pseudomorphic or deformation disrupted	Li content (weight % Li ₂ O)
1 (isoc.)	Petalite giant crystals	4.11	Spodumene + quartz pseudomorphic	3.86
2 (deut.)	Petalite	4.00	Cookeite + quartz + albite Quartz + lepidolite + muscovite + kaolinite-montmorillonite	0.20 0.71
3 (deut. to sup.)	Spodumene + quartz pseudomorphic ± relict petalite	3.78–3.50	Lepidolite + muscovite + masutomilite ± cookeite Quartz + cookeite + muscovite ± clinocllore Quartz + kaolinite + cookeite ± muscovite	3.33 0.44 0.62
3 (deut.)	Spodumene + quartz	3.71	Bikitaite + quartz	3.32
4 (deut. to sup.)	Spodumene + quartz ± lepidolite	2.35	Hectorite ± cookeite Kaolinite + cookeite + quartz	1.23 0.60
5 (sup.)	Petalite + spodumene + quartz pseudomorphic ± albite ± perthite	1.12	Gibbsite + quartz Kaolinite + quartz	0.46 0.14

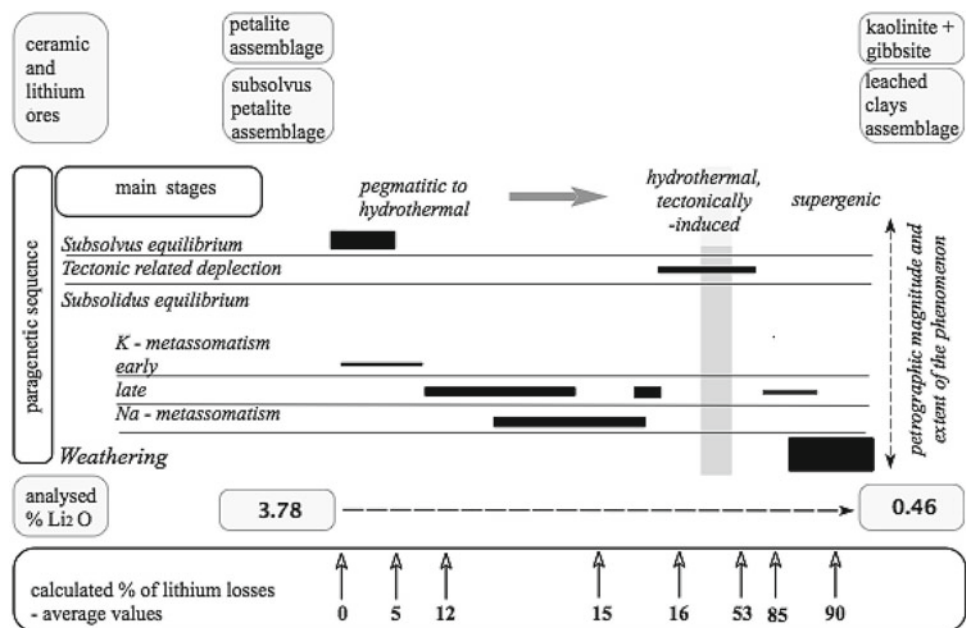
primary and the more common secondary paragenesis (Leal Gomes 2015).

The documented approach deals with representative cases of paragenetic diversification due to secondary evolution in the two LCT pegmatite groups of Lousado and Formigoso. These groups might be considered key systems since they contain the greatest lithium phases' most remarkable diversity, so far identified in an individual pegmatite body. As so, the results are extendable to the whole pegmatite belt for bodies hosted in Silurian terrenes. The isochemical transition from petalite to spodumene and quartz is already affected by some lithium loss. It partially occurs under cataclastic to mylonitic deformation, favouring limited alkali metal mobility through fluid circulation.

4 Discussion

Petrography results, Li values obtained now for the different alteration products and XRD mineralogy suggest that some secondary phases are more prevalent than previously thought (Leal Gomes and Dias 2018). The most persistent and stable allochemical-alteration minerals are: lepidolite, cookeite and masutomilite, in metasomatism; hectorite, kaolinite, montmorillonite and gibbsite, in the case of weathering (Fig. 2). In the same study, rarer late phases identified were:

- bityite—LiCaAl₂(AlBeSi₂O₁₀)(OH)₂;
- akopovaite—Al₄Li₂(OH)₁₂(CO₃)(H₂O);

Fig. 2 Calculated Li₂O decay and progressive loss by leaching associated with *subsolvus* to *subsolidus* evolution of lithium paragenesis


- dritsite— $\text{Li}_2\text{Al}_4(\text{OH})_{12}\text{Cl}_2 \cdot 3\text{H}_2\text{O}$;
- dusmatovite— $\text{K}(\text{Na}, \text{Y})_2(\text{Zn}, \text{Li})_3(\text{Mn}^{2+}, \text{Y}, \text{Zr})_2[\text{Si}_{12}\text{O}_{30}]$.

The main sequestration of Li in the end products of deuteric alteration occurs in the pair polyolithionite–trilithionite (lepidolite), cookeite and masutomilite. The other secondary minerals are so rare that the reticular Li sequestration they represent is insignificant.

The final expression of Li can occur in crystal lattices, in the case of the minerals, hectorite and lithiophorite and relict particles and adsorption in the case of montmorillonite and kaolinite. Thus, gibbsite can be regarded as a residual mineral resulting from extreme leaching of silica and alkali metals, which nonetheless can retain a relatively high Li content (average $\text{Li}_2\text{O} \sim 0.69\%$) under both the relict and submicroscopic dust inheritance of primary phases, as well as, possibly, in adsorption.

5 Concluding Remarks

In summary, the decay of Li content in pegmatites is related to isochemical transition, cataclasis, milonitization and deuteric changes: cation exchange K/Li-phyllitic alteration and microclinization; cation exchange Na/Li-albitization \pm eucryptite deposition. Weathering also has high leaching potential, as is generally the case with alkali metals. However, in general, alteration phenomena only leach and do not add Li. Only in the case of eucryptite generation, associated with albitization, this tendency is not so evident. Possibly eucryptite represents a very localized and rare case of Li fixation in some SiO_2 undersaturated spots, which are circumscribed within extensive secondary

albite masses resulting from the replacement of earlier Li phases.

A general consequence for this paragenetic diversification is the suggestion that petalite and/or spodumene routine mineralogy may face very significant impoverishment between Li's levels attributed by analysis to total pegmatite and recovered levels concentrates from the beneficiation plants.

Acknowledgements To Prof. M. R. Machado Leite and Eng. Rogério Calvo for chemical analysis in the facilities of Laboratório Nacional de Energia e Geologia (LNEG) in S. Mamede de Infesta, Portugal. To José Aldeia Lagoa e Filhos Lda, for supporting analysis performed in the laboratories of Unipasta—Pastas Cerâmicas SA and sub-contracted abroad.

References

- Černý P (1990) Distribution, affiliation and derivation of rare-element granitic pegmatites in the Canadian Shield. *Geol Rundsch* 79 (2):183–226
- Černý P, Ercit T (2005) The classification of granitic pegmatites revisited. *Canad Mineral* 43:2005–2026
- Dias P, Leal Gomes C (2005) Tipologia dos materiais cerâmicos petalíticos provenientes de aplito-pegmatitos graníticos da Cintura Centro-Ibérica. In: *Actas do IV Seminário Recursos Geológicos, Ambiente e Ordenamento do Território*, Vila Real
- Leal Gomes C, Dias P (2018) Subsídios para uma sistemática dos jazigos minerais e minérios de lítio de Portugal. *Bol Min* 52:7–47
- Leal Gomes C (1985) Pegmatitos, aproximação ao seu interesse económico. Plano para uma aula teórico-prática da disciplina “Recursos Minerais e Energéticos”, Provas de Aptidão Pedagógica e Capacidade Científica. Universidade do Minho, Braga (Unpublished Scientific Report)
- Leal Gomes C (1994) Estudo estrutural e paragenético de um sistema pegmatóide granítico: O campo filoniano de Arga-Minho (Portugal). Universidade do Minho, Braga (PhD thesis)
- Leal Gomes C (2015) O determinante petalítico dos teores máximos de lítio em pegmatitos Variscos do NW de Portugal: aproximação paragenética e geoquímica. *Comun Geol* 102(I):53–56



Nodular Sulphides in Cerdeirinha Stratiform Metasomatic Deposit—LA-ICP-MS Composition of Typomorphic Minerals

Ana Sofia Souto, Carlos Leal Gomes, Wolfgang Bach, and Patrick Monien

Abstract

In the northwest of Portugal, in Serra de Arga, a stratiform and metasomatic tungsten ore deposit known as Cerdeirinha is located in parautochthonous terrains attributed to Silurian. In its stratigraphic sequence, there are some horizons containing concentrations of spheroid sulphide nodules. The composition and origin of these nodules were poorly constrained. Co, Ni and Ag contents obtained by laser-ablation inductively coupled plasma mass spectrometry in nodular pyrite-pyrrhotite suggest a metamorphic/hydrothermal rework of a primitive sedimentary nature.

Keywords

Nodular pyrite • LA-ICP-MS • Parautochthonous terrains • Silurian

1 Introduction

Cerdeirinha mine is located in northern Portugal, more precisely in the Covas mining district. The stratiform metasomatic ore deposit is part of a mega sheath fold associated with an earlier obduction stage (2nd Variscan deformation phase)

A. S. Souto (✉) · C. L. Gomes
School of Sciences, Department of Earth Sciences, University of Minho, Braga, Portugal
e-mail: anasofiasgv@souto@gmail.com

C. L. Gomes
Landscapes, Heritage and Territory Laboratory, University of Minho, Braga, Portugal

W. Bach · P. Monien
Department of Geosciences, University of Bremen, Bremen, Germany

W. Bach
MARUM—Center for Marine Environmental Sciences, University of Bremen, Bremen, Germany

reworked in the late-Variscan 3rd deformation phase as an antiformal known as Covas Dome (Fig. 1).

The main regional formations are considered to be Silurian in age and formed during Paleothetys basin's opening. The model attributed to the evolution of NW Gondwana margin assumes the opening of the Rheic Ocean between NW Gondwana and Avalonia. That was the result of the Cambrian-Ordovician distension (500–470 Ma). Later, during Ordovician to Silurian evolution (430–390 Ma), SE margin of the Rheic Ocean would have subducted. Paleothetys backarc opening is related to this event (Pin et al. 2002; Ribeiro et al. 2007). In its sequence, the parautochthonous terrains, which correspond to the backarc basin, comprise metasedimentary sequences from the Upper Ordovician to Devonian deposited on the North-Gondwana margin (Ribeiro et al. 1990). Silurian formations suggest anoxic to euxinic deposition in confined epicontinental basins.

For the regional polymetallic mineralisations of W, Fe, As, Bi > (Au), Te, Zn, Cu, and Mo, the ore mineral assemblages in Cerdeirinha include native metals, oxides and sulphides (Leal Gomes et al. 2011; Souto 2017).

In this study, trace element analyses were conducted on nodular sulphide samples collected from a sulphide-rich horizon in the Cerdeirinha stratigraphic column, trying to clarify its nature, which, due to several stages of deformation and fluid remobilisation, is still unclear.

2 Materials and Methods

Spheroid or nodules richest levels in the Cerdeirinha stratigraphic sequence occur at the apical sulphide domain near some fossil mound structures (Leal Gomes et al. 2011). A representative nodular rock sample was studied in a thin polished section by energy-dispersive X-ray spectroscopy using a scanning electron microscope (SEM). Analyses were performed by electron microprobe (EMPA) for Fe and S

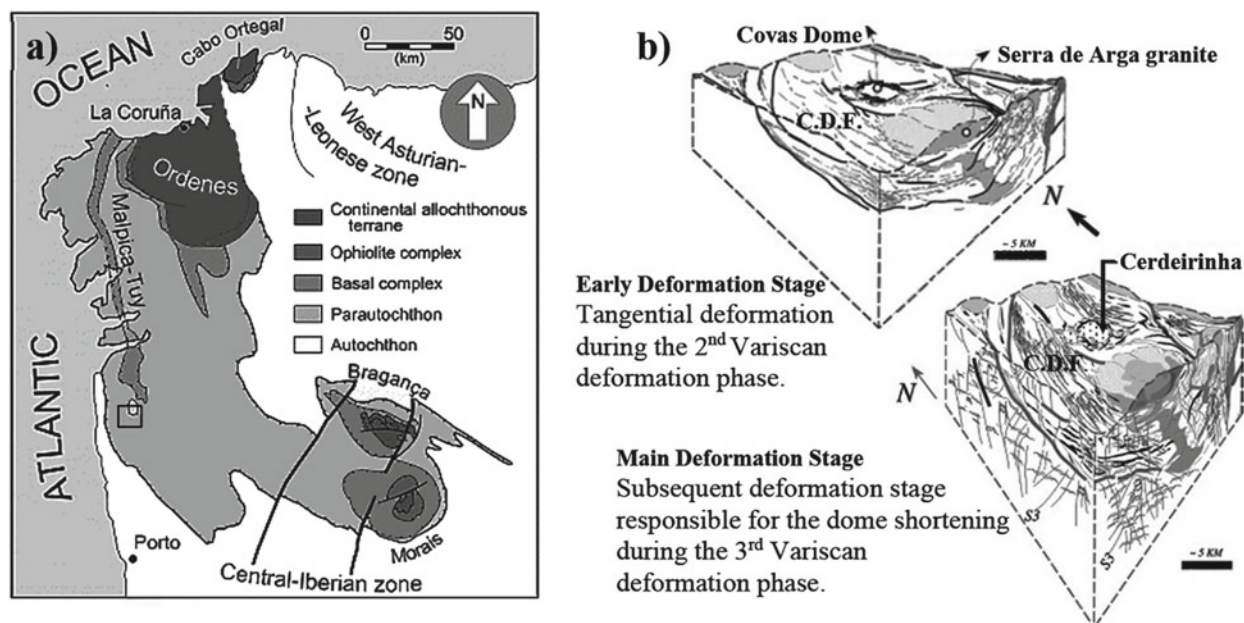


Fig. 1 Geological setting. **a** Region in NW Portugal where Cerdeirinha deposit is located (Ribeiro et al. 2007). **b** Interpretative sketch blocks for Covas Dome Formation (CDF), its evolution and where Cerdeirinha deposit has an apical location

contents. Ni, Co and Ag in sulphide minerals were measured by laser-ablation inductively coupled plasma mass spectrometry (LA-ICP-MS), at the University of Bremen, with a New Wave UP193 solid-state laser coupled to a Thermo Scientific Element2 HR-ICP-MS, using ^{57}Fe as an internal standard. NIST610 glass was analysed as an external calibration standard (Jochum et al. 2011). Data quality was assessed by analysing reference materials BCR2G, BHVO2G, and MASS-1, along with the samples (Table 1).

3 Results and Discussion

A spheroidal nodule with a diameter smaller than 4 cm, whose dominant mineral phases are pyrite ($\text{FeS}_{1.89-2.16}$) and pyrrhotite ($\text{Fe}_{0.89}\text{S}$) (Fig. 2), were analysed under SEM. This texture suggests a sedimentary related genesis due to its

spheroidal form and radial to concretionary inner crystal-growth and the graded bedding structure of its primordial sedimentation. The compositions and trace element contents measured in the sample (Fig. 2b) are shown in Table 2.

According to Xue et al. (2014), in pyrite Co and Ni isomorphously replace Fe, whilst Ag exists in its mechanical mixtures. However, in this case, Ag could more likely be present in pyrite lattice, similarly to what has been described by Leighton et al. (2019) in the MacMillan Pass Sedex district, Yukon. Co:Ni ratios in nodular Cerdeirinha pyrites range between 0.39 and 0.50 (Table 2), which is typical for sedimentary pyrites (Fig. 3), where Co:Ni ratios below 1 are expected (Bajwah et al. 1987). The minor-element contents in sedimentary pyrite are explained by: (i) its association with detrital or chemically precipitated Fe minerals, which may follow Fe in the formation of monosulphides;

Table 1 Replicate analyses of the three reference materials BHVO-2G ($n = 8$), BCR-2G ($n = 8$), and MASS-1 ($n = 3$) used during LA-ICP-MS analyses. Reference data are from the GeoRem database (<http://georem.mpch-mainz.gwdg.de>)

Element	BHVO-2G certified (mg kg^{-1})	BHVO-2G measured (mg kg^{-1})	BCR-2G certified (mg kg^{-1})	BCR-2G measured (mg kg^{-1})	MASS-1 reference (mg kg^{-1})	MASS-1 measured (mg kg^{-1})
Ni	119.8 \pm 1.2	123.8 \pm 1.9	13 \pm 2	11.8 \pm 0.6	71–109 ^b	99.2 \pm 1.8
Co	44.89 \pm 0.32	46.2 \pm 0.6	38 \pm 2	38.4 \pm 0.6	67 ^b	67.0 \pm 0.5
Ag	0.36–0.79 ^a	0.407 \pm 0.048	0.5 \pm 0.4	0.748 \pm 0.042	67 ^b	68.6 \pm 1.5

^a Ag concentration in BHVO-2G is only for information and not certified

^b Ni, Co, and Ag concentrations in MASS-1 are only for information and not certified

Fig. 2 Nodular samples.
a Nodular hand samples.
b Nodule section—representative inner texture with a pyrite-rich core surrounded by a pyrrhotite-rich rim. Py—Pyrite; Po—Pyrrhotite

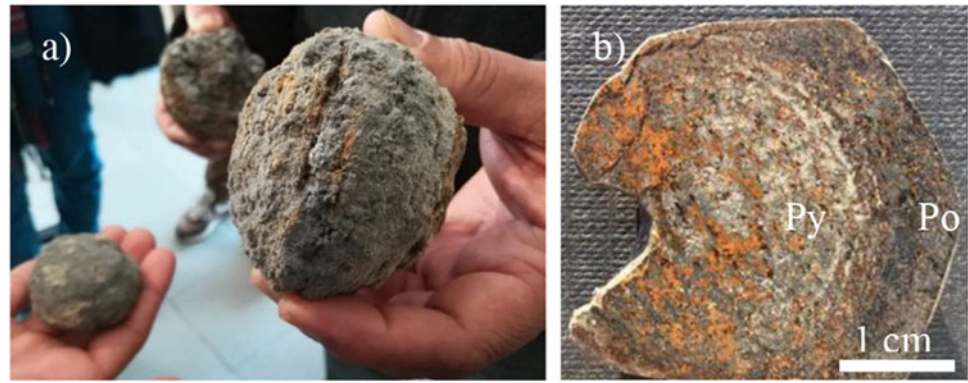


Table 2 Trace element contents in a representative nodule from the Cerdeirinha region

Mineral	Fe (%wt.)	S (%wt.)	Ni (mg kg ⁻¹)	Co (mg kg ⁻¹)	Ag (mg kg ⁻¹)	Co:Ni	Formula
Pyrrhotite	61.4	39.4	37.6	19.1	0.821	0.51	Fe _{0.89} S
	61.3	39.3	37.1	18.4	0.130	0.50	Fe _{0.89} S
	61.4	39.4	50.0	27.1	0.491	0.54	Fe _{0.89} S
Pyrite	47.6	52.1	48.4	22.0	0.190	0.45	FeS _{1.91}
	43.3	53.7	44.4	20.5	0.343	0.46	FeS _{2.16}
	47.6	52.6	43.8	18.7	0.371	0.43	FeS _{1.92}
	45.2	54.6	51.2	20.1	0.599	0.39	FeS _{2.10}
	47.9	52.1	98.7	49.6	0.377	0.50	FeS _{1.89}
	47.7	53.0	29.2	14.7	0.164	0.50	FeS _{1.93}
	47.1	52.9	27.8	14.0	0.311	0.50	FeS _{1.95}

(ii) organisms that decay in sediments; (iii) the release or acceptance of minor elements by Fe monosulphides upon conversion to pyrite. Also, trace impurities could be trapped at grain boundaries or lattice defects (Price 1972, and references therein). However, metamorphic remobilisation events may redistribute the Co and Ni contents, changing the pyrite Co:Ni ratios and masking their primary compositional signatures, consequently inducing misinterpretation of their genesis (Price 1972, and references therein).

Coelho (1993) considered the Cerdeirinha deposit as a single-stage skarn deposit. However, pyrite's Ni and Co contents do not plot in the hydrothermal field (field II in

Fig. 3). Possibly Cerdeirinha's pyrite and pyrrhotite contain a mixed signature, where a preserved sedimentary affiliation is still prevailing (field III in Fig. 3).

The Ag and Ni binary plot suggests that these pyrites have chemical similarities with orogenic-type pyrite (metamorphic/hydrothermal) (Fig. 4). The low Ag and Ni contents in pyrite that characterise this field are related to metamorphic processes, more specifically to element remobilisation via coupled dissolution-reprecipitation processes (Gourcerol et al. 2018). Note that Co, Ni, and Ag contents may vary accordingly to the chemistry of regional rocks (Price 1972; Gourcerol et al. 2018).

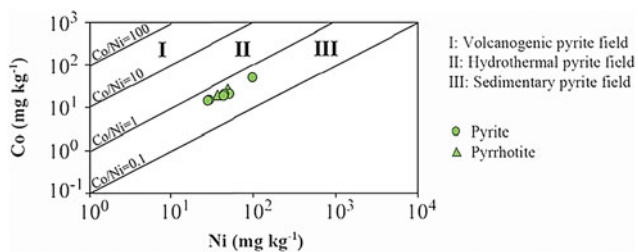


Fig. 3 Co versus Ni diagram for pyrite and pyrrhotite samples (modified after Price 1972; Bajwah et al. 1987) with the position of compositions representative of iron sulphide nodules from Cerdeirinha

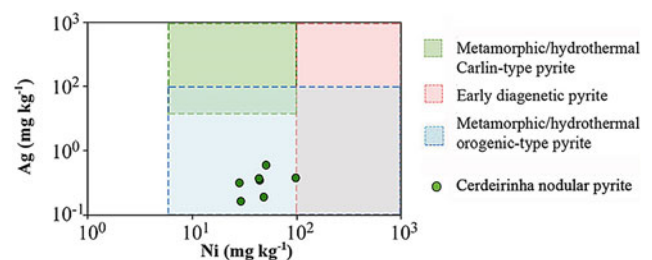


Fig. 4 Empirical binary plot of Ag versus Ni (discriminating fields are from Gourcerol et al. 2018, and references therein)

4 Concluding Remarks

Co, Ni, and Ag signatures of pyrite suggest a sedimentary origin, obscured by metamorphic/hydrothermal overprinting. Our data is consistent with a sedimentary-exhalative syn-genetic origin for the pyrite-pyrrhotite nodules, followed by metasomatic overprinting of the primary signatures (Leal Gomes et al. 2011; Dias 2011). Pyrite and pyrrhotite from Cerdeirinha's nodules suggest a primordial sedimentary setting that subsequently was reworked by metamorphism and some skarn-like evolution.

Acknowledgements We thank A. Klügel, S. Sopke and P. Witte for their help during LA-ICP-MS, EPMA, and SEM analyses. Moreover, Erasmus + scholarship is gratefully acknowledged here.

References

- Bajwah ZU, Secombe PK, Offier R (1987) Trace element distribution Co:Ni ratios and genesis of the Big Cadia iron-copper deposit, New South Wales, Australia. *Miner Dep* 22:292–300
- Coelho JMD (1993) Os “skarns” cálcicos, pós-magmáticos, mineralizados em scheelite, do distrito mineiro de Covas, Vila Nova de Cerveira (Norte de Portugal). *Mem Mus Lab Miner Geol, Fac Cienc Univ Porto, Porto* (PhD thesis)
- Dias P (2011) Análise estrutural e paragenética de produtos litológicos e mineralizações de segregação metamórfica: estudo de veios hiper-aluminosos e protólitos poligénicos Silúricos da região da Serra de Arga (Minho). University of Minho, Braga (PhD thesis). <http://hdl.handle.net/1822/19736>
- Gourcerol B, Kontak DJ, Thurston PC, Petrus JA (2018) Application of LA-ICP-MS sulfide analysis and methodology for deciphering elemental paragenesis and associations in addition to multi-stage processes in metamorphic gold settings. *Can Miner* 56:39–64
- Jochum KP, Weis U, Stoll B, Kuzmin D, Yang Q, Raczek I, Jacob DE, Stracke A, Birbaum K, Frick DA, Günther D, Enzweiler J (2011) Determination of reference values for NIST SRM 610–617 glasses following ISO guidelines. *Geostand Geoanal Res* 35(4):397–429
- Leal Gomes C, Verduzco G, Dias PA (2011) Vestígios de actividade fumaroliana litificados no nível com sulfuretos do jazigo da cerdeirinha, Caminha, N Portugal. In: *Proceedings VIII Congresso Ibérico de Geoquímica–XVII Semana de Geoquímica, Castelo Branco*, pp 1–6. <http://hdl.handle.net/1822/30356>
- Leighton C, Layton-Matthews D, Peter JM, Gadd MG (2019) Application of pyrite chemistry to recognise a distal expression of hydrothermal activity in the MacMillan Pass SEDEX district, Yukon. *Geolog Surv Can Open File* 8549:125–137. <https://doi.org/10.4095/313646>
- Pin C, Paquette JL, Santos Zalduegui JF, Gil Ibarguchi JI (2002) An Early Devonian suprasubduction zone ophiolite related to incipient collisional processes in the western variscan belt: the Sierra de Careón Unit, Órdenes Complex, Galicia. In: Martínez Catalán JR, Hatcher Jr RD, Arenas R, Diaz García F (eds) *Variscan-appalachian dynamics: the building of the late Paleozoic basement*. *Geol Soc Amer Sp Pap* 364:57–71
- Price BJ (1972) Minor elements in pyrites from the smithers map area, BC and exploration applications of minor element studies. University of British Columbia, Vancouver (MSc thesis). <http://hdl.handle.net/2429/33251>
- Ribeiro A, Pereira E, Dias R (1990) Structure of the northwest of the Iberian Peninsula. In: Dallmeyer D, Martínez García E (eds) *Pre-mesozoic geology of Iberia*. Springer, Heidelberg, pp 220–236
- Ribeiro A, Munhá J, Dias R, Mateus A, Pereira E, Ribeiro L, Fonseca P, Araújo A, Oliveira T, Romão J, Chaminé HI, Coke C, Pedro J (2007) Geodynamic evolution of the SW Europe variscides. *Tectonics* 26(6):1–24
- Souto AS (2017) Dispositivos estruturais exalativos em níveis estratiformes com sulfuretos da região de Caminha. University of Minho, Braga (BSc Final Report). <http://hdl.handle.net/1822/48987>
- Xue JL, Li SR, Sun WY, Zhang Y, Zhang X (2014) Characteristics of the genetic mineralogy of pyrite and its significance for prospecting in the Denggezhuang gold deposit, Jiadong Peninsula, China. *Sci China Earth Sci* 57:644–661



Calc-silicate Gemstones from the Meluco Region, Cabo Delgado, Mozambique

Carlos Leal Gomes

Abstract

Northeastern Mozambique, regional Proterozoic formations in the Meluco region, especially its metacarbonate members, host Mg-B-rich skarns bearing coloured dravite and other B-Mg-calc-silicate gemstones, in Micute and N'Djekwa area. Following the probable lithological precursor composition, these peculiar gemstones consistently reveal geochemical Mg-B signature that could have been inherited from an evaporite ancestry, inter-stratified in the protolithic Lalamo sequence.

Keywords

Dravite • Calc-silicates • Skarn • Evaporite • Mozambique

1 Introduction

In Northeastern Mozambique, Cabo Delgado Province, recent field studies of the small scale mining in the Messalo River Basin revealed the presence of rare semi-precious stones, which primary genesis hypothetically depend on atypical processes, complexly related, having in common, the structural relation with strike-slip and overthrust shear and the geochemical relation with acidic metasomatism.

Some of these peculiar deposits occur near Meluco and have their most significant expression in the sector of N'Djekwa and Micute (Fig. 1). Here, several mine diggings, in the calc-silicate members of a silicious–dolomitic rock, produced peculiar assemblages of coloured gemstones.

C. L. Gomes (✉)

School of Sciences, Department of Earth Sciences, University of Minho, Braga, Portugal
e-mail: carloslealdb@gmail.com

Landscapes, Heritage and Territory Laboratory, University of Minho, Braga, Portugal

Proterozoic rocks outcrop in most of the Meluco region, corresponding to gneissic-migmatitic complexes, where the different members can be distinguished by lithology, metamorphic grade, structure, and age. Often the contacts are of a tectonic type and were established from Neoproterozoic to Cambrian, already independent of Pan African Orogeny (Leal Gomes et al. 2012). Widespread orthogneisses are predominantly felsic to intermediate. They occur at lower tectonostratigraphic levels but possibly segmented, indented, or carried over other formations, mainly of the Lalamo complex, which, according to regional geological mapping, covers the entire area (Chikwanda nd) and, in its turn, serves as the basis for Cenozoic to recent deposits of the glacial and fluvio-lacustrine placers, more or less crustified as laterites.

The lithologies of the Lalamo complex itself include mesocrustal components. Also, the metamorphic features vary from low grade to amphibolite and granulitic facies. The contiguity of these formations is attributed to tectonic transport and carriage overlap. The complex's predominant rocks are meta-sandstones and meta-conglomerates, quartzites, meta-carbonate rocks and other metamorphic terms of chemical precipitation rocks, biotitic to amphibolic gneisses, amphibolites and, with less cartographic expression, metamorphic products of granite to ultrabasic protoliths.

2 Materials and Methods

In a first approach, the following studies were developed: geometric analysis of mega-structures and their regional framework and remote detection of lithological patterns compatible with the expression of gem-productive lithologies. Fieldwork included a review of the assemblages of noble minerals and the observation or deduction of the types of mineral deposits to which they could be related. The main gemstones collected were dravite, tourmaline, epidote, spinel, several garnet varieties, beryl and kornepupine (Leal Gomes

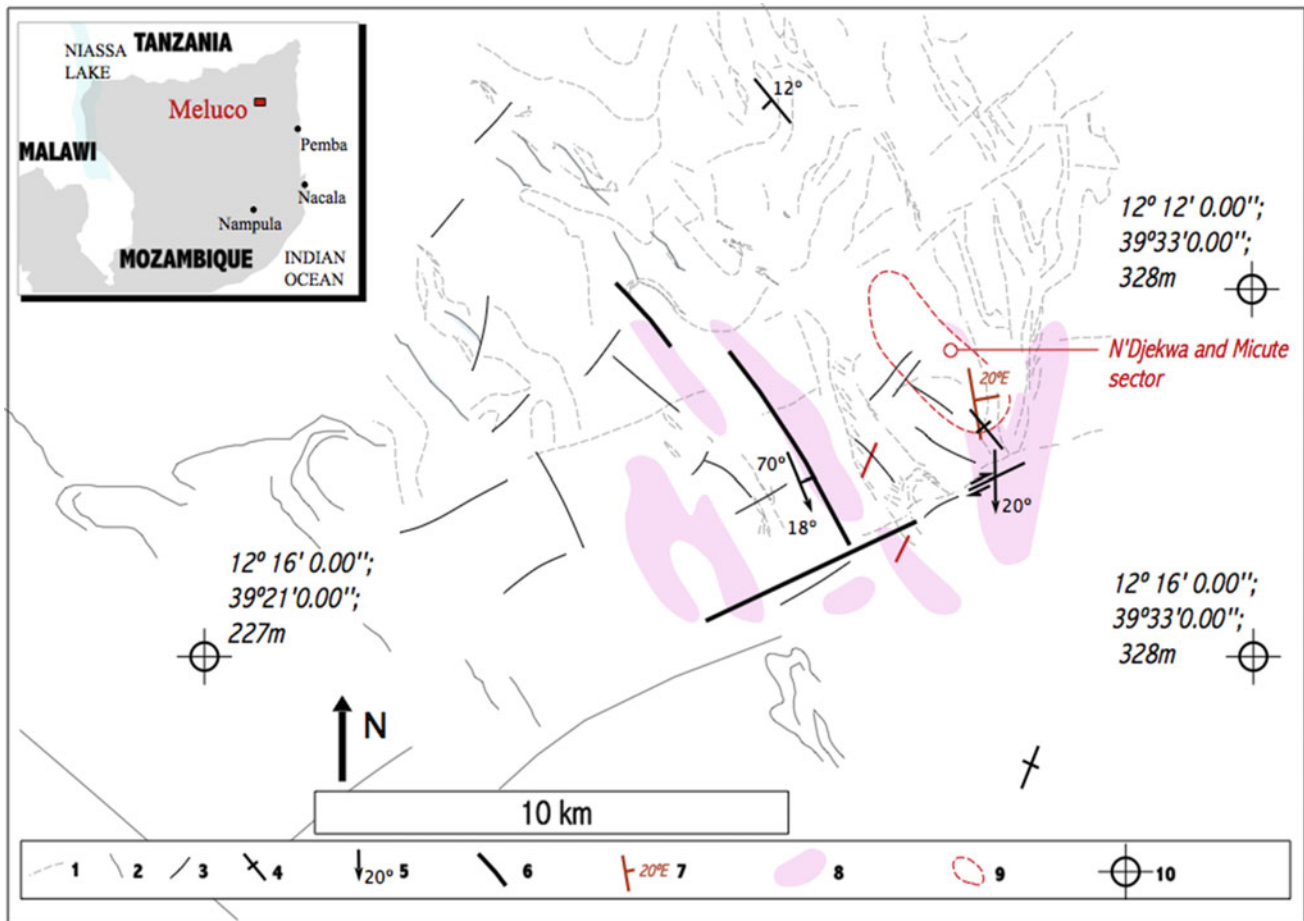


Fig. 1 Meluco location in Northern Mozambique and the structural map corresponding to this region. 1–trajectories of metamorphic surfaces; 2–trajectories of probable lithological contacts and other lineaments defined in ductile regime (established in remote sensing); 3–trajectories of ductile-fragile lineaments (confirmed in fieldwork); 4–

gneissose reference structures, measured at outcrop; 5–intersection and stretching lineations; 6–tectonic accidents reactivated in a fragile regime; 7–segregation pegmatoid or quartz veins; 8–areas with complex lithological variability; 9–limits of N'Djekwa and Micute pitted and trenched area; 10–cartographic reference points

2019). These set of minerals suggest that the main common origin could be metasomatic, producing calc-silicate rocks departing from meta-carbonate protoliths. Micute and N'Djekwa sites, meta-carbonate and calc-silicate rocks were sampled for rock and mineral specimens. These samples were studied in thin section (petrology) and separate phases for XRD. Semi-quantitative chemical analysis of individual polished grains was obtained in SEM–EDS.

3 Results

The base resources that were confirmed include gemstones of dubious nature present in secondary deposits but with uncertain primary source (Chikwanda, nd). Nevertheless, the most probable primary-secondary linkages survey from the detailed inspection of the trenches, we deduce that the gem mineralization is quite heterogeneous. There is a tendency

for its dispersion in the silicate-rich meta-carbonate rock and occasional concentration in typical skarn horizons, currently showing dravite tourmaline (Ca, Mg)-varieties of garnet, epidote, kornepupine and spinel. The most prevalent gemstones correspond to dravite and dravi-uvite tourmaline (Fig. 2), identified by XRD and semi-quantitative chemical analysis by SEM.

Much more rare is finding some specimens of corundum, chrysoberyl, ilvaite, axinite, scapolite, holmquistite, titanite, and spodumene. In Fig. 3, it is apparent that the transition stage between prograde and retrograde stages of a typical skarn and concomitant metamorphic peak materializes a threshold suitable for the main gemstones are trapping in voids related to shear.

Figure 4 synthesizes the skarn deposits' internal structure and paragenesis typically lying between meta-carbonate rocks and gneissic to migmatite formations under glacia coverage to placer type mobilization of erosional debris.

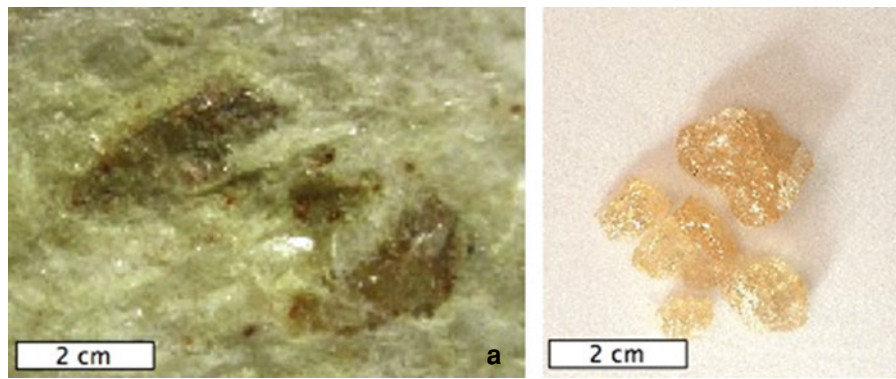


Fig. 2 Macro-images of the prevailing primary tourmalines collected from N'Djekwa and Micute sites. **a** Intergrowth of tremolite (elongated white laths) with dravi-uvite (brown to yellow, lodged in dilation, transpressive sites); **b** Blast fragments of yellow dravite extracted from a reaction rim between dolomite and tremolite asbestos

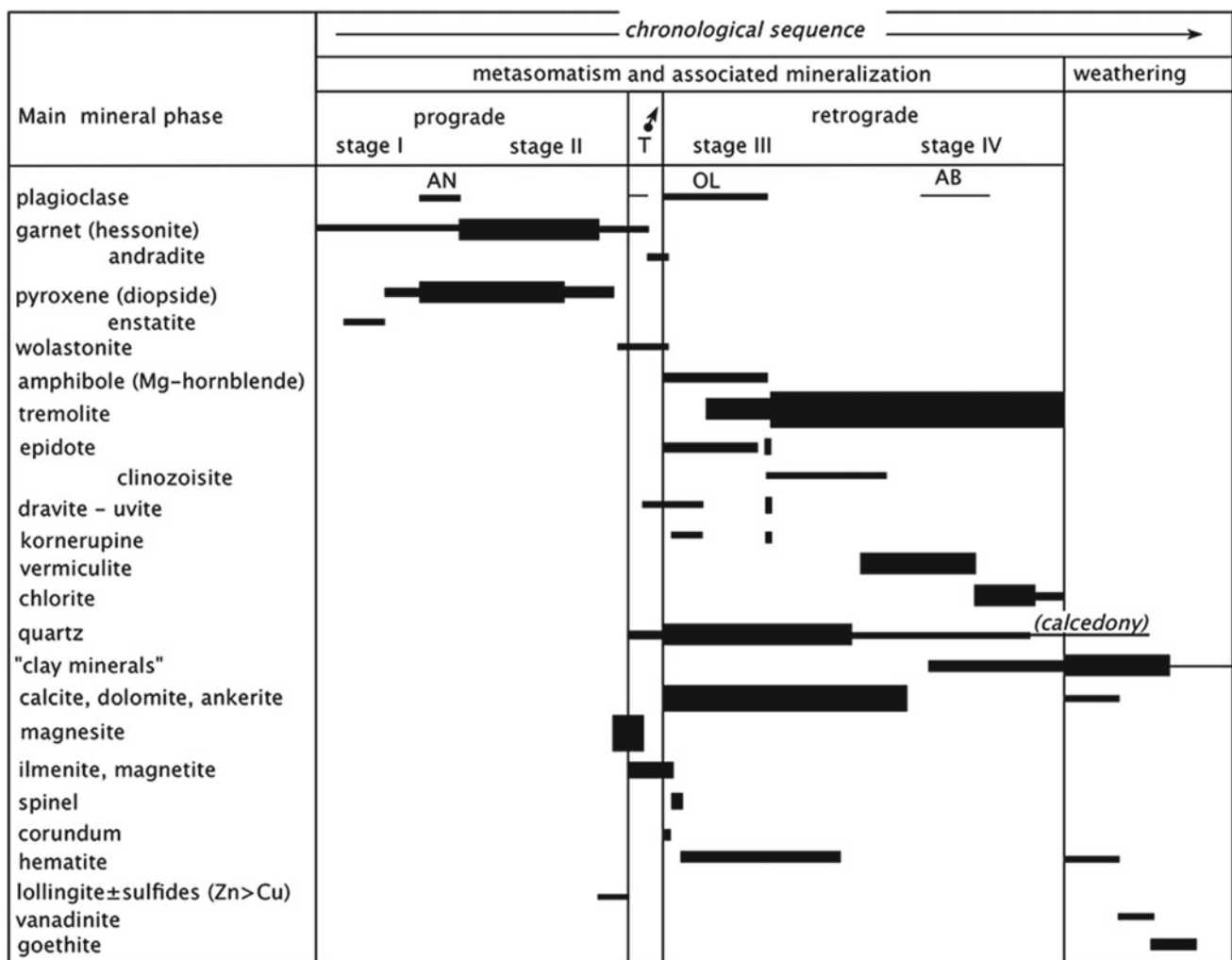


Fig. 3 Paragenetic synthesis for N'djekwa and Micute gem deposits in silicious metacarbonate rocks from Meluco. T-maximum conditions (P, T) for metamorphism and metasomatism (±630°, 5.5 kBar). AN-anortite; OL-oligoclase; AB-albite

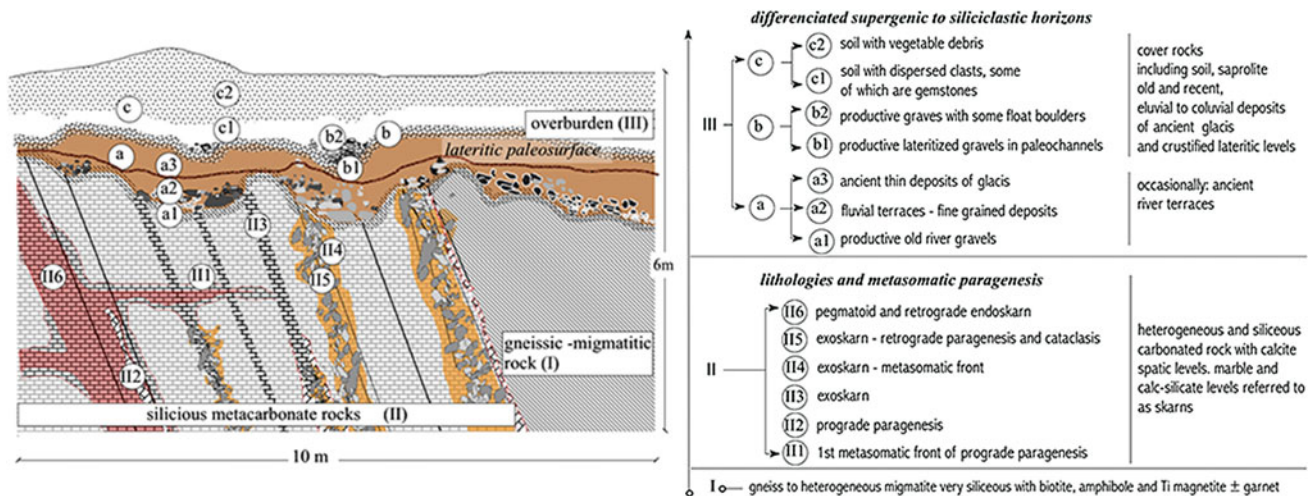


Fig. 4 Holistic and representative sketch profile for the transversal NE-SW trenches located at N'Djekwa and Micute sites: geometrical analysis of structure and paragenesis of the main calc-silicate occurrences

4 Discussion and Concluding Remarks

Hydrothermal alteration and precipitation focused on shear zones and associated dilatational volumes are critical mechanisms for deposition and maintaining the gems' quality after their deposition. From the gemological point of view, the most interesting sites and modes of deposition are: tourmaline and garnet in porphyroblasts; tourmaline matrix precipitation and recrystallization of clasts under variable deformation regimes; miarolitic precipitation in pegmatites and dilatational volumes associated with shear, inside true skarn lenses; interfaces and reaction fronts are good reception sites for typical gem minerals resulting from metasomatic reactions.

Dravite is the gem with the greatest diversity of locations. Its hydrothermal concentration in dilatational sites is likely to be the most favourable for developing larger quantities of crystals, larger crystals and better crystals. These observations stand out the importance of shear displacement to the opening of empty porosity for fluid percolation followed by voids occlusion. That also favours metasomatic reaction conditions suitable to the trapping of noble crystalline products.

Reactivity results from the interaction of acidic fluids with B-enriched metacarbonate rocks, and it is expressed as aluminoborosilicate products. The Mg content from carbonate protolith is transposed to calc-silicate rocks enriched in dolomite and magnesite. This boron-magnesian chemist suggests an evaporitic signature associated with the primordial chemical precipitation.

This subject needs further investigation as it raises new possibilities for interpretation of the primitive sedimentary petrogenesis of the Lalamo complex itself.

The genesis of boronaluminosilicates depends on the particularities of the primary composition of the protoliths, the substituted calc-silicated facies and the process of alteration, limestone—marble—silica-rich metacarbonate—skarn. The substituted minerals determine the substitution between Mg and Fe and Al, Si and B in complex and associated boronaluminosilicates (e.g., magnesite and pyroxenes) is expressed in the tourmaline (product) and later silicates.

Kornerupine is a tipomorphic mineral characteristic of deep bimetasomatic skarns. Kornerupine and tourmaline probably crystallize during the late stage of the evolution of boron mineralization, in contact with the sequences of magnesian carbonates and desilicified silicoaluminous rocks. The value $(Mg/Mg + Fe) > 0.85$ can be considered characteristic of these sequences. It was estimated in carbonated associations from the calcite, dolomite, ankerite, magnesite ratios.

There is also a good potential for the occurrence of garnet deposits hosted in this type of skarns and siliceous marbles, especially in high-grade metamorphic crustal domains, and thus also in this case.

Studying the observed typomorphic minerals, the estimated peak metamorphic conditions are $T \pm 630$ °C and $P \pm 5.5$ kbar. These are consistent with the development of the metamorphic facies, amphibolite to granulite. Figure 5 shows a first conceptual and phenomenological conjugation between regional deformation and metasomatism, involving sedimentary carbonates and acidic fluids.

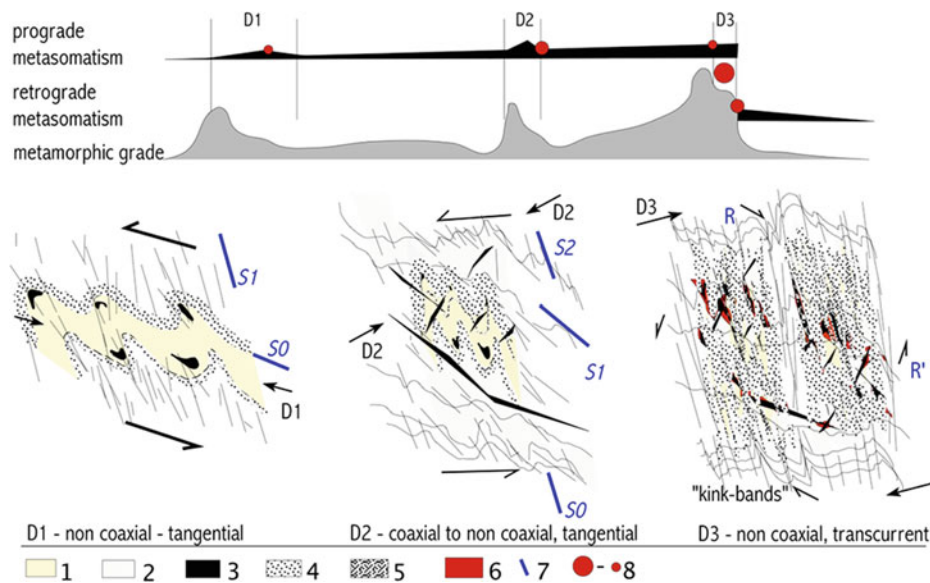


Fig. 5 Conceptual model for the generation of Mg-Al-B-calc-silicate gemstones—fluid/rock interaction in the presence of tangential to transcurrent shear deformation (note: the model is partially invariant from a scalar point of view): 1—calc-magnesian silicious metacarbonate rock; 2—magnesian calc-silicate rock; 3—dilatational environments, occasionally miarolitic; 4—masses of deformed inosilicates and

phyllosilicates with neoformation blasts; 5—cataclasites and mylonites; 6—Deposition sites for gemstones; 7—sedimentary to metamorphic surfaces; 8—probable chronological position for the genesis of gemstones, with magnitude qualitatively indicated by the diameter of the representative circle.

In the studies of petrofabric, it was possible to discriminate at least three deformation phases related to the prograde and retrograde metasomatic textures in thin polished sections and the field. This combination of geometries and processes would trap the rare gemstones.

It seems more credible an evaporitic signature for the carbonated protolith, considering the mineral-chemical composition biased to a probable magnesian and borated geochemical inheritance. The prevalence of late B and Mg gemstones, including the dravite-uvite series, is consistent with this hypothesis for at least some of the Lalamo sequence's protoliths.

References

- Chikwanda P (n/d) Minas de Meluco–Micute Project, Cabo Delgado Mozambique. Technical report on exploration work done on prospecting license, 7283L, Cabo Delgado Mozambique (Unpublished Report)
- Leal Gomes C (2019) Auto de visita à área de prospecção e pesquisa, 7283L da Empresa, Minas de Meluco SA–SE do curso médio do Rio Messalo. Relatório Inédito para Empresa Minas de Meluco SA, Moçambique (Unpublished Report)
- Leal Gomes C, Marques J, Moiana M (2012) Quadro geológico conceptual para a localização dos recursos base de gemas no Norte de Moçambique. In: Actas do Iº Congresso Nacional de Geologia de Moçambique, Maputo, Moçambique



Conceptual Genetic Model for the Primary Occurrence of Garnet and Corundum Gemstones in the Miteda Region, Cabo Delgado Province, Mozambique

Carlos Leal Gomes

Abstract

This study enhances the importance of primary, shear-related eclogite-granulite metasomatite, not only as a source of corundum and garnet gemstones for placers but also as a valuable deposit by itself. The focus of hydrothermal circulation in multistage shear zones is invoked as the main pathway to interpret the complex mineralization observed in Miteda. In this case, the structure of a corundum + garnet major spots is interpreted according to a model of pull-a-part structures associated with sinistral shear. There is a relation between the red saturation of Rubi and the content of Cr in corundum. Cr can be leached from the meta-ultramafic host rocks as a co-product of desilification.

Keywords

Ruby • Rhodolite • Eclogite • Shear zone • Mozambique

1 Introduction

In the last decade, the exploitation of rubies in Cabo Delgado and Niassa provinces in Mozambique has reached significant values in terms of the number of regular companies and informal prospectors involved and the monetary amounts that characterize local and international transactions of these gemstones. It turns out that, in most cases, mining works focus on the so-called secondary deposits, alluvial placers being considered as the most interesting. Nevertheless, some companies are beginning to devote some attention

to primary deposits. Excluding pegmatites, Leal Gomes et al. (2012) presented a first synthesis of the main conceptual models involved in the origin and structural control of primary mineralization of peraluminous gemstones (mainly ruby and garnet) in northern Mozambique. They also listed some other noble materials, which might be obtained as by-products from ruby and garnet mining. In most models, the focus of hydrothermal circulation in shear zones is invoked as the main pathway for the generation of metamorphic and metasomatic deposits. These occur in corridors of anomalous lithologies and vein swarms where peraluminous paragenesis is hosted, often related to acidic fluid desilification by the reaction with a sedimentary protolith of metacarbonated or meta-ultramafic nature in sequences of amphibolitic to granulitic facies.

A noble corundum prospect of primary generation was recently identified in the vicinity of Miteda, Cabo Delgado Province (Fig. 1). Here, a few exploration diggings intersected an anomalous concentration of garnet and corundum. In satellite imagery, this seems to be conditioned by the proximity of first-order lineaments with the azimuths referred to in Leal Gomes et al. (2012)—160, 130, and 65–70°.

Starting from the above-mentioned mega-scale organization (Fig. 1), a fieldwork mission enabled the detailed structural and paragenetic analysis of these occurrences. It also provided the collection of samples of gem minerals, carrier associations, and host rocks. These samples were studied by optical, electron microscopy, and X-ray diffraction (XRD), and the noble species were subjected to carving, polishing, and stone enhancement assays to confirm their gemological adequacy.

In the case of pink to red corundum, Cr₂O₃ contents were also estimated by scanning electron microscope analysis through energy-dispersive X-ray spectroscopy, only dedicated to this oxide and using a known standard of a Cr-rich ruby, previously analyzed in electron microprobe.

Comparing (colour, crystalline forms, and transparency) some of the corundum of this deposit with others that appear

C. L. Gomes (✉)
Department of Earth Sciences, School of Sciences, University of Minho, Braga, Portugal
e-mail: carloslealdb@gmail.com

C. L. Gomes
Landscapes, Heritage and Territory Laboratory, University of Minho, Braga, Portugal

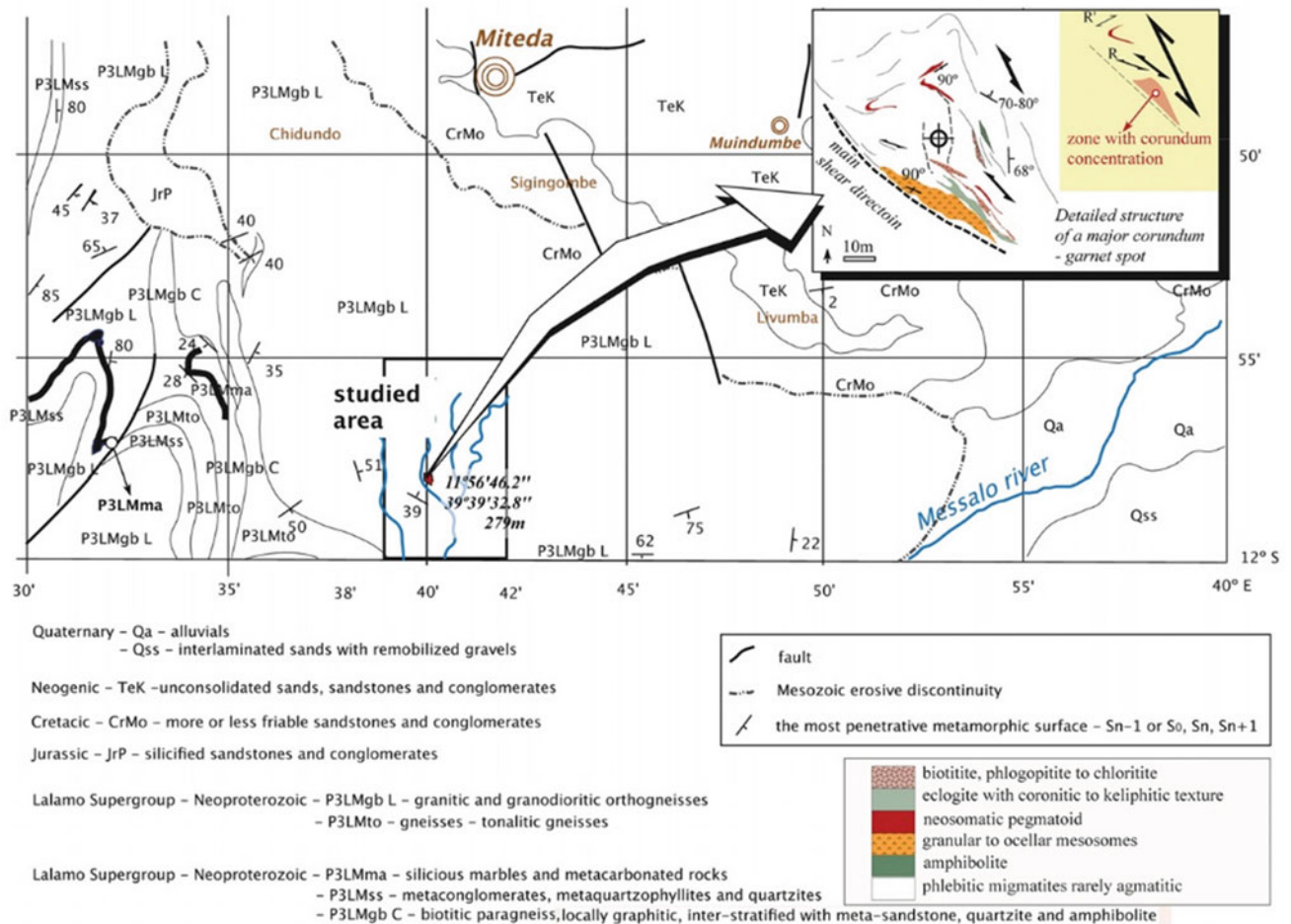


Fig. 1 Location of the garnet–ruby sites in the regional geology framework—referred to as studied area. Inset: Detailed structure of a corundum + garnet major spot, interpreted according to a model of pull-a-part structure associated with sinistral shear

in nearby placers, it is reasonable to accept that these deposits may, at least in part, be the source of ruby clasts of secondary deposits.

On the other hand, these same spots alone can represent deposits of relevant economic interest.

Thus, based on detailed structural analysis, mineralogy, and paragenesis, we sought to establish a genetic model capable of accommodating the available information and serving as a conceptual basis for the advancement of exploration and small-scale mining dedicated to ruby, pink sapphire, and other associated gemstones.

2 Results

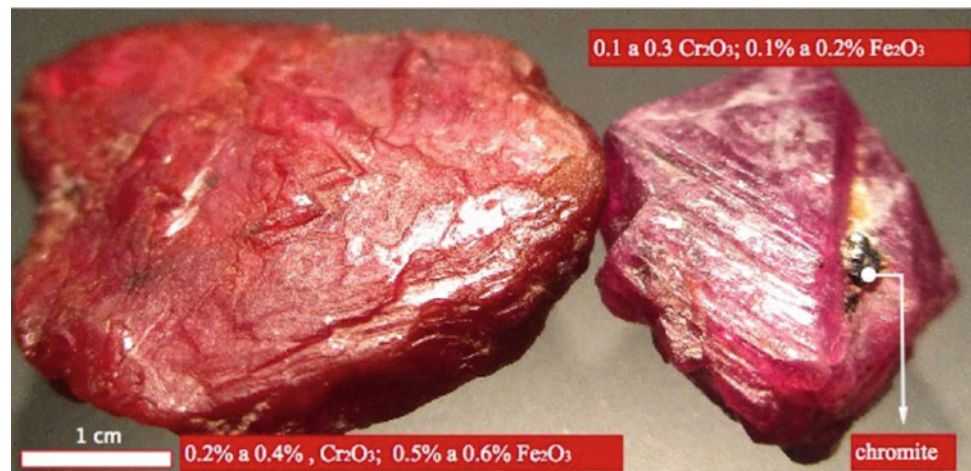
From combined cartography and structural analyses and petrology approach, it was deduced that gneissic-migmatitic terranes of Miteda present metamorphic paragenesis typical of the granulitic facies with the variations of the stability

fields of the aluminosilicate (Al_2SiO_5) being located between sillimanite and kyanite.

The metamorphic P/T stability field admits granulite—amphibolite transition due to temperature and lithostatic pressure variations in the sillimanite field—and granulite—eclogite transition, more dependent on pressure variations—sillimanite => kyanite transition. This might be facilitated by increased stress related to progressive shear (tangential to transcurrent) and fluid circulation focused on the same deformational corridors causing regional to local metasomatism.

At the petrography and paragenetic analysis of the regional metamorphic rocks, it does emerge a pattern of regional metamorphic evolution, which shows the following trends: A—pressure and temperature increase that allows the transition of the monovariant limit between amphibolite facies and granulite facies—regional metamorphism in the sillimanite stability field; B—pressure increase, in conjunction with fluid circulation, originating an eclogitic transition

Fig. 2 Relationship between red colour saturation and contents of Fe and Cr. Note: the formation of chromite seems to penalize Cr's availability for incorporating the crystalline lattice of corundum



from the granulitic facies; the transition seems to be controlled by mega-corridors, with a regional cartographic expression. Such corridors may include tectonic accidents and shear zones ductile to fragile, both tangential and transcurrent.

These conjugated structures control dynamic metamorphism in the transition from sillimanite to kyanite stability field to which metasomatism is associated. The most valuable noble minerals detected were translucent, cabochon grade rubies and pink-sapphires (Fig. 2); transparent, in various shades of red, almandine–rhodolite–pyrope garnet; iolite variety of cordierite. Typical rubies with higher concentrations of Cr_2O_3 (as in Fig. 2) are rare. The lithological and mineralogical diversity associated with these deposits can be synthesized as follows.

Regional rocks belong to Lalamo, Neoproterozoic Supergroup. It includes garnet migmatites and alkaline gneisses; occasional meta-ultramafic layers with Cr, Fe, and Mg spinels; amphibolic rocks of diverse typology and

phyllitic appearance, sometimes with sillimanite or kyanite and amphiboles; granulites and granulite gneissic rocks; graphite gneisses; eclogitic facies (Fig. 3) with coronitic and kelyphitic textures involving garnet (pyrope-almandine) and orthopyroxene (enstatite); magnesian fluorocarbonate formations and calc-silicate rocks in contact with siliciclastic formations (metaconglomerates and quartzites).

Mineralization host rocks occur along shear corridors. It includes coronitic eclogites, biotites with some phlogopite and banded iron rocks (with magnetite and ilmenite and atypical intergrowths of ilmenite, magnetite, ixiolite and almandine garnet) and transitions between these facies and regional rocks; pinch and swell boudin-like pegmatites.

Mineralogy of the deposits of gemological interest includes garnet (rhodolite and pyrope); corundum (ruby and pink sapphire) with spinel halos showing inclusions of native gold, silver-copper alloy, alumotantite, and scheelite (Fig. 4); cordierite (iolite); epidote; zoisite; glaucophane; Cr-diopside; beryl (heliodor).

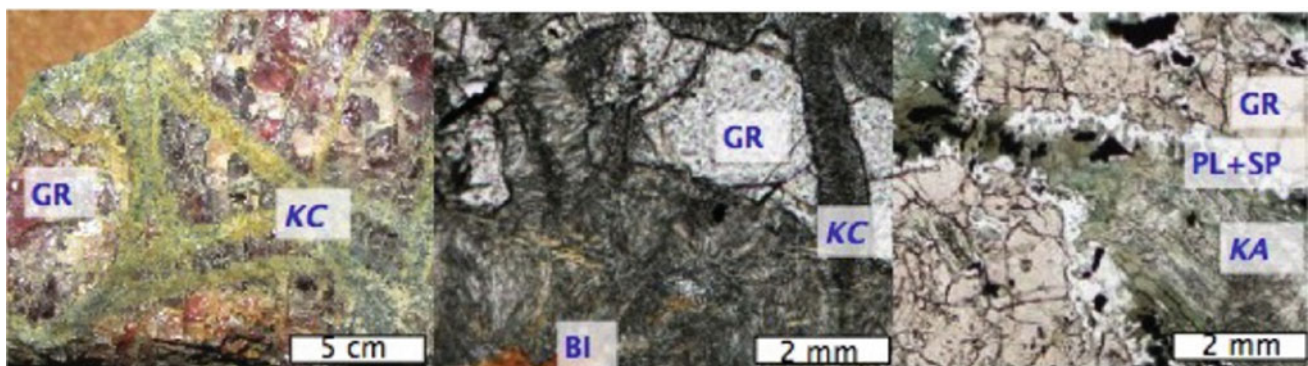
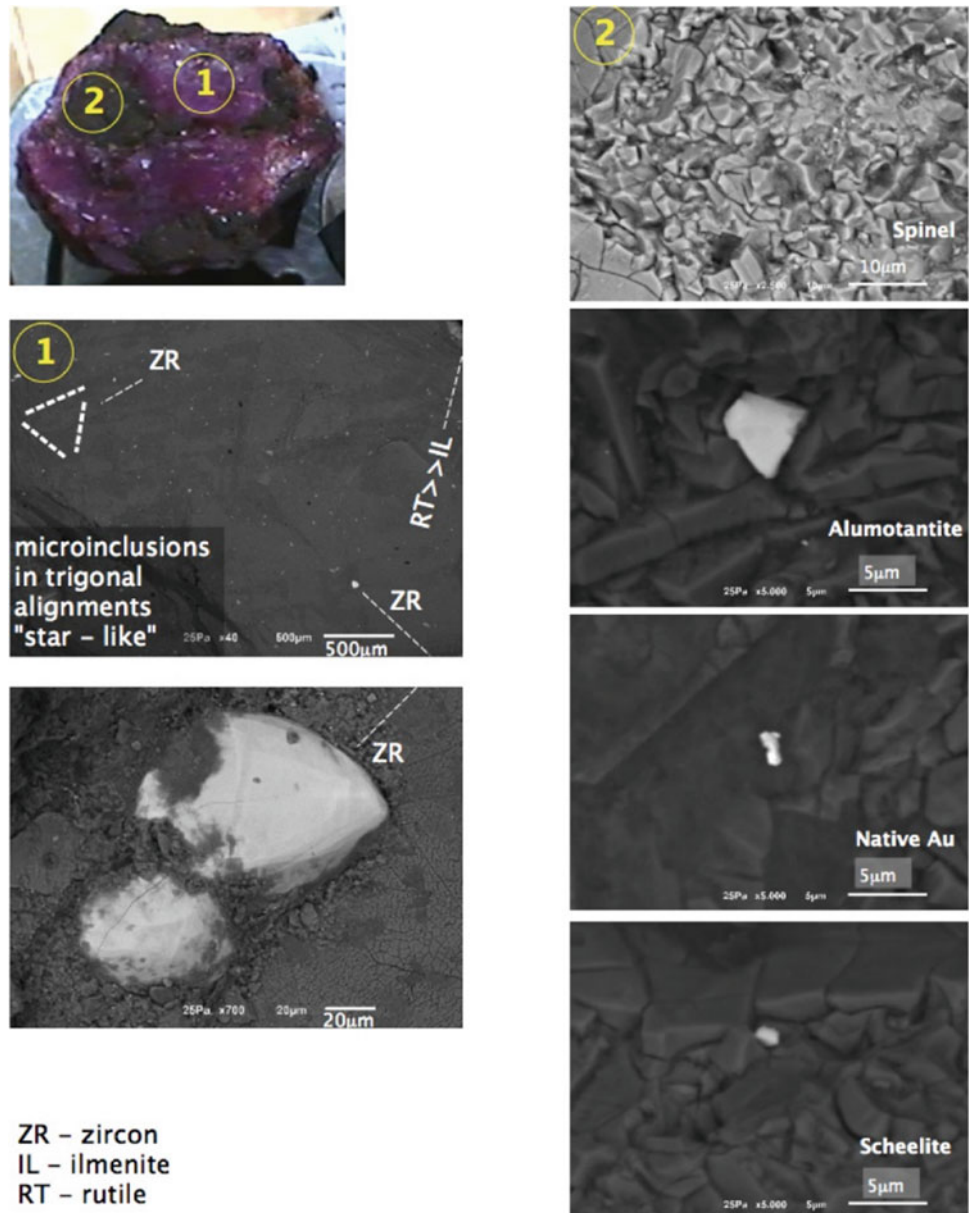


Fig. 3 Textural expression of metamorphic reactions in eclogite type lithologies: macro-image and transmitted light micrographs obtained in plane-polarized light. GR—garnet; SL—sillimanite; BI—biotite; PL +

SP—plagioclase + spinel; KC—kelyphite coronas or reaction laths with major enstatite; KA—kelyphite assemblage with diopside + albite + omphacite

Fig. 4 Domains with inclusion (1) and epitaxy (2) in red corundum; images of scanning electron microscope in low-vacuum conditions allow obtaining, simultaneously, backscattered electron contrast and secondary electron topography



3 Discussion

In what concerns ruby and garnet occurrence, much attention has been accorded to the diversity of placer deposits and less to its linkage to primary occurrences (Dill 2018). Besides that, the structure and paragenesis of primary occurrences is a less debated matter, both in the case of Cabo Delgado occurrences (Pardieu et al. 2013) as in more generalized studies (Giuliani et al. 2007). However, in general terms, shear development is faced as structural trap provider, several times considered to control the activity of parental disilicate fluids, which, in its turn, are favourable to the deposition or hyper-aluminous gemstones. The case of

Miteda reveals a new structural and paragenetic scenario where it is necessary to consider the strict spatial, and probably 42 genetic, the relation of productive shear with eclogite transition in high-grade metamorphic terranes.

4 Concluding Remarks

Shear corridors constitute structural and paragenetic anomalies to consider in the search for primary corundum gemstones. Detailed structural analysis and petrofabric studies suggest a preferential hosting of the corundum gemstones in the transpressive or transpressive spots of the vast shear zones with the adjacent eclogitic transition. As

seen in Fig. 1 (inset), the sinistral shear triggers degeneration of fluid-attracting voids in pull-apart structures and interstitial spaces between early crystals.

The desilicification of fluids that generate the ultra-aluminous signature may have been caused by loss of silica in the same metasomatic reactions that also produced calc-silicate minerals—in contact with metacarbonated rocks or with meta-ultramafic rocks hosted in granulitic sequences. Fluids and melts predictably segregated near these rocks' contact are more deficient in silica compared to fluids that would be secreted from normal granulitic metamorphic sequences.

The more or less coronitic to kelyphitic eclogitic facies with pyroxene, which is closer to the biotitic micaceous schlieren, also present the best rhodolite garnet (with best gem quality) and therefore, the association ruby + rhodolite + iolite is directly and indirectly indicated by the faciological guide, biotite (Leal Gomes 2019).

References

- Dill H (2018) Gems and placers: a genetic relationship par excellence. *Minerals* 8:470
- Giuliani G, Ohnenstetter D, Garnier V, Fallick AE, Rakotondrafa M, Schwarz D (2007) The geology and genesis of gem corundum deposits. *Geol Gem Depos*, Mineral Assoc Can 37:23–80
- Leal Gomes C (2019) Juízo sobre actos de prospecção de gemas e minérios na área correspondente à licença 7606C, Miteda, Mueda, Cabo Delgado. Relatório de fundamentação e progresso da actividade prospectiva—Inédito para GAL Resources SA Mueda (Unpublished Report)
- Leal Gomes C, Marques J, Moiana M (2012) Quadro geológico conceptual para a localização dos recursos base de gemas no Norte de Moçambique. In: Actas do Iº Congresso Nacional de Geologia de Moçambique, Maputo
- Pardieu V, Sangsawong S, Muyal J, Chauviré B, Massi L, Sturman N (2013) Rubies from the Montepuez area (Mozambique). GIA News from Research Report. https://www.gia.edu/doc/GIA_Ruby_Montepuez_Mozambique.pdf

**Geotechnologies, Engineering Geosciences,
and Geohazards**



Polish Experience in Offshore Mining: The New Concept of Transport Deep-Sea Concretions and Processing

Krzysztof Broda, Wiktor Filipek, and Barbara Tora

Abstract

This work presents new technologies used in transporting deep-sea concretions from the seabed to the surface. Transporting matter from great depths to the surface is the biggest problem for deep-sea mining. The solutions used to date, based on Continuous Line Bucket (CLB) method, hydraulic pumping (HP) method or air-lift pumping (ALP) method, are energy-intensive, thus generating high costs. This research presents transport technology based on the concept of using phase transition from solid or liquid to gas or solid to liquid as an energy source for transport from the seabed. The developed methods are less cost-intensive, and the exploitation and transport of concretion can be undertaken environmentally friendly. In addition, methods of recovering metals from concretions are presented—hydrometallurgical methods and leaching.

Keywords

Deep-sea mining • Nodules • Technology • Processing

1 Introduction

Recognising the potential benefits of exploiting submarine deposits, for several decades, many countries, including Poland, have been carrying out scientific research and developing concepts for the exploitation of these deposits (e.g., Depowski et al. 1998; Abramowski and Kotliński 2011; SPC 2013; RS 2017; Sharma 2017; Jones et al. 2019).¹

¹ See also: <http://www.blue-nodules.eu/> (accessed in January 2020).

K. Broda (✉) · W. Filipek · B. Tora
Faculty of Mining and Geoenvironment, AGH University of
Science and Technology, Krakow, Poland
e-mail: broda@agh.edu.pl

In July 2017, the Polish Council of Ministers adopted the Ocean Geological Survey Programme (“PRoGeO”) to secure the safety of our country’s raw materials and energy security, among other things, through seabed exploration. According to the plans, the programme shall run until 2033. In the nearest future, the “PRoGeO” will support the research of deposit structures specific for seabed areas in order to locate and identify undersea resources, such as massive sea-floor sulphide (SMS) deposits polymetallic nodules, cobalt crusts, gas hydrates and others. The purpose is to increase available reserves of mineral resources. More than EUR 120 million is expected to be allocated for research carried out under the programme. The amount of EUR 7.3 million is earmarked for the programme implementation in 2020.

The project involves acquiring rights to the undersea plots in the areas under the International Seabed Authority’s control (ISA). Due to the programme’s implementation, Poland will be among the countries allowed to exploit seabed deposits perspective.²

In addition to the Clarion-Clipperton Zone plot, on 12.02.2018, Poland signed a contract with the UN International Seabed Authority for searching and identifying the massive sulphide deposits on about 10 thousand km² area in the central Atlantic (Fig. 1). The concession for exploration was issued for 15 years. The efforts started in 2016, when the Polish Geological Institute purchased from the Russia Scientific Research Institute for Geology and Mineral Resources of the Ocean the exact plot coordinates with elaboration concerning staking out the coordinates for the research area of massive sulphide deposits in the Mid-Atlantic Ridge region. Our plot spreads over about 950 km along the axial part of the Mid-Atlantic Ridge of 26,010’–32,045’N latitude, and it borders French and Russian plots. ISA Council accepted the Polish application in

² Details in: <https://www.portalmorski.pl/> (accessed in January 2020); <https://www.psp.mos.gov.pl> (accessed in January 2020).

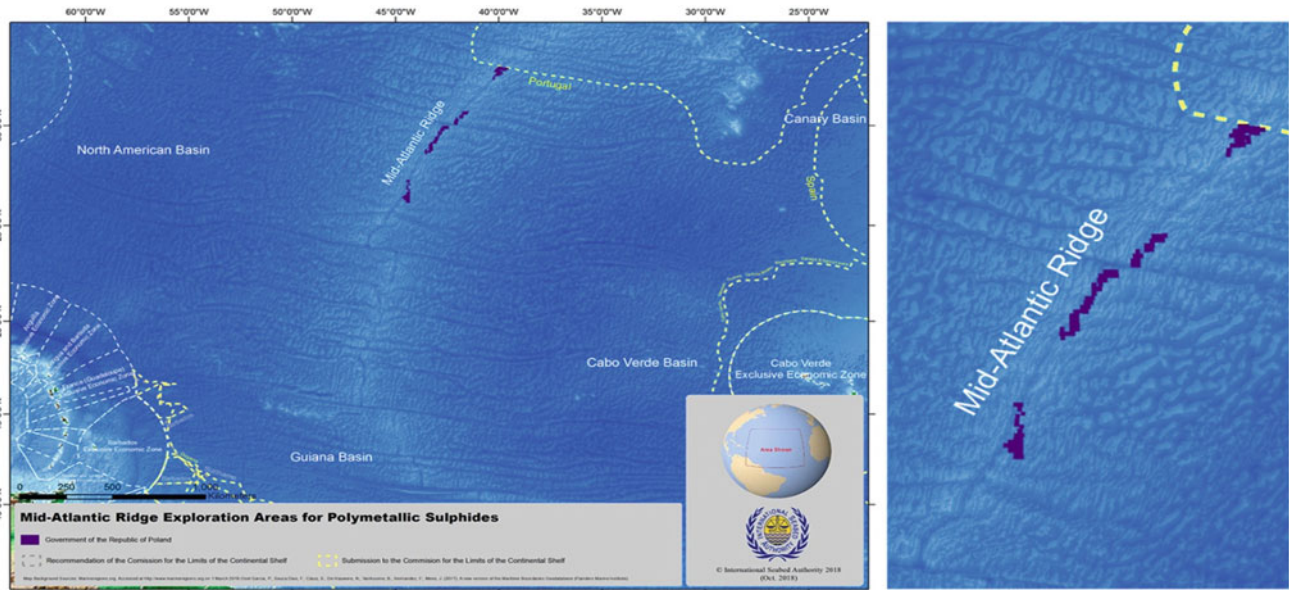


Fig. 1 The area on the Atlantic Ocean, in which Poland is allowed to conduct research (marked in violet) (<https://www.portalmorski.pl/>)

August 2017. The Atlantic seabed is covered with non-ferrous metal sulphide deposits. The deposits are supposed to be located at a depth from about 1400 to about 2800 m. The area of this plot is 10 thousand km². Forecasts indicate that the costs related to plot search and reconnaissance will be oscillating around EUR 120 million. The first research cruise of the vessel is planned for 2021. Financial outlays for the research and the uncertainty of the extraction profitability have been the source of numerous controversies concerning signing the contract with ISA, and the anticipated financial outlays (Wołkowicz and Paulo 2019).

2 The New Concept of Transport from Deep Sea

The biggest problem in sea mining (open-cast) is transporting from the great depths to the surface. Despite many existing devices, none of the solutions used to date, based on the Continuous Line Bucket (CLB) method, hydraulic pumping (HP) method or air-lift pumping (ALP) method, is far from ideal. First of all, they are energy-intensive. Second, the operation and transport are undertaken in an environment-friendly manner. Our research focused on transporting the seabed output to the surface and was to approach this problem from the perspective of a new energy source. This idea is based on the concept of using solid or liquid to gas or solid to liquid phase change as an energy source for transporting from the seabed (Filipek and Broda 2016, 2017, 2018a, b, 2019). This concept is designed for regular transport from great depths above 200 m.

The transport module's operating principle is based on the change in the mean density of the entire module, connected to the buoyancy that acts on the immersed body (Acott 1999; Wilson 2012). When the mean density of the module is greater than that of the surrounding medium, the floatability is lesser than the body weight and there occurs a descent (drowning). A specific case is when the module's mean density is equal to that of the surrounding medium. The buoyancy is equal to the body weight, and the body remains motionless. The change in the mean density of the immersed object in a given medium may be obtained in two ways. The first one, used in submarines, is based on using the so-called ballast tanks filled with water or compressed air. This method is used when the immersion depth is not too much and does not exceed several hundred metres. Under this depth, due to technical reasons, the second method is used. It consists of diving with the ballast, and then, to emerge, the ballast shall be dropped, which causes it to be irretrievably lost as it lands on the bed of the researched water tank. Figure 2 presents the idea of using phase change as an energy source for transporting in the marine environment. It shows the two crucial operation stages of the transport module, i.e. descending towards the bed and surfacing. As mentioned earlier, the process of descending towards the bed may occur only when the density of the transport module—equal to the density of the substance before the phase change of volume, assuming that neglected the mass of the structure—will be greater than the density of water surrounding the transport module. In turn, the surfacing may occur only when the density is expressed by the following relation (Filipek and Broda 2016, 2017):

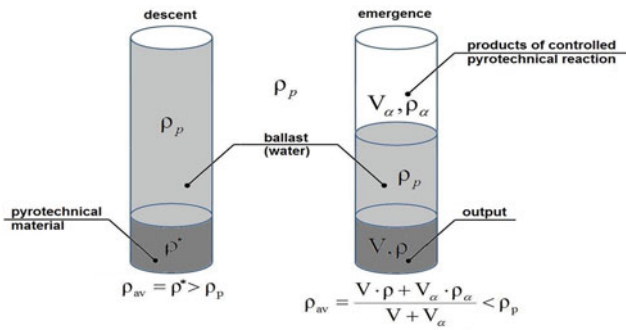


Fig. 2 The concept of using phase change as an energy source for transporting from the seabed (Filipek and Broda 2016)

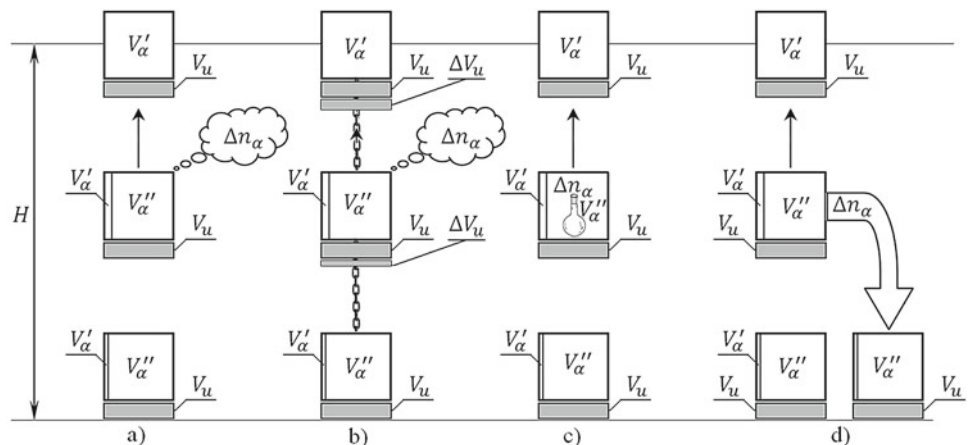
$$\rho_m = \frac{V_u \rho_u + V_\alpha \rho_\alpha}{V_u + V_\alpha} \quad (1)$$

will be smaller than the density of ρ_{H_2O} . It is assumed that the “ α ” index next to the density and volume symbol concerns the substance subjected to the phase change, which earlier, before the change, was marked with the “ s ” index. At this stage of presenting a conception of using phase change as an energy source for transporting in the marine environment, we will not go into details, substance or substance mix, and the chemical and physical processes it is subjected to during phase change. It should only be noted that by this term, we understand an initial state, marked with the “ s ” index and a final state, marked with the “ α ” index of processes occurring inside the transport module to change the mean density ρ_m of the discussed object. The “ u ” index near the density and volume symbol concerns the (widely understood) output, which is transported by the module from the seabed towards the surface. We can neglect the transport module structure’s density because it is fixed during the descent and surfacing. Thus there is no problem to balance it by the selected floats of right density so that its influence on the total density ρ_m of the transport module is negligible.

The concept of using solid or liquid to gas or solid to liquid phase change is characterised by one specific property that distinguishes it from the systems currently used. This property can use (in the next cycle) a part of the energy generated or necessary to start transport module surfacing. Transporting the seabed output using rope or hydraulic methods is linked to losing the total energy needed to fulfil the set goal. This article focuses on a short presentation of four concepts of implementing solid or liquid to gas phase change for transporting the output from the seabed. These concepts enable retrieving a part of the energy needed to initiate transport module surfacing, and these are the methods we currently research. Figure 3 shows them schematically, where the surfacing, i.e., transporting the output from the seabed stage alone, is presented. According to the relationship (1), the surfacing process is initiated when the medium subject to phase change reaches the right volume V_α at the right density ρ_α , which corresponds to the right amount of working medium mole n_α . The original volume V_α , with which the surfacing process was initiated, can be divided into two parts V'_α and V''_α , and thus $V_\alpha = V'_\alpha + V''_\alpha$ ($n_\alpha = n'_\alpha + n''_\alpha$). Wherein the volume V'_α is the minimal amount of working medium n'_α , which must be left in the system so the surfacing process may be completed. The result is that V''_α and so n''_α is the amount of working medium that, on the one hand, is necessary to initiate the surfacing process and on the other must be removed from the space V_α due to the need to preserve the safe pressure within this space, the working medium will expand during the surfacing process.

The most important issue that emerges during designing a module enabling transport of output from the seabed to the surface that uses solid or liquid to gas or solid to liquid phase change phase as an energy source is the question of what to do with the working medium excess Δn_α (Fig. 3a, b). The object’s surfacing under consideration generates an

Fig. 3 An illustration shows the four concepts of implementing solid or liquid to gas phase change for transporting the output from the seabed



unfavourable operation internal pressure increase compared to the surroundings. Of course, nothing stands in the way to dissipate the energy excess and thus to Δn_x return it to the surroundings, but this solution is disadvantageous in economics and the sea's environmental protection. However, it is the easiest solution, and besides, it is possible to use it for operation. As the working medium, such a substance can be selected, after completing the diving—surfacing cycle, it will be possible to sell it using the part Δn_x that was released to the surroundings (e.g., nitrogen) for auto-compressing the remaining working medium to use in the next cycle.

The expanding during surfacing working medium is characterised by one more desired property which is the change of its density, and so the possibility of increasing the transported load by the ΔV_u value, while maintaining the same default volume V_x . Nothing prevents connecting the transport modules, creating a kind of transport system (Fig. 3b). This system is characterised by some additional properties that are not achievable if each transport module works alone. When the modules create a cooperating system, there is a possibility to use the phase change ρ_x to compensate the mass of the additional load ΔV_u or a possibility to generate at the H depth less working medium than if the module worked alone. The considerations presented in the article (Filipek and Broda 2017) indicate that possible to achieve energy income can be even 90 (%). The system shown in Fig. 3c is a system where, to control the demand for working medium amount, an absorbent substance—absorbent system or reversible chemical reactions were used in a function of depth. This system is advantageous when hydrogen is the working medium because many known systems can be adjusted to the specificity of the sea transport we currently working on in the literature on the subject. We believe that for safety reasons, nitrogen would be a better working medium. However, no formula has been found to suit these conditions so far because nitrogen is a neutral gas, hard to react with other substances. While the last of the presented systems (Fig. 3d) is characterised by the fact that its transport modules operate in the system and that the excess Δn_x is used in the next cycle only for a different module already.

3 Metal Recovery Technologies

There are four main types of oceanic polymetallic mineral deposits: polymetallic nodules (PN), iron-manganese crusts (Fe-MnC), sea-floor massive sulphides (SMS) and metalliferous clays deposits. Polymetallic nodules (concretions) are the best recognised and described. Concretions create clusters of concentrically arranged alternating layers of iron and manganese oxides and clay minerals. Concretions are

Fe-Mn oxide clusters. The grain size of the concretion ranges from 10 to 200 mm. Based on the research (Piotrowicz et al. 2019), it appears that the density of the concretion in the dry state varies from 1.22 to 1.39 g/cm³, while the average density in the wet state is 1.94 g/cm³. The Mohs hardness is 2.5–3.0, with moisture 28–35%. In polymetallic concretions (Niedoba 2015), the greatest content has iron (6%), manganese (28%), nickel (1.4%), cobalt (0.2%), copper (1.0%), molybdenum and Au, Ag, Zn, PGE—platinum metals, REE—rare earth (Ce, Nd, Y, La, Ti, W, Zr, Bi). The prognostic resources of concretions in the Clarion-Clipperton field are estimated at 34 billion tonnes, including Mn—7,500 million tonnes; Ni—340 million tonnes; Cu—265 million tonnes; and Co—78 million tonnes. In order to obtain metals from polymetallic concretions, three main technology groups were studied (Pietrzyk et al. 2023): pyrometallurgical processes (e.g., smelting), hydrometallurgical processes (e.g., acid leaching) and combined processes. The most preferred method of processing is hydrometallurgy. Great facilitation is the easy crushing of concretes in dry conditions. Hydrometallurgy plays an essential role in recovering such metals as cobalt, nickel, copper, gold, platinum metals and lanthanides. These methods are the only way to obtain gold, platinum or palladium.

4 Concluding Remarks

A new approach to solving the problem of transporting seabed nodules concerns using a new energy source. This idea is based on solid or liquid to gas or solid to liquid phase change as an energy source for transporting. Besides, the results of theoretical research are presented and outlined how recovering metals from concretions are presented—hydrometallurgical methods and leaching.

References

- Abramowski T, Kotliński R (2011) Współczesne wyzwania eksploatacji oceanicznych kopalń polimetalicznych. *Górnictwo i Geoinżynieria* 35(5):41–61
- Acott C (1999) The diving “Lawers”: a brief resume of their lives. *S Pac Underw Med Soc J* 29(1)
- Depowski S, Kotliński R, Rühle E, Szamałek K (1998) *Surowce mineralne mórz i oceanów*. Wydawnictwo Naukowe Scholar, Warszawa
- Filipek W, Broda K (2016) Theoretical foundation of the implementation of controlled pyrotechnical reactions as an energy source for transportation from the seabed. *Sci J Marit Univ Szczec 48* (120):117–124
- Filipek W, Broda K (2017) The theoretical basis of the concept of using the controlled pyrotechnical reaction method as an energy source in transportation from the seabed. *TransNav, Int J Mar Navig* 11 (4):653–659

- Filipek W, Broda K (2018a) Experimental research on the concept of using an autonomous transport module for transport from the seabed. *New Trends Prod Eng* 1(1):267–275
- Filipek W, Broda K (2018b) Theoretical research on the gas phase density change in processes occurring during work of the transport module intended for transport from the seabed. *New Trends Prod Eng* 1(1):597–604
- Filipek W, Broda K (2019) Theoretical research on mass exchange between an autonomous transport module and the environment in the process of transport from the seabed. In: Weintrit A, Neumann T (eds) *Advances in marine navigation and safety of sea transportation*. CRC Press/Balkema: Taylor & Francis Group, pp 143–149
- Jones DO, Durden JM, Murphy K, Gjerde K, Gebicka A, Colaço A, Morato T, Cuvelier D (2019) Existing environmental management approaches relevant to deep-sea mining. *Mar Policy* 103:172–181
- Niedoba T (2015) Polymetallic concretions: long-range source of mineral raw materials. *Inż Mineralna* 1(35):61–74
- Pietrzyk S, Piotrowicz A, Tora B (2023) Recovery of non-ferrous metals from oceanic nodules by pyro and hydrometallurgical methods. In: Chaminé HI, Fernandes JP (eds) *Advances in geoenvironmental engineering, geotechnologies, and geoenvironment for earth systems and sustainable georesources management*, proceedings of the 1st conference on georesources, geomaterials, geotechnologies and geoenvironment (4GEO), Porto. Springer ASTI Series, Cham (this volume)
- Piotrowicz A, Pietrzyk S, Czarny K, Płachta P (2019) Pyro and hydrometallurgical recovery of non-ferrous metals from oceanic nodules. *Inż Mineralna* 2(44):319–325
- RS (2017) *Future ocean resources: metal-rich minerals and genetics—evidence pack*. The Royal Society, London. <https://royalsociety.org/-/media/policy/projects/future-oceans-resources/future-of-oceans-evidence-pack.pdf>. Accessed January 2019
- Sharma R (2017) *Deep-sea mining: resource potential, technical and environmental considerations*. Springer International Publishing AG
- SPC (2013) Baker E, Beaudoin Y (eds) *Deep sea minerals: sea-floor massive sulphides. A physical, biological, environmental, and technical review*, vol 1A. Secretariat of the Pacific Community, Sydney
- Wilson MR (2012) Archimedes's principle gets updated. *Phys Today* 65(9):15
- Wołkowicz S, Paulo A (2019) Blue mining on the Atlantic: real need or need for realism? *Przegląd Geol* 67(2):91–103



Recovery of Non-ferrous Metals from Oceanic Nodules by Pyro- and Hydrometallurgical Methods

Stanisław Pietrzyk, Andrzej Piotrowicz, and Barbara Tora

Abstract

The study aimed to investigate the possibilities of recovering non-ferrous metals from polymetallic nodules originating from the ocean floor by pyro- and hydrometallurgical methods. In the pyrometallurgical method, the effect of the binder's addition and the slag-forming component on the reduction process's efficiency was examined. The reduction allowed the separation of the fraction rich in Mn and Fe (slag phase) from the metallic phase containing non-ferrous metals (mainly Cu and Ni). On the other hand, the hydrometallurgical method consisted of leaching manganese and iron into the solution with mineral acid without adding organic acids. At the current research stage for each of the methods used, separation of ferrous and non-ferrous metals was obtained and concentrated of these last ones suitable for further processing by copper pyrometallurgy technologies.

Keywords

Oceanic nodules • Non-ferrous metals • Pyrometallurgical extraction • Hydrometallurgical extraction

1 Introduction

The ocean polymetallic nodules of the Clarion-Clipperton nodules field from the ocean floor were examined. Kotliński (2011) and Abramowski and Kotliński (2011) revealed

relationships and regularities of polymetallic nodules distribution occurring on the Clarion-Clipperton nodules field. The strict correlations between the region's morphostructural development with the Pacific Plate evolution in the Mesocenozoic were demonstrated. The seabed form characteristics directly reflect geological development and changing sedimentation conditions determining productive nodule deposits. The selected hydrogenetic nodule type "H" with higher relative contents of Fe and Co shows in comparison against diagenetic type "D" and transition type "HD" lower contents of Mn, Ni, and Cu. In the Interoceanmetal Joint Organization (IOM) mining area, the greatest significance has type "D" and "HD" (with increased content of REE) and high nodules abundance and metal content, occurring at a depth interval of 4200–4500 m. Adopted criteria for mining area delineation, including high nodule abundance above 10 kg/m² and Mn content (>30%), high-grade sum of Cu, Ni, Co > 2.5% and bottom slope < 7°, confirm the IOM ore deposits can be considered perspective.

2 Materials

IOM provided the study material. This material was botryoidal concretions (Fig. 1) with a brown and rough surface, porous organic layer on the top, and easily crumbled. The inner layers are light brown or grey.

The results of the sieve analysis of the raw samples are shown in Fig. 2.

The feed material's chemical composition was determined using the WD-XRF method (MiniPal 4 PANalytical), while the phase analysis was performed using the XRD method (Rigaku Miniflex II). Table 1 shows the chemical composition of the dried polymetallic concretions, which was determined by X-ray fluorescence. The material consisted mainly of manganese compounds (approx. 52% by mass), silica (approx. 19% by mass), as well as iron (12% by

S. Pietrzyk · A. Piotrowicz
Faculty of Non-Ferrous Metals, AGH University of Science and Technology, Cracow, Poland

B. Tora (✉)
Faculty of Civil Engineering and Resources Management, AGH University of Science and Technology, 30-059 Cracow, Poland
e-mail: tora@agh.edu.pl

Fig. 1 Polymetallic nodules used in the research: A—appearance, B—fracture (Piotrowicz et al. 2019)

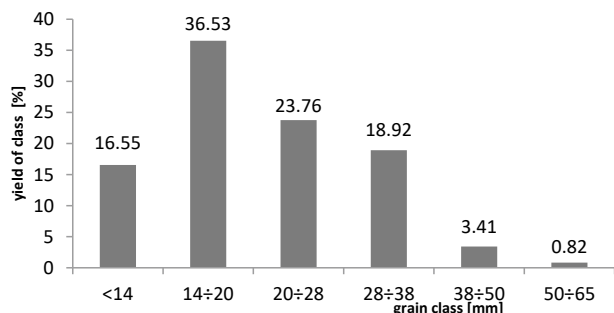
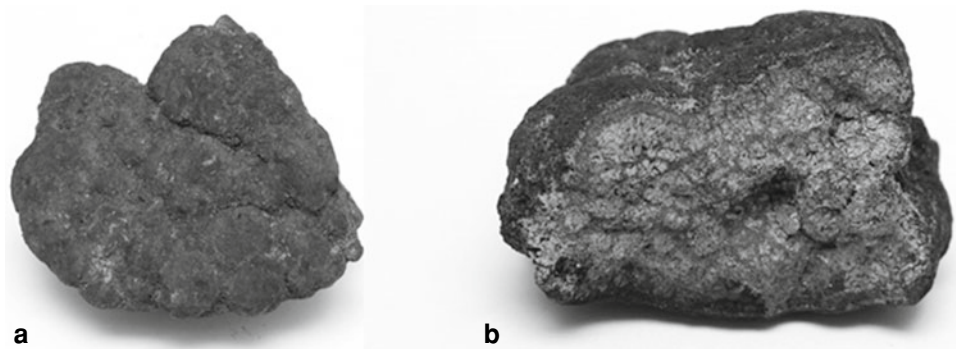


Fig. 2 Sieve analysis—fraction share in grain classes for the raw material

Table 1 Quantitative composition of raw manganese nodules (calculated as oxides)

Al ₂ O ₃	SiO ₂	CaO	MnO	Fe ₂ O ₃	NiO	CuO	Other
7.3	18.6	2.61	51.74	12.0	2.45	2.46	2.84

mass). In addition, percentages of copper compounds and nickel reach over 2% by mass.

3 Methods and Results

Pyrometallurgical tests were carried out in an electric chamber resistance furnace. A graphite crucible with an input consisting of ground concretions, flux—SiO₂, and a reducer in the form of anthracite with a grain diameter of less than 0.5 mm was placed. To improve the contact of the grains of the concretion with the reducing agent and eliminate the finest grains with gases, molasses were added as a binder. Attempts to reduction reaction were carried out at 1100 °C and lasted for 3 h, and increased to 1300 °C for 1 h. The chemical compositions of the products, both in the pyro and hydrometallurgical methods, were determined by XRF fluorescence. In the hydrometallurgical tests, the following reagents were used (all parts per): H₂SO₄ (95%,

Chempur), C₂H₄O₂ (acetic acid, 80%, POCH), C₂H₂O₄·2H₂O (oxalic acid, Chempur), and demineralized water ($\kappa = 0.05 \pm 0.01 \mu\text{S}\cdot\text{cm}^{-1}$). Leaching was carried out on a magnetic stirrer with a heating plate. The process conditions were organic acid concentration—20%, H₂SO₄ concentration—20%, duration—30 min, temperature—30 °C, $l/s = 10 \text{ ml}\cdot\text{g}^{-1}$ and stirring rate—500 rpm.

4 Results of Pyrometallurgical and Hydrometallurgical Tests

Table 2 shows the compositions of the obtained slags, which were mainly composed from manganese and silicon oxides (about 75% MnO and about 15% SiO₂, respectively). The content of non-ferrous metals (Cu and Ni) in the slag phase is lower in comparison with the starting material (approx. 0.15 vs 2.5% CuO; and 0.06 vs 2.8% NiO), so it can be assumed that these metals have passed after reduction to the metallic phase.

The XRD analysis results (shown in Fig. 3) indicate that the produced slag's main component is tephroite- manganese silicate and quartz-silicon oxide. Copper and nickel reflexes were not identified.

The metallic phase (Fig. 4) consists mainly of copper (about 28% by mass), oxygen (25% by mass), iron (18% by mass), and, to a lesser extent, manganese (19% by mass) (Table 3).

Also noteworthy is the high nickel concentration (over 7%). XRD analyzes the metallic phase (Fig. 5) to confirm that they contain mainly metallic copper, tephroite—Mn₂SiO₄, magnetite—Fe₃O₄, and quartz hausmanite—Mn₃O₄.

Table 2 Slag composition after pyrometallurgical tests (calculated as oxides)

Al ₂ O ₃	SiO ₂	CaO	MnO	Fe ₂ O ₃	NiO	CuO	BaO	Other
2.2	15.6	2.66	75.40	1.1	0.08	0.21	1.07	1.70

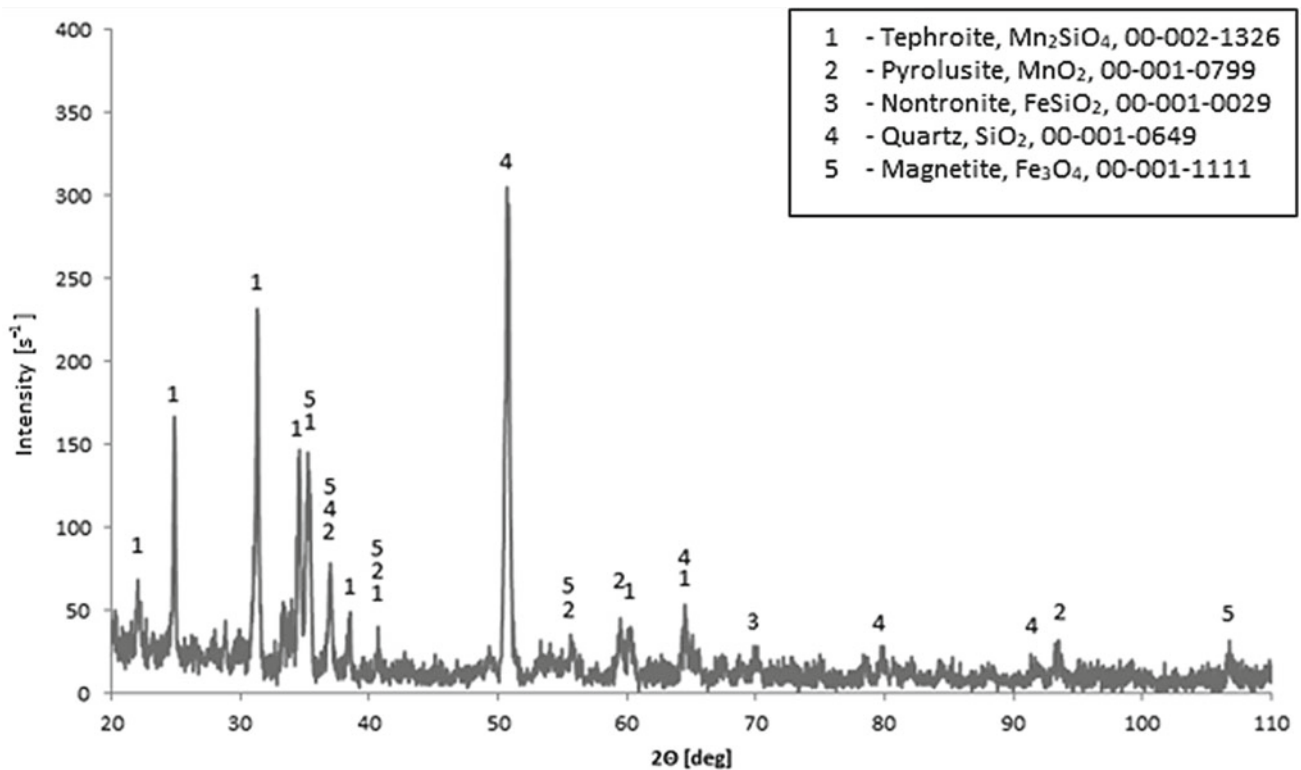


Fig. 3 X-ray diffraction analysis of the slag from the pyrometallurgical test

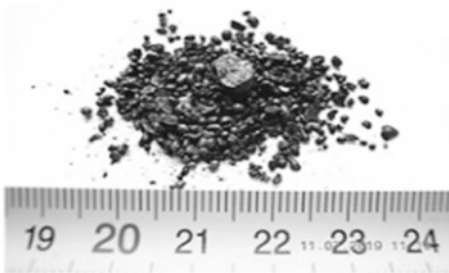


Fig. 4 The appearance of the metallic phase after the pyrometallurgical test

Table 3 The chemical composition of the metallic phases after the pyrometallurgical test (calculated as pure components)

O	Si	Mn	Fe	Ni	Cu	Other
% mass						
25.22	1.5	18.99	18.6	6.35	27.50	1.89

Hence, oxygen is associated mainly with iron, silicon, and manganese. Nickel is bound to iron (and probably also to manganese) in a mixture of oxides.

Copper extraction efficiency was 27%, but the content of metallic copper was 32% by mass. Therefore, the obtained copper extraction yields are not very high (just 27%). In further research, stages to improve the reduction parameters, probably longer process time, and higher temperatures will allow higher yields. However, preliminary research shows that the material obtained matches the copper content of industrial concentrates used in the copper smelting plant. Therefore, they are suitable for processing in the conditions of traditional copper metallurgy (shaft or slurry process). Furthermore, the obtained slags can also be a rich source for obtaining manganese (over 75% MnO).

Table 4 shows residues' compositions after leaching by sulfuric acid or a mixture with an organic acid. Comparing the results from the leaching test with sulfuric acid alone and with a mixture of acids, the impact of organic acid addition is recorded. These results confirm the phenomenon of reducing the leaching of iron and manganese. Using oxalic acid ($C_2H_2O_4$), a residue (it means concentrate) with a sufficiently high copper content was obtained—21.1% Cu. Thus, oxalic acid dissolves all metals except copper.

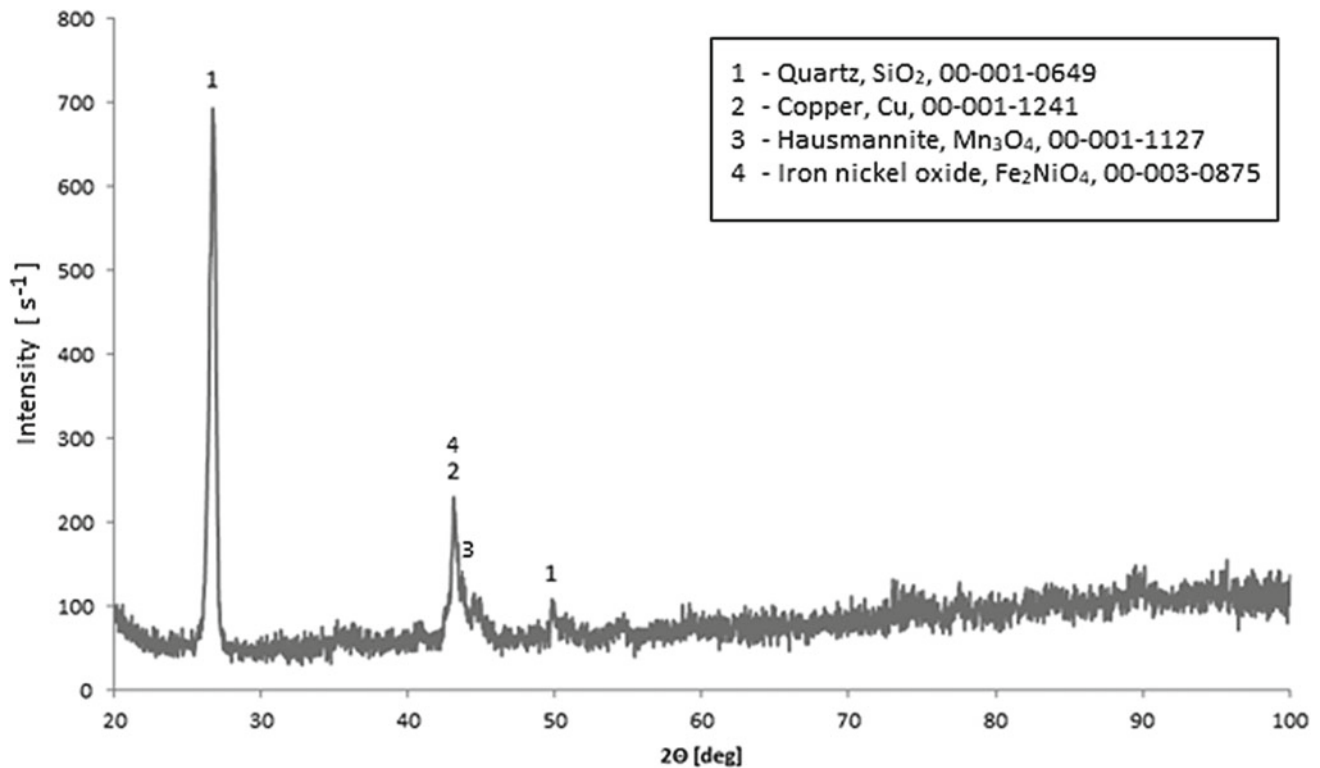


Fig. 5 X-ray diffraction analysis of the metallic phase from the pyrometallurgical test

Table 4 Chemical composition of manganese nodules residues after hydrometallurgical tests (calculated as oxides, from XRF analysis)

Content		Al ₂ O ₃	SO ₃	SiO ₂	CaO	TiO ₂	MnO	Fe ₂ O ₃	NiO	CuO	ZnO	Other
		% mass										
Feed		7.3	0.56	18.6	2.61	0.732	51.74	12.0	2.45	2.46	0.30	1.24
Acid addition	H ₂ SO ₄	1.1	5.2	5.2	0.95	0.280	71.66	9.89	2.98	1.04	0.09	0.94
	H ₂ SO ₄ + C ₂ H ₄ O ₂	4.8	14.1	27.4	2.69	1.050	6.75	28.5	0.46	0.73	0.18	6.54
	H ₂ SO + C ₂ H ₂ O ₄	4.3	11.0	23.3	2.69	0.941	7.02	21.58	0.62	21.1	0.26	0.58

5 Concluding Remarks

The following conclusions can be drawn from the obtained measurement results and their discussions:

- Proposed pyrometallurgical processing of oceanic concretions, consisting on the chemical reduction of metal oxides, i.e., the production of slag containing gangue and metal compounds from the iron group and the separation of the metallic phase, is an effective method for extracting non-ferrous metals from polymetallic concretions.
- The obtained slag consists mainly of manganese compounds (75% by mass MnO) and silicon oxide (15 wt% SiO₂). Slag contains insignificant amounts of copper (0.15% by mass CuO) and nickel (0.06% by mass NiO) in comparison to the feed material.
- Metallic phases include metallic copper (approx. 28% by mass Cu), silica, magnetite, and oxidized nickel phase. The concentrate thus obtained can be used in traditional copper metallurgy.
- The proposed method of processing concretions by hydrometallurgical method consists of reducing the leaching of manganese and iron, i.e., the main components of ore, using a mixture of sulfuric (VI) and organic acids. As a result of this process, a copper-rich concentrate was obtained.

- Among the organic acid additives used, oxalic acid turns out to be the most beneficial because it does not cause copper leaching, while it removes most of the manganese and most of the iron.
- Obtained copper concentrations in products from the pyrometallurgical method (metal fraction was containing 32.08% by weight of Cu) and hydrometallurgical (sludge containing 16.8% by weight of Cu) constitute a material that can be used in copper pyrometallurgy even without further processing.

Acknowledgements Tomasz Abramowski shared the research nodules material from the Interoceanmetal Joint Organization, for whom the authors are deeply thankful.

References

- Abramowski T, Kotliński R (2011) Contemporary challenges in the exploitation of oceanic polymetallic minerals. *Min Geoeng* 35:41–61
- Kotliński R (2011) Clarion-Clipperton concretion field—a source of future raw materials. *Min Geoeng* 35:195–214
- Piotrowicz A, Pietrzyk S, Czarny K, Plachta P (2019) Pyro and hydrometallurgical recovery of non-ferrous metals from oceanic nodules. *J Pol Miner Eng Soc* 2(44):319–326



Slope Inclinometers: Qualitative Evaluation of Probe Inclinometer Data—An Update

Luís Coimbra, Francisco Salgado, and João Paulo Meixedo

Abstract

Slope inclinometers are essential for assessing the performance and stability of a wide range of geotechnical works. These instruments are exact and easy to operate. However, credible and consistent results demand compliance with a series of operational procedures, which remain largely unknown or neglected. A state of the art and practice review on the operation of slope inclinometers in geotechnical works has been outlined. In addition, it assembles dispersed publications on the subject and discloses new methodologies for data analysis and error correction. Finally, this work summarises some aspects of the work regarding quality assurance and error correction of probe inclinometer data.

Keywords

Geotechnics • Inclinometer • Monitoring • Stability • Metrology

1 Introduction

Coimbra (2019) presents a review on the state of the art and practice of using slope inclinometers in geotechnical engineering from an operational perspective. His study aims (a) to reinforce the importance of adopting correct operating procedures and (b) to publish new methods regarding data analysis and error correction. The following topics are discussed:

L. Coimbra · F. Salgado
Division of Urban and Transportation Geotechnics (NGUT),
Department of Geotechnics, National Laboratory for Civil
Engineering (LNEC), Lisbon, Portugal

J. P. Meixedo (✉)
Department of Geotechnical Engineering (DEG), Laboratory
of Cartography and Applied Geology - LABCARGA, School
of Engineering (ISEP), Polytechnic of Porto, Porto, Portugal
e-mail: jme@isep.ipp.pt

1. A brief history of inclinometry and its adoption in geotechnical works.
2. Types of inclinometer systems available for geotechnical applications, categorised by sensor technology, system portability and (tilt) plane of reference.
3. Inclinometer casings and their installation in typical geotechnical applications.
4. Procedures for correct operation and maintenance of inclinometer systems, including general procedures for calibration and verification.
5. Data processing and obtainable results.
6. Quality assurance and error correction.

This work presents a brief introduction of the topic, addressing specifically vertical probe inclinometers.

2 Fundamentals of Inclinometer Data Processing

Most probes are biaxial, containing 2 sensors orthogonally arranged and aligned with two directions, often¹ designated A and B. Each survey requires 2 sets of readings on opposite sides of each direction. The first set of readings is taken with the probe oriented to the positive side and includes data from A0 and B0 (e.g., readings are positive if the casing is inclined to the positive side). The second set, taken with the probe rotated 180°, includes data from A180 and B180. The two sets of readings from each direction should be symmetrical at equal depths.

Nevertheless, due to several sources of error, they are not perfectly symmetrical. In good quality measurements, the main contribution for this mismatch should come from the sensors' bias. An instrument's bias refers to the reading

¹The positive and negative sides of directions A and B can be respectively designated as A0, B0, A180 and B180, as A+, B+, A- and B-, or as A1, B1, A2 and B2.

obtained at the zero position (e.g., an inclinometer perfectly aligned with its reference plane). On stable instruments, this value is well-known and can be subtracted from each reading. This is not the case for probe inclinometers. These instruments are designed with precision, speed, amplitude and thermal stability in mind, but bias stability is poor.

Equation 1 represents a reading from a standard probe inclinometer at position i , where θ is the tilt angle, b is the bias and k is a ²constant given by the manufacturer. There are four readings retrieved at each position (e.g., l_i^{A0} , l_i^{A180} , l_i^{B0} and l_i^{B180}). The tilt angle is exclusive to each reading (e.g., θ_i^{A0} , θ_i^{A180} , θ_i^{B0} and θ_i^{B180}). As a sensor characteristic, bias is exclusive to each direction (e.g., b^A and b^B).

$$l_i = k \sin \theta_i + b \quad (1)$$

Equation 2 expresses a measurement at position i from a pair of readings from direction A or B (e.g., m_i^A or m_i^B). Bias is effectively eliminated in this calculation. Though obtained from a subtraction due to symmetry, the resulting value equates to the average of two readings taken in the same direction. This redundancy allows the estimation of b and forms the basis for qualitative evaluation procedures.

$$m_i = \frac{l_i^0 - l_i^{180}}{2k} = \frac{\sin \theta_i^0 + b - (\sin \theta_i^{180} + b)}{2} = \sin \theta_i \quad (2)$$

Once m_i is known, incremental deviations in each direction can be obtained by multiplying the probe's functional length (L , usually de length between wheels). Cumulative deviations correspond to the integration of Lm_i along the surveyed axis. Displacements can then be calculated at each position by subtracting an initial survey's values from any posterior survey. For the sake of simplicity, the initial and posterior surveys will be, here, designated as reference and ordinary.

3 Qualitative Evaluation of Probe Inclinometer Data

3.1 Standard Error of an Inclinometer System

Measurement errors can be categorised as random or systematic. Random errors affect precision and cannot be corrected but can be statistically estimated. Systematic errors affect trueness and can be corrected by comparison with a standard (or reference) value. Manufacturers often report the

error in field accuracy, including both kinds of errors (Mikkelsen 2003).

The random error can be estimated from specifications or by performing a series of measurements on a verification apparatus or a stable installation (e.g., SINCO 1993; Mikkelsen 2003; Coimbra 2019). This is, here, understood as the standard error of the inclinometer system. Typical values for metric systems are ± 0.1 to ± 0.2 mm in direction A. The standard error is higher in direction B due to the lateral oscillation of the wheels in the grooves. A common practice is to consider the standard error in direction B as double the value considered in direction A (SINCO 1993; Mikkelsen 2003). Note, however, (a) the standard error in either direction increases for inclinations higher than 3–5° and (b) each *casing + probe* combination can have its variance signature (e.g., higher than the standard error, usually due to local deformations, deficient couplings, dirt or worn wheels).

The way manufacturers report field accuracy can vary substantially. Generally, field accuracy agrees well with the random error when the depth control device is a cable gate (Coimbra 2019). However, when this device is a pulley assembly, the field accuracy reported includes an additional systematic error due to the tolerance allowed for depth control (SINCO 1993; Mikkelsen 2003). By controlling depth rigorously, field accuracies achieved with these systems can be much better than those specified.

Equation 3 shows the calculation of an incremental deviation at position i with random (ε_a) and systematic (ε_s) errors discriminated. When accumulated through n positions, the corresponding cumulative deviation (D_n) takes the form of Eq. 4.

$$d_i = Lm_i \pm \varepsilon_a + \varepsilon_{s,i} \quad (3)$$

$$D_n = L \sum_i^n m_i \pm \sqrt{n} \varepsilon_a + \sum_i^n \varepsilon_{s,i} \quad (4)$$

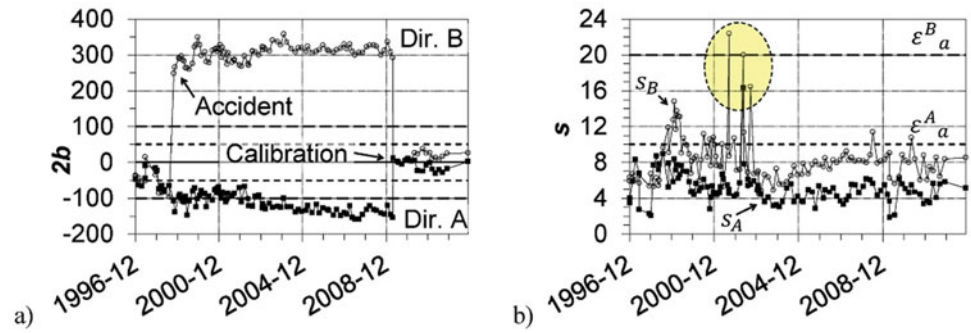
Equation 4 shows how systematic errors severely impact inclinometer measurements. Its increment is linear, so any error is replicated through all subsequent depths. Therefore, it is utterly essential to minimise the occurrence of systematic errors. They can be avoided by operating and maintaining the equipment adequately. Nonetheless, systematic errors can still occur more or less frequently, sometimes being hard to identify. For this reason, survey data should be routinely checked.

3.2 Checksums and Derived Statistical Estimates

Checksums are the sums of each pair of readings from a specific survey (SINCO 1993; Mikkelsen 2003). It will be shown that these values express an error around $2b$.

² k is related with signal gain and metrological sensitivity. Usually, $20,000 \leq k \leq 50,000$ for classic (e.g., pre-MEMS or non-solid state) sensors and $k = 100,000$ for MEMS sensors.

Fig. 1 Evolution of a $2b$ and b s through time (after Coimbra 2019)



Equation 2 can be rewritten in the form of Eq. 5 by considering ε_a and ε_s .

$$m_i = \frac{l_i^0 - l_i^{180}}{2k} = \sin\theta_i \pm \varepsilon_a + \varepsilon_{s,i}; \varepsilon_a = t \frac{\varepsilon'_a}{\sqrt{2}}; \varepsilon_{s,i} = \frac{\varepsilon'_{s,i} + \varepsilon'^{180}_{s,i}}{2} \quad (5)$$

where ε'_a is the characteristic dispersion of the system in each reading, t is a coverage factor for a certain level of confidence and ε'_s is the systematic error obtained in each reading. When taken from specifications, ε_a can be considered as a type B contribution for uncertainty estimation (JCGM 2008). If the standard value of $t = 2$ is assumed (e.g. 95% of confidence), ε'_a can be derived from Eq. 6.

$$\varepsilon'_a = \varepsilon_a / \sqrt{2} \quad (6)$$

Following the contribution of ε'_a and ε'_s in each reading, Eq. 1 is rewritten as Eq. 7. The sum of a pair of readings yields Eq. 8. As can be seen, sums beyond $2b \pm \varepsilon_a$ contain twice the systematic error introduced in the corresponding displacement. The question is knowing which reading carries the error.

$$l_i = k \sin\theta_i + b \pm \varepsilon'_a + \varepsilon'_{s,i} \quad (7)$$

$$S_i = l_i^0 + l_i^{180} = 2b \pm \sqrt{2}\varepsilon'_a + \varepsilon'_{s,i} + \varepsilon'^{180}_{s,i} = 2b \pm \varepsilon_a + 2\varepsilon_{s,i} \quad (8)$$

Following from Eq. 8, $2b$ can be estimated from the average of all the sums from a survey and ε_a can be used to establish confidence limits for the corresponding standard deviation. By monitoring these values through time, both the probe's health and data quality can be assessed (SINCO 1993; Coimbra 2019).

Figure 1a shows the evolution of $2b$ for an analogue probe from Slope Indicator Company (SINCO). It reflects the drift of the bias in reading units. The limits defined (± 50 and ± 100) stopped being published by SINCO (1993), and

references from other manufacturers are scarce. Coimbra (2019) shows that inclinometers can work reliably beyond these limits. However, depending on the casing's inclination, large drifts relative to the reference survey indicate small sensitivity changes and introduce errors in displacements upon integration. As such, $2b$ can be used as an indicator for the probe's health, as experience shows it is relatively consistent for each probe on most casings. Values off the set limits, high oscillations or static jumps are a strong indicator that the probe should be calibrated. However, acceptable limits for $2b$ are challenging to set for different probes, as they depend on several factors related to operating conditions and sensory technology. The best approach may be to keep a record of test measurements and evaluate the impact of changes.

Figure 1b shows the evolution of the standard deviation (s) for the same probe in the same casing. Coimbra (2019) analyses the sums of highlighted surveys, showing a direct relationship between abnormal s values and different kinds of systematic errors. In casings showing s signatures higher than ε_a , abnormal values can be evaluated by subtracting the reference s to each ordinary one ($\Delta s = s_p - s_r$) (SINCO 1993). In order to determine if $s_p \ll s_r$, Coimbra (2019) applies a single-tailed Fisher test (F -test) with 95% confidence. The resulting limit depends on s_r and depth (n) (Eq. 9).

$$\Delta s \leq s_r \left[\sqrt{F_{0.05}(df_1; df_2)} - 1 \right]; df_1 = df_2 = n - 1 \quad (9)$$

3.3 Known Types of Systematic Errors

Coimbra (2019) categorises errors as widespread or local. Widespread errors potentially replicate at each depth, while local errors affect isolated measurements. Mikkelsen (2003) presents a complete review of widespread errors. Coimbra (2019) proposes also new approaches to some widespread errors and some techniques directed at local errors. Table 1 presents an overview of these techniques.

Table 1 Overview of known systematic errors (after Dunncliff 1988; Mikkelsen 2003; Coimbra 2019)

Designation	Cause	Diagnosis	Correction
Bias-shift error	Malfunction of the sensory system, causing bias to change during a survey	Incremental and cumulative displacement profiles (Mikkelsen 2003). Symmetrical displacements' mismatch, sums of readings and standard error (Coimbra 2019)	Subtraction of average incremental displacement from displacements (Mikkelsen 2003) or directly from readings (Coimbra 2019)
Rotation error	Misalignment of accelerometers	Cumulative displacements and deviations of directions A and B (Mikkelsen 2003; Coimbra 2019)	Rotation of displacements (Mikkelsen 2003) or readings (Coimbra 2019) based on an estimated angle
Sensitivity error	Wear/malfunction of the sensory system, unstable temperatures or deficient sealing	Cumulative displacements and deviations of the affected survey (Coimbra 2019)	Estimation of the average drift and correction of displacements or readings (Coimbra 2019)
Depth error	Operator error, changes in the casing or the device used for depth control	Cumulative displacements of affected survey and incremental deviations of its reference (Mikkelsen 2003)	Interpolation between readings with predefined depth offset (Mikkelsen 2003)
Local error	Operator error, localised deformation, dirt, wearing of wheels or misadjusted couplings	Sums' profile and incremental deviations' change of symmetrical sides (Coimbra 2019)	Estimation of the affected reading from its pair and the global average of sums (Coimbra 2019)

4 Concluding Remarks

Operational procedures concerning slope inclinometers should include data processing techniques aiming at the evaluation of survey data. The redundancy in inclinometer data eases the development of such techniques, as shown in this work. These fundamental principles can then be extended to assess the quality and correct data. Coimbra (2019) proposes some new approaches and demonstrates their application.

Acknowledgements We are thankful to ISEP (Department of Geotechnical Engineering) and National Laboratory for Civil Engineering (LNEC) for the support given to realise this research.

References

- Coimbra L (2019) Uma perspectiva operacional sobre a aplicação de inclinómetros no âmbito da geotecnia. MSc dissertation, ISEP, Instituto Superior de Engenharia do Porto, Porto. <http://hdl.handle.net/10400.22/14770>
- Dunncliff J (1988) Geotechnical instrumentation for monitoring field performance. Wiley, USA
- JCGM (2008) Evaluation of measurement data: guide to the expression of uncertainty in measurement. Joint Committee for Guides in Metrology (JCGM 100:2008). https://www.bipm.org/utils/common/documents/jcgm/JCGM_100_2008_E.pdf. Accessed December 2020
- Mikkelsen PE (2003) Advances in inclinometer data analysis. In: Myrvoll F (ed) Sixth international symposium on field measurements in geomechanics, vol 1. A. A. Balkema Publishers, pp 555–567
- SINCO (1993) Digital DataMate and DMM Software. Manual Part No. 50310999. Slope Indicator Company (SINCO), USA



Application of Photogrammetry for Geotechnical and Structural Characterization of Carbonated Rock Mass

João Duarte, Nuno Coelho, Fernando Figueiredo, and Pedro Andrade

Abstract

This study is part of a geotechnical and structural characterisation of the rock mass of the quarry “Cabeço da Moita Negra”, located in Fátima (Central Portugal). That approach uses traditional methods of the geo-structural and photogrammetric survey based on photographic and aero-photogrammetric records. The studied quarry front was divided into sectors, and the present study focused on one sector. The traditional field survey identified and characterised the joints and grouped them in joint sets F, L and T whose orientations are, respectively, N50°W; 83 °NE, N39 °E; 76 °NE and N40 °W; 7 °NE. For the same sector, photogrammetric methods were applied to characterise the F-joint set fracturation using manual and automatic methods through computer treatment. Fracture orientation identified by both methods was represented by rosette diagrams and stereographic projection for statistical treatment and visualisation. Based on the data obtained by the different methods and on the spacing measurements, the Rock Quality Designation (RQD) index was calculated for the sector, obtaining values between 60.9% and 70.4% for the traditional survey and 68.4–77.3% for the photogrammetric survey.

Keywords

Geotechnics • Rock masses • Photogrammetric survey • Joint sets • Rock Quality Designation (RQD)

J. Duarte (✉)
IQGeo-Serviços, Lda., Coimbra, Portugal
e-mail: joao.aduarte@iqgeo.pt

J. Duarte · F. Figueiredo · P. Andrade
Geosciences Center, University of Coimbra, Coimbra, Portugal

N. Coelho · F. Figueiredo · P. Andrade
University of Coimbra, Faculty of Sciences and Technology,
Department of Earth Sciences, Coimbra, Portugal

1 Introduction

This work is part of a geotechnical and geo-structural characterisation of the rock mass of the quarry “Cabeço da Moita Negra”, located in the parish of Fátima, a council of Ourém (Central Portugal). For this purpose, the traditional geo-structural survey methods and the photogrammetric methods based on photographic and aero-photogrammetric surveys of the quarry were used. This work aims to compare and validate the data obtained by different methodologies proposed. The first stage of the work began with obtaining the necessary data to characterise the rock mass, determined in situ or through laboratory tests. The selected blasting front was divided into several sectors. Only one was considered for this work. The data obtained were processed and modelled. The results defined by the different methodologies were subsequently projected using rosette diagrams and stereographic networks for statistical and structural analysis. The discontinuity spacing, discontinuities representing a loss of cohesion of the rock material, such as joints and stratification, the Rock Quality Designation (RQD) was calculated for each of the methodologies and methods.

2 Location and Geological Characterisation

This work was carried out on the quarry of the company FassaLusa, called “Cabeço da Moita Negra”, which is located south of the city of Fátima, municipality of Ourém, district of Santarém (Fig. 1a, b).

The limestones are exploited to produce mortars and lime and belong to Serra de Aire Formation (Azerêdo 2007), which is composed of micritic limestones (Manuppella et al. 2000).

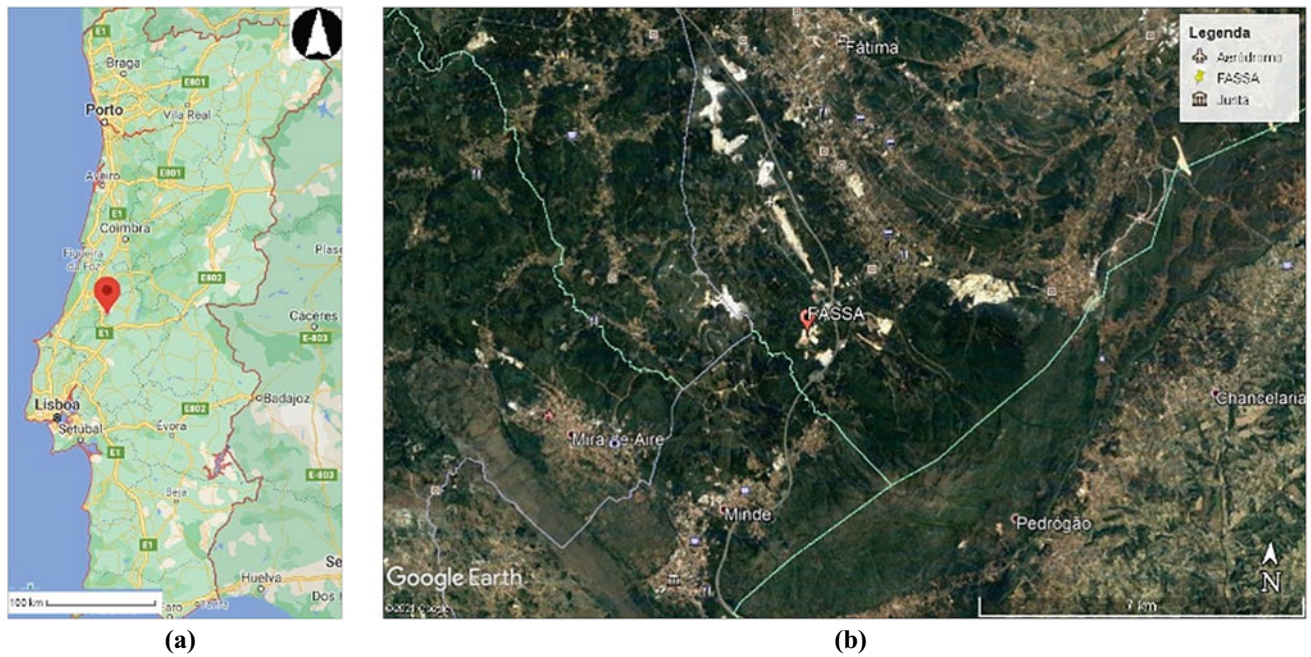


Fig. 1 **a** Location of Fátima in Portugal. **b** Representation of Fátima's area, located at the Municipality of Ourém, adapted from Google Maps (2021). Location of the study area as indicated by the red arrow, adapted from Google Earth Pro (2021)

3 Methods and Methodology

The present work is related to a geotechnical and geo-structural characterisation of the front of the quarry “Cabeço da Moita Negra”. The methodology used (Fig. 2) considers the geo-structural and photogrammetric surveys, which last use photographic and aero-photogrammetric surveys. In the first phase of the work, the data acquisition was performed through an in situ survey to obtain results that characterise the massif in structural terms and compare the results obtained by the different methods used. Simultaneously, photographic surveys and the placement of control points (GCP) were performed, according to the methodology proposed by Duarte (2018), Coelho (2019). The study fronts target was divided into 12 sectors, and only one sector data was considered for the present work.

3.1 Field Survey

At the quarry front, for the studied sector, a cartographic survey and the characteristics of the discontinuities were carried out, along different scanlines, which allowed the determination of the RQD index (Deere et al. 1967) through the methodologies proposed by Priest and Hudson (1976), Palmström (1982). 130 fractures grouped in joint sets F, L and T, which orientation is, respectively, N50 °W; 83 °NE, N40 °W; 7 °NE, N39 °E; 76 °SE. The random joints,

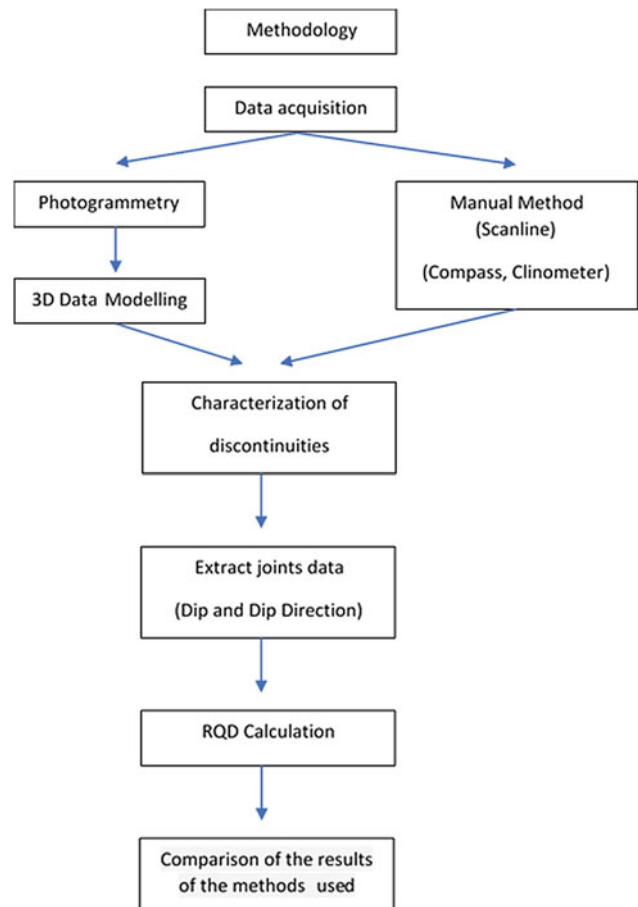


Fig. 2 Methodology workflow

although present, do not correspond to a significant part of the number of discontinuities of the studied rock mass.

3.2 Photogrammetric Surveys

The photogrammetric surveys were carried out using two methods:

1. Camera—A Fujifilm model JZ100 with the specifications indicated in Table 1 was used for the image acquisition. To obtain the photographs with the best possible orientation, a guideline parallel to the slope/front direction was marked on the quarry's base floor (scanline), along which the camera was moved to obtain sequential photographs that *overlap* horizontally by at least 80%.
2. Unmanned Aerial Vehicle (UAV)—The aerial survey was performed with a DJI Phantom 4 Pro, equipped with a camera described in Table 1. As a data acquisition methodology, the flight was initially planned for a longitudinal overlap of 80% and a lateral overlap of 60%. The GCP's georeferencing was done using a GNSS (Global Navigation Satellite System) receiver of the Geomax brand, model Zenith 10. The horizontal receiver's static accuracy is $5 \text{ mm} \pm 0.5 \text{ ppm}$ (RMS), and the vertical aesthetic precision is $10 \text{ mm} \pm 0.5 \text{ ppm}$ (RMS). The UAV flight was carried out parallel to the topographic surface with the camera placed at 75° and fully automated. The flight parallel to the surface in front of the quarry was carried out manually, and the two aerial surveys were subsequently merged with those of the photographic survey.

The photogrammetric survey modelling was performed using the software programme Agisoft PhotoScan (Agisoft 2018), which is based on the Structure from Motion (*SfM*) and dense correlation technique (Westoby et al. 2012). Extract of rock mass fracturing degree was obtained from the point node created (Fakunle 2016) using the software programme *CloudCompare* (Girardeau-Montaut 2011). Manual and automatic procedures were used for the characterisation of rock mass fracture degree.

The studied area corresponds to a quarry for aggregates. The data extraction from the point cloud was made with a

visual pre-selection to identify the natural planes and not caused by the exploratory process. After this selection, a manual classification was carried out, complemented with the automatic classification. The methodological process provides for the manual classification of the determination of the orientation of the planes (using the *CloudCompare Point list picking-Fit-Plane* functions), is subsequently compared with the automatic classification (using the *CloudCompare RANSAC-Fit-Plane* functions) (Duarte 2018), of the plans previously identified, with no cleaning or segmentation of the point cloud used. Thus, only these plans were the object of statistical analysis.

4 Results

Once the data were surveyed and processed according to the proposed methods (in situ and photogrammetry), the studied sector's discontinuity orientation results were obtained. Table 2 shows those related to joint set F. The statistical treatment of the joint orientation data, the values of its mean spacing per joint set and the respective calculation of the RQD index for the sector were obtained and indicated in Table 3.

5 Discussion

The spacing of the 3 joint sets occurring in the rock mass was considered in the calculation of RQD, namely in the selected sector. The RQD values, according to Palmström's (1982) method, allowed defining the rock mass, according to traditional survey and photogrammetry, respectively, as reasonable (70.4%) and good (77.3%). The methodology of Priest and Hudson (1976) permitted the classification of the rock mass as reasonable using both the traditional survey method (60.9%) and Photogrammetry (68.4%). Priest and Hudson (1976) relationship with the RQD uses the total frequency joint instead of the identified joint sets' average spacing. The first method can present more conservative results than the relationship of volumetric joint count with the RQD.

The coefficient of variation (CV) is a good indicator of the accuracy of the acquired data. For example, the discontinuity

Table 1 Fujifilm JZ100 and UAV camera specifications

Brand	Model	Nr. Pixels	Focal length (f)	Maximum aperture (F)	Sensitivity (ISO)
Fujifilm	JZ100	14 Megapixels	f = 4.5–36.0 mm	F2.9/F7.8	100–3200
DJI		20 Megapixels	f = 8.8–24.0 mm	F2.8/F11	100–12,800

Table 2 Discontinuity orientation of joint set F is obtained by different used methods

Parameters	Traditional survey		Manual cloud compare photogrammetry		Automatic cloud compare photogrammetry	
	Dip (°)	Dip direction (°)	Dip (°)	Dip direction (°)	Dip (°)	Dip direction (°)
Maximum	89	43	87	55	87	54
Minimum	78	39	79	40	80	40
Average	86	41	83	48	84	49
Standard deviation	3.8	1.3	2.0	4.3	2.1	4.9
Cf. variation	0.044	0.031	0.025	0.089	0.025	0.1
N° sampling	9		20		12	

Table 3 Average joint set spacing and respective Rock Quality Designation (RQD) calculation for the studied sector, using traditional survey and photogrammetry

Method	Average joint set spacing (m)			Jv	RQD (%)	
	F	T	L		Palmström (1982)	Priest and Hudson (1976)
Traditional	0.11	0.33	0.78	13.52	70.39	60.86
Photogrammetry	0.14	0.29	1.52	11.41	77.34	68.40

Jv—Volumetric fracturing count

orientation survey data (studied sector) showed that the lowest CV values for Dip were defined by the Manual and Automatic Cloud Compare photogrammetry. In contrast, for Dip direction, the lowest CV values were obtained by the traditional survey. Therefore, a relevant factor to be considered is the number of samples obtained using the photogrammetry methodology for this sector, namely when defining the discontinuity surfaces using the Manual Cloud Compare photogrammetry (20 measurements).

6 Concluding Remarks

The RQD index values defined by the photogrammetric method show an increment of 7–8% compared to those obtained by the traditional method. This difference may be explained by the loss of precision in measuring the discontinuity spacing in the point cloud due to the lack of photographic data acquisition or development process.

The photogrammetric method presents lower CV values for Dip determinations, which corresponds to higher accuracy. For the Dip Direction determination, the lower CV values are associated with the traditional geological/structural survey method. That can be partially explained by difficulties in acquiring photographic data, such as limited specifications of the camera, acquisition conditions or modelling processes; thus, the discontinuity characterisation can be affected, particularly the Dip Direction. The photogrammetric method has proved to be less time-consuming

in the discontinuity identification, presenting a time duration of approximately 20 h less, allowing the acquisition of a more significant number of data and the possible access to higher elevation survey areas. In addition, photogrammetric methods allow an increase in security conditions when carrying out studies related to the discontinuities' characterisation in rock masses. For an 11 m high heavily jointed front and part of an active quarry, the photogrammetric methods considerably increase the survey's safety levels. The proposed methodology for photogrammetric data acquisition revealed a good precision, being possible to perform several types of measurements regarding orientation, spacing and discontinuities persistence. The methodology simplifies and complements the rock masses characterisation, enabling the determination of the RQD and contributing to the determination of the Rock Mass Rating (RMR) system.

Further studies may include other joint essential characteristics, such as persistence. Furthermore, to improve photogrammetry and photography, improving the quality of acquisition conditions (brightness, resolution) is necessary. Also, the classification and segmentation of the noise-causing elements can be carried out.

Acknowledgements To IQGeo-Serviços, for the financial, material and human investment, to FASSALUSA LDA for allowing the use of the facilities and industrial. We thank FCT-MEC for its financial support through national funds and, when applicable, co-financed by the ERDF within the PT2020 partnership through the research projects UID/Multi/00073/2020 of the Geosciences Centre and UID/Multi/00308/2020.

References

- Agisoft (2018) Agisoft photoscan. Professional Edition v. 1.4, Agisoft LCC, St Petersburg
- Azerêdo A (2007) Formalização da litostratigrafia do Jurássico Inferior e Médio do Maciço Calcário Estremenho (Bacia Lusitânica). *Comun Geol* 94:29–51
- Coelho NJDS (2019) Caracterização geotécnica e estrutural de um maciço de rochas carbonatadas com aplicação da técnica de fotogrametria: caso de estudo aplicado a uma pedreira de rocha industrial. Faculdade de Ciências e Tecnologia, Universidade de Coimbra, Coimbra (Master's dissertation). <http://hdl.handle.net/10316/86706>
- Deere DU (1967) Geological considerations. In: Stagg KG, Zienkiewicz OC (eds) *Rock mechanics in engineering practice*. Wiley Sons, London, pp 1–20
- Duarte JAM (2018) Contributos para a caracterização de áreas com potencial para a extração de rochas ornamentais carbonatadas: Análise integrada de dados fotogramétricos, geológicos e geofísicos para caracterização de maciços rochosos carbonatados. Universidade de Coimbra, Coimbra, Portugal (PhD Thesis). <http://hdl.handle.net/10316/87557>
- Fakunle AA (2016) Detection of weathering signatures using VANT photogrammetry in comparison with ground-based sensors. Faculty of Geo-information Science and Earth Observation, University of Twente, The Netherlands (MSc Dissertation). <http://purl.utwente.nl/essays/83844>
- Girardeau-Montaut D (2011) Cloud compare-open-source project. OpenSource Project. <https://www.danielgm.net/cc/>
- Google Maps (2021) Accessed on 02 Apr 2021. <https://www.google.com/maps/place/Portugal>
- Manuppella G (coord) (2000) Notícia explicativa da Carta Geológica de Portugal, escala1:50.000, Folha 27-A (Vila Nova de Ourém), 2ªedição. Inst Geol Min, Lisboa
- Palmström A (1982) The volumetric joint count-a useful and simple measure of the degree of rock jointing. In: *Proceedings of the 4th international congress IAEG*. New Delhi, vol 5, pp 221–228
- Priest SD, Hudson J (1976) Discontinuity spacings in rock. *Int J Rock Mech Min Sci Geom Abstr* 13(5):135–148
- Westoby MJ, Brassington J, Glasser NF, Hambrey MJ, Reynolds JM (2012) Structure-from-motion photogrammetry: a low-cost, effective tool for geoscience applications. *Geomorph* 179:300–314



GeoTec: A System for 3D Reconstruction in Underground Environment (Aveleiras Mine, Monastery of Tibães, NW Portugal)

Ana Pires, André Dias, Paulo Rodrigues, Pedro Silva, Tiago Santos, Alexandre Oliveira, António Ferreira, José Almeida, Alfredo Martins, Helder I. Chaminé, and Eduardo Silva

Abstract

This work addresses reconstructing an ancient mining site in three-dimensional (3D) modelling with robotic systems, processing the information from two visible spectrum cameras. The developed solution, GeoTec System, was validated in an underground environment in the Monastery of Tibães (Braga, NW Portugal). This study was developed under the MineHeritage project's scope, aiming to attain society on the importance of raw materials across a historical approach. The outputs acquired from the datasets developed in a successful 3D reconstruction of the main gallery and secondary tunnels of the Aveleiras mine in Tibães. However, the investigation is still ongoing to contribute to applying 3D reconstruction technologies, GIS-based mapping and geovisualization techniques in the underground heritage environment.

Keywords

Geotechnologies • Mine Heritage • 3D reconstruction • Robotics • GeoTec system

1 Introduction

3D Reconstruction of large-scale underground environments, such as tunnels, mines, and caves, is typically highly time-consuming and challenging due to normally humid environments, mud and water, and irregular geometry and size. This time of constraints will impose restrictions on the type of sensors that could be used and the size of the system to register the information. Existing techniques based on 3D terrestrial scanners (Kwoczynska et al. 2016) provide an accurate 3D reconstruction, but the survey procedure is time-consuming and inefficient. Mobile mapping solutions overcome this limitation by being more efficient in covering more space. However, existing commercial solutions rely on pose estimation with a GPS (Global Positioning System) signal and an IMU (Inertial Measurement Unit).

This study was developed within the MineHeritage Project's scope (<https://mineheritage-project.eu/>) and supported by the EIT Raw Materials Academy within the European Institute of Innovation and Technology (EIT) community of innovation. The GeoTec system developed during the MineHeritage Project is a custom-made solution that will combine visual techniques with a stereo baseline to estimate the pose during the survey (details in Silva et al. 2020).

2 3D Reconstruction for Underground Environments

Some existing systems that are similar to GeoTec, often use laser sensors (LiDAR) without using inertial and vision sensors. In Thrun et al. (2000), two 2D laser sensors were used to compute 3D data. One sensor is mounted horizontally to obtain the robot's pose, and the other is vertical scans and estimates the 3D points using the robot's pose. Ferguson et al. (2004) present a robotic system that will autonomously map abandoned mines. The vehicle used is equipped with two actuated laser sensors. In order to move around the

A. Pires (✉) · A. Dias · P. Rodrigues · P. Silva · T. Santos · A. Oliveira · A. Ferreira · J. Almeida · A. Martins · E. Silva
Centre for Robotics and Autonomous Systems CRAS|LSA,
Department of Electrical Engineering, School of Engineering
(ISEP), Polytechnic of Porto, Porto, Portugal
e-mail: ana.c.pires@inesctec.pt

H. I. Chaminé
Laboratory of Cartography and Applied Geology (LABCARGA),
Department of Geotechnical Engineering, School of Engineering
(ISEP), Polytechnic of Porto, Porto, Portugal

Centre GeoBioTec|UA, Aveiro, Portugal

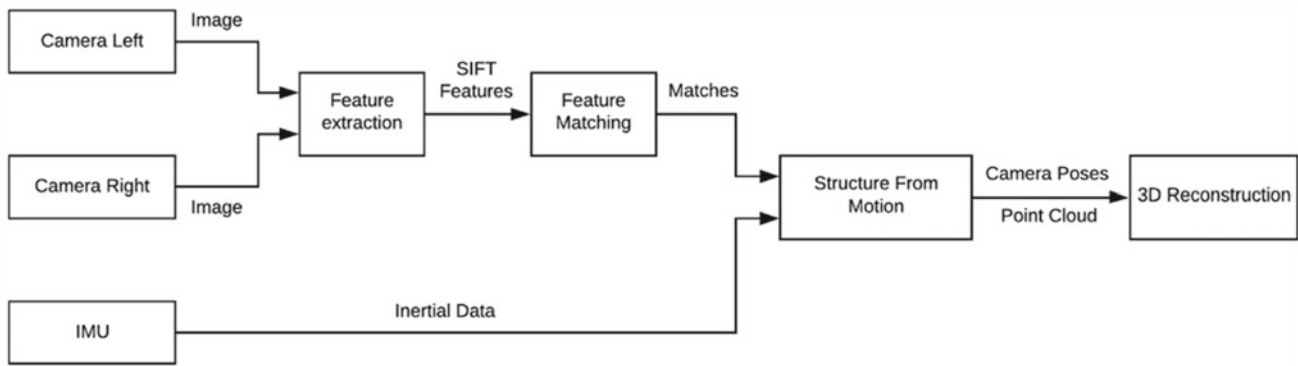


Fig. 1 3D reconstruction processing pipeline

environment, it uses a 2D laser scanner, stopping from time to time to perform a 3D scan of the area around it. The robot then plans its trajectory using fast 2D scans to determine the robot's relative position on the 3D map through these scans. Thrun et al. (2003, 2004), in addition to the robot of Ferguson et al. (2004), also referred to the use of a robotic platform pushed by humans equipped with four 2D laser scanners to provide information about the transverse section of the mine ahead of the vehicle, the structure of the roof and the ground. None of these systems uses inertial or vision sensors to estimate the pose, which is a substantial handicap. It forces the vehicle pose to be predicted only by using the information provided by laser scanners.

The 3D reconstruction pipeline developed is detailed in Fig. 1. Each image pair is obtained and run through the Scale Invariant Feature Transform (SIFT) procedure, a

feature extraction algorithm (more details in Ma et al. 2011). The SIFTs identify, on images, key points invariant to scale and therefore are very likely to be recognized in other images even with different lighting and angles. The features are identified by a descriptor that represents the key point.

The descriptors of the features are used to identify the same feature in different images, providing a match between them. This process is called feature matching. Estimating each camera pose and generating the corresponding point cloud is possible with these matches and the inertial system's information. This process is repeated for all image pairs to create a point cloud representing the whole mining gallery. Then this point cloud is processed to make a 3D mesh. That includes calculating depth maps, texturing, and meshing (Fig. 2).

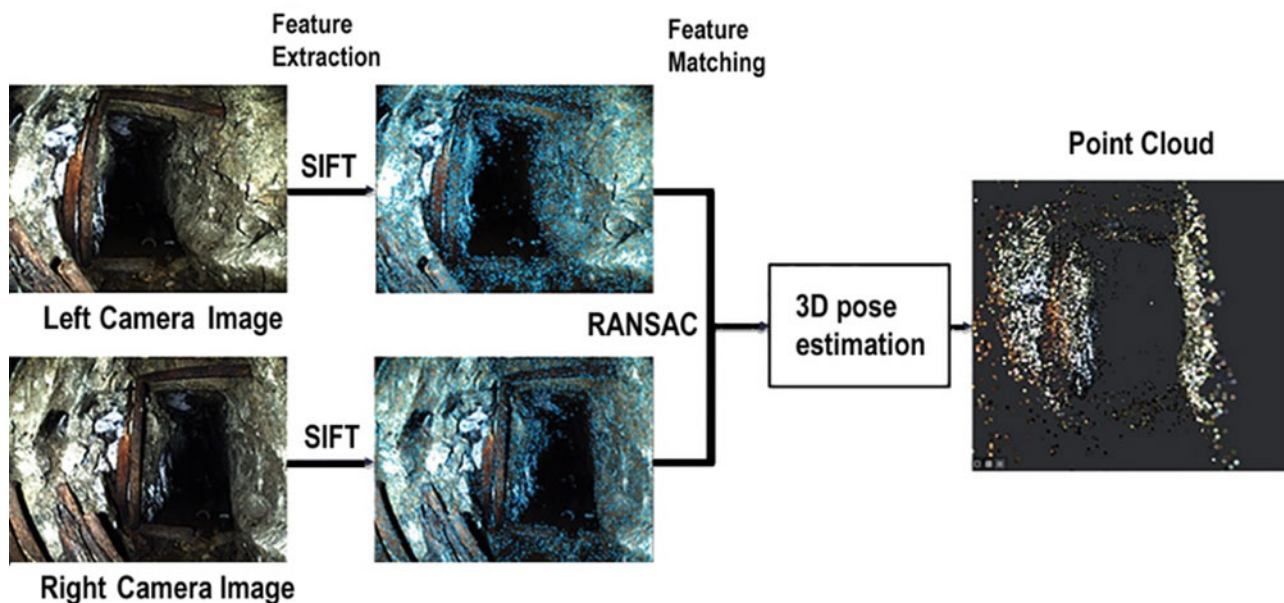


Fig. 2 Processing pipeline to achieve 3D reconstruction

3 GeoTec System

The GeoTec System was developed by the Centre for Robotics and Autonomous Systems (CRAS-INES TEC) under the MineHeritage Project framework. It is a practical, robust, and portable system. Its primary goal is to register multiple sensors, such as a camera, a LiDAR, and an IMU.

The system is presented in Fig. 3. A structure was developed to accommodate all the sensors and the needed components, consisting mainly of an aluminium Bosh profile. This structure needed to be robust, sturdy, and simple to mount/dismount, allowing easy transport of all sensors. The GeoTec System is composed of several sensors, such as a high-precision IMU (STIM 300) and two visible spectrum cameras (FLIR Blackfly GigE BFLY-PGE-31S4C-C) and a 2D LiDAR (Hokuyo UTM-30LX). The CPU (Central Processing Unit) is a 4th generation Intel i5 with an SSD. The synchronization of all data recorded is critical to consider when building this system. The cameras' trigger could be done by software, but this methodology is inaccurate due to the unpredictable delays in the control protocols and CPU saturation. The best method for triggering cameras is by hardware. The data gathered by the sensors and all data storage were developed with the ROS (Robot Operating System) framework.

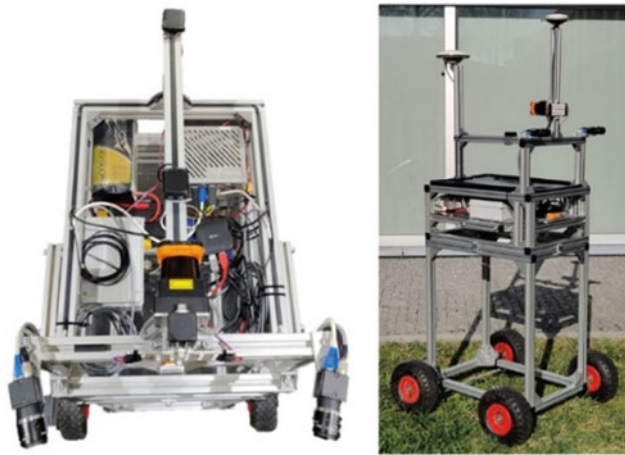


Fig. 3 GeoTec system equipment overview (details in Rodrigues 2020)

4 Field Tests Site: Preliminary Results and Discussion

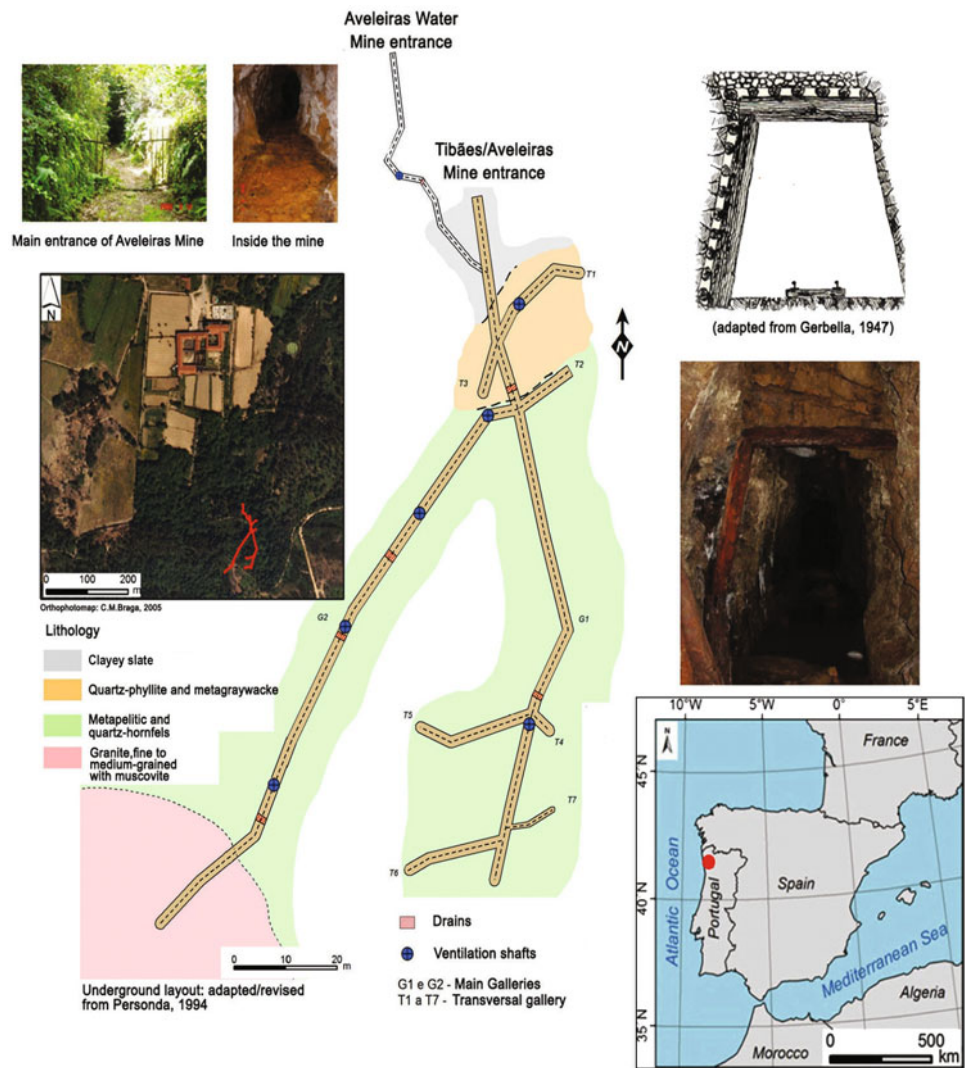
4.1 Experimental Site: Aveliras Mine

The field test site was the ancient Aveliras mine, located in Tibães Monastery close to Braga city, NW Portugal. The Monastery was the motherhouse for Portugal of the Order of Saint Benedict, and it was established at the end of the eleventh century. Most of the magnificent construction was carried out between the seventeenth and eighteenth centuries. The Monastery was closed due to liberal policies in 1834 and sold in 1864. Thirty years later, a fire devastated a section of the refectory cloister. Despite the deterioration of the Monastery over time, in 1986, the Portuguese Government invested in the property. A recovery project took place, which included a process of heritage protection and continues to be carried out until the present day (e.g., Meixedo et al. 2011; Trigo et al. 2012; Lopes et al. 2015; Chaminé et al. 2017). The mining framework of the Aveliras mine is wolfram. Nowadays, most of these mines are abandoned, but the Monastery was distributed by a complex water mine system for many centuries.

The site's geological background comprises clayey slates, quartz-phyllites, and metagraywackes interbedded with metapelites, quartz hornfels, and granitic rocks. The thick wolfram-bearing quartz-sheared veins in the region led to the exploitation of these hydrothermal deposits in the twentieth century (e.g., Lopes et al. 2015; Chaminé et al. 2017). The Aveliras mine is one of the ancient groundwater sites (dug around 1626), supplying for three centuries the cloister before being converted into a wolfram mine operating between 1940 and 1962 (Chaminé et al. 2017). Finally, it has returned to its previous function related to a water mine (Afonso et al. 2017). The Aveliras mine comprises several vertical ventilation shafts, and the main gallery width goes up to 1,50 m and a maximum height of 1,90 m. The transverse galleries have smaller sections, around 1 m in width and 1,60 m (Trigo et al. 2012).

Aveliras mine (Fig. 4) is the ideal site for testing new geotechnologies, including interesting geological, mining, and heritage features, significant biodiversity and geodiversity, and exciting spots waiting to be discovered.

Fig. 4 Underground geological map of the Aveleiras mine site and an aerial view of the Tibães Monastery enclosure (details in Trigo et al. 2012; Chaminé et al. 2017)



4.2 3D Reconstruction Results

In this preliminary stage of the investigation, the mine assessment required two campaigns: (i) gather all data with the GeoTec System and validate the 3D reconstruction in desk studies; (ii) cover all the areas that have not been done previously. Gathering field data with the GeoTec System over the mine was challenging due to water's presence (around 10–25 cm). In addition, the wheels were powerless to rotate due to the ground's rough and wet conditions. Figure 5 displays some views of the field campaign accomplished.

During the field tests, the GeoTec System gathered more than 70 Gb of raw data, composed of information provided from two cameras, with 10 FPS and an IMU at 1000 Hz. Figure 6 shows the original image of the entrance of the mine (on the left) and the development of the 3D mine digital reconstruction (on the right).

The 3D reconstruction was done in two sweeps, corresponding to the main tunnel and the transversal gallery. As a result, the main tunnel log has collected more than 3000 images from each camera and the transversal gallery with 6000 images each. The final 3D reconstruction, depicted in Fig. 7, was obtained after applying the SFM technique with 1200 pairs of images.

5 Concluding Remarks

This study presented a 3D reconstruction methodology validated along with the Aveleiras Mine, resulting in several datasets. This reconstruction has been successfully achieved. This study provided: (i) preliminary results using digital geotechnologies on Aveleiras mine (Tibães Monastery); (ii) this mining heritage site was used for the first time as an experimental field site to test the robotic systems developed;

Fig. 5 Several aspects of the field tests site with the GeoTec system data acquisition inside the Aveleiras mine



Fig. 6 Aveleiras mine entrance: the image is taken from one of the cameras, and on the right is displayed the corresponding 3D reconstruction



(iii) gathered data to develop algorithms to perform 3D reconstruction; (iv) the process and methodology can be now replicated to other MineHeritage sites along with the project; (v) GeoTec system proved its effectiveness during the operations and field campaigns.

The research is still in progress to improve the preliminary results and technology. In upcoming studies, it is challenging to combine all the data sets provided by the GeoTec System with geoheritage, geomining, hydrogeomechanical, and geotechnical mapping data within an integrated GIS-based mapping platform.

Additional Material

Geovisualization links of the 3D Reconstruction of the Aveleiras mine site (Tibães Monastery), acquired with the GeoTec System, are available at:

- Main Gallery (100,000,530 points): http://www.lsa.isep.ipp.pt/~adias/cloud/minas/projects/mineheritage/pointclouds/tibaes_mine/geotec/main_tunnel/main_tunnel

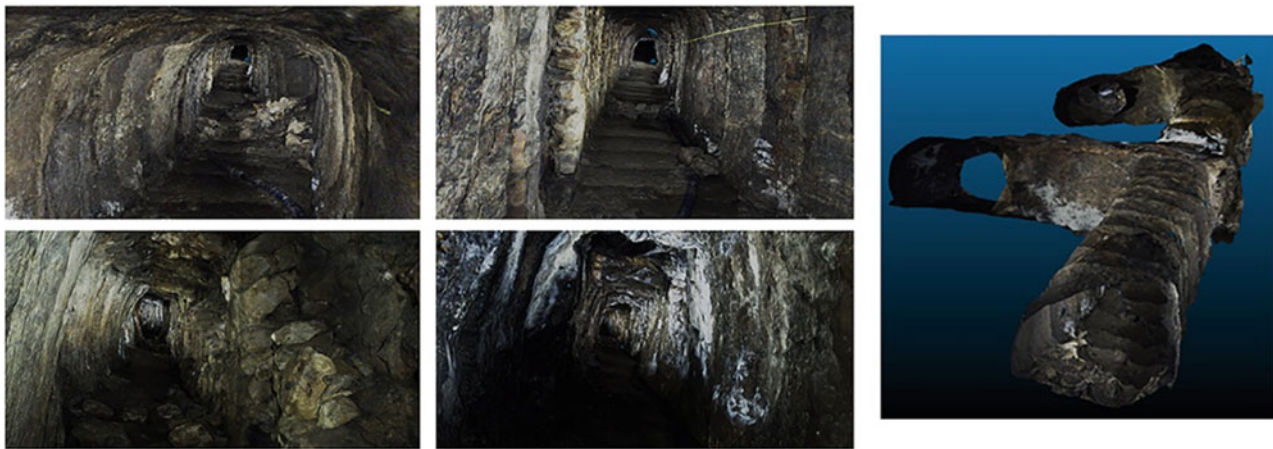


Fig. 7 Final 3D digital reconstruction of Aveleiras mine: on the left, it represents the main gallery; the transversal gallery is illustrated in the middle; on the right, the shape of the 3D reconstruction with an intersection between the main and the transversal gallery

- Secondary Gallery (99,999,858 points): http://www.lsa.isep.ipp.pt/~adias/cloud/minas/projects/mineheritage/pointclouds/tibaes_mine/geotec/secondary_tunnel/secondary_tunnel
- Promotional video with the underground mapping with GeoTec System of the Aveleiras mine site (accessed in July 2021): <https://www.youtube.com/watch?v=lgpTGcFoJCA>

Acknowledgements We are grateful to the Tibães Monastery board during the fieldwork campaigns, particularly Maria João Dias Costa and Paulo Oliveira's support. Thanks to the ISEP colleagues J.F. Trigo, M. J. Afonso, J.P. Meixedo, and M.E. Lopes for the field inputs. This study was developed within the MineHeritage Project scope (EIT/RAW MATERIALS/SGA2019/1), funded by EIT Raw Materials Academy [Nr. 18111; Main Theme 1 Exploration and raw materials resources assessment; Area D3 RM Academy; Segment D3.1 Wider Society Learning]. The investigation was funded by a research contract under the Portuguese Foundation for Science and Technology, FCT (CEECIND/00835/2018) to AP and supported by project UIDB/50014/2020. HIC was supported under the framework of the LABCARGA|ISEP re-equipment program (IPP-ISEP|PAD'2007/08) and Centre GeoBioTec|UA (UID/GEO/04035/2020). Finally, we are grateful to the anonymous reviewers for the constructive inputs which have improved the manuscript.

References

- Afonso MJ, Lopes ME, Chaminé HI (2017) Hydrogeochemical assessment of Tibães waters (NW Portugal). *Proc Eart Planet Sci* 17:790–793
- Chaminé HI, Lopes ME, Trigo JF, Dias Costa MJ (eds) (2017) *As minas de Tibães: um património hidrogeológico, geomineiro e de hidráulica monástica/The Tibães mines: a hydrogeological, geomining and monastic hydraulic heritage*. Coleção Labcarga-GEO| 3, Edição Laboratório de Cartografia e Geologia Aplicada and Departamento de Engenharia Geotécnica, Instituto Superior de Engenharia do Porto, Porto, Portugal
- Ferguson D, Morris A, Haehnel D, Baker C, Omohundro Z, Reverte C, Thayer S, Whittaker C, Whittaker W, Burgard W, Thrun S (2004) An autonomous robotic system for mapping abandoned mines. In: *Advances in neural information processing systems*, pp 587–594
- Kwoczynska B, Litwin U, Piech I, Obirek P, Sledz J (2016) The use of terrestrial laser scanning in surveying historic buildings. In: *Proceedings of the baltic geodetic congress (BGC Geomatics)*, Gdansk, pp 263–268
- Lopes ME, Afonso MJ, Teixeira J, Meixedo JP, Trigo JF, Dias Costa MJ, Gama Pereira LC, Chaminé HI (2015) Recovery of ancient groundwater supply systems and old abandoned mines: coupling engineering geosciences and geoh heritage management. In: Lollino G, Giordan D, Marunteanu C, Christaras B, Yoshinori I, Margottini C (eds) *Engineering geology for society and territory—preservation of cultural heritage*. IAEG, Springer, Cham, vol 8, pp 227–230
- Ma W, Le M, Jo K (2011) 3D reconstruction and measurement of indoor object using stereo camera. In: *Proceedings of the 6th international forum on strategic technology*. Harbin, Heilongjiang, pp 738–742
- Meixedo JP, Lopes ME, Dias Costa MJ, Trigo JF, Chaminé HI (2011) Geological and mining heritage in NW Portugal (Mire de Tibães): threats and opportunities for a sustainable second life-cycle. In: Cloughton P, Mills C (eds) *Mining perspectives: proceedings of the 8th international mining history congress 2009*. Cornwall and west devon mining landscape world heritage site. Cornwall Council, Truro, pp 110–116
- Rodrigues PMC (2020) *GeoTec: Sistema de reconstrução 3D baseado em imagem para cenários GPS-denied*. Instituto Superior de Engenharia do Porto, ISEP, Porto (MSc Dissertation). <http://hdl.handle.net/10400.22/15717>
- Silva P, Dias A, Pires A, Santos T, Amaral A, Rodrigues P, Almeida J, Silva E (2020) 3D Reconstruction of historical sites using an UAV. In: Gradetsky VG, Tokhi MO, Bolotnik NN, Silva M, Virk GS

- (eds) Proceedings of the CLAWAR 2020–23rd international conference on climbing and walking robots and the support technologies for mobile machines. Moscow, Russian Federation
- Thrun S, Burgard W, Fox D (2000) A real-time algorithm for mobile robot mapping with applications to multi-robot and 3d mapping. In: Proceedings of the IEEE international conference on robotics and automation, symposia, ICRA, millennium conference (Cat. No. 00CH37065), vol 1, pp 321–328
- Thrun S, Hahnel D, Ferguson D, Montemerlo M, Triebel R, Burgard W, Baker C, Omohundro Z, Thayer S, Whittaker W (2003) A system for volumetric robotic mapping of abandoned mines. In: Proceedings of the IEEE international conference on robotics and automation (Cat. No. 03CH37422), vol 3, pp 4270–4275
- Thrun S, Thayer S, Whittaker W, Baker C, Burgard W, Ferguson D, Hahnel D, Montemerlo M, Morris A, Omohundro Z, Whittaker RC, C, (2004) Autonomous exploration and mapping of abandoned mines. *IEEE Rob Automat Mag* 11(4):79–91
- Trigo JF, Chaminé HI, Afonso MJ, Almeida H, Lopes ME, Teixeira J, Pereira R, Pinheiro R, Meixedo JP, Gomes A, Teixeira JFA, Dias Costa MJ (2012) A antiga mina de volfrâmio das Azeleiras (Mosteiro de Tibães, NW Portugal): estudos interdisciplinares para a valorização do património geomineiro. *Bol Minas, Lisboa* 47 (2):139–156



Rock Surveys for Geological and Geotechnical Assessment in a Basic Rock Quarry (SW Dili, East Timor)

Roberto R. Varela, Luís Ramos, José Augusto Fernandes, and Helder I. Chaminé

Abstract

The quarry geotechnics on-site investigation and field surveys are challenging for developing the best practices in the rock quarry. The lithological heterogeneity, geological structures, weathering grade, fracture spacing of discontinuities, and the strength degree of the intact rock are driven parameters influencing the quarry excavation. The heterogeneity of the geological properties of rock masses is valuable in practice. In particular, block size evaluation shows an essential role in rock design projects of mining, quarrying, and highway cutting operations. Understanding the ground conditions during the excavation design is the best approach to decreasing costs and increasing safety. This work presents an exploratory study highlighting the importance of rock surveys in quarrying geotechnics practice. This study contributes to the basis of a geological and geotechnical assessment of the Jonize quarry at SW Dili (Turlio village, East Timor). Scanline surveys have been employed for rock mass characterisation and related geological, geotechnical, and geomechanical properties. That also permitted to outline of essential information about the studied rock mass and the block size parameters.

Keywords

Mapping • Geotechnical zoning • Rock surveys • Quarry • East timor

R. R. Varela · J. A. Fernandes

Laboratory of Geotechnics and Construction Materials (LGMC), Department of Geotechnical Engineering, School of Engineering (ISEP), Polytechnic of Porto, Porto, Portugal

R. R. Varela · L. Ramos · H. I. Chaminé (✉)

Laboratory of Cartography and Applied Geology (LABCARGA), Department of Geotechnical Engineering, School of Engineering (ISEP), Polytechnic of Porto, Porto, Portugal
e-mail: hic@isep.ipp.pt

J. A. Fernandes · H. I. Chaminé

Centre GeoBioTec|UA, Aveiro, Portugal

1 Introduction

Pettifer and Fookes (1994) state an impressive thought: “It is usually cheaper to break up rock masses by ripping rather than by drilling and blasting, but productivity may be lower. Blasting is often more economic for large-scale quarrying operations.” In fact, the correct knowledge of the blasting operation is essential to optimise the costs of rock mass excavability. Consequently, the inadequate performance may cause unnecessary costs in the subsequent engineering quarry operations to drilling, i.e., blasting, handling, splitting, and crushing (e.g., Langefors and Kihlström 1978; Jimeno et al. 1995; Dinis da Gama 1996; Galiza et al. 2011b, and references therein).

Drilling operations assume an essential role in balanced engineering and economic results. This operation evolves the following groups of parameters (e.g., Langefors and Kihlström 1978; Hartman 1992; Dinis da Gama 1996; Moodley and Cunningham 1996; Galiza et al. 2011a): (i) geological, geotechnical, and geomechanical characteristics and patterns; (ii) top hammer and bench drilling tools; (iii) blast design.

The structural geology features and geomechanical parameters are essential in rock mass surveys. So, it is vital to understand the drilling technologies, methodologies, and costs engaged (Galiza et al. 2011a, b). Thus, engineering geology and applied geomorphology contribute decisively to the rock mass projects (e.g., Terzaghi 1965; Oliveira 1987; Hartman 1992; González de Vallejo and Ferrer 2011; Rocha 2013; Chaminé et al. 2013; Cosgrove and Hudson 2016). Furthermore, the jointed rock masses’ behaviour is shaped by the interlocking of single rock blocks divided by faults, joints, and/or geological contacts (e.g., Goodman 1976; Priest 1993; Galiza et al. 2011a; Rocha 2013; Cosgrove and Hudson 2016).

Galiza et al. (2011a, b) highlighted that the optimisation of rock blasting operation requires prior knowledge of the fracturing degree to outline the block size. So, it is crucial to

carry on comprehensive geologic and geomechanical studies on rock masses (ISRM 1978, 1981; GSE 1995; CFCFF 1996). That approach is essential because the insufficient or lack of knowledge about the geological and geotechnical conditions of a rock quarry site interferes with the efficiency and cost of subsequent quarrying and processing operations.

This work aims to present a preliminary study of the engineering geology conditions of the Jonize rock quarry in East Timor. In situ rock surveys were performed to gather geology, geotechnics, and rock engineering data. For example, a scanline mapping was vital to help collect discontinuity and heterogeneity information on a rock mass. Moreover, it is the simplest way to take in reliable field rock data on-site investigations (e.g., Priest 1993; Palmström 1997; Peacock et al. 2003; Zeeb et al. 2013; Chaminé et al. 2013, 2015, 2021).

2 Jonize Quarry: Setting and Status

East Timor is situated in the eastern half of Timor Island (eastern Indonesian archipelago). It results from strike-slip tectonics in an arc-continent collision between the so-called Banda volcanic forearc and the Australian continental margin (e.g., Charlton et al. 1991; Audley-Charles 2004; Tate et al. 2015). It has about 15,000 km², including the Atauro and Jaco islands, and the enclave of Oecussi is located on the north coast of Western Timor. Figure 1 outlines the geological framework of East Timor.

Carvalho and Lisboa (2005) stated that East Timor has extensive clays, limestones, sand, and gravel resources, supporting small- to large-scale raw material extractive industries, including an interesting potential for ornamental stones, crush stones, and aggregates.

East Timor is a country with a long history and traditions. For locals, the use of explosives still brings very painful memories. Therefore, most explosives are only used by the police authorities or the military. Accordingly to the East Timor elders, commercial explosives were often used in the past to cut slopes for the passage of roadways. The Tibar Port project in the Kaiteu area used explosives to extract a larger quantity of rock material. In such a way, it forced the authorities to create a governmental Order No. 1:2017, which allows the implementation of explosives in some circumstances. Under this decree, authorisation is granted, provided the licensing for import, possession, transport, and use of explosives is respected, but it only applies to the Tibar Port project. Consequently, most quarry or open-pit mines are excavated or dug with mechanical means. Currently, the

mineral resources law to regulate and manage the georesources of East Timor is under preparation and discussion.

The Jonize quarry is situated on the left bank of Mota Comoro stream in southwest Dili municipality. The quarry is located in the Aileu formation, which is well exposed along the north coast of East Timor, comprising metamorphosed shales, siltstones, and arenites with minor limestones and basic rocks (Leme 1963; Audley-Charles 1968). In the studied site, outcrops include a gabbro-diorite suite with associated serpentinites and minor amphibolite and andesitic rocks (JCU 2017). The quarry is classified as large scale (Ministry Decree no. 64:2016) with a licensed area of 10 ha, and the quarry occupies an area of 4,82 ha. The Jonize quarry is mainly related to the extraction, processing, and production of crushed rock aggregates for the industry. The Jonize quarry is formed by sound, fine to medium-grained, and dark-green basic rocks, including the strategic reserves, equipment, and facilities. The rock mass is fractured and significantly weathered in the top part of the ground (Fig. 2).

3 Jonize Rock Mass: Preliminary Geotechnical Characterisation

An exploratory study of the Jonize quarry rock mass was carried out (details in Varela 2019). The investigation combined GIS mapping with applied geology and rock mechanics data. First, the field techniques, recommendations, and standards of mapping, applied geology, and geotechnics were applied at the study site (e.g., ISRM 1978, 1981; GSE 1995; CFCFF 1996; Griffiths 2002; ISRM 2007, 2015; Zhang 2017; Norbury 2020, and references therein). Then, after a detailed desk study of the quarry site and neighbouring zone, the following approach was developed: (i) field surveys to characterise the geologic and geomorphological constraints and also to perform a visual inspection of the site conditions and surrounding outcrops; (ii) thematic maps were arranged from multi-source data (i.e., remote sensing, topography, geology, and field surveys); (iii) rock surveys based on the scanline sampling technique on benches to the geotechnical description of the rock mass; (iv) definition of the expected in situ block size and interrelated parameters.

Figure 3 illustrates an example of rock surveys and a summary of the fundamental geotechnical parameters.

The computed data of Jonize rock mass allowed to define some key information (Palmström 2005; González de Vallejo and Ferrer 2011): (i) the rock mass structure of the block

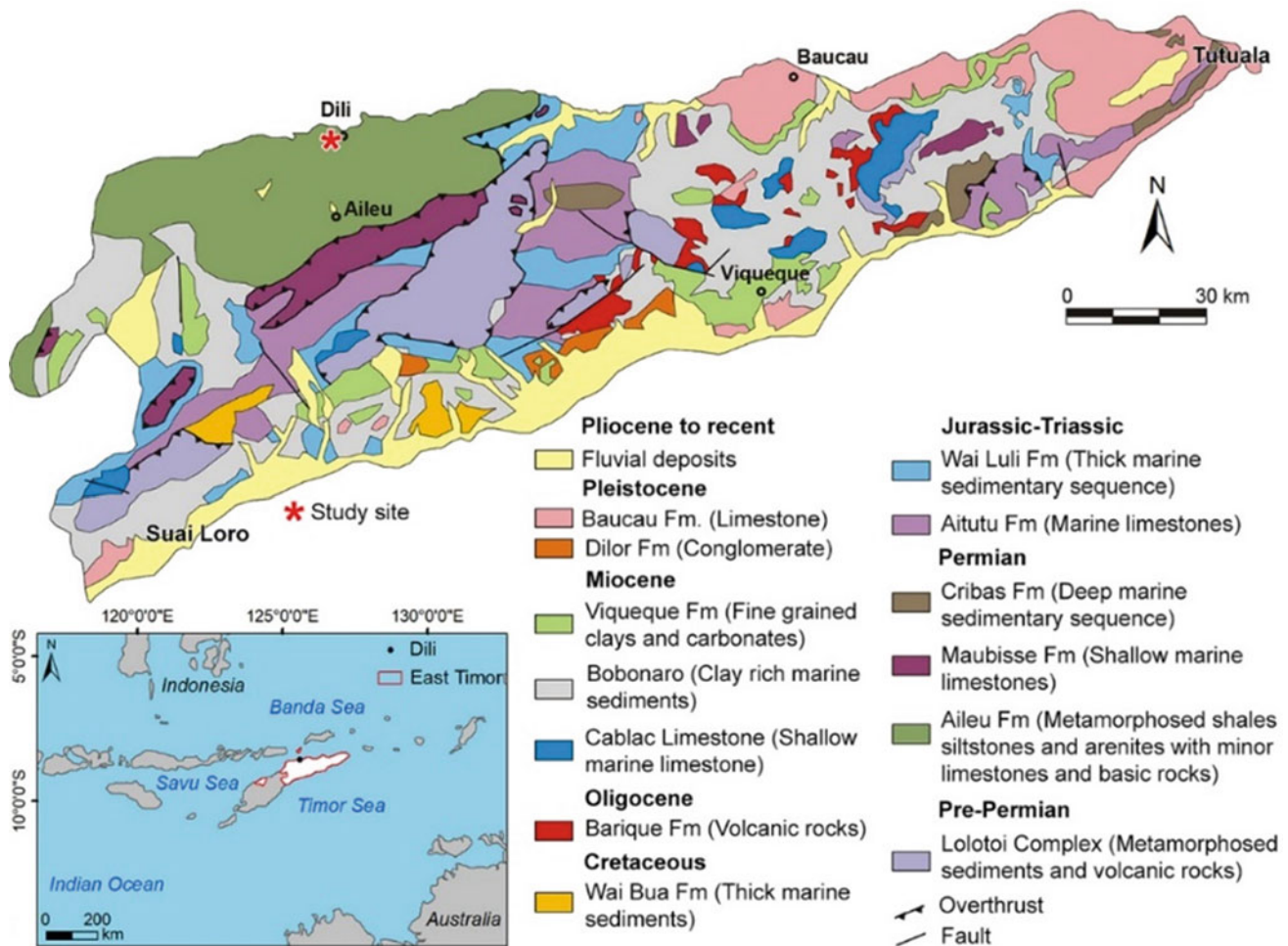


Fig. 1 Simplified geological setting from East Timor (Timor Leste) and location of the studied site—Jonize quarry, adapted from Audley-Charles (1968)

shape is irregular to blocky; (ii) J_v (volumetric joint count) of 14,2 (joints/m³), i.e., expected blocks of small size; (iii) RQD (Rock Quality Designation) based on median fracture spacing ranges from 48 to 68% (moderate to good rock quality); (iv) the GSI—Geological Strength Index (Hoek et al. 2013) ranges from 55 to 65 (i.e., “blocky, interlocked partially disturbed rock mass consisting of multifaceted angular blocks, formed mainly by orthogonal discontinuity sets and random fractures”); (v) the excavatability of rock based on the revised chart of the Pettifer and Fookes (1994) by Galiza et al. (2011b) pointed out the Jonize rock data as hard to very hard ripping rock mass class; that is also reinforced in the GSI chart for the assessment of excavatability of rock masses (Tsiambaos and Saroglou 2009) which suggests the mixed use of the hydraulic breaker hammer and blasting techniques.

The Jonize rock mass characterisation allowed a preliminary description of two geotechnical zones. Thus, it was

possible to identify distinct zones in terms of the rock quality in a practical, consistent, and pragmatic way. This geotechnical zoning represents a valuable tool for industrial rocks evaluation, as it provides crucial information for balanced management and development of the natural resource. Currently, civil explosives are not allowed in East Timor for rock blasting purposes. However, a governmental regulation for geological resources and mining activities is expected shortly. In this sense, the study developed on the basic rock mass has great relevance. For example, the orientation of the main discontinuities set identified will significantly select the best direction for blasting. Consequently, the geologic and geomechanical characteristics highlighted by the different geotechnical zones will allow each zone's distinct and suitable blasting approach. In short, decisions based on knowledge ensure greater technical and economic assertiveness, directly impacting the blasting results, both in terms of quality and efficiency.

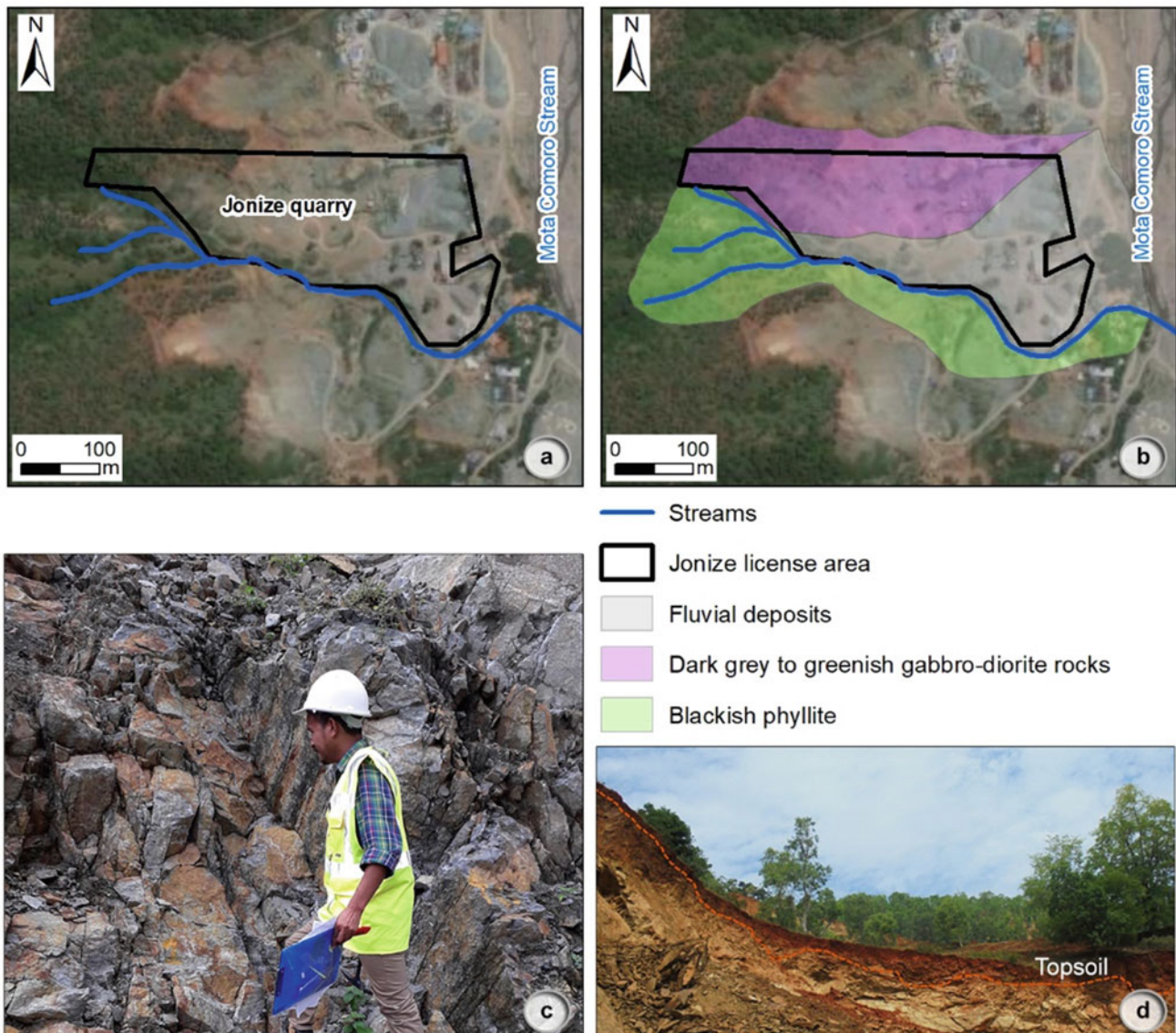


Fig. 2 Jonize quarry ($8^{\circ}34'48.14''S$; $125^{\circ}31'37.43''E$ —East Timor, SW Dili): **a** Jonize license area (orthophoto from Google Earth Pro), details in JCU (2017), **b** Geological map of Jonize quarry (updated

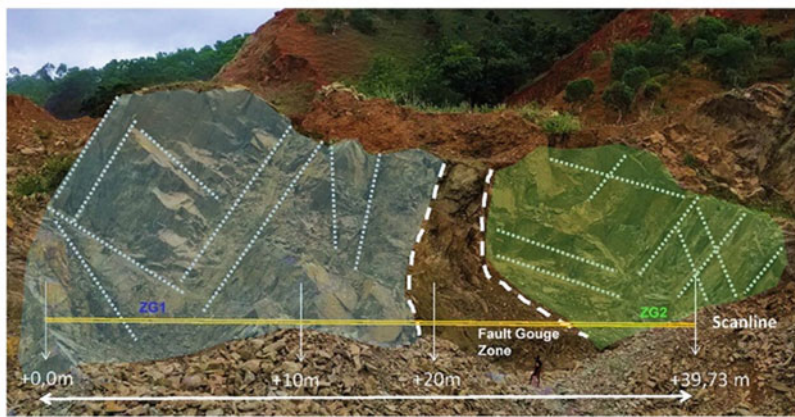
from JCU 2017, ANPM 2018); **c** Dark grey to greenish gabbro-diorite and serpentinite rocks (photo taken in January 2019); **d** Aspect of the cut-slope rock mass with brownish topsoil horizon (over a 1 m thick)

4 Concluding Remarks

Multidisciplinary studies propose a consistent multi-scale approach for on-site geotechnical investigations. The rock surveys for engineering purposes are reliable and valuable to the overall georesource assessment. That allowed mapping the geological and geotechnical features and delineating the rock mass characterisation. Rock sampling techniques are the most straightforward and reliable approach for rock mass

characterisation and related geological, geotechnical, and geomechanical properties. That approach is vital to support an appropriate blasting scheme design.

According to the so-called “Mine to Mill” framework, this study shows that the reliable multi-scale approach for on-site investigations is essential in identifying constraints and possible opportunities. In addition, it contributes to optimising different downstream processes (rock blasting and processing) to ensure the sustainability of the georesource and maximise overall profitability.



Geotechnical Zoning Units (ZG)

ZG1: fine to medium-grained, dark-greenish basic rock mass; slightly to moderately weathered (W2 to W3); moderately to widely spacing (F3 to F2; 55 - 65 cm); high to moderate strength (S2-S3; 50 - 80 MPa)

ZG2: fine to medium-grained, dark-greenish basic rock mass; highly to moderately weathered (W4 - W3); moderately to close spacing (F3 to F4; 35 - 15 cm); moderate strength (S3; 35 - 55 MPa)

Overall Geotechnical Parameters from Jonize Rock Mass: Basic Geotechnical Description (BGD) (suggested methods, terminology, techniques followed from ISRM 1978, 1981, GSE 1995, CFCFF 1996, ISRM 2007, 2015)	
Quarry cut-slope (length / height)	40 m / 5 m
Weathering grade, W	Slightly to moderately weathered (W ₂ to W ₃) Was mapped a stripping zone with highly weathered (W ₄₋₅)
Discontinuity type	Predominantly joints, but a fault gouge zone also mapped
Discontinuity set	F1: N15°E; 69° SE F2: N45°E; 61° SE F3: N155°E; 59° SW (n = 75)
Aperture	Open to close [median value: 0.3 - 0.5 mm]
Fracture spacing, F	Moderate to wide spacing (F ₃ to F ₂) [median value: 55 - 65 cm]
Persistence, L	Moderate to high (3 - 8 m)
Roughness, R	Smooth to rough (R ₃ - R ₄); Plane
Filling	Mostly none, but sometimes hard clayey
Seepage	Dry to slightly wet
Strength degree, S	High to moderate strength (S ₂ to S ₃) [median value: 50 - 80 MPa]

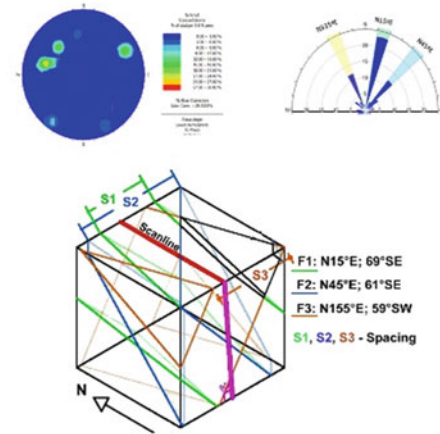


Fig. 3 Jonize quarry site: an example of scanline surveys and geotechnical parameters summary

Acknowledgements H.I. Chaminé was supported by the Centre GeoBioTec|UA (UID/GEO/04035/2020). Our thanks to the colleague P. Nogueira (University of Évora) for valuable input on the regional geology of the Dili area. Thanks to Jonize Construction company and the National Petroleum and Mineral Authority of East Timor (ANPM) for the field support, technical data, and assistance were shared. We appreciate the Jonize field inputs from Eng. R. Magno and his team from ANPM. R. Varela developed a short traineeship under the Field Study Program of the Mineral Resources Department from the ANPM and MSc Dissertation on the School of Engineering (ISEP), Polytechnic of Porto. Lastly, our appreciation to the Vice-President of ANPM, Mr J. Gonçalves, and Mr J. Filipe from Jonize Construction firm. Many thanks to the anonymous reviewers for their contributions to the manuscript.

References

ANPM–Autoridade Nacional do Petróleo e Minerais (2018) Jonize geologic map. Autoridade Nacional do Petróleo e Minerais, Dili, East Timor
 Audley-Charles MG (1968) The geology of Portuguese Timor. Mem Geol Soc Lond 4(1634):133–136

Audley-Charles MG (2004) Ocean trench blocked and obliterated by Banda forearc collision with Australian proximal continental slope. Tectonophysics 389:65–79
 Carvalho JF, Lisboa JV (2005) Construction raw materials in Timor Leste and sustainable development. In: Marker BR, Petterson MG, McEvoy F, Stephenson MH (eds) Sustainable minerals operations in the developing world, geological society, London, vol 250, no 1. Special Publications, pp 161–183
 CFCFF–Committee on Fracture Characterization and Fluid Flow (1996) Rock fractures and fluid flow: contemporary understanding and applications. National Research Council, National Academy Press, Washington DC
 Chaminé HI, Afonso MJ, Teixeira J, Ramos L, Fonseca L, Pinheiro R, Galiza AC (2013) Using engineering geosciences mapping and GIS-based tools for georesources management: lessons learned from rock quarrying. Eur Geol J 36:27–33
 Chaminé HI, Afonso MJ, Trigo JF, Freitas L, Ramos L, Carvalho JM (2021) Site appraisal in fractured rock media: coupling engineering geological mapping and geotechnical modelling. Eur Geol J 51:31–38
 Chaminé HI, Afonso MJ, Ramos L, Pinheiro R (2015) Scanline sampling techniques for rock engineering surveys: insights from intrinsic geologic variability and uncertainty. In: Giordan D, Thuro K, Carranza-Torres C, Wu F, Marinos P, Delgado C

- (eds) Engineering geology for society and territory—applied geology for major engineering projects, vol 6. IAEG, Springer, pp 357–361
- Charlton TR, Barber AJ, Barkham ST (1991) The structural evolution of the Timor collision complex, eastern Indonesia. *J Struct Geol* 13:489–500
- Cosgrove JW, Hudson JA (2016) Structural geology and rock engineering. Imperial College Press, London
- Dinis da Gama C (1996) The concept of rock mass fragmentability. In: Franklin JA, Katsabanis PD (eds) Measurement of blast fragmentation. Balkema, Rotterdam, pp 209–214
- Galiza AC, Ramos L, Fonseca L, Chaminé HI (2011a) Geomechanical control of jointed rock mass blasting by aligned drilling. In: Holmberg R (ed) Proceedings EFEE 2011 conference, European federation of explosives engineers conference, Lisbon, pp 271–280
- Galiza AC, Ramos L, Fonseca L, Teixeira J, Chaminé HI (2011b) O papel da geotecnia mineira na otimização do desmonte de maciços rochosos fraturados. *Bol Min* 46(2):103–120
- González de Vallejo LI, Ferrer M (2011) Geological engineering. CRC Press, Taylor-Francis Group, Boca Raton
- Goodman RE (1976) Methods of geological engineering in discontinuous rocks. West Publishing Company, New York
- Griffiths JS (2002) Mapping in engineering geology. Key Issues in Earth Sciences, vol 1. The Geological Society of London, London
- GSE—Geological Society Engineering Group Working Party Report (1995) The description and classification of weathered rocks for engineering purposes. *Quart J Eng Geol* 28(3):207–242
- Hoek E, Carter TG, Diederichs MS (2013) Quantification of the geological strength index chart. In: Proceedings of the geomechanics symposium, 47th US rock mechanics, San Francisco, CA, ARMA13–672, pp 1–8
- ISRM—International Society for Rock Mechanics (1978) Suggested methods for the quantitative description of discontinuities in rock masses. *Int J Rock Mech Min Sci Geom Abstr* 15(6):319–368
- ISRM—International Society for Rock Mechanics (1981) Basic geotechnical description of rock masses. *Int J Rock Mech Min Sci Geom Abstr* 18:85–110
- ISRM—International Society for Rock Mechanics (2007) The complete ISRM suggested methods for characterization, testing and monitoring: 1974–2006. In: Ulusay R, Hudson JA (eds) Suggested methods prepared by the commission on testing methods. ISRM, Ankara
- ISRM—International Society for Rock Mechanics (2015) The ISRM suggested methods for rock characterization, testing and monitoring: 2007–2014. In: Ulusay R (ed) Suggested methods prepared by the commission on testing methods, ISRM. Springer, Cham
- JCU—Jonize Construction Unipessoal (2017) Quarry andesit: annual report 2016–2018. Jonize Construction Unipessoal, Lda, Dili, East Timor (Unpublished Report in Tetum)
- Jimeno CL, Jimeno EL, Carcedo FJA, De Ramiro YV (1995) Drilling and blasting of rocks. A.A. Balkema, Taylor & Francis Group, Rotterdam
- Langefors U, Kihlström B (1978) The modern technique of rock blasting, 3rd edn. Wiley, New York
- Leme JCA (1963) The eastern end geology of Portuguese Timor. *Garcia de Orta Revista Junta Investigações Ultramar* 11(2):379–388
- Moodley L, Cunningham C (1996) Measuring the effect of blasting fragmentation on hard rock quarrying operations. In: Mohanty B (ed) Rock fragmentation by blasting. Balkema, Rotterdam, pp 353–359
- Norbury DN (2020) Soil and rock description in engineering practice. 3rd Rev. Edn., Whittles Publishing, Caithness
- Oliveira R (1987) Engineering geological investigations of rock masses for civil engineering projects and mining operations. Memórias LNEC Lisbon 693:1–28
- Palmström A (2005) Measurements of and correlations between block size and rock quality designation (RQD). *Tunn Undergr Spac Techn* 20:362–377
- Palmström A (1997) Collection and use of geological data in rock engineering. *ISRM News J*, 21–25
- Peacock DCP, Harris SD, Mauldon M (2003) Use of curved scanlines and boreholes to predict fracture frequencies. *J Struct Geol* 25:109–119
- Pettifer GS, Fookes PG (1994) A revision of the graphical method for assessing the excavability of rock. *Quart J Eng Geol* 27:145–164
- Priest SD (1993) Discontinuity analysis for rock engineering. Chapman and Hall, London
- Rocha M (2013) Mecânica das Rochas. Edição no âmbito das comemorações do centenário do nascimento do Engenheiro Manuel Rocha—1913–2013. Laboratório Nacional de Engenharia Civil, Lisboa
- Hartman HL (ed) (1992) SME mining engineering handbook, 2 edn, vol 2. Society for Mining, Metallurgy and Exploration, Colorado, USA
- Tate GW, McQuarrie N, van Hinsbergen DJJ, Bakker RR, Harris R, Jiang H (2015) Australia going down under: quantifying continental subduction during arc-continent accretion in Timor-Leste. *Geosphere* 11:1860–1883
- Terzaghi RD (1965) Sources of errors in joint surveys. *Géotechnique* 15:287–304
- Tsiambaos G, Saroglou H (2009) Excavability assessment of rock masses using the Geological Strength Index (GSI). *Bull Eng Geol Environ* 69(1):13–27
- Varela RR (2019) Implementação de desmonte com explosivos em Timor-Leste: proposta exploratória. Instituto Superior de Engenharia do Porto, Porto, URI <http://hdl.handle.net/10400.22/15773> (MSc Dissertation)
- Zeeb C, Gomez-Rivas E, Bons PD, Blum O (2013) Evaluation of sampling methods for fracture network characterization using outcrops. *AAPG Bull* 97(9):1545–1566
- Zhang L (2017) Engineering properties of rocks, 2nd edn. Elsevier, Butterworth-Heinemann, Oxford



Cut Slope Stabilization Proposals at A03 Karimbala Road, Liquiça Municipality, Timor-Leste

Oktooviano V. Tilman de Jesus and Mário Quinta-Ferreira

Abstract

In Timor-Leste (East Timor), many road cuts are a frequent cause of slope failures, requiring extensive maintenance. The failures are related to a rough topography, complex geology and intense precipitation, aggravated by recent road construction to improve the old roads. The slope stability problems were previously evaluated, and stabilisation procedures adjusted to Timor-Leste are here proposed. The leading causes of slope instability are surface weathering, discontinuities with unfavourable orientation, and intense rainfall inducing high water pressure. The computed values of the FoS below 1.5 were considered insufficient for long-term stability, and it was concluded that most slopes are prone to additional slope failures. Therefore, mitigation procedures must be urgently implemented to reduce the damages and the danger to drivers and pedestrians. Improvement stability procedures were simulated, and the ones considered best suited are proposed as it is highly recommended to use improvement techniques adjusted to the local and economic conditions of Timor, such as reshaping of the slope, reduction of the slope height or angle, drainage improvement and reinforcement of the slope using rockfill.

Keywords

Slope stability analysis • Road slopes • Slope reshaping and reinforcement • East Timor

1 Introduction

After the failure of a significant number of recent road-cut slopes, a characterisation of the geological and geotechnical local conditions of five selected slopes was done and presented elsewhere (Jesus and Quinta-Ferreira 2020). In addition to the stability analysis, stabilisation procedures, preventive or corrective (Abramson 2002), are evaluated to verify the increase in the slopes' safety conditions (Duncan 2000; El-Ramly et al. 2002) the reduction of the risk situations for the road and its users.

To mitigate future slope failures in post-failure vulnerable areas (De Blasio 2011), attempts were made to achieve a minimum factor of safety of 1.5 by (a) employing different types of improvement techniques such as reduction of slope height; reduction of slope angle; drainage improvement (reduction of pore water pressure) and (b) reinforcement of the slope increasing the shearing resistance of the slip surface by substitution of weaker materials with other presenting higher friction angle in the critical zones of failure, or by nailing.

It is considered that rockfill is a good solution, well suited to Timor-Leste because it can benefit from the abundant rock outcrops and does not need high skilled techniques or procedures. Furthermore, the use of rock bolts in the reinforcement was also evaluated and considered necessary in some cases.

As previously stated, the description of the failure and characterisation of these five slopes' geological and geotechnical local conditions was presented by Jesus and Quinta-Ferreira (2020). The procedures evaluated for stabilising each of the five slopes are presented based on the analysis performed with the Rocscience (2020) software tools, mainly Slide and RocFall (see Fig. 1).

O. V. T. de Jesus
Instituto do Petróleo e Geologia, Dili, Timor-Leste

M. Quinta-Ferreira (✉)
CGeo–Geosciences Center, Faculty of Sciences and Technology,
Department of Earth Sciences, University of Coimbra, Coimbra,
Portugal
e-mail: mqf@dct.uc.pt

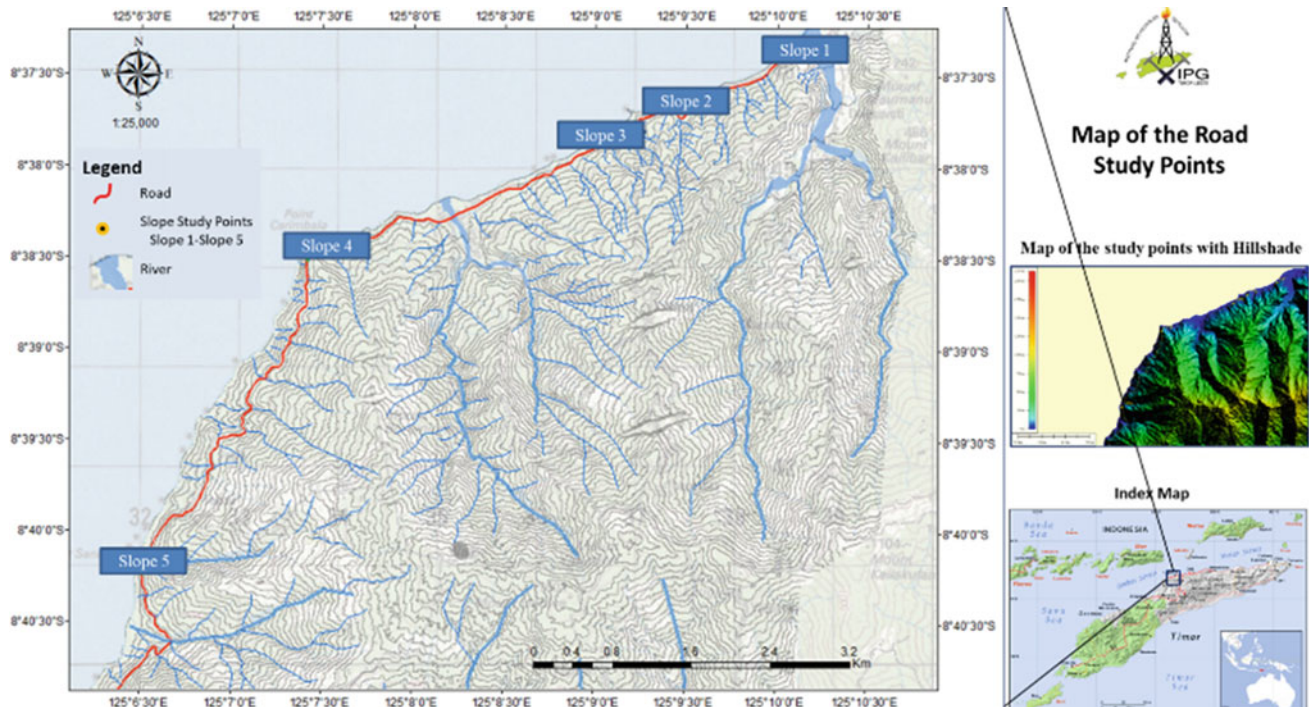


Fig. 1 Map of the A03 Karimbala road linking the Liquiça and Bobonaro Municipalities, showing the location of the five slopes (Jesus and Quinta-Ferreira 2020)

2 Proposed Slope Stabilisation Measures

2.1 Slope 1

For Slope 1, the mitigation can be achieved by using rockfill to improve the slope stability (Fig. 2-left) as it will restrain the sliding of the soil materials in Zone C. The Factor of Safety (FoS) computed is 1.52. Hence the slope can be considered in a safe condition (D'Andrea and Sangrey 1982). Rockfill is proposed because it can be easily obtainable in the surroundings at a low cost. For the Rockfall hazard mitigation (e.g., Pierson and Van Vickle 1993; Budetta and Nappi 2013; Rocscience 2020), it is required to install a rockfall barrier/protection with 2 m height, adjacent to the platform of the road.

2.2 Slope 2

The proposed mitigation solution for Slope 2 is rockfill reinforced by nailing, where the unit weight, the friction angle, and the cohesion of the rockfill materials are 28 kN/m³, 45° and 0 kPa. As shown in Fig. 2-right, the rockfill and nailing are designed to mitigate the superficial soil materials' sliding. The computed Factor of Safety (FoS) is 2.2. Consequently, the slope is in a safe condition. For the

rockfall hazard mitigation, it is required to install a rockfall barrier with 2 m height at the base of the slope adjacent to the road.

2.3 Slope 3

The proposed mitigation solution for Slope 3 is to use gabion and end-anchored rock bolts. The unit weight, friction angle, and cohesion of the gabion materials are 20 kN/m³, 50° and 20 kPa (Fig. 3-left). The gabion material is designed to protect the soil materials' sliding, as shown in Zone C. The computed Factor of Safety (FoS) is 1.6, and the slope will be in a safe condition. The Rockfall hazard mitigation was installing a rockfall barrier 2 m height at the slope's foot (Fig. 3-right).

2.4 Slope 4

The more suitable mitigation procedure for Slope 4 is considered to be the use of rockfill combined with rock bolts, end anchored. The unit weight, friction angle, and cohesion of the materials are 30 kN/m³, 45° and 0 kPa consequently, as shown in Fig. 4-left. The rockfill will prevent the sliding of the soil materials, as shown in Zone C. The computed Factor of Safety (FoS) is 1.9. Therefore, the slope will be in

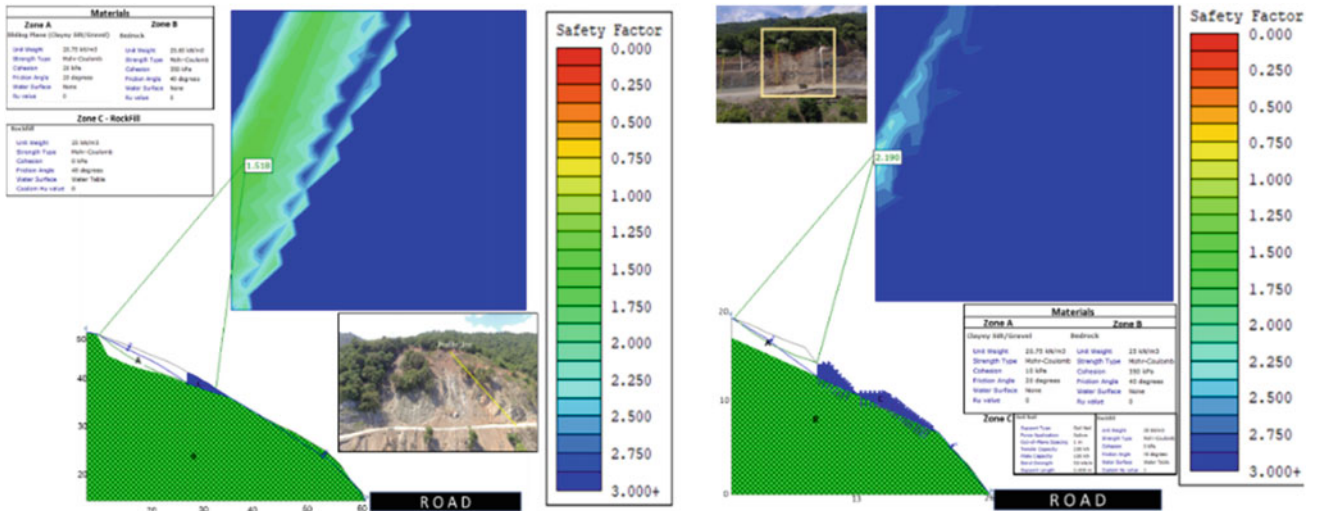


Fig. 2 Proposed slope stability improvement procedures using rockfill in Slope 1 (left) and rockfill with the combination of soil nailing for Slope 2 (right)

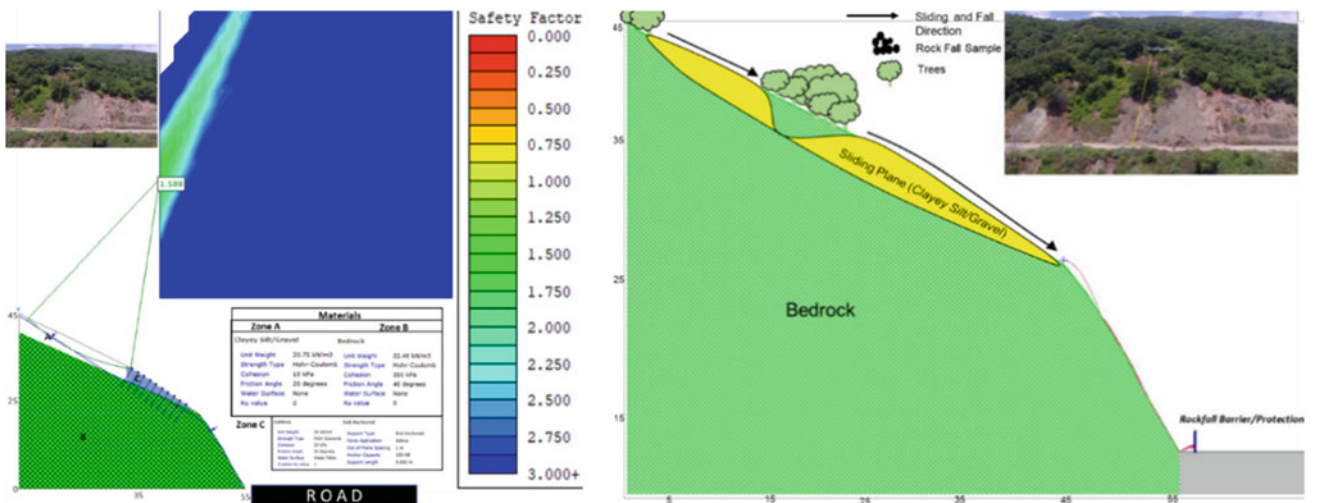


Fig. 3 Slope stability analysis of proposed procedures for slope protection using gabion combined with end anchored rock bolts for Slope 3 (left) and rockfall simulation (right)

a safe condition. For the Rockfall hazard mitigation, it is required to install a rockfall barrier 2 m height at the base of the slope, adjacent to the road platform.

in a safe condition. For the rockfall hazard mitigation, installing the rockfall barrier/protection 2 m height is required.

2.5 Slope 5

The mitigation at Slope 5 can be done using rockfill at the foot of the unstable mass, with the rock bolts' combination (end anchored). The unit weight, friction angle, and cohesion of the rockfill materials is 30 kN/m³, 45° and 0 kPa, as presented in Fig. 4-right. The parameters computed for the Factor of Safety (FoS) resulted in 1.5. Therefore the slope is

3 Concluding Remarks and Recommendations

The study performed along the A03 road in the Aileu Formation confirmed that several large slopes become unstable due to local geology and surface weathering, mainly during rainy periods, after the cuts performed at the slope's foot the beneficitation of the road. As a result, the natural balance of

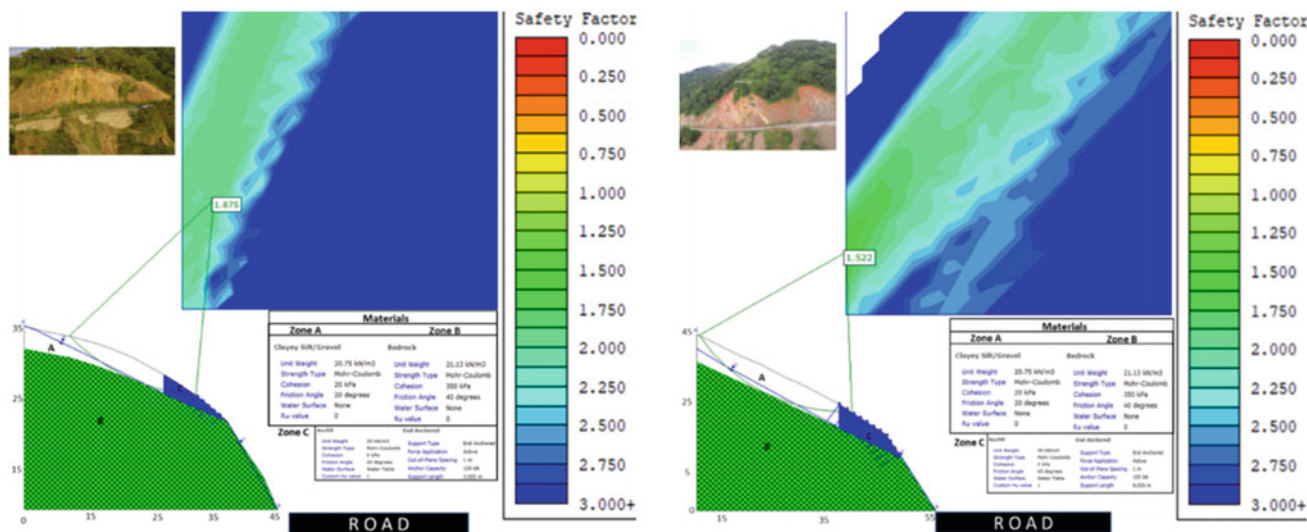


Fig. 4 Slope stability analysis results of improvement procedures proposed for slope protection using rockfill and rock bolts for Slope 4 (left) and Slope 5 (right)

the slope was modified by the excavation at the foot, generating unstable conditions. Due to the absence of remediation procedures (Table 1) and the danger to drivers and pedestrians, the present unstable condition justified the decision to study some essential unstable slopes.

To improve the efficiency of the stabilisation, nailing should be used. Rock bolts can be helpful to minimise the failure from discontinuities (joints, fractures, faults). Removal or reinforcement of the unstable materials on slope and revegetation works are highly recommended. It is also possible to use grating works at the lower parts of the landslide to increase stability. Failed ground generally presents significant strain on its inside. Therefore, removing the unstable volume and/or construct a stabilising retaining structure at the slope’s toe is recommended.

The use of bio-organic/bio-engineering stabilisation methods is quite interesting in shallow slides. Improvement of surface soil conditions and the use of plants and grass can prevent surface erosion. In some rock faces, this objective could be achieved using shotcrete.

In Timor-Leste, most of the solutions that do not use local materials will require expensive resources, so all the solutions that require more labour and local materials are best suited to developing the country’s economy.

Despite being outside the present work scope, a detailed drilling and core sampling for suitable subsurface geotechnical characterisation would be advisable and a detailed engineering study and design of the road slopes. The monitoring of the failure scars and slope movements and traffic control should be arranged and optimised. Detail study of the slopes below the road platform is also recommended. Rerouting is recommended when the slope failure remediation would be too expensive or when the maintenance cost would be unacceptable.

With the development of Timor-Leste, there is a need to improve safety, avoiding accidents related to mass movements, mainly slip slides and rock blocks fall. It is worth mention that the construction of roads in Timor-Leste is mainly done without an entire developed project, being absent a detailed geotechnical characterisation study and

Table 1 Summary table of the Factor of Safety (FoS) of slopes before adding the proposed improvement procedures. The seismic load coefficient is 0.28

Slope	Before	Improvement procedures	
	Saturated	Saturated with seismic load	After improvement procedures Saturated with seismic load
Slope 1	1.2	0.7	1.5
Slope 2	1.2	0.7	2.2
Slope 3	0.8	0.4	1.6
Slope 4	1.2	0.7	1.9
Slope 5	0.8	0.5	1.5

design. This work aims to draw attention to the urgent need to change the current approach, allowing to improve safety and to reduce the economic losses and the need to repair recently constructed roads, stressing the need to perform a detailed geological and geotechnical study in all projects, and use a minimum Factor of Safety (FoS) of 1.5 for any permanent road slope design.

Acknowledgements To “Instituto do Petróleo e Geologia” (IPG) of Timor-Leste, to Mr. Hélio C. Guterres, for the financial support. To the Director of Geo-Hazard Division, Mr Eugenio Soares, for letting us use several valuable data. To the Director of Geo-Information Division, Mr Osório da Costa, for sharing the LIDAR data from Geo-Hazard Division. To all the IPG staff, especially to Mr. José Nano, in structural geology interpretation, Eng. Abilo Fernandes and Eng. Moisés Pereira, for fieldwork and data collection, and to Eng. Emanuel Assis for the drone images captured in 2018; this work will not be successful without all support. To the Ministry of Public Works of Timor-Leste, Directorate of Roads, Bridges and Flood Control for data sharing on Detailed Engineering Design for Maubara-Karimbala Section. FCT—Fundação para a Ciência e a Tecnologia also supported this work through Portuguese funds in the research project UIDB/00073/2020 of the Geosciences Center at the University of Coimbra.

References

- Abramson LW (2002) Slope stability and stabilisation methods. Wiley, Hoboken
- De Blasio FV (ed) (2011) Introduction to the physics of landslides: lecture notes of the dynamics of mass wasting. Springer, Cham
- Budetta P, Nappi M (2013) Comparison between qualitative rockfall risk rating systems for a road affected by high traffic intensity. *Nat Haz Earth Syst Sci* 13:1643–1653
- D’Andrea RA, Sangrey DA (1982) Safety factors for probabilistic slope design. *J Geotech Eng ASCE* 108(9):1108–1118
- Duncan JM (2000) Factors of safety and reliability in geotechnical engineering. *J Geotech Geoenviron Eng ASCE* 126(4):307–316
- El-Ramly H, Morgenstern NR, Cruden DM (2002) Probabilistic slope stability analysis for practice. *Can Geotech J* 39:665–683
- Jesus OVT, Quinta-Ferreira M (2020) Slope stability analysis along A03 Karimbala road, Liquiça Municipality, Timor-Leste. In: Abrantes I, Callapez PM, Correia GP, Gomes E, Lopes B, Lopes FC, Pires E, Rola A (eds) *Uma visão holística da Terra e do Espaço nas suas vertentes naturais e humanas. Homenagem à Professora Celeste Romualdo Gomes*. CITEUC, Coimbra. <https://doi.org/10.5281/zenodo.4409370>
- Pierson L, Van Vickle R (1993) Rockfall hazard rating system: participant’s manual. US Department of Transportation, Federal Highway Administration. Publication No. MA SA-93-05, Washington DC. <https://vulcanhammer.net/files.wordpress.com/2017/01/fhwa-sa-93-057.pdf>
- Rocscience (2020) Rocscience programs: <https://www.rocscience.com/rocscience/products/>. Accessed in January 2020



Rock Slope Instability Risk Assessment in Open-Pit Quarries: A Comprehensive Approach

João Brissos, Leonor Mata, João Cruz, João Saúde, Paulo Sá Caetano, Carlos Costa, and Daniel Vendas

Abstract

This work aims to develop a simplified approach to assess slope stability in open-pit marble quarries. Each site is subject to field investigation to determine the relevant rock mass properties, using the scanline sampling technique to list the mechanic and geometric properties of the intact rock and rock mass discontinuities and collect samples for laboratory analysis of the relevant geotechnical properties. The stability conditions of each slope for planar, wedge and toppling mechanisms were then studied through kinematic analysis techniques, both qualitative and quantitatively. To determine the stability, both Limit Equilibrium Methods (LEM) and geomechanical classifications for rock masses are applied, namely the Slope Mass Rating. With the proposed approach, it is possible to determine a qualitative variable called the Risk Index, based on the *vulnerability* and the *hazard* of the slope, and address the most suitable control measures to eliminate the potential risks these sites represent.

Keywords

Rock slope stability • Risk assessment • Open-pit quarries • Dimension stone

1 Introduction

Dimension stone extraction in Portugal dates back to the Roman Period, and this resource has been widely used as construction and ornamental raw material for the country's historical monuments. In recent years, economic and market constraints forced quarry owners to focus on the homogeneity of the extracted materials rather than the exploitations' sustainable longevity. Therefore, the main difficulty facing the adequate development of an open-pit quarry nowadays is to assure the slopes' geotechnical stability, which can be achieved using slope stability analysis. That is one of the most critical steps towards ensuring safer working environments because an inadequate slope design can eventually cause severe human and material damage. Given the high number of active and inactive quarries in the country, many with multiple and, occasionally, quite complex instability issues, any imminent risks can only be fully mitigated when a detailed slope stability analysis is combined with an adequate risk assessment.

The stability of rock slopes is crucial to public safety in transport infrastructures passing through rock cuts, as well as to personnel and equipment safety in open-pit quarries. Slope instability can be induced by many preparatory factors, namely adverse slope geometries and joint sets, soft or weathered slope materials, and the presence of groundwater. External loads caused by heavy or prolonged rain, seismic events or blasting can play a significant role in slope failures, typically acting as triggering mechanisms that can initiate failure. The slope stability of the open-pit marble quarries in the region of Estremoz-Borba-Vila Viçosa (Estremoz Anticline, Portugal) has attracted major concern after a large slope collapse on the EN255 on 19th November 2018. This event motivated the inception of the Intervention Plan for Quarries in Critical Situation approved by Cabinet Meeting n°50/2019, 5th March, which requires “*the definition of urgent and priority risk mitigation measures to avoid or, at least, reduces the critical situations in quarries*”.

J. Brissos · L. Mata (✉) · J. Cruz · C. Costa · D. Vendas
eGiamb – Consultoria Geoambiental Lda, Caparica, Lisboa,
Portugal
e-mail: lepsmata@gmail.com

J. Saúde
RM –Engenharia, Geologia e Ambiente, Vila Viçosa, Évora,
Portugal

P. S. Caetano
GeoBioTec – Polo UNL and Department of Earth Sciences, FCT
NOVA, Lisbon, Portugal

2 Methodology

Several techniques and methods for slope stability analysis have been developed over the years. These methods can be grouped into four categories, i.e., kinematic analysis, limit equilibrium, numerical modelling (based on deterministic or probabilistic methods) and empirical methods. Kinematic analysis is commonly used to predict the potential structural failure mechanism by projecting the slope and discontinuities' orientation on a two-dimensional stereograph net (Hoek and Bray 1981). Rock mass classification systems or empirical methods represent an essential tool that is often used for preliminary assessment of the rock mass's engineering behaviour, with proven usefulness due to the ease with which they can be implemented and their effectiveness in interpreting stability and recommending control measures. On the other hand, risk assessment is a versatile decision-making tool, as it involves considering the sources of risk, their consequences, and the likelihood of those consequences. Therefore, a methodology for assessing the stability of open-pit quarry cuts and the associated risk is suggested using a combination of kinematic analysis and empirical methods (Fig. 1).

Each site is subject to field investigations to determine the rock mass's relevant properties (including intact rock and discontinuities). These include rock type, rock weathering, condition of discontinuities (orientation, spacing, aperture and filling, persistence, wall weathering), groundwater presence, and the geometrical description of the slope, such as slope height, face dip and dip direction. The following step involves laboratory testing to determine the relevant geotechnical properties of rock samples. In this methodology, it is suggested to perform uniaxial compressive strength tests

and tilt tests to determine the unconfined compressive strength (UCS) of the rock and the basic friction angle for discontinuities (ϕ_b), respectively (Bruce et al. 1989). For marble open-pit quarry slopes failure is, in general, structurally controlled, except in localized areas where groundwater flows through the more persistent joint sets typically form highly weathered areas filled with silty clay soil from the dissolution of CaCO_3 (karst cavities). Two types of approaches are used: kinematic analysis and the RMR (Rock Mass Rating) system (Bieniawski 1989).

Kinematic analysis is used to determine the likelihood of planar, wedge and toppling failures and assess the most critical failure surface on the rock slope. The RMR is a system that rates the rock mass quality based on five parameters that represent different conditions of the rock material and the discontinuities. These parameters are UCS of intact rock, RQD (Rock Quality Designation), the spacing between discontinuities, condition of discontinuities and groundwater. This RMR system is known as "the basic RMR", and it gives a value that ranges between 0 and 100 (Bieniawski 1989).

Based on the results of the RMR and the identification of the most critical failure from the kinematic analysis, the SMR (Slope Mass Rating) system is applied to the slope. The SMR system is derived from the RMR, where adjustment factors representing the discontinuity orientations towards the slope are subtracted from the basic RMR (RMR_b) and the effect of the excavation method (e.g., Romana 1985; Anbalagan et al. 1992). The continuous SMR system (Tomás et al. 2007) replaces the rating system adopted in the original SMR with continuous functions (Riquelme et al. 2014). Both approaches can be used.

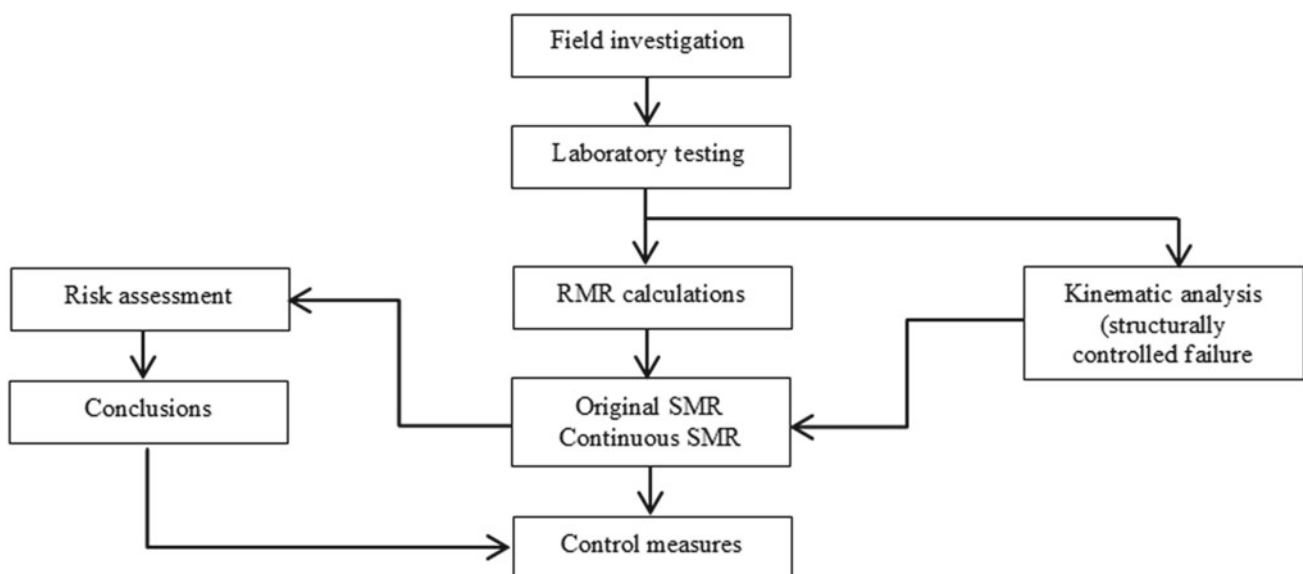


Fig. 1 Proposed methodology flowchart

Table 1 Planned control measures based on the proposed risk index

Risk Index	Classification	Planned mitigation measures
25	Critical	<ul style="list-style-type: none"> • Total or partial suspension of labour • Structural measures (slope stability) and surface drainage • Security perimeters/access restriction • Removal of unstable wedges • Monitoring measures
20-24	Very high	<ul style="list-style-type: none"> • Re-profiling/induced blasts • Structural measures (slope stability) and surface drainage • Security perimeters/access restriction • Removal of unstable wedges • Monitoring measures
15-20	High	<ul style="list-style-type: none"> • Structural measures (slope stability) and surface drainage • Security perimeters/access restriction • Periodic removal of unstable wedges • Monitoring measures
10-15	Moderate	<ul style="list-style-type: none"> • Security perimeters/access restriction • Periodic removal of unstable wedges • Monitoring measures
5-10	Low	<ul style="list-style-type: none"> • Periodic removal of unstable wedges • Monitoring measures
0-5	Insignificant	<ul style="list-style-type: none"> • Monitoring measures

The next stage consists of a qualitative risk assessment where the terms hazard (H) and vulnerability (V) are categorized on a scale of 1–5, providing a risk index adapted from the work produced by Costa et al. (2009), revised by Brissos (2013), Brissos et al. (2014) and Caetano et al. (2015), applied to instability risk assessment in natural slopes. It should be noted that H is to be understood as an apparent hazard, differing from the concept commonly used since it is not derived from a probabilistic assessment of the damaging phenomenon but rather from the obtained SMR class.

This risk classification encompasses a fair degree of subjectivity, yet it allows for the concentration of resources on sites that demand immediate intervention and implementation of control measures (Table 1). Subsequently, limit equilibrium techniques or other methods can refine the stability analysis of the sites' that shows very high or critical risk.

3 Results

The described methodology was implemented on the NE slope of an open-pit marble quarry (Site A) located in the Estremoz Anticline, Portugal (Fig. 2).

For site A, kinematic analysis, using *Rocscience* software *Dips*, indicated that the most unfavourable structural movement is planar sliding along a joint set sub-parallel to

the slope and dipping approximately 50–70°SW with a basic friction angle of 45°, as determined by tilt testing. The most critical element of this joint set (highlighted in red in Fig. 2) intersects the slope from the surface and shows itself along the slope's face until approximately 38 m from its base. The persistence of this element was estimated at approximately 50 m. Therefore, the SMR classification deemed the site prone to sliding along some of the more persistent joints and joint intersects (for wedge failure). Results are shown in Table 2.

The Risk Index for site A (Fig. 2) was found to be very high, resulting from a high H rating based on the SMR results (favouring the risk of sliding of the rock mass along the identified joint), and a high V rating, as there is an operating derrick crane on top of the slope (static and dynamic loads), while work is underway at the toe of the bench leading to the presence of operators and equipment. Furthermore, there is a substantial thickness of residual soil at the top of the slope, which can be mobilized by runoff and other erosion agents.

To refine the geotechnical model regarding the very high risk of this site, a limit equilibrium analysis (Wyllie and Mah 2004) was conducted to estimate the dimension of the unstable mass as well as the corresponding factor of safety (FS) (Fig. 3). Calculations considered a unit weight of the rock (γ) of 27 kN/m³, a mass height (h) of 46 m and a horizontal distance between the face of the slope and the outcrop (X) of 25,5 m with a dip angle (ψ) of 61°, leading to

Fig. 2 Characterization of site A. Stereographic projection and identification of the most critical fracture (in red) affecting the slope

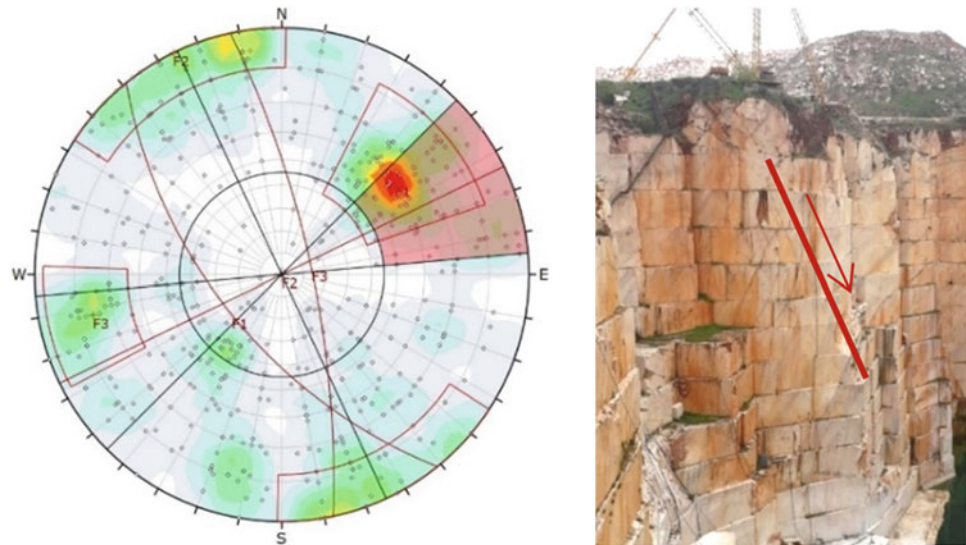


Table 2 Results obtained for site A

Site	Critical structural failure	RMRb	Original SMR	Continuous SMR	Rating SMR	Failures SMR	Stability SMR	Risk Index
A	Planar slide	69 (II)	27	26	IV	Planar or big wedges	Unstable	Very high (20)

a mass weight (triangular wedge) of 16.334 kN/m. No tension cracks were identified in the upper surface or the face of the slope. It was also considered that the area of the sliding surface was 52,59 m²/m with the cohesion of 160 kPa (the value was estimated on-field shear strength assessment and literature results by Costa 1992), which resulted in a factor of safety of 1,14, lower than that required for temporary open-pit slopes (Wyllie and Mah 2004).

4 Control and Risk Mitigation Measures

Several risk mitigation measures were discussed with the quarry owner and site engineers. Regarding the very high-risk index obtained for this specific site, risk mitigation measures proposed include:

- Slope re-profiling—controlled removal of the identified unstable rock mass.
- Periodic removal of any other potentially unstable rock masses.
- Periodic slope monitoring using high-precision topography devices (UAV).
- Instrumentation plan—Implementing fissurometers in the critical fractures of the most unfavourable joint sets considered in the SMR calculations and surface surveying techniques to detect any vertical movements.

- Access restriction/alteration (until slope re-profiling is complete). Restrict the derrick crane's use only to maintenance operations and extraordinary activities in which its use is mandatory and create a security perimeter of 30 m along the base of the slope.

If the unstable rock mass remains, other measures will need to be implemented, namely rock support bolts to increase the slope's FS. Based on the conducted calculations, to obtain a factor of safety of 2,0, the bolting force must be 1461 kN/m. The rock bolts must be placed in vertical rows of 5 bolts, horizontally spaced by 2,05 m, with as many vertical rows as required to obtain the mass's total coverage (Wyllie and Mah 2004).

Depending on the type of slope, its current status (if it is under active exploitation or if its geometry has been finalized) and the size of the unstable wedge(s), other solutions can be implemented, for example, rolled cable nets that can offer protection against small-sized but, nonetheless, hazardous rockfalls over wide areas of the slope. In the studied region, most marble quarries are exploited by different companies over small areas, which result in adjacent and very deep sub-vertical open-pit quarries whose boundaries are often subject to slope instability issues. Other alternatives can be sought in these cases, such as integrated exploitation with adjacent quarries, which can effectively eliminate the risk.

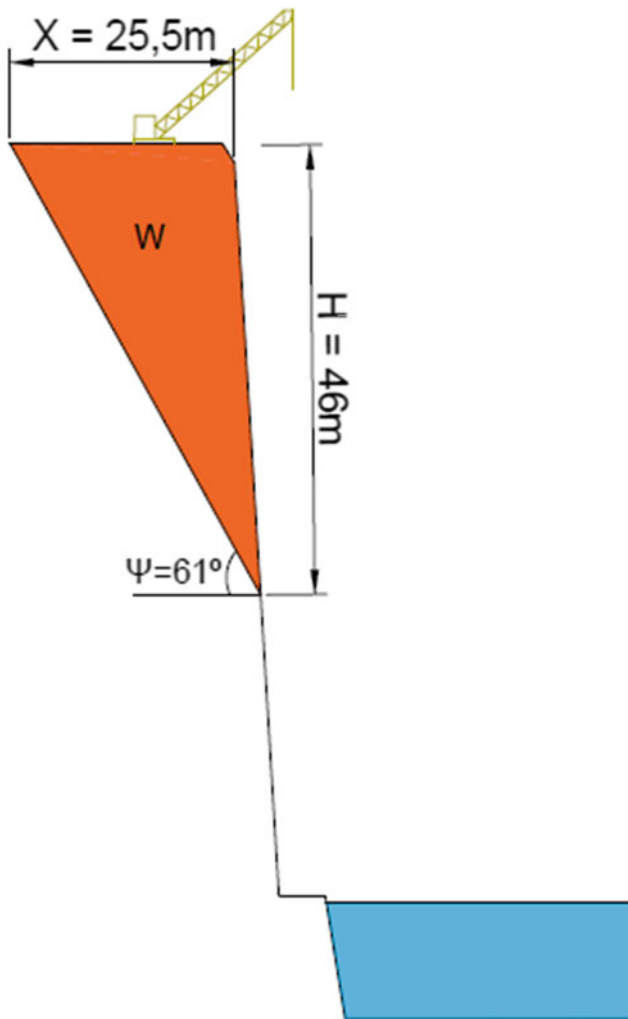


Fig. 3 Limit equilibrium model for site A

It should be noted that a given slope that, at any moment, is considered as stable, during continuing exploitation can rapidly evolve into an unstable one. Therefore, the geotechnical model of the slope must be adapted accordingly, and some adjustments must be made to update the current model if necessary, namely if tension cracks are identified.

5 Concluding Remarks

In summary, the proposed approach, combining kinematic analysis and empirical methods, allows to study of quarry slope stability and subsequently prioritize several high-risk sites over a short timeframe in order to determine the need for further studies and/or risk mitigation measures, as enforced by the Portuguese Intervention Plan for Quarries in Critical Situation.

This approach was applied to the study of several sites in the region of Estremoz-Borba-Vila Viçosa and produced

satisfactory results for both quarry owners and regulators. The conducted analysis allowed identifying many different slope stability issues that represent a risk for the existing receptors. Therefore, several control and mitigation measures were proposed for these sites, ranging from site monitoring to the temporary, total or partial, suspension of labour.

Further work is required to improve the proposed methodology. To this end, incorporating laser scanning techniques via UAV in order to improve the geological data acquisition process can be a step forward, as the traditional scanline sampling technique is highly dependent on accessibility to the study areas, which can be a severe limitation in open-pit quarries bordered by sub-vertical slopes.

References

- Anbalagan R, Sharma S, Raghuvanshi TK (1992) Rock mass stability evaluation using modified SMR approach. In: Proceedings of the 6th national symposium on rock mechanics, pp 258–268
- Bieniawski ZT (1989) Engineering rock mass classifications: a complete manual for engineers and geologists in mining, civil and petroleum engineering. Wiley, Pennsylvania
- Brissos J (2013) Avaliação de risco de instabilidade de arribas no troço Sines – Zambujeira do Mar (SW Alentejano). Faculty of Science and Technology, UNL, Monte Caparica. <http://hdl.handle.net/10362/114059>
- Brissos J, Caetano PS, Lamas P, Costa C, Rocha M (2014) Avaliação do risco de instabilidade de arribas no troço costeiro Sines-Zambujeira do Mar. *Comun Geol* 101(2):883–887
- Bruce G, Kruden D, Eaton T (1989) Use of a tilting table to determine the basic friction angle of hard rock samples. *Canad Geotech J* 26:474–479
- Caetano PS, Brissos J, Barbosa S, Lamas P, Brito MG, Fernandes C (2015) Avaliação geotécnica detalhada das arribas inseridas nos sectores Espichel-Sado e Sines-Odeceixe. Technical Report for Egiamb, Lda. and ARH-Alentejo (Évora). NOVA School of Science and Technology, Monte Caparica (Unpublished Report)
- Costa CN (1992) As pedreiras do anticlinal de Estremoz. A geologia de engenharia na exploração e recuperação ambiental de pedreiras. Ph. D. thesis. Universidade Nova de Lisboa, Monte Caparica
- Costa CN, Caetano, PS, Brito MG, Vendas D. (2009) Estudo preliminar do risco associado à instabilidade de arribas no troço entre Cabo Espichel e Setúbal. Technical Report for ARH-Alentejo (Évora). NOVA School of Science and Technology, Monte Caparica (Unpublished Report)
- Hoek E, Bray J (1981) Rock slope engineering, 3rd edn. The Institution of Mining and Metallurgy, London
- Riquelme A, Tomás R, Abellán A (2014) SMR tool beta: a calculator for determining slope mass rating (SMR). Universidad de Alicante, Alicante, Spain
- Romana M (1985) New adjustment ratings for application of Bieniawski classification to slopes. In: Proceedings of the international symposium on the role of rock mechanics. Zacatecas, ISRM, p 49–53
- Tomás R, Delgado J, Serón JB (2007) Modification of slope mass rating (SMR) by continuous functions. *Int J Rock Mech Min Sci* 44:1062–1069
- Wyllie DC, Mah CW (2004) Rock slope engineering: civil and mining, 4th edn. Spon Press, Taylor & Francis Group, Abingdon



Geological and Geotechnical Hazards in Large Infrastructures in Spain: Lessons Learned from Pajares Railway Tunnels and Castor Underground Gas Storage Project

L. I. González de Vallejo

Abstract

The analysis of two large infrastructures built in recent years in Spain highlights the importance of geological and geotechnical knowledge on large engineering projects' feasibility and cost. The first case analysed concerns the Pajares Tunnels, 24.9 km long, located in the NW of Spain. Despite completing its excavation in 2009, hydrogeological problems that arose after the tunnel's excavation have prevented the tunnels from entering in service. The environmental damage caused by water leakage has irreversibly affected a large environmental value area, with significant economic losses. In the second case, the Castor underground gas storage project is described. This facility is located under the sea in the Gulf of Valencia's Mediterranean waters on an old hydrocarbon deposit. Due to induced seismicity by gas injections, the project was closed in 2013, two months later than the injections started. The cause of the injection suspension was the social alarm in several coastal towns located near the injection area due to moderate earthquakes. The project did not consider the hazard of induced seismicity or the presence of faults with seismic potential in the area. Currently, this facility is definitely closed, leaving substantial economic losses.

Keywords

Geological hazards • Induced seismicity • Tunnel hydrogeology • Pajares Tunnels • Castor Project • Fluid injection hazards

L. I. G. de Vallejo (✉)

Department of Geodynamics, Faculty of Geological Sciences, Universidad Complutense de Madrid, Madrid, Spain
e-mail: vallejo@ucm.es

Volcanological Institute of Canary Islands (INVOLCAN), Tenerife, Spain

1 Introduction

From the second half of the last century, it is from the start of constructing large engineering infrastructures when the importance of geology in engineering is highlighted after significant dam failures related to the foundation ground. Geological and geotechnical engineering become then relevant, and courses on engineering geology, rock and soil mechanics begin to be introduced in European and American higher education institutions. However, despite the current development on geoengineering, major failures still continue to occur in infrastructures, being the leading cause of the insufficiencies in the geological-geotechnical studies on which the projects are based.

The first case analysed refers to the Pajares Tunnels Project (2009), and the second to the Castor Project for underground storage of natural gas (2013). Hydrogeological conditions were not adequately considered in the tunnel project, while in the second case, the facility was closed due to unforeseen induced seismicity. As a result, the economic losses of both projects have exceeded 5,665 million euros, in addition to causing significant environmental damage.

2 The Pajares Railway Tunnels

The excavation works for the Pajares Tunnels were completed in 2009. However, up to the present (2021), they have not entered into service mainly due to hydrogeological problems that have led to significant water seepage into the tunnels. These problems have caused critical economic losses and irreversible environmental damage.

In 2004, started the excavation of two long tunnels located in NW Spain, in the Cantabrian Mountains, between León and Asturias (Fig. 1). These tunnels are part of a new high-speed railway line. The Pajares Tunnels are 24.9 km long and are two parallel tunnels with a circular section of 8.5 m diameter, 50 m apart. The maximum overburden



Fig. 1 Left: A general view of the Pajares Tunnels portal area. Right: Tunneling Boring Machine (TBM) used in the Pajares Tunnels. *Photos* ADIF, Administrator of Railway Infrastructures

thickness is 1,100 m. The tunnels were excavated by tunnelling boring machines (TBM), although conventional methods (NATM) were also used in some sections. The most widely used support consisted of precast concrete dowels of 40–110 MPa of strength (Fig. 1).

The area crossed by the tunnels is formed by a long east-west alignment of mountains with heights exceeding 2,000 m and is located within a protected environmental reserve. The geological materials are composed of sedimentary rocks from the Paleozoic age, mainly limestones, shales, sandstones and quartzites. These rocks form a folded rock mass with sub-vertical folds and numerous faults and overthrust at great length (Angoña et al. 2009; Toyos et al. 2009). Geological conditions have given rise to highly fractured and karstified materials, with complex geotechnical behaviour reflected by the presence of water seepage, weak zones and squeezing ground in many tunnel sections (Fig. 2).

Before excavating the tunnels, geological and geomechanical site investigations were carried out for tunnel feasibility purposes. On this preliminary stage, 23 boreholes with a total length of 1.844 m were drilled, and 131 water absorption tests have been performed. Additionally, 41

dilatometer test were carried out, and geophysical site investigations and laboratory tests. For the tunnels' design project, no additional geological studies neither new boreholes were carried out (Arlandi et al. 2009).

The first geological and geotechnical studies performed to design the layout of the Pajares tunnels' alignment began in the 1970s and 1980s. Between 1980 and 1984, one of the tunnel's alignments was studied geologically and geotechnically, including site investigations and geomechanical studies to estimate the tunnel supports (Linares Rivas et al. 1984). These studies revealed the importance of hydrogeological aspects and warned of “a high risk of seepage in karstic limestones”, recommending detailed hydrogeological studies to be carried out (González de Vallejo and Oteo 1986). Subsequently, between 1998 and 2003, new geological and geotechnical studies were carried out as part of the tunnel project, but specific hydrogeological studies were not included. However, it was stated that “the interaction between the tunnels and hydrogeological environment would be low and acceptable” (Garrido et al. 2009).

Several hydrogeological studies were conducted during the excavation works between 2005 and 2008, which estimated “low to moderate leakages, between 200 and 350 L/s”

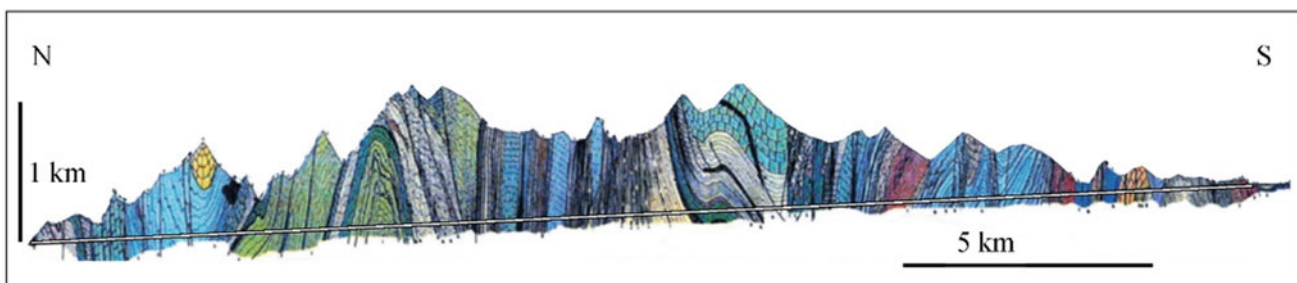
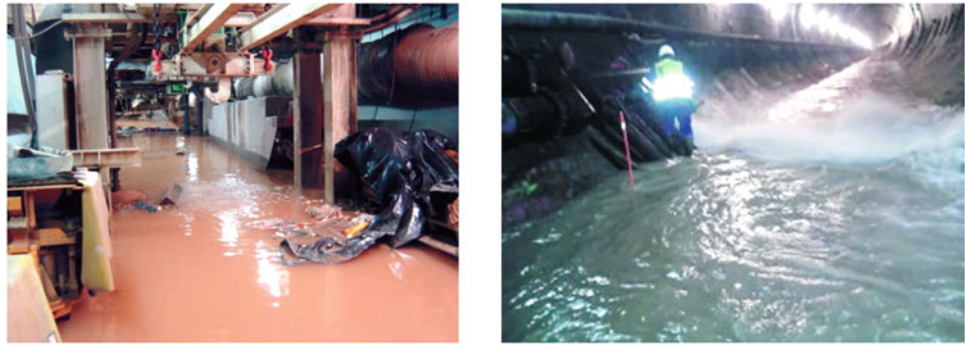


Fig. 2 Geological cross-section along with the Pajares Tunnels. Modified from Mendaña and Fernández (2009)

Fig. 3 Floods caused by leaks during the excavation works of the Pajares Tunnels (Rojo 2009)



(Rojo 2009). One of them concludes that “the results obtained during the excavations allow us to estimate with sufficient approximation the hydrogeological regime, as well as to verify the hydrogeological affections produced by the tunnels” (Álvarez-Díez et al. 2009). In summary, the hydrogeological studies considered that the water seepages would be controllable with conventional drainage and pumping measurements. However, during the excavation works, problems occurred due to significant leakages and water blows when crossing the aquifers in karstified calcareous rocks and highly fractured quartzites (Fig. 3). In 2005, leaks and water blow between 500 and 1,000 L/s were recorded. In 2006, there was a significant flood of 50,000 m³, and in 2009 leaks of up to 2,000 L/s were registered in 12 h (Álvarez-Díez et al. 2009).

Since the end of the excavation of the tunnels in 2009 and up to the present (2021), water seepages and leaks have occurred much higher than anticipated, requiring drainage, and sealing measurements, as well as reinforcement works. These seepages have produced severe environmental damage, affecting more than 20 aquifer formations, draining more than 50% of the aquifers’ water capacity, and transferring more than 12 Hm³ from the southern hydrological basin to the north. In addition, many sinkholes and ground subsidence zones have been registered, with essential changes in shallow springs and streams (Valenzuela et al. 2015). In summary, an entire ecosystem of great environmental value has been irreversibly affected.

The economic consequences of the problems caused by the water infiltration into the tunnels and their interaction with stability and safety have been extremely high. Until 2016, the works’ total costs have exceeded 3,550 million euros, compared to the initial project contracting budget of 1,085 million euros, which has meant an over cost of more than 2,460 million euros. Moreover, the magnitude of the problems that arose after the construction of the Pajares Tunnels, which have not yet entered in service, has given rise to deep social concern with critical economic consequences in Asturias, whose region still lacks a high-speed railway connection.

3 The Castor Underground Gas Storage Project

The project site is located in the waters of the western Mediterranean, 22 km from the coast and the town of Vinaroz, E Spain (Fig. 4). The underground reservoir uses an old conventional hydrocarbon deposit, exploited in the period 1973–1989. This reservoir is located at a depth of 1,750 m below sea level with a sheet of water of 60 m; its storage capacity is 1,900 million m³. The reservoir comprises porous limestones, with cover rocks formed by shales and sandstones (Fig. 5). Near the reservoir, several important faults have been identified, although the regional seismicity is low. During the project design, a maximum injection pressure of 22.9 MPa was estimated as a reference value and ruled out both reactivation of faults due to fluid injections and induced seismicity hazard.

Gas injection started in August 2013, and a few weeks later, 516 earthquakes were recorded in the vicinity of the injection area, with magnitudes between 0.7 and 4.2. Some of the earthquakes were felt in the nearby towns producing a high social alarm, and, although there was no significant damage, the injection operations were suspended. Afterwards, new technical reports were issued by governmental agencies, attributing the seismicity to the injections, being the cause to the reactivation of minor faults located in the



Fig. 4 The situation of the Castor Project (ESCAL UGS SL)

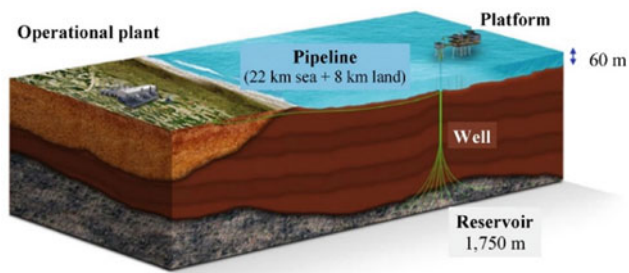


Fig. 5 Scheme of the installations for the Castor Project (ESCAL UGS SL)

vicinity of the site, warning that new injections could cause larger earthquakes. Similar conclusions have been reached by Cesca et al. (2014) but exclude the possibility that major faults could be reactivated. On the other hand, Juanes et al. (2017) did not rule out that new injections could reactivate regional faults and release enough energy to produce high-magnitude earthquakes, as high as 6.8.

Given the evidence of the relationship between the location of the epicentres around the injection area and its synchronisation with the injections, it was concluded that the injection of fluids induced the seismicity. In 2014 the facility was definitely closed. The economic consequences of the closure of the Castor Project have led to high economic losses. At the end of 2019, losses have exceeded 3,200 million euros, more than three times the initial budget of 1,085 million euros.

4 Discussion and Concluding Remarks

The importance of geological, hydrogeological, and geomechanical aspects in large engineering projects is highlighted through the cases analysed.

The experiences learned in the Pajares Tunnels show that the excavation of the tunnels started without sufficient hydrogeological knowledge, estimating water seepage much lower than that recorded during and after the excavations, even though preliminary studies warned of the hazard of significant leaks. The tunnels were completed in 2009, ruling out the possibility of significant leaks. However, the hydrogeological problems that occurred during the tunnels' construction prevented them from entering into service up to the present.

In the Castor Project, induced seismicity hazard was not considered at the project stage. The maximum injection pressure was based on a geomechanical model that did not consider the in situ tectonic stresses nor the presence of faults located near the injection area whose shear strength could be in residual conditions. Since the reservoir was an old hydrocarbon deposit previously exploited, the presence

of fractures or faults could be expected due to the stress redistribution around the reservoir. These geomechanical conditions would lead to new fractures or existing faults' reactivation (McGarr et al. 2002). Consequently, the maximum recommended injection pressures have exceeded the fractures' strength, reactivating some faults located near the site and releasing energy compatible with the seismicity registered.

In both the Castor Project and the Pajares Tunnels, the problems' leading cause was to neglect the possibility of major geological hazards, as induced seismicity and high-water inflows into the tunnels. These hazards could have been avoided if the geological, hydrogeological and geomechanical conditions had been sufficiently investigated before the tunnel excavations and the gas injections. In the Pajares Tunnels, there has been a delay of over 12 years for their construction and remedial works, while the Castor Project was definitively closed. The environmental damage in the Pajares region has been considered irreversible. The over cost of both projects exceeds 5,500 million euro, mainly due to the problems mentioned above.

These experiences show that geological factors are decisive for assessing the feasibility and the cost of engineering infrastructures. The cases presented are not unique, but they are exceptional in terms of economic losses. In all cases, deficiencies in geological and geotechnical investigations during the pre-construction stages are found as the primary cause, generally associated with the scarcity of economic resources for such investigations. Another aspect to consider is the lack of appreciation by project managers of the geological environment's complexity, whose knowledge requires not only means but sufficient time to carry out the studies. In the case of the Castor Project, the fact that the reservoir was located under the sea determines greater complexity in geological research. Simultaneously, in the Pajares Tunnels, hydrogeological studies would require long observational periods to interpret the behaviour of aquifers in the medium and long term and their interaction with the tunnels.

References

- Álvarez-Díez J, Fallesen J, Ruiz MS, Barceló M, Bermejo F, Cristóbal JC, Serrano L (2009) Hidrogeología de los túneles de Pajares. In: Míguez R (ed) Túneles de Pajares, ADIF Oviedo, pp 167–208
- Angoña AM, Bernárdez E, Fernández L, et al (2009) La geología de los Túneles de Pajares. In: Míguez R (ed) Túneles de Pajares, ADIF Oviedo, pp 53–74
- Arlandi M, Domínguez ML, Pelaez, M (2009) Génesis del proyecto de Pajares. Estudios previos, proyecto básico y proyecto constructivo. In: Míguez R (ed) Túneles de Pajares, ADIF Oviedo, pp 35–50
- Cesca S, Grigoli F, Heimann S, González A, Buforn E, Maghsoudi S, Dahm T (2014) The 2013 September–October seismic sequence

- offshore Spain: a case of seismicity triggered by gas injection. *Geophy J Int* 198(2):941–953
- Garrido M, Serrano L, Miguez R, et al (2009) El estudio hidrogeológico de los túneles de Pajares. In: Pando LA, López-Fernández C, de la Rubia Mir L (eds) *Jornadas Técnicas Variante de Pajares Oviedo*, pp 77–86
- González de Vallejo L, Oteo C (1986) Site investigations for big tunnels: an application to the Pajares railway tunnel. *Proceedings of the international conference on large underground excavations* 1:169–173
- Juanes R, Castiñeira D, Fehler MC, Hager BH, Birendra S, Shaw JH, Plesch A (2017) Coupled flow and geomechanical modeling and assessment of induced seismicity at the Castor Underground Gas Storage Project. Final Report. http://mesadelaria.es/documentos/20170424_Castor_final_report_final_signed.pdf
- Linares Rivas A, González de Vallejo L, Saint-Aubin J (1984) Estudio geológico-geotécnico del gran túnel de la variante ferroviaria de Pajares. In: VII Simposio Nacional de la SEMR sobre reconocimiento de macizos rocosos, *Memorias Sociedad Española de Mecánica de Rocas*, Madrid, vol 2, pp 235–239
- McGarr A, Simpson D, Seeber L (2002) Case studies of induced and triggering seismicity. In: *International handbook of earthquake and engineering seismology*, vol 81, pp 647–661
- Mendaña F, Fernández R (2009) *Tuneladoras de Pajares*. In: Miguez R (ed) *Túneles de Pajares ADIF Oviedo*, pp 127–152
- Rojo G (2009) Evacuaciones de caudales de agua de infiltración durante la ejecución de los túneles descendentes del Lote 2. In: Miguez R (ed) *Túneles de Pajares ADIF Oviedo*, pp 449–482
- Toyos JM, Suarez MA, Rodriguez Fernandez LR, Serrano L (2009) Perfil geológico a lo largo de los Túneles de Pajares. In: Pando LA, López-Fernández C, de la Rubia Mir L (eds) *Jornadas Técnicas Variante de Pajares Oviedo*, pp 41–52
- Valenzuela P, Dominguez-Cuesta J, Meléndez-Asensio M, Jimenez-Sanchez M, de Santa S, Maria JA (2015) Active sinkholes: a geomorphological impact of the Pajares Tunnels (Cantabrian Range, NW Spain). *Eng Geol* 196:158–170



Multiscale and Modelling Hydraulic Properties of Rock Mass Foundations: Decision Tools for Design and Construction

Vasco Gavinhos, Jorge Carvalho, João Paulo Meixedo, and Helder I. Chaminé

Abstract

This work describes the use of geostatistics in permeability data obtained by the Lugeon test at determined depths within boreholes during curtain grouting at a dam foundation. Design criteria often demand a first and a secondary stage of grouting treatment defined by a threshold permeability of 1 Lugeon unit (U.L.), above which there is a need for grouting. That implies, namely, to accurately characterise the permeability spatial variability at the foundation rock mass with minimum data collection. This study aims to assess the advantages of geostatistical modelling of permeability. A secondary goal is to compare the non-geostatistical (traditional) approach and geostatistical interpolation methods to the raw permeability data sets. Both will quantify different foundation zones needing treatment. The obtained model and the corresponding error study was analysed and correlated with the design stage's geological-geotechnical model. The results show a good correlation between the obtained model and the geological-geotechnical model, pointing out the feasibility as an optimising tool for curtain grouting design at a dam foundation. Furthermore, the cost estimates of activity, time, and materials by applying a traditional empirical approach and a modelling approach to solve it were compared. The latter showed significant enhancement, construction efficiency with reduced costs and construction time, and negligible loss in quality due to residual uncertainty in the models.

V. Gavinhos (✉) · J. P. Meixedo · H. I. Chaminé
Laboratory of Cartography and Applied Geology, Department of Geotechnical Engineering, School of Engineering (ISEP), Polytechnic of Porto, Porto, Portugal
e-mail: vasco.gavinhos@gmail.com

J. Carvalho
CERENA – UP, Department of Mining Engineering, Faculty of Engineering (FEUP), University of Porto, Porto, Portugal

H. I. Chaminé
Centre GeoBioTec|UA, Aveiro, Portugal

Keywords

Dam foundation · Hydraulic properties · Permeability · Lugeon test · Rock engineering · Geostatistics

1 Introduction

The geological and geotechnical uncertainty is one of the most common sources of risk in rock excavation and foundation projects. The variability of natural rock masses is often poorly known at the early stages of design development (e.g., Bieniawski 1989; Barton and Quadros 2015; Chaminé et al. 2015). Furthermore, the geological structures of rock masses considerably influence their hydrogeomechanical properties, such as permeability, cohesion, roughness, aperture and in situ stress (e.g., Rocha and Francis 1977; Barton et al. 1985; CFCFF 1996; Hamm et al. 2007; González de Vallejo and Ferrer 2011; Chaminé et al. 2013; Rocha 2013, and references therein).

In dams, in situ tests should involve large volumes of the rock mass, representing the overall rock mass behaviour and applying loads similar to those imposed by the dam at the depths of interest (Vieira de Lemos and Lamas 2013). Within dam construction projects, this is particularly important to consider, as the effects of accidents or other anomalies have a high impact on the project and its stakeholders. Regulation documents such as legal project, construction, and safety standards and the Eurocode7 state that information gathering and processing are due throughout all stages of these works. Given that uncertainty plays a significant role in decision processes, both in design and construction stages, real-time decisions and adaptation to natural conditions is always present when and where the rock media's interventions occur. In this context, the knowledge of the natural setting's fundamental features comes as a necessity to overcome uncertainty at the early stages of design and development and the construction stage. Data

constitute real-time updates to the decision and physical models that support decision-making at the construction stage scale.

Foundation treatment design is a crucial stage in any dam project. Concern about quality and safety regarding the foundation conditions makes most designers adopt an intensive construction stage dedicated to the ground improvement and quality control. The curtain grouting is a series of parallel drill holes along the dam foundation that, after the procedure, work as an underground barrier (i.e., curtain) to water percolation. This tridimensional element is usually inclined towards upstream, and it can be interpreted as two dimensional for modelling purposes, as in the scope of this case study. Complementary to this barrier, a parallel series of drainage holes (drainage curtain) is built downstream for pressure relief and a series of piezometers to monitor any remaining water pressure in the foundation. All these elements are materialised within the general drainage gallery on the base of the dam's structure. Another purpose of the grouting procedure is to improve the mechanical behaviour of the foundation rock mass. The usual construction methodology, namely low permeability hard fractured rock masses, consists of applying a sequentially phased drilling strategy. The curtain of drill holes is materialised by successively drilling and grouting the first line of primary boreholes and then a secondary line of in-between boreholes from the primary ones. That implies that the secondary drilling locations may be affected by permeability by the first phase of grouting (Deere 1982). This process continues to higher-order drilling campaigns if necessary.

The traditional approach (TA) for construction development in the dam foundation treatment process consists of defining a second phase drill/test/grout in two secondary positions in a primary drill's vicinity (half-distance). In the present case, whenever the permeability above 1 U.L. was detected, drilling continues up to a depth of plus 5 m (safety factor) from that level, and secondary drilling is decided. That approach was performed systematically throughout all the foundations between primary drill holes concerning the lowest position of >1 U.L. This split method results in a conservative, expensive, but effective way to assess the necessity and decide to perform the corresponding treatment.

The case study features the foundation treatment of the Feiticeiro dam (Torre de Moncorvo, NE Portugal): a conventional gravity concrete dam with 22 blocks up to 45 m high with a 290 m development along a straight axis approximately perpendicular to the river stream (details in Gavinhos 2017).

This geotechnical study explores and assesses a geostatistical methodology advantage (Goovaerts 1997; Soares 2006). Indeed, it is an effective alternative tool in identifying the zones in which the design criteria may demand a

secondary (or higher) stage of grouting treatment, defined by a threshold permeability of 1 Lugeon unit, U.L., above which there is a need for grouting. A methodological assessment of the feasibility and advantage of using geostatistical estimation procedures to support the decision and optimisation processes was used in a real-time data collection/modelling procedure in the context of the construction stage. The results are applied to the real case scenario to compare the traditional criteria performance and the tested estimation algorithm. It was made by measuring the amount of activity resulting from using each of the decision process criteria.

2 Risk Management and Decision Support

The base definition of criteria is established considering the data collected during the design studies. This follows some semi-empirical rules of thumb (Lombardi 1999; Weaver and Bruce 2007, among others) and the experience of the project design teams. The objective is always to guarantee lateral and in-depth low permeability of the foundation. The sampling is sparse at this stage and scale and represents a large rock mass volume with all its shortcomings. The reduction of uncertainty comes from collecting more data, but this occurs only at the project's construction stage.

Nevertheless, defining a starting or base point in terms of criteria will be refined by gathering more information at the construction scale. Furthermore, in this case, the study was detailed through geospatial modelling to help decision making. The following definition or criteria characterise the starting point of the foundation treatment (details in Gavinhos 2017):

Minimum depth = 30 m;
Maximum depth = 40 m;
Target permeability: < 1U.L.

Within the construction stage of the project, specifically in the foundation treatment, the process for a first and second campaign (C) flows as follows:

Primarydrilling–Permeabilitytesting(C1) –PrimaryGrouting
→ DECISION(TraditionalApproachorModelling?) →
Secondarydrilling–Permeabilitytesting(C2) –SecondaryGrouting.

The depth criterion is objective and easily applied throughout the process of construction. The permeability criterion is the one subjected to ambiguity because of the unknown extent of its lateral representativity. The traditional approach imposes a split block decision based on the value of independent tests collected in 5 m chambers, considering

neither the spatial relation nor the geological setting. Furthermore, performing geospatial analysis and identifying a geological correlation could produce a more refined distribution of the variable within a geostatistical model.

In this construction activity, the involved opposing risks are economical versus the final quality of the product. Decision support based on risk management follows the national and international standards (namely, ISO:31,000). That was focused on value optimisation regarding cost and planning at the project's construction stage. Design teams play a relevant role in the decision process by evaluating data and giving feedback to the management and construction teams. This information impacts the deconstruction process at a technical level by defining new criteria or production levels by limiting a larger or smaller quantity of predicted or contracted work and resources. The economic burden is interrelated with the safety risk resulting from the probability of foundation failure resulting from poor grouting treatment. The first is a straightforward calculation, with an objective budget and contract parameters, from which the positive outcome is to spend fewer resources on this specific activity. On the opposite side, assessing the effect of poor foundation treatment is less obvious because it includes a multivariate analysis of factors contributing to foundation failure. For this study, both risks are managed through optimisation: cost and time reduction on one side and avoid quality loss.

The decision tree uses the base definitions from the construction stage. It rigidly applies the traditional approach using discrete volumes of the rock mass to move forward with the treatment or a more adapted spatially interpolated (model) to identify the zones that need subsequent treatment. They could be defined separately, but they are integrated into the same decision tree, focusing on the permeability criterion for conceptual comparison (Table 1).

The cycle continues with Phase 2 (i.e., secondary drilling and testing). There is a higher level of information in that stage, and there is the possibility of calibrating the permeability model. The criteria are maintained throughout the treatment process towards subsequent phases (3, 4, ... n) until the criterion of <1 U.L. is met.

Table 1 Decision tree for the grouting process

Construction stage: decision process tree	Criterion	Decision
Phase 1 —primary drilling and testing – Higher level of information – Possibility to model permeability	>1 U.L.	1 or 2 more 5 m chambers (e.g., maximum 40 m total maximum depth) Secondary drilling and testing: Yes
	<1 U.L.	Stop at 30 m Secondary drilling and testing Yes, according to the traditional approach; or Yes, according to the model where >1 U.L.

Adapted from Gavinhos (2017)

2.1 Modelling Process

2.1.1 Geological Setting Assessment and Uncertainty

The Feiticeiro dam construction site, near Torre de Moncorvo, is a typical schist-greywacke complex that occurs in the Northern Portuguese region (Ferreira da Silva et al. 1989). The dam structure was settled in a complex of igneous and schist-greywacke rocks of the Palaeozoic age. The rock mass is a hard, unweathered, quartz-rich greywacke with well-developed schistosity. Faults and veins were identified in the rock mass. Those structures potentially affect the permeability of the foundation rock mass. As the rock matrix is practically impervious, the permeability occurs throughout the discontinuities network patterns and some singular structural features (like faults and weathered bands). From early studies regarding the design and construction of the Feiticeiro dam, geological and geotechnical information was collected in technical reports (EDP 2007). Figure 1 shows the geologic-geotechnical model and highlights that the foundation rock mass is generally medium to good rock quality.

There is a complementary surface mapping of the excavations in the construction stage, a thorough review of the geotechnical features, and systematic survey campaigns. As a result, further new information is added, enabling more accurate estimation of the permeability and designing an impervious curtain according to this parameter. This design is accomplished by a discrete raw utilisation of the data, using the criteria (TA) described above. In this case, this information was used in a geostatistical estimation process to assess and discuss the advantages of using the results in the decision process, reducing uncertainty with fewer amounts of data, instead of just the raw data with empirical criteria.

2.1.2 Data Collection Within the Grouting Process

The foundation treatment during the construction stage was located in the river bottom, from which two work fronts move towards the margins and up the foundation drainage

Fig. 1 Geological model from the dam project preliminary studies: an interpretive cross-section view from upstream to downstream. Adapted from EDP (2007)

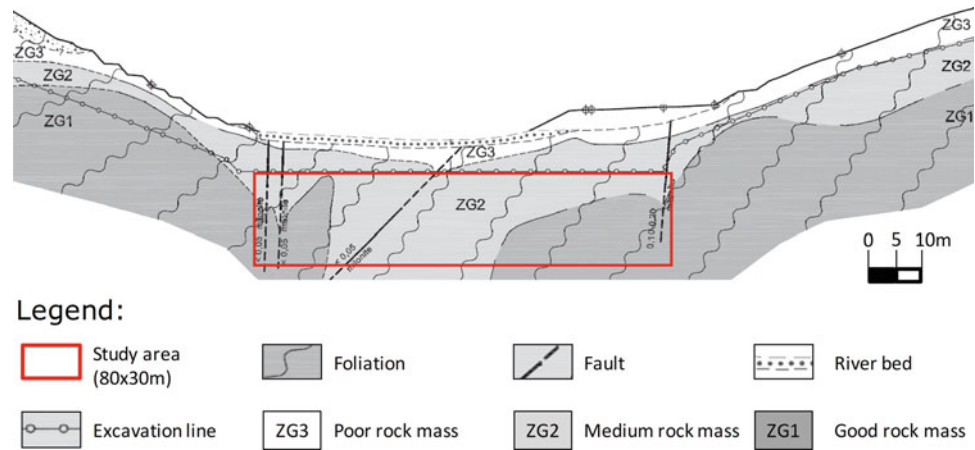
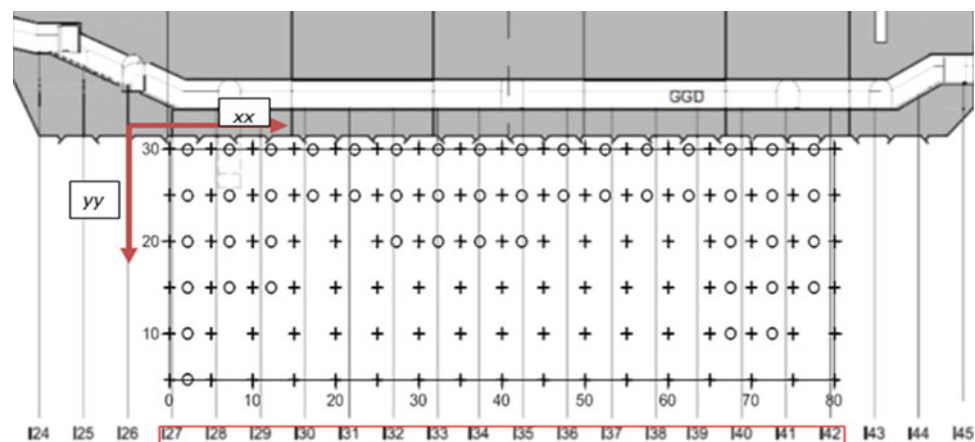


Fig. 2 Sampling area with primary C1 (+) and secondary C2 (o) drilling data sets (Surfer 12). Background adapted from EDP (2007)



gallery (GGD) (Fig. 2). The drill holes are regularly spread in a systematic core drill survey campaign. Primary drill holes are 5 m apart. Secondary drill holes are in between primary drills (e.g., 2,5 m apart from them). Higher-order drilling campaigns are made if necessary by applying the same splitting method into half the spaces available.

Permeability data were obtained by systematically performing the Lugeon test, interpreted according to (Houlsby 1976, 1990), at every five-meter depth within the wireline core drilling during curtain grouting at the dam foundation. This resulted in vertical sample lines evenly spaced along a longitudinal axis. The Lugeon test is a standard packer test primarily used in hard, fractured rock that usually occurs in dam foundations to assess the permeability and the hydraulic regimes present in the context of a foundation grouting procedure (foundation treatment). The test results' interpretation gives a value (n U.L.) for each chamber (point in the sample grid) that correlates with the hydraulic conductivity.

In practice, the foundation treatment's construction stage resulted in 17 primary drill holes (Fig. 2) spaced 5 m along the GGD at the riverbed. Each drill hole has 30 m depth, in which a total of 6 Lugeon tests were performed, one every

five meters. There was no need to drill more than 30 m in this area. A total of 102 test values were collected. Subsequently, 52 values were collected for the secondary campaign, defined using the traditional criteria (TA) described before. So, the limited data available was a challenge from the beginning of the study. Figure 2 shows the sampling area at the riverbed used in this study. It corresponds to a vertical rectangle in the foundation rock mass. The sampling grid for the first campaign (C1) is regular (5×5 m) from 0 to 80 m along X and from 5 to 30 m along Y. For the secondary drilling data set (C2), the locations are in between the primary data. The data coordinates are transformed so that the Y-axis is always positive. According to Fig. 2, $Y = 30$ is the first Lugeon test value collected at a depth of 5 m. This procedure does not affect data structure, preserving spatial relations between the positions of all sampled points.

The general assumption regarding the sampling procedure and configuration is that each 5 m chamber, where the Lugeon test was performed, is represented by a single integer that results from the test values' interpretation. A subsequent assumption is to take each value as representative of the 5×5 m cell that forms the initial data area's wide grid.

Table 2 Qualitative statistical description

C1 data (102 values of Permeability)	C2 data (52 values of permeability)
<ul style="list-style-type: none"> • Seven (7) classes of permeability: [0, 6] U.L. • High positive skewness from the log-normal distribution of the data • Low frequency of high values. High-frequency of low-values, namely 0 U.L. • High variation coefficient 	
The statistics of all population (C1C2) of values also bears similar values	

Each C1 point located off the borders represents the centre of a 25 m² cell within the vertical two-dimensional pane rectangle that comprises the sample area. This is the starting point from which the dense grids of interpolation will be computed in the estimation process. The same assumptions were made for the data set C2. The C2 data sampling grid is irregular because applying the TA decision criteria resulted in less labour (shallower drills) (Fig. 2). For the sample area, C2 data reduced representativeness to about one half of the C1 data.

2.1.3 Exploratory Statistical Study

The data exploratory statistical study follows the generally accepted good practice (Deutch and Journel 1998; Soares 2006). In addition, Gavinhos and Carvalho (2016) discussed this particular data set. The main statistical features are identical for both sets (Table 2).

Even though this previous exploratory statistical analysis is essential to data interpretation and more informed decision support, the task of finding the (spatial) locations in which to perform more treatment should benefit from a spatial analysis and estimation process. Therefore, the analysis was expanded towards a non-geostatistical primary spatial description where no trends nor drift were found. Consequently, stationarity and homoscedasticity were assumed. Given this evidence, the Ordinary Kriging algorithm

estimates the permeability in the curtain area that could be used. Moreover, compared to considering point data and empirical interpolations from the traditional criteria.

2.1.4 Continuity Analysis and Estimation

For estimation, Ordinary Kriging (OK) interpolation procedures were implemented. A grid of 100 × 32 nodes was computed for C1, C2 and C1C2 data sets. Multiple directions were tested with different angular tolerances to investigate a possible and expected anisotropic behaviour (from 22,5° up to 45°). In data set C1, the variogram highlights an anisotropic behaviour with maximum continuity (range) along 45°. That corroborates the recognised site geological characteristics, namely schistosity and discontinuities dipping 45° (EDP 2007). Figure 3 shows the fitted spherical variogram models for direction 45° of maximum continuity for the studied data sets.

The spherical model was adjusted with the appropriate parameters for each case. As stated above, the three data sets are statistically similar, but their behaviour differs in spatial analysis. In particular, the C2 data set as the same anisotropic behaviour, but the variogram was more erratic due to the reduced number of points (52). This fact reduced this set's reliability for modelling and was used in the estimation control in the calibration model. Figure 4 shows the estimation map of C1 for OK, which reveals a smoothing effect

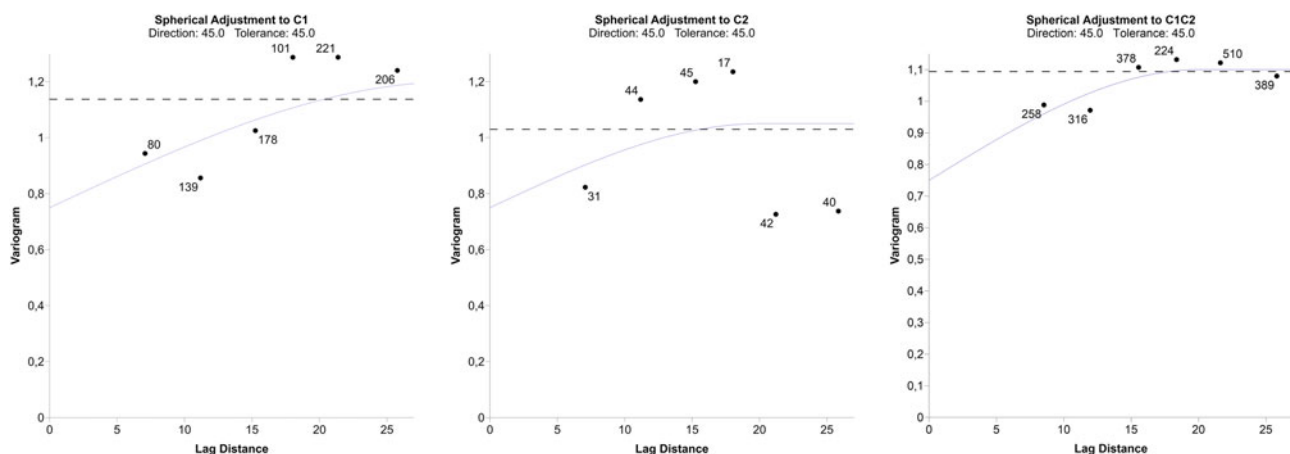


Fig. 3 Variogram models assumed for data sets C1, C2 and C1C2 along the direction of maximum continuity. Each point also indicates the number of pairs used in calculations

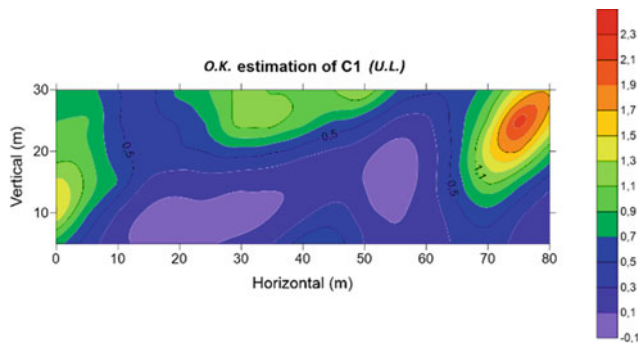


Fig. 4 Contour map (C1). **a** Ordinary kriging estimation

associated with the OK interpolator; the correlation with the natural setting is satisfactory.

2.1.5 Error Study

The cross-validation was performed in the process of variogram model adjustment in kriging. Residuals (Z_r) are calculated in the positions where estimated value ($Z_{O.K.}$) also has the real value of the data (Z_{dat}), according to the expression:

$$Z_r = Z_{dat} - Z_{O.K.} \quad (1)$$

Error statistics is an important part of the calibration process. This case shows that the OK algorithm bears a satisfactory performance in all error (residuals) parameters, given that high errors occur in permeable zones where little or no decision uncertainty exists. Furthermore, after gridding the residuals from estimating the C1 set with the corresponding OK algorithm, it is possible to produce a smooth image of the error to assess its spatial behaviour, Fig. 5.

This map shows that error is concentrated in permeability areas above 1 U.L. that most likely were treated with secondary drilling and grouting. From the OK estimation and the error location, it is possible to infer that there is no risk of overestimation or targeting areas that are not permeable. An important criterion to assess and consolidate this possibility of using only C1 data is the correlation between the obtained estimation model ($C1_{O.K.}$) and the geologic model.

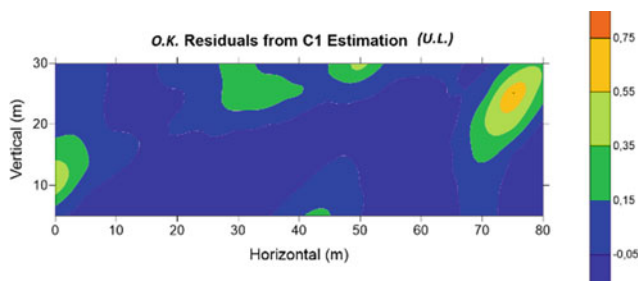


Fig. 5 Error map (residuals) from the OK estimation (Surfer 12)

2.2 Geologic-Geotechnical Model Comparison with Geostatistical Model

The estimated permeability maps of the area obtained by OK (Fig. 4) show a significant correlation with the geological profile of the foundation rock mass and the geotechnical zoning (Fig. 6). Consequently, the model (Fig. 4) and the associated errors (Fig. 5) correlate well with the geological-geotechnical model used in the design stage (Fig. 1). Therefore, there is some increase in the observed correlation with the geologic model when combining C1 and C2 data. So, this increase is not significant to change the decision of which areas to target because they are identical, i.e., the areas with permeability above 1 U.L. are the same considering the metric scale of these construction procedures. Therefore, this evidence shows that, in this case, from the management of construction or design points of view, C2 data does not change the amount of activity to execute.

The generic observed good correlation between the obtained models and the used geological-geotechnical model points to the advantage of the presented approach as an optimising tool for curtain grouting design in the dam construction stage. The apparent good correlation of the first campaign model C1 could mean that this data set would be sufficient for the estimation and decision process. That is because, as pointed above, the use of secondary data, although showing some miss estimations, would not result in demonstrating decision error as all areas (points) where computation failed were targeted using the permeability criterion, <1 U.L.

3 Application

3.1 Performance of Estimation and Decision Support

Previous sections described the context and geostatistical methodology used to obtain the (C1) models of permeability in the dam foundation's rock mass. To use this information, the following campaign positions and depths were simulated geometrically. In this case, the first campaign data, C1, was used to simulate work quantities of (C2) by applying each approach: traditional versus model. The estimation map (Fig. 4) allows identifying the grouted area with a resolution below 5 m. Nevertheless, the analysis made a unit length of 5 m (length of one Lugeon test chamber) for comparison purposes. Measurements were made with a computer-assisted design tool manually assigning intermediate positions to depths in which permeability was estimated to be above 1 U.L. and adding the 5 m drill length as a safety factor. Table 3 shows the comparison of the required quantity of work (linear drilling) after the C1 stage using the

Fig. 6 Comparison of the estimation model with the geologic-geotechnical model. Adapted from Gavinhos (2017)

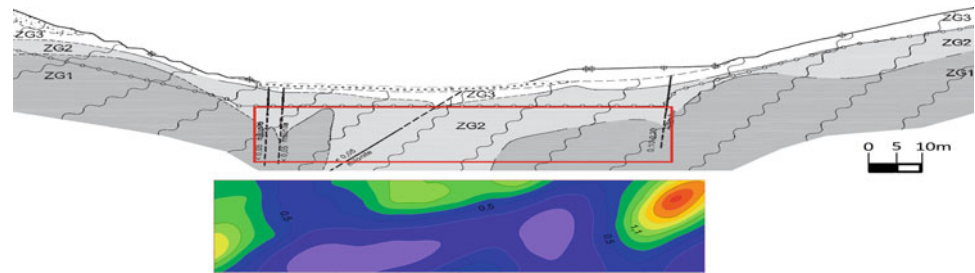


Table 3 Comparison of secondary (C2) drilling decision criteria

Criteria	Number of samples (5 m chambers)	Drill (m) Meters	%
C2 _{TA}	52	260	100
C2 _{O.K}	39	195	75

traditional approach (TA) and those inferred from geostatistical (OK) estimation maps.

Assuming the quality of the C1_{O.K.} estimation demonstrated above, the results show an impressive performance from using the OK estimation map as a decision support tool, pointing to a straightforward 25% reduction of work optimisation. Additionally, going straight forward to a second drill and grout procedure would mean more optimisation by avoiding C2 expensive data collection. Eventually, targeted verifications could be performed according to grouting data instead of (C2) systematic permeability testing data. Another direct consequence of this assumption is that the decision-makers become free to use a cheaper and faster drilling technology.

4 Discussion

All obtained estimation results appear generically consistent with each other and the known geological local site model. Ordinary kriging estimation allowed the identification of foundation zones needing treatment with satisfactory error performance. This methodology is innovative in this context and is necessary for the purposed objectives, namely early risk assessment, to enable the project manager to be aware of the accuracy of the estimation/simulation for decision making and the potential for optimisation. The models were successfully correlated with the design study, namely the geological and geotechnical. The described approach has great potential as an optimising tool for curtain grouting design dam foundation in the construction stage. Nevertheless, this case study's analysis verified that the error associated with the C1 OK estimation would not induce decision error.

The drilling and grouting work from the identified impermeable zones using OK (C1) would improve general

management features such as planning and cost control and environment and safety, indicating this methodology has great potential for support inefficiency decisions. Nevertheless, a more thorough analysis is mandatory for this approach to enable the decision responsible aware of the estimation's accuracy to ensure the final quality of the treatment. In this case, further geostatistical processing can be the answer by providing probability maps for the estimated (interpolated) values and simulation scenarios.

5 Concluding Remarks

This work describes geostatistics application to permeability data obtained by the Lugeon test at determined depths within boreholes during curtain grouting at a dam foundation. This original procedure shows interesting potential in the construction scale and decision-making tool as an optimising methodology for technical assessment and management purposes. Following a preliminary statistical, spatial continuity characterisation and error analysis, estimation maps of the first data set C1 was produced with satisfactory results. This could lead to an immediate simplification (optimisation) of the subsequent grouting stages. Nevertheless, the data collected in a calibration iterative process assesses the resulting activity differences and confirms the desired optimisations. That is not a linear procedure and should be subject to further investigation. C2 secondary data as real reference values with similar statistical and spatial behaviour should identify the combined effects of random low values and the first grouting procedure.

Further analysis is necessary to separate and quantify these effects to improve secondary data to assess estimation quality. Secondary variables, such as fracture density or the weathering degree of the rock mass, would bring more accuracy to the estimation process. In addition, obtaining

interpolated information, namely probability maps, should reduce uncertainty in the decision process. In risk analysis, further studies should also investigate using a sequential stochastic approach in model simulations of the permeability, allowing the characterisation and identification of the spatial distribution of the probability of cut-off values (1 U. L. in this case). The resulting maps would become valuable decision tools.

Acknowledgements VG is grateful for the support of EDP—Energias de Portugal, SA. HIC was supported partially under the Labcarga/ISEP re-equipment program (IPP-ISEP/PAD'2007/08) and Centre GeoBio-Tec/UA (UID/GEO/04035/2020). We are grateful to the anonymous reviewers for the valuable inputs that helped improve the manuscript focus.

References

- Barton N, Bandis S, Bakhtar K (1985) Strength, deformation and conductivity coupling of rock joints. *Int J Rock Mech Min Sci Geom Abstr* 22(2):121–140
- Barton N, Quadros E (2015) Anisotropy is everywhere, to see, to measure and to model. *Rock Mech Roc Eng* 48:1323–1339
- Bieniawski ZT (1989) Engineering rock mass classifications: a complete manual for engineers and geologists in mining, civil, and petroleum engineering. Interscience. Wiley, New York
- CFCFF—Committee on Fracture Characterization and Fluid Flow (1996) Rock fractures and fluid flow: contemporary understanding and applications. National Research Council, National Academy Press, Washington DC
- Chaminé HI, Afonso MJ, Ramos L, Pinheiro R (2015) Scanline sampling techniques for rock engineering surveys: insights from intrinsic geologic variability and uncertainty. In: Giordan D, Thuro K, Carranza-Torres C, Wu F, Marinos P, Delgado C (eds) Engineering geology for society and territory—Applied geology for major engineering projects, vol 6. IAEG, Springer, pp 357–361
- Chaminé HI, Afonso MJ, Teixeira J, Ramos L, Fonseca L, Pinheiro R, Galiza AC (2013) Using engineering geosciences mapping and GIS-based tools for georesources management: lessons learned from rock quarrying. *Eur Geol J* 36:27–33
- Deere DU (1982) Cement-bentonite grouting for dams. In: Proceedings of the ASCE specialty conference in grouting in geotechnical engineering, New Orleans, LA, pp 279–300
- Deutch CV, Journel AG (1998) Geostatistical software library and user's guide. Oxford University Press, New York
- EDP (2007) Relatório geológico geotécnico escalão jusante: empreitada geral de construção do aproveitamento hidroeléctrico do Baixo Sabor. Porto (Unpublished Report), EDP
- Ferreira da Silva AJ, Ribeiro ML, Rebelo JA (1989) Notícia Explicativa, Carta Geológica de Portugal, folha 11C – Torre de Moncorvo, escala 1:50000. Serviços Geológicos de Portugal, Lisboa
- Gavinhos V (2017) Parametrização geotécnica no melhoramento de maciços rochosos: o papel da hidrogeotecnia no tratamento de fundações. Instituto Superior de Engenharia do Porto, ISEP, Porto. <http://hdl.handle.net/10400.22/10877>
- Gavinhos V, Carvalho J (2016) Geostatistical modelling and simulation scenarios as optimizing tools for curtain grouting design and construction at a dam foundation. In: Gómez-Hernández JJ, Rodrigo-Ilarri J, Rodrigo-Clavero ME, Cassiraga E, Vargas-Guzmán JA (eds) Geostatistics Valencia 2016, Quantitative geology and geostatistics series, vol 19. Springer, Cham, pp 789–804
- González de Vallejo LI, Ferrer M (2011) Geological engineering. CRC Press, Taylor-Francis group, Boca Raton
- Goovaerts P (1997) Geostatistics for natural resources evaluation. Oxford University Press, Oxford
- Hamm S, Kim M, Cheong J, Kim J, Son M, Kim T (2007) Relationship between hydraulic conductivity and fracture properties estimated from packer tests and borehole data in a fractured granite. *Eng Geol* 92:73–87
- Houlsby AC (1976) Routine interpretation of the Lugeon water test. *Quart J Eng Geol Hydrogeol* 9(4):303–313
- Houlsby AC (1990) Construction and design of cement grouting. Wiley, New York
- Lombardi G (1999) Grouting of rock with cement mixes. In: Proceedings of the ICOLD symposium: dam foundations: problems and solutions, Antalya, Turkey, pp 1–18
- Rocha M (2013) Mecânica das Rochas. Edição no âmbito das comemorações do centenário do nascimento do Engenheiro Manuel Rocha – 1913–2013. LNEC, Laboratório Nacional de Engenharia Civil, Lisboa
- Rocha M, Franciss F (1977) Determination of permeability in anisotropic rock-masses from integral samples. *Rock Mech* 9:67–93
- Soares A (2006) Geoestatística para as Ciências da Terra e do Ambiente. IST—Instituto Superior Técnico, Lisboa
- Vieira de Lemos J, Lamas L (2013) Contribution of Manuel Rocha to rock mechanics and dam foundations. Edição no âmbito das comemorações do centenário do nascimento do Engenheiro Manuel Rocha – 1913–2013. LNEC, Laboratório Nacional de Engenharia Civil, Lisboa
- Weaver KD, Bruce DA (2007) Dam foundation grouting, Revised and Expanded (edn). American Society of Civil Engineers, ASCE Press, New York



RMR|14 Versus RMR|89: A Methodological Approach for Rock Mass Excavations (N Portugal)

Suse Mateus, Maria José Afonso, Isabel Fernandes, and Helder I. Chaminé

Abstract

The Rock Mass Rating (RMR) is one of the most widely recognised geomechanical classifications for tunnel and excavation design. This scheme was originally proposed in 1973, and it has been developed since then. Significant revisions in its characterisation and structure were made in the version 1989 and, particularly, in the 2014 version. The last version, RMR|14, maintains three parameters combining the RMR|89, i.e., the uniaxial compression strength of intact rock, the water effect, and the number of discontinuities per meter. Additionally, three new features are considered: the intact rock alterability derived from water (I_{d2}), and two adjustment factors, one related to the excavation method, F_e , and the other related to the rock mass's stress-strain behaviour tunnel face (F_s). This work compares the version RMR|89 with the RMR|14 and applies it to underground excavation engineering design and practice.

Keywords

Rock masses • Underground excavations • RMR • RMR|14

1 Introduction

Rock mass schemes and geomechanical indexes are often used for excavations, tunnels, and mining design purposes (e.g., Ritter 1879; Terzaghi 1946; Deere 1963; Wickham et al. 1972; Bieniawski 1973; Barton et al. 1974; Rocha 1976; Hoek 1994). The assessment of a rock mass based on engineering geological, geotechnical and geomechanical features encompasses multi-criteria parameters to result from quantitative classifications for rock engineering design and construction (details in Bieniawski 1997; Barton and Bieniawski 2008). The geological fieldwork data are essential for the rock mass evaluation quality, specifically in discontinuities behaviour and permeability (e.g., Hudson and Cosgrove 1997; Barton and Bieniawski 2008; Lowson and Bieniawski 2013; Pinheiro et al. 2014; Barton and Quadros 2015; Chaminé et al. 2015). The definition of rock mass behaviour in the former classification systems was primarily focused on a descriptive approach. The earliest rock mass scheme was developed for steel set support tunnels (Terzaghi 1946). The RMR is one of the most broadly recognised quantitative classifications for tunnel projects. This classification was created by Bieniawski (1973) and mainly developed in the '70s of the 20th century (1973–1979), using excavation data of heterogeneous rock media. The RMR has been targeted by several developments in the last 49 years, namely Bieniawski (1974, 1975, 1976, 1979, 1989, 1993, 2011) and Serafim and Pereira (1983). Celada et al. (2014) made several key updates, and Celada and Bieniawski (2020) proposed the RMR|14.

This work presents a methodological approach for a comparative evaluation of RMR|14 and RMR|89, applied to a deep underground excavation (321 m depth) for a hydroelectric power plant in Northern Portugal. The rock mass comprises granitic rocks and micaschists, crossed by aplitic-pegmatitic veins. The study site concerns a tunnel of circular cross-section, 4598 m long and a diameter of 8 m. The underground excavation has four linear sections (total

S. Mateus · M. J. Afonso (✉) · H. I. Chaminé
Laboratory of Cartography and Applied Geology, Department of
Geotechnical Engineering, School of Engineering (ISEP),
Polytechnic of Porto, Porto, Portugal
e-mail: mja@isep.ipp.pt

M. J. Afonso · H. I. Chaminé
Centre GeoBioTec|UA, Aveiro, Portugal

I. Fernandes
Department of Geology, IDL, Faculty of Sciences, University of
Lisbon, Lisbon, Portugal

length of 4073 m) and four curvilinear sections (total length of 526 m), with bending angles in the range of 15° – 32° (details in Mateus 2020).

2 Methodology Applied to Rock Mass Faces in N Portugal

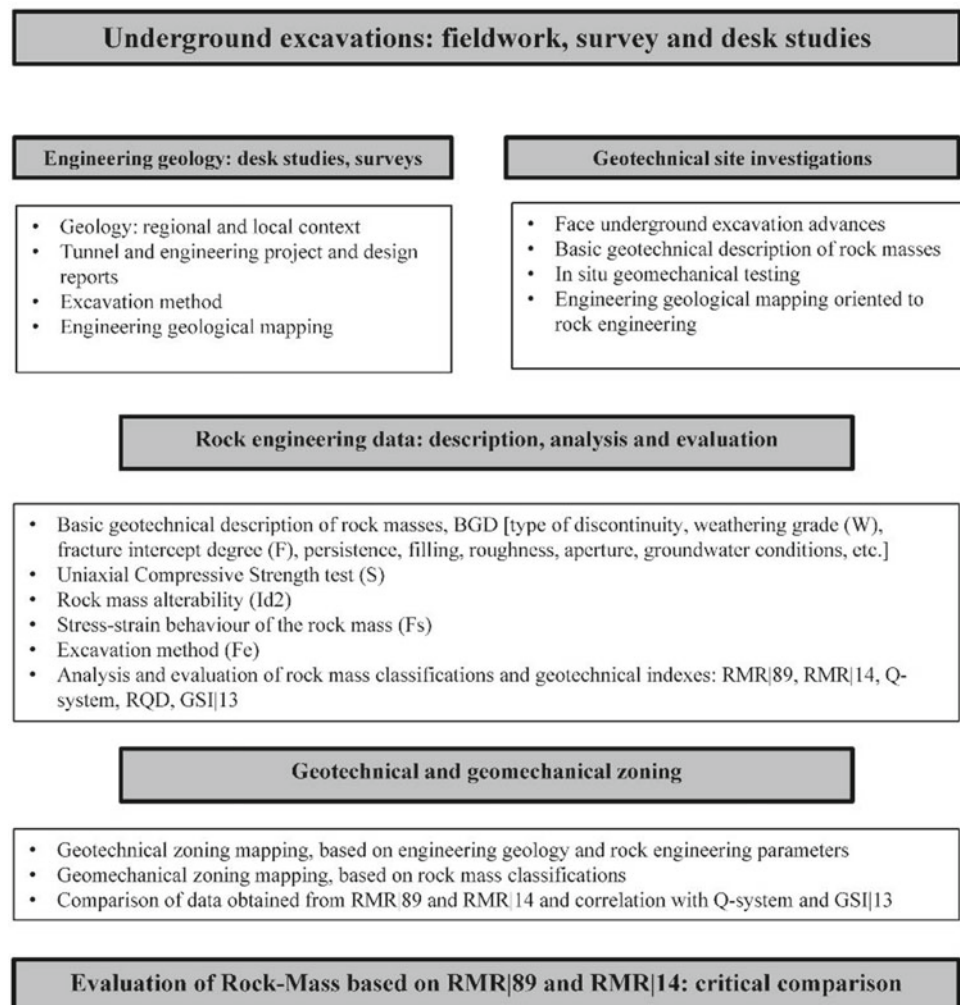
Several techniques were combined and developed in successive steps to appraise this work (Fig. 1):

- (i) Desk studies, including geological, geotechnical, and geomechanical surveys to create the geological and the geotechnical framework;
- (ii) Detailed underground engineering geology and geotechnical mapping and field surveys;
- (iii) The rock surveys were applied for each excavation advance (front, roof, and sidewalls) following the general recommendations of ISRM (1978, 1981, 2007, 2015) and CFCFF (1996). Several parameters

were recorded, namely: discontinuity type and orientation, with correction of the sampling bias (e.g., Terzaghi 1965; Priest 1993; Zeeb et al. 2013; Chaminé et al. 2015; Mahé et al. 2015; and references therein); and other geotechnical and geomechanical parameters (ISRM 1981, 2007, 2015);

- (iv) Three parameters were evaluated to develop RMR|14: alterability of the intact rock (I_{d2}), a factor related to the excavation method (F_e), and another concerning the elastic-plastic behaviour (F_s);
- (v) An engineering geological zoning map was produced (e.g., Griffiths 2002; ISRM 2007, 2015);
- (vi) The following geotechnical indexes and geomechanical classifications were used: the Rock Quality Designation (RQD) (Deere 1963; Deere and Deere 1988); the RMR (e.g., Bieniawski 1973, 1989, 1993); the Q-system (Barton et al. 1974; Barton 2002; NGI 2015); and the Geological Strength Index (GSI), (e.g., Hoek 1994; Hoek et al. 2013; Hoek and Brown 2019; Santa et al. 2019). In addition, was made a

Fig. 1 Methodological flowchart for the investigation site: a case study of a deep underground excavation (321 m depth) for a hydroelectric power plant in N Portugal



geomechanical zoning map and a comparison RMR|14 with RMR|89 (Bieniawski 1989; Celada et al. 2014; Celada and Bieniawski 2020).

3 RMR|89 Versus RMR|14

Due to mining and civil engineering developments, the RMR classification system has been updated and/or improved. Table 1 summarises the main details and upgrades in RMR. While the RMR|89 (Bieniawski 1989) is based on five parameters (A_1, A_2, A_3, A_4, A_5) and one adjustment factor (A_6), the newest version, RMR|14 (Celada et al. 2014; Celada and Bieniawski 2020) has a new structure with five basic parameters (B_1, B_2, B_3, B_4, B_5) and three adjustment factors (F_0, F_e, F_s). The main differences between RMR|89 and RMR|14 are: (i) the sum of parameters A_2 and A_3 in RMR|89 corresponds to parameter B_2 in RMR|14; (ii) the introduction of a new parameter B_4 in RMR|14 concerning the alterability of intact rock (I_{d2}); (iii) the introduction of two adjustment factors in RMR|14, one related to the excavation method, F_e , and other related to the stress-strain behaviour of the rock mass at the tunnel faces, F_s .

Parameter I_{d2} can be evaluated through the slake durability test (Franklin and Chandra 1972) or the rock

immersion in ethylene glycol (e.g., Carter et al. 2010; Piaggio 2015). Moreover, I_{d2} can be assessed by empirical correlations with other parameters, namely Uniaxial Compressive Strength (UCS), Rebound value obtained by Schmidt hammer (R), and Point Load Index (PLI) (e.g., Koncagül and Santi 1999; Parish and Borden 2001; Andrade and Saraiva 2010; Sharma et al. 2011; Ahmad et al. 2017; Fereidooni and Khajevand 2018). In the study tunnel, the correlation (1) proposed by Koncagül and Santi (1999) was applied since it fits better the rock mass conditions.

$$I_{d2} = 1.52UCS - 13.80 \quad (1)$$

The adjustment factor F_e considers that the utilisation of mechanical means (TBM, road headers, or hydraulic hammers) is less damaging to the remaining rock than blasting (Celada et al. 2014), which leads to considering this factor as 1 when the excavation is performed by blasting. When mechanical means are used, the F_e can be obtained from correlations (1), (2), or (3) (Fig. 2).

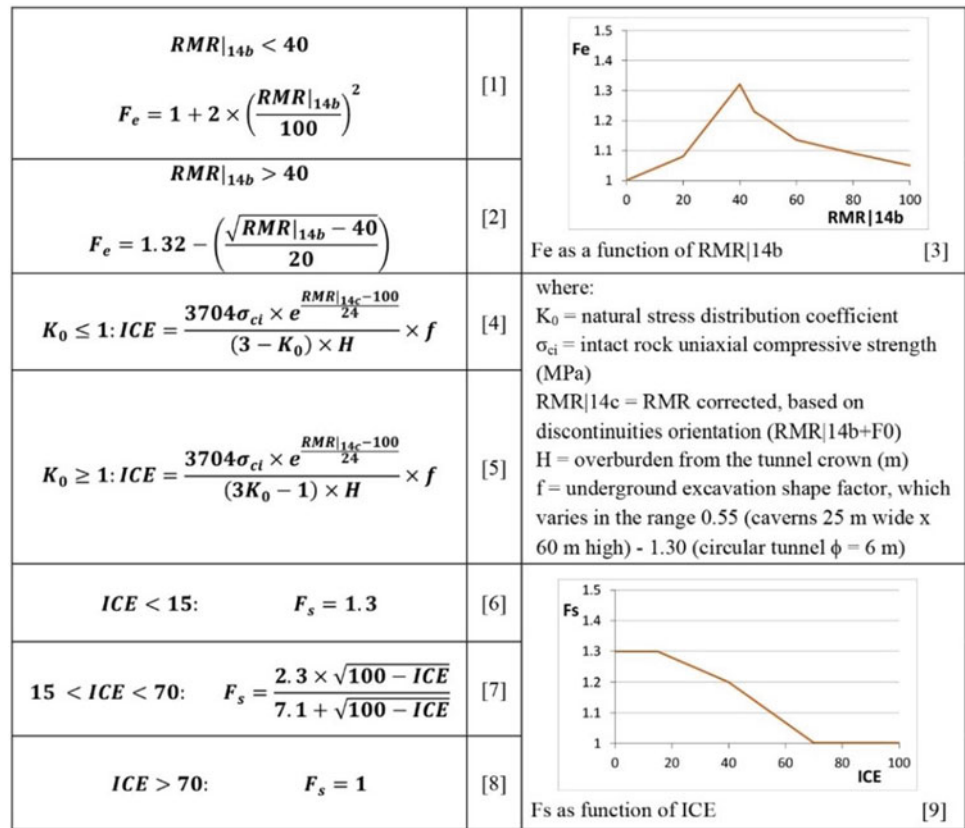
The adjustment factor F_s aims to accept the declining impact of yielding at the tunnel faces. To obtain this factor, it is necessary to calculate the Index of Elastic Behaviour (ICE, in Spanish acronym), proposed by Bieniawski et al. (2011), expressed by the correlations (4) and (5). After the determination of the ICE value, it is possible to calculate the F_s from correlations (6), (7), (8), or (9) (Fig. 2).

Table 1 Parameters, adjustment factors, and ratings in three versions of the RMR classification system

Parameters and adjustment factors		RMR ratings							
		1973	1989			2014			
			1st edition	Revised	ID		ID		
Strength of intact rock material (MPa)		0–10	0–10	0–15	A_1	0–15	B_1		
Density of discontinuities (per meter)	RQD (%)	3–16	3–20	0–20	A_2	0–40	B_2		
	Spacing of discontinuities (m)	5–30	5–20	0–20	A_3				
Condition of discontinuities	Continuity (m)	0–5	0–6	0–6	0–30	A_4	0–5	0–20	B_3
	Roughness	–	0–6	0–6			0–5		
	Aperture (mm)	1–5	0–6	0–6			–		
	Filling (mm)	–	0–6	0–6			0–5		
	Weathering	1–9	0–6	0–6			0–5		
Alterability of intact rock, I_{d2} (%)		–	–	–	–	0–10	B_4		
Groundwater		2–10	0–15	0–15	A_5	0–15	B_5		
Adjustment factors	F_0 (axis orientation of the tunnel vs discontinuities)	–12 to 0	–12 to 0	–12 to 0	A_6	–12 to 0	F_0		
	F_e (excavation method)	–	–	–	–	1.00–1.32	F_e		
	F_s (stress-strain behaviour)	–	–	–	–	1.00–1.30	F_s		
RMR 89 value		RMR 89b = $A_1 + A_2 + A_3 + A_4 + A_5$ [Basic RMR 89] RMR 89 = RMR 89b + A_6							
RMR 14 value		RMR 14b = $B_1 + B_2 + B_3 + B_4 + B_5$ RMR 14 = (RMR 14b + F_0) x F_e x F_s							

Updated from Bieniawski (1973, 1989), Celada et al. (2014)

Fig. 2 Correlations to obtain the adjustment factors F_e and F_s . Adapted from Celada et al. (2014), Celada and Bieniawski (2020)



The obtained values for RMR|89 and RMR|14 were, respectively, in the range 31–55 and 34–61. Generally, RMR|14 presents higher values than RMR|89, mainly because of the new parameter I_{d2} . Also, when the excavation method is performed by mechanical means, F_e is higher than 1, which leads to an increase in the difference between the two versions of RMR. Therefore, the correlation (2) between RMR|14 and RMR|89 was good ($R = 0.81$) and is expressed as follows:

$$RMR|_{14} = 0.84 * RMR|_{89} + 11.24 \quad (2)$$

Additionally, the Q-system and the GSI|13 values correlated with the RMR|14 and RMR|89 values. The correlation between the Q-values and RMR|14 was moderate ($R = 0.55$), while RMR|89 was good ($R = 0.82$). Moreover, the relationship between the GSI|13 and the RMR|14 was good ($R = 0.79$), while RMR|89 was very good ($R = 0.89$).

4 Concluding Remarks

This case study compares the implementation of the RMR versions (1989 and 2014) to understand the main differences between them and the new parameters' influence. It is concluded that the application of the RMR|14 results, primarily,

in higher values than when the 1989 version was applied, mainly due to the introduction of the new parameter I_{d2} . However, the new adjustment factor (F_e) also provides higher RMR values when mechanical means are used. The correlation between these two versions is good, and with the other geomechanical classifications (Q-system and GSI), a good correlation is also obtained. However, it is between RMR|89 and GSI|13 that the highest correlation is achieved. Nevertheless, this research is still ongoing, and more underground excavations must be analysed to define the importance of the RMR|14 development for the underground excavation engineering design and practice.

Acknowledgements MJA and HIC were supported by the Labcarga| ISEP re-equipment program (IPP-ISEP| PAD'2007/08) and Centre GeoBioTec|UA (UID/GEO/04035/2020). IF was supported by IDL (UIDB/50019/2020). SM is grateful for the support of the Geoárea firm. Finally, acknowledgements are owed to the anonymous reviewers for their valuable contributions to improving the manuscript.

References

Ahmad M, Ansari MK, Sharma LK, Singh R, Singh TN (2017) Correlation between strength and durability indices of rocks-soft computing approach. *Procedia Eng* 191:458–466

- Andrade PS, Saraiva AA (2010) Physical and mechanical characterisation of phyllites and metagreywackes in central Portugal. *Bull Eng Geol Environ* 69:207–214
- Barton N (2002) Some new Q-value correlations to assist in site characterisation and tunnel design. *Int J Rock Mech Min Sci* 39(2):185–216
- Barton N, Bieniawski ZT (2008) RMR and Q-setting records straight. In: *Tunnels and tunnelling international*, pp 26–29
- Barton N, Quadros E (2015) Anisotropy is everywhere, to see, to measure and to model. *Rock Mech Roc Eng* 48:1323–1339
- Barton N, Lien R, Lunde J (1974) Engineering classification of rock masses for the design of tunnel support. *Rock Mech* 6(4):189–236
- Bieniawski ZT (1973) Engineering classification of jointed rock masses. *Trans South Afr Inst Civ Eng* 15:335–344
- Bieniawski ZT (1976) Slope stability of the de Beers diamond mine. Council for Scientific and Industrial Research, Republic of South Africa, Pretoria
- Bieniawski ZT (1975) Prediction of rock mass behaviour by the geomechanics classification. In: *Proceedings of the Second Australia-New Zealand Conference on Geomechanics*, vol 75, no 4, Brisbane, Australia, pp P36–P41
- Bieniawski ZT (1976) Rock mass classification in rock engineering. In: *Proceedings of the symposium on exploration for rock engineering*, vol 1, Cape Town, Balkema, pp 97–106
- Bieniawski ZT (1979) The geomechanics classification in rock engineering applications. In: *Proceedings of the 4th congress international symposium of rock mechanics*, vol 2, Montreux, pp 41–48
- Bieniawski ZT (1989) *Engineering rock mass classifications: a complete manual for engineers and geologists in mining, civil, and petroleum engineering*. Interscience. Wiley, New York
- Bieniawski ZT (1993) Classification of rock masses for engineering: the RMR system and future trends. In: Hudson JA (ed) *Comprehensive rock engineering: principles, practice, and projects*. Pergamon Press, Oxford, pp 553–574
- Bieniawski ZT (1997) *Quo Vadis* rock mass classifications?: some thoughts on rating methods for tunnel design. *Felsbau* 15(3):177–178
- Bieniawski ZT (2011) Misconceptions in the applications of rock mass classifications and their corrections. In: *Proceedings of the ADIF seminar on advanced geotechnical characterization for tunnel design*, Madrid, Spain, pp 4–9
- Bieniawski, ZT, Aguado, D, Celada, B, Rodríguez A (2011) Forecasting tunnelling behaviour, tunnels and tunnelling international, pp 39–42
- Carter TG, Castro SO, Carvalho JL, Hattersley D, Wood K, Barone FS, Yuen CMK, Giraldo, D (2010) Tunnelling issues of Chilean Tertiary volcanoclastic rocks. In: *Proceedings of the MIR 2010, XIII Ciclo di conferenze di Meccanica ed Ingegneria de lle Rocce*, Torino, pp 215–236
- Celada B, Bieniawski ZT (2020) *Ground characterisation and structural analyses for tunnel design*. CRC Press, Taylor & Francis Group, Boca Raton
- Celada B, Tardáguila I, Varona P, Rodríguez A, Bieniawski ZT (2014) Innovating tunnel design by an improved experience based RMR System. In: *Proceedings of the world tunnel congress 2014—Tunnels for a Better Life*, Foz do Iguaçu, Brazil, pp 1–9
- CFCFF—Committee on Fracture Characterization and Fluid Flow (1996) *Rock fractures and fluid flow: contemporary understanding and applications*. National Research Council, National Academy Press, Washington DC
- Chaminé HI, Afonso MJ, Ramos L, Pinheiro R (2015) Scanline sampling techniques for rock engineering surveys: insights from intrinsic geologic variability and uncertainty. In: Giordan D, Thuro K, Carranza-Torres C, Wu F, Marinos P, Delgado C (eds) *Engineering geology for society and territory—Applied geology for major engineering projects*, IAEG, vol 6. Springer, pp 357–361
- Deere DU (1963) Technical description of rock cores for engineering purposes. *Rock Mech Eng Geol* 1(1):17–22
- Deere DU, Deere DW (1988) The rock quality designation (RQD) index in practice. In: Kirkaldie L (ed) *Rock classification systems for engineering purposes*, ASTM STP 984. American Society for Testing and Materials, Philadelphia, pp 91–101
- Fereidouni D, Khajevand R (2018) Correlations between slake-durability index and engineering properties of some travertine samples under wetting-drying cycles. *Geotech Geol Eng* 36:1071–1089
- Franklin JA, Chandra R (1972) The slake-durability test. *Int J Rock Mech Min Sci* 9(3):325–328
- Griffiths JS (2002) Mapping in engineering geology. In: *Key issues in earth sciences*, vol 1. The Geological Society of London, London
- GSE—Geological Society Engineering Group Working Party Report (1995) *The description and classification of weathered rocks for engineering purposes*. *Quart J Eng Geol* 28(3):207–242
- Hoek E (1994) Strength of rock and rock masses. *ISRM News J* 2(2):4–16
- Hoek E, Brown ET (2019) *The Hoek-Brown failure criterion and GSI—2018 edition*. *J Rock Mech Geotech Eng* 11(3):445–463
- Hoek E, Carter TG, Diederichs MS (2013) Quantification of the geological strength index chart. In: *Proceedings of the geomechanics symposium, 47th US rock mechanics*, San Francisco, CA, ARMA13–672, pp 1–8
- Hudson JA, Cosgrove JW (1997) Integrated structural geology and engineering rock mechanics approach to site characterisation. *Int J Rock Mech Min Sci Geom Abstr* 34(3/4):1361–13615
- ISRM—International Society for Rock Mechanics (1978) Suggested methods for the quantitative description of discontinuities in rock masses. *Int J Rock Mech Min Sci Geom Abstr* 15(6):319–368
- ISRM—International Society for Rock Mechanics (1981) Basic geotechnical description of rock masses. *Int J Rock Mech Min Sci Geom Abstr* 18:85–110
- ISRM—International Society for Rock Mechanics (2007) *The complete ISRM suggested methods for characterisation, testing and monitoring: 1974–2006*. In: Ulusay R, Hudson JA (eds) *Suggested methods prepared by the commission on testing methods*. ISRM, Ankara
- ISRM—International Society for Rock Mechanics (2015) *The ISRM suggested methods for rock characterisation, testing and monitoring: 2007–2014*. In: Ulusay R (ed) *Suggested methods prepared by the commission on testing methods*. ISRM. Springer, Cham
- Koncağül EC, Santi PM (1999) Predicting the unconfined compressive strength of the breathitt shale using slake durability, shore hardness and rock structural properties. *Int J Rock Mech Min Sci* 36:139–153
- Lowson A, Bieniawski ZT (2013) Critical assessment of RMR based tunnel design practices: a practical engineer’s approach. In: *Proceedings of the SME, rapid excavation and tunnelling conference*, Washington, DC, pp 180–198
- Mahé S, Gasc-Barbier M, Soliva R (2015) Joint set intensity estimation: comparison between investigation modes. *Bull Eng Geol Environ* 74(1):171–180
- Mateus S (2020) *Classificação geomecânica RMR|89 versus RMR|14: uma aplicação a frentes de escavação em maciços rochosos heterogêneos (Norte de Portugal)*. Instituto Superior de Engenharia do Porto, Porto (MSc Dissertation)
- NGI—Norwegian Geotechnical Institute (2015) *Using the Q-system: rock mass classification and support design*. Handbook Norwegian Geotechnical Institute, NGI, Oslo
- Parish DW, Borden RH (2001) Engineering properties and slake durability of weak Triassic Basin rock. In: *Proceedings of the*

- fifteenth international conference on soil mechanics and geotechnical engineering Istanbul. pp 475–478
- Piaggio G (2015). Swelling rocks characterisation: lessons from the Andean region. In: Proceedings of ITA World Tunnel Congress, Dubrovnik, Croatia
- Pinheiro R, Ramos L, Teixeira J, Afonso MJ, Chaminé HI (2014) MGC–RocDesign|CALC: a geomechanical calculator tool for rock design. In: Alejano LR, Perucho A, Olalla C, Jiménez R (eds) Proceedings of Eurock 2014, rock engineering and rock mechanics: structures in and on rock masses (ISRM European regional symposium, Vigo, Spain). CRC, London, pp 655–660
- Priest SD (1993) Discontinuity analysis for rock engineering. Chapman and Hall, London
- Ritter W (1879) Die Statik der Tunnelgewölbe. Springer, Berlin
- Rocha M (1976) Estruturas subterrâneas: túneis, cavernas e poços. LNEC, Laboratório Nacional de Engenharia Civil, Lisboa
- Santa C, Gonçalves L, Chaminé HI (2019) comparative study of GSI chart versions in a heterogeneous rock mass media (Marão tunnel, north Portugal): a reliable index in geotechnical surveys and rock engineering design. Bull Eng Geol Environ 78:5889–5903
- Serafim JL, Pereira JP (1983) Consideration of the geomechanics classification of Bieniawski. In: Proceedings of the international symposium on engineering geology and underground constructions, vol 1, Lisbon, pp 1133–1144
- Sharma PK, Khandelwal M, Singh TN (2011) A correlation between Schmidt hammer rebound numbers with impact strength index, slake durability index and P-wave velocity. Int J Earth Sci 100:189–195
- Terzaghi K (1946) Rock defects and locals on tunnel supports. In: Proctor RV, White TL (eds) Rock tunneling with steel supports, vol 1. The Commercial Shearing & Stamping Co., Youngstown, pp 17–99
- Terzaghi RD (1965) Sources of errors in joint surveys. Géotechnique 15:287–304
- Wickham GE, Tiedemann HR, Skinner EH (1972) Support determination based on geologic predictions. In: KS Lane, LA Garfield (eds) Proceedings of the 1st North American rapid excavation tunneling conference (RETC), Chicago. AIME, New York, pp 43–64
- Zeeb C, Gomez-Rivas E, Bons PD, Blum O (2013) Evaluation of sampling methods for fracture network characterisation using outcrops. AAPG Bull 97(9):1545–1566



Drilling Parameters in the Evaluation of Rock Mass Quality

Marcelo Pereira, Isabel Fernandes, Rui Moura, and Nadir Plasencia

Abstract

The production of a geotechnical model-based on-site investigation and surface mapping is particularly challenging for tunnels due to the depth at which the excavation is performed. Besides the lithology and the weathering grade, the main factors influencing the underground excavation are related to the rock mass structure, namely joints and major faults. The knowledge in advance of the conditions to be found during the excavation usually saves time and money and increases safety. In the present work, the excavation of two large tunnels was studied, aiming to obtain correlations between the rock mass properties and the parameters obtained by the drilling machine ahead of the excavation front. The study included the geological mapping of the excavation surfaces, the determination of the intact rock strength and the record of the drilling parameters, namely the penetration rate, feeder pressure, pressure in the hammer, rotation pressure and strike pressure. The variability of the results was analysed and the Pearson coefficient $|r|$ established for each parameter in order to find the most accurate correlations. It was concluded that, for deep structures, monitoring these parameters constitutes an essential complement to the previous geotechnical site investigation, contributing to a better definition of immediate support measures to apply along the excavation works.

Keywords

Measurement while drilling • Rock support • Rock mass characterisation • Tunneling • Drilling parameters

1 Introduction

The excavation of tunnels demands previous detailed site investigation and application of exploration techniques, namely core drilling, to define the geological model and produce the geotechnical zonation. The data obtained are applied in the most common geomechanical rock mass classifications—the Rock Mass Rating (RMR) and the Q-system—which suggest adequate measures of support depending on the span and the stand-up time. The uncertainty of the rock mass properties between consecutive drilling sites leads to the interpretation by the engineering geologist of large volumes of rock mass, which might sometimes not be confirmed during the construction phase. The properties of the rock mass are defined by the lithology but also depend on the weathering grade (W1–W5, ISRM 2007), the fracture spacing (F1–F5, ISRM 2007), the rock strength and the presence of major faults (Howarth and Rowlands 1987; Hoseinie et al. 2007). Furthermore, the anisotropy of the rock, the orientation of the discontinuities with the direction of drilling, the porosity, the mineralogy and the unconfined compressive strength of the intact rock influence the drilling parameters and the stability of the excavation (e.g. Yue et al. 2004; Reiffsteck et al. 2018; Vezhapparambu et al. 2018; Khorzoughi et al. 2018; van Eldert et al. 2020). The surface geological mapping performed in the early stages of the site investigation must be confirmed, detailed and complemented by the engineering geological mapping of the excavated surfaces, just the following blasting, to adapt the support design to the real behaviour of the rock mass. The drill rigs automatically collect the drilling parameters by measurements while

M. Pereira
GGC, Geologia & Geotecnia Consultores Lda, Porto, Portugal

I. Fernandes (✉)
Instituto Dom Luiz e Departamento de Geologia, Faculdade de Ciências, Universidade de Lisboa, Lisboa, Portugal
e-mail: mifernandes@ciencias.ulisboa.pt

R. Moura
DGAOT and ICT, Faculty of Sciences, University of Porto, Porto, Portugal

N. Plasencia
EDP—Gestão da Produção de Energia, Porto, Portugal

drilling (MWD), which are recognised in the construction industry to correlate with the characteristics of the rock mass (e.g. Reiffsteck et al. 2018). In this concern, drill hole depth (distance), penetration rate (distance/time), thrust (feed pressure in kN), torque pressure (bar), percussive pressure (bar) and rotation speed (RPM) (Schunnesson 1997) can assist in forecasting the behaviour of the rock mass ahead of the tunnel face contributing to save time and money in the definition of the adequate rock support. Although drill monitoring has been used for decades, it is not a standard technic in excavation works.

The present work summarises the results obtained by MWD in excavating two large tunnels in a granitic rock mass in the North of Portugal. Charts were prepared to correlate the features measured with each of the rock mass properties, namely W, F, the properties of joints, and the presence of faults. The study demonstrated the capability of the data acquisition while drilling to forecast the rock mass properties and to detect zones of weakness, such as major faults or strongly weathered rock mass which may occur unexpectedly during the excavation (Kovári and Fechtig 2000), therefore contributing to the decision processes needed during the tunnel construction.

2 Methodology

Two tunnels excavated in syn-tectonic Hercynian granitic rock mass were studied: Tunnel 1 with 740 m in length, inverted U-profile, 48 m² cross-section and dipping 11%; Tunnel 2 with 814,5 m in length, a circular profile of 113 m² cross-section and dipping 13.8%. The rock mass is a medium- to coarse-grained porphyric two-mica granite of the Galicia-Trás-os-Montes Zone, Iberian Massif.

The number of measurements recorded is 214 for Tunnel 1 and 134 for Tunnel 2. The parameters recorded by the drilling machine were correlated with the geotechnical map of the tunnel face and closest walls. The drilling of the rock mass was carried out using a three-armed drilling rig, with continuous recording of the drilling parameters. The drilling proceeded by percussion and rotation, with bits of 3 inches in diameter. The depth of each drilling hole was defined according to the geomechanical classifications obtained in the previous drilling depth.

The Jumbo was equipped with Robodrill's Drill-Analyser software, registering the main drilling parameters: penetration rate (m/min), feeder pressure (thrust), rebound hammer pressure, rotation pressure and strike pressure (all in bar). The hammer pressure, or rebound pressure, is the energy applied in the opposite direction to the direction of the forward force. The feeder pressure is the force that pushes the drill bit against the rock mass. The rotation pressure results from the pressure exerted to perform the maneuver of the

stick rotation. Finally, the strike pressure is the pressure applied for the execution of the blow exerted by the hammer. The values of these parameters are conditioned by the characteristics of the material to be drilled, which combination influences the drilling penetration rate.

For each excavation advance, the mapping of the geological and geotechnical conditions was carried out, which included the recording of the lithology, the grade of fracturing (F) and weathering (W), in accordance with the ISRM (2007) recommendations. The set of joints was defined, including orientation, spacing, roughness and infilling. The Rock Quality Designation (RQD) was calculated following Palmström (1985), using the factor of fracture frequency (Jv). The values of uniaxial compressive strength (UCS), estimated at the excavation face aiming at the application of geomechanical classification, were obtained by point load tests carried out every 10–20 m. The major faults were recorded in what concerns orientation, the thickness of the fault gauge, the composition of the gauge and water presence.

3 Results

Tunnel 1 and Tunnel 2 were excavated in a granitic rock mass mainly composed of sound (W1) to slightly weathered (W2), in particular in the vicinity of faults, with wide to moderate spacing of discontinuities (F2–F3). However, in Tunnel 1 there were also very wide spacing discontinuities (F1). The data from geotechnical characterisation show that the rock mass in Tunnel 1 is slightly more weathered and fractured (RQD 81%) than in Tunnel 2 (RQD 91%). The drilling parameters are also different for both tunnels. On average, the impact pressure and the pressure forward are higher in Tunnel 1 than in Tunnel 2, while the torque pressure is 1.5 times lower. Table 1 summarises the values of each parameter. However, the penetration rate shows similar values, and therefore, the analysis was focused on the relationship between the penetration rate and the different geotechnical properties of the rock mass.

It was verified that the major faults and the more intense fracturing of the rock mass in their vicinity have a large influence on the results of the drilling parameters, as shown in Fig. 1. The charts also stress that the weakness zones have a large impact on the penetration rate, and, in Tunnel 2, the range of values in the head pressure is increased. On the contrary, in Tunnel 1, the main variation is obtained for the strike pressure.

The Pearson correlation coefficient $|r|$ (Franzblau 1958) was calculated between the penetration rate and the various rock mass characteristics, as presented in Table 2. It shows that there is (negative) robust correlation (>0.80) with the weathering (W) and fracturing (F) grades, with the decrease

Table 1 The average, median and standard deviation of the perforation parameters for Tunnel 1 (T1) and Tunnel 2 (T2)

	Penetration rate (m/min)		Rotation pressure (bar)		Strike pressure (bar)		Feeder pressure (bar)	
	T1	T2	T1	T2	T1	T2	T1	T2
Average	1.69	1.45	86.57	128.16	147.05	33.65	98.01	89.35
Median	1.60	1.40	86.00	128.00	152.00	34.00	98.00	85.00
Standard deviation	0.25	0.26	4.85	4.23	12.13	3.03	4.40	17.56

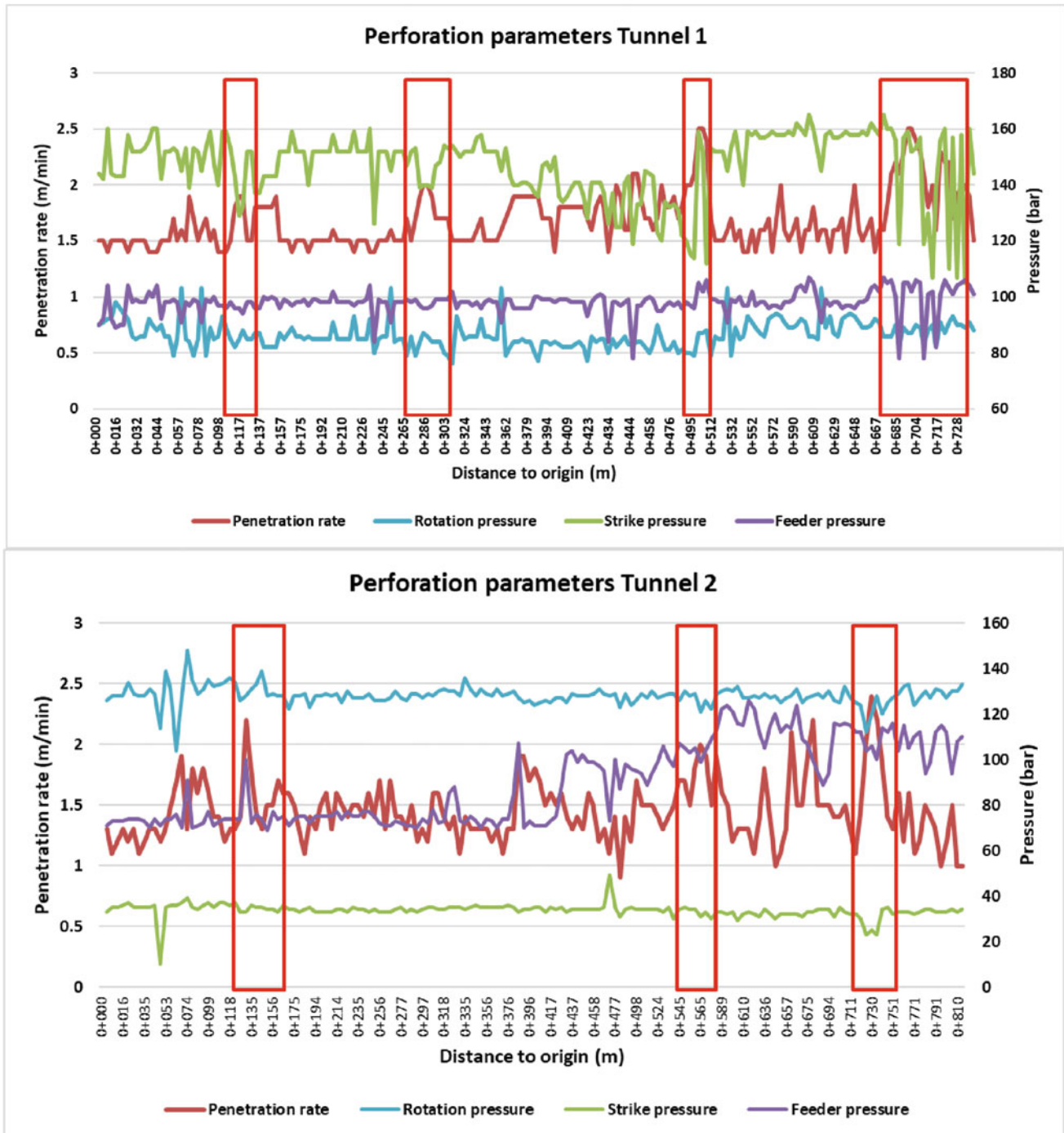


Fig. 1 Evolution of the perforation parameters along the length of both tunnels. The width of the red rectangles represents the length of intersection of the weakness zones and major faults for both tunnels (adapted from Pereira 2013)

Table 2 Pearson correlation coefficient between drilling penetration rate and the parameters (adapted from Pereira 2013)

	Tunnel 1 r	Tunnel 2 r
RQD	0.73	0.67
UCS	0.70	0.63
W	0.85	0.95
F	0.90	0.96
Joint properties	0.58	0.62

of the penetration rate as the quality of the rock mass increases. Also, there are (negative) strong correlations (0.60–0.80) with the unconfined compression strength and RQD and moderate (0.40–0.60) to strong correlation with the joint properties, namely persistence, aperture, roughness and infilling, for Tunnel 1 and Tunnel 2, respectively.

4 Concluding Remarks

Two tunnels with a total of more than 1500 m in length were studied, aiming to obtain correlations between the Measurement While Drilling (MWD) parameters and the geotechnical characteristics of the rock mass. The excavation was performed in granitic rock masses with different weathering and fracturing grades intersecting some major faults. The penetration rate shows a good correlation with the geotechnical properties and is highly affected by weak areas associated with major faults. The results obtained are intended to optimise future excavations in similar rock masses, using MDW to estimate the rock mass quality in advance of the excavation. Nevertheless, more data collected at the different geological environments must be analysed to create consistent correlations based on historical information, which must also consider the variability that might result from using different equipment.

Acknowledgements The author thanks FCT—Foundation for Science and Technology for funding UIDB / 50019/2020 project—IDL and are grateful to EDP Produção and CÊGÊ for allowing the publication of the results.

References

- Franzblau AN (1958) A primer of statistics for non-statisticians. Harcourt, Brace, New York
- Hoseinie SH, Aghababaei H, Pourrahimian Y (2007) Development of a new classification system for assessing of rock mass drillability index (RDi). *Rock Mech Rock Eng* 45:1–10
- Howarth DF, Rowlands JC (1987) Quantitative assessment of rock texture and correlation with drillability and strength properties. *Rock Mech Rock Eng* 20:57–85
- ISRM (2007) The complete ISRM suggested methods for rock characterisation, testing and monitoring: 1974–2006. In: Ulusay R, Hudson JA (eds) Suggested methods prepared by the commission of testing methods. ISRM Turkish National Group, Ankara, Turkey
- Khorzoughi MBB, Hall R, Apel D (2018) Rock fracture density characterisation using measurement while drilling (MWD) techniques. *Int J Rock Mech Min Sci* 28(6):859–864
- Kovári K, Fechtig R (2000) Historical tunnels in the Swiss Alps Gotthard Simplon Lötschberg. Society for Art of Civil Engineering, Zürich
- Palmström A (1985) Application of the volumetric joint count as a measure of rock mass jointing. In: Proceeding of international symposium fundamentals of rock joints. Björkliden, Sweden, pp 103–110
- Pereira M (2013) Utilização de parâmetros de furação para previsões geológico e geotécnicas na fase de execução de obras subterrâneas. Faculty of Sciences, University of Porto, Porto (MSc Dissertation)
- Reiffsteck P, Benoît J, Bourdeau C, Desanneaux G (2018) Enhancing geotechnical investigations using drilling parameters. *J Geotech Geoenviron Eng* 144(3):1–11
- Schunnesson H (1997) Drill process monitoring in percussive drilling for location of structural features. Lithological boundaries and rock properties and for drill productivity evaluation. Department of Environmental Planning and Design Division of Applied Geology. Luleå University of technology. Luleå
- van Eldert J, Schunnesson H, Saiang D, Funehag J (2020) Improved filtering and normalising of Measurement-While-Drilling (MWD) data in tunnel excavation. *Tunn Undergr Spac Technol* 103:103467
- Vezhapparambu VS, Eidsvik J, Ellefmo SL (2018) Rock classification using multivariate analysis of measurement while drilling data: towards a better sampling strategy. *Minerals* 8:384
- Yue ZQ, Lee CF, Law KT, Tham LG (2004) Automatic monitoring of rotary-percussive drilling for ground characterisation: illustrated by a case example in Hong Kong. *Int J Rock Mech Min Sci* 41:573–612



Methodologies for the Geological–Geotechnical Characterisation of Weathering Profiles of Granite: A Case Study

Rita Lamas, Isabel Fernandes, Jorge Espinha Marques, and António Viana da Fonseca

Abstract

Engineering works, especially those carried out in an urban environment, generally concern shallow depths in which soil or weathered rock mass is present. The assessment of a rock mass weathering grade relies on chemical and mechanical features related to the degradation of the mechanical properties and the increase of permeability. This study aims at improving the existing knowledge on the description of rock masses' weathering grade by indexing different weathering grade, namely, regarding mineralogical composition, fabric and microstructure, and its influence on the geomechanical parameters that the project of foundations and, in particular, the geotechnical structures demand, specifically, for the numerical modelling with view to constructive solutions. The permeability, deformability, and resistance of weathering horizons are underlined, and physical properties are to be evaluated closely related to the geological characteristics already mentioned. Given the environmental concerns to which society and the scientific community are increasingly alert, the final work will include new radiological measurements in the granite rock mass of the Porto urban area, which are added value to the geological and geomechanical knowledge of rock masses.

Keywords

Granite • Weathering profiles • Pedological characterisation • Geological–geotechnical characterisation • Porto granite

1 Introduction

Weathering profiles can vary widely in the area and in-depth in the same rock mass. The spatial variability and weathering intensity depend on the rock mineralogy and texture, the discontinuities, the topography, the climate, and the groundwater conditions. The description of such profiles gave rise to proposals for the classification of weathering grade classes based on colour, friability, modifications of mineralogical composition, and microfracturing. Several authors, institutions, and technical associations proposed their weathering grade classifications. However, the ISRM classification (1978, 1981, 2007) is universally used for rock masses and considers five weathering grade (W_1 – W_5) and one grade corresponding to residual soil (W_6). A similar description is found in GSE (1995) for intact rock, which is very useful for obtaining correlations with the laboratory mechanical tests.

The influence of weathering grade on petrographic, physical, and mechanical characteristics has been studied by several authors in different lithologies (e.g., Irfan and Dearman 1978; Viana da Fonseca 1996; Arel and Tuğrul 2001). According to Letto et al. (2018), the geomechanical and mineral-petrographic properties of the rocks decrease with the weathering grade increase. Therefore, the weathering profiles' mechanical characterisation must be made for the rock masses for geotechnical purposes. Knowledge of the index properties, as listed in González de Vallejo and Ferrer (2011), which can be evaluated in laboratory tests, enables the classification of intact rocks, while field tests are

R. Lamas (✉) · J. E. Marques
Instituto Ciências da Terra, Faculdade de Ciências da
Universidade do Porto, Porto, Portugal
e-mail: rita_rocha_lamas@hotmail.com

I. Fernandes
Instituto Dom Luiz e Departamento de Geologia, Faculdade de
Ciências da Universidade de Lisboa, Lisboa, Portugal

A. V. da Fonseca
Departamento de Engenharia Civil, Faculdade de Engenharia da
Universidade do Porto, Porto, Portugal

usually needed for the characterisation of rock masses according to various technical criteria.

For the Portuguese granitic rock masses, widely outcropping in the country, the hypothesis arose that radon gas could be used as a plotter for geological materials' transformation processes, both due to weathering or when subjected to stresses (Koike et al. 2015). Pereira et al. (2017) showed a possible relationship between weathering grade in granitic rocks and exhaled gas concentration.

The Granite of Porto presents weathering profiles in which the entire range of weathering grades (W_1 – W_5) is found and a variable and erratic thickness of residual soil (W_6). The main objective of this work is to present the methodologies which are used in the research being carried out, aiming to establish correlations between the geological characteristics of Granite of Porto, namely, the weathering grade, mineralogy, geochemistry, porosity, and microstructure, with the hydraulic and geomechanical properties of the rock mass, namely, the parameters of stiffness and shear strength of the granite for the various weathering grade.

The present work aims to present the methodology of the work developed in the scope of the ongoing research project. Results are not available yet and are planned to be published soon.

2 Methodology

In order to thoroughly characterise the geological–geotechnical variability of the Porto granite weathering profiles, it is fundamental that the amount of data is sufficiently broad. Furthermore, it is necessary to conduct tests that consider the mineral and chemical composition and determine the physical and mechanical properties for better characterisation. Thus, in order to carry out this study, a strategy was defined: first, the selection of sites for sampling, followed by the careful sampling and preparation of specimens; finally, the laboratory and in situ testing. For the first step, it was essential to take advantage of new excavation works in Porto city due to its extensive urban network. Moreover, the lack of outcrops available, namely, the excavation for constructing a building in the D. João I block in the city centre (Fig. 1), complemented a former sampling during the site investigation works for Metro do Porto tunnels, underground stations, and other infrastructures.

In order to minimise the samples disturbance, among the several existing sampling techniques, the block sampling method was selected, using excavation and manual moulding. This method is the most recommended for residual soils, while for un-weathered rock, the ideal sampling is obtained by drilling with continuous coring.

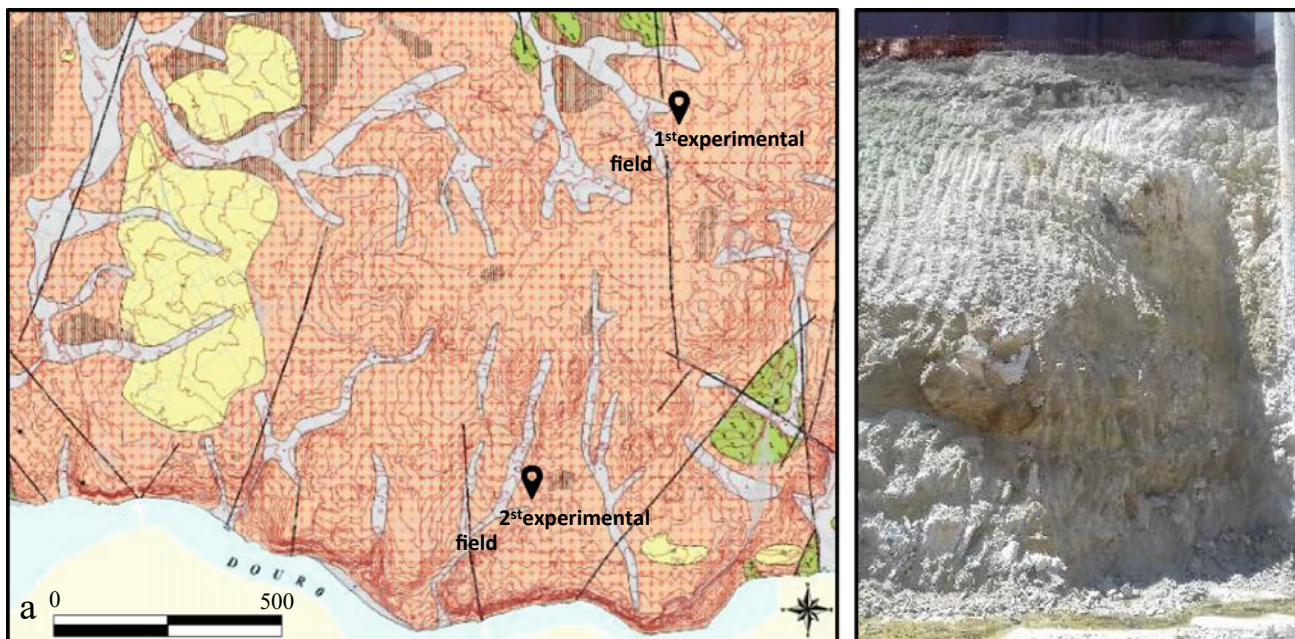


Fig. 1 Excavation works in Porto City: **a** Location of two experimental fields (adapted from COBA 2003); **b** Stone-wall in the D. João I city block

2.1 Pedological Characterisation and Associated Trials

The pedological characterisation is based on the FAO soil classification system—World Reference Base for Soil Resources (FAO 2015), using the internationally accepted FAO guidelines for soil description—Guidelines for Soil Description (FAO 2006)—to describe soils and their characteristics (Table 1).

2.2 Mineralogical and Geochemical Properties

For evaluating the mineralogical and textural characteristics, the petrographic analysis of thin sections, X-ray diffraction, and scanning electron microscopy are used (Table 2).

2.3 Physical Properties

The evaluation of physical properties includes water content, porosity, voids index, unit weight, and rock permeability. In addition, the size distribution and the consistency limits

(Atterberg limits) are determined for the residual soils. Finally, in Table 3, the properties and respective standards, considering the need to apply the soil geotechnical classifications.

2.4 Mechanical Properties

In order to characterise the residual soil and the rock material, various mechanical properties will be determined. These tests are listed in Table 4, and the equipment used is listed.

2.5 Radiometric Methods

It is intended to use the radon accumulator method, which allows obtaining radon concentration in the samples to show the variations it presents according to the rock weathering grade. The method is based on measuring the exhalation of radon and is obtained using an Alphaguard Pro2000 equipped with an ionisation chamber (University of Coimbra). Subsequently, the exhalation rate of radon is calculated.

Table 1 Methods of pedological characterisation

	Properties	Methods of determination
Field pedological characterisation	Soil profile description	Guidelines (FAO 2006)
	Unsaturated hydraulic conductivity and infiltration rates	Mini-disk infiltrometer
	Saturated hydraulic conductivity	Guelph permeameter
Laboratory pedological characterisation	Colour	Munsell Soil Colour maps
	Texture	FAO (2006)
	Bulk density	FAO (2006)
	Porosity	Volumetric ring method
	pH	pH metre—(FAO 2006)
	Electrical conductivity	Method of Benton Jones

Table 2 Methods for determining mineralogical and geochemical characteristics

Properties	Methods of determination
Mineralogy, texture, microfracture index, and microphotographic index	Petrographic analysis under optical microscope—NIKON Eclipse E400 POL (University of Porto)
Chemical analysis of major oxides and determination of the mineralogical composition	X-ray fluorescence and X-ray diffraction (University of Alicante)
High-resolution images with verification of the composition of cryptocrystalline components	SEM/EDS/EPMA-JEOL JXA-8200 (University of Lisbon)

Table 3 Methods for determining physical properties

Properties	Methods of determination
Water content	Portuguese standard NP-84 1965 (University of Porto)
Porosity, void index, and weight volume	Portuguese standard NP EN 1936 2008 (University of Porto)
Size distribution	LNEC Specification E196-1966 (University of Porto)
Consistency limits (Atterberg limits)	Portuguese standard NP-143 1969 (University of Porto)

Table 4 Methods for determining mechanical properties

Properties	Methods of determination
Seismic wave velocity (Longitudinal and transverse waves- V_p , V_s)	Laboratory ultrasonic pulse wave velocity Proceq® system—ASTM D2845-08 (Labgeo-University of Porto)
Unconfined compressive strength (σ_c)	Uniaxial compression test (TRIAx 500KN)-ASTM D7012-14e1 Point load tester (Controls-D550)—ASTM D5731-16 Schmidt Hammer L-Proceq (Labgeo-University of Porto)
Tensile strength (σ_t)	Diametrical test (Clockhouse DIX20)-ASTM D3967-16
Resistance (cohesion- c , friction angle- Φ)	Triaxial compression test-ASTM D7012—14e1 (PUC of Rio de Janeiro)
Deformability (static and dynamic elastic deformation modules: Young's modulus— E , Poisson ratio- ν)	Uniaxial compression test (TRIAx 500KN)—ASTM D7012-14e1 (Labgeo-University of Porto) Seismic test—ASTM D2845-08 (University of Porto)
Abrasiveness	Cerchar Abrasiveness Index—ASTM D7625-10 (Federal University of Viçosa)
Soil compressibility	Edometric test (Wykeham Farrance 24,251)-ASTM D-2435/D2435M-11 (Labgeo-University of Porto)

3 Concluding Remarks

The proposed programme will contribute to the evolution of knowledge globally since, in most cases presented in the literature, the evaluation is based on a limited number of tests and samples. There is a wide variety of papers regarding laboratory tests due to the need to define the best method to reflect the variability of the geotechnical properties with the granitic rock masses' weathering grade profiles.

The methodology proposed above intends to obtain a complete characterisation to establish correlations between the rock mass's geological, hydrogeological, and geotechnical characteristics. The aim is to achieve comprehensively relevant results in granitic rock masses with varying weathering grade and in residual soils with similar properties to the materials studied in the present work.

Acknowledgements RL thanks FCT-Foundation for Science and Technology for funding granted under the Ph.D. scholarship SFRH/BD/131120/2017. The authors are grateful for the support of ICT through the COMPETE 2020 project (UIDB/GEO/04683/2020) of reference POCI-01-0145-FEDER-007690. This work was financially

supported by: Base Funding—114 UIDB/04708/2020 and Programmatic Funding—UIDP/04708/2020 of the CONSTRUCT—Instituto de I&D Estruturas e Construções—funded by national funds through the FCT/MCTES (PIDDAC) and by the FCT -UIDB/50019/2020- IDL project.

References

- Arel E, Tuğrul A (2001) Weathering and its relation to geomechanical properties of Cavusbasi granitic rocks in northwestern Turkey. *Bull Eng Geol Environ* 60:123–133
- COBA—Consultores de Engenharia e Ambiente (2003) Carta geotécnica do Porto. 2nd edition, COBA/FCUP/CMP, Porto
- FAO (2006) Guidelines for soil description. Food and agriculture organisation of the United Nations, 4 edn. Rome
- FAO (2015) International soil classification system for naming soils and creating legends for soil maps—Update 2015. World reference base for soil resources. Rome, Italy
- González de Vallejo LI, Ferrer M (2011) Geological engineering. CRC Press
- GSE—Geological Society Engineering Group Working Party Report (1995) The description and classification of weathered rocks for engineering purposes. *Quart J Eng Geol* 28(3):207–242
- Irfan TY, Dearman WR (1978) Engineering classification and index properties of a weathered granite. *Bull Eng Geol Environ* 17:79–90

- ISRM—International Society for Rock Mechanics (1978) Suggested methods for the quantitative description of discontinuities in rock masses. *Int J Rock Mech Min Sci Geom Abstr* 15(6):319–368
- ISRM—International Society for Rock Mechanics (1981) Basic geotechnical description of rock masses. *Int J Rock Mech Min Sci Geom Abstr* 18:85–110
- ISRM—International Society for Rock Mechanics (2007) The complete ISRM suggested methods for characterisation, testing and monitoring: 1974–2006. In: Ulusay R, Hudson JA (eds) Suggested methods prepared by the commission on testing methods. ISRM, Ankar
- Koike K, Yoshinaga T, Suetsugu K, Kashiwaya K, Asaue H (2015) Controls on radon emission from granite as evidenced by compression testing to failure. *Geophys J Inter* 203(1):428–436
- Letto F, Perri F, Cella F (2018) Weathering characterisation for landslides modeling in granitoid rock masses of the Capo Vaticano promontory (Calabria, Italy). *Landslides* 15:43–62
- Pereira A, Lamas R, Miranda DF, Neves L, Ferreira N, Costa, (2017) Estimation of the radon production rate in granite rocks and evaluation of the implications for geogenic radon potential maps: A case study in Central Portugal. *J Environ Rad* 166(2):270–277
- Viana da Fonseca A (1996) Geomecânica dos solos residuais do granito do Porto. Critérios para o dimensionamento de fundações directas. Universidade do Porto, Porto (PhD Thesis). <http://hdl.handle.net/10216/11101>



Characterisation of Coastal Granitic Sector Using Geomorphological and Hardness Measurements (Galicia, NW Iberian Peninsula)

Alejandro Gómez-Pazo and Augusto Pérez-Alberti

Abstract

This investigation analyses the erosion degree in the coastal edge sector of Punta Couso, a granitic area in the Galician coast (NW Iberian Peninsula). For this purpose, high-resolution images were used; geomorphological parameters, such as joint density or terrain ruggedness (calculated from LiDAR data) and fieldwork information obtained with Proceq's Equotip 3 portable hardness tester. Based on this information, this research could verify that the mean joint direction is oriented to the main wave component (Western). Also, there is a negative correlation between rock hardness values and the joint density (-0.43). This correlation increases significantly when the measurements are grouped in 10 m areas since the low tidal water edge (an estimated shoreline) reaches -0.87 . With this aggrupation method, the relation between rock resistance and joint density is clear. On the other hand, it is necessary to do a more detailed analysis of the rock composition, especially in granitic sectors, to improve these relationships' understanding.

Keywords

Granitic rocks • Coastal geomorphology • Hardness tester • Equotip • Galicia

1 Introduction

The characterisation of coastal sites has great importance in understanding the past coastal evolution and possible future changes. In this way, the scientific and technological advances allowed that coastal studies increase their detail level.

In this work, it was used two primary data sources. On the one hand, remote sensing data include high-resolution aerial images obtained by photogrammetric flights and LiDAR (Light Detection and Ranging) data. The other data source was in situ information obtained through fieldwork surveys. In this survey, an Equotip hardness tester was used to collect the values about rock resistance, which is a non-destructive technique employed in several investigations in littoral sectors as Coombes et al. (2013) or Pires et al. (2014). The field data and the parameters calculated by remote information analysed the relation between the different variables for a precise characterisation of the littoral area and the relationship between the different parameters.

The investigation concerned a granitic coastal site named Punta Couso, placed at the north part of the Ría de Arousa (NW Iberian Peninsula) (see Fig. 1). It is an excellent example of a granitic shore platform with boulders and mega-boulders dispersed above the platform.

The Galician coast is the most energetic in the Iberian Peninsula context and has mesomareal behaviour. The daily mean wave height in this area is 1.52 m (Point SIMAR 3010013, Puertos del Estado 2019). During the winter period, this value increases to 2.02 m. Storms are pretty frequent in this area, especially in the winter months (October–March). The energetic events include 3% of the days in the period 2000–2018 based on Puertos del Estado's data (2019). The dominant wave direction in this site is from the western, particularly for the highest waves. In waves above 3.83 m (level $H_{s,95}$), the mean approach direction comes from 262° .

A. Gómez-Pazo (✉)
AMBIOSOL - Departamento de Xeografía, Universidade de Santiago de Compostela, Santiago de Compostela, Spain
e-mail: a.gomez@usc.es

A. Gómez-Pazo · A. Pérez-Alberti
AMBIOSOL - Departament of Soil Science and Agricultural Chemistry, Universidade de Santiago de Compostela, Santiago de Compostela, Spain

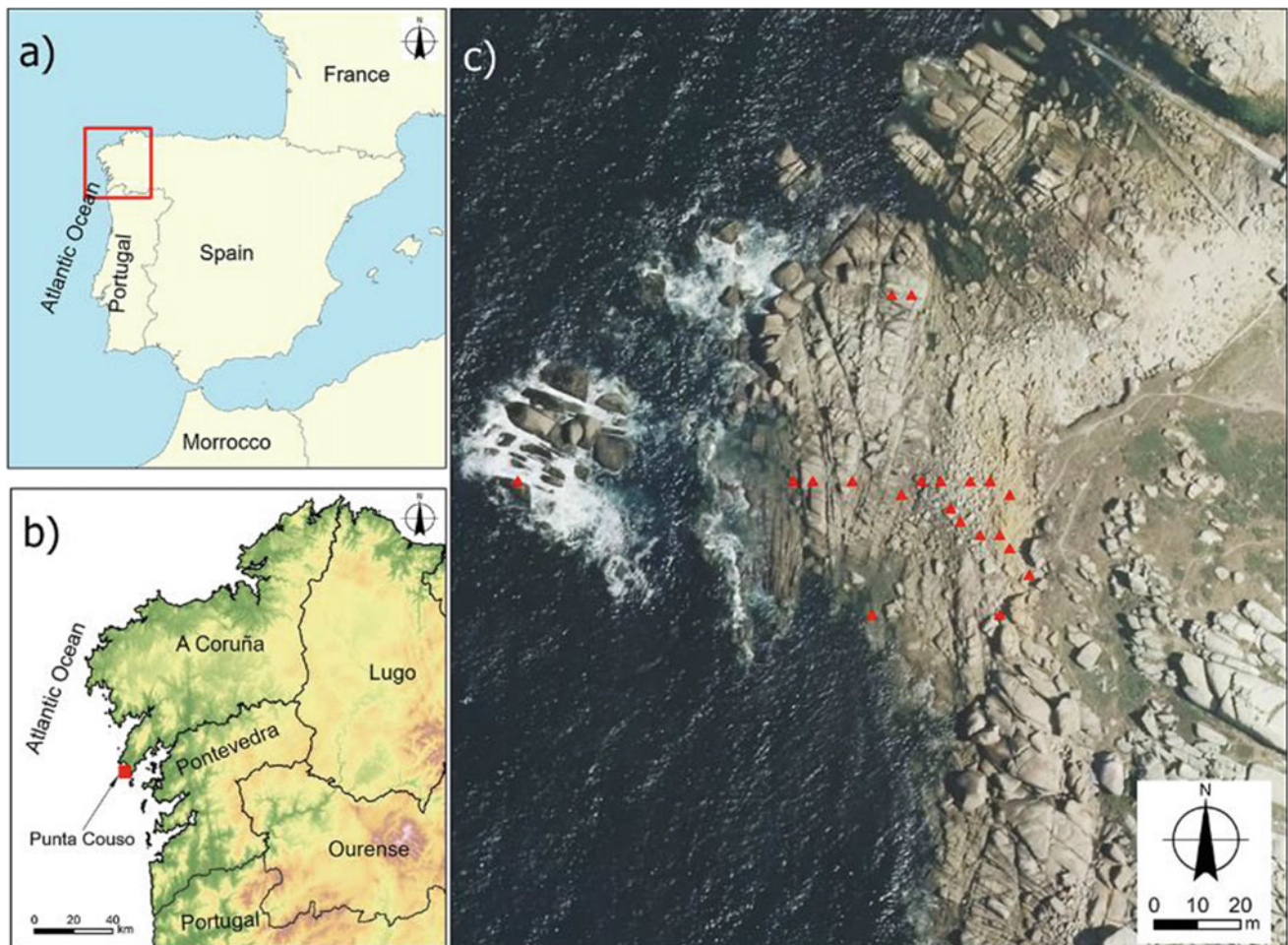


Fig. 1 Location of the study area location. **a** Peninsular context of Galicia in Iberia; **b** Punta Couso site in Galicia and **c** Sample positions represented with red triangles, background orthoimage of 2017 (IGN 2019)

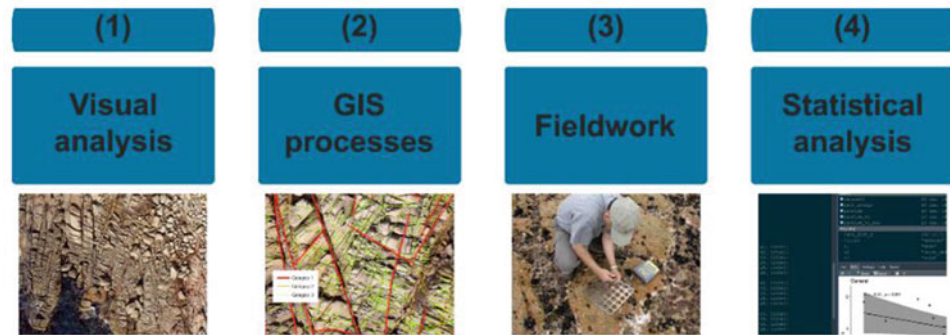
2 Materials and Methods

This investigation is based on high-resolution aerial images and orthophotographs from Spanish PNOA (Plan Nacional de Ortofotografía Aérea), IGN (2019). LiDAR information was used for the generation of high-resolution DSMs (Digital Surface Models). Concerning the fieldwork survey, it was applied a Proceq Equotip 3 to hardness assessment.

The methodology of this research combined four phases, as shown in Fig. 2.

1. The aerial images available in the study site were analysed. Definition of boundaries to the study zone to the spatial resolution and the tidal levels and register the most critical changes in this sector.
2. Definition of the structures and joints in the study area with GIS techniques and visual interpretation, categorising the joints in three levels according to their relative importance (depth and width) like Pires et al. (2016). The first level represents the structural joints, the second the joints with relevance in the mesoscale and the third level shows the superficial joints. In this phase, the Terrain Ruggedness Index (TRI) of the analysis site was calculated with the method explained by Riley et al. (1999). It was also estimated the joint density and the distance between each sample point and the sea edge (shoreline in low tidal level).
3. Design and development of fieldwork to obtain the hardness values of each rock section. This analysis employed an Equotip 3 and was selected for 20 sample points scattered through the analysis area (see Fig. 1). Each sample point was recorded 25 measurements and extracted the mean HLD (hardness value obtained with the D probe) and the standard deviation for each sample point following a similar process to Pérez-Alberti et al. (2013).
4. The information about rock hardness was processed, their relation to the other geomorphological parameters and the sea distance was calculated at this moment. This

Fig. 2 Flowchart with investigations phases



phase obtained the correlation values through Pearson's correlation coefficient at the 95% confidence level. This statistical analysis allows a complete characterisation of the Punta Couso site.

3 Results

There is a parallelism between the waves direction component, especially the most energetic waves, and the mean joint direction in the study area. In both cases, the orientation is W-E. However, there are joints in other directions, particularly in the shorter length and last joint categories (especially in category 3) (see Fig. 3b, c).

Mean values of HLD, in the Equotip measurements, are about the sea distance (shoreline) of each sample point and represented with values 1–20 (see Fig. 3d). These values do not follow a linear pattern with the sea distance. The hardness is strongly associated with joints in individual sample points. For example, in sample points 3, 5 and 13, the lower Equotip values are related to a high joint density sector, while in sample points 10 and 14, the high HLD values are linked with the low presence of joints. Analysing the mean values of sample points in intervals about 10 m from the shoreline, observed as the values are very similar in all categories (365–411). That is concerning the significant variability between each sample point.

The correlation was checked between these values from the evaluated parameters used in this study (see Table 1). The correlation between mean hardness values (HLD) and joint density was significantly negative, though this value is not too high (-0.43). If the correlation with the mean values of 10 m aggrupations from the shoreline is analysed, this negative correlation increases to -0.87 . The correlation to other parameters shows lower rates in all cases. It can highlight the negative correlation between the joint density and the sea distance, whose behaviour is similar to the relation between rock hardness and joint density.

4 Discussion

In the case of Punta Couso, the wave patterns are related clearly to the predominantly joints orientation. That generally occurs in the Galician coast context. Therefore, the waves and storms in conjunction with the lithological control have great importance in the coastal evolution, and their distinctive design is explained in previous works (e.g., Pires et al. 2016).

The importance of joint density was analysed carefully in several previous works (Naylor and Stephenson 2010). As a result, it has been verified that the lower joint density is related significantly to the higher HLD values recorded through Equotip measurements.

It is essential to highlight that the analysis in granitic platforms with an Equotip could show important variations in the mean values considering the mineralogical heterogeneity. This fact is observed in the standard deviation values, represented in the sample points graph (see Fig. 3d) (Viles et al. 2011). Grouping the values in areas in function to their distance to the sea, the importance of values moving further away from the average is smoothed.

In terms of outlook and future fieldwork surveys, it would be very interesting to apply a methodology to minimise these variations by selecting a specific number of samples in previously delimited sectors.

5 Concluding Remarks

With the information shown in this study, it is possible to extract relevant conclusions for the Punta Couso site and extrapolate them to other areas. First, the hardness values decrease according to the rise of the number of joints in the rock surface. This relation is more clearly analysing the sample values in the groups defined previously. Second, the mineralogical diversity of granitic rocks has a negative impact on the correlation values between parameters. The variation of mean values is significant for using the Equotip

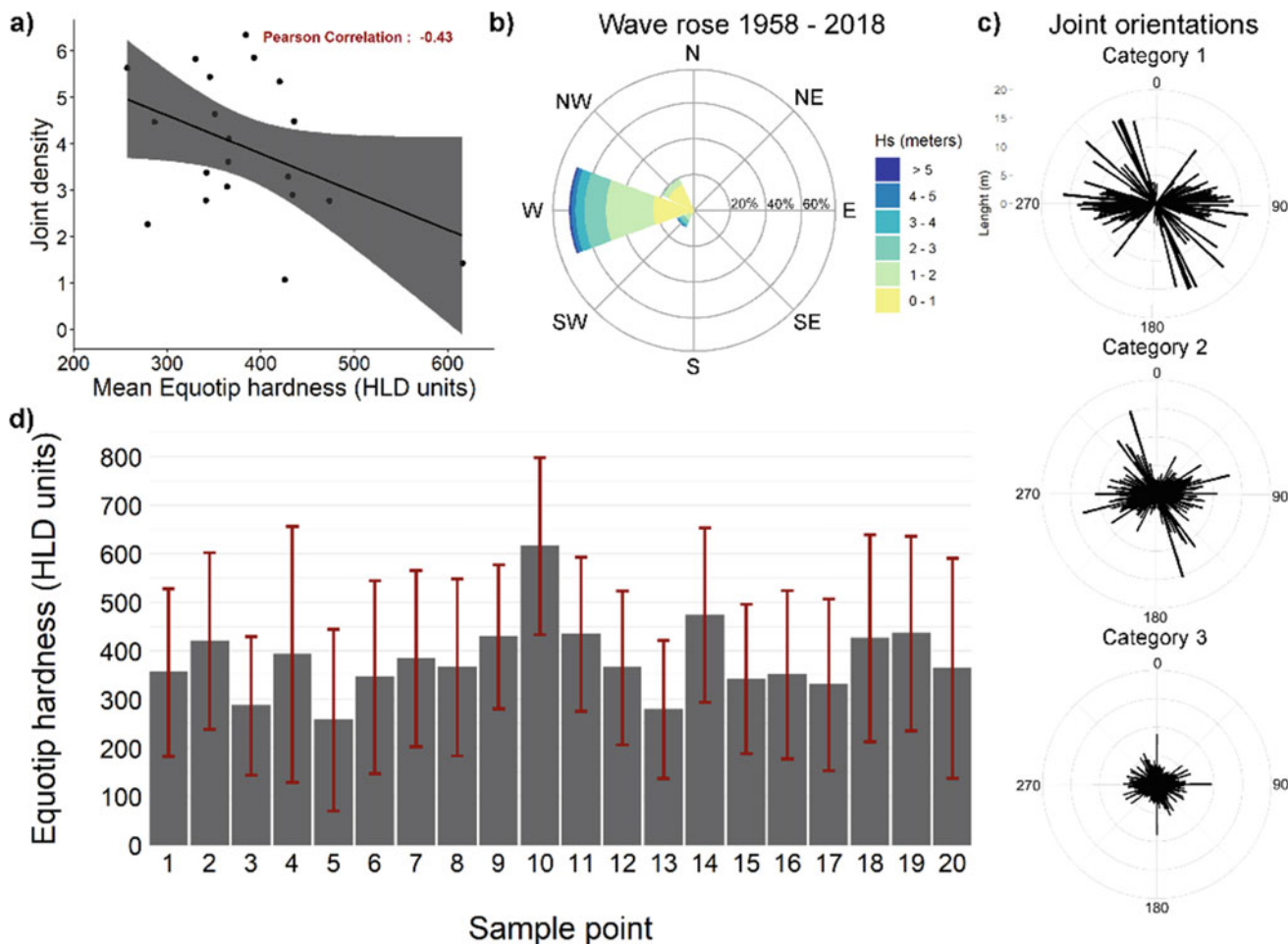


Fig. 3 a) Pearson's correlation graph between mean HLD and joint density; b) Wave rose of Point SIMAR 3,010,013 Puertos del Estado (2019); c) Joints orientation in each category and d) Bars represent the mean HLD values, and dark red lines show the standard deviation in each sample point

Table 1 Pearson's correlation coefficient values between all analysed parameters

	Joint density	TRI	Sea distance
Mean (HLD)	-0.43	0.09	0.19
Joint density		0.21	-0.35
TRI			-0.21

in minerals with different properties. Third, effects such as bioerosion have significant relevance to explain the hardness of rock values in coastal areas, as the zone of this study. Also, bioerosion could have essential effects on the hardness of rock values.

Acknowledgements This work was supported by CRETUS Institute. Alejandro Gómez-Pazo received an FPU predoctoral contract from the Spanish Ministry of Education and Innovation with reference FPU16/03050. Currently, the work of A.G-P was supported by a postdoctoral contract from the program named “Programa de axudas de apoio á etapa inicial de formación posdoutoral (2022)” founded by Xunta de Galicia (Government of Galicia, Spain). Reference number: ED481B-2022-090.

References

Coombes MA, Feal-Pérez A, Naylor LA, Wilhelm K (2013) A non-destructive tool for detecting changes in the hardness of engineering materials: application of the Equotip durometer in the coastal zone. *Eng Geol* 167:14–19

IGN–Instituto Geográfico Nacional (2019) <https://www.ign.es/web/ign/portal>. Last accessed 12 March 2020

Naylor LA, Stephenson WJ (2010) On the role of discontinuities in mediating shore platform erosion. *Geomorphology* 114(1–2):89–100

Pérez-Alberti A, Gomes A, Trenhaile A, Oliveira M, Horacio J (2013) Correlating river terrace remnants using an Equotip hardness tester:

- an example from the Miño River, northwestern Iberian Peninsula. *Geomorphology* 192:59–70
- Pires A, Chaminé HI, Pérez-Alberti A, Gomes A, Rocha F (2014) Rock strength assessment and structural features analysis on rocky coasts. In: Alejano LR, Peruchó A, Olalla C, Jiménez R (eds) *Proceedings of the Eurock'2014, rock engineering and rock mechanics: structures in and on rock masses (ISRM European Regional Symposium, Vigo, Spain)*. CRC Press/Balkema, Taylor & Francis Group, London, pp 1267–1272
- Pires A, Chaminé HI, Piqueiro F, Pérez-Alberti A, Rocha F (2016) Combining coastal geoscience mapping and photogrammetric surveying in maritime environments (Northwestern Iberian Peninsula): focus on methodology. *Environ Earth Sci* 75(3):1–17
- Puertos del Estado (2019) <http://www.puertos.es/en-us/oceanografia/Pages/portus.aspx>. Last accessed 12 March 2020
- Riley SJ, Degloria SD, Elliot R (1999) A terrain ruggedness index that quantifies topographic heterogeneity. *Intermountain J Sci* 5(1–4):23–27
- Viles H, Goudie A, Grab S, Lalley J (2011) The use of the Schmidt Hammer and Equotip for rock hardness assessment in geomorphology and heritage science: a comparative analysis. *Earth Surf Proc Landfor* 36(3):320–333



Hardness Tester for Analog Planetary Rocks: A Preliminary Assessment in Microgravity Flight

Ana Pires, Catarina Costa, Rui Moura, Aaron H. Persad, Jason Reimuller, Derek Gowanlock, Shahrukh Alavi, Heather Wright Beatty, José Almeida, Fernando Almeida, Eduardo Silva, Augusto Pérez-Alberti, and Helder I. Chaminé

Abstract

This research is focused on the study and comparison of different methods to select the most suitable non-destructive hardness-measuring equipment capable of assessing the hardness of analog planetary rocks in space environments. Proceq's Equotip 3 equipment proved to be the most suitable alternative, and it was possible to carry out, for the first time, a microgravity experiment inside a Falcon 20 aircraft during parabolic flight. Studying the rebound principle and recognizing that this value is affected by the variation in gravity, it was essential to propose compensation values to correct it,

based on previous works regarding impact direction change. This study addresses the preliminary results of ongoing research in the area of rock hardness detection.

Keywords

Hardness tester • Equotip • Geomaterials • Astrogeology • Gravity compensation

A. Pires (✉) · J. Almeida · E. Silva
Centre for Robotics and Autonomous Systems CRAS|LSA, DEE,
School of Engineering (ISEP), Polytechnic of Porto, Porto,
Portugal
e-mail: ana.c.pires@inesctec.pt

C. Costa · F. Almeida
Faculty of Engineering, University of Porto, Porto, Portugal

R. Moura
ICT and DGAOT, Faculty of Sciences, University of Porto, Porto,
Portugal

A. H. Persad
Massachusetts Institute of Technology (MIT), Cambridge, USA

J. Reimuller
International Institute of Astronautical Sciences, Boulder, CO,
USA

D. Gowanlock · S. Alavi · H. W. Beatty
National Research Council (NRC), Aerospace, Flight Research
Laboratory, Ottawa, Canada

A. Pérez-Alberti
AMBIOSOL—Departament of Soil Science and Agricultural
Chemistry, University of Santiago de Compostela, Santiago de
Compostela, Spain

H. I. Chaminé
Laboratory of Cartography and Applied Geology, Department of
Geotechnical Engineering, School of Engineering (ISEP),
Polytechnic of Porto, Porto, Portugal

Centre GeoBioTec|UA, University of Aveiro, Aveiro, Portugal

1 Introduction and Background

Human activities related to space are no longer merely understood as 'looking at planted flags'. From the moment that the potential of space was recognized in all sectors, a continuing number of nations and private companies have been encouraging its exploitation as a technological asset, potentially profitable, which tends to motivate global cooperation. Planetary geology, also called Astrogeology, is the science centered on the connection between astronomy, astrophysics, and geology, explaining the evolution of celestial bodies based on the study of geological processes. Several space missions focused on Astrogeology have visited the Moon, Mars, Venus, and other celestial bodies. The increasingly recurrent use of automatic and/or remote systems in most industries is a global reality, either to allow mankind to concentrate on more complex activities, to ensure their safety, or even to make some process possible that would not be in a manual way. The space industry has always been a strong reason for several robotizing processes: transmission of information, geopositioning, or scientific experiments.

The number of unmanned missions prior to the first manned Apollo 11 mission exceeds three dozen. Most Luna missions emphasized geological milestones such as Luna 2 by measuring the magnetic field, Luna 9 that took the first images of the surface, or Luna 16 that sampled it. The Surveyor missions took those geological objectives as the primary scientific goal, some of them going into the field of

soil mechanics. The Surveyors' main objectives were to obtain better images of the lunar surface and determine if the terrain was safe for human landings. The Surveyors were equipped with a television camera.

Additionally, missions such as Surveyors 3 and 7 took soil mechanics experiments and a surface sampling scoop that could both excavate and perform soil mechanics tests. Surveyors 5, 6, and 7 had magnets attached to the footpads and an alpha particle instrument to perform the lunar material's chemical analysis. Some simple experiments, such as the footpad prints, allowed for estimates of soil bearing calculations. Thus, it was proven that space research could no longer be understood as a theoretical scientific study without a sound practical foundation. These missions included numerous scientific experiments onboard, collecting information, and transmitting it in real time (Siddiqi 2000). In this sense, both ESA (European Space Agency) and NASA (National Aeronautics and Space Administration), together with large international companies, have already shown interest in initiating the construction of space infrastructures. Applied geology, in-situ geotechnical investigations, and in-depth knowledge of the planet's geological materials or celestial body become entirely essential for this effect. Although destructive laboratory assessments have been replaced by portable devices capable of characterizing and evaluating rock materials in-situ, analysis of data on Earth is still relevant and conducting manned missions justified by the weight of human observation. For example, on the Apollo 17 mission, Harrison Schmitt, the first and only lunar astronaut with a background in geology, had the opportunity to directly observe and confirm many geologic features, such as soil type and texture, lithology (Bailey and Ulrich 1975). Also, H. Schmitt observed and confirmed the Moon's geomorphology and recognizes signs of impact cratering, mass movements, and volcanic activity (Bailey and Ulrich 1975).

1.1 The Rationale: Space Geo-Exploration

Lunar exploration is becoming more and more critical in recent space missions. Planetary exploration is not limited to the Moon or Mars, but it is essential to include asteroids, comets, and meteors. Sampling and analysis have posed significant past and present challenges in such a low gravity environment as comets and asteroids. The Philae's failure to land on the 67P/Churyumov–Gerasimenko comet is one example of how very low gravity coupled with the heterogeneity of geology of such planetesimals can impair a mission. Recent missions to Ryugu (performed by Hayabusa 2) and Bennu (performed by the OSIRIS-REx mission) demonstrate how microgravity research on Earth is important to geological sampling's planning and success. To further highlight that microgravity platforms are important in

assessing geological conditions, one of the experiments carried out during a microgravity campaign was an experiment related to asteroid exploration (Parker et al. 2019). Moura et al. (2019, 2020) highlight another geophysical nature experiment that was also relevant to be carried out successfully in that environment. The past 50 years of research has shown that the development related to space robotic exploration and planetary geology is becoming increasingly innovative. Those missions comprehend several science instruments and state-of-the-art tools for acquiring information about the geology, atmosphere, environmental conditions, and other relevant geo-data. The measurement of hardness of ground, samples, geomaterials, or rocky surfaces can extrapolate several mechanical characteristics of the material under test, namely on its compressive strength. Various space missions included soil mechanics measurements using penetrometers. It is worth mentioning Luna 17 and 21, which included robotic penetrometers on the Lunokhod rovers and Apollo 14, 15, and 16, whose penetrometers required manual operation by astronauts.

2 Microgravity Flight and Research: BIO103 Campaign

This study presents a preliminary approach within the Polar Suborbital Science in the Upper Mesosphere (PoSSUM) Project, a NASA-supported citizen science astronauts research program (projectpossum.org), and PoSSUM BIO103 Microgravity Research Campaign of 2019, promoted by the International Institute of Astronautical Sciences (IIAS) educational program in Bioastronautics with Extravehicular Activity (EVA) Concentration. The rock hardness experiment was carried out under the microgravity campaign framework at the National Research Council (NRC) of Canada (Ottawa) and is featured in Fig. 1. During the Falcon 20 aircraft flight, this type of investigation completed several parabolas to create microgravity and lunar gravity environments. The data gathered enabled researchers to understand the geological material behavior of rocks in a microgravity environment. This research aimed to evaluate the rock hardness testing function of the Proceq's Equotip 3 (www.proceq.com), particularly the equipment behavior in microgravity and lunar gravity environments, well as to carry out a preliminary approach for data correlation. The experiment used rock samples (namely, basalt and limestone) collected from Flagstaff (San Francisco Volcanic Field, Arizona, USA). The Flagstaff area is on the Colorado Plateau's southern margin and is dominated by the San Francisco volcanic field underlying the limestone-capped plateau (Bezy 2003). The rock samples from the Flagstaff area (San Francisco Volcanic Field) are: (i) basalt from the crater; (ii) gray limestone from Kaibab formation.

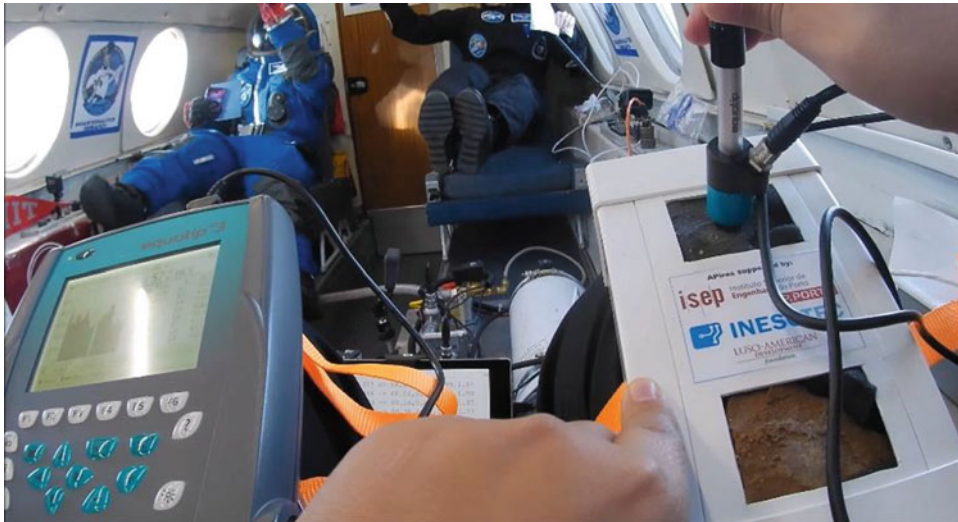


Fig. 1 Experimental set-up inside the National Research Council (Ottawa, Canada) FALCON20 aircraft, under the scope of PoSSUM Project microgravity campaign: Proceq's Equotip 3 apparatus from the University of Santiago de Compostela, Spain (on the left); and rock

sample box developed by CRAS|LSA-INESC TEC|School of Engineering (ISEP), Polytechnic of Porto (on the right). The rock sample box is visible with the dark-colored, fine-grained basalt, and the gray limestone from the Flagstaff area (Arizona, USA)

3 Hardness Measurement Methods

Hardness is defined as a material's ability to resist plastic deformation when in contact with another material. Also, hardness is not a mechanical property, but its value depends directly on the method, scale, and parameters defined within the same test. Compressive strength is one of the essential material characteristics for the design of structures. The technique that tests this property is a destructive practice that requires a significant sample of the material under study. It is often not possible to obtain samples, and above all, in space exploration, non-destructive and portable methods are preferred (Kılıç and Teymen 2008). The hardness measurements are directly related to the compressive strength to provide quick, easy, and reliable information on the material's condition. The measurement of metal hardness is fully regulated, from the practice itself to conversion between scales. However, the same does not happen with rocky materials, therefore the need for this study. There is a lack of investigations aimed at selecting the most appropriate hardness measurement method for Astrogeology. In-depth studies were carried out on the following hardness methods (ISRM 2007, 2015): Vickers test, Brinell test, Rockwell test, Knoop test, Shore durometer, dynamic and static penetrometers, Schmidt hammer, and Equotip. The Brinell, Vickers, Rockwell, and Knoop tests do not present adequate loads for measurements

on rocky materials (according to ISO 6506, ISO 6507, ISO 6508, and ISO 4545: www.iso.org).

The Shore durometer excelled in the low price and low mass of the equipment yet only permits measurements on rocks of high or very high resistance. On the other hand, the static penetrometers showed advantages, such as the lack of sample preparation, the continuous registration of the applied force, and the possibility of operating in any direction. However, the high price and the possibility of only evaluating rocks with extremely low, very low, and low resistance are the main drawbacks of static penetrometers. On the other hand, dynamic penetrometers are cheaper; still, they have the same disadvantages as static and are heavier (e.g., ISRM 1980, 2007, 2015).

Schmidt's hammer (type L—rock type) presented itself as a very light, cheap, and versatile alternative (e.g., Schmidt 1951; Poole and Farmer 1980; Pires et al. 2014a, b). However, the related high impact energy requires large samples and only test medium and high strength rock materials. Equotip, despite being more expensive and sensitive to roughness, has established itself as the most general possibility, capable of testing from low to very high resistant rocks and with very small minimum sample sizes (e.g., Viles et al. 2011; Pérez-Alberti et al. 2013). The biggest problem regarding using rebound equipment in hardness measurements is gravity and orientation on its operating principle, changing the results' quality.

4 Chosen Method and Discussion: Proceq's Equotip Apparatus

From an applied geologist or geotechnical engineer's perspective, the most relevant attribute of a hardness-measuring instrument used in space is the range of materials that it can test. Suppose it is possible to include a one instrument solution for soils or soft rocks, miscellaneous, spaceship components, and any other material that will suffer wear and tear and should be evaluated. In that case, it will be the best alternative. The apparatus covering a more significant number of degrees of resistance of the rocks is the Equotip, as displayed in Fig. 2.

4.1 Compensation Proposal for the Change in Gravitational Acceleration

The selection of Proceq's Equotip as the most suitable instrument for measuring hardness in an extreme environment requires recognizing that its principle of operation is affected by changes in gravity. Thus, it is necessary to propose a solution to adapt the results to the environment in which it is utilized. The proposal presented consists of developing, just like the compensation tables for the variation of orientation presented in ISO 16859 (2015), rules to correct the gravity allocation (Proceq 1985; Frank et al. 2019). The hardness measurement is a function of the speeds at which a magnet passes through the coil before and after impact with the sample. This coil is located, in the case of impact device D, 2 mm (h_1) from the impact point, as shown in Fig. 3. It is intuitive to understand that the difference

between the measured speed and the effective impact speed (v_i) depends directly on the measurement orientation (θ) and gravity (G), as shown in Eq. (1), in which E_m refers to the elastic potential energy and m to the mass of the impact body.

$$v_i = \sqrt{2Gh_1 \cos\theta + \frac{2E_m}{m}} \tag{1}$$

To outline the possibility that this theoretical model can justify the compensation values, a study was carried out to determine if the tabulated factors are only related to the variation in the amount of movement (or the impact speed). In this sense, vertical measurements were evaluated, with movement ascending ($\theta = 180^\circ$) and descending ($\theta = 0^\circ$) of the impact body. The chosen angles are justified by eliminating the friction contribution, which must be the same in both situations.

Table 1 presents the compensation values obtained based on the change in movement by altering the impact direction.

It appears that the normalized compensation contains correction factors numerically superior to those obtained, which indicates that there were more influential elements in the variation of the direction of impacts, such as friction between the impact body and the inner walls of the guide tube. Then, it was found that this simplified model does not fully justify the orientation compensation, making it necessary to carry out a detailed model of Equotip and its measurement process capable of predicting the tabulated values. One of the models containing the necessary information is Digital Twin, which consists of an iterative digital simulator of the real process. This model requires an enormous level of detail, representing all components with high precision and connections between them, which possibly only would be attainable with the collaboration of Proceq. Likewise, not having the necessary information for elaborating the Digital Twin model, it is impossible to propose a relationship between the direction tables and the influence of gravity or even conjecture gravity compensation. The development of this model and the degree of its detail do not suppress the need, as far as possible, for empirical tests to validate the values obtained, for example, in a microgravity campaign.

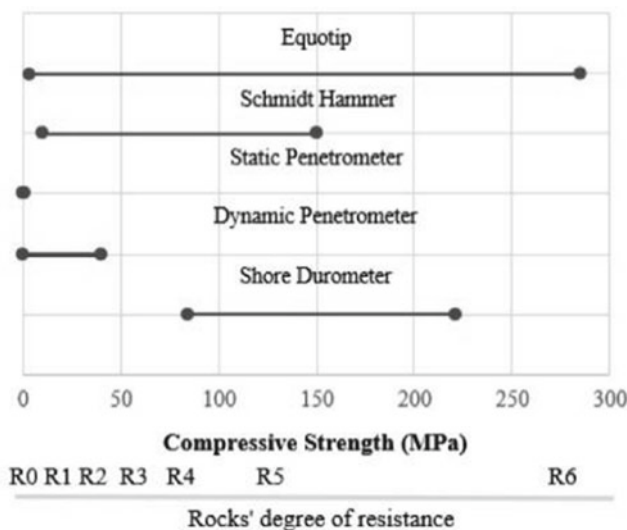


Fig. 2 Compressive strength range for hardness measurer (R degree scale from ISRM 1980, 2007)

Fig. 3 Proceq's Equotip hardness measurement scheme

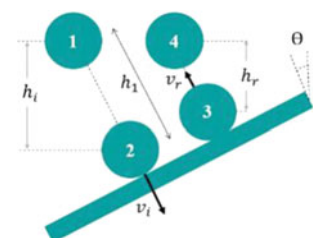


Table 1 Compensation for orientation changes for $\Theta = 180^\circ$ for de impact device D of Proceq’s Equotip portable hardness tester (HLD stands for the impact device D Leeb hardness value)

HLD	Regulated compensation from ISO 16859	Calculated compensation
200	-33	-21
300	-29	-14
400	-25	-11
500	-22	-10
600	-19	-4
700	-17	-4
800	-15	-4

5 BIO103 Campaign Results

Considering that it is not possible to propose a relationship between the direction tables and the influence of gravity, as well as to quantify the anticipated variation in a hardness measure conducted on Earth or the Moon, it is expected to obtain higher values in lunar gravity compared with the ground truth (Earth) values, and even higher values in microgravity. That is justified because a lower gravity causes a lower impact speed, such as a higher orientation angle.

Figure 4 illustrates the measurements carried out on Earth and during lunar gravity and microgravity in parabolic flight on NRC's Falcon 20 aircraft (including 2G) on both samples (limestone and basalt). For the ground truth sampling, 50 measurements were taken since the prior studies pointed to this value as the minimum number for a representative sample. The measurements collected in the BIO103 campaign were gathered in the Equotip memory and confirmed by a camera that was recording the flight and the gravity measurer. To develop a quantitative preliminary consideration, the measurements that distance more than 2 standard deviations for every experiment were treated as outliers.

The HLS (Hardness Conversion Table) unit stands for the conversion from Leeb to Shore is based on an Equotip measurement using a standard conversion for metallic

materials. Although this scale or conversion is not the most used to represent rocky materials, it was predefined in Equotip 3, has not changed, and the comparisons remain valid.

The median results of the hardness measurements HLS can be summarized in Table 2.

These values should not be used as accurate absolute hardness values because the number of measurements and the samples’ roughness value were not respect the applicable standards. However, relative comparisons are interesting. Besides, according to Proceq’s booklet (Frank et al. 2019), the device’s load movement must be carried out a short distance from the sample and never be in contact with it. This principle could not be guaranteed due to the difficulty of operating under reduced gravity.

Comparing the ground truth values to the ones measured in reduced gravity, all the hardness measurements tend to be higher on both samples. Although this meets the predictions based on orientation compensation, it would be expected to obtain higher hardness values in microgravity simulation than in lunar.

This experiment and the preliminary data obtained were essential to understanding better the portable hardness tester’s behavior under extreme environments and the same manual actuation. Equotip proved effective in different acceleration environments, acquiring a low number of empty

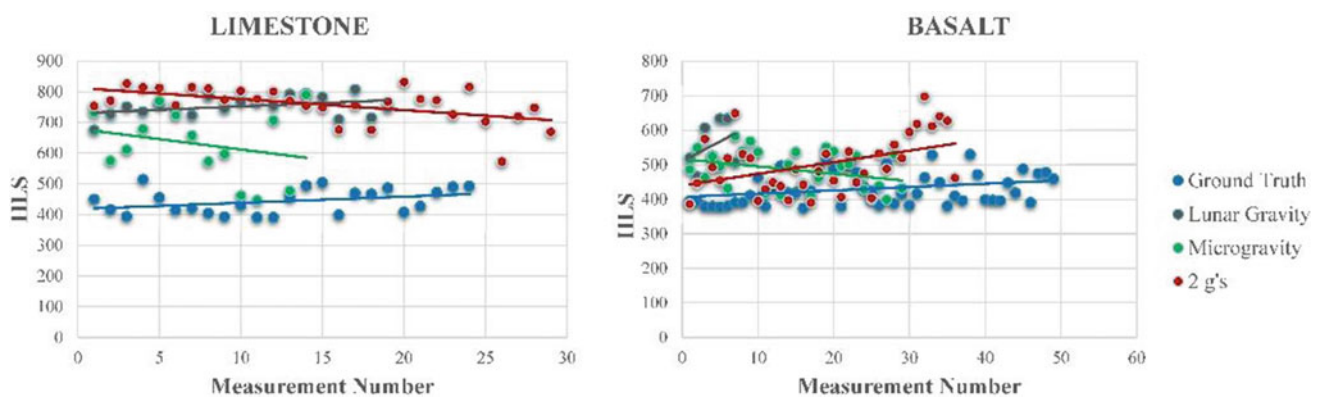


Fig. 4 BIO103 campaign results of limestone and basalt on Earth and simulation of lunar gravity, micro, and 2 g’s

Table 2 Median of the results obtained in the BIO103 campaign. The rock samples are from the Flagstaff area (Arizona, USA)

	Limestone	Basalt
Ground truth	440	418
Lunar gravity	751	525
Microgravity	634	494
2 g's	770	487

values during the measurements, even in 2 g's acceleration. On the other hand, it is possible to see that the movement precision required to perform a correct hardness measurement is difficult to accomplish manually under lower gravity.

6 Concluding Remarks and Outlook

Despite all the hardness measurements carried out outside the terrestrial environment until now having used penetrometers, the instrument's maximum value was reached several times during the Apollo 14 mission. In the Venera 14 mission, there were also doubts about the veracity of the results. Transporting a hardness meter with low maximum hardness directly compromises the space mission's benefits (NASA 1973). The use of Equotip increases the possibility of testing rock materials whose hardness is unknown and evaluating structural metals (e.g., vessels). To include Equotip in space exploration is an enormous advantage to ensure the proper compensation for the change in gravity in its operation. The beginning of the construction of infrastructures in space depends on the geology of celestial bodies. In-situ analyses are essential, complemented with further laboratory studies, as well as manned missions. It would be essential to develop the Equotip equipment's automation to improve its performance and meet the operating requirements, avoiding inconsistencies in the measurements. The Equotip could easily be reformulated and installed in a geo-robotic Rover or in a spacesuit to carry out total or partially automatic measurements.

Acknowledgements Our thanks are due to the National Research Council (NRC) of Canada for providing all the safety requirements during the flight campaign and all the land support. Special thanks are also due to Dariusz Burnat (Proceq), Sonia Girón, and Marcel Poser (Screening Eagle Technologies) for all the support concerning Equotip's equipment. AP was partially sponsored by Luso-American Development Foundation (FLAD). The investigation was funded by a research contract under the Portuguese Foundation for Science and Technology, FCT (CEECIND/00835/2018) to AP and supported within project UIDB/50014/2020. HIC was supported under the framework of the LABCARGA|ISEP re-equipment program (IPP-ISEP|PAD'2007/08) and Centre GeoBioTec|UA (FCT-UID/GEO/04035/2020). In addition, APA received support from CRETUS—AMBISOL|USC (Spain). Finally, we acknowledge the anonymous reviewers for the constructive comments that helped to improve the manuscript.

References

- Bailey NG, Ulrich GE (1975) Apollo 17 voice transcript pertaining to the geology of the landing site. U.S. Geological Survey, Branch of Astrogeology Flagstaff, Arizona
- Bezy JV (2003) A guide to the geology of the Flagstaff area. Arizona Geological Survey, Tucson
- Frank S, Frehner C, Akhlaghi A (2019) Equotip application booklet: portable hardness testing – Leeb, Portable Rockwell and UCI. Proceq SA, Switzerland
- ISRM – International Society for Rock Mechanics (2007) The complete ISRM suggested methods for characterization, testing and monitoring: 1974–2006. In: R Ulusay, JA Hudson (eds.) Suggested Methods Prepared by the Commission on Testing Methods, ISRM, Ankara
- ISO 16859 (2015) Metallic materials — Leeb hardness test — Part 1: Test method; Part 2: Verification and calibration of the testing devices; Part 3: Calibration of reference test blocks (www.iso.org)
- ISRM – International Society for Rock Mechanics (2015) The ISRM suggested methods for rock characterization, testing and monitoring: 2007–2014. In: R Ulusay (ed.) Suggested Methods Prepared by the Commission on Testing Methods, ISRM, Springer, Berlin
- ISRM – International Society for Rock Mechanics (1980) Rock characterization, testing and monitoring: ISRM suggested methods. In: ET Brown (ed.) suggested methods prepared by the Commission on Testing Methods, ISRM, Pergamon Press, Abstracts 15(6), 319–368
- Kılıç A, Teymen A (2008) Determination of mechanical properties of rocks using simple methods. *Bull Eng Geol Environ* 67:237–244
- Moura R, Almeida F, Persad A, Ferreira A, Teixeira L, Gowanlock D, Sant'Ovaia H, Reimuller J (2019) Preliminary results of compressional seismic wave velocity measurements of lunar regolith simulant (JSC-1) during a microgravity flight campaign. In: Proceedings of the 19th International Multidisciplinary Scientific GeoConference, SGEM, Albena, Bulgaria
- Moura R, Almeida F, Ferreira A, Persad A, Teixeira L, Gowanlock D, Sant'Ovaia H, Reimuller J, Parkhill M, Pires A (2020) Microgravity geophysical experiments with JSC-1 lunar regolith simulant: results and future developments within project PoSSUM. In: Proceedings of the Next-Generation Suborbital Researchers Conference, Broomfield, Colorado
- NASA (1973) Apollo 17: preliminary science report. National Aeronautics and Space Administration, NASA-SP 330, Washington DC [<https://www.hq.nasa.gov/alsj/a17/as17psr.pdf>] (last accessed October 2020)
- Parker AH, Walsh KJ, Durda DD, Nowicki K, Project ESPRESSO Team (2019) Magnetic grapples for asteroid regolith sample collection, anchoring, and mobility. In: 50th Lunar and Planetary Science Conference 2019 (LPIContrib.No.2132) [<https://www.hou.usra.edu/meetings/lpsc2019/pdf/3111.pdf>] (last accessed December 2020)
- Pérez-Alberti A, Gomes A, Trenhaile AS, Oliveira M, Horacio J (2013) Correlating river terrace remnants using an Equotip hardness tester:

- an example from the Miño River, northwestern Iberian Peninsula. *Geomorphology* 192:59–70
- Pires A, Chaminé HI, Pérez-Alberti A, Gomes A, Rocha F (2014a) Rock strength assessment and structural features analysis on rocky coasts. In: LR Alejano, A Perucho, C Olalla, R Jiménez (Eds.) *Proceedings of the Eurock'2014, Rock Engineering and Rock Mechanics: Structures in and on Rock Masses (ISRM European Regional Symposium, Vigo, Spain)*, CRC Press/Balkema, Taylor & Francis Group, London, pp. 1267–1272
- Pires A, Chaminé HI, Piqueiro F, Rocha F (2014b) Coastal geo-engineering techniques for the assessment of rock armour structures. *Mar Georesour Geotech* 32(2):155–217
- Poole RW, Farmer IW (1980) Consistency and repeatability of Schmidt hammer rebound data during field testing. *Int J Rock Mech Min Sci Geomech Abst* 17:167–171
- Proceq (1985) *Equotip hardness tester: conversion tables, impact device D*. Proceq SA, Switzerland
- Schmidt E (1951) A non-destructive concrete tester. *Concrete* 59 (8):34–35
- Siddiqi AA (2000) *Challenge to Apollo: The Soviet Union and the space race 1945–1974*. NASA History Series SP-2000-4408, Washington DC
- Viles H, Goudie A, Grab S, Lalley J (2011) The use of Schmidt Hammer and Equotip for rock hardness assessment in geomorphology and heritage science: a comparative analysis. *Eart Surf Proc Land* 36(3):320–333

Geoenvironment, Water, and Climate Change



Environmental and Productive Applications of Tailor-Made Technosols: Biosphere Learnings

Felipe Macías García, Isabel Macías García, and Felipe Macías Vázquez

Abstract

A review of the origin and evolution of the concept, foundations, capabilities, and technology of tailor-made Technosols and reactive wetlands and their possible environmental and productive applications is carried out. Among them, highlights the possibility of its use in the rehabilitation of soil, water, and ecosystems degraded/contaminated by mining processes, public works, industrialization, or forest fires that lead to a deficiency of the soil fulfilment of its environmental and productive functions. Tailor-made technosols, being designed “to measure” and depending on the needs, can significantly reduce or eliminate the risks derived from organic and inorganic pollutants in soil, water, and biota, modify the physicochemical acid–base conditions, redox and surface reactions, increase fertility, productive capacity, biodiversity, biotic activity, durable carbon sequestration, buffer capacity against pollutants, and improve the availability of helpful water and resistance to soil erosion, favouring human health and the conservation of the ecosystems. As they are designed and produced “at the image” of natural soils, tailor-made Technosols perform the same biogeochemical reactions, processes, and functions as their models, magnifying certain properties, which increases their efficiency and usefulness. They evolve as natural soils, being subject to the Circular Economy imposed by the biosphere.

Keywords

Biosphere • Tailor-made Technosols • Biogeochemical systems and cycles • Environment • sustainability

1 Introduction: Biogeochemical Cycles—Soil Formation and Its Functions

In the terrestrial biosphere, soils are the great regulators of biogeochemical cycles, protecting the quality of water and biota and decisively influencing human health and conserving ecosystems. However, many human activities have been and are causing the elimination or deterioration of soil's quality and the loss or reduction of their environmental and productive functions, as defined by the European Soil Protection Strategy (Commission of the European Communities 2006) and recognized as ecosystem services in the European Green Deal (European Commission 2020). Some examples are mining processes, high-intensity fires, agronomic and/or livestock over-exploitation, urban planning, industrialization, inadequate waste management, deforestation, desertification, etc. There are also many mechanisms by which soil deterioration occurs: erosion, acidification, excess inorganic and organic pollutants, loss of organic matter and carbon sink capacity, compaction, salinization, structure degradation and sealing, which have been recognized among potential soil threats. The degree of deterioration is variable, being able to reach the complete elimination of the soils by erosion (conditions of extreme Rhexistaxy) and, in the worst case, to become a source of transmission of pollutants towards the most sensitive systems with a less buffer capacity of their environments such as water and biota.

As defined by Vernadsky (1929), the biosphere uses the soil to control the mobility of all species that can generate the chemical elements present in the earth's lithosphere, in the atmospheric and hydrosphere systems of living beings. For the biosphere, nothing is considered waste, only components

F. M. García · I. M. García
Recursos y Valorización Ambiental, Santiago de Compostela,
Spain

F. M. Vázquez (✉)
AMBIOSOL, Universidad de Santiago de Compostela, Santiago
de Compostela, Spain
e-mail: felipe.macias.vazquez@usc.es

that are reused, recycled, and transformed to adapt to the demands imposed by the search for thermodynamic balance. Through biogeochemical cycles, exchanges between the different biospheric compartments occur, and the soil is formed by transforming the lithosphere produced by the joint action of living beings and weather over time. Whatever the composition of the surface materials, the biosphere always tries to put soil in the epidermis of the lithosphere, with a porous structure and aggregates with organic and inorganic colloids, mostly flocculated, within which it reproduced again the organization of the lithosphere, hydrosphere, atmosphere, and biosphere elements that constitute them. The aggregates, dominated by organic and inorganic fine fractions, have a substantial internal and external specific surface in which the presence of permanent and/or pH-dependent electrical charges is frequent, which continuously interact with other edaphic components through reactions with variable kinetics, from microseconds to millennia (Sparks 1991, 1999) transforming energy through metabolic cycles. The microporous structure allows infinite simultaneous reactions between organic and mineral nanoparticles, microorganisms, and the dissolution of the soil. It is the great invention of the biosphere and what differentiates soils from other surface formations, such as rocks or sediments, in which the energy received from the sun is rapidly dissipated. In contrast, this energy is lost more slowly in soils, descending through metabolic cycles, allowing further development of biocenoses and organo-mineral interactions (Kleber et al. 2015).

The interaction set inside the soil increases its differentiation concerning the starting material and progressively increases its potentialities. This improvement in the capacities of the soil to fulfil its functions is called biostaxia conditions (Erhardt 1967). Soils in biostaxy progress until they are eroded or conditions close to thermodynamic equilibrium are reached in all their mineral composition (Pédro (1968) (Geric soils, FAO (2006, 2014)) or residual system (Chesworth 1973), closing the cycle of edaphogenesis and transforming itself back into the lithosphere. Maintaining the biostatic conditions for as long as possible and on the largest possible surface is the main objective that can be achieved by following the guidelines of the Circular Economy of the biosphere, which is the main model we must follow if we want to harmonize our actions with those produced by the natural systems in which we are included.

When soils are eroded, degraded, or polluted, natural processes restart their formation or recovery of functions, but this process is usually slow. It does not work at the rate of human needs but rather with natural cycles, which leads to the formation of small thicknesses of soils over long periods (of the order of cm/century, when starting from original consolidated materials). They can occur more quickly under certain conditions, especially when a loose material of fine size, easily alterable, and with high contents of bioavailable

nutrients is deposited on the lithosphere. This is the case of wind loess deposits, volcanic ash, or alluvium transported by rivers, where, if the climatic conditions are favourable, soil can be formed very quickly.

There have also been experiences of rapid soil formation with human intervention. In most cases, soils with negative characteristics have been formed since most of the materials have developed residues of human activities, whose composition did not have enough nutrients or contained abnormally high concentrations of bioavailable pollutants mobilized, affecting their water and biotic environment. These anthropic soils are what FAO (2006, 2014) called Technosols when their content in materials made, modified or moved by humans (artefacts, previously anthropogeomorphic materials; FAO 1998), exceeds 20% by weight or volume. Most of these soils, products of negligence or mismanagement, are environmentally unsuitable, unproductive, and a source of polluting risks, so they must be rehabilitated. However, in certain situations, human intervention has contributed to the formation of productive anthropic soils, which exceed the qualities of the natural soils in their surroundings. This is the case of the historical soils of the Maori, many of the plaggen soils, the Brazilian sambaquis, the Mexican chinampas, the Horticultural horizons, and, above all, of the Amazonian “Terras pretas” (Sombroek et al. 1993), among other examples of success. The case of the “Terras pretas” (black soils) is, perhaps, the most paradigmatic, since they have been able to generate productive soils in a context of aged, ferralitic soils, with very low fertility and the capacity to regenerate their properties after fire stress or after massive logging that eliminate the already scarce recycled and retained fertility in its surface horizon. Hence, Win Sombroek’s dream that each farmer makes his black soil and creates “new Terra preta” (Glasser and Wood 2004) and the importance of understanding the processes of edaphogenesis as a learning system to improve waste management activities and their consequences in the processes of transformation and biogeochemical recovery (Macías 2004; Macías et al. 2007; Macías and Camps Arbostain 2010). These examples show that, under certain conditions, the soil can begin its functions, or at least part of them, in much shorter times than those normally recognized, and that human activity can promote the formation, and even “make soil”, relatively quickly and with edaphic conditions that improve those of the surrounding natural soils.

2 Evolution of the Fundamentals of the Recovery of Degraded Soils

When soil is eliminated by erosion, degradation, or contamination, it can be expected to regenerate itself, apply corrective systems, or use tailor-made Technosols.

“Self-regeneration” consists of letting natural processes take charge of the recovery of degraded soils. It has been the most followed procedure when there is no adequate knowledge or means and when the use of the degraded area has not been immediately necessary.

Recovery based on amendments and fertilizers has been the most used procedure in regenerating recently degraded or contaminated areas. It is based on the knowledge of the positive effects of incorporating foreign materials with the appropriate properties, such as liming substances, organic and inorganic residues, and fertilizers. Although they had already been used in classical and mediaeval cultures, especially manures and carbonate materials, their use on a large scale increased with the progress of Agricultural Chemistry from the eighteenth century. This knowledge is behind the great success in the food production capacity of current agricultural systems. Therefore, it is not surprising that agricultural techniques were direct and widely used to recover soils degraded by mining activities, public works, or urban planning. The progressive increase in the raw materials and fertilizers cost urged the search for new sources of cheaper resources for recovery activities, like by-products and residues, such as foundry slags, ashes, and other industrial waste, which complemented the action of manure and fertilizers and, later, of composts, vine waste and other organic biomass and necromass waste, which provided energy for soil microorganisms, as well as some nutrients.

3 Tailor-Made Technosols: Composition, Properties, Environmental, Productive Applications, and Outlook

Agricultural experiences since the Neolithic period, knowledge about the properties of certain geological materials, especially carbonate materials and, much later, phosphate materials, and the application of Agricultural Chemistry, meant a considerable advance in food and plant production and degraded soils recovery possibilities, although not so much of the contaminated ones. In any case, it involved the use of scientific knowledge of first or second-generation sciences, such as Chemistry, Geology, or Agricultural Chemistry, whose knowledge and applications should continue to be encouraged, but to which concepts and strategies derived from the sciences of the third generation, such as Soil Science, Biogeochemistry, or Ecology.

Observing natural processes, it can be easily appreciated that when soil disappears, becomes contaminated or degrades, recovery can begin through indigenous or allochthonous materials, but the clear objective of the biosphere is to reuse them to build new soil. Whatever the starting material and even if it contains abnormally high concentrations of pollutants, as happens in reservoirs with

high contents of toxic elements, such as As, Se, and/or heavy metals, edaphic processes are responsible for transform, passivate, inert, and dilute pollutants, reducing their mobility and bioavailability. In this case, the toxic elements do not disappear and remain in situ, but the chemical species in which they occur change, progressively favouring those with less solubility and greater chemical inertness. When it comes to organic pollutants, soil microorganisms transform them through metabolic reactions, eliminating them or integrating them into complexes or associations of less active organic components, such as humins and other humic substances. It can take some time, but the biosphere will continuously transform the different surface materials, continuously trying to achieve an edaphic system with the appropriate properties to develop environmental and productive functions efficiently. The problem is the time it takes, which may be too long for human needs.

An alternative that develops from the application of third-generation sciences is learning and imitating the biosphere and carrying out the recovery or rehabilitation of degraded or contaminated soil by incorporating soils with its organization and reactive constituents. Not materials, nor disorganized mixtures of them, but a soil, designed, formulated, and elaborated to correct the existing deficiencies and limitations and recover the capacity and quality of the environmental and productive functions of the natural soils in the shortest possible time of the climatic environment. This designed anthropic soil, not the accidentally produced after land abandonment, is called tailor-made technosol because it is a soil built mostly or totally with non-toxic or dangerous artefacts, whose composition, properties, and functions are established after a careful analysis of the situation of the degraded or contaminated system and the constituents, organization, and properties that it should receive in order to carry out the physical–chemical and biotic corrections that limit it and, at the same time, encourage a faster and more efficient recovery. It is the biogeochemical processes with mineral alteration, neof ormation (Pédro 1968; Chesworth 1992), and meta-stabilizing transformation of plant and animal remains into soil organic matter (Senesi and Loferodo 1999; Kleber et al. 2015) that lead to adequate and more favourable aggregation and functioning conditions for the evolution of the terrestrial biosphere, in compliance with natural laws. Therefore, if the soil does not exist or is contaminated or degraded, it can be substituted or mixed with another soil that eliminates the limitations, performs ecosystem services, and evolves over time, converging with natural soils, by the same laws of alteration and edaphogenesis and by the same biogeochemical reactions.

Tailor-made Technosols are soils, not raw materials or mixtures, that may have one or more valuable properties for rehabilitation. They are complex and heterogeneous edaphic systems, which are designed and elaborated by applying the

knowledge of Soil Science and Biogeochemistry replicating natural soils and that, like them, have active solid fractions: inorganic and organic colloids, dissolution of the soil and microorganisms, and skeletal fractions that contain the nutrients reserve to be released and that help in drainage and compaction control. For them to act like natural soils, they must have an adequate microporous organization and reactive surfaces, which allow them not only the rehabilitation of the affected soils but also their subsequent operation under biostatic conditions, simultaneously carrying out a multitude of biogeochemical reactions (multifunctional reactor) that accelerate the rehabilitation and lead the systems to the recovery of the soil functions and their edaphodiversity (Fig. 1) (Macías and Camps Arbestain (2010, 2020).

Tailor-made Technosols are means of life that contain numerous beneficial organisms from their constituents and/or from the air. Those most beneficial for their intended purposes may be incorporated in their preparation, such as nitrogen-fixing bacteria, ligninolytic fungi, etc. As they are designed, formulated, and elaborated “tailor-made”, faster kinetic reactions can be encouraged, from microseconds to days or months (Sparks and Suarez 1991, 1999) so that they exceed the reactive capacity of the natural soils that they imitate (hypertechnosols) or the opposite, so that they slow down or inhibit vegetative development if desired (hyperdystrophic). The concentration of pollutants can be reduced to tolerable limits so that the generic reference levels of the area of action are not exceeded so that they cannot act as sources of contamination. It is also possible to concentrate and balance the nutrient elements necessary for more efficient development of biota, avoiding, if necessary, the super concentration of eutrophying elements and always considering that productivity follows the “Law of the Minimum”. They can fix C in their biota and, in the organic compounds from the degradation of their components, can be favoured

relationships that encourage aggregate stability, erosion resistance, durability, or even recalcitrance of organic matter, biodiversity, and biotics activity. In the current context of climatic forcing and loss of organic matter from a large part of the soils, especially in arid, mining, or burned areas and where surface horizons have disappeared, tailor-made Technosols can make an essential contribution of C labile, metastabilized, and recalcitrant (Glasser & Woods 2004; Lal 2004; Lehmann et al. 2006; Lehmann 2007; Lehmann and Joseph 2009; Lutzow et al. 2006; Macías and Camps Arbestain 2010) that helps to restore C edaphic reservoirs and minimize the significant N losses that occur in management systems of waste (see Fig. 2).

In synthesis, adequately designed, formulated, and elaborated Technosols can change the physical–chemical and biotic conditions of contaminated or degraded soils through the modification of acid–base dissolution–precipitation reactions, redox processes, surface reactions of ionic exchange, adsorption and/or occlusion, metabolic reactions, enzymatic activity, fertility, and the increase in helpful water, or its more efficient use, and, through the transformations they produce, can modify the conditions of the drainage and infiltration waters and biotic systems. They can act by recovering contaminated systems and avoiding contamination processes through prevention in a much more efficient way. An example is a preventive control of the oxidation of metallic sulphides and the leaching of As and heavy metals carried out in some landfills of high-speed laying tunnels (ADIF 2019) that can and should be applied in mining and civil works.

Tailor-made technosols can be used isolated or in associations, mixed, overlaid in situ, or spatially distributed, imitating different types of soil catenas generated in the different topographic positions of the relief. The set of different tailors made technosols along a topographic



Fig. 1 Recuperation of 1,200 ha of hyperacid, hyper sulphated, heavy metal bearing tailings. Design and EIA of 10 km² lake. Rehabilitation of spoiled Technosols and first tailor-made Technosol



Fig. 2 Cu sulphide mine (Touro). Recovery of hyperacid cuttings with tailor-made Technosols (1998–2021). Surface runoff waters moved from pH < 3.5 to 7.0, recovering the whole trophic chain and

passing from only extremophile organisms to the existence of the complete trophic chain up to raptors

sequence allows geomorphological recovery and the differentiation of landscape areas with different vocations and aptitudes in their possibilities of use. A particularly successful arrangement in the rehabilitation of waters, soils, and ecosystems is their combination with water, plants, and microorganisms, in systems called “reactive wetlands” (Fig. 3). Formations that imitate natural or artificial wetlands that base their purifying efficiency on increasing the residence time of the waters and favouring the multiple biogeochemical reactions that microorganisms can

develop. The importance, positive effects on biota and landscape, and the purification capacity of the wetlands are widely accepted, but their effectiveness is often restricted by the long time they require for their correct operation and the vast area of the surface that must be used. A large part of these problems can be reduced by incorporating the wetlands of the appropriate Technosols for the functions that want to be prioritized. Some examples of successful implementation of these new technologies are shown in Figs. 4 and 5.

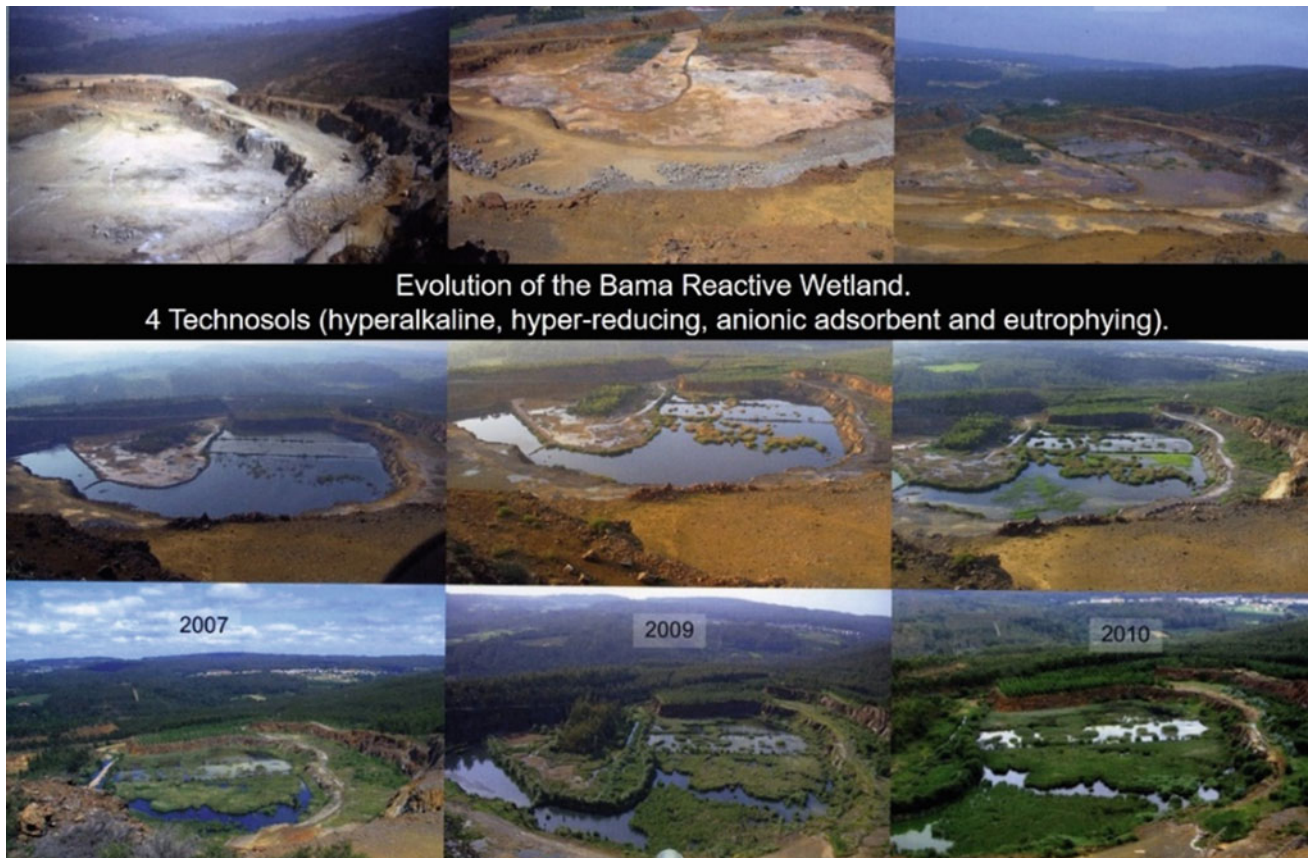


Fig. 3 Evolution of the first Bama “reactive wetland”, Touro Mine. From hyperacid to drinkable water with class 1 invertebrates (2004–2008)

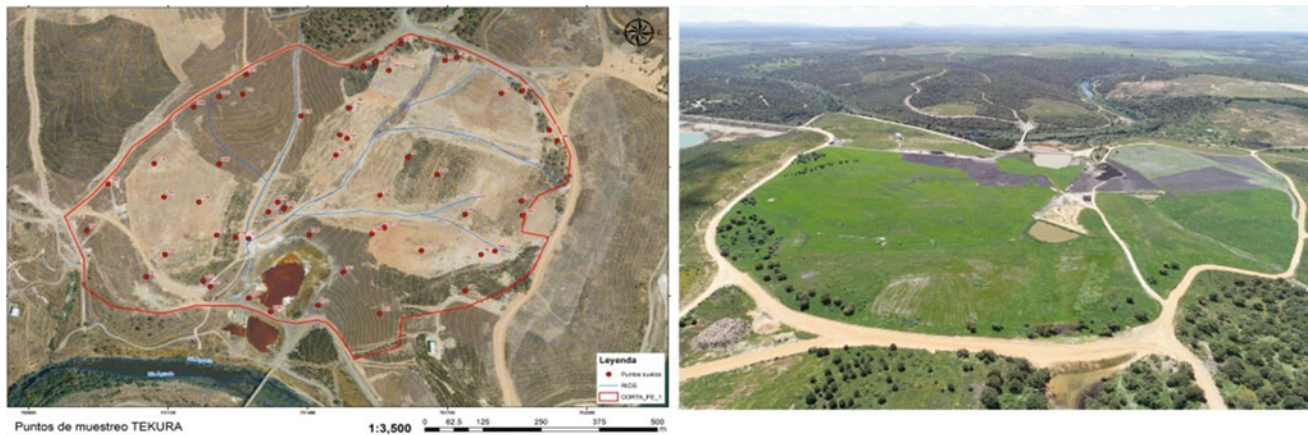


Fig. 4 Soil and water evolution of the TEKURA project in 3 years



Fig. 5 Construction and evolution of a reactive wetland in the uranium mine of Saelices (Salamanca)

References

- ADIF (2019) Vídeo: tratamiento ambiental con tecnosoles. Línea del tren de alta velocidad Madrid-Galicia
- Commission of the European Communities (2006) Thematic Strategy for Soil Protection. COM(2006)231 final, Brussels, 22.9.2006, 12 p
- Chesworth W (1973) The parent rock effect in the genesis of soil. *Geoderma* 10:215–225
- Chesworth W (1992). Weathering Systems. In: Martini, I.P., Chesworth, W. (eds). *Developments in Earth Surface Processes*. vol 2. Elsevier, pp. 19–40
- Erhardt H (1967) La genèse des sols en tant que phénomène géologique: esquisse d'une théorie géologique et géochimique, biostasie et rhexistase: exemples d'application. Masson. No. 551:305
- European Commission (2020). A European Green Deal. [online] European Commission. Available at: https://commission.europa.eu/strategy-and-policy/priorities-2019-2024/european-green-deal_en
- FAO (2006) World reference base for soil resources. Rome
- FAO (2014) World reference base for soil resources. Rome
- FAO, IUSS, ISRIC (1998) World reference base for soil resources. Rome
- Glasser B, Woods, (eds) (2004) *Amazonian dark earths: explorations in space and time*. Springer, Berlin, Heidelberg
- Kleber M, Eusterhues K, Keiluweit M, Mikutta C, Mikutta R, Nico PS (2015) Mineral–organic associations: formation, properties, and relevance in soil environments. In: *Advances in Agronomy*, vol 130. Academic Press, pp. 1–140
- Lal R (2004) Soil carbon sequestration to mitigate climate change. *Geoderma* 123:1–22
- Lehmann J (2007) A handful of carbon. *Nature* 447:143–144
- Lehmann J, Gaunt J, Rondon M (2006) Biochar sequestration in terrestrial ecosystems. A review. *Mitig. Adapt Strategies Glob Chang* 11:403–427
- Lehmann J, Joseph S (eds) (2009) *Biochar for environmental management*. Earthscan Publications Ltd., Sterling
- Lutzow MV, Kogel-Knaber I, Ekechmitt K, Matzner E, Guggenberger G, Marschner B, Flessa H (2006) Stabilization of organic matter in temperate soils: mechanisms and their relevance under different soil conditions. *Rev Eur J Soil Sci* 57: 426–445
- Macías F (2004) Recuperación de suelos degradados, reutilización de residuos y secuestró de carbono. Una alternativa integral de mejora de la calidad ambiental. *Recursos Rurais* 1, 49–56
- Macías F, Bao M, Macías-García F, Camps Arbstein M (2007) Valorización biogeoquímica de residuos por medio de la elaboración de Tecnosoles con diferentes aplicaciones ambientales. *Aguas Residuos* 5:12–25

- Macías F, Camps Arbestain M (2010) Soil carbon sequestration in a changing environment. *Mitig Adapt Strat Glob Chang* 15:511–529
- Macías F, Camps Arbestain M (2020) A biogeochemical view of the world reference base soil classification system. *Adv Agron* 160:295–345
- Pédro G (1968) Distribution des principaux types d'alteration chimiques à la surface du globe : présentation d'une esquisse géographique. *Rev Geograph Phys Geol Dynam* 10(5):457–470
- Senesi N, Loffredo E (1999) The chemistry of soil organic matter. In: Sparks DL (ed) *Soil Physical Chemistry*, 2nd ed. CRC, Boca Raton, pp. 239–370
- Sombroek WG, Nachtergaele FO, Hebel A (1993) Amounts, dynamics and sequestering of carbon in tropical and subtropical soils. *Ambio* 22:417–426
- Sparks DL, Suarez DL (1999) Rates of soil chemical processes. SSSA Special Publications, Number 27, Soil Sci Soc Amer, Inc. Madison.
- Sparks DL, Suarez DL (1991) Rates of Soil Chemical Processes Soil Science Society of America Madison, WI, USA
- Vernadsky V (1929) *La biosphère*. Felix Alcan. Nouvelle Collection Scientifique, Paris



The Multi-incremental Sampling Methodology in the Study of Potential Contaminated Sites

Celeste Jorge

Abstract

Environmental sampling of soils is carried out to monitor or characterise the concentration of substances in this environmental compartment. In potentially contaminated sites, sampling is used to characterise the quality of soils, general or specificity, depending on the historical activity developed in an area. The need to assess potentially contaminated areas by the most diverse substances (compounds or chemical elements), some of the less common, such as explosives, or the contamination (with some diffuse character) resulting from the deposition of substances by air, has led to the requirement to establish different strategies to approach the evaluation of these areas. Instead of a discrete sampling (D.S.) distributed at random, conditioned, or in mesh, there may be the convenience or the need for an incremental sampling (I.S.). This sampling strategy is appropriate for certain specific conditions, sampling objectives, and particular contaminants to obtain a single sample for analysis (at least three field replicates), representing the mean concentrations of elements and compounds of the decision unit adopted. This work intends to present the major features of the I.S. strategy and its advantages and disadvantages when comparing it with the common practice of the D.S. strategy.

Keywords

Incremental sampling • Soil • Contamination • Methodology

1 Introduction

The study of contaminated areas is a complex and expensive task that should be appropriately planned. As is well known and assumed by the community of experts (Hewitt et al. 2007), an environmental characterisation programme's essential aspect is collecting samples. It is usually implemented in stages, allowing knowing the conditions in a given site or area, going from the general to the detail. However, many of the potentially contaminated or contaminated areas are too vast and the most common sampling approaches, referred to in NSW-EPA (USEPA 1995) and by U.S. Environmental Protection Agency (USEPA 2010), are not feasible, because of financial and temporal issues, due to the significant number of samples to collect and analytical determinations to be made. However, the reliability of the results must be a warranty. In these cases, instead of a discrete sampling (DS-collection at a point) distributed randomly, conditioned, or in mesh, there may be the convenience or the need for an incremental sampling (IS). Nowadays, IS is also used in small areas.

The theory behind Incremental Sampling Methodology (ISM) was developed by Pierre Gy in the early 1990s (Esbensen 2004). This theory was first used in mining prospecting and adapted to study military training areas, and USEPA adopted it. Interstate Technology Regulatory Council (ITRC 2020) refers that USEPA continued to refine the description of ISM in different publications for almost two decades [from procedures in SW846 Method 8330B (USEPA 2006) until Polychlorinated Biphenyl (PCB) Cleanup Sites (USEPA 2019)]. In addition, the U.S. Army Corps of Engineers produced guidance for sampling for munitions in surface soil using ISM (USACE 2009), among other significant publications. All these approaches intend to reduce the potential source for such “decision errors” (deciding that cleanup is needed) and to give significant attention to quality assurance (QA), and to quality control (QC) for laboratory analytical methods that have resulted in accurate

C. Jorge (✉)

Advisory Group of the Board of Directors, Laboratório Nacional de Engenharia Civil (LNEC), Lisbon, Portugal
e-mail: cjorge@lnec.pt

and reproducible methods for analysing small subsamples (aliquots) of soil (adapted from ITRC 2020). According to ITRC (2020), ISM is a statistically supported technique for assessing the mean contaminant concentration in soil, sediment, and other environmental media.

2 Incremental Sampling Methodology

ITRC produced guidance for ISM in 2012, which was reviewed and updated in 2020 (ITRC 2012 and 2020). These publications mention that ISM is a structured composite sampling and processing protocol that reduces data variability and provides a reasonably unbiased estimate of mean contaminant concentrations in a volume of soil targeted for sampling (Fig. 1) because contamination distribution is a heterogeneous process on a set of variables. “ISM provides representative contaminant concentrations in samples from the specific soil volumes, defined as decision units (DUs) or sampling units (SU), by collecting numerous increments of soil (typically 30–100 increments to form a mass sample with 1–2 kg dry weight). (...) According to a specific field and laboratory approach, protocols are combined and processed, and subsampling is used in laboratory analysis” (ITRC 2012 and 2020) (Fig. 1). In the author’s opinion, the total sample mass (multi-incremental mass) should be greater to compensate for the variation in the grain size (granulometry) of soil or a greater number of increments. It will also depend on the mass of the subsample (increment).

According to Hewitt et al. (2007), as it is well known, sampling activity is the core of a site investigation for the characterisation of contamination status. The sampling strategy and design should be planned using all data available and the knowledge and expertise of training technicians. All details must be considered, and conservative approaches

should be assumed (additional samples should be collected). The number of increments for multi-increment samples constitution should be maximised rather than minimised. To ensure that an expected value of the presence of contamination is obtained, it is imperative to collect triplicate field samples. This is mandatory to assess the uncertainty of sampling strategy and the design for a specific scenario. In the aerial deposition of certain components, it is also fundamental not to remove surface vegetation before collection. When the extent of the area influenced by an activity is unknown or in dispute, more decision units should be added to the sampling plan, and these sub-areas should be sampled. Adopting this systematic approach will reduce the number of times the field sampling team is assigned to a given site investigation, saving time and money.

The IS strategy can be done on a 2D (surficial) or 3D (at different depths) approach and is appropriate for specific conditions, sampling objectives and peculiar contaminants. That minimises spatial heterogeneity and aims to obtain a single sample for analysis (at least three field replicates). That represents mean concentrations of elements and compounds representative of the DU they were adopted (a cell of defined area based on the area’s available size to be evaluated, the land’s characteristics, the properties of the contaminants under study, the present climatic conditions, etc.). In the author’s opinion, this kind of procedure is not appropriate for volatile sampling compounds, but in the USA, several states practice it (i.e., Hawaii). A cold territory could be acceptable, but not in a warm territory (warm and windy climacteric conditions).

The ISM process is illustrated in Fig. 2. The flow chart shows the main steps of the three phases: Planning, Implementation, Data Analysis and Decision-making (Fig. 2a). ISM planning is usually based on the preliminary conceptual site model (CSM). It will contribute to the “final” CSM

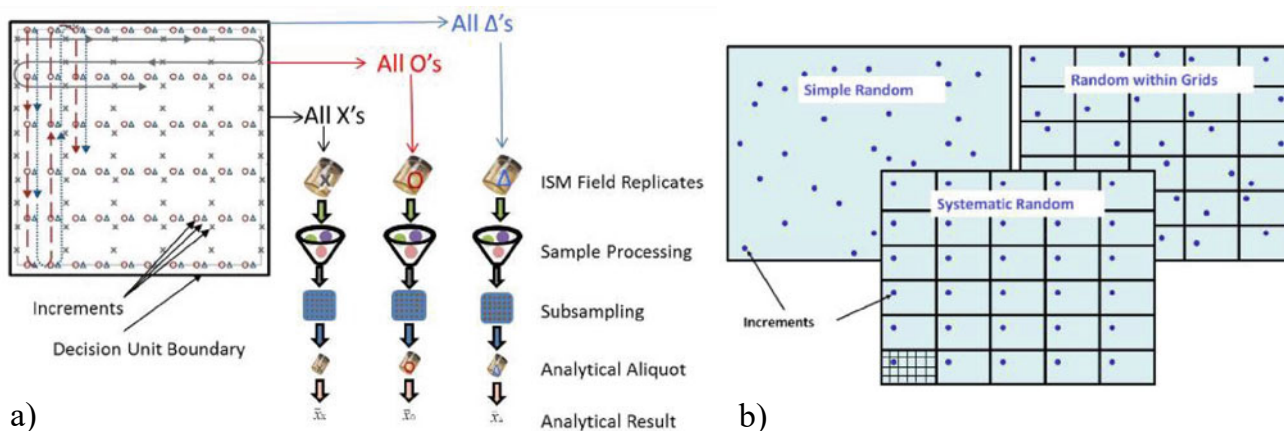
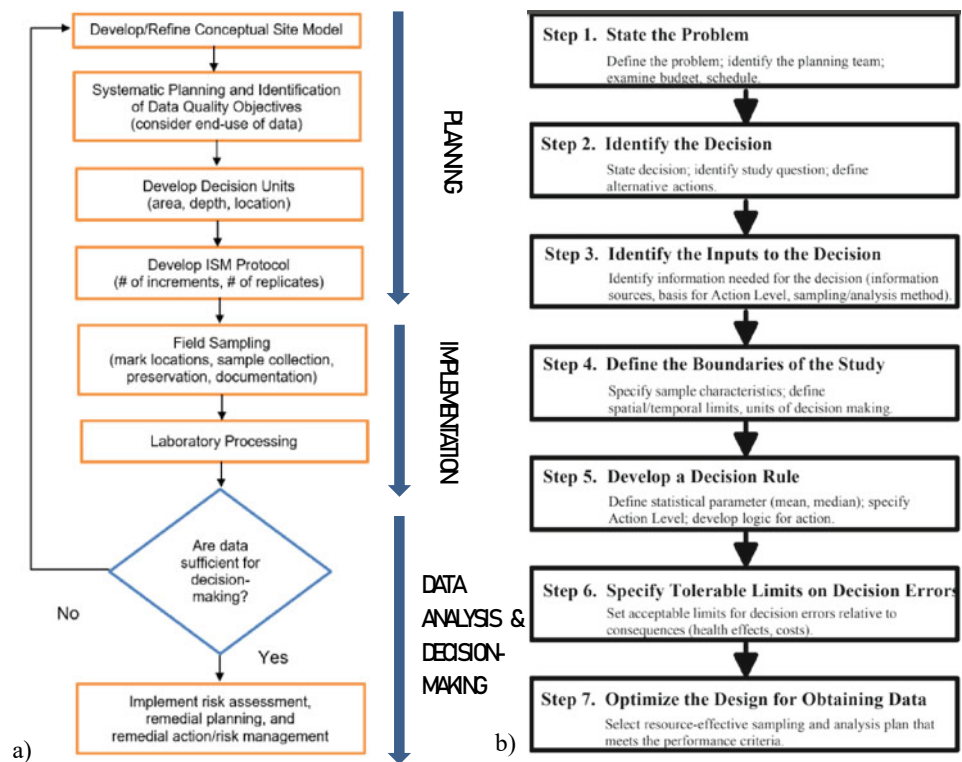


Fig. 1 a Simplified scheme of the procedure for incremental sampling and incremental processing of the sample collected for analytical determination (ITRC 2012) and b unbiased increment collection designs for decision unit (ITRC 2020)

Fig. 2 a ISM flow chart (ITRC 2012) and b Steps of the DQO Process (USEPA 2002)



definition to help decision-makers protect human health and the environment. The Data Quality Objectives definition is essential (Fig. 2b). Following the different steps, it is essential to mention that the process is iterative.

According to Hewitt (2007), concerning the processing and analysis of field samples, the entire field sample must be powdered and, after being conveniently subsampled (multi-incremental procedure), the entire field sample should be extracted. This laboratory procedure must be audited visually, and a triplicate aliquot should be taken at a regular intervals to control the uncertainty associated with this task. In addition, QA/QC criteria must be implemented.

Data for small subsamples of soil tested by a laboratory represent the mean for that soil volume included in the subsample (ITRC 2020). As part of this process, representative sample data is compared with decision criteria, such as numerical regulatory cleanup standards for a given contaminant (ITRC 2020).

The sampling results should be interpreted statistically. In general, if the results indicate a lack of hot spots and the 95% upper confidence level (UCL) of the arithmetic average contaminant concentration (with at least three replicates) of the site (a DU) is below a threshold limit. Then, the site can be considered uncontaminated or successfully remediated for specific end uses (NSW-EPA 1995). All the statistical data treatment can be seen in ITRC (2020).

3 Advantages and Disadvantages of ISM

The ISM procedure has advantages and disadvantages. According to USACE (2013), the advantages are (1) a soil sample is a representative of the area of interest (i.e., DU), (2) the procedure allows for quantification of the uncertainty for field sampling and laboratory sample and analysis and (3) there is a reduction in the number of field samples collected for laboratory analysis. In opposition, the disadvantages of ISM comprise (1) an increased volume of individual samples sent to the analytical laboratory, (2) the necessity of a particles size reduction step (e.g., milling,) and (3) the possibility of modifying the availability of some metals during acid digestion, due to the milling operation.

This method provides the researcher with more accurate and reproducible data on the average concentrations on/in the D.U. This type of sampling aims to study heavy metals, PCBs, pesticides and PAHs and most explosives. However, in explosives, specific treatment procedures (screening and sieving) of the samples are limited to avoid losses due to volatilisation and thermal decomposition.

Brewer et al. (2017) carried out a critical review of discrete soil sampling and corroborated the adoption of the DU and multi-increment sampling method. However, replacing the practice of DS with IS cannot be carried out linearly

while considering several fundamental aspects, such as the reliability, representativeness and meaning of the analytical results and their interpretation.

4 Concluding Remarks

According to the author's experience, applying the IS strategy depends on convenient planning. Consequently, the amount of soil to be collected in each increment, the number of increments needed, the size of the DUs and the protocol defined for treating the samples, which precedes the analytical procedure, are supreme parameters of success, decreasing the errors introduced by heterogeneity.

However, it should be noted that this type of strategy for approaching contaminated areas may require further stages of the investigation, iterative ones, for fully supported decision-making. Therefore, surface sampling is the most practicable and economically feasible.

The specificity of the IS strategy resides quite a lot in laboratory treatment, which precedes the analysis. In this strategy, laboratory processing employs procedures to produce a uniform fine-grained sample and uses multi-incremental subsampling to obtain a representative sample for analysis. These procedures make it possible to achieve a highly reproducible average concentration. The IS strategy improves the sampling data's reliability and reduces its variability compared with conventional DS strategies. The data distribution for the replicated IS samples tends to be normally distributed.

References

- Brewer R, Peard J, Heskett M (2017) A critical review of discrete soil sample data reliability: part 1—field study results. *Soil Sedim Cont Int J* 26(1):1–22
- Esbensen KH (2004) 50 Years of Pierre Gy's theory of sampling—WCSB1: a tribute. *Chem Intellig Laborat Syst* 74(1):3–6
- Hewitt AD, Jenkins TF, Walsh ME, Walsh MR, Bigl SR, Ramsey CA (2007) Protocols for collection of surface soil samples at military training and testing ranges for the characterisation of energetic munitions constituents. Technical Report ERDC/CRREL TR-07-10. U.S. Army Corps of Engineering
- ITRC (2012) Incremental sampling methodology. Interstate Technology Regulatory Council, Washington
- ITRC (2020) Incremental sampling methodology—2. Interstate Technology Regulatory Council, Washington
- NSW-EPA (1995) Contaminated sites—sampling design guidelines. New South Wales Environment Protection Authority, Contaminated Sites Section, Hazardous Substances Branch, Sydney
- USACE (2009) Implementation of incremental sampling (I.S.) of soil for the military munitions response program. Interim Guidance 09-02. Environmental and Munitions Center of Expertise. U.S. Army Corps of Engineers
- USACE (2013) Demonstration of incremental sampling methodology for soil containing metallic residues. Project ER-0918. ERDC TR-13-9. U.S. Army Corps of Engineers and Engineering Research and Development Center
- USEPA (2002) Guidance on choosing a sampling design for environmental data collection—for use in developing a quality assurance project plan. EPA QA/G-5S. EPA/240/R-02/005. U.S. Environmental Protection Agency
- USEPA (2006) Method 8330B—Nitroaromatics, nitramines, and nitrate esters by high performance liquid chromatography (HPLC). Test Methods for Evaluating Solid Waste: Physical/Chemical Methods/ SW-846 Compendium
- USEPA (2010) Sampling design—modulo at a glance. Environmental Protection Agency, Sampling design and optimisation. U.S.
- USEPA (2019) Incremental sampling methodology (ISM) at polychlorinated biphenyl (PCB) Cleanup Sites. Environmental Protection Agency, U.S.



Contaminated Soil Management in Urban Earthworks in Portugal: Solutions for Treatment and Valorisation of Hazardous and Non-hazardous Wastes

Carlos Costa and Daniel Vendas

Abstract

Due to the tight execution timetable of the urban development earthworks, the most commonly used decontamination technique in Portugal is excavation and transport to a suitable final destination through a properly licensed carrier. The goal of this work is to present the efficiency of the solutions offered by Integrated Centres for Recovery, Valorisation and Disposal of Hazardous Waste (CIRVER) in the treatment of contaminated soil classified as hazardous waste and co-processing by replacing raw materials in clinker production in cement kilns for the treatment and valorisation, of non-hazardous contaminated soils.

Keywords

Contaminated soil • Waste management • Hazardous • Non-hazardous • Valorisation

1 Introduction

The urban expansion due to population growth and the increasing consumer demand for larger houses, more vacation homes and more commercial and industrial facilities has severely increased the impacts on the available soil in the Portuguese metropolitan areas. On the other hand, due to the tight execution timetable of the urban development earthworks, there is rarely time for in-situ treatment in most real estate sectors. Therefore soil decontamination, treatment and/or valorisation is almost always performed ex-situ, as it is more cost-effective.

This work intends to present and discuss the efficiency of the solutions offered by Integrated Centres for Recovery and Disposal, Valorisation of Hazardous Waste (CIRVER) in the treatment of contaminated soil classified as hazardous waste resulting from excavation works and by co-processing in clinker production in cement kilns by replacing raw materials for contaminated soils classified as non-hazardous waste.

2 Treatment of Contaminated Soil Classified as Hazardous Waste

CIRVER are integrated industrial units for recovery, valorisation and disposal of hazardous waste that combine the best available technologies at affordable costs, enabling a specific solution for each type of waste, in order to optimise treatment conditions and minimise the costs for its national and international clients (ECODEAL 2019; EGEO 2019). The creation of these facilities was a decisive milestone towards the principle of self-sufficiency and proximity to treat hazardous industrial waste in Portugal. The legal provisions resulting from Decree-Law No. 3/2004, dated January 3rd, which established the legal regime for licensing, installation and operation of this type of establishment, lead to the construction of two CIRVER units, both in the Chamusca region (Central Portugal) and equipped with a series of support units for the treatment of hazardous waste. One of these units is precisely a Soil Decontamination Unit.

For soil contaminated with hydrocarbons, decontamination is carried out in bio-piles, promoting the biodegradation of hydrocarbons present in the soil through microorganisms. This operation is optimised by controlling the following parameters:

- TPH aliphatic: <50,000 mg/kg (no PAH, PCB or halogenated);
- Heavy metals: <2500 mg/kg;

C. Costa (✉) · D. Vendas
eGiamb – Consultoria Geoambiental Lda, Caparica, Lisboa,
Portugal
e-mail: carlos.costa@egiamb.pt

- Humidity: 12–30%;
- Nutrients (C:N:P): (100:10:1);
- pH soil: 6–9;
- Temperature: 10–45 °C;
- Clay: <25%.

Figure 1 illustrates the construction of a biopile at CIRVER ECODEAL.

In addition to the Soil Decontamination Unit, the two CIRVER have seven other waste treatment units: Classification, Sorting and Transfer Unit, Contaminated Packaging Recovery Unit, Organic Waste Treatment Unit, Alternative Fuel Preparation Unit, Chemical Treatment Plant, Stabilisation Unit and Landfill of Hazardous Industrial Waste (ECODEAL 2019; EGEO 2019). Having all these treatment units in just a single facility ensures access to the best available technologies and maximum security, selecting appropriate treatment solutions for each case, synergies resulting from the common use of different treatment units and rationalising resources.

3 Treatment and Valorisation of Contaminated Soil Classified as Non-hazardous Waste

Co-processing consists of replacing fossil fuels and/or conventional raw materials in energy and material-intensive industries to introduce alternative fuels and secondary raw materials from waste. It provides the destruction of the contamination present in soils classified as non-hazardous waste—previously prepared and identified as suitable for replacing raw materials (clay, marlstone, limestone) in clinker production in cement kilns, ensuring product quality standards, energy efficiency and environmental protection in line with the official certification of these facilities. This is possible due to the cement kiln characteristics, which are characterised by the long residence time and high temperatures that allow the complete and safe recovery of waste without resulting in environmental liabilities.

Co-processing shows many advantages, namely (3DRIVERS 2018):

Fig. 1 Construction of a biopile (Photos kindly shared by CIRVER ECODEAL). From top to bottom and from left to right: 1—Spreading of the soil; 2—Installation of gas monitoring pipes watering system; 3—Biopile before impervious cover; 4—HDPE sheet extended over the biopile; 5—Watering system connection; 6—Gas monitoring pipe (detail)



- Provision of a waste recovery service through its integration in the cement production process, without the need for investments in new infrastructures, unlike other dedicated energy recovery solutions (e.g. waste incinerators);
- Reduction of the amount of waste sent to landfill;
- Increased recycling levels, ensuring a solution for materials with no recycling potential and total recovery of the mineral fraction;
- Reduction of the extraction of natural resources.

Co-processing of secondary raw materials in resource-intensive industries, such as cement plants or foundries, is an old industrial practice. Use of sludge and limestone in the Portland cement and granulated slag from the iron furnaces as aggregate for the construction industry is mentioned in 1881 (Desrochers 2005), being the benefits associated with the saving of raw materials and the prevention of environmental and health damages caused by the uncontrolled waste dumping.

Presently the advantages of co-processing are widely recognised (Saveyn et al. 2016) and have led to the publication of specific guidelines for co-processing under the United Nations “Basel Convention” (UNEP 2011). Figure 2 illustrates the position of co-processing in the European waste hierarchy (EEA 2019).

In Portugal, the co-processing of waste in cement plants is an issue since 1997. Since then, the evolution of the national and the EU legislative and strategic framework has ensured the strong regulation of the cement industry and waste co-processing and has promoted the transition of the sector to a low-carbon, resource energy-efficient circular economy (3DRIVERS 2018). Six types of cement plants in

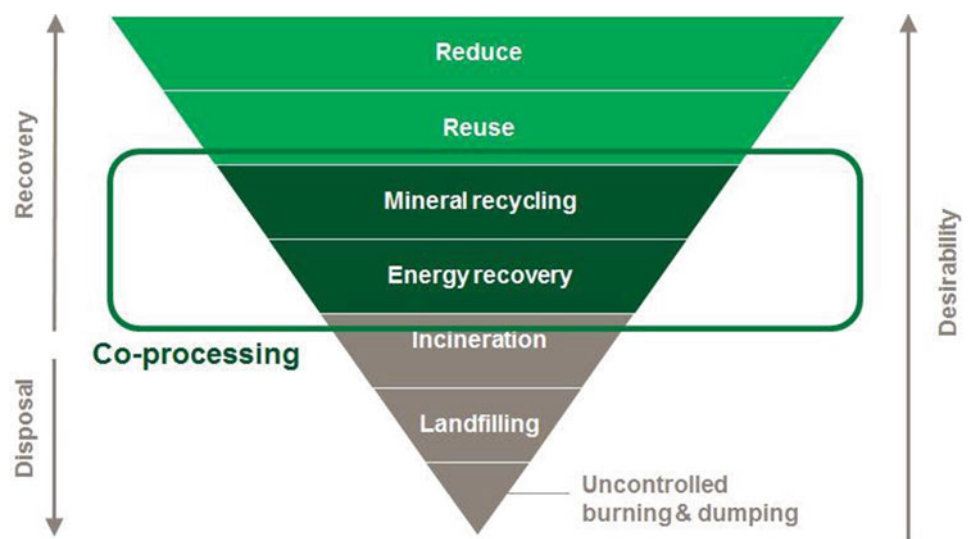
Portugal are equipped to incorporate alternative raw materials in cement production. The quantities of secondary raw materials valued in the cement industry have increased in recent years and are estimated to exceed 100,000 tons in 2019. The use of waste resulting from contaminated soil excavation in urban earthworks as alternative or secondary raw material contributes to preserving limited and not renewable natural resources extracted from quarries. Despite being part of an industrial process, co-processing of waste in cement kilns does not imply any excess—since there is no residual waste—or any environmental liabilities (CEM-BUREAU 2017).

Waste management operations are harmonised at the European level and published in Annex III of the European Waste List, through Ordinance No. 209/2004, of March 3, as amended by Decree-Law No. 73/2011, June 17th. In the case of secondary raw materials used upstream and downstream of the cement kilns, with an incorporation rate of about 10%, these operations are typically classified as R5 (recycling/reclamation of other inorganic materials). That includes contaminated soil cleaning resulting in the recovery of the soil and recycling of inorganic construction materials. Therefore, it accounted for overall recycling targets at the national level, minimising the deposition of non-hazardous waste in landfill.

4 Waste Management Operations in Urban Earthworks

Contaminated soils resulting from an excavation in urban operations are subject to previous licensing under the Waste Management Legal Regime (Decree-Law No. 178/2006

Fig. 2 Position of co-processing in the European waste hierarchy (EEA 2019)



The principles of the waste management hierarchy set out in the EU Waste Framework Directive and the Basel Convention, the United Nations

amended by Decree-Law No. 73/2011) by the Regional Spatial Planning Authorities (CCDR). To classify excavated soil (as waste) and define its LoW (List of Waste) code, the provisions of the annexe to Commission Decision 2014/955/EU, of 18 December, imply concerning its delivery to a duly licensed waste management operator. More recently, a guide with measures and recommendations to be adopted in terms of licensing, monitoring the execution and inspection of urban operations, issued in July 2019 (version 2), was prepared by a commission integrating the National Environmental Agency (APA), the Directorate-General for Health (DGS), the Commission for Regional Development and Coordination of Lisbon and Tagus Valley (CCDR-LVT), the Lisbon Municipality (CML), the Municipal Civil Protection Service (SMPC) and the General Inspection of Agriculture, Sea, Environment and Spatial Planning (IGAMAOT).

In the context of the management of soils resulting from the excavation of contaminated areas, the classification of this particular type of waste as hazardous or non-hazardous, and the understanding of under which circumstances a waste should be considered hazardous is a crucial decision for proper waste management. Therefore, it is not sufficient to perform landfill admissibility tests in Decree-Law No. 183/2009, of August 10th. It is also essential to classify the hazardousness of the soil as waste for its disposal to a duly licensed waste management operator, according to EU Regulation No. 1357/2014 published for the replacement of Annex III to Directive 2008/98/EC on the criteria for hazardous waste.

Figure 3 illustrates the operations for excavation and transport to a duly licensed waste management operator.

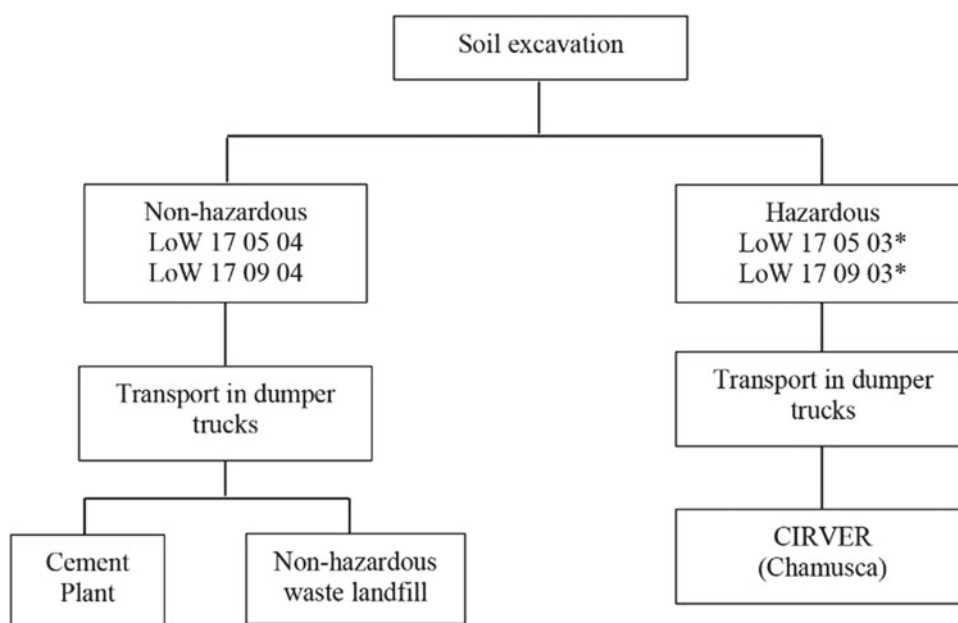
In Portugal, the absence of specific legislation for soil protection is considered the major obstacle to the correct management of contaminated soils, favouring the adoption of discretionary procedures for managing contaminated soils by less scrupulous operators. However, positive steps have recently been made to ensure greater control of the entire waste path (e.g., the electronic waste tracking guides—e-GAR—implemented in 2018).

5 Concluding Remarks

In opposition to the traditional disposal of contaminated land in industrial waste landfills, the solutions offered by Integrated Centres for Recovery, Valorisation and Disposal of Hazardous Waste (CIRVER) in the treatment of contaminated soil classified as hazardous waste resulting from excavation works and the co-processing in clinker production in cement kilns by replacing raw materials for contaminated soils classified as non-hazardous waste, meet the principles and sustainable practices of remediation projects. Sustainable remediation seeks to minimise the impacts of construction on human health and the environment. To accomplish this aim, it is important, at least to the most possible extent, to develop an approach that results in the reuse or recycling of contaminated soil or other undesirable materials and therefore minimise the energy consumption of other natural resources (Ellis and Hadley 2009).

Inorganic non-metal wastes, including construction and demolition waste such as contaminated soil, represent a large proportion of the total waste generated. The reduction in the rate of incorporation of clinker necessary for the

Fig. 3 Operations for excavation and transport to a duly licensed waste management operator



manufacture of cement, through the increase in the consumption of alternative fuels and decarbonated raw materials, and consequently the decrease in specific thermal consumption, also makes it possible to respond to the challenge of climate change, by reducing specific CO₂ emissions.

Acknowledgements The authors would like to thank AVE (Gestão Ambiental e Valorização Energética, S.A.), ECODEAL (Gestão Integral de Resíduos Industriais, S.A.) and SISAV (Sistema Integrado de Tratamento e Eliminação de Resíduos, S.A.) for the key information provided.

References

- 3DRIVERS—Engenharia, Inovação e Ambiente Lda (2018) 13 Years of co-processing in Portugal: assessment of the contributions of waste co-processing in cement plants to the socioeconomic and environmental development of Portugal. Promoter AVE—Gestão Ambiental e Valorização Energética SA, Lisboa
- CEMBUREAU—European Cement Association (2017) Status and prospects of co-processing of waste in EU cement plants: case studies. <http://www.cembureau.eu/library/reports/status-and-prospects-of-co-processing-of-waste-in-eu-cement-plants/>
- Desrochers P (2005) Learning from history or from nature or from both? Recycling networks and their metaphors in early industrialisation. *Progr Industr Ecol Int J* 2(1):19–34
- ECODEAL—Integrated Waste Management (2019) Decontamination of soils (“In-Situ” and “Ex-Situ”). <https://www.ecodeal.pt/servicos/descontaminacao-de-solos-in-situ-e-ex-situ>
- EEA—European Environmental Agency (2019) Land and soil in Europe: why we need to use these vital and finite resources sustainably. EEA Signals 2019, European Environment Agency, Copenhagen. <https://www.eea.europa.eu/publications/eea-signals-2019-land>
- EGEO—Hazardous Industrial Waste (2019) Homepage content. <http://www.egeo.pt/servicos/area/113>
- Ellis DE, Hadley PW (2009) Integrating sustainable principles, practices, and metrics into remediation projects. *Remed J* 19:5–114
- Saveyn H, Eder P, Ramsay M, Thonier G, Warren K, Hestin M (2016) Towards a better exploitation of the technical potential of waste-to-energy. EUR 28230 EN, Publications Office of the European Union, Sevilla, Spain. <https://doi.org/10.2791/870953>
- UNEP—Secretariat of the Basel Convention on the Control of Transboundary Movements of Hazardous Wastes and Their Disposal (2011) Technical guidelines on the environmentally sound co-processing of hazardous wastes in cement kilns: as adopted by the 10th meeting of the Conference of the Parties to the Basel Convention on the Control of Transboundary Movements of Hazardous Wastes and their Disposal (decision BC-10/8), Cartagena, Colombia. <https://digitallibrary.un.org/record/737419?ln=en>



Decommissioning of Potentially Polluting Activities in São Paulo: A Petrol Station Case Study

Erika von Zuben and Carlos Costa

Abstract

The activities developed by the commerce of motor fuels, combined with other petrol station activities such as oil change and vehicle washing, are considered potentially polluting and may cause risks to human health and the environment. Due to the growing expansion of the real estate market, urbanised areas in large cities have been restructured. Urban expansion often advances over areas with several previous polluting activities, requiring actions not to expose the population to risk situations. The degradation of these areas and their decommissioning is a concern that led the Brazilian Government to encourage their revitalisation to protect human health and rehabilitate the environment. The solution for this problem involves the consolidation of a set of technical measures to be taken: preventive, aiming to minimise the occurrence of spills of these products; corrective, for emergency and remediation phase of contaminated areas; and health promotion in order to reduce the health effects of those exposed. The presented case study is a petrol station located in a prime area of São Paulo, which operated for approximately 40 years. It is currently abandoned without any studies for the proper deactivation of the area.

Keywords

Decommissioning • Petrol station • Remediation • Monitoring

E. von Zuben (✉)

Hera – Consultoria e Treinamento, S. Paulo, Brazil
e-mail: erika.zuben@heraconsultoria.com.br

E. von Zuben · C. Costa

AECSAS—Associação para o Estudo da Contaminação de Solo e Água Subterrânea, Lisboa, Portugal

C. Costa

eGiamb—Consultoria Geoambiental Lda, Caparica, Lisboa, Portugal

1 Introduction

The activities developed by the commerce of motor fuels, combined with other activities developed in petrol stations such as oil change and vehicle washing, are considered potentially polluting and may cause risks to human health and the environment.

At the end of 2017, 41,984 petrol stations operated in Brazil, of which 9,175 are located in the State of São Paulo alone, according to data from the National Petroleum Agency (ANP 2018). On a national level, 42.8% are considered white flags (they can be supplied by any distributor). The degradation of these areas, as well as their decommissioning, is a concern that has led the Government to encourage their revitalisation in order to ensure the protection of human health and the rehabilitation of the environment, according to the National Environment Policy, instituted by the Federal Law 6938 /81, which establishes the remediation of derelict areas among other principles.

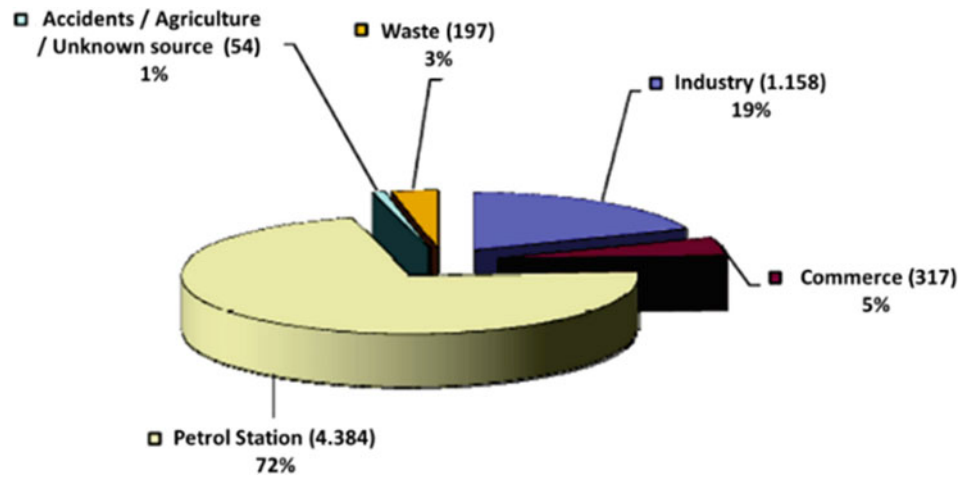
Due to the growing expansion of the real estate market, the urbanised spaces in large cities have been restructured, and urban expansion in medium and small municipalities often advances over areas with several previous polluting activities requiring adequate actions to avoid the exposure of the population to risk situations.

2 Materials and Methods

The municipality of São Paulo, with an area of 1,521.11 km², has 12.18 million inhabitants. From the exploratory survey of the State Environment Agency—CETESB database (CETESB 2018), 6,110 areas were listed as contaminated in December 2018, of which 4,384 (72%) correspond to petrol stations (Fig. 1). Of these, 1,608 are located in the city of São Paulo.

The deactivation of areas where potentially polluting activities were historically established should be done in

Fig. 1 Registered areas: distribution by activity (December 2018), (CETESB 2018)



tandem with the need to develop and improve legal and institutional mechanisms to avoid unregulated occupation of such spaces, enabling the rehabilitation of degraded environments, reducing the risks to the population, and ensuring environmental control.

As shown in Fig. 2, between 2013 and 2018, it was possible to increase 425 to 1,453 the number of rehabilitated areas for declared use, very similar to the number of areas in the remediation process (1,441), while 1,397 are still being monitored for closure.

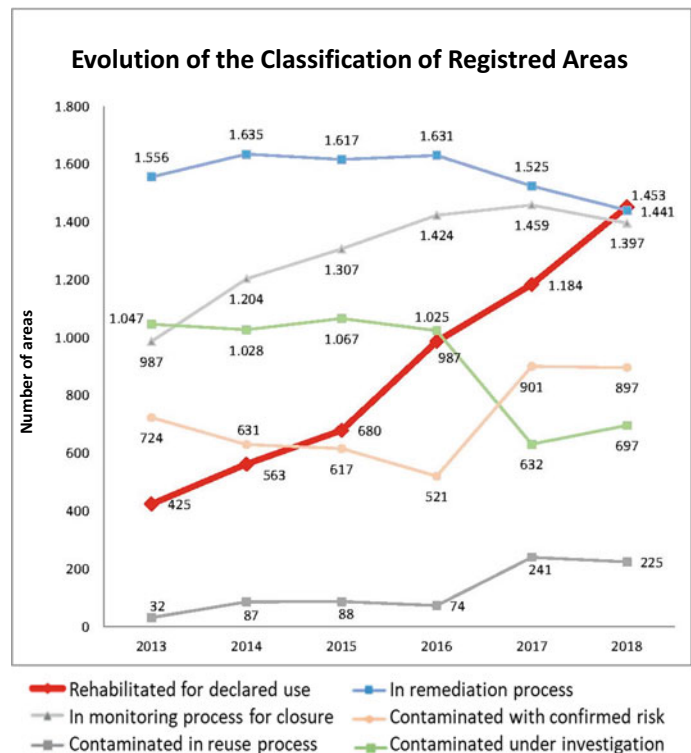
The legislation of the State of São Paulo provides the obligation to follow the guidelines established in State

Decree nº 59.263/13—Chap. III, Sect. IV, Articles 56 to 59 when an industrial activity is total or partially deactivated. A Deactivation Plan is mandatory and must ensure that all equipment, structures, pipes and utilities are decontaminated and suitable for environmentally correct disposal.

The Deactivation Plan should specify:

- Description and map identification of:
 - Equipment,
 - Structures,
 - Installations (water and oil separator box),
 - Pipes,

Fig. 2 Evolution of classification of registered areas in S. Paulo (CETESB 2018)



- Aerial and/or underground tanks,
- Contamination identification on floors, walls, and other structures with sample collection for NBR 10.004 (ABNT 2004) characterisation.
- The final destination of:
 - Decontaminated and decommissioned equipment,
 - Solid wastes that are still in place,
 - Masonry/metal demolition plan, if any.

The Deactivation Plan report must contain:

- Preliminary Evaluation and Confirmatory Investigation
- Study area characterisation
- Solid waste inventory
- Identification and description of equipment, materials, structures, lines, utilities
- Future use of area.

3 Case Study

The case study is a petrol station located in a prime urban area of São Paulo (Fig. 3), which operated for approximately 40 years upstream of a hotel and a shopping mall. It is currently abandoned without any studies for the proper deactivation of the area.

The main activities of the petrol station were:

- Fuel supply and storage area,
- Oil change, tyre change, repair, and mechanical maintenance workshop.

Besides the fuel supply area, other contaminants source areas considered were:

- Vehicle washing area,
- Storage of used lubricating oil,
- Contaminated tow and cloth,
- Automotive filters,
- Lube Oil Packaging,
- Vehicle wash effluent generation.

A Phase II Environmental Site Assessment was performed to evaluate the soil and groundwater quality, and benzene concentration detected near the fuel supply area was 491 µg/L (reference value is 5 µg/L—CETESB 2016). Although the groundwater level is rather shallow (0.9 m), the contamination was considered local (Fig. 4).

4 Discussion and Concluding Remarks

The analysis of the São Paulo scenario regarding the decommissioning of areas with potentially polluting activities indicates that environmental contamination resulting from leaks in petroleum-based above-ground and underground tanks induce constant impacts on environmental quality. Furthermore, the current state legislation has not been sufficient to prevent change using the areas with the necessary environmental liability control measures.

Regarding the case study above presented, several flaws can be identified:

- tanks have not been removed, nor all of the product lines or products within the tank,
- no screening was made in the shallow excavations along with the dispenser islands and between the tank basin and dispenser islands,
- no soil vapour intrusion approach was taken (pavement made with permeable concrete blocks),



Fig. 3 Site aerial photography



Fig. 4 Potentiometric surface map with benzene (in Portuguese Benzeno) contamination

- the investigation did not include the hotel and shopping mall (downstream),
- no human health risk assessment was made.

The solution for this problem requires the consolidation of a set of technical measures to know the actions to be taken:

- Preventive measures, aiming to minimise the occurrence of product spills;
- Corrective measures for emergency and remediation phase of contaminated areas;
- Health promotion measures to reduce the health effects of those exposed.

The risk-based management framework is used to address the current or potential adverse impacts of a contaminant of concern (COC) present in the soil and/or groundwater on human health and the environment by evaluating the linkage between:

- a release of a chemical from a source;
- the transport or exposure pathway; and
- the exposure to and uptake of the chemical contaminants by the receptor.

The corrective action selection process should also consider effectiveness for the impacted media, the required remediation time frame, reliability of the technique,

contractors' expertise, stakeholder views, business needs, accessibility, sustainability, and costs.

Risks associated with petroleum sources can be managed via different techniques applied to mitigate risks by removing or preventing exposures to the COC.

In many cases, the remedial approach can be divided into two general categories: (a) containment or plume stabilisation and/or institutional controls such as land-use restrictions, alternative water supply or permit requirements, and (b) source removal/treatment. Containment is often used for immediate receptor protection, while source removal/treatment is conducted to eliminate or reduce the need for continued containment and monitoring (EPA 2013).

A conceptual site model is developed to understand the site conditions, the extent of the contamination, and the potential impact on receptors. A conceptual site model represents the physical, chemical, and biological conditions and the processes that control the transport, migration, and current/potential impacts of contamination on human and/or ecological receptors for a particular site.

The conceptual site model should include the following (EPA 2013):

- description of the site, environment and Areas of Concern (AOC),
- nature and extent of contaminants,
- potential release mechanisms for such contaminants,
- evaluation of migration pathways and locations at which environmental media are most likely to have been impacted by a release,
- identification of the AOC in which releases have occurred (as well as the AOC in which no releases have occurred),
- data and rationale to support the conclusion.

Once the conceptual site model and risk assessment indicate that remediation is necessary, a suite of remedial techniques is available (EPA 2013).

While specific criteria must be established for each project, typical screening criteria can be followed (NICOLE 2010):

- Stakeholder
- Technical performance
- Resources availability
- Equipment and materials availability
- Cost
- Sustainability factors

References

- ABNT (2004) NBR 10004:2004 Resíduos sólidos – Classificação. ABNT, Brazil
- ANP (2018) Anuário estatístico brasileiro do petróleo, gás natural e biocombustíveis. Agência Nacional do Petróleo, Gás Natural e Biocombustíveis, ANP, Rio de Janeiro [<https://www.gov.br/anp/pt-br/centrais-de-conteudo/dados-abertos/anuario-estatistico-2020-dados-abertos>] (accessed January 2021)
- CETESB (2016) Decisão de Diretoria nº 256/2016/E, de 22 de Novembro de 2016 - Valores Orientadores para Solos e Águas Subterrâneas no Estado de São Paulo, Brazil
- CETESB (2018) Relatório de Áreas Contaminadas e Reabilitadas no Estado de São Paulo, São Paulo, Brazil [<https://cetesb.sp.gov.br/areas-contaminadas/relacao-de-areas-contaminadas/>] (accessed January 2021)
- DE-SP (2013) Decreto Estadual 59.263 de 05 de junho de 2013. Regulamenta a Lei nº 13.577, de 8 de julho de 2009, que dispõe sobre diretrizes e procedimentos para a proteção da qualidade do solo e gerenciamento de áreas contaminadas [<https://www.al.sp.gov.br/repositorio/legislacao/decreto/2013/decreto-59263-05.06.2013.html>] (accessed January 2021)
- EPA (2013) Contaminated site clean-up information. Available online at www.clu-in.org/techdirect/ (accessed March 2021)
- NICOLE - Network for Industrially Contaminated Land in Europe (2010) NICOLE road map for sustainable remediation. Network for Industrially Contaminated Land in Europe. Available at: www.nicole.org/uploadedfiles/2010-wg-sustainable-remediation-roadmap.pdf (accessed March 2021)



Tailings Dams: The Environmental Risks and Failures Management

Maria de Lurdes Dinis and António Fiúza

Abstract

The increasing severity of tailings dam failures and potential impacts of the existing ones require more stringent safety criteria at mining operations. There is a significant degree of underreporting of tailings dam failures. In many cases, when reported, there is no information on many critical factors, compromising the efficient development of safety regulations. Several studies have tried to identify the causes of major tailings dam failures worldwide. Different approaches have been used based on a statistical analysis of the available data, focusing on time and space, causes, and consequences. This work proposes a data analysis of failures based on the severity coding system and mining economic growth metric. The reported cases of tailings dam failure in the past have been collected and re-evaluated thoroughly to understand the distribution of the incident better and establish relationships or identify patterns. The analysis focused on the characteristics of the tailings storage facilities, the causes for failure, the type of accident, and the regulatory framework, both in mining and environmental fields.

Keywords

Tailings dam failures • Mine waste • Economic factors • Consequences and impacts • Severity

1 Introduction

Tailings storage is typically considered the main source of environmental impact for many mining operations. This is due to the volume of pulp requiring storage and the fine ground particles' reactivity. The management of a tailing storage facility presents significant engineering, safety and environmental challenges. The consequences of a dam failure can be severe, both in social and economic aspects, with significant loss of lives. The damages are extremely difficult and costly to address through remedial measures in most cases. Therefore, the risks of dam failures must be minimised by rigorously improving safety criteria at each step of the dam lifecycle (Roca et al. 2019).

The increasing frequency of dam failure incidents and the potential impact and risk of an incident from the existing ones require an awareness urgently from all stakeholders to identify the causes, and understand the different types of risk that tailings facilities pose, as well as their potential for collapse. Significant dam failures remain unreported, which has impeded efficient safety regulations. At the same time, the challenges associated with tailings storage are continually growing. Lower-grade ores can now be exploited thanks to modern technology, resulting in larger volumes of waste that must be safely stored (Owen et al. 2020).

The potential causes of the significant tailings dam incidents have been studied worldwide: UNEP (1996), ICOLD (2001), Bowker and Chambers (2016), and Roca et al. (2019). Different methodologies have been used to analyse the available data on the tailings dam failures. Simple statistical techniques and correspondence analysis infer dam features, failure causes and types of disasters (Rico et al. 2008). The multivariate statistics explore root causes and ascertain which areas of change in legislation and policies, and regulatory enforcement, could be more successful in anticipating general loss and liabilities (Bowker and Chambers 2017).

M. de Lurdes Dinis (✉) · A. Fiúza
Centre for Natural Resources and the Environment
(CERENA-Porto), Faculty of Engineering (FEUP), Porto
University, Porto, Portugal
e-mail: mldinis@fe.up.pt

This study aims to analyse tailings storage facility failures based on the severity coding system and the mining economic history metric. In addition, an extended analysis of the reported cases of tailings dam incidents was performed to better understand the distribution of the incident and establish relationships or identify patterns.

2 Methods

The databases on tailings dam incidents contain information compiled by the United Nations Environmental Protection (UNEP), the International Commission on Large Dams (ICOLD), the World Information Service of Energy (WISE) and the United States Committee on Large Dams (USCOLD).

The ICOLD/UNEP database content resulted from an international expert panel (1995–2001) released in 2006. WISE continued its global compilation by consolidating all failures from ICOLD (2001) and including all newly reported failures. World Mine Tailings Failures (WMTF) has extended the original compilation with independently investigated compiled failures since 1915, incorporating all WISE updates and supplements up to 2015. Missing descriptors in the WISE and ICOLD/UNEP compilations were filled in, element by element, from multiple sources, primarily legal documents and technical reports (Bowker and Chambers 2015, 2016, 2017).

The information was extracted and analysed for: (i) dam characteristics; (ii) failure causes; (iii) types of incidents; (iv) existing mining regulations and environmental protection laws; (v) consequences and impacts. The comparative studies were performed with constant duration, as “averaging” through an extended timeframe. However, so many conditions have changed during this timeframe, which may mislead the conclusions.

3 Results

The ICOLD (2001) database registers 135 failure events from 1917 through 2000. The causes of the reported failures for active and inactive dams are reported as being due to slope stability (23%), overtopping (21%), earthquakes (13%), foundation failure (9%), structure failure (9%), seepage and internal erosion (7%), erosion (2%), mine subsidence (2%) and unknown causes (13%) (Roca et al. 2019). The WMTF registered 246 tailings dam incidents between 1908 and 2017. Twelve more tailings dam failures occurred between February 2018 and January 2019, and WISE registered six more dam failures between March 2019 and March 2020. The data was aggregated in ten years (decade by decade).

A severity coding system with four levels was created for dam tailings failures taking into account three severity variables: release (million m^3), runout (km), and deaths (count) (UNEP 1996, ICOLD 2001). The code system allows examining how often a specific type of severity incident occurs over time but does not evaluate the severity. The levels are classified as “*very serious failures*”, “*serious failures*”, “*minor failures*”, and “*potential failures*”. Severe failures are defined as “*having a release of at least 1 million m^3 and/or a release that travelled 20 km or more and/or multiple deaths (generally = 20)*”. Serious failures are defined as “*having a release of greater than 100,000 cubic m^3 and loss of life*”. Minor failures refer to “*a release lower than 100,000 m^3 and no loss of life*”. Finally, potential failure represents “*an observed condition that could evolve to failure over time if left unattended*” (Bowker and Chambers 2015).

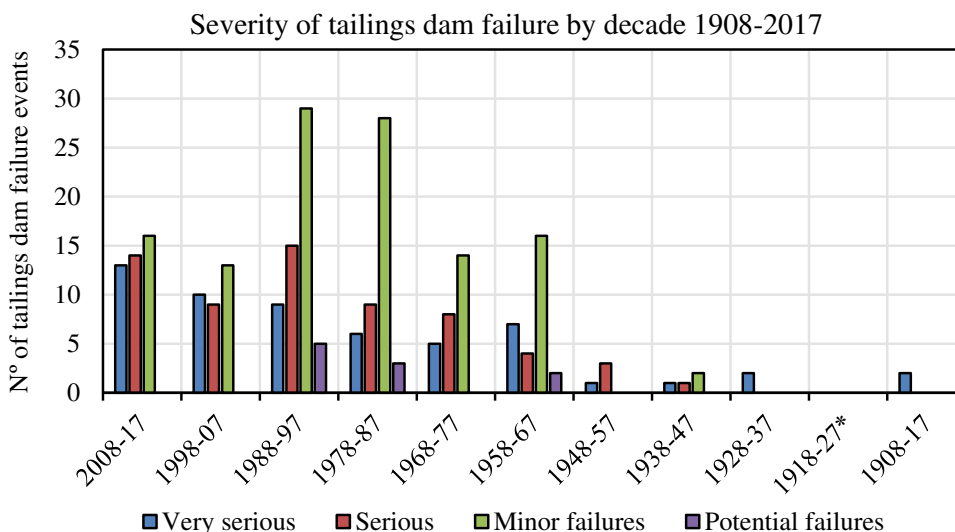
A total of 56 dam failures were classified as very serious, 63 as serious, 117 as minor failures, and 10 as potential failures between 1908 and 2017 (Fig. 1). Failures registered from 2018 to 2020 account for one very serious, one serious and three minor failures events. No classification was given for the remaining twelve failure events.

Published statistics have shown that failure events have increased considerably during the 1960s, 1970s, and 1980s, with 50 events per decade registered against eight to nine in the 1940s and 1950s (Bowker and Chambers 2015). The frequency of tailings dam incidents decreases in the post-2000 events, but serious and very serious failures increase through the following decades. Data on previously reported trends and descriptive statistics were revised (Bowker and Chambers 2017) and updated with data from 2009–2015, including identified data from previously unreported failures. A linear trend was adjusted to the frequency of very serious and serious failures with an r-square of 0.79 and 0.70, respectively. Projecting the overall severity profile up to 2025 will be 67% higher for both failure categories (Bowker and Chambers 2017).

Bowker and Chambers (2015, 2016, 2017) explored the relationship between the economic parameters of mining and the observed trend toward failure incidents of more significant consequence (high severity). Price, production costs, ore production, metal production, and grade were considered economic factors. Copper production was the only commodity with publicly available data for ore production. Data on this economic parameter was collected from the World Bank/Raw Materials Group.

Bowker and Chambers (2015) observed that the correlation between the incident failure and the commodity price was lower than the correlation with the production cost. Copper production’s cost, grade, yearly ore production volume, and metal production strongly correlated with the four failure variables. Only the two most severe failure

Fig. 1 The severity of tailings dam failures by decade (*no data for this decade)



severity categories had significant correlations. Copper metal production presented a stronger correlation with both very serious and severe failures (0.881 and 0.826, respectively) than copper ore production.

According to Bowker and Chambers (2015), projected future failures estimate that very serious and serious tailings dam failures will continue to rise for the next decade if the present mining metric continues. Therefore, only copper production (Mton), production cost (U.S. \$,) and grade were considered in the analysis (Fig. 2).

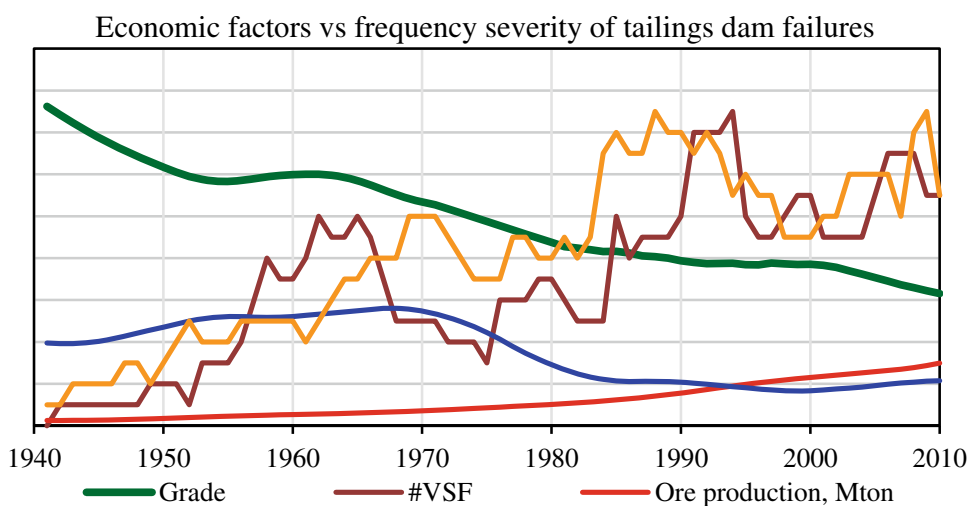
The relationship between the economic history of mines and tailings dam failures at which failures occurred was analysed by Bowker and Chambers (2017) through a multivariate technique known as Canonical Correlation Analysis (CCA). Contrary to a previous interpretation of the frequency and severity of catastrophic failures, these are more common during rapid and sustained price rise periods.

Bowker and Chambers (2017) pointed out the stronger influence of grade and production cost on failure severity categories. Besides, failure events often occur in developing countries with rapidly developing economies, meaning countries that do not meet the United Nations’ socio-economic criteria (e.g. Brazil, Chile, and China).

4 Discussion

There is no complete global database of all tailings dam incidents. Public information, made available by ICOLD, is mostly for large dam incidents. The WISE database addresses only “large” dams (height > 15 m). The USCOLD database or reports (dam incidents in the U.S.) cover a larger scope with very small dams. The WISE, the official global record keepers of significant unplanned incidents at tailings

Fig. 2 Variation of the mining economic factors: Cu grade, Cu ore production (per 100 000 million metric tonnes), Cu production cost (U.S. \$), and the severity of the tailings dam failures from 1940-49 to 2010-19 decades (Bowker and Chambers, 2017)



impoundments, displays a considerable degree of underreporting in their ICOLD and WISE compilations, even for the most significant incidents. The impact of the tailings dam incidents is increasing, with increased runout and emissions affecting a larger area. The high r-square values for very serious and serious failures foreseen the same pattern for the present decade reaffirmed in Bowker and Chambers (2017) through the correlation between failure severity and mining economics parameters.

It is widely recognised that regulatory and legal gaps and inadequacies are common core causes determining the failure's severity. Without clear standards in law and regulation requiring the application of the best available techniques (BAT), the best practices and technical solutions, and economic considerations will continue to lead to choices that can contribute to tailings dam incidents. Therefore, an independent expert review of the safety and economic viability decisions should also be a mandatory request.

5 Concluding Remarks

The tailings dam incidents are often caused by a conjunction of aspects related to the characteristics of the storage facility itself (e.g. type of construction—the upstream method is more prone to instability due to seismic loading than the downstream method), of elements from the external environment (e.g. climate—abnormal intense rainfall events may be the cause of overtopping) and mining economic factors that may lead to sub-standard aspects throughout each stage in the tailings dam lifecycle. Current tailings storage facilities are drafted with operational aspects in mind but rarely consider a long-term and post-closure view, even though they will remain perpetually. Efficient monitoring techniques are vital for risk management of the tailing facility, but although there are robust guidelines for monitoring tailings dams, they are not explicitly included in the legislation. Commercial operations work within a given economic context and have to be profitable. Additional optimisation

measures are only undertaken if there is a financial benefit or compliance with regulatory requirements. Tailings storage facilities should give priority to safety. Safety requirements should be essential in management actions and operations, assessed independently from costs. Ultimately, costs should not be the decisive criterion. Also, *the strengthening of waste regulation at the international level* should be implemented, including penalties (financial and criminal) for non-compliance.

References

- Bowker LN, Chambers DM (2015) The risk, public liability, and economics of tailings storage facility failures. *Earthworks Action* (<https://www.resolutionmineeis.us/documents/bowker-chambers-2015>)
- Bowker LN, Chambers DM (2016) Root causes of tailings management failures: the severity of consequence of failures attributed to overtopping 1915–2015. In: 2nd International Seminar on Dam Protection Against Overtopping. Ft. Collins, Colorado, USA
- Bowker LN, Chambers DM (2017) In the dark shadow of the supercycle: tailings failure risk & public liability reach all time highs. *Environments* 4(4):75
- ICOLD—International Commission on Large Dams (2001) Tailings Dams—Risk of dangerous occurrences, lessons learnt from practical experiences. Bulletin 121, International Commission on Large Dams
- Owen JR, Kemp D, Lèbre É, Svobodova K, Pérez Murillo G (2020) Catastrophic tailings dam failures and disaster risk disclosure. *Int J Disast Risk Reduct* 42:101361
- Rico M, Benito A, Salgueiro R, Díez-Herrerod A, Pereira HG (2008) Reported tailings dam failures: a review of the European incidents in the worldwide context. *J Hazard Mater* 152(2):846–852
- Roca M, Murphy A, Walker L, Vallesi S (2019) A review of the risks posed by the failure of tailings dams. HR Wallingford Ltd, Oxfordshire, U.K., p. 1–63 (<https://damsat.com/2019/01/30/a-review-of-tailings-dams-risks/>)
- UNEP—United Nations Environment Programme (1996) Environmental and safety incidents concerning tailings dams at mines: results of a survey for the years 1980–1996 by the Mining Journal Research Services. United Nations Environment Programme, Paris (file:///C:/Users/Gil/AppData/Local/Temp/EnvDM.pdf)



Geochemical Background in Heavy Metals on Basaltic Soils from the Lisbon Volcanic Complex

Andrei Spiridon, Paulo Sá Caetano, Graça Brito, André Sanches, and Ricardo Manuel

Abstract

Anthropic activities have increasingly influenced soil quality due to growing urban development. This study aims to establish a methodology for determining reference levels for heavy metal concentrations in soils by using X-ray fluorescence, an analysis technique that relies on simple and relatively fast sample preparation. To test the proposed methodology, a study was carried out on soils and outcrops originating from the basalts of the Lisbon Volcanic Complex in Odivelas. To verify the concentrations of heavy metals obtained via X-ray fluorescence, soil samples were also tested by atomic emission spectrometry. The results compare favourably between the pairs of V, Cr, and Pb measurements, showing a concordance between the methods. The obtained concentrations and their cumulative frequency curves were used to determine the upper limit for the background concentration in V, Cr, Ba, Ni, Zn, Cu, and Pb. The 95th percentile was chosen as the upper limit of background for the studied soils. These soils show a large variability in their composition that prevents a clear definition of the boundary between which of them correspond to natural concentrations, and which are most likely caused by anthropogenic influences. Some of the values obtained are higher than those found in guidelines for use at contaminated sites and deserve further investigation to confirm contamination or not.

Keywords

Geochemical background • Heavy metals • X-ray fluorescence • Basaltic soils

1 Introduction

Considering that urban environments are always in constant change, with the construction of new infrastructures that increasingly occupy natural areas, it becomes essential to recognize which geochemical parameters of urban soils might relate to natural features, thus allowing to distinguish them from those which might result from anthropic activity (Zgłobicki et al. 2011). Over time, the quantification of the geochemical background of soils was performed mainly using analytical techniques that rely on complicated and time-consuming sample preparation, often involving the destruction of the sample, high costs, chemical waste production, daily calibration of equipment, and long periods until results are obtained (McComb et al. 2014). Therefore, this study intends to investigate the geochemical background of soils formed by weathering of the basaltic rocks from the Lisbon Volcanic Complex (LVC), using X-ray fluorescence (XRF), an analysis technique which relies on an expeditious preparation of soil samples.

2 Materials and Methods

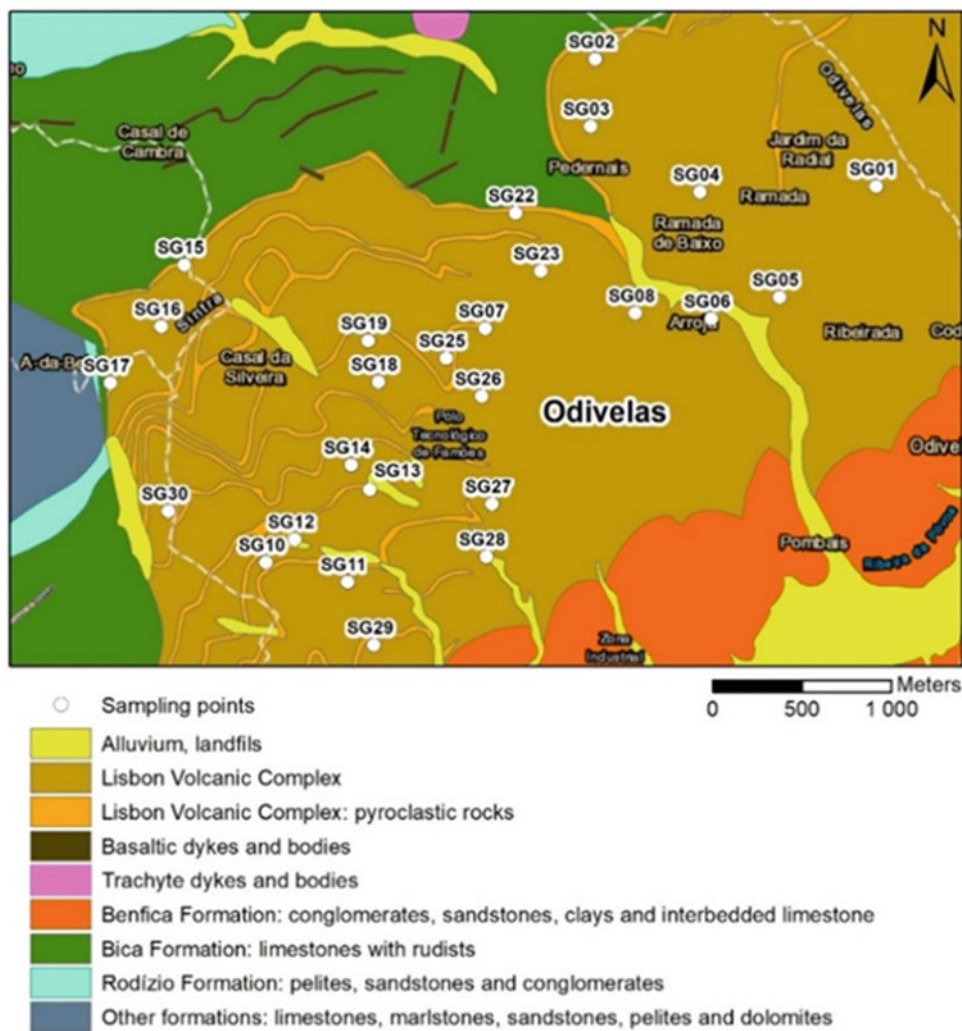
Soil sampling was performed in 26 separate locations in Odivelas, near Lisbon, at two distinct depths: 0.5–1.5 m (top level) and 2–3 m (bottom level). On the samples from both these levels, chemical analyses were performed on two separate granulometric fractions, the total fraction, under 2 mm, and the fine fraction, under 63 μm . The sampling points' location and the region's geological setting are shown in Fig. 1.

A. Spiridon (✉)
NOVA School of Science & Technology, Caparica, Portugal
e-mail: a.spiridon@campus.fct.unl.pt

P. S. Caetano · G. Brito · A. Sanches
GeoBioTec|NOVA, Department of Earth Sciences, NOVA School of Science & Technology, Caparica, Portugal

R. Manuel
eGiamb-Consultoria Geoambiental Lda, Caparica, Portugal

Fig. 1 Location of the sampling points and geology (geological setting adapted from Zbyszewski et al. 2008)



Additionally, basaltic rock samples were collected from outcrops in the immediate vicinity of some of the soil samples. These rock samples were ground and sieved before being submitted for chemical analysis, and the obtained results were compared with previous results from Palácios (1985). Finally, using Niton XI3t GOLDD equipment for XRF analyses, the chemical concentrations of the heavy metals V, Cr, Ni, Cu, Zn, Ba, and Pb were selected for further analysis.

3 Results

During the sampling campaign, different types of basaltic soils were identified: pyroclastic soils, amygdaloid basalt-derived soils, and fine-textured basalt-derived soils. The XRF analysis results for the 23 samples collected at the top level are shown in Table 1.

Regarding the results of the XRF analysis for the 16 samples collected from the bottom level, these are shown in Table 2.

To verify the existence of similarities between results obtained by different methods of analysis, the XRF concentrations of elements V, Cr, Zn, and Pb from the collected basaltic soils were compared with the results obtained by atomic emission spectrometry (ICP-AES), for the same elements, in duplicates of the samples. As an outcome, it was found that the pair of results XRF/ICP-AES obtained for V shows a good correlation. The results obtained by the two methods (XRF and ICP-AES) for V in the collected top-level (T) soil samples are illustrated in the chart in Fig. 2. The correlations for Cr and Pb turned out worse, and no correlation was found for Zn.

To study the similarities between the chemical elements in basaltic soils, in order to make a comparison of their behaviour, Principal Component Analysis was performed.

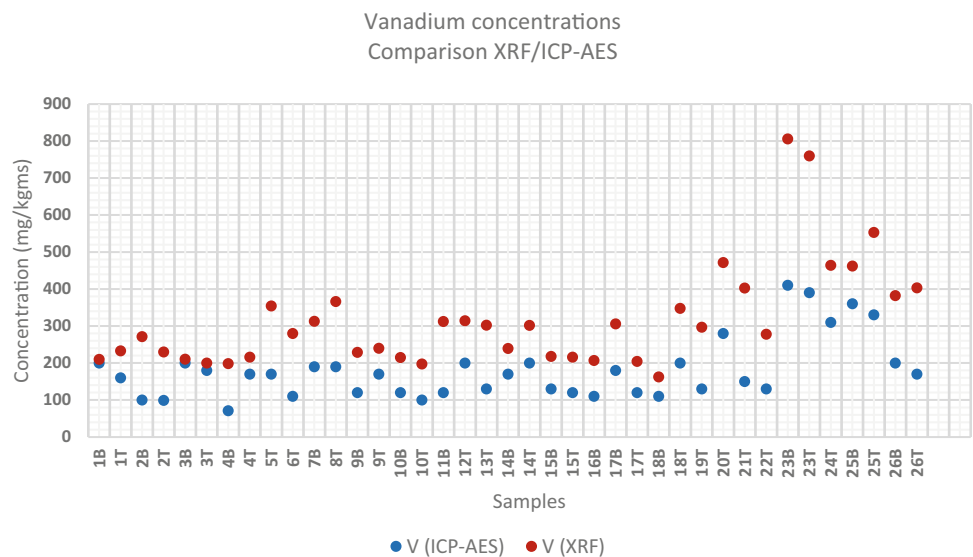
Table 1 Concentration of elements measured in top-level soils by XRF (23 samples)

Element (ppm)	Average	Minimum	1st Quartile	2nd Quartile	3rd Quartile	Maximum	Std. deviation	Variation coefficient	Skewness
V	331.9	197.5	229.8	302.0	402.6	759.8	134.4	0.4	1.7
Cr	236.3	24.1	77.2	214.0	358.9	568.7	178.6	0.8	0.5
Ni	163.8	11.1	80.8	185.3	250.7	329.7	97.0	0.6	-0.1
Cu	55.2	23.6	45.1	53.1	64.9	91.9	16.3	0.3	0.4
Zn	102.3	71.9	93.1	101.5	106.4	138.1	15.1	0.2	0.6
Ba	663.7	443.9	515.2	651.1	732.9	1516.7	218.6	0.3	2.8
Pb	9.9	4.2	6.3	8.6	11.7	21.0	4.7	0.5	1.2

Table 2 The concentration of elements measured in bottom level soils by XRF (16 samples)

Element (ppm)	Average	Minimum	1st Quartile	2nd Quartile	3rd Quartile	Maximum	Std. deviation	Variation coefficient	Skewness
V	296.3	162.3	210.4	239.3	312.7	805.6	156.3	0.5	2.6
Cr	158.8	21.1	80.4	145.2	244.0	402.5	111.5	0.7	0.7
Ni	144.9	31.0	84.4	157.8	208.2	281.5	78.5	0.5	0.2
Cu	51.8	4.5	45.4	50.6	62.8	96.0	21.2	0.4	-0.2
Zn	92.5	70.8	84.3	90.3	98.0	144.2	18.5	0.2	1.5
Ba	660.0	260.8	481.0	662.6	819.2	1528.6	308.2	0.5	1.3
Pb	6.8	3.9	5.4	6.1	8.9	12.5	2.4	0.4	1.1

Fig. 2 Comparison between XRF and ICP-AES V results from top-level (T) soil samples



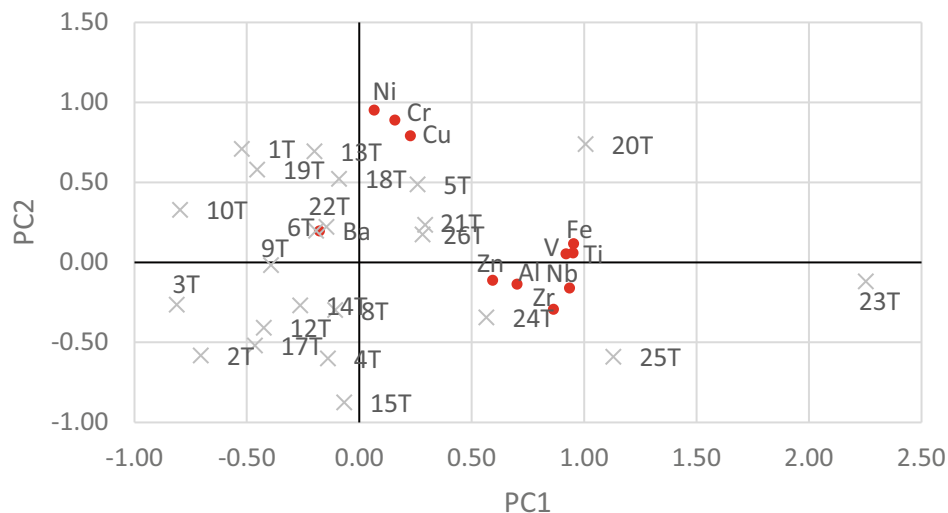
An example of the contributions on the factorial plane PC1/PC2 provided by the chemical elements V, Fe, Ti, Zn, Al, Nb, Zr, Ni Cr, Cu, and Ba, determined in samples of top-level (T) soils, is represented in Fig. 3.

It can be noticed that the first axis explains a group formed by the elements Al, Ti, V, Fe, Zn, Zr, and Nb, with an explanation percentage of 47.58% of the variance, meaning that these elements are closely related to each other in the chemistry of the basaltic soils. The second axis

explains the group of elements Cr, Ni, and Cu, with a percentage of explanation of 22.95% of the variance. The element Ba is explained by the third axis, as opposed to the other variables.

Despite many studies of the geochemical background in several locations around the world, there is still no consensus among researchers as to the methods of determination. To define the upper guideline values and check the differences between results obtained by different methods, background

Fig. 3 Projection of the 11 variables assessed in 23 samples of basaltic soils on the factorial plane PC1/PC2



concentrations were calculated using statistical frequency analysis techniques.

In the first stage, upper guidelines values were calculated following recommendations from the English and Finnish legislation (Ander et al. 2013), based on the percentiles of the measured concentration's cumulative frequency curves, as presented in Table 3.

In the second stage, because the percentile values are subject to some uncertainty, based on the number of data points and the shape of the distribution, additional methods can be used to calculate the background interval upper limits, based on statistical measures of central tendency (mean, median) associated with σ —standard deviation and MAD—median absolute deviation.

For this purpose, iterative methods such as $[\text{mean} \pm 2\sigma]$ and $[\text{median} \pm 2\text{MAD}]$, presented by Matschullat et al. (2000), and Reimann et al. (2005), were also implemented. These methods repeatedly apply the exclusion of values that exceed the limits of the interval defined by the statistical parameters. The operation is iterated until the same subset of data is repeated in two successive iterations, thus approximating a normal distribution. The results obtained by all previously mentioned methods are presented in Fig. 4 for the V concentrations in the soils collected from the top levels. To allow a comparison between the results, only the upper limits of the interval are considered for the iterative method cases.

For all the studied elements (V, Cr, Ni, Cu, Zn, Ba, Pb), it can be seen that the limits of the calculated geochemical background are affected by the type of distribution that the element concentrations exhibit and the implementation of different methods can lead to widely varying results. Methods based on mathematical formulas that use more than one parameter, in conjunction with high compositional variability of the investigated soils, can set background limits higher than the maximum obtained concentration value of a chemical element. Therefore, the results obtained by the English method (P95) were selected as adequate for the studied basaltic soils. A comparison between these limits and the lowest reference levels specified by the Ontario Standards (agricultural use) is shown, for the top-level sampled soils, in Table 4.

4 Discussion

Considering the studied area geology, the soils were formed on basaltic mantles intercalated with pyroclastic levels. Although formed on a single geological unit (the LVC), the soils show significant heterogeneity in textures and chemical composition. That may derive from the fact that the study area shows a hydrographic network that is well embedded in the ground. It may induce different degrees of alteration of the parent rocks (basalts) and, consequently, the formation of

Table 3 Methods based on percentiles

Method	Calculation
English legislation	B = P95
Finnish legislation	BL = P75 + 1.5 (P75 - P25)

B—Geological background upper limit; BL—Baseline; P95—95th percentile of measured concentrations; P75—75th percentile of measured concentrations; P25—25th percentile of measured concentrations

Fig. 4 Example of a frequency distribution plot used in the data exploration—cumulative probability plot of V results from the top-level soils

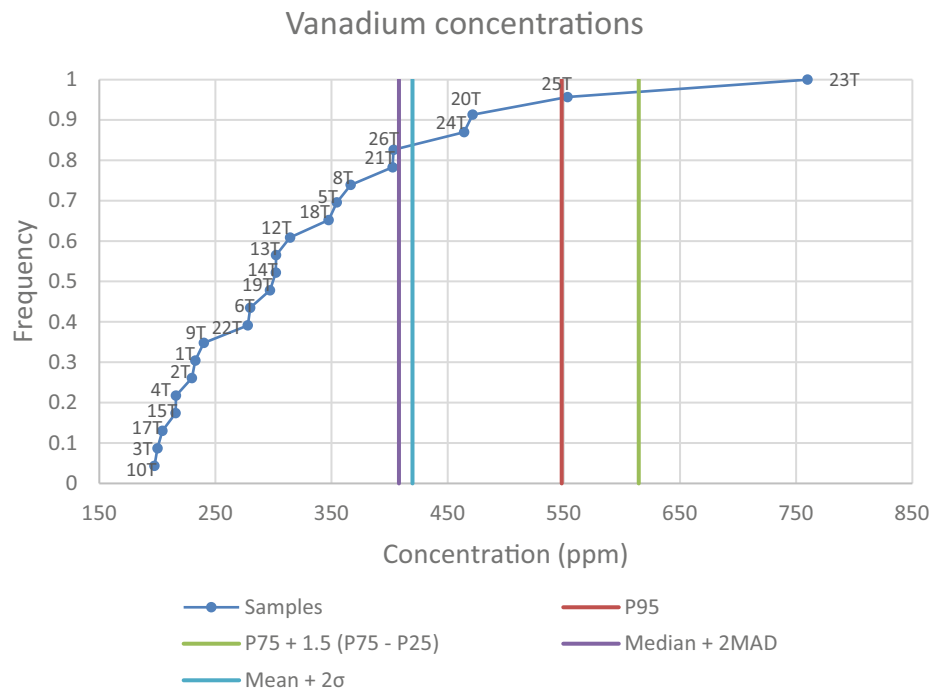


Table 4 Calculated background interval upper limits for soil samples from the top levels (23 samples). Numbers in bold represent background concentrations higher than reference levels

Element (ppm)	Background interval upper limit	Ontario Standards (agricultural use)
V	548	86
Cr	332	67
Ni	262	37
Cu	84	62
Zn	124	290
Ba	1018	210
Pb	11	45

different types of soils through its erosive power. There is a strong dependence between the Ti, V, and Fe elements, as shown in Fig. 3. These elements are most likely derived from the titanomagnetite found in the parent rock (basalts). Although on a smaller scale, these elements (Ti, V, and Fe) display correlations with the elements Zn, Zr, and Nb. Among all the elements analysed, Ti, V, Fe, Zr, and Nb are the ones that best correlate with the fine fraction of the superficial top-level soils, indicating that the studied soils, of basaltic origin, tend to show reduced mobility of the respective elements and, therefore, what seems a residual character. In the same soils, there is a strong correlation between Cr and Ni and an average correlation between these elements and Cu (Fig. 3).

5 Concluding Remarks

The chemical analyses performed on basaltic soil samples with the portable XRF equipment enabled the gathering information on a relatively extensive set of chemical elements. The upper limits of the geochemical background interval, based on P95, exceed the lowest reference limits specified for land use by the Ontario Standards (agricultural use) for V, Cr, Ni, Cu, and Ba. In these cases, special attention should be given to the history of anthropogenic activity to confirm the anthropogenic contribution to high levels of these elements and thus be able to influence the decision on adequate future land use.

Acknowledgements The authors are thankful to Centre GeoBioTec (UID/GEO/04035/2020-FCT) and Professor Fernanda Pessoa for their support and availability of the handheld XRF usage spectrometer and assistance in the sample preparation technique.

References

Ander EL, Johnson CC, Cave MR, Palumbo-Roe B, Nathanail CP, Lark RM (2013) Methodology for the determination of normal background concentrations of contaminants in English soil. *Sci Tot Environ* 454(455):604–618

Matschullat J, Ottenstein R, Reimann C (2000) Geochemical background: can we calculate it? *Environ Geol* 39(9):990–1000

McComb JQ, Rogers C, Han FX, Tchounwou PB (2014) Rapid screening of heavy metals and trace elements in environmental

- samples using portable X-ray fluorescence spectrometer, a comparative study. *Wat Air Soil Poll* 225:2169
- Palácios T (1985) Petrology of the Lisbon Volcanic Complex. PhD Thesis, University of Lisbon
- Reimann C, Filzmoser P, Garrett RG (2005) Background and threshold: critical comparison of methods of determination. *Sci Tot Environ* 346:1–16
- Zbyszewski G, Manupella G, Ferreira OV, Rodrigues L, Rodrigues A (2008) Geological Map of Portugal on the scale 1/50,000 Sheet 34-B—Loures. Serviços Geológicos de Portugal, Lisbon
- Zgłobicki W, Lata L, Plak A (2011) Geochemical and statistical approach to evaluate background concentrations of Cd, Cu, Pb and Zn (case study: Eastern Poland). *Environ Earth Sci* 62:347–355



Bioaugmentation and Biostimulation for Remediation of BTEX—Polluted Soils: Study Case

Manuela M. Carvalho, Maria Cristina Vila, Teresa Oliva-Teles, Cristina Delerue-Matos, and António Fiúza

Abstract

Soils are a sensitive biomineral layer on top of the Earth's crust and are a complex ecosystem. They are used and requested by various human activities, and this intensive use can affect their characteristics and functions, causing erosion, compaction, and contamination. Contamination of soils with petroleum hydrocarbons is still common in many places on our planet, and, also, there are old contaminations that have not yet been remedied. This work evaluated the efficiency of remediation of soils contaminated with BTEX using assisted bioremediation techniques, applying bioaugmentation and biostimulation. The results highlight that the consortium of microorganisms used and the applied methodologies were adequate. Furthermore, the achieved remediation efficiencies were high, varying the remediation time with the contaminant and the number of clay minerals present in the soil.

Keywords

Soils • Standardization • Laboratory testing • Particle size distribution

1 Introduction

Soils are natural resources that provide nutrients for plants and also provide critical ecosystem services to sustain life on Earth; they are used daily, whether as a base for solid waste disposal facilities, as a filter for water, or even as a foundation for cities, thus soils are often subject to degradation

and contamination. Over time, the extensive use of chemicals in human activities has caused soil contamination. When soil pollutants reach some levels, they are contaminated, and loss of function and deterioration can occur (ESDAC 2019). This problem is common and dangerous for the environment, also presenting a significant risk to human health, which requires attention. When the health risk is unacceptable, soil contamination must be dealt with (EEA 2019). In European Union countries, the types of contaminants that appear in groundwater and soils are similar; mineral oils and heavy metals are the main categories; reports from countries across Europe indicate that polycyclic aromatic hydrocarbons (PAH), aromatic hydrocarbons (BTEX), phenols and chlorinated hydrocarbons (CHC) are also found very often (EEA 2019). In addition, petroleum hydrocarbon spills have been occurring in the last decades, causing soil contamination. Their presence in the environment is harmful to health (EPC 2017).

Contaminated sites are commonly managed using “traditional” remediation techniques, such as excavation and off-site disposal. Nonetheless, the development of advanced remediation techniques, new policies, and increased operations control are changing these practices (EEA 2019). In this perspective, bioremediation techniques present themselves as appealing, simple, and useful methods of remediating petroleum hydrocarbons in contaminated soils, and they enable the effective destruction of the contaminant (Carvalho 2014; Carvalho et al. 2015).

Aromatic hydrocarbons present high microbial degradability, and if appropriate nutrients and aerobic conditions are available, microorganisms convert these organic contaminants to carbon dioxide, water, and microbial cell mass (EPA 2019). However, the autochthone microorganisms are, in most cases, unable to degrade hydrocarbons in a timely way, and the contaminated sites do not have, usually, favourable environmental conditions for the microorganism's development. This situation can be improved with assisted bioremediation, such as bioaugmentation and

M. M. Carvalho (✉) · T. Oliva-Teles · C. Delerue-Matos
REQUIMTE|LAQV, ISEP, Polytechnic of Porto, Porto, Portugal
e-mail: mmc@isep.ipp.pt

M. C. Vila · A. Fiúza
CERENA|FEUP, Faculty of Engineering, University of Porto,
Porto, Portugal

biostimulation (Carvalho et al. 2015). Usually, these techniques are used together (Tyagi et al. 2011).

In the present study, assisted bioremediation lab-scale tests were made by applying a consortium of heterotrophic microorganisms from a crude oil-contaminated site. The consortium was extracted from contaminated soil (BSoil), and the microorganisms were developed in a liquid mineral medium enriched with xylene as a carbon source. The obtained microbial cultures were used for bioaugmentation in the tests performed. In bioremediation trials made without ventilation, biostimulation was accomplished solely by adding nutrients contained in the mineral medium of the microbial culture, whereas, in the bioventing tests, oxygen supply was also included. The main objectives of the trials were to evaluate the remediation time and the remediation efficiency for both methodologies in three different residual soil types, granite (SR), limestone (CL), and schist (XT), artificially contaminated by BTEX. To achieve the objectives, several experiments were performed in stainless steel reactors containing the contaminated soils; in bioventing tests, columns were connected to a respirometric circuit to provide oxygen, which also allowed daily monitoring of oxygen and carbon dioxide concentrations in the system. In addition, BTEX concentrations in the gas phase were also determined daily by gas chromatography (GC-FID).

2 Materials and Methods

Four natural soil were used: a petroleum-contaminated soil (BSoil) to obtain the microbial consortium and three different residual soils (SR, CL, and XT) for the bioremediation tests as a substratum. Standard methodologies were used for geotechnical, physical, chemical, and biological soil characterization and several properties were determined, namely: mineral composition, particle size distribution, particle density (G), bulk density (ρ), porosity (η), permeability (k), water content (W), water-holding capacity (WHC), pH, conductivity (σ), total organic carbon, nitrogen, and phosphorus content (C:N:P), total hydrocarbons (TPH) content and biomass content. In addition, pro-analysis benzene, toluene, ethylbenzene, and xylene with purity $\geq 99.5\%$ were used to contaminate the soils with BTEX artificially.

To develop and adapt the microbial consortium obtained from BSoil to the contaminants under study, successive transfers in a liquid medium were done. Microbial cultures (first and second transfers) were developed in a mineral media enriched with xylene (280 mgL^{-1}). The microbial cultures were maintained under aerobic conditions, at a controlled temperature of $28 \text{ }^\circ\text{C}$, and shaken at 150 rpm. At the end of the second transfer, these cultures were used as

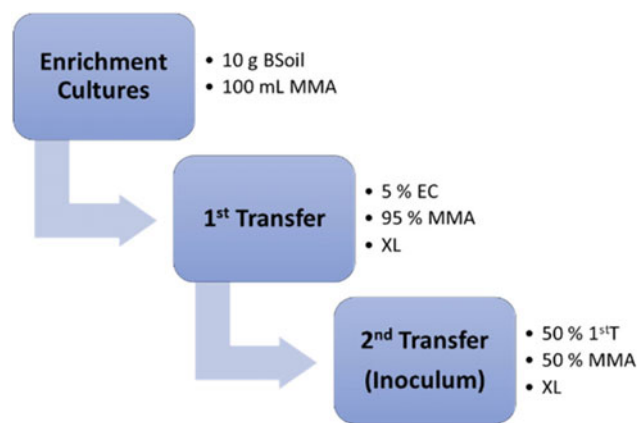


Fig. 1 Microbial cultures preparation. BSoil: petroleum-contaminated soil MMA: mineral media; XL: xylene

inoculum for the bioaugmentation in the bioremediation assays (Fig. 1).

The bioremediation tests were done in stainless steel reactors (Fig. 2a) partly filled with 2 kg of wet soil, kept at $25 \text{ }^\circ\text{C}$. In the two assisted bioremediation methodologies implemented, bioventilation, and bioremediation without ventilation, inoculated assays and non-inoculated assays (blank) were performed (Fig. 2b). In the inoculated tests (B and BV), the previously dried soil was moistened by adding the produced inoculum to proceed with the system bioaugmentation and biostimulation. Sterilized demineralized water was added to moisten the soil in the blank tests (Bb and BVb). After introducing the wet soil into the reactors, they were closed and sealed. Afterwards, 400 mg of contaminant (benzene, toluene, ethylbenzene, xylene, or a mixture of the four (BTEX)) were introduced through the reactor sampling ports. During bioventing experiments, oxygen was supplied daily, using an airflow of $3.33\text{E}-7 \text{ m}^3/\text{s}$, in open circuit mode, for 15 min.

To monitor bioremediation rate and microorganisms activity, the concentration of contaminants in the gas phase was assessed daily in all experiments, and, in the bioventing ones, carbon dioxide and oxygen concentrations were also measured. The contaminant concentration was determined by isothermal gas chromatography ($200 \text{ }^\circ\text{C}$) using a GC-Shimadzu-2010 chromatograph equipped with an FID detector and TRB-5 Teknokroma column; N_2 was used as carrier gas. The carbon dioxide and oxygen concentrations were assessed with Servomex—5200 Multipurpose respirometers. Inoculated trials were considered complete when a residual concentration of 0.5 mg/L in the gas phase was reached; the corresponding blank trials were concluded on the same day, regardless of contaminant concentration. The final biomass content was determined in all experiments by serial dilution in plates of LB broth medium (Luria–Bertani).

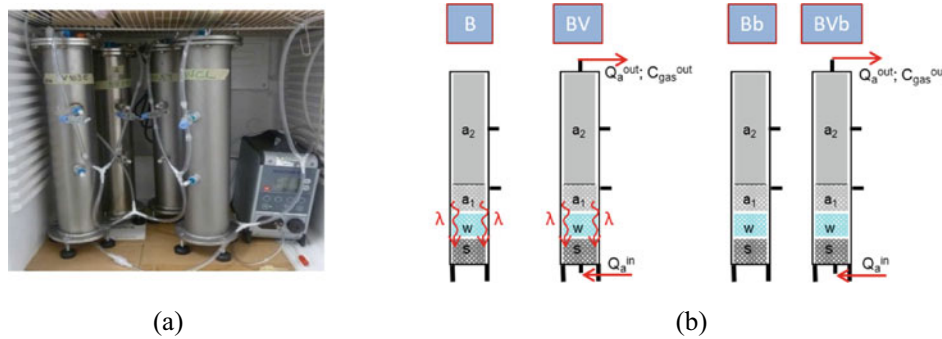


Fig. 2 a Stainless steel reactors at controlled temperature (bioventing); b Schematic representation of assisted bioremediation lab-scale tests: B—bioremediation test; BV—bioventing test; Bb—bioremediation control test (blank), and BVb—bioventing control test (blank)

3 Results

The main results obtained in the soil characterization are summarized in Fig. 3, grain size distribution, mineralogical composition, and evaluated physical–chemical characteristics were presented.

The results from assisted bioremediation tests performed in limestone soil (CL), granitic soil (SR), and schist soil (XT) are presented in Fig. 4; remediation time and final efficiency were presented for all tests.

4 Discussion

As it turns out from the presented soil characterization: (i) XT contains the highest fine fraction (82% < 0.074 mm), predominantly silty (79%), but it does not contain clay minerals; (ii) CL has the highest clay fraction (15% < 0.002 mm) and contains kaolinite; (iii) SR has the lowest fine fraction

(35% < 0.074 mm) but contains kaolinite and montmorillonite and the highest clay activity; (iv) porosity and water-holding capacity present the highest values in SR; (v) CL showed the highest pH and conductivity; (vi) SR presents the lowest values of pH and conductivity; (vii) the initial permeability value has the same order of magnitude in SR, CL, and XT; (viii) the initial biomass content value has the same order of magnitude (E4 CFUg⁻¹) in SR, CL, and XT; (ix) BSoil has the highest total petroleum hydrocarbons content (TPH), a significant quantity of organic matter, and the highest biomass content (E7 CFUg⁻¹).

Final efficiencies in inoculated assays were always very high, both in bioremediation and bioventilation. In addition, the remediation time required to reach the established residual concentration is, in most cases, shorter in bioventilation tests.

The different contaminants in the same soil showed that xylene always needed the longest remediation time, sometimes *ex aequo* to benzene. In limestone and granite, toluene and ethylbenzene were the contaminants that required the

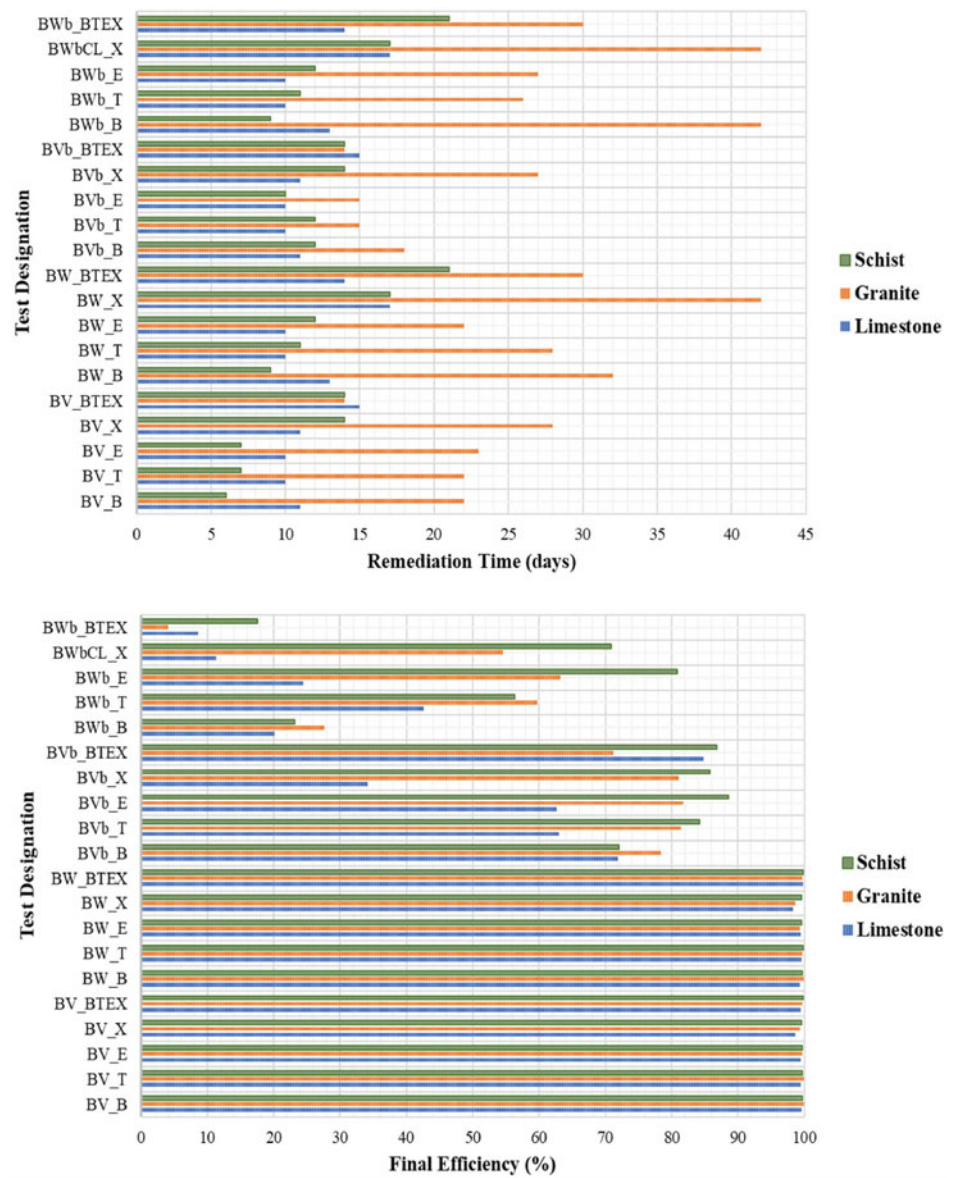
Fig. 3 Synthesis of the results obtained in the characterization of soils

	Clay (%)	Mud (%)	Sand (%)	Gravel (%)
SR	7	28	60	5
CL	15	30	35	20
XT	3	79	18	0

	Mineral Composition
SR	Kaolinite, muscovite, montmorillonite, quartz, potassium feldspars and hematite.
CL	Calcite, kaolinite, mica, quartz and hematite.
XT	Chlorite, mica, quartz and sodium feldspars.

	WHC (%)	W (%)	η (%)	K (ms ⁻¹)	G	ρ (Kgm ⁻³)	TPH (mg kg ⁻¹)	C:N:P	pH	σ (μS cm ⁻¹)	Biomass (CFUg ⁻¹)
SR	46	25	60	7.6E-6	2.68	1.1	0.35	120:7:52	5.8	24	4.1E4
CL	20	11	44	7.9E-6	2.73	1.5	0.46	120:3:13	6.8	295	1.8E4
XT	29	14.5	47	9.9E-6	2.80	1.5	0.55	120:3:13	6.1	67	3.6E4
BSoil							296	120:5:4			8.9E6

Fig. 4 Synthesis of the results obtained in assisted bioremediation tests in limestone, granite, and schist soils. Remediation time (days) and final efficiency (%)



B - benzene
 E - ethilbenzene
 T - toluene
 X - xylene
 BWb - bioremediation tests without ventilation, control test
 BVb - bioremediation tests with ventilation (bioventing), control test
 BW - assisted bioremediation tests without ventilation
 BV - assisted bioremediation tests with ventilation (bioventing)

shortest remediation time, almost always *ex aequo*. In schist, the benzene always had the shortest remediation time.

Comparing similar inoculated experiments in different soils, it is possible to notice that SR had the longest remediation time in most cases. The inoculated tests' remediation time was 26.4 days in SR, 12.1 days in CL, and 11.8 days in XT. These results did not directly correlate with the respective clay fraction since the limestone and schist have very different clay fractions, 15% and 3%, respectively, and

presented similar remediation times. Granite with a clay fraction of 7% presented much longer remediation times. The organic matter content is very low and similar in all soils, so it cannot be considered a determining factor in this difference. Instead, the mineralogical composition, namely the clay mineral content, appears critical for the different remediation times since the granitic soil presents a high percentage of kaolinite in its mineralogical composition, which does not happen in the other two soils.

5 Concluding Remarks

The results outline that the developed microbial consortium can degrade BTEX in aerobic conditions and the applied assisted bioremediation techniques were suitable for the soil remediation. However, the remediation time was shorter with bioventing experiments in all soils and contaminants. The most significant difference in the remediation time between ventilated and non-ventilated assisted bioremediation tests was verified in residual granitic soil; this soil was, in all tests conditions, the one with the slowest remediation rate, which could be related to the more significant presence of clay minerals. In all inoculated tests, the final efficiency was very high, between 98.2% and 99.9%. In non-inoculated control tests, lower remediation efficiencies were obtained, with the highest values in bioventing tests. It can also be concluded that in bioventing, as expected, in addition to bioremediation, contaminant removal by advection also occurs. Therefore, the analytical methods implemented to determine the contaminants, carbon dioxide, and oxygen concentrations in the gas phase were appropriate. This work proved that bioaugmentation and biostimulation were appropriate strategies for the remediation of BTEX-polluted soils.

References

- Carvalho MM (2014) Análise fenomenológica da bio-remediação de solos contaminados com compostos orgânicos: perspectiva multidisciplinar. PhD thesis, Faculdade de Engenharia da Universidade do Porto, Porto. <https://hdl.handle.net/10216/95741>
- Carvalho MM, Vila C, Delerue-Matos C, Oliva-Teles T, Fiúza A (2015) Assisted bioremediation tests on three natural soils contaminated with benzene. *Euras J Soil Sci* 4(3):153–160
- EEA (2019) Progress in management of contaminated sites. Retrieved from <https://www.eea.europa.eu/data-and-maps/indicators/progress-in-management-of-contaminated-sites-3/assessment> (accessed on 2019/10/29)
- EPA (2019) Bioremediation. Retrieved from [https://clu-in.org/techfocus/default.focus/sec/Bioremediation/cat/Aerobic_Bioremediation_\(Direct\)/](https://clu-in.org/techfocus/default.focus/sec/Bioremediation/cat/Aerobic_Bioremediation_(Direct)/) (accessed on 2019/10/29)
- EPC (2017) Oil Spill Pollution. Retrieved from <https://www.environmentalpollutioncenters.org/oil-spill/> (accessed on 2019/10/29)
- ESDAC (2019) Soil Contamination. Retrieved from <https://esdac.jrc.ec.europa.eu/themes/soil-contamination> (accessed on 2019/10/29)
- Tyagi M, Fonseca MM, Carvalho CCR (2011) Bioaugmentation and biostimulation strategies to improve the effectiveness of bioremediation processes. *Biodegradation* 22(2):231–241



Microplastic-Like Debris and Biomarkers in the Fish *Pseudochondrostoma duriense*: Preliminary Findings

M. A. Martins, L. R. Vieira, L. G. A. Barboza, J. Costa, C. Antunes, and L. Guilhermino

Abstract

The contamination of the freshwater fish *Pseudochondrostoma duriense* from the Minho River estuary by anthropogenic debris suspect of being microplastics (MP-S) was investigated. Biomarkers (neurotoxicity, energy-related, biotransformation, oxidative stress, and damage) were also determined. Twelve fish were analyzed for MP-S presence in the gastrointestinal tract (GT), gills, liver, and dorsal muscle. A total of 207 MP-S was recovered from fish with sizes between 79 and 48,900 μm (94% had size $<5000 \mu\text{m}$, and 6% were larger debris). The predominant shape was fiber-like (89%), followed by fragments (11%). The most common color was black/brown, but other colors were also found. The frequency of MP-S ingestion by fish was 100%. The frequency of specimens with MP-S in gills, liver, and muscle was 8%, 25%, and 25%, respectively. The means (\pm standard deviation) of the number of MP-S items per fish were 16 ± 9 in the GT, 0.3 ± 1.2 in gills, 0.3 ± 0.5 in the liver, 0.4 ± 0.8 in the muscle, 17 ± 9 in total. The results provide baseline values for *P. duriense* MP-S contamination and biomarkers in the Minho estuary, and further investigation concerning long-term contamination and climate changes is ongoing.

Keywords

Microplastics-like debris • Freshwater fish • Very high contamination • Baseline biomarkers

1 Introduction

Studies in different regions have shown that fish populations are contaminated with microplastics (MP) (Wang et al. 2020). Most parts of the studies on wild fish investigated MP ingestion (e.g., Bessa et al. 2018). The presence of MP in gills and internal tissues was investigated in a limited number of works (e.g., Abbasi et al. 2018). Laboratory experiments demonstrated that MP could induce toxic effects on fish (Luis et al. 2015). Adverse effects of MP contamination in wild fish populations were also found (Barboza et al. 2020). Fish are an essential component of the human diet, and their contamination by MP may decrease fish health and be a route of exposure to humans through the ingestion of contaminated parts of the fish as food (Barboza et al. 2018). More studies on the topic are needed.

The goal of the present study was to perform a preliminary assessment of the contamination by anthropogenic debris suspect of being microplastics (MP-S) in a wild population (Minho River estuary, NW Iberian Peninsula) of *Pseudochondrostoma duriense* (Coelho 1985). This freshwater fish is consumed as food by humans. Baseline values for biomarkers indicative of fish health were also determined.

2 Methods

Fish ($N = 12$) from the Minho estuary's freshwater tidal area were obtained from the local fishery (September–October 2018). Fish whole bodies were transported in cold conditions to the laboratory, measured (total length—length), and

M. A. Martins · L. R. Vieira · L. G. A. Barboza · L. Guilhermino (✉)

Department of Populations Studies, Laboratory of Ecotoxicology and Ecology (ECOTOX), ICBAS—Institute of Biomedical Sciences of Abel Salazar, University of Porto, Porto, Portugal
e-mail: lguilher@icbas.up.pt

M. A. Martins · L. R. Vieira · L. G. A. Barboza · J. Costa · C. Antunes · L. Guilhermino

CIIMAR—Interdisciplinary Centre of Marine and Environmental Research, University of Porto, Research Team of Ecotoxicology, Stress Ecology and Environmental Health (ECOTOX), Research Team of Estuarine Ecology and Biological Invasions, Matosinhos, Portugal

C. Antunes
Aquamuseu do Rio Minho, Vila Nova de Cerveira, Portugal

weighed (body weight). The samples' preparation was done under conditions aimed at avoiding sample contamination, and blanks were included (Barboza et al. 2020). From each fish, the whole gastrointestinal tract (GT) and the liver were isolated and weighed. Samples of gills, brain, liver, and dorsal muscle were collected for this and other studies and weighed. Samples for MP-S analyses were frozen at -20°C , and samples for biomarkers were frozen at -80°C . The extraction of MP-S, measurements of individual debris, and sorting by shape, color, and size classes were done as indicated in Barboza et al. (2020) with minor modifications. Biomarkers were lipid peroxidation levels (LPO) and the activity of the enzymes acetylcholinesterase (AChE), cholinesterases (ChE), lactate dehydrogenase (LDH), isocitrate dehydrogenase (IDH), glutathione *S*-transferases (GST), catalase (CAT), glutathione reductase (GR), glutathione peroxidase (GPx) and superoxide dismutase (SOD). They were determined according to the original techniques with adaptations (Luis et al. 2015; Barboza et al. 2020). Enzymatic activities were expressed in nanomoles of substrate hydrolyzed per minute per mg of protein (nmol/min/mg prot), except SOD that was expressed in Units per mg of protein (U/mg prot) (1 U = amount of enzyme needed to inhibit the cytochrome *c* reduction rate by 50%). LPO levels were indicated as thio-barbituric acid reactive species per mg of protein (TBARS/mg prot). The correlation between fish length (or body weight) and the number of MP-S in the GT, liver, muscle, or total (sum of MP-S in all body sites) and between tissue weight and MP-S content were analyzed using the Spearman correlation coefficient (*r*). The SPSS (version 25) was used for data analyses. The significance level was 0.05.

Table 1 Mean and standard deviation of sample weight and MP-S concentrations and properties of the MP-S. Twelve samples per body location (12 fish) were analyzed. GT—whole gastrointestinal tract; *n*—number of MP-S items; Freq.—frequency of fish with MP-S. Conc—MP-S concentration expressed as the mean of the number of MP-S items per individual fish (MP-S *n*/ind) or as the mean of the number of MP-S items per individual fish per weight of the analyzed tissue (MP-S *n*/g); Max.—the highest number of MP-S found in a single individual

Parameter	GT	Gills	Liver	Muscle	Total
MP-S (<i>n</i>)	195	4	3	5	207
Freq. fish MP-S (%)	100	8	25	25	25
Conc (MP-S <i>n</i> /ind)	16 ± 9	0.3 ± 1.2	0.3 ± 0.5	0.4 ± 0.8	17 ± 9
Max. MP-S in ind	31	4	1	2	31
Sample weight (g)	37 ± 11	1.6 ± 0.9	0.6 ± 0.4	15 ± 12	54 ± 15
Conc (MP-S <i>n</i> /g)	0.5 ± 0.4	0.3 ± 0.9	0.9 ± 2	0.04 ± 0.07	0.3 ± 0.2
Mean size (μm)	1458 ± 3961	679 ± 839	561 ± 484	1210 ± 654	1424 ± 3850
Lowest size (μm)	79	254	79	190	79
Highest size (μm)	48,900	1937	1048	1873	48,900
Fibers (%)	89	100	67	100	89
Fragments (%)	11	0	37	0	11
Transparent (%)	0	0	0	9.7	9
White/whitish (%)	0	0	0	27.7	26
Black/brown (%)	25	67	40	58.5	58
Blue/blueish (%)	50	33	60	3.6	6
Red/reddish (%)	25	0	0	0.5	1

3 Results

The mean and standard deviation (SD) of fish length, body weight, and liver weight was 28 ± 2 cm, 366 ± 61 g, and 4 ± 2 g, respectively. The weight of the samples is shown in Table 1. A significant and positive correlation ($N = 12$, $r = 0.586$, $p = 0.045$) between fish length and the number of MP-S in the liver was found. All the other correlations were not significant ($p > 0.05$). The total number of debris recovered from fish was 207. Because 94% of debris suspected of being plastic items had a size lower than <5000 μm, for simplicity, all the debris is indicated as MP-S. The frequency of MP-S ingestion by fish was 100%. The frequency of specimens with MP-S in other body sites, mean concentrations of MP-S, properties of the MP-S, and other indications are shown in Table 1. The distribution of MP-S per size classes is displayed in Fig. 1. The mean of biomarkers determined in the fish is shown in Table 2.

4 Discussion

The significant and positive correlation between fish length and the number of MP-S in the liver suggests that fish length may influence MP-S liver storage. The lack of other significant correlations indicates that morphometric parameters did not influence MP-S ingestion, gill retention, or muscle storage in the analyzed ranges of size and weight. In the intervals tested, the differences in sample weight did not influence the likelihood of finding MP-S.

Fig. 1 Distribution of MP-S per size classes according to their longest dimension (μm)

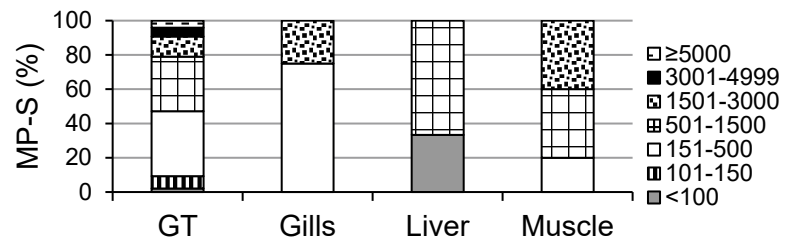


Table 2 Mean and standard deviation of the biomarkers determined in the fish ($N = 12$)

Parameter	Gills	Liver	Brain	Muscle
AChE (nmol/min/mg prot)	–	–	35 ± 6	–
ChE (nmol/min/mg prot)	–	–	–	22 ± 6
LDH (nmol/min/mg prot)	–	–	–	29 ± 6
IDH (nmol/min/mg prot)	–	–	–	1.5 ± 0.2
GST (nmol/min/mg prot)	9 ± 2	104 ± 11	–	–
GR (nmol/min/mg prot)	8.6 ± 0.7	10 ± 4	–	–
GPx (nmol/min/mg prot)	5 ± 1	4 ± 1	–	–
CAT (nmol/min/mg prot)	15 ± 3	48 ± 7	–	–
SOD (U/mg prot)	52 ± 11	4 ± 2	–	–
LPO (TBARS/mg prot)	0.2 ± 0.8	0.1 ± 0.3	0.3 ± 1.1	0.5 ± 0.6

The predominant shape (fiber-like) and colors of the MP-S are in agreement with findings in other estuarine fish, such as three fish species from the Mondego River estuary, also located on the Portuguese coast, where fibers were predominant (96%) over other shapes. Blue was the most common color of the MP recovered from the GT, accounting for 47% of the particles (Bessa et al. 2018). The 100% of fish with MP-S in the GT and the GT concentrations of MP-S were determined to indicate very high ingestion and contamination of the population. These findings and the diversity of MP-S colors and sizes also indicate the high availability of different MP-S in the Minho estuary. Considerable MP's availability in other estuaries of the Portuguese coast (Bessa et al. 2018) and in other aquatic ecosystems (Wang et al. 2020) was documented. The percentage of fish with MP-S and the mean number of particles per individual are higher than those reported for the most contaminated species in the Mondego River estuary, namely 73% of fish with MP in the GT and 3.14 ± 3.25 particles per fish. The lower frequency of fish with MP-S and MP-S concentrations in gills than in the GT suggests that fish may ingest actively MP-S by confusion with prey and uptake MP-S through contaminated prey and/or from sediment

additionally to passive ingestion from the water. *P. duriense* is a benthopelagic species and may be exposed to MP-S through water, sediment, and pelagic and benthic prey. The MP-S recovered from liver and muscle samples indicate that absorption and storage of some MP-S occurred. As in studies with other fish species (Abbasi et al. 2018; Barboza et al. 2020), large MP-S (mainly fiber-like) in the liver and muscle were found. The mechanisms allowing large MP to cross-protective barriers and reach internal organs and tissues of fish have been discussed (e.g., phagocytosis, endocytosis, lesions) but were not yet demonstrated (Barboza et al. 2020). The presence of MP-S in internal tissues, including muscle which is the main fish tissue ingested by humans, is of high concern regarding fish and human health. MP can cause physical and chemical toxic effects, decrease the nutritional value of fish, and carry other toxic chemicals and pathogenic microorganisms that can also induce adverse effects (Barboza et al. 2018, 2020).

The means of the biomarkers determined in *P. duriense* from the Minho estuary are in the range of corresponding values documented for other fish species (e.g., Luis et al. 2015; Barboza et al. 2020) and constitute baseline values for the population of the Minho River estuary.

5 Concluding Remarks

Very high frequency of MP-S ingestion (100%) and MP-S concentration in the GT (16 ± 9 MP-S items/ind) of *P. duriense* from the Minho River estuary was found, indicating significant contamination of the population and availability of MP-S in the ecosystem. These findings raise concern because the Minho estuary has great conservation and ecologic value due to its biodiversity and habitat variety, and high socio-economic interest. The MP-S found in the liver and muscle indicates that MP-S absorption and storage in internal organs and tissues occurred, contributing to the existing concern concerning fish health and human exposure through food. The preliminary data on *P. duriense* MP-S contamination and biomarkers constitute baseline values for further studies on long-term contamination and effects on the Minho estuary population concerning climate change and contribute to the overall knowledge on the paradigm of wild fish contamination by MP and other debris.

Acknowledgements This study was funded by FCT, Portugal (PTDC/MAR-PRO/1851/2014), and ERDF European funds (COMPETE 2020, POCI-01-0145-FEDER-016885) through the project PLASTICGLOBAL.

References

- Abbasi S, Soltani N, Keshavarzi B, Moore F, Turner A, Hasanaghaei M (2018) Microplastics in different tissues of fish and prawn from the Musa Estuary, Persian Gulf. *Chemosphere* 205:80–87
- Barboza LGA, Lopes C, Oliveira P, Bessa F, Otero V, Henriques B, Raimundo J, Caetano M, Vale C, Guilhermino L (2020) Microplastics in wild fish from North East Atlantic Ocean and its potential for causing neurotoxic effects, lipid oxidative damage, and human health risks associated with ingestion exposure. *Sci Total Environ* 717:134625
- Barboza LGA, Vethaak AD, Lavorante BRBO, Lundebye A-K, Guilhermino L (2018) Marine microplastics debris: an emerging issue for food security, food safety and human health. *Mar Pollut Bull* 133:336–348
- Bessa F, Barria P, Neto JM, Frias JP, Otero V, Sobral P, Marques JC (2018) Occurrence of microplastics in commercial fish from a natural estuarine environment. *Mar Pollut Bull* 128:575–584
- Luis LG, Ferreira P, Fonte E, Oliveira M, Guilhermino L (2015) Does the presence of microplastics influence the acute toxicity of chromium (VI) to early juveniles of the common goby (*Pomatoschistus microps*)? A study with juveniles from two wild estuarine populations. *Aquat Toxicol* 164:163–174
- Wang W, Ge J, Yu X (2020) Bioavailability and toxicity of microplastics to fish species: a review. *Ecotoxicol Environ Saf* 189:109913



Impact of Agriculture and Livestock on Quality of the Tagus Alluvial Groundwater Body: Evolution of Nitrate Concentration

Joel Zeferino, Maria do Rosário Carvalho, Ana Rita Lopes, Rosário de Jesus, José Martins Carvalho, and Helder I. Chaminé

Abstract

Groundwater contamination by nitrates is a public health problem worldwide due to the intensive demand for food products. Under Portuguese Law, groundwater quality targets are set by Water Framework Directive 2000/60/EC and Nitrates Directive (Directive 91/676/EEC). The Nitrates Directive indicates a risk of water contamination caused or induced by nitrates from the agricultural origin; when NO_3 concentration is above 50 mg/L, the state organism that is responsible for water management creates a Nitrate Vulnerable Zone (NVZ) to avoid the spread of this kind of pollution, where minimization measures must be applied. To evaluate the long-term effect of the water quality measures of an alluvial aquifer under agricultural practices and livestock production, numeric flow and mass transport modelling was carried out using the software FEFLOW. The model domain resembles the area of the Tagus alluvial groundwater body. The productive units are constituted by sands and gravels of the Quaternary age. The mean values of the samples collected from March to September 2018 (6 months) were used to define the initial nitrate concentrations in the numerical model. The nitrate loads of agriculture and livestock origins were estimated, considering the land use and the average amount of nutrients excreted by animals. The forward simulations show decreasing nitrate concentrations and consequently

reducing the contaminating plume's extent. However, some parts of the aquifer still have nitrate concentrations above 50 mg/L, even in 2040, proving that the mitigation measures are not entirely effective. So, this groundwater body is always at risk of pollution by nitrates.

Keywords

Groundwater modelling • Nitrates • Tagus alluvium aquifer • Agricultural pressures • FEFLOW

1 Introduction

The contamination of groundwater by nitrates is a serious environmental and public health problem of growing concern, given the high demand for this resource. In the European Union, it is estimated that 61% of agricultural land puts water bodies under pressure and at risk of contamination by nitrates of agricultural origin (EC-European Parliament 2018). Council Directive 91/676/EEC of 12 December 1991 emerged to protect the water quality from this type of pollution across Europe by promoting good agricultural practices. As a result, the designation of Nitrate Vulnerable Zones (NVZs) is assigned in areas where the concentration of nitrate in water exceeds or is at risk of exceeding 50 mg/L. To prevent the dispersion of nitrates in the waters, a set of mandatory rules displayed in Action Programs must be applied.

In Portugal, diffuse agricultural pollution and livestock effluents are the main causes of water pollution by nitrates. According to the last four-year report (2012–2015) (DGADR-APA 2016), nine NVZs are approved, covering fourteen groundwater bodies, including the Tagus alluvial groundwater body (Tagus NVZ). A periodic assessment of the water quality must be carried out in these areas. Predictions should be performed to evaluate the mitigation measures' effectiveness and estimate the time needed to restore the quality of the groundwater bodies.

J. Zeferino (✉) · M. do Rosário Carvalho
IDL and Department of Geology, Faculty of Sciences, University
of Lisbon, Lisbon, Portugal
e-mail: jfzeferino@fc.ul.pt

A. R. Lopes · R. de Jesus
Portuguese Environment Agency (APA), Lisbon, Portugal

J. M. Carvalho · H. I. Chaminé
Laboratory of Cartography and Applied Geology (LABCARGA),
Department of Geotechnical Engineering, School of Engineering
(ISEP), Polytechnic of Porto, Porto, Portugal

Centre GeoBioTec|UA, Aveiro, Portugal

2 Setting and Methods

2.1 Approach to Quality Assessment

Groundwater quality goals under Portuguese Law are set by the Water Framework Directive (WFD) 2000/60/EC and Nitrates Directive (ND, Directive 91/676/EEC). However, the criteria used in these documents to classify the chemical status of a groundwater body are different. For example, the WFD indicates that contamination of a groundwater body should not exceed 20% of its total area, using the terms “mediocre” and “good” for chemical status labelling. On the other hand, the ND considers a risk of contamination by nitrates from agricultural sources whenever the concentration in groundwater exceeds 50 mg/L, proposing the creation of an NVZ to prevent its spread and facilitate the application of mitigation measures.

The data for evaluating mitigation measures’ effectiveness (Action Programs) are obtained from the water quality monitoring network. However, it is not enough to estimate the time required for the groundwater body’s quality recovery. Therefore, to evaluate the measures’ long-term effect, the FEFLOW software (Diersch 2013) was used to simulate the transport of contaminants in the aquifer. The results obtained will evaluate the effectiveness of the measures in force, while the comparison with historical records will define evolution patterns of the nitrate content in the aquifer.

2.2 Aspects of Groundwater Modelling

The model domain resembles the Tagus alluvial groundwater body area, given that administrative boundaries outline Tagus NVZ. The aquifer’s productive units are sands and gravels of alluvial deposits and terraces of fluvial origin. Groundwater flow occurs towards the Tagus river, the basin’s primary drainage axis, towards the Tagus estuary in the terminal phase, and occasionally to valleys that limit the high areas covered by terraces. The aquifer is a discharge area for adjacent systems and can thus be fed at several points (Simões 1998; Almeida et al. 2000; Mendonça 2010). To reproduce the aquifer hydraulic behaviour, boundary conditions were applied to the Tagus river, its main tributaries, and probable lateral feeding areas. The hydraulic behaviour of the aquifer shown in Fig. 1 is essential to understanding some conditioning factors of mass transport, such as pollutant dispersion or dilution.

Parametrization was focused on three main aspects: vertical recharge, hydraulic conductivity, and (effective) porosity. A methodology proposed by LABCARGA (2017) to evaluate groundwater bodies’ recharge in mainland Por-

tugal was applied to import the recharge values into the numerical model. Reference values were introduced for the remaining parameters based on hydraulic tests and normative values (Portuguese Law No. 382/99). Through a zonation procedure (Carrera et al. 2005), the hydraulic conductivity was calibrated for several aquifer parts using observation points from the SNIRH (Portuguese Information Services of Water Resources) quantity network. At a steady-state flow regime, the effective porosity cannot be calibrated at this stage. These values were first adjusted using the normative values and later by analysing nitrate samples in different aquifer materials in different samples of aquifer materials. Finally, pressure zones were identified in borehole reports and added to the model, matching the extraction volumes from APA (Portuguese Environment Agency) database (APA 2016).

2.3 Nitrate Sources and Concentrations

The nitrate concentration in the groundwater is analysed semi-annually in the quality network spots by the SNIRH. The mean values of the semi-annual (March and September) samples from 2018 were used to define the initial nitrate concentrations in the numerical model. The spatial distribution of NO_3 levels was obtained by kriging, interpolating the sample values for the remaining area of the model.

It is not easy to control the amount of nitrogen applied to soils over such vast areas. To circumvent this problem, APA (2016) proposed a method based on the calculation of diffuse loads as a function of land occupation. The total diffuse pollutant load affluent to a body of water (CT_i) is calculated by multiplying the unit loads assigned to each land occupation class (C_{ij}) (DCEA-FCT 2015) by the respective area (A_j). For the livestock sector, the county’s quantification of nitrogen surpluses is carried out according to the number of nutrients excreted annually by each “livestock unit” (Annex II, Portuguese Law No. 214/2008, Annex XII of Portuguese Ordinance No. 259/2012). The same methodological approach was used to determine agricultural sector surpluses, considering that 12% of the total gross load generated can reach aquifers.

Approximately 2125 tons of nitrogen can reach the aquifer every year, with around 60% of the agricultural sector (Table 1). Agricultural producers must respect these values, as they are considered by managing authorities to be sufficient for sustainable food and livestock production. In numerical terms, agricultural loads are replicated by 4th-order boundary conditions (mass nodal sink/source), the best available option, as a set of equispaced source points of a given land-use class.

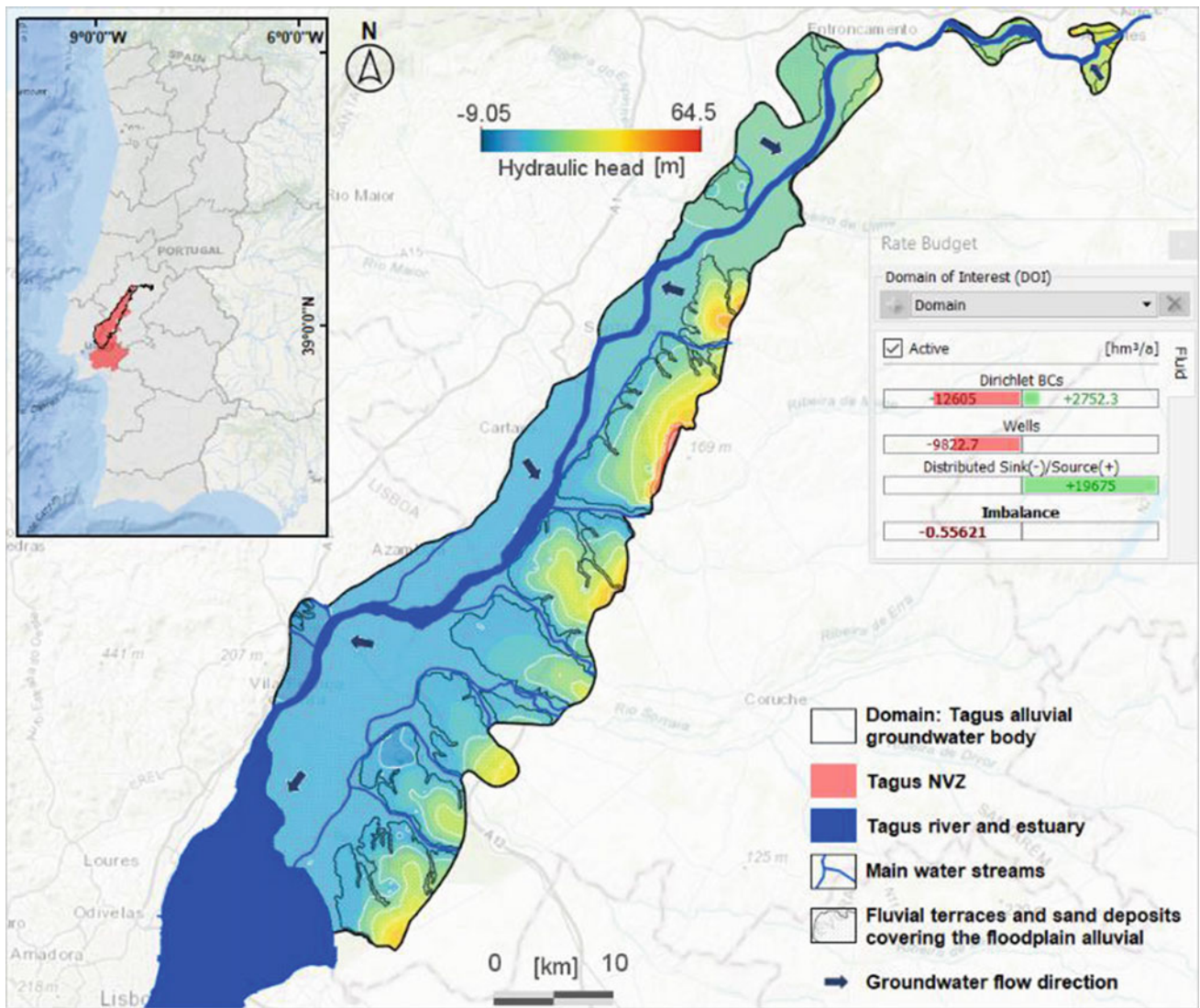
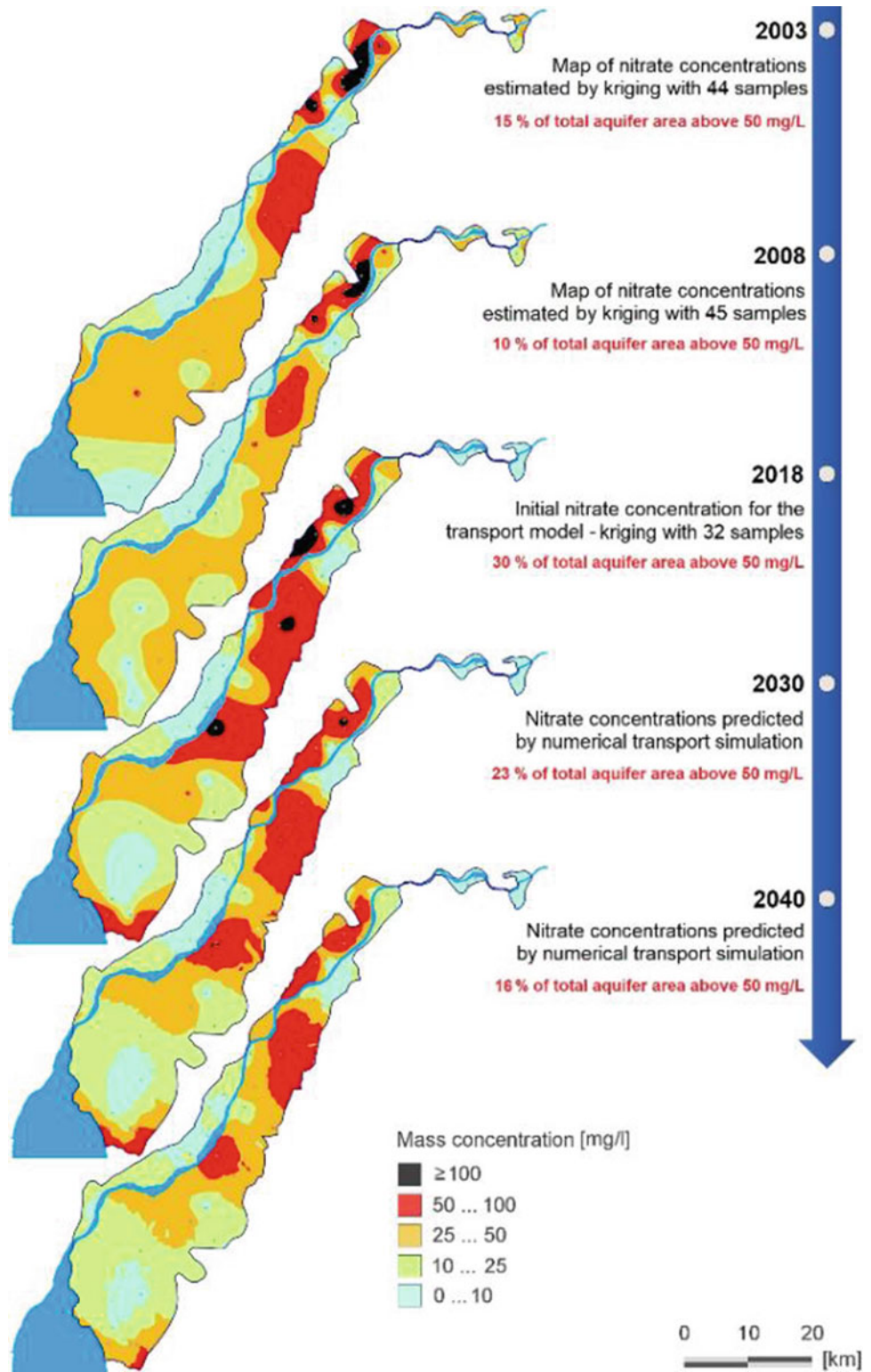


Fig. 1 Geographic settings of the Tagus Nitrate Vulnerable Zone (NVZ) and Tagus alluvial groundwater body, simulated piezometric level in the aquifer, and rate budget within the model domain

Table 1 Nitrogen loads that could potentially reach the aquifers used in the numerical model

Land-use classes	C_{ij} (kg/ha/year)	A_j (ha)	CT_i (kg/year)	Total (kg/year)
Agriculture activity				
Heterogeneous agricultural areas	11.94	21,182	252,809	1,261,482
Agricultural areas with temporary crops	15.50	54,860	850,332	
Agricultural areas with permanent crops	8.37	7915	66,252	
Permanent pastureland	4.65	3436	15,975	
Forest area	6.20	12,276	76,114	
Others (non-agricultural areas)	0	9702	0	
Livestock activity				
Total Livestock Loads	13.59	119,615	863,414	863,414

Fig. 2 Evolution of nitrate concentrations in the Tagus alluvial groundwater body



3 Results

Figure 2 shows the evolution of the NO₃ concentrations in the aquifer, estimated from historical series for current and past scenarios and simulated by a numerical model.

4 Discussion and Concluding Remarks

Among forecasts and spatial distributions by kriging historical records, the 2018 scenario (used as initial concentration) is the most alarming and where the contamination is more dispersed in the aquifer. It is challenging to identify evolution patterns in nitrate content since it has decreased and increased over the years.

The forward simulations show decreasing nitrate concentrations and consequently reducing the contaminating plume's extent. However, some parts of the aquifer still have nitrate concentrations above 50 mg/L, even in 2040, proving that the mitigation measures are not entirely effective. This decrease is sluggish, and the environmental goals defined by the legislation in force are far from being achieved. Under the WFD criteria, the groundwater body's chemical status can be classified as good post-2030. However, according to the Nitrates Directive, nitrates from agricultural sources are always a risk of pollution.

Acknowledgements The authors thank APA for financing this project through the POSEUR program (Portugal 2020) and FCT through the UID/GEO/50019/2020–IDL. In addition, HIC and JMC were supported under the LABCARGA|ISEP re-equipment program (IPP-ISEP|PAD*2007/08) and Centre GeoBioTec|UA (UID/GEO/04035/2020).

References

- Almeida C, Mendonça JL, Jesus MR, Gomes AJ (2000) *Sistemas aquíferos de Portugal Continental*, vol 3. Instituto da Água e Centro de Geologia da Universidade de Lisboa, Lisboa
- APA–Agência Portuguesa do Ambiente (2016) *Plano de Gestão de Região Hidrográfica 2016/2021 da Região Hidrográfica do Tejo e Ribeiras do Oeste (RH5A)*, Lisboa
- Carrera et al., 2005 Carrera J, Alcolea A, Medina A, Hidalgo J, Slooten LJ (2005) Inverse problem in hydrogeology. *Hydrog J* 13 (1): 206–222
- DCEA-FCT (2015) *Avaliação das cargas de poluição difusa gerada em Portugal continental. Relatório para a Agência Portuguesa do Ambiente*, IP. Departamento de Ciências e Engenharia do Ambiente, Faculdade de Ciências e Tecnologia da Universidade Nova de Lisboa, Monte da caparica. (Unpublished Report)
- DGADR-APA (2016) *Poluição provocada por nitratos de origem agrícola—Diretiva 91/676/CEE, de 12 de dezembro—Relatório 2012–2015*. Direção Geral de Agricultura e Desenvolvimento Rural e Agência Portuguesa do Ambiente, Lisboa (Unpublished Report)
- Diersch HJ (2013) *FEFLOW: finite element modelling of flow, mass and heat transport in porous and fractured media*. Springer Science & Business Media, Berlin
- EC–European Parliament (2018) Report from the commission to the council and the European Parliament. On the implementation of Council Directive 91/676/EEC concerning the protection of waters against pollution caused by nitrates from agricultural sources based on Member State reports for the period 2012–2015. Brussels, 4.5.2018 COM (2018) 257 final, p 4
- LABCARGA–Laboratório de Cartografia e Geologia Aplicada (2017) *Desenvolvimento de métodos específicos para a avaliação da recarga das massas de águas subterrâneas, para melhorar a avaliação do estado quantitativo. Relatório para a Agência Portuguesa do Ambiente*, IP. Laboratório de Cartografia e Geologia Aplicada, ISEP, Porto (Unpublished Report)
- Mendonça JP (2010) *Sistema aquífero aluvionar do Vale do Tejo (V. N. da Barquinha a Alverca): Características e Funcionamento Hidráulico*. Universidade de Coimbra, Coimbra (Ph.D. Thesis). <https://estudogeral.uc.pt/handle/10316/1869>
- Simões M (1998) *Contribuição para o conhecimento hidrogeológico do Cenozóico na Bacia do Baixo Tejo*. Universidade Nova de Lisboa, Monte da Caparica (Ph.D. Thesis). <http://hdl.handle.net/10362/1152>



Use of Drill Cuttings for Hydrogeological Water Well Logging Reconstruction: A Practical Approach

José Teixeira, José Martins Carvalho, and Helder I. Chaminé

Abstract

In hard rock terrains, down-the-hole hammer drilling is a method commonly used. Consequently, it is a destructive method, and the resulting drill cuttings are crushed rock and rock dust. A low-cost and valuable methodology to reconstruct the water well logs from drill cuttings is presented. That approach encompasses lithological, mineralogical, geo-structural, and hydrogeotechnical data. A comprehensive study of the site's geology, engineering geology, and hydrogeology constraints supports the water wells design at an early stage. The cuttings were systematically collected and described during the drilling process, and they were registered hydrogeological field parameters for every 3 m drilled. The drill cutting samples were carefully described at the laboratory with a binocular microscope's assistance. The design of the water well potentially intersects the fracture zone trending NNE-SSW. The groundwater flow seems to be associated preferentially with this orientation. That was confirmed in the drilling data and related to the productive groundwater zones. The synthesis and integration of this information allowed a significant improvement in the hydrogeological conceptual site model, thus contributing to efficient groundwater resource management.

Keywords

Water well • Log reconstruction • Drill cuttings • Hydrogeotechnics • NW Portugal

J. Teixeira (✉)
Centre CEGOT(UP), Department of Geography, Faculty of Arts,
University of Porto, Porto, Portugal
e-mail: jateixeira@letras.up.pt

J. Teixeira · J. M. Carvalho · H. I. Chaminé
Laboratory of Cartography and Applied Geology (LABCARGA),
Department of Geotechnical Engineering, School of Engineering
(ISEP), Polytechnic of Porto, Porto, Portugal

J. M. Carvalho · H. I. Chaminé
Centre GeoBioTec|UA, Aveiro, Portugal

1 Introduction

In hard rock terrains, the down-the-hole hammer (DTH) method is commonly used to drill water wells and other boreholes (e.g., Bresson 1977; Atlas-Copco 1979; Plote 1985; Driscoll 1986; ADITC 2015; Missstear et al. 2017; Glotfelty 2019, and references therein). Several button bits could be mounted at the end of the drill pipe, combined with a down-the-hole air percussion hammer to cut the rock. Then, high-pressure air is pumped through the drill pipe to lubricate the cutting surfaces and blow the broken-down rock material (cuttings) to the surface. The drill cuttings consist of rock dust and fragments up to 3 cm in diameter (e.g., USACE 2001; Sterrett 2007; Marjoribanks 2010). These destructive drilling methods are well described in the scientific and technical publications (e.g., Davis and Turk 1964; Summers 1972; Bresson 1977; Plote 1985; Driscoll 1986; Clark 1988; Hartman 1992; Yin and Brook 1992; USACE 2001; Doesburg 2005; Eustes et al. 2009; Ahmed et al. 2014; ADITC 2015; Rix et al. 2019; Zhang 2016; Missstear et al. 2017; Dassargues 2019; Patel 2019; Glotfelty 2019). Still, systematic sampling is not treated with equal importance. Nevertheless, Harvey and Lovell (1998), Marjoribanks (2010), Monnet (2015), and Kyzym et al. (2015) highlight the sampling and logging procedures for destructive drilling methods, clearly stating that it is only possible if undertaken when the water well is being drilled.

This preliminary study shows how a low-cost and prompt methodology greatly supports the water well log reconstitution from drill cuttings. Furthermore, that comprehensive approach based on lithological, mineralogical, geo-structural, and hydrogeotechnical data is reliable. This data has crucial importance for the development of the hydrogeological conceptual site model.

The geology of the study site—Noninha, Montemuro Mountain, North Portugal—is dominated mainly by granitic rocks (Fig. 1). At the bottom of the Noninha stream valley, some alluvia deposits are also present. Additionally, quartz

veins outcropped the granite bedrock and quartz hornfels (Teixeira 2011). The granitic rocks are dominated by two major fault sets, mainly trending to NNE-SSW and conjugated systems, NW-SE to WNW-ESE. The field studies conducted in the area have integrated geological, morphostructural, and hydrogeological data to support a series of exploration works. In the former S. Pedro das Meadinas spring vicinities, two exploration sub-horizontal (5° dip) water wells were drilled, trending $N160^\circ E$ and $N90^\circ E$, respectively (Fig. 1).

2 Material and Methods

At the Noninha site, was carried out a comprehensive hydrogeological study. Field surveys, such as regional and local geological mapping, morphotectonical, hydrogeological inventory, and hydrogeotechnical surveys. Besides, desk studies and laboratory analysis were performed, namely GIS (Geographical Information Systems) mapping and hydrogeochemical analysis. Therefore, was design two sub-horizontal exploration water wells (5° dip) and drilling with the DTH method. Figure 2 presents a practical methodology for water well logs reconstruction based on drill cuttings in hydrogeological studies to support the conceptual site model.

The studies performed at the investigation site were structural geology and geomorphology mapping, on-site fracturing scanline surveys, hardness testing evaluation on exposed rock surfaces, and hydrogeological field surveys. In addition, the suggested methods for characterisation and testing of rock masses proposed by ISRM (1981, 2007, 2015) were followed. This information was necessary to design the water wells, later integrated with the data collected during the drill cuttings sampling and log reconstruction stage.

The water wells were drilled using the down-the-hole hammer (DTH) method, employing 3 m drill pipes mounted with button bits. The cuttings sampling was made during the drilling process, following the methodology proposed by Marjoribanks (2010). The collected samples for every 3 m drilled are stored in a wooden box (Fig. 3a). Several parameters were recorded from the drill cuttings, namely: Depth (or length, since the water wells are sub-horizontal), Geological description (lithology, mineralogy, colour, grain size, among others), Weathering grade (W) and Fracturing degree (F). At the end of the drilling works, the samples were packaged and labelled into individual plastic bags to be carried out to the laboratory. Also, during the drilling process, other hydrogeological parameters were recorded, namely the measurement of flow (L/s), pH, temperature ($^\circ C$), and electrical conductivity ($\mu S/cm$) of the water. To accomplish this task were followed several recommendations, highlighted, for example, by Clark (1988), CFCFF (1996), Assaad et al. (2004), Doesburg (2005), Brassington (2017), Rix et al. (2019) and Kowalska et al. (2020).

The samples were carefully analysed in the Laboratory of Cartography and Applied Geology—LABCARGA (School of Engineering ISEP, Polytechnic of Porto). A macroscopic characterisation was carried out, with an accurate scale observation of rock/mineral cutting samples (description, identification, and evaluation) and a binocular microscope (10 and 30 x magnification) observation and description. For each sample, were taken three photos: real scale, 10 x magnification and 30 x magnification (Fig. 3b, c, and d). Complementary mineralogical tests and geochemical evaluation were also carried out, such as handheld XRF spectrometer, X-ray fluorescence spectroscopy technique, chemical, and pyrognostics tests. The collected information supports the water well logging process, namely lithological reconstruction and description with geological, geotechnical, and hydrogeological data.

Fig. 1 Location of the Noninha stream valley: schematic geological profile and FH2 horizontal water well position (adapted from Teixeira 2011)

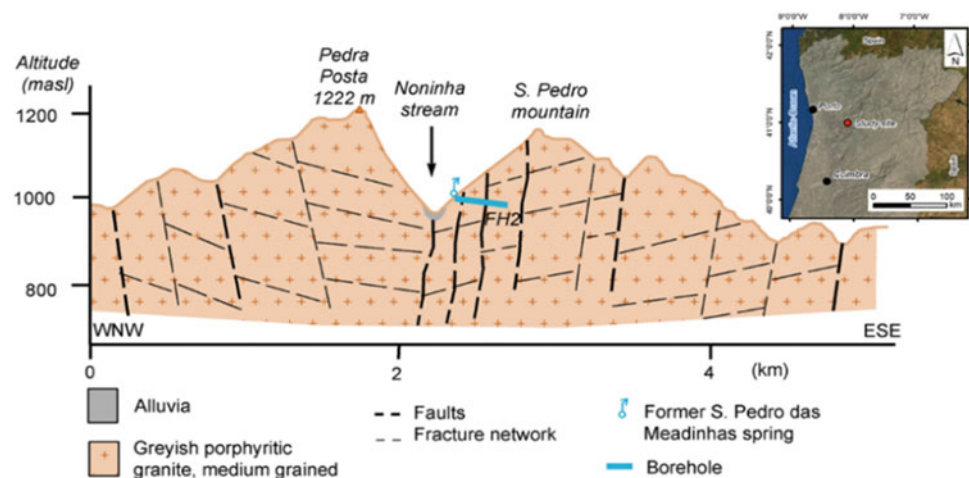
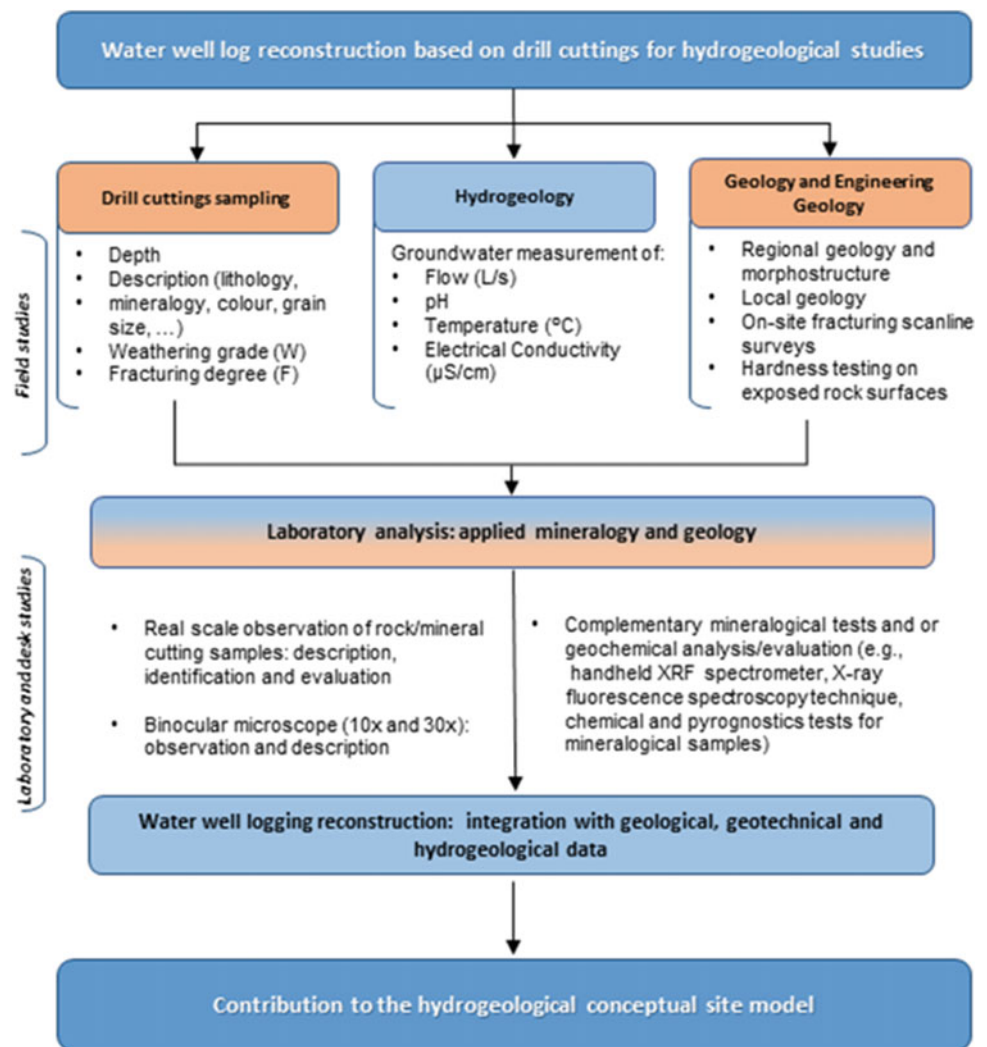


Fig. 2 Practical methodology for water well logs reconstruction based on drill cuttings



3 Results

The hydrogeological inventory in the area has shown that most groundwater manifestations (springs, fountains, dug wells, wells, and others) are in the granitic rocks. That highlights a thick horizon of weathered granite (W_{4-5}) to a residual soil (W_6). This weathered horizon is sometimes over 20 m and plays an essential role in improving the quantity of groundwater stored in this shallow aquifer system. Locally, when geo-structural conditions are favourable, this groundwater flows to the deeper aquifer system. The area's water manifestations also seem to be highly correlated with tectonic lineament nodes or some preferential orientations at a local scale, and mainly near the valleys' bottom. The tectonic lineaments primarily trending NE-SW and ENE-WSW appear to be the most important hydrogeological traps. Therefore, the water wells were designed to intersect these geostructures (Teixeira 2011).

Figure 4 shows the database created with comprehensive information that permits the water well log reconstruction. Also, it added a photo of each sample. The log drawn was also added to the database. Thus, the collected data allowed the reconstruction of the logs of FH1 and FH2 water wells. At the FH1 water well, some alternating zones of fresh to slightly weathered granite (W_{1-2}) with highly weathered granite zones (W_{4-5}), up to 81 m. The identified fractures belong to the specified NNE-SSW orientation and are also present mainly until 81 m. The main productive groundwater zones (where the drilling flow increases significantly) were determined at 50 and 120 m.

Additionally, the FH2 water well has similar characteristics, and the alternating zones of fresh to slightly weathered granite with zones of highly weathered rock mass (Fig. 4) go up to 120 m. Still, the fracture density is higher until 50 m. The productive groundwater zones were identified at 30 and 70 m. The gravitic groundwater flows measured after the drilling process finished is 4–6 L/s for each well.

Fig. 3 Field samples in the wooden boxes, collected during drilling (a); Sample from a fractured zone (b); Aspect of some muscovite crystals (c); Portion of chlorite crystals, seen through a binocular microscope with 10 × magnification (d). (Images adapted from Teixeira 2011)



Fig. 4 Extract of the database and the final result of the log reconstruction for water well FH2

Depth (m)	Lithology	Minerals		Colour/ton	Granularity						Weathering						Observations	Schematic log	Photo
		Essential	Accessory		VC	C	M	F	VF	I	B	III	IV	V	VI				
3	Medium grained granite	Quartz, Feldspar, Biotite, Muscovite		Yellowish				X				X							
6	Medium grained granite	Quartz, Feldspar, Biotite, Muscovite		Yellowish				X				X					Large muscovite grains		
9	Medium grained granite	Quartz, Feldspar, Biotite, Muscovite		Yellowish				X				X							
12	Medium grained granite	Quartz, Feldspar, Biotite, Muscovite	Tourmaline, chlorite?	Yellowish, greyish	X	X	X					X	X				Large muscovite grains, slickenside lineations on rock surface cuttings, highlighting probable fractures		
15	Medium grained granite	Quartz, Feldspar, Biotite, Muscovite	Tourmaline, chlorite?	Yellowish, greyish				X				X							
18	Medium grained granite	Quartz, Feldspar, Biotite, Muscovite	Tourmaline (few minerals)	Greyish	X		X					X					slickenside lineations on rock surface cuttings, highlighting probable fractures		
21	Medium grained granite	Quartz, Feldspar, Biotite, Muscovite	Tourmaline, chlorite (few)	Greyish			X	X	X			X							
24	Medium grained granite	Quartz, Feldspar, Biotite, Muscovite	Tourmaline, chlorite (few)	Greyish				X	X			X							
27	Medium grained granite	Quartz, Feldspar, Biotite, Muscovite	Tourmaline, chlorite (few)	Greyish				X				X							
30	Medium grained granite	Quartz, Feldspar, Biotite, Muscovite	Tourmaline, chlorite (few)	Greyish	X		X	X				X					Fractures?		
33	Medium grained granite	Quartz, Feldspar, Biotite, Muscovite	Tourmaline	Greyish	X			X				X					Quartz vein? Fractures?		
36	Medium grained granite	Quartz, Feldspar, Biotite, Muscovite	Tourmaline	Greyish	X		X	X				X					Iron oxide? Quartz vein?		

The in situ hydrogeochemical studies revealed hyposaline water and sodium bicarbonate facies. However, during the rainy season and relatively short residence times, the Non-inha's waters turn to sodium chloride facies. As a result, the analysed waters' silica/total mineralisation ratio is around 30–35%.

4 Concluding Remarks

The practical methodology applied to reconstitute water well logs from drill cuttings and the database created has proven reliable. That integrates the lithological, mineralogical, geo-structural, and hydrogeotechnical data. The discontinuity orientations were confirmed in the interpretation of the drilling data, characterised in the drilling logs carried out, and correspond, in general, to the productive groundwater zones of the water wells. Combining and integrating this information allowed a substantial improvement in the hydrogeological conceptual site model, thus contributing to more efficient water well completion and groundwater resources management.

Acknowledgements Acknowledgements are due to JAPP Lda firm, namely Eng. J. Pinto Pereira for all support. JT holds a doctoral scholarship from the Portuguese Foundation for Science and Technology, FCT (SFRH/BD/29762/2006). This study was supported partially by LABCARGA|ISEP re-equipment program (IPP-ISEP|PAD'2007/08) and FEDER EU COMPETE Funds and FCT (CEGOT|FLUP – UIDB/04084/2020, GeoBioTec|UA - UID/GEO/04035/2020).

References

- ADITC–Australian drilling industry training committee, (2015) The drilling manual, 5th edn. CRC Press, Boca Raton
- Ahmed N, Taylor SW, Sheng Z (eds.) (2014) *Hydraulics of wells: design, construction, testing, and maintenance of water well systems*. Task committee on hydraulics of wells, American society of civil engineers, manuals and reports on engineering practice number 127. Reston, Virginia
- Assaad FA, LaMoreaux PE, Hughes TH, Wangfang Z, Jordan H (2004) *Field methods for geologists and hydrogeologists*. Springer-Verlag, Berlin
- Atlas-Copco (1979) *Foration fond-de-trou avec les marteaux COP. Méthodes d'Exploitation de Mine et de Construction*, AHB, COP 00–16, Stockholm
- Brassington R (2017) *Field hydrogeology*. Geological field guide series, 4th edn. Wiley-Blackwell, Chichester
- Bresson G (1977) *Technique et utilisation du marteau fond-de-trou pour la recherche et l'exploitation des eaux souterraines*. In: *Colloque Nationale sur les Eaux Souterraines et l'Apport en Eau de la France*, BRGM, Nice
- CFCFF–Committee on Fracture Characterization and Fluid Flow (1996) *Rock fractures and fluid flow: contemporary understanding and applications*. National Academy Press, Washington DC, National Research Council
- Clark L (1988) *The field guide to water wells and water wells*. The Geological Society of London Handbook series, Wiley, London
- Dassargues A (2019) *Hydrogeology: groundwater science and engineering*. CRC Press, Taylor and Francis, Boca Raton
- Davis SN, Turk LJ (1964) *Optimum depth of wells in crystalline rocks*. *Ground Water* 2(2):6–11
- Doesburg J (2005) *Operating and maintaining horizontal wells*. *Wat Well J* 59(12):40–42
- Driscoll FG (1986) *Groundwater and wells*. Johnson Screens, St. Paul, Minnesota
- Eustes AW III, Fleckenstein WW, Gertsch L, Lu N, Stoner MS, Tischler A (2009) *Ground drilling and excavation*. In: Bar-Cohen Y, Zacny K (eds) *drilling in extreme environments: Penetration and sampling on earth and other planets*. Wiley-VCH Verlag, Weinheim, pp 141–220
- Gloftelty MF (2019) *The art of water wells: technical and economic considerations for water well siting, design, and installation*. NGWA Press, Westerville, Ohio
- Hartman HL (ed.) (1992) *SME mining engineering handbook*. Society for mining, metallurgy, and exploration. Littleton, Colorado
- Harvey PK, Lovell MA (1998) *Core-log integration*. Geological Society Special Publication N° 136. The Geological Society London, London
- ISRM–International Society for Rock Mechanics (1981) *Basic geotechnical description of rock masses*. *Int J Rock Mech Min Sci Geom Abstr* 18:85–110
- ISRM–International Society for Rock Mechanics (2007) *The complete ISRM suggested methods for characterisation, testing and monitoring: 1974–2006*. In: Ulusay R, Hudson JA (eds.), *Suggested methods prepared by the commission on testing methods*. ISRM, Ankara
- ISRM–International Society for Rock Mechanics (2015) *The ISRM suggested methods for rock characterisation, testing and monitoring: 2007–2014*. In: Ulusay R (ed.), *Suggested methods prepared by the commission on testing methods*, ISRM. Springer, Cham
- Kowalska S, Kubik B, Skupio R, Wolansk K (2020) *Downhole lithological profile reconstruction based on chemical composition of core samples and drill cuttings measured with portable X-ray fluorescence spectrometer*. *Minerals* 10:1101
- Kyzym I, Reyes R, Rana P, Molgaard J, Butt S (2015) *Cuttings analysis for rotary drilling penetration mechanisms and performance evaluation*. In: *Proceedings of the 49th US Rock mechanics and geomechanics symposium*. American Rock Mechanics Association, ARMA 15–764, San Francisco
- Marjoribanks R (2010). *Rotary percussion and auger drilling*. In: Marjoribanks R (Ed.) *Geological methods in mineral exploration and mining* Springer Berlin Heidelberg, pp 85–97
- Missteat B, Banks D, Clark L (2017) *Water wells and boreholes*, 2nd edn. Wiley-Blackwell, Chichester
- Monnet J (2015) *In situ tests in geotechnical engineering*. ISTE. London and John Wiley & Sons, Hoboken
- Patel A (2019) *Geotechnical investigation*. In: Patel A (ed) *Geotechnical investigations and improvement of ground conditions*. Woodhead Publishing, London, pp 87–155
- Plote H (1985) *Sondage de reconnaissance hydrogéologique: méthode du marteau fond-de-trou, exécution et surveillance*. *Séries Manuels et Méthodes n 12*, BRGM, Orléans
- Rix GJ, Wainaina N, Ebrahimi A, Bachus RC, Limas M, Sancio R, Fait B, Mayne PW (2019) *Manual on subsurface investigations*. The National Academies Press, Washington DC
- Sterrett RJ (ed.) (2007) *Groundwater and wells*. 3rd edn. Johnson Screens, A Weatherford Company, New Brighton
- Summers WK (1972) *Specific capacities of wells in crystalline rocks*. *Ground Water* 10(6):37–47

- Teixeira J (2011) Hidrogeomorfologia e sustentabilidade de recursos hídricos subterrâneos. University of Aveiro, Aveiro (Ph.D. Thesis)
- USACE (2001) Engineering and design: geotechnical investigations. EM 1110-1-1804, Department of The Army, U.S. Army Corps of Engineers, Washington, DC
- Yin GU, Brook GA (1992) The topographic approach to locating high-yield wells in crystalline rocks: does it work? *Ground Water* 30(1):96-102
- Zhang Z-X (2016) Rock drilling and boring. In: Zhang Z-X (ed) *Rock fracture and blasting*. Butterworth-Heinemann, Oxford, pp 155-175



A Case Study on the Use of Ground Source Heat Pumps (GSHP) in Heating and Climatization of the Military Academy—Amadora Quarters (Portugal)

Diogo Gonçalves, Rui Costa Neto, José Manuel Marques, Paula Figueiredo, Paula Carreira, and Maria Orquídia Neves

Abstract

The viability study of the use of a vertical closed Ground Source Heat Pump (GSHP), as well as a Groundwater Heat Pump (GWHP) open-circuit system, to climatize the student house edifice of the Military Academy, Amadora Quarters (Portugal), and to develop Domestic Hot Waters (DHW), is described. The quantity of energy necessary for space heating and cooling was 27.83 and 25.76 MWh/year, correspondingly, and for the development of DHW was 46.36 MWh/year. The evaluation of the existing technology, a natural gas boiler with a coefficient of performance COP = 0.68 and the climatization system with a COP = 3.5, when compared with the GSHP system to be put in place with a COP = 4, displayed primary energy savings of € 4,476/year. The economic balance achieved for the GSHP and GWHP systems, permitting a 15 years project life, was an NPV of € 24,117 and € 32,450, an IRR of 18 and 34%, and a PP of about 5 and 3 years, correspondingly.

Keywords

Renewable Energy • Geothermal Energy • Ground Source Heat Pumps • Payback Period • Climatization

D. Gonçalves · R. C. Neto
Center for Innovation, Technology and Policy Research (IN+),
Instituto Superior Técnico, University of Lisbon, Lisbon, Portugal

J. M. Marques (✉) · M. O. Neves
Centro de Recursos Naturais e Ambiente (CERENA), Instituto
Superior Técnico, University of Lisbon, Lisbon, Portugal
e-mail: jose.marques@tecnico.ulisboa.pt

P. Figueiredo
Academia Militar, Lisboa, Portugal

P. Carreira
Centro de Ciências e Tecnologias Nucleares (C2TN), Instituto
Superior Técnico, University of Lisbon, Lisbon, Portugal

1 Introduction

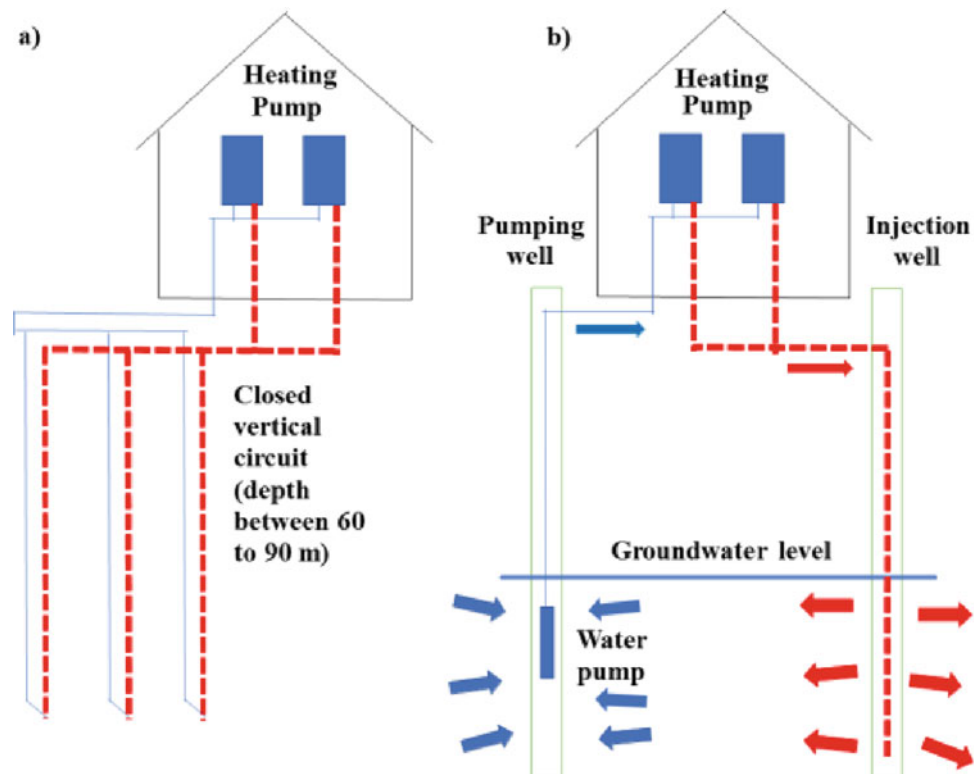
This study arises to meet two attractive energy needs at the Military Academy—Amadora Quarters (Portugal): (i) change the present useless system for climatizing the dormitory edifice, and (ii) use a renewable font of energy (geothermal) in order to fit the projected European Community objectives in reducing carbon dioxide discharges by 20% in 2020 (Schibuola and Scarpa 2016). Furthermore, this study aims to assess current external accommodations and the thermal loads that can be switched by geothermal energy and the viability study of the best development for geothermal pilot equipment.

2 Framework and Methodological Approach

In Europe, most soils about 50 m in depth show approximately steady temperatures (around 10 °C and 15 °C) (Moel et al. 2010; Carvalho et al. 2015). Gonçalves (2017a, b) referred to the study area the soil temperature is 18.5 °C, data supplied through the *RETSscreen* software (RETSscreen 2015), which gathers and analyzes recent satellite data operated by NASA. From the energy efficiency point of view, such soil temperatures can be used for the building's air conditioning using a Geothermal Heat Pump system (GHP). In order to provide adequate energy all over the year, to warm up and cool down a middle-sized housing, shallow groundwaters should be faced as another essential supply of renewable energy, with a steady temperature (≈ 17 °C) under a given depth (Kim and Nam 2016). This paper was designed for the viability study of using a Ground Source Heat Pump (GSHP) closed-circuit (Fig. 1a) and a Groundwater Heat Pump (GWHP) open circuit (Fig. 1b).

The study region fits the temperate Mediterranean climate, typical of the Iberian Peninsula (Kutiél and Trigo 2014; Gonçalves 2017a,b). As stated by Gonçalves (2017a, b), the hot period (from June to September) is characterized

Fig. 1 Scheme of **a** GSHP and **b** GWHP (Adapted from Kavanaugh and Rafferty 2014)



by monthly mean temperatures in the range of 20–22 °C. Monthly average temperatures are below 15 °C from November to March, and January is the coldest month. The study region is dominated by the Lisbon Volcanic Complex (LVC). The LVC consists of a sequence of lava flows, mainly basalts, separated by pyroclastic levels (e.g., breccias, tufts, cinerites, and ashes) and sedimentary layers (e.g., conglomerates and clays). The LVC overlies both the Holocene argillaceous limestones and the reef limestones of the Upper Cretaceous, covered by the Paleogene conglomeratic layers of the “Benfica Complex” formation (Zbyszewski 1963, 1964; Ramalho et al. 1993, 2001). The geotectonic activity responsible for forming the LVC resulted in fracture systems trending NNE-SSW and NNW-SSE (Zbyszewski 1963, 1964; Ramalho et al. 1993, 2001; Crucho 2013). Special attention was put into assessing the geothermal capability of the Military Academy—Amadora Quarters region. Correia and Ramalho (2010) stated that a reasonable estimate for the average geothermal gradient and heat flux density in this region is 31 °C/km and 91 mW/m². However, suppose there is a significant groundwater flow in a given area. There is a high probability that the thermal energy will flow away from the GSHP systems, which will not allow the maximum yield associated with this technology (e.g., Kim and Nam 2016). In low permeability soils/rocks, as in this case study (Crucho 2013), the groundwater flow is usually low, and, consequently, the

convection involved will be minimal. In the LVC, the pyroclastic materials intercalated basaltic spills caused some springs that led to the construction of wells and boreholes for groundwater extraction (e.g., Carreira et al. 2017). As the result of the water–rock interaction of local meteoric waters with the upper LVC geological formations (Carreira et al. 2017), the main hydrogeochemical facies of the local shallow groundwaters is Ca/Na–HCO₃. Such shallow groundwater systems show temperatures between 17 and 22 °C, likely to support GSHP systems. However, flow rates are usually low (0.5–1 L/s).

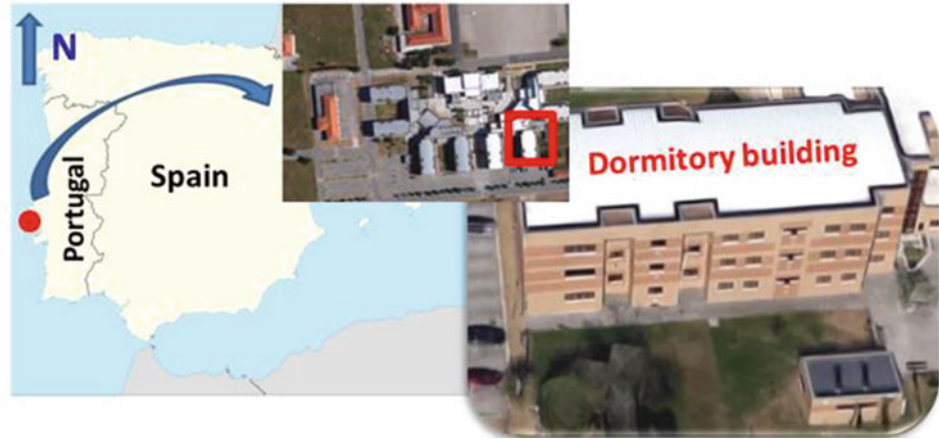
3 Results and Discussion

3.1 Military Academy—Amadora Quarters Dormitory Building

The dormitory building for the Military Academy’s internal students (Fig. 2) comprises three floors (ground, 1st and 2nd floor) with a functional area of 535 m² and a right foot of 2.70 m per floor.

This construction presents a full capability for 78 cadets. The construction’s shape is made of reinforced concrete. Passageways and sanitary facilities for the student’s support were regarded as non-working spaces. The sum of the spaces to be climatized has 279.8 m² on every floor. The

Fig. 2 Location of amadora quartering (·) and the building under study (adapted from Gonçalves 2017a, b)



construction has three floors of equivalent house plants, so the overall space to be climatized corresponds to 839 m². The construction exterior, the rooftop of the 2nd floor, and the ground footpaths were regarded as external envelopes. The interior side of the building measured the wall area of the outer envelope on every floor, agreeing to the No. 15793-E/2013 Portuguese Regulation. The whole space outside is 542.0 m² since the three floors have equal dimensions. The coefficient of thermal transmittance U , of the several opaque components ascribed to both outer, not including glazing elements, and inside envelopes, was estimated agreeing to the ISO 6946:2007 2017 European standard through the Eq. (1) in W/m². °C,

$$U = \frac{1}{R_{si} + \sum_j R_j + R_{se}} \quad (1)$$

where R_j stands for the thermal resistance of stratum j , in m². °C/W, since the envelope components comprise various materials in layers of regular thickness. R_{si} and R_{se} stand for the interior and outside surface thermal resistances, correspondingly, in m². °C/W (Table 1).

3.2 Annual Valuable Energy Demands for Space Heating (N_{ic}), Refrigeration (N_{vc}), and Domestic Hot Water Provision (Q_{DHW})

The present Portuguese Regulation of Energy Performance of Domestic Edifices was employed to properly quantify the

construction's thermal loads. Consequently, due to the construction's local climatic and physical signatures, it was feasible to calculate the valuable energy demands for space heating, refrigeration, and household hot water requirements. This approach defined the annual nominal thermal energy requirements and the EN ISO 13790:2008 2016 European Standard. According to Gonçalves (2017a, b), Eqs. 2, 3, and 4 were applied to estimate the annual valuable energy requirements for space heating (N_{ic}), refrigeration (N_{vc}), and household hot water provision (Q_{DHW}), correspondingly:

$$N_{ic} = \frac{(Q_{tr,i} + Q_{ve,i} - Q_{gu,i})}{A_p} \quad (2)$$

where according to Gonçalves (2017a, b), " $Q_{tr,i}$ stands for the heat transfer by transmission in the heating season through the building envelope in kWh, $Q_{ve,i}$ represent the heat transfer by ventilation in the heating season in kWh, and $Q_{gu,i}$ represents the useful thermal gains in the season, resulting from solar gains through windows, lighting, equipment and occupants in kWh". According to Gonçalves (2017a, b) " A_p is the conditioned interior area of the building floor measured in m²",

$$N_{vc} = \frac{(1 - \eta_v) Q_{g,v}}{A_p} \quad (3)$$

where " $Q_{g,v}$ represents the gross thermal gains in the cooling season in kWh, and η_v the utilization factor of the thermal gains in the cooling station" (Gonçalves 2017a, b),

Table 1 Coefficients of thermal transmittance were achieved for the various components of the construction envelope (Gonçalves 2017a, b)

Envelope	Element	U (W/m ² . °C)
External	Double external wall	0.460
	Ceiling, 2 nd Floor	0.651
	Pavement, Ground Floor	0.600
Internal	Interior walls	1.587

$$Q_{DHW} = \frac{M_{DHW} \cdot 4187 \cdot \Delta T \cdot n_d}{3600 \cdot 10^6} \quad (4)$$

where ΔT is the temperature growth necessary for the DHW, being 35 °C agreeing to the Portuguese Regulation. The term n_d stands for the number of days of DHW consumption, 365 days/year. The thermal energy needed for DHW development is 46.36 MWh/year. The DHW every day mean volume used in the construction M_{DHW} , allowing for 40 L/student, is 3120 L. Utilizing the former equations, the estimates give 33.17 kWh/m² for N_{ic} , 18.44 kWh/m² year for N_{vc} and 46.36 MWh/year for DHW development. N_{ic} and N_{vc} take the values of 27.83 and 15.48 MWh/year, correspondingly, considering the total construction area to be climatized (839 m²).

3.3 Dimensioning the Ground Source Heat Pump (GSHP)

The approach to designing the key elements of the GSHP was the *RETScreen* software (RETScreen 2015). By adding up all the annual sound thermal energy needed for space heating and DHW requirements, the value obtained is 74.19 MWh, 62.5% of the energy used in the provision of DHW. When correcting the energy balance during the year, sound energy required to cool 25.76 MWh/year was obtained. The peak loads for the space heating and refrigeration, which are 21.01 and 6.37 kW, were equally reached by the *RETScreen* software. The selected characteristics for DHW heating and cooling are power supply—3-phase; nominal cooling 29 kW; nominal heating 25 kW; energy efficiency ratio 5; coefficient of performance COP 4.9. To project the geothermal heat exchanger system, it was necessary to delimit some crucial parameters to be included in the *RETScreen* software, such as (data from Gonçalves 2017a): soil properties (temperature 18.5 °C; thermal conductivity 2.4 W/(m · °C); thermal diffusivity 1.03×10^{-6} m²/s; and specific heat capacity 0.84 kJ/(kg · °C)), and the energy requirements (peak load 21.01 kW and the average for the heating season 12.7 kW, as well as, the COP for which the system is scaled 4.9). The software's soil properties were chosen to approximate the values of the different rock types (mainly basalts) present in the Amadora region. The energy requirements presented were obtained according to the energy balance previously made for the building (Gonçalves 2017a, b). The vertical GSHP system was necessary to define the minimum distance between each borehole (6.1 m) since more than one borehole is required. In the GWHP system, it was necessary to define the typical groundwater depth supplying the well (piezometric level) at the site under study (10 m). This maximum flow rate is expected to be

Table 2 Main sizing parameters were obtained for the two systems considered (Gonçalves 2017a, b)

Vertical GSHP system—Closed loop	
Required land area	146 m ²
Total borehole length	579 m
Total geothermal loop length	1157 m
GWHP—Open loop	
No. of supply wells	1
Necessary groundwater flow	1 L/s
Power of well water pump	0.5 kW
Central heat exchanger	23.7 kW

supplied continuously by the well (1.5 L/s) and the depth at which the pump should be installed in the well (9 m). The separation between vertical boreholes of 6.1 m chosen for the Vertical GSHP system represents the minimum distance that the *RETScreen* software model considers appropriate. The considerations for specific parameters for the open-circuit GWHP system were made according to the region's hydrogeological characteristics under study, previously presented. Table 2 can examine the estimated outcomes of the main design parameters of the two types of geothermal heat exchangers to be assessed, following the introduction of all required variables in the *RETScreen* software. The heat pump capacity was chosen to cover 100% of the peak load needs during the respective seasons.

3.4 Economic Viability: Results

For both systems, using Eq. (5), the annual cost estimation (in €) of the primary energy utilized was performed:

$$\text{Annual energy cost}_i = \left(\frac{\text{Total energy}_i}{\text{COP}_j} \right) \times \text{Energy cost} \quad (5)$$

where “i” stands either for heating or cooling, and “j” stands for the different technologies. Amadora region's natural gas cost is 0.0588 €/kWh and 56.88 €/year for the constant tax. In Portugal, the electricity cost is 0.13 €/kWh in intermediate voltage. A COP = 4 was used to estimate the annual GSHP system primary energy cost, considering the intermittent operation of the Heat Pump unit (EN ISO 13790:2008 2016). Considering the amount of the boiler direct energy costs and air conditioning, excluding GSHP primary energy costs, annual savings are 4476 €. Although the NPV obtained was 24117 and 32450 € for the GSHP and GWHP, the IRR estimate is comparatively high (18 and 34%, respectively) in 15 years of operation. These results confirm the heat pump's energy efficiency.

4 Concluding Remarks

This paper demonstrates the *RETScren* software applicability for sizing and evaluating the implementation of the Geothermal Heat Pump (GHP) technology to improve the energy efficiency of the student's house edifice at Amadora Quarters of the Military Academy (Portugal). Two types of GHP systems were evaluated: the vertical closed-loop GSHP system and the GWHP open-circuit system. It was crucial to establish the area necessary to fix the closed-loop GSHP (142 m²) with four boreholes, obtain the central exchanger power in GWHP (23.7 kW), and expenses ascribed to system substitution the edifice by GHP. As the investing costs have a payback of 3 years for the GWHP open-circuit and five years for the closed-loop GSHP, both systems are viable. The profits will be 32450 and 24117 € for the GWHP and GSHP, respectively, after 15 years of operation. Although the GWHP could be considered the most attractive, it is essential to consider that groundwater must be fairly available in quantity from an economic perspective. Therefore, fieldwork campaigns should be enhanced by carrying out pumping tests and monitoring to study the feasibility of using shallow groundwater wells. Thus, it was assumed that the GSHP presents the most applicability.

Acknowledgements This research was developed during the R&D Project GHAMA (Contract No. P.4459), funded by the Ministry of National Defense/Portuguese Army Staff. CERENA/IST researchers thankfully recognize FCT by the UIDB/04028/2020 Project, and C²TN/IST researchers gratefully recognize FCT by the UIDB/04349/2020 Project. Two anonymous reviewers critically read a preliminary version of this work, and the authors gratefully acknowledge their contribution.

References

- Carreira PM, Neves MO, Figueiredo P, Marques JM, Nunes D, Rei JCM, Caracho AJE (2017) Geochemistry and environmental isotopes as natural tracers of groundwater flow in shallow aquifer systems within Lisbon Volcanic Complex (Portugal). *Proceed Earth Planet Sci* 17:634–637
- Carvalho AD, Moura P, Vaz GC, de Almeida AT (2015) Ground source heat pumps as high efficient solutions for building space conditioning and for integration in smart grids. *Energ Convers Manag* 103:991–1007
- Correia A, Ramalho EC (2010) Update heat flow density map for Portugal. In: *Proceedings world geothermal congress 2010*. Bali, Indonesia, pp 1–7
- Crucho EAL (2013) Caracterização física do concelho da Amadora e suscetibilidade às inundações. Universidade de Lisboa, Instituto de Geografia e Ordenamento do Território, Lisboa. <http://hdl.handle.net/10451/20515> (MSc Dissertation)
- EN ISO 13790:2008 (2016) Energy performance of buildings: calculation of energy use for space heating and cooling. Available in <https://www.iso.org/obp/ui/#iso:std:iso:13790:ed-2:v1:en>. Accessed on 04 Jan 2020
- Gonçalves DJP (2017a) Utilização de bombas de calor geotérmico no aquecimento e climatização da academia militar: aquartelamento da amadora (um caso de estudo). Instituto Superior Técnico, Universidade de Lisboa, Lisboa. <https://fenix.tecnico.ulisboa.pt/cursos/mege/dissertacao/1691203502342894> (MSc Dissertation)
- Gonçalves DJP (2017b) Use of ground source heat pumps (GSHP) in heating and climatization of the military academy: Amadora quartering (a case study). Instituto Superior Técnico, Universidade de Lisboa, Lisboa. <https://fenix.tecnico.ulisboa.pt/cursos/mege/dissertacao/1691203502342894> (Extended Abstract)
- ISO 6946:2007 (2017) Building components and building elements—Thermal resistance and thermal transmittance: calculation method. Available in http://www.iso.org/iso/catalogue_detail.htm?csnumber=40968. Accessed on 04 Jan 2020
- Kavanaugh S, Rafferty K (2014) Geothermal heating and cooling: design of ground-source heat pump systems. American Society of Heating, Refrigerating and Air-Conditioning Engineers, Atlanta, ASHRAE
- Kim J, Nam Y (2016) A numerical study on system performance of groundwater heat pumps. *Energies* 9(1):4
- Kutiél H, Trigo RM (2014) The rainfall regime in Lisbon in the last 150 years. *Theor Appl Climatol* 118:387–403
- Moel M, Bach PM, Bouazza A, Singh RM, Sun JO (2010) Technological advances and applications of geothermal energy pile foundations and their feasibility in Australia. *Renew Sustain Energy Rev* 14:2683–2696
- Ramalho M, Pais J, Rey J, Berthou PY, Alves CAM, Palácios T, Leal N, Kullberg MC (1993) Notícia Explicativa da Carta Geológica de Portugal, 1:50 000, No. 34-A (Sintra). Instituto Geológico e Mineiro, Lisboa
- Ramalho M, Rey, J, Zbyszewski G, Alves CM, Almeida FM, Costa C, Kullberg MC (2001) Notícia Explicativa da Carta Geológica de Portugal, vol 1:50 000, No. 34-C (Cascais). Instituto Geológico e Mineiro, Lisboa
- Regulation No. 15793-E/2013 3 December (2013) *Diário da República*, 2.ª série N.º 234. Available in <https://dre.pt/application/dir/pdf2sdip/2013/12/234000003/0001400025.pdf>. Accessed on 04 Jan 2020
- RETScren (2015) Clean energy management software system for energy efficiency, renewable energy and cogeneration project feasibility analysis as well as ongoing energy performance analysis. Natural resources Canada. Available in <https://www.nrcan.gc.ca/maps-tools-publications/tools/data-analysis-software-modelling/retscreen/7465>. Accessed on 04 Jan 2019
- Schibuola L, Scarpa M (2016) Experimental analysis of the performances of a surface water source heat pump. *Energ Build* 113:182–188
- Zbyszewski G (1963) Carta geológica dos arredores de Lisboa, 1:50000. Notícia explicativa da Folha 4 (Lisboa). Serviços Geológicos de Portugal, Lisboa
- Zbyszewski G (1964) Carta geológica dos arredores de Lisboa, 1:50000. Notícia explicativa da Folha 2 (Loures). Serviços Geológicos de Portugal, Lisboa



The Hydromineral and Geothermal Field of Chaves (NE Portugal): A Prospective Approach Updated

José Martins Carvalho and Helder I. Chaminé

Abstract

The main goal of this essay is to outline a prospective approach related to the hydromineral and geothermal field of Chaves (NE Portugal). The Verin–Régua–Penacova megastructure, trending NNE–SSW, controls the Chaves basin. The thermal water springs in the Chaves urban area have been well known since Roman times with magnificent Roman Bath buildings. Since 1983, the geothermal power available in Caldas de Chaves in three production wells supports a small heat network. Currently, with a long delay of over 35 years, Chaves will enter the roadmap of European cities benefiting from a geothermal district-heating network. The Roman Baths legacy suggests the design and development in Chaves of a geothermal project for direct, continuous, and sustainable use. This project must be adjusted to the resource and demand to promote the region, Chaves city, and the Thermal Bath and comfort its inhabitants and visitors.

Keywords

Geothermics • Hydromineral resources • Conceptual models • Sustainability • Chaves basin • N Portugal

1 Introduction

Groundwater plays an essential role in the sustenance of the inhabitants and the economic activity of the Trás-os-Montes region (NE Portugal). Evidence of this importance can be seen in the water wells, springs, and fountains standing in

the centres of villages. Also, the wells with their shadoofs (or well sweep) are common irrigation systems in areas where the groundwater occurs near the surface (Dias and Galhano 1986). Nowadays, the fields and the surroundings of the villages are dotted with small cottages sheltering many water wells used mainly for the irrigation of small areas. Moreover, thousands of other boreholes operate or are abandoned inside the backyards of houses or even inside them. Nevertheless, plentiful springs and horizontal/vertical wells supply small towns and villages in North Portugal (Carvalho et al. 2023). The shared knowledge and intuition attained many generations ago about some groundwaters are different from those used for drinking, cooking, or irrigation purposes. Therefore, popular wisdom has attributed healing powers to these different and/or atypical waters, and small crowds have gathered around these events, people eager to know about these virtues. Some of these were meeting and socialising spots giving rise to thermal water baths. That is a unique paradigm in the Trás-os-Montes region, particularly in the Caldas de Chaves site, due to the splendour of Roman civilisation (e.g., Henriques 1726, Carneiro 2016, Vaz et al. 2015, Houten 2021). About a hundred of these occurrences are well known in popular culture for their therapeutic benefits (Almeida and Almeida 1970; Termared 2011). Some of them are mineral waters or natural mineral waters in the technical-scientific sense (e.g., Acciaiuoli 1952/53, Carvalho 1993a, 1996, 2006, TERMARED 2011, Eggenkamp et al. 2015, Carvalho et al. 2016, 2023). Lastly, the thermal waters of Trás-os-Montes are genetically associated with deep, fractured crustal reservoirs, where seeping meteoric waters acquire mantle fluids emerging according to deep geological fault zones and related geostructural nodes, which allow a rapid rise up to the surface (e.g., Choffat 1917, Zbyszewski 1938, Carvalho and Silva 1988, Aires-Barros et al. 1994, 1995, 1998, Carvalho 1996, Baptista et al. 1998, Marques et al. 1999, 2010 2012, Portugal Ferreira et al. 2003, Carvalho and Chaminé 2016, Marques and Carreira 2019, Carvalho et al. 2023).

J. M. Carvalho (✉) · H. I. Chaminé
Laboratory of Cartography and Applied Geology (LABCARGA),
Department of Geotechnical Engineering, School of Engineering
(ISEP), Polytechnic of Porto, Porto, Portugal
e-mail: jmc@tarh.pt

Centre GeoBioTec|UA, Aveiro, Portugal

The geothermal power currently available in Caldas de Chaves (NE Portugal) in three production wells with depths up to 200 m, located in Largo do Tabolado, is 7.3 MWt which currently supports a small heat network in operation since 1983. The pumping flow is 15 L/s, and the temperature is 77 °C. Nowadays, with a long delay of more than 35 years, Chaves will finally enter the roadmap of European cities benefiting from a geothermal district-heating network. The Support Fund for Innovation ('Fundo de Apoio à Inovação'—FAI) has supported an essential non-refundable grant to the Municipality of Chaves to construct a 1.5 km long district-heating system (heating of twenty public buildings in Chaves city centre). The work has already been consigned, and it started in the first quarter of 2021. The total energy replaced will be 47.5TJ, which corresponds to an average power of 1.51 MWt with a reduction in greenhouse gas emissions of 1330ton CO² Eq/year. For around one million euro investments, the simple payback time of the operation will be around four years.

It should be noted that the district heating network now being installed is the most important in the Iberian Peninsula, with considerable growth capacity, given that the energy consumption replaceable by geothermal energy in the centre of the city of Chaves is at least in the order of 3 000 toe, annual energy that corresponds to a power of about 4 MWt. Finally, the emblematic Roman Bath building will be geoheated (heating and dehumidification) from a small inclined geothermal borehole 66 m long located on the facility's outskirts in Largo do Arrabalde. In a flow test in July 2019, this borehole delivered a flow rate of 5.3L/s at a temperature of 66.5 °C with a drawdown of only 1.15 m. Therefore, the operation will run with 1L/s since the heating power will be 110 kW. The HVAC (Heating, Ventilation, and Air Conditioning) work is underway, and it is expected that the Roman Baths Museum will start operating in 2021.

That essay is a revised, deepened, and updated version of the previous work of Carvalho (2015) and Carvalho and Chaminé (2017).

2 Geological and Hydrogeological Background (N Portugal): A Brief Outline¹

The Iberian basement represents the best westernmost exposure of the European Variscides (Ribeiro et al. 2007). The human occupation—about 4 million people living in the

North region of mainland Portugal—is quite diversified and includes the mega-conurbation of Porto with concentrated small industrial activities, sparse settlements around the main towns in the north-eastern and central inner areas, and natural mountainous protected areas such as Peneda-Gerês, Montesinho, Estrela and S. Mamede (North and Central Portugal). Groundwater plays a significant role in the economic activities and the quality of life of this population. The public water supply of main cities and villages is nowadays dependent on surface water. However, several hundred of small villages have underground origins. In addition, small-scale agriculture is highly dependent on groundwater resources and other human economic activities (Carvalho 1993b; Carvalho et al. 2005, 2023).

Some major rivers drain the northeastern region with a mean altitude of 700 m of the Iberian 'Meseta' fundamental surface. Three main morphotectonic units from the basement comprise the study region (e.g., Ribeiro et al. 1990; Cunha et al. 2019): (i) the 'Meseta Surface', an almost perfect planation surface which in the Portuguese territory stretches both northwards and southwards of the river Douro; (ii) the 'Central Plateaux'; and, (iii) the 'Western mountains' correspond to several stepped levels.

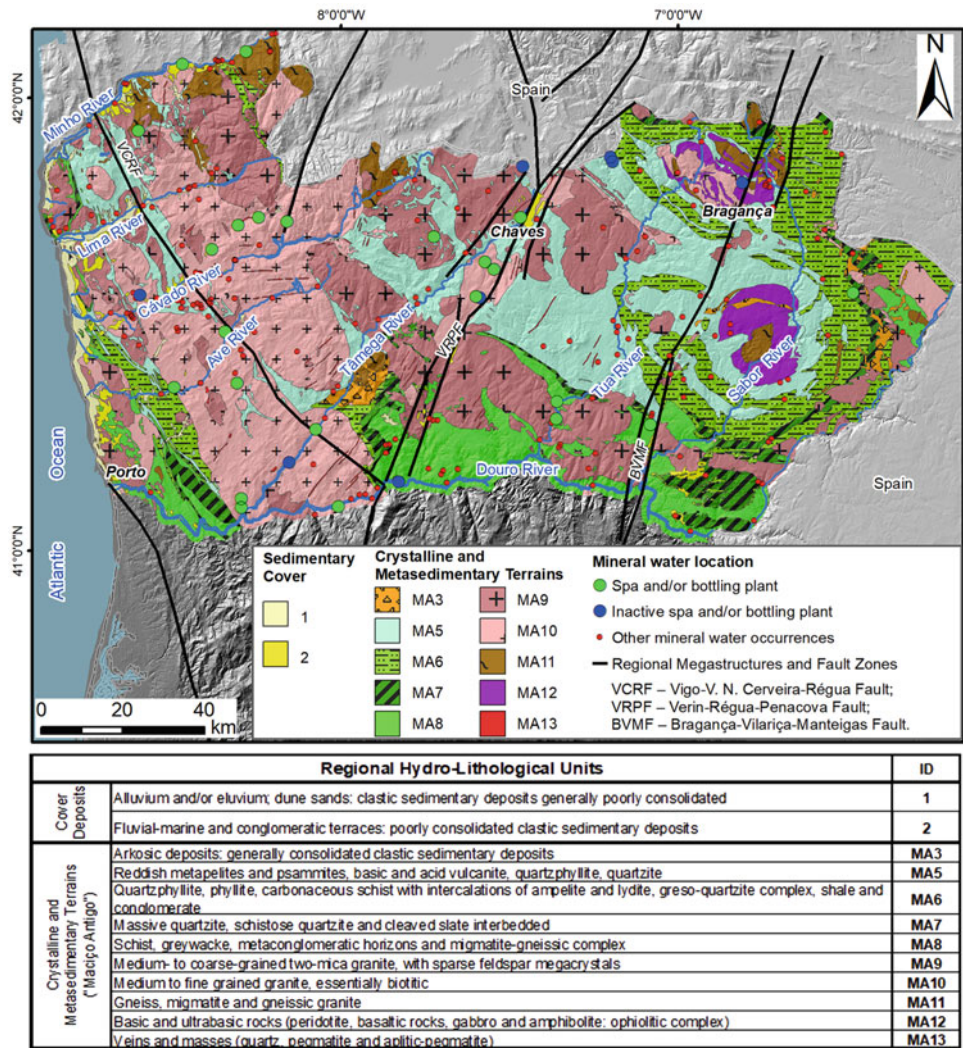
The Iberian basement in the Northern Portuguese sector comprises autochthonous and allochthonous metasedimentary sequences imbricated with major thrusts and other structures. The autochthonous litho- and tectonostratigraphic units are black shales, slates, greywackes, micashists and quartzites. The major allochthonous units in NE Portugal are characterised by an ophiolite complex sequence of nappes comprising serpentinites, flaser gabbros, sheeted dikes, and basalts. The igneous rocks include pre-orogenic and syn-orogenic suites, which occupy an extensive exposure of granitic rocks (e.g., Pereira 2006; Ribeiro et al. 2007).

The active Régua-Verin fault zone (e.g., Ribeiro et al. 1990; Baptista et al. 1998; Cunha et al. 2019) defines the main hydrogeological division in the Northern Portugal region. The mean annual rainfall to the West of this megastructure is over 1000 mm, reaching 3000 mm in the mountainous National Park PenedaGerês. Towards the East and South, aridity conditions occur, and precipitation decreases, i.e., a minimum of 500 mm is attained in the Douro River valley, near the Spanish border. These contrasts determine remarkable changes in the recharge conditions. The relative occurrence of metasedimentary rocks is very sparse in the Northwestern area (e.g., Carvalho et al. 2005, 2023).

Regional groundwater path flows are governed mainly by fissured hydraulic conductivity, faulting, and weathering, resulting in non-continuous productive zones. The spatial hydraulic connectivity of reservoirs is poor, so it is not appropriate to designate these zones, at the scale of regional investigation, as aquifers because there is no flow continuity.

¹ Details about Chaves geology and surrounding area: (i) regional geology and morphotectonics, seismotectonics and neotectonics in Feio (1951), Teixeira (1948), Ribeiro et al. (1990, 2007), Brum Ferreira (1991), Baptista et al. (1998), Pereira (2006), Cunha et al. (2019); (ii) regional hydrogeology and thermal water resources in Rego Lima (1892), Choffat (1917), Zbyszewski (1938), Freire de Andrade (1952), Almeida and Almeida (1970), Carvalho (1996), Portugal Ferreira et al. (2003), Carvalho et al. (2005, 2023, 2023).

Fig. 1 Outline of the regional geology and hydro-lithological units of northern Portugal (adapted from INAG 1997; Carvalho 2006; Carvalho et al. 2023). Geological background is adapted and simplified from Oliveira et al. (1992) and Pereira et al. (1989, 2001)



In addition, that path flows are mainly dependent on fracture connectivity. Nevertheless, it is clear that in the Variscan Iberian basement, lithological heterogeneity plays a significant role in the productivity of regional geological units and related water wells (e.g., Carvalho 1996, Carvalho et al. 2003, 2005, 2023, Carvalho and Chaminé 2016), Fig. 1.

3 Hydrothermal and Geothermal Field of Chaves: General Overview

Chaves’s hydrothermal and geothermal field is located in Chaves municipality, in the charming Trás-os-Montes region, district of Vila Real, near the Northern border of Portugal’s mainland (e.g., Acciaiuoli 1952/1953, Almeida and Almeida 1970, TERMARED 2011).

The thermal water springs in Caldas de Chaves (or *Aquae Flaviae*, named by Romans) have a glorious past, revealed

by the latest discovery, in 2006, of the Roman Baths, right next to the Trajano’s Bridge, in the historical city centre. In the Roman Empire, those from the Galicia region (roughly corresponding to Hispania Nova, later renamed ‘Callaecia’) crossed the Tâmega River and found it at the city’s entrance. This vast facility housed several swimming pools and other bathing structures fed by two thermal springs (Rego Lima 1882, Vasco et al. 2015, Carneiro 2016, Paiva et al. 2022). As seen today in the museum built on the archaeological remains rediscovered in 2006, the technology was outstanding and straightforward. Everything worked by gravity, and there was no mixing of the thermal waters with the ‘normal’ waters of the surroundings other than that necessary to achieve dilution and cooling, suitable for healing, well-being, and leisure (e.g., Vasco et al. 2015, Joukes and Costa 2015; Carneiro 2016). All the ingredients that are part of the modern thermal spas were present. The thermal environment was supposed to be warm, welcoming those

who, like the Roman soldiers of the so-called ‘Legio Septima Gemina’ (i.e., The Twins’ Seventh Legion; Le Roux 2000),² vigorously harnessed the surrounding roads and the residents’ comfort, lovers of conviviality in thermal spaces (Houten 2021). It still impresses the accuracy and cares with which the thermal resource was managed, including the careful sewage disposal by a conduit (still available today) to the Tâmega river that at those times would pass in the immediate vicinity. The impressive balneological station (Roman Bath building), whose foundations we enjoy nowadays as if it were still active, such as the conservation quality of the structures, constitutes a geothermal operation for multiple purposes combining heating, thermal heating, and thermal healing, and well-being.

The Caldas de Chaves area is included in the HM-09 Caldas de Chaves hydromineral and hydrothermal concession, with 50 hectares centred on the current thermal spa in Caldas do Tabolado, about 500 m WSW of the Roman Baths. This concession is the most significant Portuguese geothermal occurrence of the ante-Mesozoic crystalline basement. Henriques (1726) stated impressive words related to the Chaves: ‘... these are the best thermal bath, that there is in the kingdom [of Portugal]’.

Recorded discharge temperatures up to 77 °C and remarkable flow rates for aquifer systems in crystalline rocks (from 5 to 15 L/s per well), together with its situation in the city centre of a town with 18,500 inhabitants, make this concession, and surrounding area, a place with unique conditions to constitute a European-level geothermal operation. There is no industrial geothermal energy without coexistence between resources and consumers. In Chaves, this coexistence exists almost perfectly for direct uses.

4 Conceptual Model of the Geothermal Resource

The natural mineral water of Chaves is sodium bicarbonate–CO₂-rich mineral water with a total mineralisation of 2560 mg/L, pH 7, free CO₂ of about 350–500 mg/L, the electrical conductivity of 2,3 µS/cm, emerging at a temperature of around 74 °C in the former wells (AC1 and AC2) included in the official Exploitation Plan. Additionally, with a 190 m depth new borehole carried out in 2014 (CC3), the total operating flow rate should be up to 30 L/s. Although the total mineralisation of water is relatively low, large precipitates occur when cooling the fluid. This circumstance

requires preventive maintenance measures to control the quality of the readings in the monitoring devices and maintain the heat exchangers’ efficiency.

The original discharge of the springs is not documented, but inside a large part of the city of Chaves, in an area of about 30 hectares, hot springs were known (Fig. 2), which shows the quantitative importance of the resource and the role it played in securing the population. At the level of the natural discharges, the hydromineral aquifer in Tabolado is generally referred to have a flow rate of 1–2 L/s under pristine conditions (Carvalho 1993a, 1996, 2006).

The Chaves basin, on the western edge of which is located the hydrothermal and geothermal concession of Chaves, is controlled by the Verin-Régua-Penacova megastructure (Rego Lima 1892, Choffat 1917, Zbyszewski 1938, Freire de Andrade 1952, Carvalho and Silva 1988, Portugal Ferreira et al. 2003, Carvalho et al. 2023). This regional fault zone corresponds to an active NNE-SSW active structure with a maximum horizontal separation of approximately 3.4 km, developing an extensive crustal blocks system due to the structural complexity (e.g., Baptista et al. 1998, Portugal Ferreira et al. 2003, Cunha et al. 2019, and references therein). Thus, the basin corresponds to the abatement of a block (graben) due to the curvature of the main structure, which trends from NNE-SSW to N-S. Thus, the first rational tectonic model of the Chaves Basin in the discharge zone has been namely defined by the studies of ACavaco (1982), Grade and Casal Moura (1982), Portugal Ferreira et al. (1982) and Hidroprojecto et al. (1987).

The detailed geoelectric surveys at the local scale (ACavaco 1982; OCSA 2012) show that the existing thermal water discharge is related to a regional tectonic node, resulting in an NNE fracture intercepting with an important NNW fault structure (ACavaco 1982, Portugal Ferreira et al. 1982). The previous authors also inferred in 1982 the existence of another favourable sector in the Outeiro Seco area, where effectively, some potable water wells have found water with abnormal chemistry. Some of these deep-fault structures (related to tectonic damage and ductile–brittle rock fracture zones) are proven by measurements of water conductivity of the aquifer(s) at the level of the Chaves basin, revealing conductive anomalies along the main geostructural axes (Hidroprojecto et al. 1987).

More recently, the City Council of Chaves carried out high-resolution reflection seismic and high-resolution electrical surveys (OCSA 2012) that have made it possible to clarify better the role of fracturing at the local scale to depths of about 600 m in the Tabolado area.

In the classical perspective, the Chaves geothermal field would be controlled by a typical fissural quartz veins mechanism activated by recent tectonics in quartzphyllite and slate rocks, which bear hydrothermal quartz veins. This mechanism would allow the rapid rise of geothermal fluids

² It was founded in 68 AD in Hispania by the general Galba to take part in his rebellion against the emperor Nero. “Gemina” means the legion was dedicated to the legendary twin founders of Rome, Romulus and Remus [http://worldebooklibrary.org/articles/eng/Legio_VII_Gemina (accessed in May 2021)].

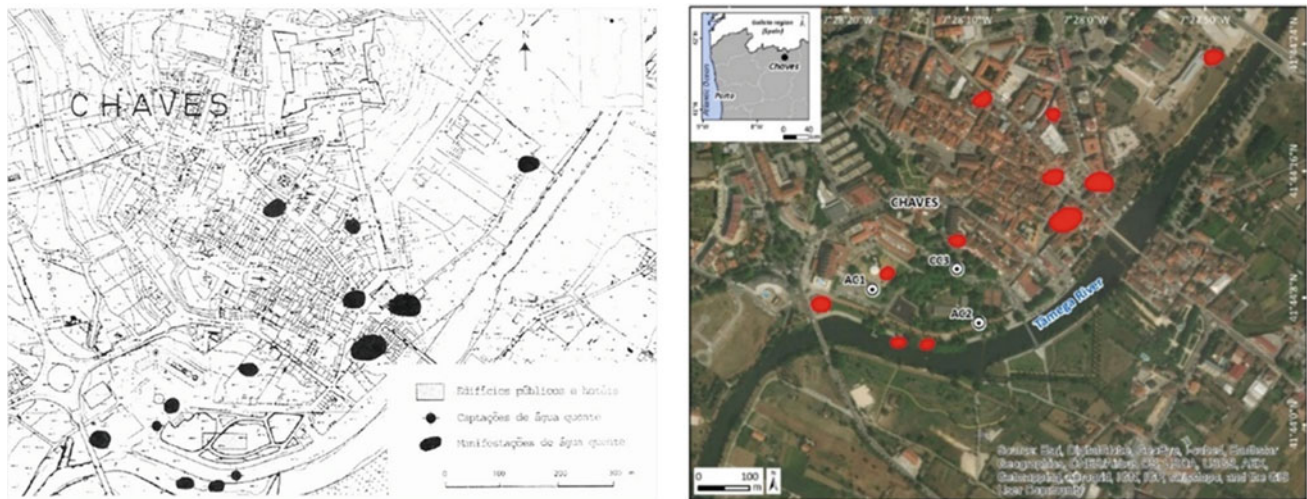


Fig. 2 Location of thermal water occurrences in the Chaves urban area: (i) early 80's, twentieth century, adapted from Carvalho and Silva (1988) (based on Rego Lima 1892; Choffat 1917; Almeida and Almeida 1970; Varet 1979). Explanation: Public buildings and hotels;

thermal water wells; thermal water occurrences; (ii) current days, aerial photo after Google Earth Pro. (wells–AC1/AC2/CC3; red spots–inventoried thermal waters occurrences, after Rego Lima 1892; Choffat 1917; Almeida and Almeida 1970)

from meteorically heated waters in-depth at temperatures of $123\text{ }^{\circ}\text{C} \pm 10$ to the surface (Moitinho de Almeida 1982). In the CC3 drilling operation on the Tabolado field, granitic rocks were recognised from -190 m deep. In addition, the granitic occurrences, with the support of the seismic reflection surveys, can be attributed to the granite substrate over which the metasedimentary rocks lay.

The recharge area, according to geochemical models based on environmental isotopes (e.g., Aires-Barros et al. 1994, 1998; Carreira et al. 2008; Marques and Carreira 2019; Marques et al. 2019, and references therein), should be located on the Bolideira Plateau in the Serra da Padrela, located east to the discharge zone in the centre of Chaves city. However, the reality of this interpretation is still to be validated with hydrodynamic and geological approaches. The known precipitation data at the Padrela Mountain (850 mm) and a conservative 0.03 recharge rate (Plasencia et al. 2015) for deep aquifers in the northern Portuguese Variscan basement are compatible with the available recharge area, and a 15 L/s extraction in the Tabolado area. However, the future will pass through the system's hydrodynamic investigations, including extensive hydrogeological fieldwork and flow and heat transport modelling. To develop such an investigation, sound activities have to be done to design a realistic hydrogeological model in order to fully understand the water flow paths to depths of about 3000 m and residence times of 8000 years as generally is accepted (e.g., Aires-Barros et al. 1994; Carreira et al. 2008; Marques and Carreira 2019; Marques et al. 2019).

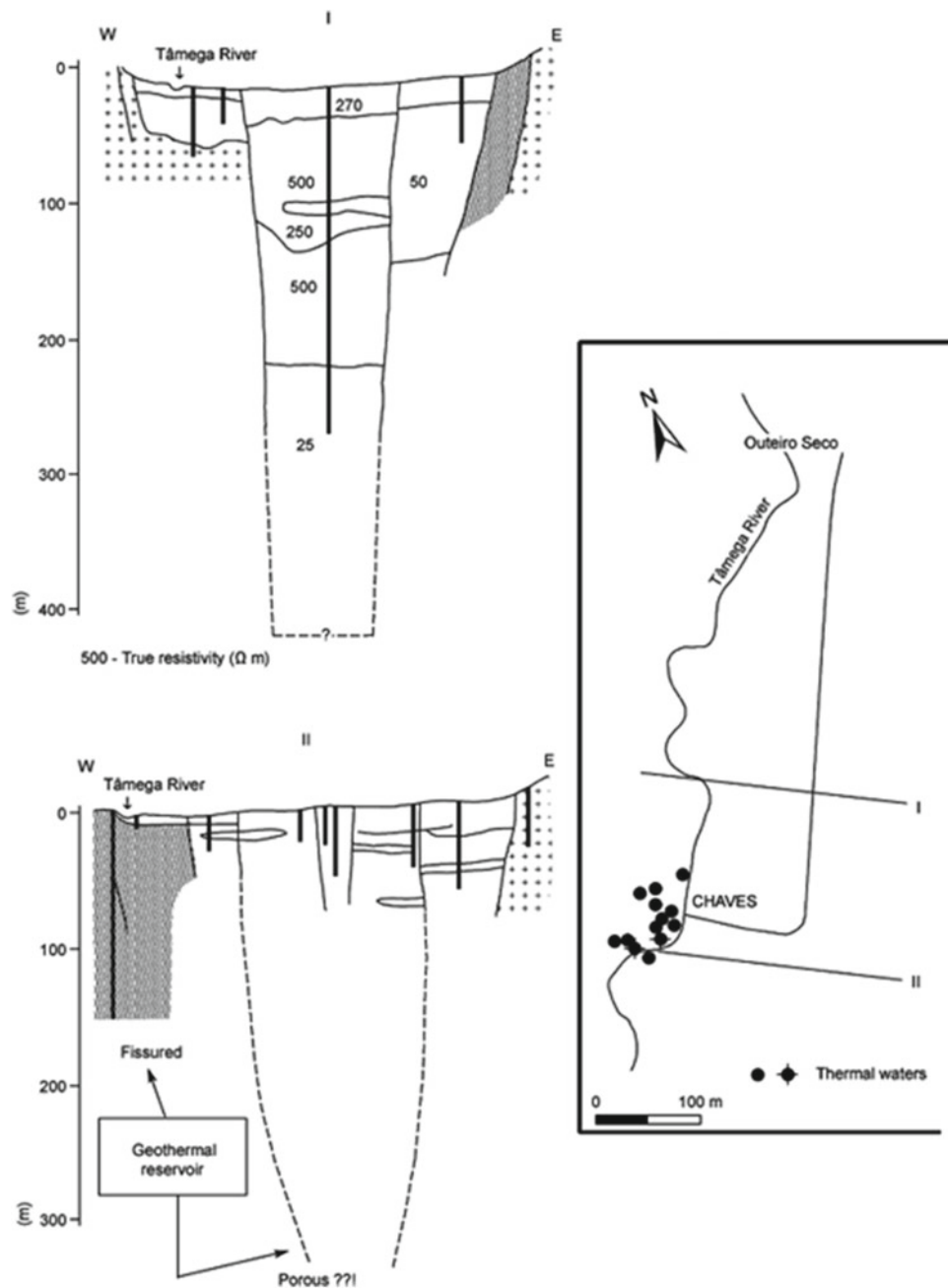
As previously stated, the hydrothermal and geothermal fluid of Chaves has a long, slow, and deep circulation path, and, for the moment, only the conditions of the discharge

zone in the Tabolado area are known with a low degree of uncertainty. Therefore, excluding infiltration on the graben edges (GeothermEx 2010).

Till the mid-1980s, there was no reference to the thickness of the valley's sedimentary infill, and it was accepted that it would not exceed a few tens of meters and that tectonic control would not be decisive in its occurrence. However, Carvalho and Silva (1988) show that the thickness of the graben should be at least 450 m (Fig. 3) using geoelectric surveys.

Later, recurring to MT and AMT geophysical exploration, Andrade Afonso et al. (1995), Monteiro Santos et al. (1996, 1997), Duque et al. (1998), and GeothermEX 2010) reported that the maximum thickness of the sedimentary deposits in the centre of the graben should range from 1100 to 1600 m, which can consolidate the perspective of Carvalho and Silva (1988): *'the possibility of deep occurrence in the central part of the graben of sedimentary materials, possibly in communication with an important fissural trap responsible for the emergence of geothermal fluids. This model, to be confirmed, will put in prospect, in a new way, the exploration and exploitation of geothermal fluids in Chaves. In fact, in terms of the geothermal reservoir, rather than the classical binomial of fractured media (high transmissivity, very high in this case, very low coefficient of storage), it can be expected that much higher storage coefficients will occur, certainly permitting more flexible exploitation conditions. We would thus have a fissural geothermal system feeding sedimentary formation with interstitial permeability in which geothermal abstraction wells with relatively small geological risk would be constructed'* (see Figs. 3 and 4). Furthermore, the studies by

Fig. 3 Hydromineral and geothermal circuit of Chaves in the discharge zone: a hydrogeological conceptual model proposed by Carvalho and Silva (1988)



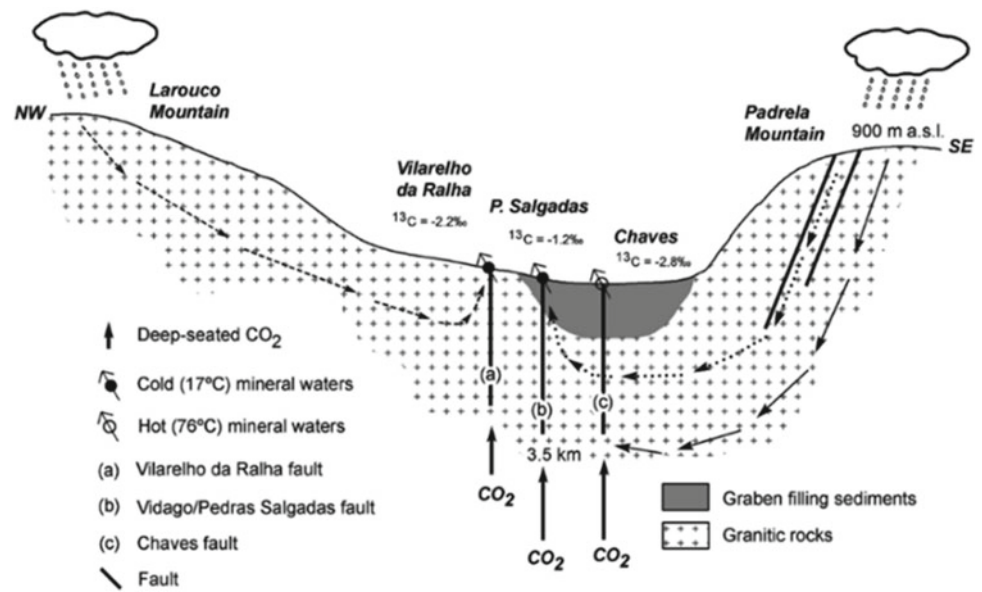
Represas et al. (2013) highlight a gravimetric anomaly (reaching up to more than -55 mGal), trending NNE–SSW orientation, centred on the Veiga de Chaves, which seems well evidenced.

5 Extractions and Available Power

Freire de Andrade (1952) designed shallow wells installed directly on the Silurian metamorphic rocks punctually cut by a dense network of hydrothermal quartz, providing water at 74 °C. Quaternary alluviums of the Tâmega River have a

maximum thickness of about 10 m. Carvalho and Silva (1988) pointed out that the piezometric surface of the thermal aquifer was superior to that of the shallow phreatic waters, which allowed to explain the occurrence of the thermal occurrences in a restricted area of lower dimension in the embankment of the Tâmega river. At present, the piezometric level of the geothermal aquifer is close to, or slightly lower than, the water table of the alluvial aquifer. However, this variation may not mean a decrease in the piezometric level of the geothermal system but a rise in the level of the alluvial water table after the nearby construction of the Tâmega reservoir.

Fig. 4 The conceptual model of the thermo-mineral waters of Chaves and other non-thermal carbogaseous waters of the region focused on the environmental isotopic approach (Carreira et al. 2008; Marques and Carreira 2019)



The current exploitation wells AC1, AC2, and CC3 of the hydromineral and geothermal resources of Chaves reach -100, -150, and -190 m deep, respectively 10.5, and 15 L/s flow rates. In CC3 well, the specific flow rate is 3.2 L/s/m, corresponding to first-order transmissivities of 740 m²/day and storage coefficients of 7.5×10^{-3} . To have an idea of the magnitude of this transmissivity and the quantitative value of the Chaves geothermal resource, it should be noted that the average transmissivity of water wells considered productive in the Central-Iberian Zone (s.l.) in normal waters is in the range of 2–4 m²/day (Carvalho 2006). Furthermore, the transmissivity in S. Pedro do Sul (the second recognised the high geothermal potential in the Portuguese Old Massif) does not exceed 100 m²/day (Carvalho 1996). Thus, from the reservoir point of view, Henriques (1726) had a reason. Indeed, in Chaves, there are the highest hydraulic transmissivities and the highest temperatures in the thermo-mineral waters of mainland Portugal.

The thermometric electrical logs show gradient inversions under the large, fractured zones crossed (from 150 m in the deepest CC3 hole). This circumstance should be considered normal in fractured media. Carvalho (1995) stated that: 'Chaves constitutes an exceptional location, with substitutable consumption of around 3,000 toe. For more than a dozen years, the municipal swimming pool has been heated by water from the AC2 borehole with a depth of 150 m carried out for this purpose in 1982. A hotel and the new Thermal Bath use geothermal hot water. A greenhouse is under construction. They are disconnected uses without dimension or studied design, of questionable energy efficiency. A project financed by the European Union in 1989 included: (i) one or two geothermal boreholes, and (ii) the construction of an urban district heating network that was

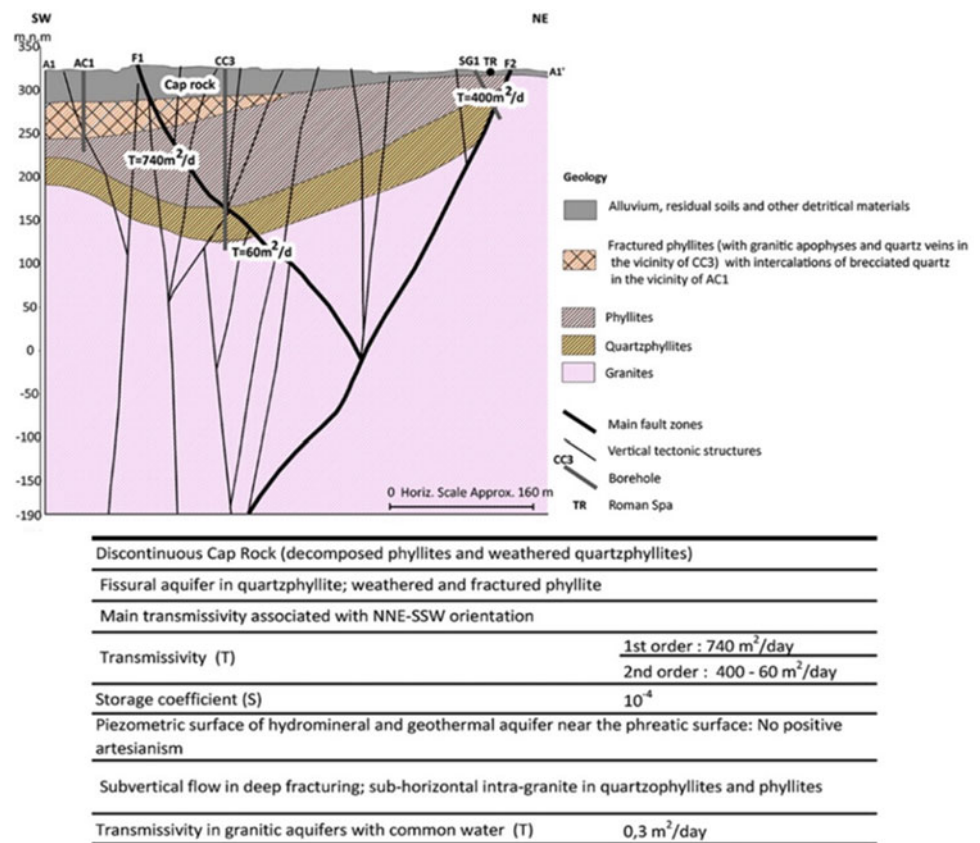
not even started despite the very low technical risk and the financial funds been made available to the promoter, the Chaves Municipality. A research program funded by the Joule Programme promoted knowledge on the reservoir conceptual model, Aires-Barros et al. (1994) and Andrade Afonso et al. (1995)'. Indeed, over twenty-five years later, the situation has hardly evolved.

Figure 5 shows the conceptual model of the hydromineral and geothermal circuit of the Caldas de Chaves site in the discharge zone.

The geothermal greenhouse, built after the Joule Project mentioned above, in the Outeiro Jusão site (Cruz and Lourenço 2006), operated for only one year and was abandoned and dismantled. However, the swimming pool heating system, which has been in operation for more than 30 years, continues to operate without interruption using the AC2 borehole but with new and more efficient heat exchangers. The heat distribution network to the *Acqua Flaviae*, Jaime (now Hotel Geriátrico) and Ibis hotels, and the heating of the thermal building, operates regularly based on the AC1 borehole. Nevertheless, the uses are insufficient to efficiently take advantage of the resource: water is often rejected for sewage at 60 °C, and there is still a need to run electric cooling towers to produce 'cold thermal water' for use in the thermal bath.

During the year 2014, the energy performance of the Chaves geothermal project corresponds to the installed capacity of 3.6 MWt (considering a use of up to 15 °C, the average groundwater temperature in surface aquifers in the region), a total energy utilisation of 7 088 471 kcal \times 103 and utilisation coefficients of 18 and 42% in AC1 and AC2, respectively. Thus, available power amounts now to 7.3 MWt with the three wells.

Fig. 5 Conceptual model of the Caldas de Chaves hydromineral and geothermal circuit in the discharge zone



The shallow resource formed by the thermal water must be added to these availabilities until now discharged by the geothermal system in the Tâmega alluvium and in the weathered upper zone of the metasedimentary materials that have not deserved any geothermal use. So, the shallow resources have been evaluated with a geoelectric exploration campaign followed by hydrogeological exploration boreholes up to about -30 m deep. It is planned to use these resources in the future Water Palace near the municipal swimming pool. In this context, we must also consider the use of effluents from thermal baths, a fluid of great energetic value, the use of which could be envisaged in the context of a surface geothermal operation with heat pumps.

6 The Future of the Chaves Geothermal Project: Final Remarks and Outlook

The 7.3 MWt power currently available in Chaves far exceeds the needs of balneotherapy and should be oriented to direct uses (heating, dehumidification, preparation of hot tap water, and, in a thermal cascade, greenhouses and fish farming). Furthermore, the heating station in Chaves runs from October to April, making the geothermal resource particularly suitable for district heating. So, it is time to

recreate the cancelled 1989 DG-XVII-EC Demonstration Project to develop the incipient existing heat network, extending it to new users, such as some of the city's public buildings, hotels, Roman Baths, etc. A minimalist hydrogeological intervention in the springs of the Roman Baths was boosted by the fact that it is not convenient to empty the Roman swimming pools nor degrade the quality of the thermal water that occurs there for museological reasons. The thermal water resource, in our view, is part of the museological approach.

This goal is incompatible with on-site geothermal resource extraction. It is recalled here that low-enthalpy geothermal energy at Chaves is highly adequate to meet the current needs already identified in previous interventions. Generally, it does not encourage new activities, such as fish farming and greenhouses, if not already installed. This fact was well evident in the clamorous failure of the greenhouses of the Joule Project. The eventual extraction of shallow geothermal fluids at a small depth (ongoing project) will further increase the availability of geoheat. In this regard, it is also essential to emphasise the possibility of integrating the effluents of the thermal bath, a fluid of great energetic value, into a rational system of the utilisation of existing resources. This use could be envisaged in an additional operation with geothermal heat pumps.

The joint use of all these resources raises the question of the sustainability of the Chaves geothermal system, considering the uncertainty of the overall conceptual model. The adequate monitoring of the resource in the discharge zone is essential, but it is also imperative to move towards numerical modelling, supported by new fieldwork, to identify possible recharge zones and resource renewal rates.

The question of geothermal production of electric energy in the region of Chaves can be posed. This issue has already been considered previously, and there has been a license to develop geothermal resources in an area of 200 km² in the surrounding region of Chaves granted by the Portuguese State in 2009 (GeothermEx 2010). GeothermEx took over and developed the model of Carvalho and Silva (1988) and proposed to the license holder (Galena International Resources) to carry up investigations to about 2000 m, trying to explore deep aquifers on the granite underlying the graben where temperatures will occur at 123 °C (Moitinho de Almeida 1982). Fluids with temperatures of this magnitude can be used to generate electricity in binary fluid geothermal power stations. GeothermEx (2010) evaluated in situ thermal energy with the Monte Carlo method and concluded that for an area of 2.5–7 Km², in the Chaves graben, there would be thermal power available of 11 MWe (20 years). The same document considered that this power could be extended from 2.6 to 5 MWe per km² for 20 years. These results suggest that the available electrical power is relatively modest and that investments would be very high.

There is heat in the Chaves geothermal field, and there is water available for recharge, but the limits of the reservoir, its permeability, and its typology are not known. Whether it concerns a classical project with fluid extraction or a stimulated system (EGS), how to conciliate the existence of this new exploitation with the balneotherapy and its direct uses?

New improvements in converting low-temperature heat to electricity could be applied to the existing Chaves geothermal resource and are economically feasible. However, caution must be taken in order to integrate this kind of solution in order to maintain the sustainability of the system. The technical and sociological legacy of the Roman Baths suggests, as a priority, the development in Chaves of a geothermal project for direct, sustained, and sustainable use. This project must be adjusted to the existing resource and demand to promote Chaves city and the Thermal Bath and comfort its inhabitants.

Acknowledgements This work was partially supported by: (i) LABCARGA|ISEP re-equipment program (IPP-ISEP|PAD'2007/08); (ii) Centre GeoBiotEc|UA through FEDER-EU COMPETE Funds and the Portuguese Foundation for the Science and Technology, FCT (UID/GEO/04035/2020); (iii) 'La Caixa' Foundation–FCT (Programme 'Promove 2020', Aqueae Vitae R&D Project—'Thermal waters as a natural resource and with therapeutic applications'). Many thanks to colleagues J.A. Teixeira and L. Freitas

to support the final editing of the figures. Our thanks to Chaves municipality for all data and for sharing historical information. Lastly, a special thanks to all the colleagues, technicians, and managers of the companies, contractors, academia, state laboratories, and central administration we have contacted over the years, who have made it possible to exchange learning, perspectives, and various information.

References

- ACavaco (1982) Estudo hidrogeológico das emergências de águas minero-medicinais de Chaves—Tarefa 2. Estudo geofísico e execução de furos de pesquisa. Câmara Municipal de Chaves Lisboa. (Unpublished Report)
- Acciaiuoli LMC (1952/1953) Le Portugal hydromineral. Direction Générale des Mines et des Services Géologiques, Lisbonne, I Vol. 1952, 284 p; II Vol. 1953, 574 p
- Aires-Barros L, Graça RC, Marques JM (1994) The low temperature geothermal system of Chaves (Northern Portugal): a geochemical approach. In: Geothermics'94 in Europe. Doc Bur Rech Géol Min 230:67–74
- Aires-Barros L, Marques JM, Graça RC (1995) Elemental and isotopic geochemistry in the hydrothermal area of Chaves-Vila Pouca de Aguiar (Northern Portugal). Environ Geol 25(4):232–238
- Aires-Barros L, Marques JM, Graça RC, Matias MJ, Weijden CH, Kreulen R, Eggenkamp HGM (1998) Hot and cold CO²-rich mineral waters in Chaves geothermal area (Northern Portugal). Geothermics 27:89–107
- Almeida A, Almeida J (1970) Inventário hidrogeológico de Portugal, vol 2. Trás-os-Montes e Alto Douro. Instituto de Hidrologia, Lisboa
- Andrade Afonso J, Mendes-Victor LA, Portugal Ferreira M, Dupis A, Aires-Barros L, Monteiro Santos FA, Trota A, Marques JM, Moreira M, Ribeiro J, Oliveira A (1995) Evaluation of geothermal resources in the Chaves region (North Portugal). Proc World Geoth Congr 2:1349–1353
- Baptista J, Cabral J, Ribeiro A (1998) Seismotectonics of Chaves and Moledo mineral springs in Penacova-Régua-Verin Fault Zone. Comun Inst Geol Min 84(1):D69–D72
- Brum Ferreira A (1991) Neotectonics in Northern Portugal: a geomorphological approach. Zeitschr Geomor 82:73–85
- Carneiro S (2016) The water supply and drainage system of the roman healing spa of Chaves (*Acquae Flaviae*). In: Failde-Garrido JM, Formella A, Fraiz-Brea JA, Gómez-Gesteira M, Pérez-Losada F, Rodríguez-Vázquez V (eds) Libro de Actas del I Congreso Internacional del Auga, Termalismo y Calidad de Vida. Vicerrectoría del Campus de Ourense, Universidade de Vigo, Ourense p, Campus da Auga, pp 289–298
- Carreira PM, Marques JM, Graça RC, Aires-Barros L (2008) Radiocarbon applications in dating “complex” hot and cold CO²-rich mineral water systems: a review of case studies ascribed to the northern Portugal. Appl Geochem 23(10):2817–2828
- Carvalho JM (1993a) Mineral and thermal water resources development in the Portuguese Hercynian Massif. In: Banks SB, Banks D, (eds.), Proceedings of the XXIV of the International Association of Hydrogeologists, Hydrogeology of Hard Rocks, vol 24, no 1. IAH, Oslo, pp 548–561
- Carvalho JM (1993b) Ground water exploration in hard rocks for small scale irrigation in Trás-os-Montes, Portugal. In: Banks SB, Banks D, (eds.), Proceedings of the XXIV of the International Association of Hydrogeologists, Hydrogeology of Hard Rocks, vol 24, no 1. IAH, Oslo, pp 1021–1030
- Carvalho JM (1995) Recursos geotérmicos de Portugal Continental: da utopia à realidade. In: Borges FS, Marques M (coords.), Resumos Alargados do IV Congresso Nacional de Geologia Memórias do

- Museu e Laboratório Mineralógico e Geológico, vol 4. Universidade do Porto, Porto, pp 851–856
- Carvalho JM (1996) Mineral water exploration and exploitation at the Portuguese Hercynian Massif. *Environm Geol* 27:252–258
- Carvalho JM (2006). Prospecção e pesquisa de recursos hídricos subterrâneos no Maciço Antigo Português: linhas metodológicas. Universidade de Aveiro, Aveiro. <http://hdl.handle.net/10773/5016> (Ph.D. Thesis)
- Carvalho JM (2015) O campo hidromineral e geotérmico de Chaves (NE de Portugal): uma visão prospectiva. *PPGS Newsletter* 5:4–9
- Carvalho JM, Chaminé HI (2016) Mineral water resources development in crystalline rocks: challenges and possible solutions. In: Failde-Garrido JM, Formella A, Fraiz-Brea JA, Gómez-Gesteira M, Pérez-Losada F, Rodríguez-Vázquez V (eds) *Libro de Actas del I Congreso Internacional del Auga, Termalismo y Calidad de Vida*. Vicerrectoria del Campus de Ourense, Universidade de Vigo, Ourense, Campus da Auga, pp 39–53
- Carvalho JM, Chaminé HI (2017) The hydromineral and geothermal field of Chaves (NE Portugal): a prospective approach. In: Sousa R, Abrunhosa M, Chambel A, (eds.), *Abstract Book & Field Guide GwFR'2017–International Conference on Groundwater in Fractured Rocks (5–7 June 2017)*, Chaves, pp 16–24
- Carvalho JM, Chaminé HI, Afonso MJ, Espinha Marques J, Medeiros A, Garcia S, Gomes A, Teixeira J, Fonseca PE (2005) Productivity and water costs in fissured-aquifers from the Iberian crystalline basement (Portugal): hydrogeological constraints. In: López-Geta JA, Pulido-Bosch A, Baquero-Úbeda JC (eds) *Water, mining and environment Book Homage to Professor Rafael Fernández Rubio*. Instituto Geológico y Minero de España, Madrid, pp 193–207
- Carvalho JM, Paiva M, Carvalho R, Freitas L, Teixeira J, Chaminé HI (2023) Uma visão integrada dos recursos hídricos subterrâneos e dos recursos hidrogeológicos de Trás-os-Montes. In: Balsa C, Sobrinho Teixeira J (eds.), *Recursos geológicos de Trás-os-Montes: passado, presente e perspetivas futuras*. 2a edição, Instituto Politécnico de Bragança, Bragança (in press)
- Carvalho JM, Paiva M, Carvalho R, Fonseca PE, Freitas L, Teixeira J, Chaminé HI (2023) Uma visão integrada dos recursos hídricos subterrâneos e dos recursos hidrogeológicos de Trás-os-Montes. In: Balsa C, Escudeiro M, Rodrigues O (eds) *Recursos Hídricos e Geológicos de Trás-os-Montes*. Instituto Politécnico de Bragança Edições, Bragança, Portugal, pp 1–84
- Carvalho JM, Silva LF (1988) Pólos geotérmicos de Trás-os-Montes: recursos e metodologias de desenvolvimento. *Anais Da UTAD, Vila Real* 2:23–45
- Choffat P (1917) La ligne de dépression Régua-Verín et ses sources carbonatées: remarques et considérations. *Comun Serv Geol Portg* 12:35–69
- Cruz J, Lourenço C (2006) Os recursos geotérmicos de baixa entalpia em Portugal Continental e seu tipo de aproveitamento. *Bol Min* 41 (2):175–186
- Cunha PP, Vicente G, Martín-González F (2019) Cenozoic sedimentation along the piedmonts of thrust related basement ranges and strike-slip deformation belts of the Iberian Variscan Massif. In: Quesada C, Oliveira JT (eds) *The geology of Iberia: a geodynamic approach–*, vol 4. *Cenozoic Basins*. Springer, Cham, pp 131–165
- Dias J, Galhano F (1986) Aparelhos de elevar a água de rega: contribuição para o estudo do regadio em Portugal. Edições D. Quixote, Lisboa
- Duque R, Monteiro Santos FA, Mendes-Victor LA (1998) Heat flow and deep temperatures in the Chaves Geothermal system, northern Portugal. *Geothermics* 27:75–87
- Eggenkamp HGM, Marques JM, Neves O (2015) A geochemical atlas of the Portuguese mineral waters. *Onderzoek en Beleving*, Bussum, The Netherlands
- Feio M (1951) Notas geomorfológicas: a depressão de Régua-Verín. *Comun Serv Geol Portg* 32:181–222
- Freire de Andrade C (1952) Algumas observações sobre a captagem das águas termais de Chaves. *Imprensa médica*, Lisboa
- Freitas HN (2015) Investigações hidrogeológicas da sondagem CC3 do aquífero termomineral de Chaves: implicações para o modelo conceptual. Instituto Superior de Engenharia do Porto, Porto. <http://hdl.handle.net/10400.22/8037> (MSc Dissertation)
- GeothermEx, (2010) Resource evaluation of the Chaves geothermal prospect. Richmond, California (Unpublished report), Galena International Resources
- Grade J, Casal Moura A (1982) Bacia de Chaves: Estudo prospectivo dos seus corpos argilosos. *Geonovas Rev Assoc Portg Geol* 1 (3):79–84
- Henriques FF (1726) *Aquilégio medicinal*. Edição fac-similada. Inst Geol Min, Lisboa
- Hidroprojecto, ACavaco, Tahal, (1987) Estudo das águas subterrâneas do Vale de Chaves e seus vales secundários. Relatório inédito para a DRATM, Mirandela e Lisboa (Unpublished Report), Tomo I - Vale de Chaves
- Houten P (2021) *Urbanisation in Roman Spain and Portugal: Civitates hispaniae in the early empire*. Routledge, Taylor and Francis Group, London
- INAG (1997) Definição, caracterização e cartografia dos sistemas aquíferos de Portugal continental. Instituto da Água, INAG, Divisão do Recursos Hídricos, Lisboa
- Joukes V, Costa I (2015) Eurocity Chaves-Verín: regional development strengthened by spa-linked research and professional education. In: Peris-Ortiz M, Álvarez-García J (eds) *Health and wellness tourism: Emergence of a new market segment*. Springer, Cham, pp 47–62
- Le Roux P (2000) *Legio VII Gemina (pia) felix*. In: Le Bohec Y, (ed.), *Les légions de Rome sous le Haut-Empire*, Lyon, p. 383–396
- Marques JM, Aires-Barros L, Graça RC (1999) Geochemical and isotopic features of hot and cold CO₂-rich mineral waters of northern Portugal: a review and reinterpretation. *Bull Hydrogéol* 17:175–183
- Marques JM, Carreira PM (2019) Geosciences in the assessment of thermal and mineral groundwater systems in N-Portugal: a review. *Sust Wat Res Manag* 5:1511–1523
- Marques JM, Carreira PM, Aires-Barros L, Monteiro Santos FA, Antunes da Silva M, Represas L (2019) Assessment of Chaves low-temperature CO₂-Rich geothermal system (N-Portugal): using an interdisciplinary geosciences approach. *Geofluids*, ID:1379093. <https://doi.org/10.1155/2019/1379093>
- Marques JM, Carreira PM, Espinha Marques J, Chaminé HI, Fonseca PE, Monteiro Santos FA, Eggenkamp HGM, Teixeira J (2010) The role of geosciences in the assessment of low-temperature geothermal resources (NPortugal): a review. *Geosci J* 14(4):329–446
- Marques JM, Carreira PM, Goff F, Eggenkamp HGM, Antunes da Silva M (2012) Input of 87Sr/86Sr ratios and Sr geochemical signatures to update knowledge on thermal and mineral waters flow paths in fractured rocks (N Portugal). *Appl Geochem* 27:1471–1481
- Moitinho de Almeida F (1982) Novos dados termométricos sobre as águas de Chaves e de S. Pedro do Sul. *Comun Serv Geol Portg* 68:179–190
- Monteiro Santos FA, Andrade Afonso AR, Mendes-Victor LA (1997) A study of Chaves geothermal field using 3D resistivity modelling. *J Appl Geophys* 37:85–102
- Monteiro Santos FA, Dupis A, Andrade Afonso AR, Mendes-Victor LA (1996) An audio-magnetotelluric survey over the Chaves geothermal field (NE Portugal). *Geothermics* 25(3):389–440
- OCSA (2012) Prospecção geofísica com sísmica de reflexão e tomografia eléctrica no Largo do Tabolado do Chaves. tomo 1:

- Trabalho de campo, interpretação e resultados. OCSA Prospecciones y Estudios SL, Madrid (Unpublished Report)
- Oliveira JT, Pereira E, Ramalho M, Telles Antunes M, Monteiro JH (coords.) (1992) Carta Geológica de Portugal, escala 1/500.000, 5ª edição. Serviços Geológicos de Portugal, Lisboa
- Paiva M, Carvalho R, Nogueiro R, Casal B, Carvalho JM (2022) Projeto geotérmico das termas Romanas de Chaves. In: Mendes MP, Monteiro JP, Simões M et al (eds) Livro de Resumos do 13º Seminário sobre Águas Subterrâneas, Associação Portuguesa dos Recursos Hídricos, APRH, Lisboa, pp 5–7
- Pereira E (coord) (2006). Notícia explicativa da Carta Geológica de Portugal, na escala de 1/200.000, folha 2 (Trás-os-Montes), Inst Nac Eng Tecnol Inov, Lisboa
- Pereira E, Ribeiro A, Carvalho GS, Noronha F, Ferreira N, Monteiro JH (1989) Carta Geológica de Portugal, escala 1/200000. Folha 1, Serv Geol Portg, Lisboa
- Pereira E, Ribeiro A, Marques F, Munhá J, Castro P, Meireles C, Ribeiro MA, Pereira D, Noronha F, Ferreira, N (2001) Carta Geológica de Portugal, escala 1/200000. Folha 2, Serv Geol Portg, Lisboa
- Plasencia N, Carvalho JM, Cavaco T (2015) Groundwater monitoring impacts of deep excavations: hydrogeology in the Venda Nova repowering schemes (MW Portugal). *Envir Eart Sci* 73:2981–2995
- Portugal Ferreira M, Carvalho JM, Mendonça JL (1982) Águas termo-minerais de Chaves (Trás-os-Montes, NE Portugal. In: Resumos III Semana de Hidrogeologia, Lisboa
- Portugal Ferreira M, Oliveira AS, Trota AN (2003) Termas de Chaves: I-as bases tectónicas e litoestratigráficas para a modelação física e química do sistema hidrotermal. In: Portugal Ferreira M (coord.), *A Geologia de Engenharia e os Recursos Geológicos: recursos geológicos e formação*, vol 2. Volume de Homenagem ao Prof. Doutor Cotelto Neiva, Imprensa da Universidade, Série Investigação, Coimbra, pp 277–294
- Rego Lima JM (1892) Reconhecimento geo-hidrológico de Chaves. Imprensa Nacional, Lisboa
- Represas P, Monteiro Santos FA, Ribeiro J, Ribeiro JA, Almeida EP, Gonçalves R, Moreira M, Mendes-Victor LA (2013) Interpretation of gravity data to delineate structural features connected to low-temperature geothermal resources at Northeastern Portugal. *J Appl Geoph* 92:30–38
- Ribeiro A, Kullberg MC, Kullberg JC, Manuppella G, Phipps S (1990) A review of Alpine tectonics in Portugal: foreland detachment in basement and cover rocks. *Tectonophysics* 184:357–366
- Ribeiro A, Munhá J, Dias R, Mateus A, Pereira E, Ribeiro L, Fonseca PE, Araújo A, Oliveira JT, Romão J, Chaminé HI, Coke C, Pedro J (2007) Geodynamic evolution of the SW Europe Variscides. *Tectonics* 26:TC6009
- Teixeira C (1948) A depressão de Chaves: génese e evolução. *Bol Mus Miner Geol Univ Lisboa* 2:15–16
- TERMARED (2011) Catálogo de mananciales termales del espacio Sudoe GALICIA/Catálogo de nascentes termais do espaço Sudoe GALIZA/Catalogue des sources thermales de l'espace Sudoe GALICE. Xunta de Galicia, Santiago de Compostela
- Varet J (1979) Projet géothermique dans la région du nord du Portugal: proposition d'étude de faisabilité. Rapport BRGM/RR-00119-FR, 79-SGN-822-GTH, Service Géologique National, Orléans. <http://infoterre.brgm.fr/rapports/79-SGN-822-GTH.pdf>
- Vaz FC, Martin-Seijo M, Carneiro S, Tereso JP (2015) Waterlogged plant remains from the roman healing spa of *Acquae Flaviae* (Chaves, Portugal): utilitarian objects, timber, fruits and seeds. *Quatern Int* 30:1–18
- Zbyszewski G (1938) Observations sur un cas d'hydrologie souterraine dans le Nord du Portugal: le bassin de Chaves. *Rev Géogr Phys* 11 (3):286–292